

Государственное образовательное учреждение
высшего профессионального образования
**«Томский государственный университет
систем управления и радиоэлектроники»**

ТЕМАТИЧЕСКИЙ РЕФЕРАТИВНЫЙ СБОРНИК № 49-2/1

“НЕМТ”

(«Транзисторы с высокой подвижностью электронов»)

Публикации в трудах конференций

Источник: *Digital Library IEEEExplore*

Язык: *английский*

Глубина поиска: *2007 – 2011 гг.*

Дата формирования: *март 2011 г.*

Составитель: *В.И. Карнышев*

Томск – 2011

ТЕМАТИЧЕСКИЙ РЕФЕРАТИВНЫЙ СБОРНИК № 49-2/1

"HEMT"

(«Транзисторы с высокой подвижностью электронов»)

Публикации в трудах конференций

"Terahertz-capability nanoscale InGaAs HEMT design guidelines by means of full-band Monte Carlo device simulations"

We provide design guidelines for InGaAs HEMT nanoscale scaling from the analysis of results obtained through our full band Cellular Monte Carlo simulator. In particular, improved RF performance can be obtained preserving a minimum aspect ratio of 5, limiting in such way short channel effects and reducing the electron transit time through the reduction of the effective gate length. Further improvement can be obtained reducing the source-gate access region length. Thus, the effective gate length relative increase and the parasitic intrinsic access region resistance are found to be the main factors limiting nanoscale scaling in THz InGaAs HEMTs. [C1]

"A concurrent dual band 870 and 1970 MHz 10 W envelope tracking PA designed by a WCDMA probability distribution conscious approach"

In this paper we propose a novel approach for the design of a concurrent dual-band power amplifier (PA) optimized for envelope tracking (ET) operation. The design was based around the WCDMA probability distribution function and implemented through a multi-section transmission line matching technique. This technique was applied to a concurrent 870 and 1970 MHz ET PA designed around a GaAs HEMT. The ET friendly design method has proven capable to enhance the average efficiency by a 2.2 factor over a signal bandwidth of 140MHz and 60MHz in the two carrier frequency bands respectively for the specific WCDMA signal. A detailed discussion of the design method and the validating experimental results are reported. [C2]

"A 2GHz GaN Class-J power amplifier for base station applications"

The design and implementation of a high efficiency Class-J power amplifier (PA) for basestation applications is reported. A commercially available 10W GaN HEMT device was used, for which a large-signal model and an extrinsic parasitic model were available. Following Class-J theory, the needed harmonic terminations at the output of the transistor were defined and realised. Experimental results show good agreement with simulations verifying the class of operation. Efficiency above 70% is demonstrated with an output power of 39.7dBm at an input drive of 29dBm. High efficiency is sustained over a bandwidth of 140MHz. [C3]

"Characterization of broadband Monolithic Gallium Nitride distributed power amplifier using thermal imaging technique"

A thermal imaging technique is used to characterize a Monolithic Gallium Nitride distributed power amplifier under DC and RF drive conditions. The temperature difference among the active cells (transistors) in distributed power amplifier is observed under RF drive conditions. It is believed that this non-uniform performance of individual cells in broadband distributed power amplifier results in its lower efficiency and lower power output comparing to narrowed band design. The experimentally observed results match with the results of large signal simulation. The technique can be used to optimize the distributed power amplifier design in the future. [C4]

"HEMT GaAs/GaN power amplifiers architecture with discrete dynamic voltage bias control in envelope tracking RF transmitter for W-CDMA signals"

A new approach to the average efficiency improvement based on a combined 2-PAs architecture is presented. It uses discrete power control and dynamic supply voltage, which allows enhanced efficiency at low power level. It enables envelope tracking RF transmitter with higher average efficiency than classical approach. At 2.14 GHz CW we got an average efficiency of 42.5%, 6.1% better than the classical approach with equal peak Pout= 35 dBm. The peak increment of PAE is 13.3% at 16.4 dB of power back-off. [C5]

"Characterization of GaN cantilevers fabricated with GaN-on-silicon platform"

In this article, Gallium nitride (GaN) cantilevers integrated with AlGaIn/GaN high electron mobility transistors (HEMTs) are fabricated with a GaN-on-silicon platform, which is fully compatible with the standard HEMTs fabrication process. A type of micro-bending test was used to characterize the piezoresponse of AlGaIn/GaN HEMT on the GaN cantilever. The modulation capability of the AlGaIn/GaN heterostructures under different gate bias voltages for either high sensitivity or large output signals was demonstrated. A pulsed vibration measurement technique was used to evaluate the Young's modulus of the suspended GaN cantilevers, yielding a Young's modulus of 293 GPa. [C6]

"Gallium nitride approach for MEMS resonators with highly tunable piezo-amplified transducers"

The properties of a new class of electromechanical resonators based on GaN are presented. By using the two-dimensional electron gas (2-DEG) present at the AlGaIn/GaN interface and the piezoelectric properties of this heterostructure, we use the R-HEMT (Resonant High Electron Mobility Transistor) as an active piezoelectric transducer up to 5MHz [1]. In addition to the amplification effect of piezoelectric detection, we show that the active piezoelectric transduction has a strong dependence with the channel mobility that is controlled by a top gate. This allows to envision highly tunable sensors with co-integrated HEMT electronics. [C7]

"Broadband and compact 3-dB MMIC directional coupler with lumped element"

This paper proposed a broadband and compact 3-dB MMIC edge-coupled directional coupler. The proposed coupler consists of eight stepped-impedance coupled sections and a tiny capacitor. The capacitor is constructed by using the MIM capacitor process and is located on the center of the coupler. The capacitor and stepped structure effectively realize 3-dB coupling and enhanced amplitude/phase characteristics. A millimeter-wave prototype MMIC coupler is fabricated on the 100- μm thick GaAs substrate by using the GaAs pHEMT process. The total coupler length is only 440 μm . The fabricated coupler achieves a coupling loss of $-4\text{dB} \pm 0.5\text{dB}$ from 30 GHz to 69.3 GHz. The output amplitude and phase imbalances are less than 1.4 dB and 90 degrees \pm 5 degrees at the same frequency range, respectively. The proposed MMIC coupler promises very compact and broadband MMIC. [C8]

"Nonlinear characterization techniques for improving accuracy of GaN HEMT model predictions in RF power amplifiers"

In this paper, two vector nonlinear characterization procedures are presented, aimed at improving available GaN HEMT models for an accurate reproduction of the device behavior operating as a current source and in switched-mode RF power amplifiers (PAs). In the case of the more traditional linear amplifying classes, a technique for simultaneously extracting the higher order derivatives of the $I_{ds}(V_{gs})$, $I_{gs}(V_{gs})$ and $C_{gs}(V_{gs})$ transistor nonlinearities, along a desired load line, is described. This procedure conveniently isolates and models their contributions to the device intermodulation distortion (IMD) behavior. In the case of highly efficient switched-mode PAs, employed under drain modulation condition, a modified procedure for isodynamically measuring the higher order derivatives of the Vdd-to-AM and Vdd-to-PM amplifier profiles is put into consideration, as a way to refine the triode region reproduction for ON-OFF operation. The test set-ups, based on the combination of vector signal analysis and vector signal generation capabilities, are described in detail, together with some analytic expressions for the parameter extraction. Measured results for a 15 W device from Cree are finally included. [C9]

"High power, high conversion gain frequency doublers using SiC MESFETs and AlGaIn/GaN HEMTs"

High power, high conversion gain microwave frequency doublers using wide bandgap semiconductor devices are developed. A method of determining the optimal harmonic terminations using accurate nonlinear computer models and load- and source-pull simulations is described. Synthesis of these impedances using matching and reflector networks have produced doublers with increased output power, conversion gain and very high suppression of the first and third harmonics. A SiC MESFET-based frequency doubler at $f_0=2.00\text{GHz}$ producing up to 10.00dB conversion gain and 6.31 Watts 2fo output power is presented. An AlGaIn/GaN HEMT-based frequency doubler at $f_0=3.33\text{GHz}$ producing up to 14.80dB conversion gain and 4.14W 2fo output power is also presented. The second harmonic power measurements confirm the accurate predictions made by the nonlinear model. [C10]

"Empirical modeling of GaN FETs for nonlinear microwave circuit applications"

A new approach for the electro-thermal modeling of GaN FETs is presented. The model is identified on-wafer through static I/V curves measured at different base plate temperatures and small-signal parameters.

Improvements in the prediction of the dc drain current component under large-signal operation can be obtained by taking into account nonlinear dynamics of charge trapping phenomena. The use of measured pulsed-I/V characteristics is avoided in the model extraction phase. Identification procedures and a wide experimental validation for a 0.25 μm AlGaIn/GaN HEMT on SiC with 600 μm periphery are provided in the paper. [C11]

"HEMT MMW MMICS for radiometer sensor applications"

This paper will review the progress of HEMT MMW MMIC technologies developed for radiometer sensor applications at Northrop Grumman Aerospace Systems. Specific HEMT MMIC functions that have been developed for the radiometer front-end include the RF LNA, IF LNA and LO driver power amplifiers. We will report recent advancements in both room temperature and cryogenically operated InP HEMT low noise amplifiers and power amplifiers that have reached above 300 GHz for the first time. [C12]

"Novel MMIC architectures for tunable microwave wideband active filters"

This paper reports on two novel architectures for designing tunable microwave active bandpass filters in MMIC technology. The 1stMMIC concerns a frequency-tunable active bandpass filter based on the principle of "actively-coupled passive resonators". Starting from a specific synthesis method developed for fixed-frequency high-order filters, the frequency tuning ability is now performed by the use of varactor-diodes. This new feature is illustrated by the design of a tunable 3-pole active bandpass filter centered at 12 GHz on GaAs. The 2ndMMIC implements a frequency-selective wideband active bandpass filter with the ability to select the required band. This feature is achieved by the use of a channelized configuration. To demonstrate this ability, a GaAs chip has been designed using 3 active filtering channels, embedded in a distributed topology to perform a 3-pole bandpass response in the [9-15] GHz range. The 1stchip was designed using the UMS PH25 process [1] (0.25 μm GaAs P-HEMT) whereas the 2ndone used the OMMIC ED02AH process (0.2 μm GaAs P-HEMT). [C13]

"100 W GaN HEMT power amplifier module with > 60% efficiency over 100-1000 MHz bandwidth"

We have demonstrated a decade bandwidth 100 W GaN HEMT power amplifier module with 15.5-18.6 dB gain, 104-121 W CW output power and 61.4-76.6 % drain efficiency over the 100-1000 MHz band. The 2 Ч 2 inch compact power amplifier module combines four 30 W lossy matched broadband GaN HEMT PAs packaged in a ceramic SO8 package. Each of the 4 devices is fully matched to 50 Ω and obtains 30.8-35.7 W with 68.6-79.6 % drain efficiency over the band. The packaged amplifiers contain a GaN on SiC device operating at 48V drain voltage, alongside GaAs integrated passive matching circuitry. The four devices are combined using a broadband low loss coaxial balun. We believe this combination of output power, bandwidth and efficiency is the best reported to date. These amplifiers are targeted for use in multi-band public mobile radios and for instrumentation applications. [C14]

"Reliable GaN HEMTs for high frequency applications"

This paper describes our team's efforts to develop a manufacturable 0.2 μm T-gate process for GaN HEMTs that enables high performance and enhanced reliability at high frequencies. Our team has demonstrated highly repeatable and uniform HEMT performance measured at 40 GHz with 3.6 W/mm median output power densities, 36.6% median PAE, and 8.4 dB associated gain. RF-driven, temperature-accelerated life tests show a mean-time-to-failure (MTTF) > 6 Ч 10⁷ hours at 150°C junction temperature. Using this GaN HEMT process our team has demonstrated V-band circuits with output power of 1.13 W (2.83 W/mm) with 23.3 % power-added-efficiency measured under CW operation. Furthermore, by increasing the drain bias to 38 V, the circuit demonstrated state-of-the-art power density of 3.96 W/mm (1.58 W total power). [C15]

"43W, 52% PAE X-Band AlGaIn/GaN HEMTs MMIC amplifiers"

This paper presents the results obtained on X-Band GaN MMICs developed in the frame of the Korrigan project launched by the European Defense Agency. GaN has already demonstrated excellent output power levels, nevertheless demonstration of excellent PAE associated to very high power in MMIC technology is still challenging. In this work, we present State-of-the-Art results on AlGaIn/GaN MMIC amplifiers. An output power of 43W with 52% of PAE was achieved at 10.5 GHz showing that high power associated with high PAE can be obtained at X-band using MMIC GaN technology. [C16]

"Frequency-tunable high-efficiency power oscillator using GaN HEMT"

In this paper, a frequency tunable, high-efficiency power oscillator using GaN HEMT for the RF power source applications is presented. The steady state oscillation occurs in a delay line feedback loop which length is adjusted to tune oscillation frequency. A harmonic-tuned matching network is employed to obtain high conversion

efficiency of the oscillator. The measured output power and conversion efficiency of the fabricated oscillator are 44.63 ± 0.2 dBm and better than 62%, respectively, across the 890-950 MHz band with a drain bias voltage of 40 V. Then a hair-pin resonator is employed into the oscillator to improve phase noise characteristics and frequency selectivity. The experimental results of the oscillator with the hair-pin resonator exhibit the output power of 43.55 dBm, corresponding to the conversion efficiency of 61% at 920 MHz. The measured phase noise characteristics are -64 dBc/Hz and -81.24 dBc/Hz at 10 kHz offset without and with the hair-pin resonator, respectively. [C17]

"Doherty amplifier with envelope tracking for high efficiency"

A Doherty amplifier assisted by a supply modulator is presented using 2.14 GHz GaN HEMT saturated power amplifier (PA). A novel envelope shaping method is applied for high power-added efficiency (PAE) over a broad output power range. Experimental comparison with the Doherty and saturated PAs with the supply modulator is carried out. For the 8 dB crest factor WCDMA 1FA signal, the Doherty PA supported by the modulator presents the improved PAE over the broad output power region compared to the standalone Doherty PA. In addition, it achieves better PAE than the saturated PA with the supply modulator due to the lower crest factor envelope signal applied to the Doherty PA. At the maximum average output power, back-off by 8 dB from the peak power, the Doherty amplifier employing bias adaptation shows the PAE of 50.9%, while the comparable saturated PA with supply modulator and standalone saturated Doherty amplifier and saturated PA provide the PAEs of 42.3%, 49.7%, and 35.0%, respectively. [C18]

"N-polar GaN-based MIS-HEMTs for Mixed Signal Applications"

GaN-based transistors are attractive for the next generation RF power and mixed signal electronics due to their high breakdown field and high carrier saturation velocity. III-N high electron mobility transistors (HEMTs) fabricated on the N-face of GaN are well-suited to address the problems of poor electron confinement and high ohmic contact resistance in the highly scaled transistors. At 4 GHz, N-polar metal-insulator-semiconductor (MIS)-HEMTs with a gate length of 0.7 micron exhibited a highest output power density (Pout) of 8.1 W/mm and a highest power-added efficiency (PAE) of 71%, while a Pout of 4.2 W/mm and a PAE of 49% were achieved at 10 GHz. A high speed N-polar MIS-HEMT fabricated with a gate-first self-aligned InGaN-based ohmic contact regrowth technology was characterized, demonstrating an ultra-low contact resistance of 23 ohm-micron and a state-of-the-art fTxLG product of 16.8 GHz-micron with a gate length of 130 nm. [C19]

"Fabrication of AlGaIn/GaN HEMT with the improved ohmic contact by encapsulation of silicon dioxide thin film"

We compared to the characteristics of fabricated AlGaIn/GaN HEMTs on a Si substrate with conventional ohmic contact and improved ohmic contact. In conventional ohmic contact with metal scheme of Ti/Al/Ni/Au or Ti/Al/Ti/Au, generally ohmic contact resistance is good but, surface topography has bad morphology due to ball-up by low Al melting point at high temperature RTA over 800°C. In order to improve that, we applied the encapsulation of silicon dioxide thin film in ohmic contact process and fabricated AlGaIn/GaN HEMT with improved ohmic contact better than surface morphology and resistance of the conventional. As the results, ohmic metal morphology was improved more over 50% than the conventional and contact resistance was also low. Besides, at the T-gate formation, the alignment mark detection of e-beam lithography system was improved. The fabricated AlGaIn/GaN HEMT with conventional ohmic contact has obtained Idssof 260mA/mm, Vpof -1.7V, Gm,maxof 230mS/mm, BVgdof over 90V, fTof 31GHz and fmaxof 51GHz, while it has obtained Idssof 350mA/mm, Vpof -1.6V, Gm,maxof 280mS/mm, BVgdof over 100V, fTof 34GHz and fmaxof 50GHz for improved ohmic contact, relatively. [C20]

"N-polar GaN-based MIS-HEMTs for mixed signal applications"

GaN-based transistors are attractive for the next-generation RF power and mixed signal electronics due to their high breakdown field and high carrier saturation velocity. III-N high electron mobility transistors (HEMTs) fabricated on the N-face of GaN are well-suited to address the problems of poor electron confinement and high ohmic contact resistance in the highly scaled transistors. At 4 GHz, N-polar metal-insulator-semiconductor (MIS)-HEMTs with a gate length of 0.7 μ m exhibited a highest output power density (Pout) of 8.1 W/mm and a highest power-added efficiency (PAE) of 71%, while a Pout of 4.2 W/mm and a PAE of 49% were achieved at 10 GHz. A high speed N-polar MIS-HEMT fabricated with a gate-first self-aligned InGaN-based ohmic contact regrowth technology was characterized, demonstrating an ultra-low contact resistance of 23 Ω - μ m and a state-of-the-art fT·LGproduct of 16.8 GHz- μ m with a gate length of 130 nm. [C21]

"Over 10W C-Ku band GaN MMIC non-uniform distributed power amplifier with broadband couplers"

A 6-18 GHz monolithic microwave integrated circuit (MMIC) power amplifier (PA) was successfully developed using a quarter wavelength short stub and a monolithic broadband coupler for a non-uniform distributed power amplifier (NDPA) topology. This topology improved the output power at 18 GHz and attained a flat output power profile over 6-18 GHz. It also achieved filtering characteristics for both lower and higher cut-off frequencies. A fabricated MMIC PA with 0.25 μm GaN HEMTs delivered an output power of more than 10 W with average power added efficiency (PAE) of 18% over 6 to 18 GHz. To the best of our knowledge, this is the best combination of output power and bandwidth for any solid-state MMIC amplifier operating up to the full Ku-band. [C22]

"A versatile and cryogenic mHEMT-model including noise"

A versatile scalable small signal model for high electron mobility transistors (HEMTs) of gate length 50 nm and 100 nm has been developed. The model covers a large bias range and includes the temperature dependence from 300 K to 15 K. Especially, it is capable to predict the noise behaviour of the transistor in dependence of ambient temperature and frequency. [C23]

"Evaluation of a GaN HEMT transistor for load- and supply-modulation applications using intrinsic waveform measurements"

In this paper, the efficiency of a GaN HEMT transistor and its intrinsic waveforms are measured at 0.9 GHz and investigated for load- and supply-modulation applications. The results show that both techniques perform equally well for back-off levels ≤ 6.5 dB. At higher back-off levels, the efficiency improvements achieved by supply modulation outperform load modulation. At 10 dB back-off, supply, and load modulation provide a power-added efficiency (PAE) of 68%, and 58%, respectively. Using measured intrinsic waveforms, it is shown that PAE degradations in load modulation can be mainly attributed to parallel losses rather than series losses, which are dominant in supply modulation. The harmonic contents of the intrinsic waveforms, in both techniques, are equally strong in back-off and peak power operations. There is, therefore, a great potential for further efficiency enhancement by circuit-level optimization of harmonic terminations for back-off. [C24]

"Single-chip integration of electronically switchable bandpass filter for 3.5GHz WiMAX application"

This paper demonstrates the design and implementation of a miniaturized bandpass filter integrated with switch function in commercial GaAs pHEMT process for 3.5GHz WiMAX application. A tapped-input, capacitive-loaded hairpin-comb bandpass filter is proposed to benefit from the high-density metal-insulator-metal capacitor in the GaAs process, such that the required electrical length of coupled-line is only 13.3 degree at the center frequency and the filter size can be largely reduced. The proposed integrated bandpass filter features low in-band insertion loss as well as a wide 30-dB rejection-band up to 33.8 GHz. The filter size is only 1.22 mm \times 0.61 mm, and is realized in a chip size of 1.5 mm \times 1.0 mm. Then, by adding two D-mode FETs in the pHEMT process, the proposed filter can be switched on and off electronically. Low-loss bandpass response with wide rejection band in the "filter on" state and wideband 35-dB isolation from DC up to 28.7 GHz in the "filter off" state are achieved. The chip size of this switchable bandpass filter is only 2.0 mm \times 1.0 mm. [C25]

"Laser driver switching 20 A with 2 ns pulse width using GaN"

A GaN-HEMT-based circuit is presented capable of switching 20 A of current with less than about 0.5 ns rise and fall time. This demonstrates the potential of GaN transistors for high-current switching applications, even if breakdown voltage requirements are low. The current driver is used to realize an optical pulse picker generating 10 ps optical pulses of more than 30 W with a variable repetition rate between 1 kHz and 100 MHz. [C26]

"Laser driver switching 20 A with 2 ns pulse width using GaN"

A GaN-HEMT-based circuit is presented capable of switching 20 A of current with less than about 0.5 ns rise and fall time. This demonstrates the potential of GaN transistors for high-current switching applications, even if breakdown voltage requirements are low. The current driver is used to realize an optical pulse picker generating 10 ps optical pulses of more than 30 W with a variable repetition rate between 1 kHz and 100 MHz. [C27]

"Current collapse, memory effect free GaN HEMT"

Current collapse (drain current dispersion, gradual power saturation, or memory effect) encountered during microwave GaN HEMT power amplifier operation remains to be a major reliability and stability issue for the highly promising, emerging III-nitride, polar semiconductor based technology. Current collapse leads to bias condition induced memory effect, which is particularly detrimental to broad band RF amplifiers operating with large peak-to-average signal level. Loss of polarization induced, surface mobile holes, accompanied by the

reduction of transistor channel electron density have recently been identified as the root cause of these undesirable, transient effects exhibited by the polar semiconductor based transistors, in which charge carriers are primarily originated from the built-in electric dipoles of the nitride material. A novel ohmic metal contact scheme, presenting low energy barrier for both the transistor channel electrons, and the surface mobile holes, is found to be effective in eliminating the undesirable, time and signal strength dependence behavior of the transistor performance characteristics. A GaN MISHEMT with such compound ohmic contacts is found to be capable of operating at higher saturation current density, compared to that of a GaN HEMT with traditional ohmic contacts. The new finding represents a major breakthrough in polar semiconductor device technology for microwave power amplification. [C28]

"RF class-S power amplifiers: State-of-the-art results and potential"

This paper reports recent results on a current-mode class-S power amplifier for the 450 MHz band, based on GaN-HEMT MMICs. We achieve a peak output power of 8.7 W for a single tone at 420 MHz, encoded in standard band-pass delta-sigma modulation with 1.68 Gbps sampling frequency. The respective efficiency is 34%. We find that these values strongly vary with coding efficiency of the modulation and reach 19 W with 59% for square-wave excitation. In order to clarify the potential of the PA in more detail, the S-class characteristics at power back-off and with varying oversampling ratio are presented as well. [C29]

"TCAD optimization of field-plated InAlAs-InGaAs HEMTs"

High-voltage InGaAs-InAlAs HEMTs featuring optimized field-plate structures are being developed. A TCAD approach has been adopted for their design. Two-dimensional device simulations have preliminarily been calibrated by comparison with DC and RF measurements from the baseline InP HEMT technology into which the field plate is being incorporated. Simulations have then been used to design field-plate structures with optimal length and passivation thickness. [C30]

"Plasma-resonant THz detection with HEMTs"

In this work, by means of Monte Carlo simulations we analyze the dependence of the DC drain current value in a 80 nm-gate InAlAs/InGaAs HEMTs on the frequency of a sinusoidal signal superimposed to the DC gate bias. Interestingly, a resonant peak appears in the drain current response, which lies in the THz frequency range, in good agreement with recent experiments made on similar devices. Moreover, the frequency of the resonant peak is dependent on the length of the source-gate region, but independent of the length of the drain-gate region, thus indicating that the source-gate region acts as the plasma wave cavity leading to the resonant detection of THz radiation in HEMTs. [C31]

"An optoelectronic mixer based on composite transparent gate InAlAs/InGaAs metamorphic HEMT"

In this work, we have fabricated the first transparent gate using sputtered ITO/Au/ITO composite films InAlAs/InGaAs metamorphic HEMT (CTG-MHEMT) on GaAs substrate. The CTG-MHEMT has been demonstrated to increase front side optical coupling efficiency as an optoelectronic mixer. By optimizing the bias condition, the optoelectronic mixing efficiency can be enhanced. The photodetection mechanism of CTG-MHEMT is clarified by investigating the internal photovoltaic gain (G_{pv}) and photoconductance gain (G_{pc}). For comparison of the optical characteristics, the transparent gate MHEMT (TG-MHEMT) has been fabricated. The CTG-MHEMT as an optoelectronic mixer is a promising candidate that can simplify the base station architecture in fiber-optic microwave transmission systems. [C32]

"Current collapse, memory effect free GaN HEMT"

Current collapse in GaN HEMT leads to bias condition induced memory effect, and gradual power saturation, which are particularly detrimental to broadband RF amplifiers operating with large peak-to-average signal level. A novel ohmic metal scheme presenting low energy barrier to both the polarization induced, transistor channel electrons, and the surface mobile holes, is found to be effective in eliminating the undesirable, time and signal strength dependent behavior of the transistor performance characteristics. The new finding represents a major breakthrough in polar semiconductor device technology for microwave power amplification. In this paper, the root cause of current collapse is also briefly described. [C33]

"Isolated-gate InAs/AlSb HEMTs: A Monte Carlo study"

In this work we present a Monte Carlo study of the influence of the presence of a native oxide which isolates the gate in InAs/AlSb high electron mobility transistors (HEMTs) on their dc and ac performance. A good agreement between simulations and experimental results of I-V curves and small signal equivalent circuit

parameters has been found for low VDS, where impact ionization is not of importance. The comparison between intrinsic MC simulation results for isolated-gate and Schottky-gate HEMTs reveals a strong influence of the native oxide on the dynamic behavior of the devices, mainly on Cgs, gmand fc. [C34]

"Logic characteristics of 40 nm thin-channel InAs HEMTs"

We have experimentally investigated the trade-offs involved in thinning down the channel of III-V FETs with the ultimate goal of enhancing the electrostatic integrity and scalability of these devices. To do so, we have fabricated InAs HEMTs with a channel thickness of $t_{ch} = 5$ nm and we have compared them against, InAs HEMTs with $t_{ch} = 10$ nm. The fabricated thin-channel devices exhibit outstanding logic performance and scalability down to 40 nm in gate length. $L_g = 40$ nm devices exhibit $S = 72$ mV/dec, DIBL = 72 mV/V, and $I_{ON}/I_{OFF} = 2.5 \times 10^4$, all at $V_{DS} = 0.5$ V. However, there are trade-offs of using a thin channel which manifest themselves in a higher source resistance, lower transconductance, and lower f_T when compared with InAs HEMTs with $t_{ch} = 10$ nm. [C35]

"A 68% efficiency, C-band 100W GaN power amplifier for space applications"

This paper describes a high efficiency (68%), high output power (100W), high reliability GaN HEMT amplifier for C-band space applications. The high efficiency is achieved by 2nd-harmonic frequency ($2f_0$) tuning circuits in the input and output matching circuits. The input circuit uses open-ended stubs located nearby FET gate terminals for setting the $2f_0$ reflection-phase at the optimum phase. In the output circuit, the optimum $2f_0$ reflection phase is realized using three transmission-line transformers while matching loss is kept low at fundamental frequency. In addition, a 3000 hour's RF overdrive life test reveals that an estimated mean time to failure (MTTF) is 14107 hours at 150°C channel temperature, proving that the amplifier has sufficient reliability for space applications. To the best of our knowledge, the efficiency of 68% is the highest of 100-W class C-band amplifiers ever reported, and is also comparable to that of commercially available traveling wave tube amplifiers. [C36]

"Semi-insulating iron-doped InP buffer layers for Al-free GaInP/GaInAs pHEMTs"

InP buffer layers for Al-free HEMT applications were deposited by metal-organic vapor-phase epitaxy (MOVPE) on semi-insulating InP substrates. The challenge posed by the production of insulating buffers on InP substrates is a well-known problem. Different growth conditions were chosen to achieve highly insulating layers. Our experiments show that regardless of growth conditions, impurities arising from reactor parts and from the starting substrate lead to an n-type background doping decreasing exponentially from 1.4×10^{17} at the substrate to $4.4 \times 10^{14} \text{ cm}^{-3}$ for sufficiently thick layers. Highly resistive buffer layers could only be obtained doping InP with iron at a concentration of $6.4 \times 10^{16} \text{ cm}^{-3}$. Consequently, the sheet resistance of InP could be increased from $R_S = 3000 \Omega/\square$ for undoped layers to $R_S = 9.4 \times 10^7 \Omega/\square$, resulting in InP buffer layers that are suitable for high-speed HEMTs. Non-optimized Al-free GaInP/GaInAs pHEMTs with a T-gate footprint of 100 nm achieved a cutoff frequency of $f_T = f_{max} \sim 250$ GHz, with a channel mobility and electron density of $10,000 \text{ cm}^2/\text{Vs}$ and 10^{12} cm^{-2} , respectively. [C37]

"Front cover"

This paper dealt with the following topics: photonic-electronic convergence; CMOS technologies; semiconductor growth; quantum optics; LED; quantum dots; MOSFET; III-V semiconductors; lasers; modulators; nanostructured devices; epitaxy; HBT; high-speed switches; Sb-based alloys; heterostructures; towards THz; nitrides; optoelectronic devices; integrated light sources; photodetectors; HEMT; MMIC; integrated receivers; heteroepitaxy; photonic crystal devices; FET for logic; MOS; and other related semiconductor devices. [C38]

"DC and RF cryogenic behaviour of InAs/AlSb HEMTs"

DC and RF properties are reported for InAs/AlSb HEMTs operating under cryogenic conditions (6 K) for a drain source bias up to 0.3 V. Compared to room temperature (300 K), a large improvement in device properties was observed: lower R_{on} , lower g_{ds} , a more distinct knee in the $I_{ds}(V_{ds})$ characteristics, increased f_T and a reduction of the gate leakage current of more than two orders of magnitude. This makes InAs/AlSb HEMT technology of large interest in cryogenic low-noise amplifier designs with high constraints on power dissipation. [C39]

"Frequency-tunable high-efficiency power oscillator using GaN HEMT"

In this paper, a frequency tunable, high-efficiency power oscillator using Gallium Nitride High Electron Mobility Transistor (GaN HEMT) for the RF power source applications is designed and fabricated. The steady state

oscillation occurs in a delay line feedback loop which length is adjusted to tune oscillation frequency. A harmonic-tuned matching network technique is employed to obtain high conversion efficiency characteristic of the oscillator. The measured output power and conversion efficiency of the fabricated oscillator are 44.63 ± 0.2 dBm and better than 62%, respectively, across the 890-950 MHz band with a drain bias voltage of 40 V. Then a hair-pin resonator is designed and employed into the oscillator in order to improve phase noise characteristics and frequency selectivity. The experimental results of the oscillator with the hair-pin resonator exhibit the output power of 43.55 dBm, corresponding to the conversion efficiency of 61% at 920 MHz. The measured phase noise characteristics are -64 dBc/Hz and -81.24 dBc/Hz at 10 kHz offset without and with the hair-pin resonator, respectively. [C40]

"HEMT MMW MMICs for radiometer sensor applications"

This paper will review the progress of HEMT MMW MMIC technologies developed at Northrop Grumman Aerospace Systems for radiometer sensor applications. Specific HEMT MMIC functions that have been developed for the radiometer front-end include the RF LNA, IF LNA and LO driver power amplifiers. We report recent advancements in room and cryogenically operated InP HEMT low noise amplifiers and power amplifiers operating from 1 GHz to 300 GHz and discuss past and present system applications of these MMICs. [C41]

"A 68% efficiency, C-band 100W GaN power amplifier for space applications"

This paper describes a high efficiency (68%), high output power (100 W), high reliability GaN HEMT amplifier for C-band space applications. The high efficiency is achieved by 2nd-harmonic frequency ($2f_0$) tuning circuits in the input and output matching circuits. The input circuit uses open-ended stubs located nearby FET gate terminals for setting the $2f_0$ reflection-phase at the optimum phase. In the output circuit, the optimum $2f_0$ reflection phase is realized using three transmission-line transformers while matching loss is kept low at fundamental frequency. In addition, a 3000 hour's RF overdrive life test reveals that an estimated mean time to failure (MTTF) is 14107 hours at 150°C channel temperature, proving that the amplifier has sufficient reliability for space applications. To the best of our knowledge, the efficiency of 68% is the highest of 100-W class C-band amplifiers ever reported, and is also comparable to that of commercially available traveling wave tube amplifiers. [C42]

"Characterization of trapping and thermal dispersion in GaN HEMTs"

Dispersion in a GaN HEMT, including gate and drain lag, is related to a new trapping model based on SRH theory. Measurements and SPICE simulation are used to verify the capability of this model to explain the bias- and terminal-potential dependency of the turn-on transients and their time constants. The models of both drain current and trapping need to consider temperature and power dissipation versus time. The interaction between two different trap mechanisms and two different self-heating processes is shown to adequately explain the different characteristics of the turn-on transient of the transistor under test. [C43]

"RF class-S power amplifiers: State-of-the-art results and potential"

This paper reports recent results on a current-mode class-S power amplifier for the 450 MHz band, based on GaN-HEMT MMICs. We achieve a peak output power of 8.7 W for a single tone at 420 MHz, encoded in standard band-pass delta-sigma modulation with 1.68 Gbps sampling frequency. The respective efficiency is 34%. We find that these values strongly vary with coding efficiency of the modulation and reach 19 W with 59% for square-wave excitation. In order to clarify the potential of the PA in more detail, the S-class characteristics at power back-off and with varying oversampling ratio are presented as well. [C44]

"Behavioral model analysis of active harmonic load-pull measurements"

This paper outlines the formulation of a mixing based behavioral model, capable of capturing the nonlinear response of microwave transistors to fundamental and harmonic load pull effects for use in Computer Aided Design tools. The key to the model formulation was the experimental identification of the dominating mixing terms. The model is able to accurately compute the voltage and current waveforms present at a Transistors Terminals. The formulation lends itself to economical use of measured data, reducing data storage required within the CAD environment. In this paper the modeling approach has been demonstrated on a $10 \times 75 \mu\text{m}$ GaAs HEMT operating at 9 GHz. [C45]

"Nonlinear HEMT model direct formulated from the second-order derivative of the I-V/ Q-V characteristics"

In this paper, an empirical nonlinear model for high electron mobility transistors (HEMTs) is presented. Unlike the

conventional large-signal models whose fitting parameters are coupled to the measured I-V and C-V characteristics, the proposed modeling equations are directly formulated from the second-order derivative of drain current (I-V) and gate charge (Q-V) with respect to gate voltage. As a consequence, the proposed large-signal model is kept continuously differentiable and accurate enough to the higher-order I-V and Q-V derivatives. Measured and modeled results are compared for the 0.25 μm gate-length GaAs pseudomorphic HEMTs (pHEMTs), and good agreement is obtained. [C46]

"W-Band GaN MMIC with 842 mW output power at 88 GHz"

We report W-band GaN MMICs that produce 96% more power at a frequency of 88 GHz in continuous wave (CW) operation than the highest power reported in this frequency band for the best competing solid state technology, the InP HEMT. W-band power module containing a single three stage GaN MMIC chip with 600 μm wide output stage produced over 842 mW of output power in CW-mode, with associated PAE of 14.7% and associated power gain of 9.3 dB. This performance was measured at MMIC drain bias of 14 V. [C47]

"W-band GaN MMIC with 842 mW output power at 88 GHz"

We report W-band GaN MMICs that produce 96% more power at a frequency of 88 GHz in continuous wave (CW) operation than the highest power reported in this frequency band for the best competing solid state technology[1], the InP HEMT. W-band power module containing a single three stage GaN MMIC chip with 600 μm wide output stage produced over 842 mW of output power in CW-mode, with associated PAE of 14.7% and associated power gain of 9.3 dB. This performance was measured at MMIC drain bias of 14 V. [C48]

"Nonlinear modeling of compound semiconductor HEMTs state of the art"

This paper will review the state-of-the-art for modeling compound semiconductor HFETs and HEMTs for microwave power applications. Some simple physics shows why SPICE models, or compact models, cannot contain all aspects of the device operation. Because the models are incomplete, any given model may always be improved and thus, modifiable user-defined compact models are preferred. In particular, Verilog-A coded models are shown to have many desirable features. Minimum modeling requirements for accurate system and circuit simulation are described, as well as present modeling techniques. [C49]

"Fabrication of AlGaIn/GaN HEMT with the improved ohmic contact by encapsulation of silicon dioxide thin film"

We compared to the characteristics of fabricated AlGaIn/GaN HEMTs on a Si substrate with conventional ohmic contact and improved ohmic contact. In conventional ohmic contact with metal scheme of Ti/Al/Ni/Au or Ti/Al/Ti/Au, generally ohmic contact resistance is good but, surface topography has bad morphology due to ball-up by low Al melting point at high temperature RTA over 800°C. In order to improve that, we applied the encapsulation of silicon dioxide thin film in ohmic contact process and fabricated AlGaIn/GaN HEMT with improved ohmic contact better than surface morphology and resistance of the conventional. As the results, ohmic metal morphology was improved more over 50% than the conventional and contact resistance was also low. Besides, at the T-gate formation, the alignment mark detection of e-beam lithography system was improved. The fabricated AlGaIn/GaN HEMT with conventional ohmic contact has obtained I_{dss} of 260mA/mm, V_{pof} – 1.7V, $G_{\text{m,max}}$ of 230mS/mm, BV_{gd} of over 90V, f_{T} of 31GHz and f_{max} of 51GHz, while it has obtained I_{dss} of 350mA/mm, V_{pof} – 1.6V, $G_{\text{m,max}}$ of 280mS/mm, BV_{gd} of over 100V, f_{T} of 34GHz and f_{max} of 50GHz for improved ohmic contact, relatively. [C50]

"Reliable GaN HEMTs for high frequency applications"

This paper describes our team's efforts to develop a manufacturable 0.2 μm T-gate process for GaN HEMTs that enables high performance and enhanced reliability at high frequencies. Our team has demonstrated highly repeatable and uniform HEMT performance measured at 40 GHz with 3.6 W/mm median output power densities, 36.6 % median PAE, and 8.4 dB associated gain. RF-driven, temperature-accelerated life tests show a mean-time-to-failure (MTTF) 6e7 hours at 150°C junction temperature. Using this GaN HEMT process our team has demonstrated V-band circuits with output power of 1.13 W (2.83 W/mm) with 23.3 % power-added-efficiency measured under CW operation. Furthermore, by increasing the drain bias to 38 V, the circuit demonstrated state-of-the-art power density of 3.96 W/mm (1.58 W total power). [C51]

"Experimental study on current collapse of GaN MOSFETs, HEMTs and MOS-HEMTs"

We report on the experimental results of current collapse measurements, using both conventional pulse method and a new DC method, performed on GaN MOSFETs, HEMTs and MOS-HEMTs. The current collapse

phenomena were measured and compared between the different device types, epilayer dopings, RESURF region lengths and MOS channel lengths, at both room temperature and elevated temperatures. [C52]

"Channel scaling of hybrid GaN MOS-HEMTs"

In this paper, we have studied the effect of systematic downscaling of MOS channel length of the performance of the hybrid GaN MOS-HEMT with numerical simulations. The improvement in on-state conduction, together with concomitant short channel effects, such as Drain Induced Barrier Lowering (DIBL) and velocity saturation, is quantitatively evaluated. A specific on-resistance of $2.1 \text{ m}\Omega\text{-cm}^2$ has been projected for a MOS channel length of $0.38 \text{ }\mu\text{m}$. We also have assessed the impact of high-k gate dielectrics, such as Al_2O_3 . In addition, we have found that adding a thin GaN cap layer on top of AlGaIn barrier can help reducing DIBL. [C53]

"High voltage AlGaIn/GaN High-Electron-Mobility Transistors (HEMTs) employing oxygen annealing"

The blocking characteristics of AlGaIn/GaN High-Electron-Mobility Transistors (HEMTs) were considerably improved by an oxygen (O_2) annealing. This proposed annealing, which was performed before Schottky contact formation, successfully decreased the leakage current through the buffer region by about six orders of magnitude and had no effect on the current capability of the active region. The suppressed leakage current may be due to the improved surface condition induced by the reaction between oxygen and the AlGaIn/GaN heterostructure. The proposed device employing the O_2 annealing exhibited a suppressed leakage current and a high breakdown voltage of 1140 V without any surface passivation or edge termination structure. [C54]

"AlGaIn/GaN microwave transistors for wireless communication systems and advanced nanostructures for high-speed sensor applications"

We presented a systematic study of the impact of a layer structure design on the performance of AlGaIn/GaN high electron mobility transistor structures. The new mechanism of strain relaxation by twisted nanocolumns was revealed. The experimentally obtained results were found to be in good agreement with the proposed model. Device layer structures were optimized to obtain a minimum overheating temperature at high dissipated power in HEMT channels. It was shown that the room-temperature spectra can be used to determine the activation energy of the traps. In addition, the impact of layer structure design on the properties of the $1/f$ flicker noise was studied and the phase noise performance of test microwave HEMT-based oscillators was discussed. The noise and capacitance spectroscopy of double-barrier RTDs were found to be a powerful and sensitive tool for the exploration of transport features and structural quality. The results can be used to design AlN/GaN RTD-FETs with optimized layout, to conduct a more efficient analysis of resonant tunneling processes, and to improve the peak-to-valley ratio of NDR regions. [C55]

"Breakdown voltage enhancement for GaN high electron mobility transistors"

This paper presents a high voltage AlGaIn/GaN HEMTs with remarkable breakdown voltage enhancement by introducing a magnesium doping layer under the 2-DEG channel. The surface electric field is distributed more evenly when compared to a conventional device structure with the same dimensions. This is primarily due to the presence of a charge balanced magnesium doping layer acting as a floating field plate. By optimizing the layer's length, L and the doping concentration, a breakdown voltage of 900 V with specific on-resistance of $4 \text{ m}\Omega\text{-cm}^2$ was obtained with $L = 1.5 \text{ }\mu\text{m}$, a peak concentration of $8.4 \times 10^{17} \text{ cm}^{-3}$ and a drift region length of $10 \text{ }\mu\text{m}$. Comparing with previously published breakdown optimization techniques, this work achieved a 100% improvement in specific on-resistance without any area overhead penalty. [C56]

"Enhancement-mode GaN MIS-HEMTs for power supplies"

In this paper, we present the current status of GaN-high electron mobility transistor (HEMT) for power-supply applications. Advantages of GaN HEMT are summarized with discussing required characteristics applying for power supplies. Then, we introduce our Enhancement-mode (E-mode) GaN MIS-HEMT technology. We focused on realizing both normally-off operation and high current density with high breakdown voltage. Detailed results are discussed in this paper. In particular, we developed a unique device structure called triple layer cap structure. High current density with normally-off mode was successfully achieved, which is preferable for power-supply application. We also demonstrated high speed performance with low on-resistance. [C57]

"Achievement and perspective of GaN technology for microwave applications"

This paper gives an overview of some recent results obtained by Alcatel-Thales III-V Lab using emerging AlGaIn/GaN HEMT technology. This technology is very suitable up to Ku-Band and offers impressive power

performances. The second part of the presentation will give an overview of results obtained using new InAlN/GaN heterostructures, which is expected to offer similar output power but with improved efficiencies and to cope with higher working frequencies. [C58]

"Normally-off AlGaIn/GaN HFET with p-type Ga Gate and AlGaIn buffer"

A 1.5 A normally-off GaN transistor for power applications in p-type GaN gate technology with a modified epitaxial layer structure is presented. A higher threshold voltage is achieved while keeping the on-state resistance low by using an AlGaIn buffer instead of a GaN buffer. Additionally, the AlGaIn buffer acts as a back-barrier and suppresses source-drain punch-through currents in the off-state. P-GaN gate GaN transistors with AlGaIn buffer will therefore yield higher breakdown voltages as compared to standard GaN buffer versions which results in an excellent VBr-to-ROn ratio. The proposed normally-off technology shows safe operation under elevated ambient temperature up to 200°C without thermal runaway. In contrast to standard Schottky-gate AlGaIn/GaN HEMTs, a reverse diode operation is possible for off-state conditions which may enable improved inverter circuits. [C59]

"Influence of electric field upon current collapse phenomena and reliability in high voltage GaN-HEMTs"

This paper reports that the maximum electric field is a dominant factor for current collapse phenomena and reliability in high-voltage GaN-HEMTs. The relation between the dynamic on-resistance increase caused by the collapse phenomena and the maximum electric field peak showed universality, which was independent from the field plate (FP) structure and the wafer. The gate-edge electric field strongly affects the increase of the dynamic on-resistance. After the continuous switching test for 7 hours, the change of the dynamic on-resistance also depended on the maximum electric field. The optimal FP structure minimized the increase of the dynamic on-resistance and realized high reliability due to minimization of the electric field peaks. [C60]

"Self-protected GaN power devices with reverse drain blocking and forward current limiting capabilities"

Self-protected GaN power devices were realized using AlGaIn/GaN-on-Si platform, where two built-in intelligent functions were demonstrated for "Smart Discrete" applications. First, an AlGaIn/GaN normally-off high electron mobility transistor (HEMT) with reverse drain blocking capability was realized, featuring a Schottky contact controlled drain barrier. Compared to the Schottky drain structures, the new design exhibits only a 0.55 V onset voltage in the forward biased "ON" state, while effectively blocks the reverse current conduction. The device fabrication is also free of extra photomask and process steps. Second, an AlGaIn/GaN lateral field-effect rectifier (L-FER) with intrinsic "ON" state current limiting capability was fabricated, featuring a depletion-mode (D-mode) Schottky controlled depletion-mode channel extension (length of LD) beyond the ohmic contact at the cathode electrode, where the on-state current of the new rectifiers are self-limited at 4.59 kA/cm² (LD= 1.3 μm) and 3.56 kA/cm² (LD= 1.9 μm) at room temperature. The current limiting level shows a negative temperature coefficient (TC) that is desirable for thermal stability. [C61]

"Current sensitivity of Si mosfet to terahertz irradiation"

There is an increased interest in the use of terahertz (THz) radiation (frequency range 0.1-10 THz) for various applications in the fields of security screening, medicine, radio astronomy, etc. Nowadays main concepts of THz radiation detection are well-studied which allowed to create such types of THz receivers as low temperature quasiparticle detectors, Schottky diodes, micro-bolometers, MOSFET and HEMT-detectors, etc. [C62]

"Large-signal modeling of AlGaIn/GaN HEMTs based on DC IV and S-parameter measurements"

In this paper, a large-signal model for GaN HEMT transistors for designing RF power amplifiers is presented. This model is relatively easy to construct and implement in CAD software since it requires only DC and S-parameter measurements. The modeling procedure is applied to a 4-W packaged GaN-on-Si HEMT and the developed model is validated by comparing its large-signal simulation to measured data under different classes of operation. [C63]

"Genetic algorithm based extraction method for distributed small-signal model of GaN HEMTs"

In this paper, an improved small-signal model parameter extraction method, using genetic algorithm (GA), is presented and implemented for GaN HEMT. The GA optimization is used to generate a high quality reliable starting values for the elements of distributed model. This value are then refined using local optimization technique to find optimal value for each model element. The developed extraction method is validated by

simulating S-parameter measurements of a 84125- μm gate width GaN HEMT over a wide bias range. [C64]

"Analysis of transient radiation effects in III-V compound high electron mobility transistors using mixed-mode 3D simulations"

The paper presents details of our physics-based three-dimensional (3D) device modeling coupled in mixed-mode with external load circuit and parasitics, which enabled accurate simulation of single-event effects (SEEs) in III-V compound high electron mobility transistors (HEMTs). We show the importance of correct device physics models, such as Schottky barriers and tunneling, as well as effects of parasitics modeling, for correct computation of both steady-state and transient characteristics of III-V HEMTs. Mixed-mode coupling of a realistic load circuit, including experimental parasitics, with the 3D TCAD device model, is critical to be able to compute single-event transient current waveforms and charge collection characteristics that reflect well experimental results. [C65]

"Self-consistent electro-thermal simulation of AlGaIn/GaN HEMTs for reliability prediction"

In this paper, we have developed the first fully-coupled electro-thermo-mechanical simulation of AlGaIn/GaN HEMTs to study the reliability of these devices as a function of bias voltage and operating temperature. In addition, we have compared the numerical results of our simulations with high resolution thermo-reflectance measurements, obtaining excellent agreement. [C66]

"Capabilities and limitations of equivalent circuit models for modeling advanced Si FET devices"

The most common approaches for modeling semiconductor devices are compact modeling and equivalent circuit based modeling. The former approach has its origin in analogue Si circuits, whereas the latter stems from high-frequency applications using III-V compound devices, such as HEMTs. Due to the increasing RF performance of Si devices, RF modeling engineers have been tailoring equivalent circuit based modeling techniques for Si devices over the past decade. Nevertheless, Si circuit designers continue to prefer compact models. In this paper, we critically evaluate the capabilities and limitations of equivalent circuit based models as applied to Si FET devices. To focus the discussion, the selected device of interest is the advanced FinFET. It is shown that equivalent circuit based models are well suitable for linear and non-linear RF circuit design, but that they are less appropriate for analogue design approaches that rely heavily on flexible scalability. [C67]

"Small-signal and noise parameters of heterotransistor with quantum dots"

In this work small-signal and noise parameters for heterotransistor with quantum dots were presented. These parameters were extracted from electrons' velocity and concentration distributions from two-dimensional physical-topological modeling. Noise parameters were found from average values for electron temperature for corresponding areas. Also, results for double-channel heterotransistor with quantum dots were presented. It was shown that embedding quantum dots even into the one of two channels leads to power gain increasing. [C68]

"Parametric instability of mobile elastic gate in tera- and nano- high electron mobility transistor"

Effective excitation of the micro and nanometer-size resonators has number of applications at various fields of science and technology. In particular, they include wireless telecommunication technologies, high sensitivity measuring systems, quantum information processing devices. At the present report we consider the mechanical cantilever oscillations parametric excitation that serves as the gate electrode of a high electron mobility transistor (HEMT). The parametric coupling between the mechanical resonator (cantilever) and the oscillations of two-dimensional electron gas (2DEG) with high electron mobility is considered. In the capacity of the mechanical resonator a clamped nanobeam or a carbon nanotube might be used. 2DEG can arise in GaAs/AlGaAs heterostructures on the basis of which high electron mobility transistors (HEMT) are produced. [C69]

"Selecting an optimal structure of artificial neural networks for characterizing RF semiconductor devices"

At present, there are many various microwave structures for which their nonlinear models for CAD are necessary. However, in the recent PSpice family programs, only a class of five types of MESFET model is available. In the paper, a method is suggested for modeling miscellaneous RF semiconductor devices by exclusive neural networks or by corrective neural networks working attached to a modified analytic model. An accuracy of the proposed modification of the analytic model is assessed by extracting model parameters of the AlGaAs/InGaAs/GaAs pHEMT. An accuracy of procedures with neural networks is generally assessed by extracting their parameters in static and dynamic domains. An approximation of the AlGaAs/InGaAs/GaAs pHEMT output characteristics is carried out by means of both exclusive and corrective artificial neural networks. A systematic sequence of analyses is also performed for examining an optimal structure of the artificial neural

network from the point of view its structure and complexity. The tests have been performed on both five- and four-layer artificial neural networks that serve for modeling a P-channel JFET and for the AlGaAs/InGaAs/GaAs pHEMT. [C70]

"Gateless-FET undoped AlGa_N/Ga_N HEMT structure for liquid-phase sensor"

A gateless field-effect-transistor (FET) device fabricated on undoped AlGa_N/Ga_N high-electron-mobility-transistor (HEMT) structure is investigated as a liquid-phase sensor. Good gate controllability for typical current-voltage (I-V) characteristics of FET is observed. This result shows that an undoped-AlGa_N surface at the open-gate area is effectively controlled by the isolated gate voltage via chemical solution. Stable pH sensing operation in aqueous solution is observed where this device exhibits a high linear sensitivity of 3.88 mA/mm/pH at drain-source voltage, V_{DS}= 5 V. Due to the occurrence of large leakage current, the Nernstian's like sensitivity is not observed. It is also found that the device is sensitive to changes in electrostatic boundary conditions of the polar liquids. This indicates that the change in dipole moment in each liquid causes the potential change at AlGa_N surface. [C71]

"The sensing performance of hydrogen gas sensor utilizing undoped-AlGa_N/Ga_N HEMT"

The response of Pt-circular Schottky diodes fabricated on undoped AlGa_N/Ga_N high-electron-mobility-transistor (HEMT) structure to hydrogen gas at various temperatures, ranging from 25°C to 200°C has been investigated. A 5 nm-thick of catalytic Pt Schottky contact is formed by electron beam evaporation. Both forward and reverse currents of the device increase upon exposing to hydrogen gas. Although a slight change of forward and reverse current is obtained at room temperature upon exposure to hydrogen but both currents drastically increase with the increase of temperatures. The time-transient characteristics show the average current increment and decrement speed of 27.6 nA/sec and 17.6 nA/sec, respectively at constant forward bias of 1V and temperature of 200°C. [C72]

"High temperature stability of nitride-based power HEMTs"

The temperature stability of InAlN/Ga_N heterostructure FETs has been tested by a stepped temperature test routine under large signal operation conditions. Devices have been successfully operated up to 900 °C for 50 hrs. Failure is thought to be contact metallization related, indicating an extremely robust InAlN/Ga_N heterostructure. [C73]

"The microwave noise characteristics of InAlN/Ga_N HEMTs"

The microwave noise characteristics of InAlN/Ga_N heterojunction HEMTs are analysed by using an equivalent circuit model in this paper. It shows that the minimum noise figure of InAlN/Ga_N HEMTs can be comparable with that of AlGa_N/Ga_N HEMTs at X-band and higher frequency band. However, at the lower microwave frequency band, the minimum noise figure of InAlN/Ga_N HEMTs is a little worse, the reason of which is because of its high gate-leakage current. At last, three proposals are provided to improve the noise characteristics of InAlN/Ga_N HEMTs. [C74]

"100 mm GaN-on-SiC RF MMIC technology"

100 mm diameter 4H-SiC High Purity Semi-Insulating (HPSI) substrates are now being manufactured in high volume. Ga_N HEMT layers grown on 100 mm SiC substrates have shown excellent sheet resistivity and AlGa_N thickness uniformities of 1.3 and 1.1%, respectively. The fabrication process for MMIC manufacture was adapted to the larger diameter wafers without requiring any change to the process design kits for the foundry. MIM capacitor processes were optimized, and resistor process, wafer thinning and slot via etching were all adapted to the larger platform. These 100 mm wafers are now being used in high volume production of both high power discrete Ga_N devices, as well as MMICs. Commercially available MMICs have been released to production using this 100 mm platform. A wide band 25 Watt power amplifier is discussed, along with a 3 watt driver capable of DC-4 GHz operation. [C75]

"Design of an X-band high power solid state power amplifier based on Ga_N HEMT"

Based on Ga_N HEMT's high output power, low power loss and efficient heat dissipation, an X-band, 50W solid state power amplifier is designed. Slotted-waveguide directional coupler is designed as a 2-way power divider/combiner. At last, the output power, 165W, is combined through three power combiners by four 50W solid state power amplifiers. [C76]

"Characterization of high-frequency noise performance of GaN double heterojunction HEMT"

A systematic GaN single heterojunction HEMT (SH-HEMT) physical based numerical model is established in this paper. This model includes field-dependent mobility, polarization effect, interface state, surface state, and traps. The model has been implemented into TCAD Silvaco. And the simulated DC and RF characterization fit the measured results well. The high frequency noise performance of AlGaIn/GaN/AlGaIn double heterojunction HEMT (DH-HEMT) is studied based on the established SH-HEMT model. The results show that, because of the enhancement of carrier confinement in DH-HEMT, better high frequency noise performance can be achieved.

[C77]

"A broadband low noise amplifier MMIC in 0.15 μ m GaAs pHEMT technology"

This paper describes the design and simulated performance of 18-40GHz MMIC low noise amplifier (LNA). A three stages amplifier has been designed and developed using 0.15 μ m gate length GaAs/InGaAs/AlGaAs pHEMT technology. Self-biased and resistive matching technologies have been used to enhance the electrical specifications like return loss and gain flatness. The simulated data shows better than 3.1 dB of noise figure with an associated gain of more than 17.5 dB over the frequency band of 18-40 GHz. Over the range of 19-40 GHz, it could achieve better than 2 dB of noise figure with an associated gain of 22 \pm 2dB. [C78]

"100 W GaN HEMT power amplifier module with 60% efficiency over 100-1000 MHz bandwidth"

We have demonstrated a decade bandwidth 100 W GaN HEMT power amplifier module with 15.5-18.6 dB gain, 104-121 W CW output power and 61.4-76.6% drain efficiency over the 100-1000 MHz band. The 2 $\frac{1}{2}$ inch compact power amplifier module combines four 30 W lossy matched broadband GaN HEMT PAs packaged in a ceramic SO8 package. Each of the 4 devices is fully matched to 50 Ohms and obtains 30.8-35.7 W with 68.6-79.6% drain efficiency over the band. The packaged amplifiers contain a GaN on SiC device operating at 48V drain voltage, alongside GaAs integrated passive matching circuitry. The four devices are combined using a broadband low loss coaxial balun. We believe this combination of output power, bandwidth and efficiency is the best reported to date. These amplifiers are targeted for use in multi-band public mobile radios and for instrumentation applications. [C79]

"Doherty amplifier with envelope tracking for high efficiency"

A Doherty amplifier assisted by a supply modulator is presented using 2.14 GHz GaN HEMT saturated power amplifier (PA). A novel envelope shaping method is applied for high power-added efficiency (PAE) over a broad output power range. Experimental comparison with the Doherty and saturated PAs with the supply modulator is carried out. For the 8 dB crest factor WCDMA 1FA signal, the Doherty PA supported by the modulator presents the improved PAE over the broad output power region compared to the standalone Doherty PA. In addition, it achieves better PAE than the saturated PA with the supply modulator due to the lower crest factor envelope signal applied to the Doherty PA. At the maximum average output power, back-off by 8 dB from the peak power, the Doherty amplifier employing bias adaptation shows the PAE of 50.9%, while the comparable saturated PA with supply modulator and standalone saturated Doherty amplifier and saturated PA provide the PAEs of 42.3%, 49.7%, and 35.0%, respectively. [C80]

"An ultra-broadband robust LNA for defence applications in AlGaIn/GaN technology"

The design, fabrication and test of a 2-18 GHz monolithic Low Noise Amplifier utilizing 0.25 μ m AlGaIn/GaN HEMT technology is reported. The measured noise figure of the amplifier is less than 4.7 dB over the 2-18 GHz frequency range, exhibiting a minimum of 3.3 dB at 3 GHz. The LNA gain is 23 dB. Even being a low-noise amplifier, the MMIC can withstand 10W input CW RF power, demonstrating no apparent degradation: to the authors knowledge this is the best RF LNA survivability reported to date in this frequency range using GaN technology. [C81]

"Empirical modeling of GaN FETs for nonlinear microwave circuit applications"

A new approach for the electro-thermal modeling of GaN FETs is presented. The model is identified on-wafer through static I/V curves measured at different base plate temperatures and small-signal parameters. Improvements in the prediction of the dc drain current component under large-signal operation can be obtained by taking into account nonlinear dynamics of charge trapping phenomena. The use of measured pulsed-I/V characteristics is avoided in the model extraction phase. Identification procedures and a wide experimental validation for a 0.25 μ m AlGaIn/GaN HEMT on SiC with 600 μ m periphery are provided in the paper. [C82]

"High power, high conversion gain frequency doublers using SiC MESFETs and AlGaIn/GaN"

HEMTs"

High power, high conversion gain microwave frequency doublers using wide bandgap semiconductor devices are developed. A method of determining the optimal harmonic terminations using accurate nonlinear computer models and load- and source-pull simulations is described. Synthesis of these impedances using matching and reflector networks have produced doublers with increased output power, conversion gain and very high suppression of the first and third harmonics. A SiC MESFET-based frequency doubler at $f_0=2.00\text{GHz}$ producing up to 10.00dB conversion gain and 6.31 Watts $2f_0$ output power is presented. An AlGaIn/GaN HEMT-based frequency doubler at $f_0=3.33\text{GHz}$ producing up to 14.80dB conversion gain and 4.14W $2f_0$ output power is also presented. The second harmonic power measurements confirm the accurate predictions made by the nonlinear model. [C83]

"The performance of thin barrier InAlN/AlN/GaN MIS HEMT with high dielectric insulators"

High quality thin barrier InAlN/AlN/GaN heterostructure was grown by metal-organic chemical vapor deposition (MOCVD). The metal-insulator-semiconductor (MIS) structure devices were fabricated with high dielectric constant material barium strontium titanate (BST). The gate leakage current is reduced more than one order of magnitude under 40 V reverse bias, by using the high dielectric constant material. High transconductance 200 mS/mm was obtained with 1 μm gate length. The influence of the high dielectric BST material on the performance of the MIS structure is also investigated. [C84]

"Design of a dual-band GaN Doherty amplifier"

In this paper, the design, realization and test of a dualband Doherty power amplifier (DPA) will be presented. The design has been realized in hybrid technology using a packaged GaN HEMT as active devices. A special attention will be focused on the passive structures involved in the DPA design (input power splitter, impedance transformer network, impedance inverter network and phase compensation network) showing several possible implementations and the related tricky aspects. The DPA has been designed to operate simultaneously at 2.14GHz and 3.5GHz with 6 dB of output power back off (OBO) at both frequencies. [C85]

"Enhancement of comparator operation speed by using negative-differential-resistance devices"

Enhancement of comparator operation speed by using negative-differential-resistance (NDR) devices has been investigated. A clocked comparator including resonant-tunneling diodes (RTD) as the NDR devices as well as high-electron-mobility transistors (HEMT) is designed. Theoretical analysis based on equivalent circuits and transistor-level circuit simulation are carried out to estimate the regeneration and recovery times, as figures of merit. It is found that the regeneration time is reduced by 50% by using the RTDs, while the recovery time remains almost at the same value. [C86]

"Doherty power amplifier and GaN technology"

In this paper, the features of GaN HEMT technology and Doherty Power Amplifier architecture will be investigated, as a possible answer for the stringent requirements of the next generation of wireless systems. In particular, the attention will be focused on the capabilities and the relevant drawbacks of a GaN HEMT technology when designing DPAs. The discussion of the most important DPA's design aspects will be done through the presentation of several hybrid prototypes. Experimental results will be also given to support the theoretical aspects. [C87]

"Design and simulation GaN based class-S PA at 900MHz"

A Class-S Power Amplifier architecture seems to be an attractive alternative for classical PAs due to offered very high efficiency operation. Switching mode PA principle assumes combined operation based on digital, single-bit Delta-Sigma ($\Delta\Sigma$) modulated signals and RF analog signals, what complicates design and analysis procedures. However the Class-S PA topology is known, there are not any universal design methods which can be unambiguously applied to considered architecture. Presented work defines and describes design method for Class-S PA based on GaN HEMT transistors. Moreover main simulation results for Class-S architecture based on Current Switching Class-D (CSCD) configuration at the carrier frequency of 900 MHz have been performed. [C88]

"Development strategy for GaN-based high-efficiency hybrid medium-power RF amplifiers through low-cost substrate prototyping"

Two high-efficiency power amplifiers have been designed, fabricated, and tested using a commercially available

GaN HEMT transistor and a low-cost hybrid microstrip PCB. The designed hybrid modules are a "tuned load" Class B amplifier and a Class F amplifier. The simulated performances show a peak efficiency of 72 and 78 % with an output power of 5 and 4.5W respectively. The measured performance, although still satisfactory, exhibits an efficiency of 60 and 55 %, respectively, for the two stages. The paper presents a discussion on the design approach, on the intrinsic/extrinsic load to be presented to the active device, and on the cause of the efficiency drop occurring between the simulated and measurement performances. [C89]

"Quadrature regenerative frequency dividers using HEMT technology"

Using two high electron mobility transistor (HEMT)-based technologies, divide-by-two quadrature regenerative frequency dividers (RFDs) are demonstrated. One is the 0.15- μm AlGaAs/InGaAs pseudomorphic HEMT (pHEMT) technology with 85-GHz cutoff frequency and the other is the 0.15- μm InAlAs/InGaAs metamorphic HEMT (mHEMT) technology with 110-GHz cutoff frequency. The demonstrated 22~26-GHz pHEMT quadrature RFD consumes 28.4 mA at the supply voltage of 7 V while the 36.5~38.1-GHz mHEMT one consumes 16.9 mA at the supply voltage of 6V. Thus, the mHEMT quadrature RFD operates at high frequency and has lower power consumption as compared to the pHEMT one. [C90]

"A 5.25GHz GaAs PHEMT power amplifier for 802.11a application"

A 5.25 GHz GaAs PHEMT power amplifier for 802.11a application has been realized in the OMMIC 0.2 μm AlGaAs/InGaAs/GaAs PHEMT process. To guarantee the PHEMT unconditionally stable, a combined stabilizing circuit is used. Under a single supply voltage of +3.5V, this power amplifier exhibits linear output power of 24.8 dBm (P1dB), small signal gain of 25.6 dB and the power added efficiency (PAE) of 22% at P1dB. The die size is only 1.5 mm \times 1.0 mm. [C91]

"InAlN/AlN/GaN HEMTs on sapphire substrate"

High quality InAlN/AlN/GaN heterostructure is grown by metal organic chemical deposition (MOCVD) on sapphire substrate. A high two-dimensional electron gas (2DEG) density of $2.54 \times 10^{13} \text{cm}^{-2}$ was measured in this structure. To character the electric property of this heterostructure, a 1- μm -long gate InAlN/AlN/GaN high-electron mobility transistors (HEMTs) were fabricated. A maximum output current density of 1.19 A/mm and a peak extrinsic transconductance of 240 mS/mm were measured with the InAlN/AlN/GaN HEMTs. Compare to the normal AlGaAs/AlN/GaN HEMTs, the maximum current density and transconductance is greatly improved due to the high 2DEG density and thin barrier layer. [C92]

"Design of X-band low-noise amplifier for optimum matching between noise and power"

High Electron Mobility Transistors (HEMT) plays a crucial role in microwave low noise receivers. Low noise HEMTs are used extensively in the ultra low noise amplifier (LNAs). Design the LNA is difficult for the radio astronomical observations, especially the realization of the simultaneous about the noise matching and the power matching, as well as the full band unconditional stability. With the Agilent Advanced Design System (ADS) simulation tools, the X-band three-stage LNA using NEC-NE3210S01 HEMTs has been designed: Noise Figure < 0.6dB; power Gain > 30dB at X-band (7.8~9.4GHz), full band unconditional stability. [C93]

"High conversion gain broadband frequency doubler design"

This paper focuses on the design of frequency doublers operating in the RF and microwave frequency ranges. To reject the fundamental and third harmonic signal over a broadband frequency range, an active balun was employed in the broadband frequency doubler which has resulted in fundamental signal and third harmonics signal rejection better than 12 dB from 12 to 30 GHz input frequency. More than 9.5dBm output power was achieved over the 24-60GHz doubled frequency band for 2dBm input power. The circuit was designed with a 0.15 μm gate-length InGaAs based on Pseudomorphic High Electron Mobility Transistor (pHEMT) Microwave and Millimeter IC (MMIC) technology. [C94]

"Progressive Schottky junction reaction induced degradation in Pt-sunken gate InP HEMT MMICs for high reliability applications"

Reliability performance of 0.1- μm Pt-sunken gate InP HEMT MMICs on 4-inch InP substrates was evaluated under elevated temperature life testing. The primary degradation mechanism was observed to be the progressive Schottky junction reaction with the Schottky barrier InAlAs and the InGaAs channel. Despite the progressive Schottky junction reaction with the InAlAs and InGaAs materials, the lifetest at Tambient of 280°C projects the median-time-to-failure exceeding 14106hours at Tchannel of 125°C. This result indicates that the promising initial reliability performance was achieved on Pt-sunken gate InP HEMT MMICs on 4-inch InP substrates. [C95]

"Investigation of deep levels in AlGaIn/GaN HEMTs on silicon substrate by conductance deep level transient spectroscopy"

We report investigation of electron traps in AlGaIn/GaN HEMTs, grown on silicon by molecular beam epitaxy. Deep levels analysis was performed by conductance deep level transient spectroscopy (CDLTS) under a drain pulse. CDLTS measurements reveal three traps with the energy levels of 0.11, 0.17 and 0.22 eV. [C96]

"Electrical stress induced degradation in InAs-AlSb HEMTs"

InAs-AlSb HEMTs stressed with hot electrons may exhibit shifts in the peak transconductance towards more negative gate voltages. The devices are most degradation prone in operating conditions with high vertical gate field. Annealing trends and theoretical calculations indicate the possible role of an oxygen-induced metastable defect. [C97]

"Reliability assessment of state-of-the-art GaN HEMT by means of cellular Monte Carlo Simulation"

Here we discuss how Monte Carlo Simulations can be exploited to investigate reliability issues in GaN high electron mobility transistor (HEMT) devices. In particular, we report simulation results for high-frequency, high-power state-of-the-art GaN HEMTs focusing our analysis on the effects of that threading edge dislocations on the DC and RF performance of state of the art technologies. A complete characterization of an InGaIn back-barrier device has been performed, and the influence of dislocation density on device performance analyzed. Furthermore, a device structure based on the N-face configuration is analyzed. [C98]

"Temperature assessment of AlGaIn/GaN HEMTs: A comparative study by Raman, electrical and IR thermography"

The accuracy of different thermography techniques for the determination of AlGaIn/GaN HEMT channel temperature was investigated. Micro-Raman thermography, a novel electrical testing method, and IR thermography were applied to measure the temperature in the active region of AlGaIn/GaN HEMTs with different device geometries. Due to its accepted accuracy, micro-Raman thermography was performed on different devices in order to validate thermal simulation results. When compared to the validated thermal model, pulsed I-V measurements underestimated channel temperature to some degree, while IR thermography determined unrealistically low device temperatures. [C99]

"Compact GaAs HEMT D flip-flop for the integration of a SAR MMIC core-chip digital control logic"

The paper presents a novel, ultra-compact, reduced-area implementation of a D-type flip-flop using the GaAs Enhancement-Depletion (ED) PHEMT process of the OMMIC with the gate metal layout modified, at the device process level. The D cell has been developed as the building block of a serial to parallel 13-bit shifter embedded within an integrated core-chip for satellite X band SAR applications, but can be exploited for a wide set of logical GaAs-based applications. The novel D cell design, based on the Enhancement-Depletion Super-Buffer (EDSB) logical family, allows for an area reduction of about 20%, with respect to the conventional design, and simplified interconnections. Design rules have been developed to optimize the cell performances. Measured and simulated NOR transfer characteristics show good agreement. A dedicated layout for RF probing has been developed to test the D-type flip-flop behaviour and performances. [C100]

"Temperature dependent memory effects on a drain modulated GaN HEMT power amplifier"

In this paper, the impact of self heating on the linearity of a drain modulated GaN HEMT power amplifier (PA) is studied. After characterizing the frequency response of junction temperature rise to power dissipation, as well as the effect of this variable on the PA modulation profiles, the dynamic envelope trajectory, under a two-tone test signal, appears to be slightly dependent on frequency spacing. Self heating related effects are shown to be negligible in presence of other nonidealities, as the case of feedthrough. In this way, punching a vector hole in the two-tone I/Q diagram and applying memoryless digital predistortion (DPD), will allow identifying the influence of self heating effects, over adjacent channel distortion. Finally, this long-term memory effect is proved to be responsible for only a minor residual distortion in a linearized EDGE polar transmitter. [C101]

"A very compact power amplifier using GaN HEMTs in multilayer thin-film technology"

In this paper, a compact power amplifier module integrated in a thin film multi-chip module (MCM-D) interconnect technology is presented. The active device of the amplifier is a SiC based AlGaIn/GaN high electron mobility transistor (HEMT). Measurement results show that the prototype module can exhibit an output power of

1.6 W and a drain efficiency of 28% at 5.5 GHz. The major advantage of using a system-in-package (SiP) approach with MCM-D technology is the dramatic cost reduction compared to an MMIC and the size reduction compared to a hybrid PCB approach. [C102]

"Experimental investigation of LF dispersion and IMD asymmetry within GaN based HEMT technology"

An experimental investigation of the low-frequency dispersion affecting the behaviour of microwave devices is reported in this work. The study has been carried out by exploiting two different measurement techniques and experiments have been performed on a GaN based HEMT. In particular, bias and frequency dependence of dynamic characteristics has been clearly observed. Moreover, asymmetric behaviour not exclusively ascribed to the measurement environment (e.g., termination impedance networks) manifests in the non-linear response of the considered device. [C103]

"Semi-physical nonlinear model for HEMTs with simple equations"

A Nonlinear Circuit Model (NCM) combined with device/physical parameters was developed by using hyperbolic tangent (tanh) function and applied to GaN high electron mobility transistors (HEMTs). The equations for the NCM were constructed to reproduce the results of a device physical simulation. Model parameters are similar with the parameters used in the device design. The simulated DC and capacitance characteristics agree well with the measurement data over wide voltage range. Furthermore, numbers of the parameters were reduced to only 17 by using common physical parameters to both drain current and capacitance models. [C104]

"High temperature on- and off-state stress of GaN-on-Si HEMTs with in-situ Si₃N₄ cap layer"

In this work the stability of Gallium Nitride based high electron mobility transistors grown on 4-in Si substrate (GaN-on-Si HEMTs) were tested both in off-state at high drain voltage (200 V) and in on-state at large gate voltage (+2 V) with low drain bias (5 V). In each stress experiment the ambient temperature was fixed at 200°C. Remarkably, despite the considerably large drain voltage used in the off-state stress on only 5 µm gate-drain spaced transistors, negligible signs of degradation were observed after more than 350 hours of testing. Similar results were obtained after the on-state stress. In fact, only small degradation signs were reported in spite of the large gate current and high junction temperature the devices have to withstand during the on-state stress. These results show the robustness of these devices to operate under high electric field conditions, high temperature and to withstand also a large gate current for considerable time. [C105]

"Effects of the drain width on the electrical behavior of deep defect in AlGaIn/GaN/SiC HEMTs"

The transient behaviors of AlGaIn/GaN HEMTs were studied by conductance deep level transient spectroscopy. Deep levels in HEMTs are known to be responsible for trapping processes like: kink effect and degradation in saturation current. Three electron traps were observed. An additional "hole-like" level with activation energy of 0.43 eV is obtained. They were attributed these levels with surface states. [C106]

"Reducing R_{ext} in laser annealed enhancement-mode In_{0.53}Ga_{0.47}As surface channel n-MOSFET"

High mobility, narrow band gap group IV and III-V materials are strong contenders to replace strained-Si channels for logic applications beyond the 16 nm node [1-3]. While there are many research efforts evaluating III-V channels in HEMT and MOSFET forms, model based understanding and control of the FET properties such as channel mobility, series resistance, and off-state leakage are still lacking [4-8]. In this work, we address the aforementioned issues, by investigating laser annealing to control thermal budget and lower series resistance. Additionally we also report on preliminary material analysis and demonstrate the low temperature measurement to the performance of In_{0.53}Ga_{0.47}As MOSFETs. The electrical and material characteristics of TaN/ZrO₂/In_{0.53}Ga_{0.47}As self-aligned n-MOSFETs with high I_{on}/I_{off} (> 5 Ч 10⁴), high mobility (~ 3000 cm²/V-sec) and promise for low R_{ext} are presented and discussed. [C107]

"Effect of temperature on the electronic current of two dimensional quantum well in AlGaIn/GaN high electron mobility transistors (HEMT)"

An analytical-numerical model for the electronic current of two dimensional quantum well AlGaIn/GaN in HEMTs has been developed in this paper that is capable of accurately predicting the effect of temperature on the electronic current of two dimensional quantum well. Salient features of the model are incorporated of fully and partially occupied sub-bands in the interface quantum well. In addition temperature dependent of band gap, quantum well electron density, threshold voltage, mobility of electron, dielectric constant, polarization induce

charge density in the device are also taken into account. The calculated model results are in very good agreement with existing experimental data for HEMTs device. [C108]

"2.45 GHz GaN HEMT Class-AB RF power amplifier design for wireless communication systems"

GaN based RF transistors have been drawing interest of many researchers over the recent years due to their advantages e.g. high breakdown voltage, high efficiency, high power density and large bandwidth. They are expected to replace Lateral-Diffused Metal-Oxide Semiconductor field effect transistors (LDMOS FET) that are presently popular power device for wireless and mobile communications but have a small bandwidth [1], [2], [3]. A GaN HEMT 2.45 GHz Class-AB RF power amplifier is proposed for wireless communication systems. The power device used is Gallium Nitride High Electron Mobility Transistor (GaN HEMT) with Silicon as substrate material. The fabricated prototype of class-AB RF power amplifier fabricated can generate the maximum output power of 2.9 Watts and offer a power added efficiency (PAE) of 42.5%. [C109]

"The effect of depletion layer on the cut off frequency of AlGaIn/GaN high electron mobility transistors"

An analytical model for I-V characteristics of AlGaIn/GaN based HEMTs has been developed that is capable to predict accurately the effects of depletion layer thickness on the cut off frequency in drain currents, gate biases and gate length. Salient features of the model are incorporated of fully and partially occupied sub-bands in the interface quantum well, combined with a self-consistent solution of the Schrodinger and Poisson equations. The calculated model results are in very good agreement with existing experimental data for AlGaIn/GaN based HEMTs device. [C110]

"Effect of trapping on the critical voltage for degradation in GaN high electron mobility transistors"

We have performed $V_{DS} = 0$ V and OFF-state step-stress experiments on GaN-on-Si and GaN-on-SiC high electron mobility transistors under UV illumination and in the dark. We have found that for both stress conditions, UV illumination decreases the critical voltage for the onset of degradation in gate current in GaN-on-Si HEMTs in a pronounced way, but no such decrease is observed on SiC. This difference is attributed to UV-induced electron detrapping, which results in an increase in the electric field and, through the inverse piezoelectric effect, in the mechanical stress in the AlGaIn barrier of the device. Due to the large number of traps in GaN-on-Si, this effect is clearer and more prominent than in GaN-on-SiC, which contains fewer traps in the fresh state. [C111]

"Identification of electronic traps in AlGaIn/GaN HEMTs using UV light-assisted trapping analysis"

UV light-assisted trapping analysis in conjunction with electroluminescence studies was employed to identify the location of traps generated in AlGaIn/GaN HEMTs submitted to on-state stress. Our results indicate that UV light-assisted trapping is closely related to traps in the access region close to the gate edges. An increase in the dominant electronic trap density spatially located within the AlGaIn layer underneath the gate and in the access region close to the drain side of the gate edge was found to be the most pronounced degradation mechanism for the stress conditions investigated. This trap level was found to be located 0.5 eV below the AlGaIn conduction band. [C112]

"Reliability assessment in different HTO test conditions of AlGaIn/GaN HEMTs"

This study reports on a reliability investigation of AlGaIn/GaN HEMTs submitted to life tests in High Temperature Operating (HTO) conditions at 150°C, 175°C, 275°C and 320°C. These life tests showed two different degradation steps of the drain current. One is occurring in the first tens of hour of the life test and characterized by a decrease of the drain current. The evolution of the electrical characteristics during ageing does not depend on the bias conditions but rather on the channel temperature. This degradation mode is characterized by a high activation energy of 1.2 eV. The small changes of electrical characteristics observed during the life tests results from a combination of trap-related effects before stabilization sets in. The second failure mechanism observed during the HTO tests at 275°C and 320°C results in a higher drain current decrease. Moreover, no stabilization of the parameter drifts was observed before the end of the tests. Pulsed I-V measurements show a large evolution of gate lag and drain lag rates after HTOT275 and HTOT320 life tests. LF 1/f noise after the life tests at high temperature drastically increased by more than two orders of magnitude while it hardly changed after 2000 hours of life test at 150°C and 175°C. It results that the temperature is considered as an acceleration factor of the degradation affecting the conduction channel. TEM observations revealed similar damages in the gate finger cross-section of aged devices after the HTOT275 and HTOT320 life tests. These results could point out a degradation mechanism associated with the inverse piezoelectric effect. [C113]

"GaN-on-Si power field effect transistors"

GaN-on-Si has become the most promising technology for next-generation power switching devices to overcome intrinsic Si limits for high temperature operation, high efficiency at high operating voltage, and high switching frequency. Depletion-mode devices are already offering more than one order of magnitude lower specific on-resistance above 600V. Further, we have recently demonstrated e-mode devices ($V_t > 0.5V$) with high current density, thanks to a unique in-situ SiN passivation approach. This in-situ SiN layer is further shown to be a key parameter for device stability at elevated temperatures, significantly enhancing the device reliability in high temperature accelerated lifetime tests. [C114]

"Reliability status of GaN transistors and MMICs in Europe"

Recent DC- and RF-reliability results of European GaN HEMTs for high frequency power and MMIC applications between 2 and 18 GHz will be presented. The DC-stress test experiments have been performed at high current and high voltage settings in order to test the devices in the different regimes during large signal operation. GaN HEMTs and one stage MMICs have also been tested under RF-operation conditions and the correlation to DC-stress tests has been investigated. [C115]

"Large-signal characterization of GaN-based transistors for accurate nonlinear modelling of dispersive effects"

A large-signal measurement setup with sinusoidal excitation is used for the characterization of low-frequency dispersive phenomena in III-V FET devices. This low-cost setup operates in the MHz frequency range and its components are easily available in most research laboratories. A dispersive model of the dynamic drain current, taking into account the non linear behaviour of charge trapping phenomena, is identified for an AlGaN/GaN HEMT on the basis of the proposed characterization setup. [C116]

"FPGA-based set-up for RF power amplifier dynamic supply with real-time digital adaptive predistortion"

This paper presents an exhaustive description of a field programmable gate-array (FPGA) based set-up for envelope tracking and dynamic biasing of RF power amplifiers (PA). The system includes digital adaptive predistortion (DAPD) and gain compensation deployed in a FPGA device. For testing purposes a GaN HEMT RF PA operating at 3.5 GHz was considered. Preliminary experimental results are provided showing the DAPD compensate for the steady-state PA nonlinear distortion arising as a consequence of varying the power supply. [C117]

"A 2.14 GHz GaN power amplifier with 1-bit discrete power control"

This paper focuses a GaN HEMT power amplifier with 1-bit power control and provides experimental data. It relies on a new concept of power combining allowed by an adaptive gate bias control scheme. At 2.1 GHz CW the discrete power control technique enables a linear factor 3.3 efficiency enhancement at the maximum power back-off of 7 dB, while a maximum output power of 34 dBm and a peak drain efficiency of 35%. [C118]

"A 1mm² flip-chip SP3T switch and low noise amplifier RFIC FEM for 802.11b/g applications"

This paper presents a 1mm²Cu pillar flip chip SP3T/LNA RFIC targeted for use in 802.11b/g front-ends. The SP3T switch enables WLAN transmit/receive and Bluetooth modes of operation. This switch exhibits 0.6dB insertion loss per branch and delivers 802.11g linear performance up to +21dBm output power. A single-stage LNA with a bypass mode is connected after the WLAN Rx branch to increase overall receiver sensitivity and dynamic range. The LNA achieved 1.9dB NF with a typical 11.5dB small-signal gain, including the switch loss. This die occupies only 25% of the footprint of similar existing QFN style WLAN front ends. [C119]

"A class E power amplifier design for drain modulation under a high PAPR WiMAX signal"

This paper describes the design of a class E power amplifier (PA) destined to be used as the final stage of a polar transmitter under IEEE 802.16e Mobile WiMAX signal excitation. Based on a 60 W GaN HEMT device, the load condition for optimum efficiency is set close to the maximum value of the power generating function, as defined in, for an OFDMA modulating signal. The possible impact of such average-based design on the AM profile is also put into consideration. [C120]

"Ultra wideband high gain GaN power amplifier"

A three-stage power amplifier will be described which was designed for 5 W or better power over many octaves.

A mixed topology was chosen to obtain the best bandwidth and power. First two stages are single-ended feedback designs for best gain and linear drive for the output. The last stage is a distributed PA, which is optimized to achieve high output power and high drain efficiency. The PA is designed and fabricated using discrete 2W GaN transistor die in all stages in a mixed hybrid and softboard medium. The design was fully simulated. Both measurement results and the theoretical predictions will be presented. This GaN PA has over 43 dB linear gain with good port match and it provides greater than 37 dBm of saturated power and over 20% PAE in the 0.02 to 3 GHz frequency range. [C121]

"Linearity performance of an RF power amplifier under different bias-and load conditions with and without DPD"

Adjusting the biasing- and loading conditions in a power amplifier affects the linearity and efficiency of the PA. If an accurate nonlinear model for the transistor does not exist, load-pull measurements are necessary for a high-performance PA design. In this work load-pull measurements are performed under different biasing conditions in order to utilize the fully potential of the transistor in the PA. Two different linearity criteria, one strict at -40 dB ACPR and one more relaxed at -33 dB for a 16 QAM signal, should be met by the PA, and the best bias point and load are found for these criteria from load pull measurements with single tone and digitally modulated signal. The impact on the results when linearizing the PA with DPD are also investigated. The measurements on a 1 W pHEMT transistor show that by utilizing sweet spots when biasing in deep class AB the most output power and PAE could be achieved with an ACPR level of -33 dB. With an ACPR limit of -40 dB biasing toward class A maximizes the output power. At this criterion there is much to gain by performing load pull measurements with a digitally modulated signal. When applying DPD the output power is almost independent of the biasing conditions for both linearity criteria and the load should be chosen to maximize output power at 1 dB compression. [C122]

"Research on mechanical-electrical coupling characteristics of GaAs HEMT build-in cantilevers-mass"

The micro-structure of GaAs HEMT build-in cantilevers-mass was designed and fabricated. GaAs HEMTs were embedded at the root of cantilevers for increasing the sensitivity to external force. In our experiments, it has been proved that the sensitivity of GaAs HEMT is higher than that of silicon by the Mechanical-Electrical coupling characteristics. The magnitude of the external force was then calculated according to the out-put voltage of GaAs HEMT. This research would be good for developing a new sensor technology. [C123]

"Kahn-technique transmitter for L-band communication/radar"

This Kahn-technique (Envelope Elimination and Restoration) transmitter operates at 1.2 GHz and produces a PEP output of 50 W. It employs a GaN-HEMT class-F RF-power amplifier, class-S modulators, and a digital signal processor. An overall (driver + final) efficiency of 50 percent or more is maintained over the top 6 dB of the output range. The driver and final are operated to maximize overall efficiency and the predistortion corrects for amplitude and phase errors. While originally intended for pulsed radar applications, the transmitter is capable of producing a wide variety of signals with good linearity and average efficiency. [C124]

"Multi-level QAM single-carrier high-efficiency broadband wireless system for millimeter-wave applications"

In preparation for achieving the millimeter-wave ultra-broadband wireless system aimed at seamless connection with the optical communication network, we have developed key devices such as baseband signal processing SoC (System-On-Chip) with the built-in ultrahigh-speed multi-level QAM (Quadrature amplitude modulation) modem (modulator and demodulator), SiGe I/Q quadrature modulator and demodulator MMIC (Microwave Monolithic Integrated Circuit), and GaAs HEMT frequency converter MMIC. We have also prototyped the micro-mini and ultra-broadband 38 GHz band point-to-point wireless system using TDD (Time Division Duplex) mode with dynamic bandwidth assignment that adopts the configurations of separate transmission and receiving antennas capitalizing on the characteristic of smaller antenna area in the millimeter-wave band to achieve the performance that the radio clock frequency is 200 MHz and the maximum effective throughput on 16 QAM is 600 Mbps. [C125]

"Advanced design of high-linearity analog predistortion Doherty amplifiers using spectrum analysis for WCDMA applications"

This paper represents the advanced design methods of a high-linearity analog predistortion Doherty power amplifier (DPA) using spectrum analysis for WCDMA applications. For the analog predistortion linearization, the DPA utilizes the bandwidth reduction of the error signal, linear AM/AM characteristic without any abrupt change,

and memory effect reduction. To verify our methods, the asymmetrical Doherty amplifier using a RFHIC RT440 40-W push-pull type GaN HEMT and the analog predistorter with a diode-based error generator and three-branch nonlinear paths are implemented at 2.14 GHz. From the measured one-carrier WCDMA results at an average output power of 34 dBm (11-dB back-off power from the saturation power), the analog predistortion DPA with a drain bias voltage of carrier cell of 34V shows an ACLR of -54 dBc at $\Gamma_B \pm 2.5$ offsets with a power-added efficiency of 18.9%. [C126]

"Power amplifier architectures with discrete power control for high average efficiency"

This paper focuses and provides experimental data for reconfigurable class-AB power amplifiers capable to adjust their linear power handling capability according with the application requirements. This feature is aimed at optimizing the energy requirement of the PAs. Two architectures and technologies have been considered. The first is based on SiGe HBTs with different sizes, it shows a CW PAE around 38% for the state 1 and 42% for state 2 respectively when terminated with optimum terminations. This circuit is conceived to be involved in a 1-bit step envelope tracking architecture, in which a factor two of improvement in terms of average PAE has been demonstrated. The second technique consists in controlling the output back-off of a GaN HEMT PA resulting in a significant increase of the efficiency through an, in principle, arbitrary power dynamic range. The prototype demonstrated an average PAE enhancement at 7 dB back-off of 2.1 and a maximum linear output power can be achieved up to 30 dBm, when driven by a 2.14 GHz WCDMA signal. [C127]

"Thermal and electrical layout optimisation of multilayer structure solid-state devices based on the 2-D Fourier series"

In this paper a 2-D Fourier transform-based analytical method for the thermal and electrical layout optimisation of multilayer structure solid-state devices is proposed. Compared with previous models presented in literature, it is general and can be easily applied to a large variety of integrated devices, provided that their structure can be represented as an arbitrary number of superimposed layers with a 2-D embedded thermal source, so as to include the effect of the package. The proposed method is independent of the specific physical properties of the layers, hence GaAs MESFETs and HEMTs as well as Silicon and Silicon-On-Insulator MOSFETs and heterostructure LASERS can be analysed. Moreover, it takes into account the dependence of the thermal conductivity of all the layers on the temperature; the heat equation is solved coupled with the device current-voltage relation in order to give physical consistence to the experimental evidence that a temperature increase causes a degradation of the electrical performances and that the electrical power is not uniformly distributed. [C128]

"Equivalent circuit modeling of terahertz devices and resonant MEMS with two-dimensional electron gas system"

Equivalent circuit models have been developed to study the performance of the devices with two-dimensional electron gas (2DEG) system for terahertz (THz) applications (single- and grid-grating-gated high-electron-mobility transistor (HEMT)) and for sensing (micromachined HEMT with the array of resonant floating gates). The components of the equivalent circuits were related to physical and geometrical parameters of the devices under consideration. The developed equivalent circuits were used to simulate frequency performance of the devices under consideration invoking IsSpice circuit simulator. The results of IsSpice simulation reveal that the highly doped cap layer can cause the fundamental resonant frequency reduction. It is shown that the increase in the number of fingers in gridgrating-gated HEMT-structures is accompanied by the decrease in mode separation between adjacent harmonics which results in spectrum broadening. Possible approach to realize single-mode operation of such plasma wave grid-grating-gated HEMT, i.e., to narrow its spectrum at around a certain frequency, is proposed. IsSpice simulation of the performance of recently proposed micromachined HEMT with the array of floating gates (FGs) over 2DEG channel demonstrates its capability to operate as a multi-target sensor. [C129]

"A 150MHz, 84% efficiency, two phase interleaved DC-DC converter in AlGaAs/GaAs P-HEMT technology for integrated power amplifier modules"

This paper presents a high efficiency, high switching speed, two-stage interleaved DC-DC buck converter with negatively-coupled inductors in AlGaAs/GaAs technology, targeting integrated power amplifier modules. The flip chip DC-DC converter is implemented in 0.5 μm GaAs pHEMT process and occupies 2 Ч 2.1mm² without the output network. The inductors in the output network are implemented in 65 μm thick top copper metal layer and have a quality factor of 25 at 150 MHz. The interleaved DC-DC converter achieves 84% efficiency when operating at 150MHz switching frequency with 4.5V/3.3V conversion ratio and 1A load current. [C130]

"The impact of baseband electrical memory effects on the dynamic transfer characteristics of microwave power transistors"

The inter-modulation distortion products can vary both in terms of amplitude and asymmetry due to the effects of baseband and 2nd harmonic impedance. This paper presents an investigation into the relationship between the IMD asymmetries caused by baseband impedance variation and the looping or hysteresis that can sometimes appear in the dynamic transfer characteristics of microwave power devices when subjected to modulated excitation. The investigation is carried out using a 2W GaN HFET bare die device characterized at 2.1GHz, and using IF active load-pull to clarify the role of baseband impedance on observed hysteresis in the dynamic transfer characteristics. Analysis is performed using the envelope domain in order to more effectively reveal the DUT's sensitivity to impedance environments and specifically electrical baseband memory effects. [C131]

"60 GHz broadband image rejection receiver using varactor tuning"

A pHEMT broadband image rejection receiver with an image rejection ratio (IRR) more than 20 dB from 54 GHz to 66 GHz is presented using varactor tuning topology. Tunable varactors connected in shunt between an RF coupler and mixers are used to control the phase and amplitude of two RF signals. It offers the IRR improvement of 3.1~21.4 dB in the cost of gain degradation below 1.1 dB from 54 GHz to 66 GHz except for 65 GHz. To the best of authors' knowledge, this work shows the best image rejection performance of V-band receivers. At 61 GHz, this circuit achieves an 18.3 dB conversion gain (C.G) and a 49.3 dB IRR. It shows a noise figure of 5.6~8.1 dB from 56 GHz to 64 GHz. [C132]

"Modeling GaN power transistors"

Modeling GaN transistors is still a matter of research. The technology is still quite young and not yet fully mature. A second issue is the fact that GaN transistors are commonly used as packaged power devices. This paper discusses modeling results obtained for different GaN devices from a small HEMT to a 60-W packaged power transistor. It is shown that the performance state-of-the-art GaN HEMTs are no longer strongly impacted by dispersion effects. Therefore, the well-known HEMT models can be successfully used for these transistors. Beginning with this finding, the model extraction for the 60-W packaged device is discussed step-by-step. [C133]

"Determination of channel temperature of AlGaIn/GaN HEMT by electrical method"

In this paper, the linear relationship of forward Schottky junction voltage of AlGaIn/GaN HEMT with temperature was investigated. It was used as temperature sensitive parameter to determine the channel temperature at its normal working state by fast switch circuit technique. The regress of tested data was used to reduce the scatter error too. The thermal resistance constitution was extracted from the transient heating response curves. [C134]

"Design of GaN HEMT based Doherty amplifiers"

In this paper the design of high efficiency unsymmetrical Doherty power amplifiers (PAs) will be presented. The Doherty PAs were designed to achieve high average efficiency for digitally modulated signals with high peak to average power ratio (PAR) used in third (3G) and fourth (4G) generation systems. The Doherty amplifiers have been designed using two unequal sized GaN devices for the main Class-AB and peaking Class-C amplifiers. In the first narrow band design, a 50 W Doherty amplifier has been implemented at 2.5 GHz. A drain efficiency of 54% (48% power added efficiency (PAE)) has been measured at its maximum output power of 47 dBm. The efficiency remains constant up to the 6 dB output power back-off. Moreover, the Doherty PA has been linearized to achieve an Adjacent Channel Leakage Ratio (ACLR) of -46 dBc at 10 MHz offset for a 10 MHz (UMTS-LTE) signal with a PAR of 8.5 dB, and an average output power of 40 dBm. 44% PAE was measured for this signal constellation. In a second design, the status of a wideband unsymmetrical Doherty PA with 31% fractional bandwidth will be reported. [C135]

"Design and Analysis of an X-band Low Noise Amplifier"

This paper reviews the procedure of designing an X-band Low Noise Amplifier (LNA). Design the LNA is difficult for the radio astronomical observations, especially the realization of the simultaneous about the noise matching and the power matching, as well as the full band unconditional stability. With the software, an X-band three-stage LNA using NEC NE3210S01 HEMTs has been designed: Noise Figure < 0.6 dB; power Gain > 30dB at 7.8 ~ 9.4 GHz, full band unconditional stability. The noise figure, associated gain and stability factor have been optimized while building the input and output matching network. [C136]

"4-8 GHz LNA design for a highly adaptive small satellite transponder using InGaAs pHEMT technology"

The ever increasing global space activity is characterised by emerging space systems, operation and applications challenges. Hence, reliable RF and microwave receivers for in-orbit highly adaptive small satellites are needed to support reconfigurable multimedia/broadband applications in real-time with optimal performance. Though other parameters of the small satellite communication system may be critical, the noise level of the receiver determines the viability, reliability and deliverability of the project. Thus, a good design that delivers low noise performance, high gain and low power consumption for multipurpose space missions is inevitable. This paper describes a 0.15 μm InGaAs pseudomorphic high electron mobility transistor amplifier with low noise and high gain in the frequency band 4-8 GHz. The monolithic microwave integrated circuit LNA design presented here shows the best performance known using this technology; noise figure of 0.5 dB and gain of 37 dB \pm 1 dB over the characterised bandwidth. [C137]

"Design of 140-170 MHz class E power amplifier with parallel circuit on GaN HEMT"

The class E power amplifier is a prominent switched-mode power amplifier. It is well known as being a high efficiency amplifier that provides a long operation time for mobile and nomadic devices powered by batteries. Moreover, it reduces the power dissipation of power transistor and cooling system requirement. The switching device that is used in the design is an important factor to provide maximum efficiency of the power amplifier. This paper introduces the design steps of a 140-170 MHz class E power amplifier with parallel load circuit using Gallium Nitride High Electron Mobility Transistor (GaN HEMT). The design methodology and simulation result are also provided. To match the output impedance of the load network with the output port with 50 Ohms reference impedance, the load-pull technique was utilized. The proposed design methodology provides a peak Power-Added Efficiency (PAE) of 81% with a power gain of 15 dB at an output power of 34.4 dBm. Considering the broadband performance, the power gain of 14 dB and PAE of 77.6% can be achieved. [C138]

"Nonlinear characterization techniques for improving accuracy of GaN HEMT model predictions in RF power amplifiers"

In this paper, two vector nonlinear characterization procedures are presented, aimed at improving available GaN HEMT models for an accurate reproduction of the device behavior operating as a current source and in switched-mode RF power amplifiers. In the case of the more traditional linear amplifying classes, a technique for simultaneously extracting the higher order derivatives of the $I_{ds}(V_{gs})$, $I_{gs}(V_{gs})$ and $C_{gs}(V_{gs})$ transistor nonlinearities, along a desired load line, is described. This procedure conveniently isolates and models their contributions to the device intermodulation distortion (IMD) behavior. In the case of highly efficient switched-mode PAs, employed under drain modulation condition, a modified procedure for isodynamically measuring the higher order derivatives of the Vdd-to-AM and Vdd-to-PM amplifier profiles is put into consideration, as a way to refine the triode region reproduction for ON-OFF operation. [C139]

"10-Gbit/s QPSK modulator and demodulator for a 120-GHz-band wireless link"

This paper describes a 120-GHz-band quadrature phase shift keying (QPSK) modulator and demodulator fabricated on microwave monolithic integrated circuits (MMICs) for a 10-Gbit/s wireless link. The MMICs were fabricated using 0.1- μm -gate InP HEMTs and coplanar waveguides. The direct-conversion modulator consists of hybrid couplers, gain-control amplifiers, and combiners. The delay demodulator has a 200-ps delay line, distribution amplifiers, a voltage-controlled phase shifter, and detectors. The modulator and demodulator MMICs were mounted in WR-8 waveguide modules to evaluate the characteristics of 10-Gbit/s transmission. The bit error rate (BER) for 10-Gbit/s pseudorandom binary sequence (PRBS) 27-1 data was smaller than 10⁻¹⁰. [C140]

"Behavioral model analysis of active harmonic load-pull measurements"

This paper outlines the formulation of a mixing based behavioral model, capable of capturing the nonlinear response of microwave transistors to fundamental and harmonic load pull effects for use in Computer Aided Design tools. The key to the model formulation was the experimental identification of the dominating mixing terms. The model is able to accurately compute the voltage and current waveforms present at a Transistors Terminals. The formulation lends itself to economical use of measured data, reducing data storage required within the CAD environment. In this paper the modeling approach has been demonstrated on a 10475 μm GaAs HEMT operating at 9 GHz. [C141]

"Nonlinear HEMT model direct formulated from the second-order derivative of the I-V/ Q-V"

characteristics"

In this paper, an empirical nonlinear model for high electron mobility transistors (HEMTs) is presented. Unlike the conventional large-signal models whose fitting parameters are coupled to the measured I-V and C-V characteristics, the proposed modeling equations are directly formulated from the second-order derivative of drain current (I-V) and gate charge (Q-V) with respect to gate voltage. As a consequence, the proposed large-signal model is kept continuously differentiable and accurate enough to the higher-order I-V and Q-V derivatives. Measured and modeled results are compared for the 0.25 μm gate-length GaAs pseudomorphic HEMTs (pHEMTs), and good agreement is obtained. [C142]

"Improved parameter extraction method for GaN HEMT on Si substrate"

An improved parasitic elements extraction method applied to GaN on Si devices is presented. Genetic-algorithm based procedure is used to determine a high quality reliable starting values for the extrinsic parameters of proposed small-signal model. Local optimization technique is then used to refine the initial value and find the optimal value for each model element. The validity of the developed method and the proposed small-signal model is verified by comparing simulated small-signal S-parameters with measured ones of a 2-mm (104200 μm) GaN HEMT-on-Si. [C143]

"A C-band GaAs-pHEMT MMIC low phase noise VCO for space applications using a new cyclostationary nonlinear noise model"

This paper describes the design and implementation of a C-band MMIC VCO developed in the framework of activities oriented to the improvement of products for space applications. The circuit exploits a single device with a microstrip integrated resonator coupled with varactors. The exploited technology is a space-qualified GaAs 0.25- μm pHEMT process. The MMIC exhibits 350-MHz bandwidth at 7.3 GHz, with 14 dBm output power and -86 dBc/Hz single side-band phase noise at 100 kHz from the carrier. Measured performances are in good agreement with simulations. The active device adopted for the design was characterized in terms of both low-frequency noise in quiescent bias-dependent operation and its up-conversion into phase noise under large-signal RF oscillating conditions, using in-house developed measurement setups. A new compact nonlinear noise model was identified, implemented and exploited for phase noise simulations. The model features cyclostationary equivalent noise generators. Comparisons between measurements and simulations show that the nonlinear cyclostationary modeling approach is more accurate than conventional noise models in oscillator phase noise analyses of pHEMT based circuits. [C144]

"Characterization of trapping and thermal dispersion in GaN HEMTs"

Dispersion in a GaN HEMT, including gate and drain lag, is related to a new trapping model based on SRH theory. Measurements and SPICE simulation are used to verify the capability of this model to explain the bias- and terminal-potential dependency of the turn-on transients and their time constants. The models of both drain current and trapping need to consider temperature and power dissipation versus time. The interaction between two different trap mechanisms and two different self-heating processes is shown to adequately explain the different characteristics of the turn-on transient of the transistor under test. [C145]

"A 50 mW 220 GHz power amplifier module"

In this paper, a 220 GHz solid-state power amplifier (SSPA) module is presented. Eight-way on-chip power combining is used to achieve a saturated output power ≥ 50 mW over a 217.5 to 220 GHz bandwidth, representing a significant increase in SSPA output power at this frequency compared to prior state of the art. The amplifier MMIC is implemented in coplanar waveguide (CPW) technology and uses sub 50 nm InP HEMT transistors. Two levels of power combining, a 2:1 tandem coupler and a 4:1 Dolph-Chebyshev transformer, are realized in CPW. The module demonstrates ≥ 11.5 dB small signal gain from 207 to 230 GHz. Saturated output power ≥ 40 mW was measured from 216 to 222.5 GHz. [C146]

"A 206-294GHz 3-stage amplifier in 35nm InP mHEMT, using a thin-film microstrip environment"

We present a compact, 3-stage millimeter-wave monolithic integrated circuit (MMIC) amplifier with an operating frequency of 206-294GHz, formed by common-source configured 35nm Lg InP mHEMTs and a multi-layer thin-film microstrip (TFM) wiring environment. The amplifier S₂₁ mid-band gain is 11-16dB, 3dB bandwidth at 294GHz, and 82.5mW P_{dc}. This is the first reported InP HEMT MMIC operating in G-,H-band employing thin-film microstrip. Because the TFM ground-plane shields the signal interconnects from the substrate, well behaved device (0.1-67, 140-200, 210-310GHz) and amplifier (210-320GHz) measurements are presented from an unthinned, 25mil substrate. The total size of this 3-stage amplifier is only 0.77mm \times 0.40mm. [C147]

"A 50 mW 220 GHz power amplifier module"

In this paper, a 220 GHz solid-state power amplifier (SSPA) module is presented. Eight-way on-chip power combining is used to achieve a saturated output power ≥ 50 mW over a 217.5 to 220 GHz bandwidth, representing a significant increase in SSPA output power at this frequency compared to prior state of the art. The amplifier MMIC is implemented in coplanar waveguide (CPW) technology and uses sub 50 nm InP HEMT transistors. Two levels of power combining, a 2×1 tandem coupler and a 4×1 Dolph-Chebyshev transformer, are realized in CPW. The module demonstrates ≥ 11.5 dB small signal gain from 207 to 230 GHz. Saturated output power ≥ 40 mW was measured from 216 to 222.5 GHz. [C148]

"Multi-octave GaN MMIC amplifier"

A broadband multi-octave, 0.1-20 GHz, 10 dB ± 2 dB amplifier was implemented in the GaN/SiC technology. The amplifier design relies on a series DC/RF HEMTs (SHEMTS) configuration. This configuration offers an alternative to the traveling wave amplifier (TWA), uses a smaller chip area, and readily extends the gain to the low frequency region. The amplifier is power matched at Ku-band and has an output power of 1 W at 1-dB compression, 17 GHz, and 17% drain efficiency. [C149]

"Aluminum-free GaInP/GaInAs pHEMTs for low-noise applications with peak $f_T = 256$ GHz and peak $f_{MAX} = 360$ GHz"

Al-free HEMTs show advantageous characteristics in terms of LF-noise, low-temperature performance, breakdown behavior, high-frequency power performance as well as reliability. In the present work, we report the technology and performance of 100 nm gate length Al-free GaInP/GaInAs pseudomorphic HEMTs grown by MOVPE on semi-insulating InP substrates. The epitaxial layer structure involves an In-rich channel achieving room temperature mobilities of 8,300 cm²/Vs. The fabrication of 100 nm T-Gate HEMTs gives rise to the highest reported $f_T = 256$ GHz and $f_{MAX} = 360$ GHz for Al-free GaInP/GaInAs InP pHEMTs. DC characterization yields shows saturation currents < 400 mA/mm and a maximum transconductance of 640 mS/mm. [C150]

"High reliability performance of 0.1- μ m Pt-sunken gate InP HEMT low-noise amplifiers on 100 mm InP substrates"

Accelerated temperature lifetesting at $T_{channel}$ of 240, 255, and 270°C was performed on 0.1- μ m Pt-sunken InP HEMT low-noise amplifiers fabricated on 100 mm InP substrates. The reliability performance was evaluated based on $\Delta S_{21} < -1$ dB at 35 GHz. The lifetesting results exhibit activation energy of approximately 1.8 eV and lifetime projection of 99% reliability and 90% confidence exceeds 1×10^8 hours at $T_{channel}$ of 125°C. The high reliability demonstration of 0.1- μ m Pt-sunken gate InP HEMT low-noise amplifiers on 100 mm InP substrates is essential for advanced military/space applications requiring high reliability performance. [C151]

"Sub-50NM InGaAs/InAlAs/InP HEMT for sub-millimeter wave power amplifier applications"

An InGaAs/InAlAs/InP HEMT with sub-50nm EBL gate has been developed for sub-millimeter wave (SMMW) power amplifier (PA) applications. In this paper, we report the device performance including high drain current, high gain, high breakdown voltage and scalability to large gate periphery, which are essential for achieving high output power at these frequencies. Excellent yield, process uniformity and repeatability are also demonstrated, which is critical for power amplifiers employing large number of devices and gate fingers. 10mW output power is demonstrated from a fixtured 338 GHz PA module. [C152]

"Metamorphic HEMT technology for submillimeter-wave MMIC applications"

Metamorphic high electron mobility transistor (mHEMT) technologies with 50 and 35 nm gate length were developed for the fabrication of submillimeter-wave monolithic integrated circuits (S-MMICs) operating at 300 GHz and beyond. Heterostructures with very high electron sheet density of 6.14×10^{12} cm⁻² and 9800 cm²/Vs electron mobility were grown on 4" GaAs substrates using a graded quaternary InAlGaAs buffer layer. For proper device scaling channel-gate distance and source resistance were reduced. Maximum transconductance of 2500 mS/mm and a transit frequency of 515 GHz were achieved for the 35 nm mHEMT with $2 \times 10 \mu$ m gate-width. Already the 50 nm technology allows the realization of S-MMIC operation frequencies up to 320 GHz, the current limit of on-wafer probe availability. A compact four-stage H-band amplifier circuit based on a grounded coplanar waveguide (GCPW) layout is presented in 50 and 35 nm technology, respectively. The 50 nm mHEMT amplifier has a linear gain of 19.5 dB at 320 GHz and more than 15 dB between 240 and 320 GHz. The same amplifier utilizing 35 nm gate-length transistors achieves more than 20 dB gain within the entire H-band from 220 to 320 GHz. [C153]

"Improvement in noise figure of wide-gate-head InP-based HEMTs with cavity structure"

Dependences of minimum noise figure at 94 GHz on gate-head length were studied using InP-based HEMTs. The noise figure was improved effectively by using a cavity structure even though a wide gate-head was employed. Wide gate-head InP-based HEMTs with a cavity structure are promising candidates for improving low-noise properties at millimeter-wave frequencies. [C154]

"100 mm GaN-on-SiC RF MMIC technology"

100 mm diameter 4H-SiC High Purity Semi-insulating substrates are now being manufactured in high volume. GaN HEMT layers grown on 100 mm SiC substrates have shown excellent sheet resistivity and AlGaIn thickness uniformities (σ/mean) of 1.3 and 1.1%, respectively. The fabrication process for MMIC manufacture was adapted to the larger diameter substrates without requiring any change to the process design kits for the foundry. MIM capacitor processes were optimized, and resistor process, wafer thinning and slot via etching were all adapted to the larger platform. These 100 mm wafers are now being used in high volume production of both high power discrete GaN devices, as well as MMICs. Commercially available MMICs have been released to production using this 100 mm platform. A wide band 25 Watt power amplifier is discussed, along with a 3 watt driver capable of DC-4 GHz operation. [C155]

"Toward practical applications over 100 GHz"

This paper discusses practical applications of the frequency band starting at 100 GHz—a band that has yet to be fully exploited. It considers the feasibility of future applications driven by the sub-terahertz and terahertz bands, examining this feasibility from two perspectives: (1) market needs and the standards being released to meet these needs mainly in the area of communications applications, and (2) advances in semiconductor technologies and their peripheral technologies. To discuss approaches to implementing these applications, we present two transmission technologies that we are developing. [C156]

"A 206-294GHz 3-stage amplifier in 35nm InP mHEMT, using a thin-film microstrip environment"

We present a compact, 3-stage millimeter-wave monolithic integrated circuit (MMIC) amplifier with an operating frequency of 206-294 GHz, formed by common-source configured 35 nm LgInP mHEMTs and a multi-layer thin-film microstrip (TFM) wiring environment. The amplifier S₂₁ mid-band gain is 11-16 dB, 3 dB bandwidth at 294 GHz, and 82.5 mW PDC. This is the first reported InP HEMT MMIC operating in G-, H-band employing thin-film microstrip. Because the TFM ground-plane shields the signal interconnects from the substrate, well behaved device (0.1-67, 140-200, 210-310 GHz) and amplifier (206-320 GHz) measurements are presented from an unthinned, 25 mil substrate. The total size of this 3-stage amplifier is only 0.77 × 0.40 mm². [C157]

"Optical control of InP-based HEMT 60GHz oscillators with sub-harmonic injection locking"

Optical control and sub-harmonic-injection-locking of a 60 GHz millimeter-wave oscillator using InP-based HEMTs are reported. The oscillation frequency locking by the injection of several order sub-harmonic signals was clearly observed. In addition, the modulation of the frequency-locked 60 GHz signals by the illumination of a tightly focused laser beam with intensity modulation was also demonstrated. This oscillator can lead to a key device for the base station in millimeter-wave wireless systems with optical fiber links. [C158]

"Sub 50 nm InP HEMT with $f_T = 586$ GHz and amplifier circuit gain at 390 GHz for sub-millimeter wave applications"

In this paper, we report recent advances on sub-50 nm InP HEMT have achieved new benchmarks of 586 GHz f_T and 7 dB amplifier circuit gain at 390 GHz. [C159]

"An ultra-broadband robust LNA for defence applications in AlGaIn/GaN technology"

The design, fabrication and test of a 2-18 GHz monolithic Low Noise Amplifier utilizing 0.25 μm AlGaIn/GaN HEMT technology is reported. The measured noise figure of the amplifier is less than 4.7dB over the 2-18 GHz frequency range, exhibiting a minimum of 3.3 dB at 3 GHz. The LNA gain is 23dB. Even being a low-noise amplifier, the MMIC can withstand 10W input CW RF power, demonstrating no apparent degradation: to the authors knowledge this is the best RF LNA survivability reported to date in this frequency range using GaN technology. [C160]

"GaN large-signal oscillator design using Auxiliary Generator measurements"

This paper describes the usage of the Auxiliary Generator (AG) method in the large-signal design process of a microwave oscillator. The oscillator circuit is based on a high power Gallium-Nitride (GaN) High Electron Mobility Transistor (HEMT) as active component and is used to ignite and maintain a plasma, which acts as a built-in non-linear load. The oscillator works in class A-AB in the range of 2.3 GHz. The AG method is used to monitor and optimize the oscillation characteristics under large-signal oscillation conditions. [C161]

"Comparative analysis of RF wide bandgap technologies for UMTS applications"

In this paper, we report the benefits of wide bandgap technology in UMTS applications. For this purpose, three, 10 W, 2.14 GHz class AB power amplifiers based on SiC MESFET and GaN HEMTs have been designed. A model based design procedure with simulated load pull characterization was used and the achieved results of the implemented amplifiers show an excellent performance from the efficiency/ linearity point of view. A small signal gain of 9, 13 and 15 dB for PA1(SiC MESFET, Cree), PA2(GaN HEMT, Eudyna) and PA3(GaN HEMT, Cree), respectively have been obtained. An output power of (40-41.5 dBm) and Max. PAE of (43-56%) have been achieved, too. Linearity performance based on gain compression, phase distortion, two-tone intercept points and finally ACLR characterization has been done. The results are compared and discussed in detail. It is found that, among state-of-the-art WBG transistor technologies, WBG offers the optimum solution for highly linear, high efficient power amplifiers in wireless communications to date. [C162]

"A 4W GaN power amplifier for C-band application"

In this contribution, design of a 4W GaN HEMT power amplifier (PA) for C-band application for instance of Car to Car communications will be reported. The PA design procedure considers the characteristics of digital modulated signals planned to be used in C-Band. Such signals have a high peak to average ratio (PAR), which requires highly efficient and linear PA. A 4W low cost and small size class-AB PA has been designed and fabricated for the 5.6 to 5.9 GHz band using GaN on Si. The designed PA has maximum output power of 36 dBm with 8 dB of gain. An ACPR of -30.5 dBc has been measured using a 64 QAM signal of 9.6 dB PAR at an average output power of 27 dBm with power added efficiency (PAE) of about 18%. [C163]

"A 2 W GaAs Doherty power amplifier for WiMAX applications"

This paper presents a GaAs Doherty power amplifier (DPA), designed and implemented at 5.6 GHz, for WiMAX applications. The designed DPA uses two identical 1 W packaged GaAs HEMTs for the main and peaking amplifiers. A maximum output power of 34.4 dBm (2.8 W) was measured, with a maximum power-added efficiency of PAE = 31% ($\eta = 42\%$). The efficiency was maintained higher than PAE = 23% ($\eta = 29\%$), over 6 dB of output back-off range, and higher than PAE = 16% ($\eta = 21\%$) over 10 dB output back-off. The linearity performance of the designed Doherty PA was experimentally tested with a 9-carrier, 64-QAM digitally modulated signal with a peak-to-average-power ratio of PAR = 9.6 dB. An adjacent-channel-leakage ratio of ACLR = -33 dBc was measured at an average output power of Pout, avg. = 24 dBm. To the best knowledge of the authors, this is the first Doherty PA designed and implemented in the 5-6 GHz frequency range, in hybrid technology. [C164]

"A W-band active frequency-multiplier-by-six in waveguide package"

We demonstrate a broadband active frequency-multiplier-by-six for the W-band (75-110 GHz), mounted in a waveguide package. The frequency-multiplying function is performed in a single MMIC using a cascade of balanced tripler and doubler stages. The MMIC, realized in metamorphic HEMT technology, is mounted by wire bonding and high performance waveguide-to-microstrip transitions into a split-block waveguide module containing an integrated voltage supply board. The module achieves an output power of 2.5 dBm, with an associated conversion gain of 0.5 dB, and a 3-dB output bandwidth of 21.5%, corresponding to a frequency range from 83 to 103 GHz. Unwanted harmonics in the output spectrum are suppressed by more than 18 dB. The application of the employed packaging technique to frequencies up to 325 GHz is discussed. [C165]

"An intelligence driven active loadpull system"

This paper describes how the application of the PHD model can add intelligence to an open loop active loadpull system. This intelligence driven approach by providing for an improved prediction of the operating conditions required to emulate a specified load speeds up the load emulation convergence process by minimizing the number of iterations to predict the injected signal, therefore making more efficient use of a measurement system. The results were validated by carrying out loadpull measurements on the fundamental tone of a 10 Ч 75um GaAs HEMT, operating at 3 GHz. [C166]

"Development of a GaN HEMT class-AB power amplifier for an envelope tracking system at 2.45 GHz"

A class-AB power amplifier was designed for an envelope tracking (ET) application. Class-AB amplifier is widely used in wireless communication systems due to the compromise between linearity and efficiency. As a power device, Cree Gallium Nitride High Electron Mobility Transistor (GaN HEMT) CGH4010F was chosen. The input and output matching networks were designed and simulated with Advanced Design System (ADS). After some optimization, the amplifier was fabricated using a Rogers RT/Duroid 5880 substrate. The amplifier together with a MAX2247 preamplifier as a driver was measured. A good agreement between the simulation and measurement results was observed. The maximum power added efficiency (PAE) is around 50 percents with the supply voltage $V_{sup} = 10$ V and the maximum drain efficiency is around 75 percents with $V_{sup} = 5$ V. An output power up to 42 dBm and good linearity of the output voltage with respect to the supply voltage in the range $0 < V_{sup} < 20$ V were achieved. Thus, the amplifier is suited for ET applications. [C167]

"Impact of the pulse-amplifier slew-rate on the pulsed-IV measurement of GaN HEMTs"

The influence of the non-ideal response of the pulse-amplifier on the trap and self-heating dynamics, and hence, on the drain-current transient in a GaN HEMT is studied with new trap and self-heating models. It is shown that the study of the trap and self-heating dynamics requires a proper correction technique that accounts for the change in trap-potential, trap time-constant and thermal response due to the non-ideal response of the pulse-amplifier. Several post-measurement data correction techniques are discussed and shown to be incapable of predicting the true drain-current transient. A pre-measurement terminal correction technique using a new version of the pulse measurement system is used to solve the problem. [C168]

"Harmonic termination of AlGaIn/GaN/(Al)GaN-single-and double-heterojunction HEMTs"

This paper gives a systematic comparison of input-and output-second-harmonic termination in X-frequency-band MMICs (8-12 GHz) based on advanced single- and double-heterojunction AlGaIn/GaN/(Al)GaN high electron mobility transistors (HEMTs) on SiC substrates. High-efficiency design-strategies are key to make use of the outstanding power capability in group-III-nitride MMICs. The study deals with the bandwidth trade-offs associated with reaching very high PAE-values beyond 55% at 10GHz in cw-operation to a 50 Ohm-load.

[C169]

"Design of 50MHz-1GHz low noise and high linearity MMIC amplifier"

A 50MHz-1GHz low noise and high linearity amplifier monolithic-microwave integrated-circuit (MMIC) is presented in this article. The circuit was designed with 0.15 μ m InGaAs PHEMT process. The ADS simulation results showed it gave excellent Noise Figure of 1.36dB and high linearity up to 17dBm IIP3 with 75Ohm systems. It is especially suitable in the applications such as cellular telephone base station driver amplifiers, the Cable TV etc. [C170]

"Optical Sensing Characteristics in a Transparent Al-Doped Zinc Oxide-Gated Al_{0.2}Ga_{0.8}As/In_{0.2}Ga_{0.8}As High Electron Mobility Transistor"

A three-terminal optical sensor by using an aluminum-doped zinc oxide (AZO)-gated Al_{0.2}Ga_{0.8}As/In_{0.2}Ga_{0.8}As high electron mobility transistor (AZO-HEMT) on a GaAs substrate is demonstrated in this report. Optical responses under illumination of different wavelengths are investigated, as compared to a conventional Au-gated HEMT device. Experimental results demonstrate that the present design is promising for tunable optical sensing applications. [C171]

"DARPA's GaN technology thrust"

DARPA/MTO has sponsored III-N electronics programs to combine associated high intrinsic breakdown voltages, high electron saturation velocities, and large sheet carrier densities. The WBGs-RF program has developed GaN HEMTs for high power RF electronics resulting in sufficiently mature transistors to confidently predict > 10E6 hours of MTTF for up to 40 GHz power device operation. The latest NEXT program further pushes III-N-based HEMTs toward its frequency (size) scaling limits by simultaneously minimizing carrier transit time, maximizing electron density, and reducing access resistances with innovative epitaxial structures and dielectric heterointerfaces. The goals of the Phase I of NEXT project are to demonstrate 300 GHz D-mode and 200 GHz E-mode HEMTs while maintaining the breakdown voltage and transistor cutoff frequency product ≥ 5 THz·Volt. The final goal of the NEXT program is to enable 1000-transistor, high-yield, 500 GHz E/D-mode GaN technology for mixed signal applications. [C172]

"High-efficiency class E MMIC power amplifiers at 4.0 GHz using AlGaIn/GaN HEMT technology"

Two high-efficiency Class E MMIC power amplifiers designed at 4 GHz using AlGaIn/GaN HEMT technology are presented. The first circuit was designed using a 0.5 mm (4 Ч 125 μm) HEMT and when biased at 25 V drain bias it produced 61 % PAE, 33.8 dBm of output power and maximum gain of 14.8 dB. The second circuit used a 1 mm (8 Ч 125 μm) HEMT and at 30 V drain bias it produced 57% PAE, 36 dBm of output power, and maximum gain of 13 dB. The key to obtaining the high gain, PAE and output power produced by these circuits is accurate modeling of the HEMTs and the passive components. [C173]

"Solid-state amplifiers for terahertz electronics"

With the fMAX of current generation InP transistors pushing above 1-THz and new transistor scaling in progress, the operational frequency of solid-state amplifiers is being pushed towards THz frequencies. In this paper we present our latest work towards demonstrating THz frequency amplifiers, including measured gain and noise performance of a 0.48 THz low noise amplifier using scaled InP transistors. Initial performance of next generation transistors is also presented, along with infrastructure necessary to package and operate solid-state amplifiers at THz frequencies. [C174]

"High-efficiency class E MMIC power amplifiers at 4.0 GHz using AlGaIn/GaN HEMT technology"

Two high-efficiency Class E MMIC power amplifiers designed at 4 GHz using AlGaIn/GaN HEMT technology are presented. The first circuit was designed using a 0.5 mm (4 Ч 125 μm) HEMT and when biased at 25 V drain bias it produced 61 % PAE, 33.8 dBm of output power and maximum gain of 14.8 dB. The second circuit used a 1 mm (8 Ч 125 μm) HEMT and at 30 V drain bias it produced 57% PAE, 36 dBm of output power, and maximum gain of 13 dB. The key to obtaining the high gain, PAE and output power produced by these circuits is accurate modeling of the HEMTs and the passive components. [C175]

"Evaluation of a GaN HEMT transistor for load- and supply-modulation applications using intrinsic waveform measurements"

In this paper, the efficiency of a GaN HEMT transistor and its intrinsic waveforms are measured at 0.9 GHz and investigated for load- and supply-modulation applications. The results show that both techniques perform equally well for back-off levels 6.5 dB. At higher back-off levels, the efficiency improvements achieved by supply modulation outperform load modulation. At 10 dB back-off, supply, and load modulation provide a power-added efficiency (PAE) of 68%, and 58%, respectively. Using measured intrinsic waveforms, it is shown that PAE degradations in load modulation can be mainly attributed to parallel losses rather than series losses, which are dominant in supply modulation. The harmonic contents of the intrinsic waveforms, in both techniques, are equally strong in back-off and peak power operations. There is, therefore, a great potential for further efficiency enhancement by circuit-level optimization of harmonic terminations for back-off. [C176]

"Large-Periphery AlGaIn/GaN High Electron Mobility Transistors for High-Power Operation"

We report on AlGaIn/GaN high electron mobility transistors (HEMTs) for high-power operation achieved by selective-area growth (SAG) technique based on plasma-assisted molecular beam epitaxy (PAMBE). Significant improvements in current density and on-state resistance were observed when SAG was employed. Maximum current of 1.75A and on-state resistance of 4.76mΩ cm² were demonstrated for a large-periphery HEMT with total gate width of 5.2mm. Low Schottky gate leakage current was also realized by the suppression effect of SAG and the use of Si₃N₄/SiO₂ gate insulators, leading to a high gate breakdown voltage of over 200V at a short gate-to-drain distance of 6μm. [C177]

"Frequency-reconfigurable mobile terminal antenna with MEMS switches"

In this paper a frequency-reconfigurable mobile terminal antenna with a tuning range of one octave is presented. The antenna is based on a capacitive coupling element (CCE) and switching between two separate matching circuits controlled with RF MEMS switches. The tuning concept using MEMS is compared with similar tuning cases using HEMT switches. The MEMS tuning circuit outperforms the transistor switch based circuits in both efficiency and linearity, but it is shown that also the nonidealities of the MEMS components have to be considered when designing MEMS based circuits. [C178]

"Energy efficient power MOSFETs"

An overview is given of the main technology trends and innovations in Power MOSFET transistors ranging from LV (<50V), MV (50V-200V) to HV (200V-1000V), in view of the needs for high energy efficient power

management systems. Alternatives to MOSFET, like IGBT and GaN-HEMT, are briefly highlighted and discussed. [C179]

"Advanced design of double Doherty power amplifier with a flat efficiency range"

This paper reports a new double Doherty power amplifier (DDPA) with a flat efficiency range, which consists of two-stage amplifiers. When the two-way DPA is used as the main peaking amplifier, the driving peaking cell with class-C bias turns the DPA off before the saturation of the main carrier amplifier. Three efficiency-peaking points are achieved with the additional Doherty operation by the main peaking amplifier after the saturation of the main carrier amplifier. For verifications, the driving and main amplifiers are designed and implemented with 2-W and 10-W GaN HEMTs, respectively, at 2.14 GHz. From the continuous wave (CW) results, three efficiency-peaking points are obtained at approximately 9-, 5-, and 0-dB back-off powers with over 42% drain efficiency. For one-carrier wide-band code division multiple access (WCDMA) signal, the DDPA shows good digital predistortion linearization performance. [C180]

"Improved parameter extraction method for GaN HEMT on Si substrate"

An improved parasitic elements extraction method applied to GaN on Si devices is presented. Genetic-algorithm based procedure is used to determine a high quality reliable starting values for the extrinsic parameters of proposed small-signal model. Local optimization technique is then used to refine the initial value and find the optimal value for each model element. The validity of the developed method and the proposed small-signal model is verified by comparing simulated small-signal S-parameters with measured ones of a 2-mm (10 \times 200 μ m) GaN HEMT-on-Si. [C181]

"Reliability evaluation of Schottky contact of AlGaIn/GaN HEMT, based on two AC voltages with different frequencies"

This paper presents a reliability evaluation of Schottky contact of AlGaIn/GaN HEMT. The Schottky barrier height (SBH) and ideality factor are investigated through the current-voltage (I-V) characteristics. Two kinds of ac voltages with different frequencies (10 kHz and 1 MHz) are applied on the two similar Schottky contacts of AlGaIn/GaN HEMT, and the I-V curves are measured. From the measured results, we find that the SBH increases and the ideality factor decreases after the same time. The 1 MHz ac voltage applied on device leads to a more and faster increase of SBH than that of 10 kHz. And the decrease of ideality factor for 1 MHz is more than that of 10 kHz. The reverse I-V characteristics of Schottky contact of AlGaIn/GaN HEMT also present a larger change for 1 MHz than that of 10 kHz. In addition, we give a simple explanation why the values of ideality factor are greater than 2.0 for both two Schottky contacts of AlGaIn/GaN HEMT. [C182]

"High performance SOI RF switches for wireless applications"

This paper describes 0.18 μ m CMOS silicon-on-insulator (SOI) technology and design techniques for SOI RF switch designs for wireless applications. The measured results of SP4T (single pole four throw) and SP8T (single pole eight throw) switch reference designs are presented. It has been demonstrated that SOI RF switch performance, in terms of power handling, linearity, insertion loss and isolation, is very competitive with those utilizing GaAs pHEMT and silicon-on-sapphire (SOS) technologies, while maintaining a cost and manufacturing advantage. [C183]

"0.3- μ m gate-length metamorphic AlInAs/GaInAs HEMTs on Silicon substrates by MOCVD"

Fabrication and performance of high-frequency 0.3- μ m gate-length depletion-mode metamorphic Al_{0.50}In_{0.50}As/Ga_{0.47}In_{0.53}As high electron mobility transistors (mHEMT) grown by Metalorganic Chemical Vapor Deposition (MOCVD) on n-type silicon substrates is reported. Using a combined optical and e-beam photolithography technology, submicron mHEMT devices on Si have been achieved. A maximum trans-conductance up to 739 mS/mm was measured. The unity current gain cut-off frequency (f_T) and the maximum oscillation frequency (f_{max}) were 72.4 and 77.3 GHz, respectively. An input capacitance to gate-drain feedback capacitance ratio, C_{gs}/C_{gd} , of 6.8 and a voltage gain, gm/g_o , of 6.9 are observed in the device. [C184]

"Effect of field plate length on DC characteristics of high breakdown voltage GaN HEMTs for power switching application"

High breakdown voltage GaN HEMTs was developed for power electronics application. The device with source connected field plate (FP) was fabricated, which demonstrated perfect hard breakdown characteristics. A high breakdown voltage of 740V was obtained in air ambient while gate-drain spacing L_{gd} and FP length L_{FP} equaled to 20 μ m and 2 μ m respectively. Specific on-resistance of the device was 14 m Ω .cm² far below that of Si-

based MOSFET with similar breakdown voltage. The influence of FP length on the on-state characteristics, off-state breakdown characteristics, and specific on-resistance R_{onA} was discussed. [C185]

"GaN Smart Discrete power devices"

GaN "Smart Discrete" power devices were realized using the AlGaIn/GaN-on-Si platform, where two built-in intelligent self-protection functions were demonstrated. First, an AlGaIn/GaN normally-off high electron mobility transistor (HEMT) with reverse drain blocking capability was realized, featuring a Schottky contact controlled drain barrier. Compared to the Schottky drain structures, the new design exhibits only a 0.55 V onset voltage in the forward biased "ON" state, while effectively blocks the reverse current conduction. The device fabrication is also free of extra photomask and process steps. Second, an AlGaIn/GaN lateral field-effect rectifier (L-FER) with intrinsic "ON" state current limiting capability was fabricated, featuring a Schottky controlled depletion-mode (D-mode) channel extension (length of LD) beyond the ohmic contact at the cathode electrode, where the on-state current of the new rectifiers are self-limited at 4.59 kA/cm²(LD= 1.3 μm) and 3.56 kA/cm²(LD= 1.9 μm) at room temperature. The current limiting level shows a negative temperature coefficient (TC) that is desirable for thermal stability. [C186]

"SIMS depth profile characterisation of InAlN/GaN structures"

This contribution reports on properties and characterization of InAlN/GaN structures prepared by metal organic chemical vapour deposition (MOCVD) using secondary ion mass spectroscopy (SIMS). The SIMS revealed the vertical cross section of the InAlN/GaN sample structures on SiC substrate and also visualizes the different growth procedure results. The SIMS comparison of the structures shows the Al, In and Si incorporation to the neighbouring layers and has influence on the in-plane stress in AlN layer and measured electrical properties of the fabricated HEMT devices. [C187]

"Inter-digitated AlGaIn/GaN Schottky diode for monolithic integration"

New construction of the AlGaIn/GaN/semi-insulating Schottky diode was proposed for operation at gigahertz regime. Based on the performed numerical simulations the planar diode with inter-digitated lay out was elaborated. The test structures of the diode was fabricated in AlGaIn/GaN heterostructures grown on a c-plane sapphire by MOVPE technique. The d.c. and high frequency characteristics of the device were measured. The cut-off frequency, f_T , of the diode was 8.2 GHz. The obtained results proved that inter-digitated Schottky diode fabricated in AlGaIn/GaN heterostructure grown on semi-insulating substrate is suitable for high frequency operation at gigahertz regime and could be also monolithically integrated with HEMT. [C188]

"100mV noise performances of Te-doped Sb-HEMT"

In this paper, we present the noise measurement results of InAs/AlSb HEMTs at room temperature under very low drain bias (100mV) at 30GHz. Under these dc bias conditions the transistor exhibit NF_{min} =1.56 dB and G_{ass} =5.3dB @30 GHz for P_{dc} = 7.3μW/μm. These results are compared to our previous work and the great improvements observed open up the possibility to develop a 100mV electronics at room temperature. [C189]

"Breakdown voltage enhancement in lateral AlGaIn/GaN heterojunction FETs with multiple field plates"

It has been proposed in the literature to use metal field plates (FPs) in order to increase the breakdown voltage (BV) of AlGaIn/GaN HEMTs. In this article we analyze the possibility of using multiple FPs to increase the gate-to-drain BV. We show that FPs with variable oxide thickness (with thinner oxide towards the gate electrode and thicker oxide thickness towards the drain electrode) increase the BV more efficiently than a single FP. FPs with variable oxide thickness can be built using multiple FPs with increasing oxide thickness from gate to drain and, when all FPs are connected to the source electrode. [C190]

"GaN high electron mobility transistors with localized Mg doping and Drain Metal Extension"

A Magnesium Doped Layer (MDL) under the 2-DEG channel and a Drain Metal Extension (DME) are proposed to provide a new degree of freedom in the optimization between breakdown voltage (BV) and specific-on-resistance (R_{on-sp}) in AlGaIn/GaN HEMTs. The surface electric field of the proposed structure is distributed more evenly when compare to the MDL-only structure with the same dimensions. A breakdown voltage of 1390V with specific-on-resistance of 4mΩ·cm² was obtained with L_M = 1μm, a peak concentration of 8.4×10^{17} cm⁻³, L_{pd} = 3μm and a drift region length of 10μm. Comparing with the conventional MDL-only HEMT structure, the MDL-DME is shown to deliver comparable specific-on-resistance while featuring a 54% BV improvement without any area overhead penalty. [C191]

"High-breakdown voltage field-plated normally-off AlGaIn/GaN HEMTs for power management"

The high breakdown voltage AlGaIn/GaN HEMTs with source-terminated field plate was firstly fabricated for high frequency and high power application, employing by CF₄plasma treatment for enhancement-mode (E-mode). The results showed that by adding the distance of gate to drain, LGD from 5 μm to 15 μm , the breakdown voltage of the device was rapidly increased 350V, whose value is from 50V to 400V while the threshold voltage of the device, V_{TH} was +0.5V by the charge modulation technology of CF₄plasma. When the distance of source-terminated field plate, LFP was about 3 μm , the breakdown voltage of the device was apparently improved because the electric field near the gate edge was effectively shielded. The breakdown voltage and the specific on-resistance for the LGD and LFP distance of the device about 15 μm and 3 μm were about 475V and about 2.9 $\text{m}\Omega \cdot \text{cm}^2$ respectively. The results from RF measurement showed that with the variation of V_{GS} , the f_{T} and f_{MAX} parameters of the device with source-terminated field plate were the order of Gigahertz frequency. The DC, AC and transient characteristics of E-mode Power AlGaIn/GaN HEMTs were satisfied and its forward current was about 90 mA. Therefore the E-mode AlGaIn/GaN HEMTs was very suitable as the novel power switch technology in energy management application. [C192]

"Impact of doping concentration and donor-layer thickness on the dc characterization of symmetric double-gate and single-gate InAlAs/InGaAs/InP HEMT for nanometer gate dimension-A comparison"

The aim of this paper is to investigate the impact of gate-length (L_g) and doping concentration (N_d) of the donor layer and its thickness (d_a) on the performance of double-gate (DG) InAlAs/InGaAs/InP HEMT. A comparison of the impact of donor-layer doping concentration, donor-layer thickness and gate-length on the channel current, transconductance, gate-to-source capacitance and cut-off frequency for the DG-HEMT has been studied with that for SG-HEMT. As a result of this comparison the DG-HEMT has been seen to exhibit more sensitivity to these device parameters. This is due to greater sheet-carrier concentration and better gate-control. Thus, the optimization of the donor-layer doping, donor-layer thickness and gate-length in the case of DG-HEMT is crucial. [C193]

"Cellular Monte Carlo study of RF short-channel effects, effective gate length, and aspect ratio in GaN and InGaAs HEMTs"

An investigation of RF short-channel effects in state-of-the-art GaN and InGaAs HEMTs, in relation to effective gate length and aspect ratio, is performed through our full band Cellular Monte Carlo simulator. In particular, the short-circuit current gain cut-off frequency, f_{T} , is extracted using two different methods for several gate lengths. The first method relates f_{T} to the electron transit time in the gate region, and from the electron velocity profile allows a direct estimation of f_{T} , the effective gate length L_{eff} , and the investigation of the nanoscale carrier dynamics in the channel. The second extraction methods derives f_{T} through small-signal analysis. Our results indicates that the increasing difference between effective gate length and metallurgical gate length, as the device is scaled, plays a major role in limiting the RF performance. Moreover, maintaining a minimum aspect ratio of 5 for InGaAs HEMTs, and 10 for GaN devices, helps mitigating the short-channel effects. [C194]

"Consideration of impact of GaN HEMT for class E amplifier"

This paper demonstrates GaN HEMT as the transistor switch for 13.56 MHz class E amplifier. It is shown that GaN HEMT has capability of realizing very high efficiency class E amplifier at higher frequency than Silicon MOSFETs. Problem of negative threshold voltage, i.e., "normally on" characteristics, is considered. It is considered using second voltage supply, GaN HEMT can be driven properly. Experimental demonstration of 13.56 MHz 1 W class E amplifier achieved 82% efficiency. [C195]

"High-speed driver for pin diode microwave switch"

This article discusses the design of high-speed driver for PIN-diode microwave switches. The driver is built on a normally open pHEMT and controlled with TTL level signals. [C196]

"AlGaIn/GaN MOS-HEMTs with ZnO gate insulator and chlorine surface treatment"

AlGaIn/GaN metal-oxide-semiconductor high-electron-mobility transistors (MOS-HEMTs) were fabricated with ZnO gate insulator and chlorine surface treatment. It is revealed that the chlorine treatment reduced the gate lag phenomenon and enhanced the device performance. The gate leakage current was also reduced about one order of magnitude in comparison to the conventional one. The chlorine-treated MOS-HEMTs exhibited a saturation drain-source current of 0.85 A/mm, a peak extrinsic transconductance of 207 mS/mm, and an off-state

breakdown voltage larger than 100V. This significant improvement was owing to the reduction in surface state density, which was resulted from the decrease of Ga dangling bonds and the passivation of N vacancies on the AlGa_N surface. [C197]

"AlGa_N/Ga_N HEMT TCAD simulation and model extraction for RF applications"

GaN devices have significant advantages in power density, thermal characteristics, and voltage range over those based on conventional compound semiconductors or Silicon. With GaN, as in other materials systems there are significant advantages in cycle time and strength of design from use of TCAD. Here TCAD simulations of AlGa_N/Ga_N HEMTs are shown to accurately match measured DC and small signal AC data. For large signal RF applications it is necessary to use modeling to extend the application of this TCAD solution. Proprietary models are extracted from TCAD data and demonstrated. [C198]

"Analytical models of the transition layer in HEMTs on silicon substrate for device simulation"

One way to increase the breakdown voltage in heterojunction field-effect-transistors (HFETs) on silicon substrate is to introduce a transition (buffer) layer made of a sandwich of thin AlN/AlGa_N layers between the silicon substrate and the GaN well. The effect of this transition layer is to average out and, in this way, to reduce the local mechanical stress that appears between the silicon substrate and the GaN layer because of the different lattice constants of the two layers. In this article we present an analytical model for the simulation of the transition layer in AlN/AlGa_N transistors. The model is based on writing explicitly the interface conditions at each boundary and solving the resulting system of equations analytically. The final equation is written in the form of a standard mixed-type boundary condition that can be relatively easy implemented in device simulators. [C199]

"Double δ -doped AlGaAs/InGaAs MOS-pHEMTs by using ozone water oxidation treatment"

This work investigates device performances of an AlGaAs/InGaAs metal-oxide-semiconductor pseudomorphic high electron mobility transistor (MOS-pHEMT) by using ozone water oxidation treatment. Experiment results indicate that the studied MOS-pHEMT has demonstrated superior device characteristics as compared to a conventional pHEMT without oxidation treatment on the same epitaxial structure. The studied MOS (conventional)-pHEMT exhibits improved power-added-efficiency (P.A.E.) of 39.6 (36)%, unity-gain cut-off frequency (f_T) of 19.3 (16.8) GHz, maximum oscillation frequency (f_{max}) of 30.6 (26.7) GHz, minimum noise figure (NF_{min}) of 1.21 (1.48) dB, and excellent two-terminal gate-drain breakdown voltage (BV_{GD}) of -43.1 (-7.9) V, respectively [C200]

"Handshaking multiscale thermal model of nanostructured devices"

In this work we present a multiscale method to model self-heating effects in nanostructured devices. While the heating is modeled within the drift-diffusion approximation, the heat dissipation is computed by means of a concurrent coupling between a Phonon Boltzmann Transport Equation (PBTE) based method and the Fourier model. We develop the way to connect the two models to each other and apply the implemented scheme to a GaN based High Electron Mobility Transistor (HEMT). [C201]

"A 900 MHz 10 mW monolithically integrated inverse class E power amplifier"

This work demonstrates a new integrated inverse class E amplifier circuit, employing a pHEMT switching device and fully integrated output network for pulse shaping. The circuit is particularly suitable for full integration, since it does not need any RF choke for biasing, and no DC blocking capacitor is needed between the switch and the output network parallel resonance circuit. The back plate capacitances of the additional capacitors are not connected to nodes that carry RF voltage signals. A commercial GaAs monolithic microwave integrated circuit process was used for fabricating the prototype circuit. 11.5 mW output power and 39% drain efficiency with 0.9 V supply voltage was measured at 895 MHz operating frequency. The output power remains over 10mW across 850-925 MHz, and the drain efficiency remains above 32% across this frequency range. [C202]

"Noise in the InAlN/GaN HEMT transistors"

This paper deals with measuring and analyzing input and output low-frequency noise spectra of Gallium Nitride (GaN) based High Electron Mobility Transistors. Low-frequency noise spectral densities of drain noise voltage and gate noise current are shown. The three different measurements of input low-frequency noise of GaN HEMT transistor were measured for better revealing G-R noise sources in gate region and their influence to the output noise voltage. The long-term voltage off-stress was accomplished on the HEMT and impact to the low-frequency noise characteristics shown. [C203]

"Thermal modeling and measurements of AlGa_N/Ga_N HEMTs including Thermal Boundary Resistance"

In this paper an analysis of thermal behavior of microwave power AlGa_N/Ga_N HEMTs has been carried out through pulsed current-voltage (PIV) measurements and S parameters. A special care about trapping effects has been followed where it is shown Error! Reference source not found. that the thermal resistance of the device can be accurately determined provided that some assumptions on the trapping behavior of the device are verified. The values obtained have been checked by three dimensional finite element (3D-FE) simulations. Finally, the Thermal Boundary Resistance (TBR) between Ga_N/SiC has been extracted and compared to literature. The results we have obtained are in line with what can be found. [C204]

"Production of 150 NM T-gate on basis of Ti/Mo/Cu for p-HEMT"

Technology of manufacturing of 0,15 μm T-gate Ti/Mo/Cu on heterostructure GaAs/AlGaAs/InGaAs using the electron-beam lithography in the tri-layer resist mask 950PMMA/ LOR 5B/ 495PMMA is described in the work. [C205]

"2D Thermal propagation analysis of discrete power devices based on an innovative distributed model technique and CAD framework"

Stress and reliability analysis through accurate predictive models is required in order to guarantee higher levels of quality in terms of robustness of discrete power devices. This paper focuses on thermal modeling and simulation of Power MOSFETs, Power Bipolars, Schottky Diodes and HFETs made with both consolidated silicon technologies and advanced ones on new materials. These devices, due to their peculiar characteristics, are used in a wide range of products, such as SMPS (Switched-Mode Power Supply), AC/DC converters (traditional silicon) and microwave wireless applications. The objective of this work is to describe an innovative distributed model technique and the development of a thermal-aware modeling framework covering thermal modeling issues and simulation aspects that can be found in the industrial context. A methodology for generating a lumped-element distributed model for a silicon power MOSFET device that takes into account the effects of layout parasites will be shown. The proposed technique exploits the high-frequency modeling approach of microstrips and striplines to describe the effects of the passive parts on active elementary transistor cells. The strategy described could be relevant in order to improve the design of new generations of devices; in the absence of careful design considerations, devices may cause reliability problems. [C206]

"Active UWB antenna"

This paper presents a novel scheme for development of an active Ultra-Wide Band (UWB) antenna. A single pulse of 133 ps and amplitude 530 mV peak to peak was obtained using High Electron Mobility Transistor (HEMT) as a generation circuit. This generation circuit was next integrated with a newly proposed UWB planar microstrip antenna. Transmission and reception characteristics of the UWB antenna were measured using a high speed oscilloscope. The short pulse generation circuit and the UWB antenna were fabricated using standard photolithography technique on Neltec soft substrate having $\epsilon_r = 2.2$ and thickness $= 0.254$ mm. The design and optimization of the UWB planar microstrip antenna were carried out using CST simulation software and experimental verifications done using Automatic Network Analyzer. The short pulse generation circuit was simulated using Agilent ADS software. The proposed scheme of active UWB antenna shows good agreement between simulation and measured results. [C207]

"Electromagnetic short pulse generation techniques"

Novel simple techniques are proposed in this paper to generate extremely short electromagnetic pulses using HEMT devices. The proposed circuits are simulated using Agilent ADS software and fabricated on Neltec ($\epsilon_r = 2.2$) soft substrate of thickness $= 0.254$ mm using standard Microwave Integrated Circuit (MIC) fabrication techniques. These circuits are tested in the time domain using high frequency oscilloscope and in the frequency domain using spectrum analyzer. The generated short pulse has 0.171 ps duration with peak to peak amplitude of 544.8 mV. The measured results show good agreement with the simulation results. [C208]

"Fractal nature of resistance of the drain-doped channel of the gan-based heterostructure of the field effect transistor with bidimensional electron gas"

It is shown that the specific resistivity of p 2D-channel of the drain-doped HEMT-transistor based on Ga_N heterostructure in local approximation depends on its linear dimensions l and d and if they are getting smaller it may become even bigger, that specifies the fractal nature of this effect. In course of the experiment there was

defined that the limit value of local approximation $L=60\text{ }\mu\text{m}$ specifies that linear sizes of the active elements of modern HEMT-transistors come into the sphere of local approximation and should subject to fractal geometry laws. To these laws we refer the dependence of electrophysical parameters of the facilities being measured on their sizes and slower dependence on the characterization sizes usually associated with linear dependence.

[C209]

"A novel AlGaIn/GaN HEMTs technology for intelligent electric network application"

The AlGaIn/GaN HEMTs with source-terminated field plate was firstly fabricated, employing by CF₄ plasma treatment for enhancement-mode (E-mode). The results showed that by adding LGD from 5 μm to 15 μm , the breakdown voltage of the device was rapidly increased 350 V, whose value is from 50 V to 400 V while the threshold voltage of the device, V_{TH} stayed about 0.5 V by the technology of CF₄ plasma modulating electron sheet density of the channel. When the distance of source-terminated field plate, LFP was about 3 μm , the breakdown voltage of the device was further improved because the electric field near the gate edge was effectively shielded. The breakdown voltage and the specific on-resistance for the device with the distance of LGD about 15 μm were about 475 V and about 2.9 $\text{m}\Omega \cdot \text{cm}^2$ respectively. The results from RF measurement showed that with the variation of V_{GS} , the f_{T} and f_{MAX} parameters of the device with source-terminated field plate were the order of Gigahertz frequency. The dynamic characteristic of E-mode power device was excellent and its forward current was about 80 mA. Therefore E-mode AlGaIn/GaN technology was very suitable for the application of intelligent electric network. [C210]

"An experimental recovery of GaAs and GaN PHEMT linear equivalent circuits and noise models"

In the present article an experimental recovery of GaAs and GaN PHEMT linear equivalent circuit and noise model are presented. The linear equivalent circuit and noise mode for two types of PHEMT manufactured by FSUE RPC "Istok" (molecular beam epitaxy structure on GaAs and GaN) are recovered. [C211]

"Nitride gallium high power integrated heterostructure FETs"

The heterostructures AlGaIn/AlN/GaN, grown on sapphire substrates, the standard design of the integrated power HFET and the design with the additional field-plate, and its technology have been developed. The HFETs have given output power 4,5-5,5 and 3-4 W/mm, and power gain 4,5-7,5 N 3,8-6,0 dB at frequencies 12 and 17,5 GHz. [C212]

"Approach to formation of cell libraries of MMIC and automatic layout generation for electromagnetic simulation"

A systematical approach to formation of cell libraries (PDKs) of MMIC is presented. Also, a procedure allowing automatic MMIC layout generation for specified foundry process is developed in Microwave Office (MWO) CAD tool. These results are used in developing of a pilot version of PDK for 0.15 μm pHEMT/mHEMT GaAs process. [C213]

"Thermal optimisation of GaN flip chip power transistors"

This paper demonstrates thermally optimized flip-chip designs for high power GaN-based normally-off transistors laterally scaled in two dimensions and suitable for high current loads and a breakdown voltage of 250 V. An adapted transistor layout takes the heat spreading capability of the SiC substrate into account and provides an efficient heat sinking via the bumps. [C214]

"Modelling and optimisation of a sapphire/GaN-based diaphragm structure for pressure sensing in harsh environments"

GaN is a potential sensor material for harsh environments due to its piezoelectric and mechanical properties. In this paper an 8mm diameter sensor structure is proposed based on a GaN/AlGaIn/sapphire HEMT wafer. The discs will be glass-bonded to an alumina package, creating a 'drumskin' type sensor that is sensitive to pressure changes. The electromechanical behaviour of the sensor is studied in an attempt to optimise the design of a pressure sensor (HEMT position and sapphire thickness) for operation in the range of 10-50 bar (5 MPa) and above 300°C. [C215]

"On the identification of trap location in AlGaIn/GaN HEMTs during electrical stress"

Location and properties of traps generated in AlGaIn/GaN high electron mobility transistors submitted to electrical stress was studied using an integrated electrical and optical methodology. A spatial and spectral

electroluminescence study reveals traps generated during both OFF- and ON-state stress to be located in the gate and access region close to the drain side of the gate edge, while UV-light assisted detrapping analysis in conjunction with photoluminescence illustrate these dominant traps located mostly within an AlGaIn subsurface layer. [C216]

"Analysis of structure geometry and interface charge on electrical characteristics of InAlN/GaN HEMTs"

In this paper the results obtained from simulations and measurements on InAlN/GaN HEMTs are presented. The HEMT material structure was modelled by Synopsys TCAD tools and electrical characteristics of the device were simulated by DESSIS. Several effects of the geometry and concentration of interface charges on the electrical characteristics are studied. The interface and surface charges as well as deep level traps were taken into account for the numerical simulations. An influence of variation of several structure parameters on the transfer and output characteristics was studied. The results can contribute to better understanding and further calibration of electro physical models used for InAlN/GaN heterostructures. [C217]

"Role of the gate-to-drain distance in the performance of the normally-off InAlN/GaN HEMTs"

We correlate dc maximal drain current I_{DSmax} , pulsed output characteristics, rf small-signal and breakdown performance of normally-off InAlN/GaN HEMTs with varied gate-to-drain distance d_{GD} . It is found that parasitic lag effects which are related to the possible surface states are not appearing at longer d_{GD} . On the other hand compromise need to be found between the improved gate performance and impaired I_{DSmax} and f_{Tas} as the d_{GD} is increased. The leakage current of the 0.5 μm -long gate may be reduced by up-to three orders of magnitude, down to $\mu A/mm$ at -20 V bias if d_{GD} increases from 3 to 15 μm . On the other hand I_{DSmax} and f_{Tdrop} by about one third of the original value (from about 0.6 A/mm and 34 GHz down to 0.4 A/mm and 21 GHz, respectively) if d_{GD} changes. [C218]

"Model for evaluation of terahertz plasma resonances in HEMT-based devices with grating gate"

We propose simple analytical model for calculation of spatial distribution of the sheet electron density in the channel of high-electron mobility transistor (HEMT) periodically modulated by the bias voltage applied to grid-grating gate. The contribution of ungated regions of two-dimensional electron gas (2DEG) channel is taken into account. The developed model allows to evaluate resonant frequencies of plasma oscillations excited in such periodically modulated 2DEG channel. The proposed model can be useful in the interpretation of experimentally obtained data and optimization of the grating-gated HEMT-like structures for THz applications. [C219]

"Characterisation of electrical properties of AlGaIn/GaN Schottky diode at very high temperature"

Recent progress in GaN based high electron mobility transistors (HEMTs) has revealed them to be strong candidates for future high power devices at high frequency operation. In order to extract and utilize the favorable GaN material properties, however, there are still a lot of areas to be investigated. Among them the most important is to develop new processes, structure design and characterization techniques. Determination of the effective Schottky barrier height ϕ_{bon} on GaN and related compound semiconductors with higher precision is important for further analysis of new combinations of metals and semiconductors and better understanding of physical behaviour at the interface. In this paper we present the modified method of evaluation of the selected parameters on the AlGaIn/GaN heterostructure from the I-V measurement in a wide temperature range. [C220]

"Scalable HEMT model for small signal operations"

The aim of this work is to develop a scalable small signal HEMT model. We propose a general intrinsic model "unit cell" to build larger transistor devices according to our need and model the metal according to individual geometry using a lumped element network. The challenge we address is extraction of this network from measurement. The parameters of the intrinsic part of the transistor have been extracted from different size of transistors and scaling rule applied to the unit cell. We used MathCAD worksheet to de-embed the TriQuint transistor parameters. Multiple cells are used to build larger devices and we showed that coupling between cells with lumped element affects the S-parameter responses. The interconnection with lumped elements was varied according to the need to fit with larger device responses. [C221]

"Study of temperature distribution in the channels of AlGaIn/GaN HEMT devices by μ - Raman characterization techniques"

AlGaIn/GaN and InAlN/GaN high electron mobility transistors (HEMTs) were fabricated and their electrical and thermal properties were examined. The influence of irradiation to direct current (DC) and low-frequency noise

properties of these devices have already been investigated and published. However, the thermal processes in the active layers of these devices can also induce significant changes in the performance of devices. Since thermal processes are directly associated with temperature distribution, temperature mapping in the devices has been suggested using a μ -Raman technique. Considering that the phonon frequencies are sensitive to the sample temperature, the shift of first-order Raman scattering can conveniently be used to directly measure the device temperature with a high spatial resolution. In this context, we report time resolved and sample mapping Raman spectra inside the HEMTs channel as measures of temperatures. [C222]

"HEMT-SAW structures for chemical gas sensors in harsh environment"

A growing thirst for highly sensitive and sufficiently selective sensors for extremely harsh conditions can be seen. This fact excludes the use of conventional sensing devices and gives a space for Surface Acoustic Wave sensors with monolithically-integrated electronics. We have chosen the AlGaN/GaN material as a suitable material due to its excellent chemical inertness and stability of piezoelectric parameters. In this paper we test the possible HEMT transistor/SAW transducer monolithic integration and propose the design of an oscillator based on SAW. [C223]

"AlGaN/GaN HEMT on Si (111) substrate for millimeter microwave power applications"

This paper reports the capability of AlGaN/GaN HEMTs on Si (111) substrates for microwave power applications above 30 GHz. A current gain cut-off frequency $f_t=90$ GHz and a maximum power gain cut-off frequency $f_{max}=135$ GHz are obtained for a 80 nm gate-length transistor. These results, associated with low lag effects, demonstrate the capability of these transistors for high performance, cost effective, MMIC fabrication on a Si substrate for high frequency microwave power applications. [C224]

"GaN-based lamb-wave mass-sensors on silicon substrates"

Lamb-wave mass-sensors were fabricated with MOCVD-grown GaN-based thin films on silicon substrates. Crystalline GaN provides an alternative choice of material for fabricating Lamb-wave sensors. The advantageous properties of this material include high acoustic velocity, high chemical, mechanical and thermal stability, and the potential to integrate with a wide range of GaN-based devices such as high electron mobility transistor (HEMT) circuits, light emitting diodes (LED) and other photonic devices. We successfully developed GaN based Lamb-wave mass-sensors in small size (membrane size of $\sim 1\text{mm} \times 1\text{mm}$). The sensors showed good signal strength and mass sensitivity, comparable to other mass-sensors using conventional materials. This novel approach not only allows robust low-cost sensors to be fabricated, but also enables future integration with generic GaN-based devices on the same chip (i.e. lab-on-a-chip). [C225]

"Complete electromagnetic simulation of HEMT switch circuit"

Electromagnetic (EM) only HEMT model was been proposed in [1]. In this paper, complete EM simulation has been performed on entire switch circuit. The dependences of switch performances on distributed and coupling effects can be quantitatively explained, and the prediction accuracy can be remarkably improved. Further, the EM simulation has been applied to an assembled switch with bond wires. Since a closed loop is formed by bond wires and the shunt HEMT at off switch arm, isolation is degraded when loop currents is induced by the coupling among bond wires. It has been noticed that there are two kinds of couplings, and the loop currents induced by these two couplings are in the opposite phase. The isolation degradation can be reduced or eliminated by current cancellation when the bond wire configuration is properly designed. [C226]

"Novel designs for high-efficiency millimeter-wave zero-bias detectors"

Novel designs for high-efficiency millimeter wave zero-bias detectors are presented. As the renowned backward diodes are extensively exploited in the utilization of zero bias detectors due to its preferable conduction for small reverse biases, the single-handed diode detectors reveal its inherent capabilities by the semiconductor processes which the detectors are made from. The selected process chiefly dominates the detectors' performances before take any circuit design techniques. Here we present novel designs that employ Schottky diodes in conjunction with field effect transistors (FETs) throughout zero bias condition in $0.15\mu\text{m}$ GaAs pseudomorphic HEMT (pHEMT) process. Through computational estimations, the novel designs show remarkable results of that the proposed designs surpass the conventional Schottky diode only structures in rectified current levels by four orders, and the isolation of RF-DC also be improved at millimeter wave frequencies. [C227]

"Distortion reduction of a GaN HEMT Doherty power amplifier with a series connected load"

Doherty introduced two types of concepts for high-efficiency linear amplifiers in 1936. One has a shunt connected load and the other has a series connected load. We fabricated a 1.9 GHz GaN HEMT Doherty power amplifier with a series connected load using baluns. The amplifier realized high power efficiency with a wide dynamic range in comparison with a conventional push-pull amplifier. In this paper, we propose distortion reduction method for the amplifier and achieved reduction of the third-order intermodulation distortion (IMD3) more than 15 dB at the output power from 5 to 20 dBm. The amplifier realized power-added efficiency (PAE) of 31 % at the output power of 24 dBm at 10 dB input backoff from the saturated output power of 31 dBm with PAE of 58 %. [C228]

"Experimental investigation on wideband intermodulation distortion compensation characteristics of 3.5-GHz band 140-W class feed-forward power amplifier employing GaN HEMTs"

This paper presents an experimental investigation on the wideband intermodulation distortion compensation characteristics of a 3.5-GHz feed-forward power amplifier for mobile base stations. The fabricated 3.5-GHz band 140-W class feed-forward power amplifier employing gallium nitride high electron mobility transistors (GaN HEMTs) achieves the intermodulation distortion compensation bandwidth of 160 MHz at the output power of 12.5 W and the adjacent channel leakage power ratio of -45 dBc using a long term evolution test signal with the bandwidth of 5 MHz. The results confirm that the feed-forward power amplifier with GaN HEMTs is a worthwhile linearizer because it offers wideband intermodulation distortion compensation performance to 3.5-GHz band mobile base stations. [C229]

"A Dual-gate subharmonic injection-locked oscillator using 0.5 μ m GaAs pHEMT technology"

A dual-gate subharmonic injection-locked oscillator (SILO) designed for Q-band millimeter-wave applications has been implemented in 0.5 μ m GaAs pHEMT process. Based on the dual-gate circuit topology, a wide-bandwidth and high-frequency negative resistance can be easily obtained for determining the free-running oscillation frequency by a proper resonator. The free-running frequency is designed around 49 GHz. The power consumption is 75 mW from a 5 V supply. The measured frequency tuning range is from 48.7 GHz to 49.7 GHz with 8 dBm output power. By injecting a 2nd-order subharmonic signal into the oscillator without any frequency tuning, the maximum locking range can reach to be 2.8 GHz. The measured output phase noise under locking status is close to -121 dBc/Hz at 1-MHz offset frequency. [C230]

"Design and development of an S-band Low Noise Amplifier"

This paper describes the design and development of a single stage Low Noise Amplifier (LNA) working at 3 GHz frequency. The single stage amplifier is designed by using commercially available p-HEMT, Filtronic (RFMD) FPD6836P70. The LNA makes use of plated through holes (PTH) to obtain good high frequency grounding of the transistor. The prototype LNA is tested at room temperature, and the measured Noise Figure (NF) and Gain is obtained as 1.03 dB and 16.3 dB respectively. The realized amplifier with distributed matching networks is found to perform reasonably well in the tests of gain, return loss and noise figure measurements in the desired frequency band. The practical results are also found to closely match with the simulated results. We present a description of the LNA design, results obtained from the measurements, and their comparison with simulated results. [C231]

"Degradation of sub-micron gate AlGaIn/GaN HEMTs due to reverse gate bias"

GaN High Electron mobility transistors (HEMTs) were electrically step-stressed under high reverse gate bias conditions. Once a threshold voltage is reached, gate current increases about two orders of magnitude. Though critical voltage was determined to be linear with increasing gate length, electrical simulations show that the maximum electric field was similar at the critical voltage (~ 2 MV.cm⁻¹). Electroluminescence and photoluminescence performed on the degraded samples exhibited a decrease in intensity along the periphery of the gate. Transmission electron microscopy shows a thin native oxide layer present under that gate before stressing, and the first stages of gate metal reacting with the underlying AlGaIn after stressing. [C232]

"Progress on distributed resistance model for pHEMT"

With increasing scale and complexity in pHEMT circuit and dimension shrinking in unit pHEMT devices, distributed effects are becoming more crucial than ever. During design of amplifiers, precise prediction of the resistances of a device is vital to simulation result due to the direct impact on impedance. This work reports a set of experiments utilizing different testing structures to reveal how a pHEMT device's layout affects its gate-to-source/drain resistances due to distribution of resistance along electrodes and the consequent current crowding. As an example, a distributed resistance model of source-side gate bar is quantitatively analyzed. It is shown that the prediction of the model coincides with the measurement data obtained from a variety of testing devices with

different numbers of gate fingers. [C233]

"2.4 GHz medium power amplifier for wireless LAN applications using GaAs PHEMT"

A 2.4GHz medium power amplifier (MPA) using 0.15 μ m GaAs PHEMT technology for wireless local area network (LAN) applications is demonstrated. At 3.0 V of drain voltage (VDS), a fabricated MPA exhibits the output power at 1dB gain compression (P1dB) of 15.20 dBm, power-added efficiency (PAE) of 12.70% and gain of 9.70 dB, respectively. The maximum current, I_{max} of this amplifier is 84.40mA and the power consumption for the device is 253.20mW. [C234]

"3-stage 15 GHz p-HEMT power amplifier design for MMIC applications"

This paper present the design of 3-stage 15 GHz power amplifier (PA) using 0.15 μ m GaAs p-HEMT technology. At operating frequency of 15 GHz (Ku-band), each single PA stage was designed for optimum power and efficiency of the transistor, with 50 Ω input and output impedance matching. In this design, the active devices were selected from the depletion p-HEMT type with voltage supply of 4.5 V and DC bias of -0.2 V. The PA delivers maximum linear output power of 22.29 dBm while achieving maximum power-added-efficiency (PAE) of 31.21 %. The PA has an input and output return loss at 29.80 dB and 31.05 dB respectively. Having a current consumption of 155 mA, this PA achieves a small signal gain of 32.50 dB. The proposed PA is designed within a die size of about 3.0 Ч 1.0 mm² on GaAs substrate. [C235]

"Minimization of baseband electrical memory effects in GaN HEMTs using active IF load-pull"

This paper presents a rigorous way to quantify the role played by higher baseband impedances in determining baseband electrical memory effects observed in power transistors under two-carrier excitation. These effects typically appear not only as asymmetrical distortion terms in the frequency domain, but also more reliably as a recognizable hysteresis or looping in the dynamic transfer characteristics extracted from measured input voltage and output current envelopes of a power device. Investigations have been carried out using a commercially available 10W GaN HEMT device characterised at 2GHz within a high-power modulated waveform measurement system. Active IF loadpull has been employed to present specific baseband impedance environments, allowing the sensitivity of IMD symmetry to baseband impedance variations to be investigated. [C236]

"Analysis and implementation of inverse class-F power amplifier for 3.5GHz transmitters"

In this paper, a theoretical analysis of inverse class-F power amplifier is carried out based on maximally flat drain current and voltage waveforms with the third-harmonic current and second-harmonic voltage peaking. The transistor is modeled as a switch in analysis, in which including non-zero switch-on resistance in parallel with an output capacitance. Therefore, the equations of drain efficiency and output power are derived. An inverse class-F power amplifier for 3.5GHz transmitter application based on CGH40010 GaN HEMT is designed and measured in this paper. Experimental results show that over 70% maximum drain efficiency and around 40dBm output power can be achieved. And a good broadband performance of the fabricated amplifier is also presented. [C237]

"Analysis of dispersion in intermodulation distortion in GaN HEMT devices"

The considerable variation in intermodulation across wide bandwidths due to trapping and self-heating mechanisms are considered here as a dispersion of linearity that is bias dependent. This is of interest to designers because the dispersion gives intermodulation a strong dependence on center and spacing of test frequencies, which requires an interpretation of intermodulation measurements and specifications across the whole signal bandwidth. Detailed intermodulation distortion and pulse measurements were performed for this study. New self-heating and trapping models are used to characterize intermodulation distortion and pulse measurements. [C238]

"A high efficiency VHF GaN HEMT class E power amplifier for public and homeland security applications"

Power efficiency is a very important specification of power amplifiers for mobile and wireless communication systems. High power efficiency leads to long lasting connection time for mobile, nomadic and wireless devices using battery energy. Especially for public and homeland security applications, long connection time of wireless communication devices is desirable for emergency situations. This paper proposes a high efficiency class E power amplifier with a Gallium Nitride High Electron Mobility Transistor (GaN HEMT) as a power device. A parallel load circuit is used in this class E power amplifier which operates in the frequency range of 140-170 MHz. Furthermore, load-pull technique was applied during the design process to determine the optimal load impedance for the maximum Power-Added Efficiency. Simulation and measurement results of the fabricated

class E power amplifier are provided with a peak Power-Added Efficiency (PAE) of 72.5% and power gain of 16.4 dB at 33.9 dBm output power. [C239]

"Implementation of new SP6T switch achieving high quality and small size at same time"

SP6T switch achieving low loss, high isolation and small size at same time was developed. For the excellent RF performance, optimization of p-HEMT unit cell which improves the trade-off between On/Off states, and employment of optimal additional passive components was introduced. To achieve high isolation, specially, capacitors of large size was used in switch, size increase by these components was considered by common voltage control and back via process leading increase of size efficiency. The entire layout was designed as suitable structure for miniaturization and high integration in RF front-end. Chip size was below 1 mm², and stable performance was confirmed in covering frequency. [C240]

"DC and RF performance of AlN/GaN MOS-HEMTs"

This paper reports the DC and RF characteristics of AlN/GaN MOS-HEMTs passivated with thin Al₂O₃ formed by thermal oxidation of evaporated aluminium. Device fabrication involved wet etching of evaporated Al from the ohmic contact regions prior to metal deposition. This approach yielded an average contact resistance of 0.76 Ω mm extracted from transmission line method (TLM) characterisation. Fabricated two-finger AlN/GaN MOS-HEMTs with 0.2 μ m gate length and 100 μ m gate width showed good gate control of drain currents up to a gate bias of 3 V and achieved a maximum drain current, I_{DSmax} of 1460 mA/mm. The peak extrinsic transconductance, G_{max} , of the device was 303 mS/mm at $V_{DS} = 4$ V. Current-gain cut-off frequency, f_T , and maximum oscillation frequency, f_{MAX} , of 80 GHz and 65 GHz, respectively, were extracted from S-parameter measurements. For longer gate length, $L_G = 0.5$ μ m, f_T and f_{MAX} were 40 GHz and 55 GHz, respectively. These results demonstrate the potential of AlN/GaN MOS-HEMTs for high power and high frequency applications.

[C241]

"A 5.9 GHz-8.5 GHz 20 Watts GaN HEMT"

A 20 Watts GaN high electron mobility transistor (HEMT) has been developed for C-band radio applications. The device consists of a single die of 0.35 μ m-gate GaN HEMT of 12 mm gate periphery together with input and output 2-stage impedance transformers into a conventional package. The developed GaN HEMT provides 20 watts output power and 40 % power added efficiency over 5.9 GHz to 8.5 GHz with small signal gain of 13.5 dB.

[C242]

"Internally-matched GaN HEMT high efficiency power amplifier for Space Solar Power Stations"

In this paper, an internally-matched GaN HEMT high efficiency amplifier for Space Solar Power Stations/System (SSPS) is presented. The internal matching circuit was designed so that 2nd and 3rd harmonics are tuned to obtain maximum power added efficiency (PAE). PAE of 70% was successfully obtained with 7W output power at 5.8GHz. All matching circuit is in a hermetically sealed package and no external matching component is necessary. It will enable to shrink volume and mass of modules loaded onto SSPS satellites. [C243]

"Development of 150W S-band GaN solid state power amplifier for satellite use"

150W S-band gallium nitride solid state power amplifier (GaN SSPA) has been developed for satellite use. GaN devices have been already used for various fields in lower frequency bands (L-band and S-band) such as ground station amplifier and radar system. For space application, there is great interest in realizing high power solid state power amplifier using GaN devices to achieve higher output power compare with current GaAs devices. Also there is very much interest for the performance comparison between GaN SSPA and traveling wave tube amplifiers (TWTAs). Development result shows that, with an electrical power conditioner (EPC), the GaN SSPA achieves output power of 148.6W with power added efficiency (PAE) of 53.8% which are almost equivalent to TWTAs. Moreover, footprint and mass of this SSPA are much less than those of a TWTAs. Also we confirmed through qualification testing that the GaN SSPA meets the environment requirements for satellite use.

[C244]

"An X-band 50% bandwidth high-power GaN HEMT T/R switch"

An X-band high-power T/R switch utilizing GaN HEMT has been developed. The switching circuit employed an asymmetric series-shunt/shunt configuration with bandwidth extension circuits. By using the circuit topology, the switch circuit can achieve high-power and low-loss performance at Tx-mode and low insertion loss at Rx-mode in broad bandwidth. To verify this methodology, we have fabricated a GaN HEMT switch, and the circuit has achieved the power handling capability of 20W and the insertion loss of 1.2dB at Tx-mode, 1.8dB at Rx-mode in

7-12GHz range. [C245]

"Cost effective, high performance GaN technology"

Gallium Nitride HEMT transistors are the future solid state technology that is presently advancing the performance of state-of-the-art RF power amplifiers from HF frequencies through low mmW applications. Further developments in the basic HEMT material structure, including the choice of substrate, will continue to push the RF performance, output power, frequency response, and bandwidth; availability; and affordability in the microwave marketplace for this newest semiconductor. [C246]

"Class-E Doherty power amplifier based on harmonic tuning"

This letter reports a high-efficiency gallium nitride (GaN) high-electron mobility transistor (HEMT) Doherty power amplifier (DPA) based on the Class-E topology for 3GPP-FDD applications. The harmonic controlling network (HCN) applied in the proposed DPA provides the impedance transformation for the harmonic components so that it achieves significant harmonic suppression. For the proposed DPA, the power added efficiency (PAE) is 62.1% at 37.03 dBm, 5-dB backoff power from saturation output power. For a 1-carrier 3 GPP-FDD signal, the adjacent channel leakage ratio (ACLR) and error vector magnitude (EVM) are achieved 32.16 dB and 6.59%, respectively, at 37.03 dBm. The results prove that the proposed DPA can deliver high efficiency with proper linearity for 3 GPP applications. [C247]

"GaN-AlGaIn high electron mobility transistors for multiple biomolecule detection such as photosystem I and human MIG"

This paper demonstrates a novel way of using a single type of high electron mobility transistor (HEMT) device for detecting two kinds of biomolecules (Photosystem I and recombinant human monokine induced by interferon gamma, MIG). MIG was successfully detected in 150 mM concentration of phosphate buffer solution (PBS). Floating gate configuration used for biomolecule detection eliminates the need of external gate voltage and represents purely the effect of biomolecules immobilization and binding events on the gate surface. [C248]

"Modeling of AlGaIn/GaN HEMT based stress sensors"

GaN based devices show great potential for high power, high frequency and extreme-environment applications. Due to spontaneous and piezoelectric polarization properties, these devices are also suitable for pressure monitoring or detection of biomolecules causing surface stress. Therefore, GaN based monolithic sensor system can be applied for the detection of biomolecules or pressure imaging for biomedical applications, sensor data processing and transmission of the sensor data even in extreme environmental conditions. This paper investigates the analytical performance of GaN high electron mobility transistor (HEMT) device for the induced strain due to external pressure and surface stress. Analytical expressions for the conductance-stress behavior of the sensor have been developed. The change in two-dimensional electron gas density at the heterointerface of AlGaIn/GaN layers resulting from the change in polarizations causes change in the output current of the device. The effects of both the tensile and the compressive strains due to the external force have been studied. This model can be effectively applied to the measurement of target force and to the detection of polar or nonpolar biomolecules. [C249]

"Ultra-high sensitivity gas sensors based on GaN HEMT structures"

This paper presents simulation of GaN high electron mobility transistor (HEMT) based device structures for the detection of toxic and hazardous gases like carbon monoxide (CO) and hydrogen (H₂), respectively. AlGaIn/GaN heterostructures show large potential as sensors due to the presence of 2-dimensional electron gas (2-DEG) at the heterointerface. Due to widebandgap material properties, GaN based devices are highly suitable for extreme-environment applications. The sensors are proposed selective towards specific targets by the two different gate structures. The simulated AlGaIn/GaN based HEMT with Pt/AlGaIn Schottky gate structure can detect hydrogen gas with the concentrations as low as ppb level and with the linear output variations from ~ ppb to 100 ppm level. A new gate structure based on nanocrystalline stannic oxide (α -SnO₂) layer for the selective and sensitive detection of CO gas is proposed. We report that the AlGaIn/GaN HEMT structure with Pt/ α -SnO₂/AlGaIn Metal-Oxide-Semiconductor (MOS) gate can be used to detect sub-ppm level of CO with the linear response upto 500 ppm. [C250]

"Characterization of liquid-phase sensor utilizing GaN-based two-terminal device"

In this paper, the sensitivity of GaN surfaces in aqueous solutions and polar liquids has been investigated. For this purpose, two terminal devices fabricated on bulk Si doped-GaN structures and undoped-AlGaIn/GaN

heterostructures with unpassivated open area are used to measure the responses to the changes of the H⁺ concentration in aqueous solutions and the dipole moment in polar liquids. Two material structures are used in this study. They are Si-doped GaN bulk structures and undoped AlGaN/GaN HEMT. The same structures, conditions and fabrication processes have been applied for both material samples. The fabricated devices are shown. The mesa channel is patterned using photolithography and reactive ion etching where SiO₂ layer is applied as a mask. [C251]

"Logic performance of 40 nm InAs/In_xGa_{1-x}As composite channel HEMTs"

Current Si-CMOS technology has come to a limit that novel semiconductors as alternative channel materials (Ge, InSb, In_xGa_{1-x}As) are urgently needed for high-speed and low-power logic devices for post CMOS era. Recent research shows III-V heterostructure field-effect transistors demonstrate aggressive merits due to its high electron mobility and rather mature process technology. The outstanding low field electron transport characteristics of III-V materials make ultrahigh-speed switching at very low supply voltage possible. Here, we present the latest advancement of 40 nm InAs/In_xGa_{1-x}As composite channel High Electron Mobility Transistor (HEMT) devices that have achieved excellent digital logic characteristics at very low power level. [C252]

"SiO₂/Si₃N₄ bilayer sloped etching for 20nm InAlAs/InGaAs metamorphic HEMTs"

We developed a 20 nm gate process using SiO₂/Si₃N₄ bilayer sloped etching. Selective and sloped etching of bilayer makes this technology realizable. A HEMT with this technology has merits of fine length definition beyond the limit of electron beam (E-beam) lithography system. Using this technology, we experimentally demonstrated that a 20 nm gate length from initial 50 nm line pattern. The fabricated InAlAs/InGaAs metamorphic HEMTs (MHEMTs) with 20 nm T-gate pattern have high DC and RF performance characteristics, a transconductance of 1.67 S/mm, a cutoff frequency f_t of 460 GHz. [C253]

"Reduction of negative differential conductivity effect of AlGaN/GaN HEMTs using gate scaling"

Gate characteristic is one of the most important parts for the HEMTs. In this paper the DC and RF performance improvement using gate length scaling has been presented. The results show that reduction of the gate length from 1 μ m to 0.15 μ m, the current gain cutoff frequency increases from 12 GHz to 56 GHz and power gain cutoff frequency increases from 20.5 GHz to 63 GHz respectively. In this paper we report the first ever simulation based device structure design for reduction of Negative Differential Conductivity (NDC) effect in AlGaN/GaN HEMTs by gate length scaling. [C254]

"Embedded HEMT/metamaterial composite devices for active terahertz modulation"

The first gallium arsenide (GaAs) High Electron Mobility Transistor (HEMT) based metamaterial is demonstrated and used to modulate an electromagnetic signal of 0.55 THz at speeds up to 10MHz. The devices are constructed using a commercial GaAs technology primarily used for mobile phone technology. The metamaterial was constructed using a classical Double Electric Split Ring Resonator (DESRR) using a gold metal layer available in the technology. The Scanning Electron Microscope (SEM) photograph shows one element of the array. The HEMT was placed underneath the split gap with the drain and source connected to the split gap of the resonator. This allows to change the property of the metamaterial by applying gate bias voltage to the HEMT switch. [C255]

"Effects of cap layer on 2DEGs in InN-based heterostructures"

This paper describes the effects of cap layer on sheet carrier concentration and mobility of two dimensional electron gases (2DEGs) in InN-based InN/InGa(Al)N/InN heterostructures. Addition of a InN cap layer in InGa(Al)N/InN heterostructure leads to a very interesting dependence of 2DEGs. The sheet carrier concentration decreases and mobility increases with increase of the InN cap layer thickness. The calculated values of sheet carrier concentration are found to be decreased from 6×10^{13} to $1.2 \times 10^{13} \text{ cm}^{-2}$ with increase of the cap layer thickness from 1 to 60 nm for a 10 nm barrier. The 2DEGs mobilities are found to be around 3.3×10^3 , 3.5×10^3 , and $4.8 \times 10^4 \text{ cm}^2 \text{ V}^{-1} \text{ s}^{-1}$, respectively, without, with 10 nm and 100 nm cap layer. The cap layer also enhances the peak drift velocity. The above calculated results indicate that addition of cap layer is very promising for the fabrication of high performance HEMTs. [C256]

"A de-embedding procedure oriented to the determination of FET intrinsic I-V characteristics from high-frequency large-signal measurements"

In this work a de-embedding technique oriented to the determination of FET I-V dynamic characteristics is reported. It exploits high-frequency large-signal measurements and a model based description of the reactive

nonlinearities. The proposed technique allows one to gather information about the intrinsic I-V dynamics, including traps related dispersion and thermal phenomena, directly from high-frequency large-signal measurements. Moreover, the actual waveforms exciting the FET active area can be monitored and, for instance, related to the boundaries imposed by reliability issues under dynamic operation. In order to validate the proposed approach, experiments carried out on a gallium nitride HEMT are reported. [C257]

"Development of high-k dielectric for antimonides and a sub 350°C III-V pMOSFET outperforming Germanium"

InGa_{1-x}Sb channel materials have the highest hole and electron mobility among all III-V semiconductors, high conduction and valence band offsets (CBO/VBO) with lattice matched AlIn_{1-x}Sb for heterostructure MOSFET design and allow low thermal budget MOSFET fabrication (Figure 1). While buried channel HEMT-like devices with excellent electron and hole transport have been demonstrated, realization of an Sb-channel MOSFET has remained elusive due to the highly reactive nature of the Sb-surface (Figure 2). In this paper we overcome these challenges (Figure 1) and fabricate an InGa_{1-x}Sb pMOSFET with high hole mobility (μ_b): a bottleneck for III-V complimentary logic. Synchrotron Radiation Photoemission Spectroscopy (SRPES) is used to aid the development of ALD Al₂O₃ on GaSb with a mid bandgap Dit of $3 \times 10^{11}/\text{cm}^2\text{V}^{-1}$. A p+/n diode with ideality factor of 1.4 and $\text{ION}/\text{IOFF} > 5 \times 10^4$ is developed. pMOSFETs with various channel configurations to optimize the hole transport are fabricated using a sub 350°C gate-first process. Surface (buried) channel pMOSFETs with peak μ_{hof} 620 (910) cm^2/Vs and having more than 50 (100) % higher mobility than Germanium over the entire sheet charge (N_s) range are demonstrated and analyzed. [C258]

"220GHz fT and 400GHz fmax in 40-nm GaN DH-HEMTs with re-grown ohmic"

We report record RF performance in 40nm-gate GaN-HEMT technology. Through vertical scaling in an AlN/GaN/AlGaIn double heterojunction (DH) HEMT structure and reduction of access resistance using MBE re-growth of n+-GaN ohmic contacts, fully-passivated 40-nm devices exhibited excellent DC characteristics, such as an R_{on} of $0.81 \Omega \cdot \text{mm}$, an I_{dmax} of 1.61 A/mm , a BV_{off} of 42V, and a peak extrinsic g_{m} of 723 mS/mm , resulting in a peak f_T of 220GHz and a peak f_{max} of 400GHz. The measured f_T and f_{max} are the highest ever reported in a GaN-HEMT technology. Small signal model and delay time analysis showed that the parasitic charging time was only 10% of total delay time and the gate transit time scaled with the gate length (L_g) down to 40nm, demonstrating high scalability of the new technology. [C259]

"Reliability of enhancement-mode AlGaIn/GaN HEMTs under ON-state gate overdrive"

The ON-state reliability of enhancement-mode AlGaIn/GaN HEMTs fabricated by fluorine plasma implantation technology under gate overdrive is reported. A critical gate forward voltage (V_{GC}) is observed, beyond which the turn-on voltage of the 2DEG channel exhibits a negative shift. This phenomenon is proposed to be caused by the impact ionization of the F ions in the barrier layer by hot electron injection. The proposed physical model is further validated by the temperature-dependent characterization of V_{GC} that shows an eventual stabilization at higher temperatures ($> 125^\circ\text{C}$), owing to the efficient removal of hot electrons by phonon scattering. The determination of V_{GC} provides valuable guideline for the design of gate drive circuits of GaN power circuits. [C260]

"Advanced gate technologies for state-of-the-art fT in AlGaIn/GaN HEMTs"

In this paper, the lower-than-expected frequency performance observed in many AlGaIn/GaN high electron mobility transistors (HEMTs) has been attributed to a significant drop of the intrinsic small-signal transconductance (g_m) with respect to the intrinsic DC g_m . To reduce this g_m -collapse and improve high frequency performance, we have developed a new technology based on a combination of vertical gate-recess, oxygen plasma treatment, and lateral gate-etch which has allowed us to fabricate AlGaIn/GaN HEMTs with a record current-gain cutoff frequency (f_T) of 225 GHz for a gate length (L_g) of 55 nm, and 162 GHz for an L_g of 110 nm. [C261]

"60 nm self-aligned-gate InGaAs HEMTs with record high-frequency characteristics"

We have developed a new self-aligned gate technology for InGaAs High Electron Mobility Transistors with non-alloyed Mo-based ohmic contacts and a very low parasitic capacitance gate design. The new process delivers a contact resistance of $7 \text{ Ohm} \cdot \mu\text{m}$ and a source resistance of $147 \text{ Ohm} \cdot \mu\text{m}$. The non-alloyed Mo-based ohmic contacts show excellent thermal stability up to 600°C . Using this technology, we have demonstrated a 60 nm gate length self-aligned InGaAs HEMT with $g_m = 2.1 \text{ mS}/\mu\text{m}$ at $V_{\text{DS}} = 0.5 \text{ V}$, and $f_T = 580 \text{ GHz}$ and $f_{\text{max}} = 675 \text{ GHz}$ at $V_{\text{DS}} = 0.6 \text{ V}$. These are all record or near record values for this gate length. [C262]

"High-performance monolithically-integrated E/D mode InAlN/AlN/GaN HEMTs for mixed-signal applications"

Monolithically-integrated E- and D-mode InAlN/AlN/GaN HEMTs for mixed-signal applications have been demonstrated. For devices with gate lengths of 144 nm, peak transconductances of 0.92 S/mm and 0.84 S/mm have been obtained for E- and D-mode devices, respectively, while maximum drain currents of 1.84 A/mm and 1.9 A/mm have been measured for E- and D-mode devices. RF performance is also well-matched, with E-mode devices exhibiting f_t 's of 94 GHz and f_{max} 's of 176 GHz, while D-mode devices had f_t 's of 94 GHz and f_{max} 's of 174 GHz. Ring oscillators have been fabricated to demonstrate the technology. [C263]

"Diamond-like carbon (DLC) liner with highly compressive stress formed on AlGaIn/GaN MOS-HEMTs with in situ silane surface passivation for performance enhancement"

In this work, a highly compressive DLC liner (~ 6 GPa) was applied on AlGaIn/GaN MOS-HEMTs for the first time. The compressive stress induced by DLC liner effectively reduces the tensile stress in the AlGaIn layer, thus reducing the 2-DEG density. Devices with DLC show 22 % and 19% increase in drive current and peak transconductance, respectively, at $V_G = 2$ V and $V_D = 10$ V. Threshold voltage reduction of ~ 1 V was also observed for devices with DLC liner, as compared to ones without DLC liner. Devices in this work were also integrated with in situ silane (SiH_4) passivation technology. [C264]

"A surface-potential based model for GaN HEMTs in RF power amplifier applications"

We present the first surface-potential based compact model for RF GaN HEMTs and benchmark our work against both numerical simulations and device measurements. It is expected that such an approach will be superior to other modeling techniques in terms of scalability and model performance for applications where accurate distortion modeling is of paramount importance. [C265]

"AlGaIn/GaN transistors for power electronics"

The focus of GaN based devices has expanded beyond LEDs and lasers to the large market of power electronics where the materials properties of high electron mobility, high breakdown field and good thermal conductivity make it attractive in ultra-high efficiency applications ranging from power supplies, PV inverters to motor drives. [C266]

"A comprehensive reliability investigation of the voltage-, temperature- and device geometry-dependence of the gate degradation on state-of-the-art GaN-on-Si HEMTs"

In this work, the gate degradation of GaN-based HEMTs is analyzed. We find that the gate degradation does not occur only beyond a critical voltage, but it has a strong voltage accelerated kinetics and a weak temperature dependence. By means of a statistical study we show that the time-to-failure can be fitted best with a Weibull distribution. By using the distribution parameters and a power law model it is possible to perform lifetime extrapolation based on the gate degradation at a defined failure level and temperature for the first time. From this elaboration, the lifetime of a given device geometry can also be extracted. Eventually, the strong bias dependence of the gate degradation reported here implies that this phenomenon should be assessed by means of a voltage-based accelerated investigation as described in this work. [C267]

"Spatially-discriminating trap characterization methods for HEMTs and their application to RF-stressed AlGaIn/GaN HEMTs"

New constant drain-current deep level optical/transient spectroscopy (CID-DLTS/DLOS) methods to quantify trap energies and concentrations in AlGaIn/GaN high electron mobility transistors (HEMTs) are described. These methods are applied to RF stressed HEMTs to characterize the impact of stressing on traps and identified a significant increase in virtual gate related levels. [C268]

"Power detectors and envelope detectors in mHEMT MMIC-technology for millimeterwave applications"

Two types of microwave and millimeterwave power detectors realized in a commercial mHEMT MMIC-process is presented for the first time. The detectors are based on either a gate Schottky diode or active mHEMT. Possible application are microwave/millimeterwave power detectors, and multi Gb/s high speed demodulators for OOK, BPSK, QPSK etc. [C269]

"Development of a neural approach for bias-dependent scalable small-signal equivalent circuit modeling of GaAs HEMTs"

This paper presents an approach for small-signal modeling of microwave FETs. The model is based on an equivalent circuit whose elements are extracted by an analytical approach. In order to make model bias-dependent and scalable, artificial neural networks are exploited for modeling of the dependence of the equivalent circuit elements on the bias voltages and the transistor gate width. The proposed approach is exemplified on modeling of three scaled on-wafer GaAs HEMT devices. [C270]

"Dependence of FET/HEMT reliability on substrate thickness and gate length"

The transistor substrate has a significant role on RF losses, device heating, and reliability. The substrate thickness, and the gate length, among other parameters, have direct implications on the transistor lifetime. This paper presents an analytical expression relating the reliability to gate length and to substrate thickness for a field effect transistor (FET), or a high electron mobility transistor (HEMT), based on thermal considerations. Experimental observations support the model's predicted results. The derived methodology and analytical expressions are useful for device/MMIC designers to assess the device/circuit reliability performance. [C271]

"Current density dependence of minimum noise figure for gallium nitride HEMTs"

This paper discusses recent work in noise characterization of gallium nitride high electron mobility transistors (HEMTs). The excellent noise performance of gallium nitride-based HEMTs has been discussed previously in the scientific literature. In this paper, we discuss observations that show that the best minimum noise figure is found at a constant current density, regardless of the physical dimensions of the transistor. These results resemble a previous report using CMOS processes, which found that a specific current density leads to minimum noise figure, regardless of fabrication process and gate length. We have found that the best minimum noise figure is found at a constant current density of 0.3 mA/ μm , regardless of transistor size. [C272]

"Improved measurement-based extraction algorithm of a comprehensive extrinsic element network for large-size GaN HEMTs"

This paper presents an algorithm for extrinsic element extraction of GaN-HEMTs with physically meaningful parameters calculated from S-parameters measurements at pinch-off. An improved algorithm to extract a 12-element parasitic network is presented, which allows proper modelling of the complex parasitic effects present in devices with large gate periphery. The extraction algorithm is found on a novel way to scan of the best extrinsic capacitance distribution, clear insight of the new supporting considerations of this scan is presented, as well as their derivation and physical interpretation. Results of the algorithm application with measured data of a 3.2-mm gate-periphery GaN HEMT successfully confirm its consistency. [C273]

"Low noise, low power dissipation mHEMT-based amplifiers for phased array application"

In this paper, we present two mHEMT-based low noise, low power dissipation amplifiers (LNAs) for X-band phased array applications. These LNAs provide ultra low noise figures while yielding over 20 dB of gain and dissipating less than 50 mW of DC power. The designs include both a standard, single ended topology as well as a balanced topology with novel current sharing that provides excellent return losses at the expense of only 0.3 dB of noise figure as compared to the single ended design. [C274]

"Terahertz detection by InGaAs HEMTs in quantizing magnetic fields: Relation between magnetoresistance and photovoltaic response"

THz detection by plasma wave mechanism in InGaAs HEMTs is studied in high/quantizing magnetic fields regime. The correlation between the photovoltaic response and magnetoresistance is revealed. It allows to explain the nature of strong oscillations observed in the transistor Terahertz photoresponse. [C275]

"Potentiality of commercial metamorphic HEMT at cryogenic temperature and low voltage operation"

We present in this paper, a study of Dc, RF and Noise characteristics of an industrial metamorphic HEMT (High Electron Mobility Transistor) operating under low voltage at cryogenic temperature. The results at 300K are compared with the obtained results at cryogenic temperature. Temperature decrease makes device characteristics improve. This improvements allow to expect to develop a low power cryogenic electronic (LNA), featuring high frequency/noise performances below 100 mV DC biasing. [C276]

"Development of enhancement mode AlGaIn/GaN MOS-HEMTs using localized gate-foot oxidation"

A new method for realising enhancement mode AlGaIn/GaN devices using a localized gate-foot oxidation is described. Thermal oxidation of the AlGaIn barrier layer converts the top surface/part of this layer into aluminium and gallium oxides, which serve as a good gate dielectric and improve the gate leakage current by several orders of magnitude compared to a Schottky gate. The oxidation process leaves a thinner AlGaIn barrier which can result in normally off operation. Without special precaution, however, the oxidation of the AlGaIn barrier is not uniform from the top but occurs at higher rates at the defect/dislocation sites. This makes it impossible to control the barrier thickness and so rendering the barrier useless. To avoid the problem of non-uniform oxidation, a thin layer of Aluminum is first deposited on the barrier layer and oxidized to form Al₂O₃ on top. This additional oxide layer seems to ensure uniform oxidation of the AlGaIn barrier layer underneath on subsequent further oxidation. Preliminary results of the fabricated 2 μm × 100 μm AlGaIn/GaN MOS-HEMTs with a partially oxidized barrier layer showed a maximum drain current of more than 700 mA/mm at high gate bias of 5V with very less current compression. [C277]

"New process for low sheet and ohmic contact resistance of AlN/GaN MOS-HEMTs"

This paper reports a novel method for producing low ohmic contact resistance, RC, as well as low sheet resistance, Rsh, on AlN/GaN MOS-HEMT structures. The method relies on the protection of the very sensitive AlN epi-layer from exposure to liquid chemicals during processing using evaporated Al, which on thermal oxidation forms Al₂O₃. The Al₂O₃ acts as a surface passivant and as a gate dielectric for transistors that are then fabricated. In contrast to previous approaches, the ohmic contact regions are prepared for metal deposition only using wet etching with 16H₃PO₄:HNO₃:2H₂O aluminium etch solution and so no damage to the surface associated with dry etching techniques occurs. From the ohmic contact optimisations, low average values of RC and Rsh of ~0.49 Ω.mm and ~159 Ω/□, respectively, extracted from transmission line method (TLM) characterisation. Fabricated two-finger AlN/GaN MOS-HEMTs with 3 μm gate length and 100 μm gate width showed good gate control of drain currents up to a gate bias of 3 V and achieved a maximum drain current, IDSmax of ~1000 mA/mm. The peak extrinsic transconductance, Gmax, of the device is ~230 mS/mm at VDS = 4 V. Current gain cut-off frequency, fT and maximum oscillation frequency, fMAX were 2.8 and 7.9 GHz respectively. This approach provides a simple fabrication process for realising high performance AlN/GaN MOS-HEMT for high power and high frequency applications. [C278]

"Trapping related degradation effects in AlGaIn/GaN HEMT"

Reliability in GaN based devices still motivates numerous studies because the involved degradation mechanisms are different from that in III-V narrow bandgap devices. Direct investigations on high electron mobility transistors (HEMT) are performed with low frequency noise (LFN) measurements and pulsed electrical characterization. Undoped AlGaIn/GaN devices grown on silicon substrate are stressed at a junction temperature of 175°C. Gate-lag and drain-lag measurements method have been performed versus different quiescent bias points and under different pulse conditions. This method allows the discrimination of each lag phenomenon as well as the thermal contribution. Thus it is possible to track and model the trapping mechanisms versus bias conditions. This electrical modelling is completed with LFN measurements, which is largely used for reliability investigations. [C279]

"High-isolation low-loss SP7T pHEMT switch suitable for antenna switch modules"

In this paper the design, fabrication and measurement of a high performance SP7T GaAs pHEMT switch for cellular phone applications is discussed. The antenna switch design uses a state of the art E/D-mode pHEMT process with an Ron*Coeff Figure of Merit of 145 Ohm-fF. Excellent broadband insertion loss measurements across all cellular bands are less than 0.5dB, isolations are greater than 32dB while maintaining minimum harmonic distortion levels. Matching the switch to specific bands yielded insertion losses of 0.35dB at 0.915 GHz and 0.4dB at 1.95 GHz. [C280]

"High frequency performance of Tellurium σ-doped AlSb/InAs HEMTs at low power supply"

In this paper, we present a set of characteristics (DC, ft, fmax, extrinsic and intrinsic parameters) of a 120 nm gate length InAs/AlSb high electron mobility transistor (HEMT) with a doping plane of Tellurium (Te) operating at room temperature (RT) and low power conditions. A cut-off frequency ftequal to 103 GHz has been achieved at 100 mV through the reduction of gate-channel distance and the change of dopant type. It opens up the possibility to develop an ultra low power electronics, featuring excellent high frequency performances below 100 mV DC biasing. [C281]

"High power, fully integrated SMT amplifiers with +47dBm OIP3 at 15 GHz and 6W, 38% efficiency at 30GHz using low cost, high volume PHEMT"

The system power amplifier's linearity sets the maximum bit rate and the efficiency determines the maximum output power possible given a fixed heat dissipation or DC supply. This paper demonstrates that using a GaAs PHEMT 0.15 μ m gate process, industry leading performance can be attained. Shown is a 15GHz linear power amplifier capable of -52dBc IM3 at 21dBm output power (+47dBm OIP3). Also demonstrated is a 30GHz saturated power amplifier capable of making 38dBm (6W) output power at 38% peak power added efficiency. Both are fully matched to 50 Ω and have over 20dB of gain. Both are housed in a low cost laminate surface mount package. [C282]

"AlGaIn/GaN mixer MMICs, and RF front-end receivers for C-, Ku-, and Ka-band space applications"

AlGaIn/GaN HEMTs have been widely used in RF power circuits such as high power amplifiers. This is mainly due to the capability to handle large power. Besides this main advantage, this technology demonstrates good performances in terms of noise, linearity, and robustness. This paper presents the design, and measurement results of different mixers operating at C-, Ku-, and Ka-band. All designs make use of 0.25 μ m, and 0.15 μ m AlGaIn/GaN microstrip technology. The best measured conversion losses (CL) are 10dB, 9dB, and 11dB, and the 1dB compression points referred to the output (P1dBout) are measured at -1dBm, 1dBm, and -1dBm for the C-, Ku-, and Ka-frequency band respectively. Three breadboards of RF front-end receiver have been as well manufactured to evaluate the robustness of such technology. The measured conversion gain are +21dB, +20dB, and +14dB, and the P1dBout are 10dBm, 11dBm, and 3dBm for the C-, Ku-, Ka-band respectively. [C283]

"Temperature dependent degradation modes in AlGaIn/GaN HEMTs"

This work is a study of the degradation of AlGaIn/GaN HEMTs generated by different ageing tests. The methodology is based on cross-characterisation analyses. The life tests (HTO 175°C, HTO 250°C, HTO 275°C and HTO 320°C) have mainly caused a strong decrease of the drain current at the very beginning of the test, then its partial recovery and finally its collapse. No evident degradation of the Schottky contact is observed after stress at different temperatures. Moreover, pulsed I-V measurements show an important evolution of gate lag and drain lag rates after ageing. Low frequency drain current noise increases after the life test and the highest the life test temperature, the highest the noise level increase. [C284]

"A high efficiency and multi-band/multi-mode power amplifier using a distributed second harmonic termination"

This paper proposes a new broadband saturated power amplifier (SPA) with a distributed second harmonic termination supporting multi-band/multi-mode operation. The proposed network is composed of a fundamental matching circuit and multiple second harmonic termination circuits. Due to the multiple harmonic terminations, the proposed PA improves the frequency range where the PA can achieve a high efficiency. The proposed PA is fabricated using a 45 W Cree CGH40045 GaN HEMT. Drain efficiencies of greater than 60% (average 66%) are achieved between about 1.8 GHz and 2.3 GHz (500 MHz bandwidth). When driven with long term evolution (LTE) and two carrier wideband code division multiple access (WCDMA) signals at DCS1800, PCS1900, and WCDMA bands, the linearity specifications of the corresponding standards are satisfied using the digital predistortion linearization technique, and it attains an efficiency of greater than 30%. [C285]

"Improved microwave noise and linearity performance in GaN MISHEMTs on silicon with ALD Al₂O₃ as gate dielectric"

In this work, enhanced noise and linearity performance in 0.25 μ m gate-length AlGaIn/GaN metal-insulator-semiconductor high electron mobility transistors (MISHEMTs) on high-resistivity silicon substrate using atomic-layer-deposited (ALD) Al₂O₃ as gate dielectric is reported. High current gain cut-off frequency f_{Tabove} 40 GHz and low minimum noise figure NFmin of ~1.0 dB at 10 GHz were achieved. This noise performance is believed to be the best ever reported for GaN MISHEMT on Si at this gate-length. In addition, bias dependent DC, microwave and noise characteristics were measured on both the MISHEMT and convention HEMT with Schottky gate, and it was found that the microwave small signal and noise performance in MISHEMT have less dependence on the drain current as compared to the conventional HEMT. These results demonstrate that the ALD Al₂O₃/AlGaIn/GaN MISHEMT on high-resistivity silicon substrate is promising for high-linearity low-noise-amplifier (LNA) applications. [C286]

"Electrothermal and large-signal modeling of switchmode AlGaIn/GaN HEMTs"

We report in this paper on the improvement of the model presented in [1] for AlGaIn/GaN HEMT especially focused on switch applications. We developed a new method to measure accurately the ON resistance R_{on} versus the junction temperature, and will compare here our thermal model to the measurements realized in pulsed I(V) and in [S]-parameters. We also focused on the influence of drain and gate impedances and biases for large signal switch applications, and performed extensive measurements and simulations comparisons to demonstrate the good accuracy of the proposed electrothermal model. [C287]

"A non linear power HEMT model operating in multi-bias conditions"

This paper presents a non linear model of HEMT device which operate in multi-bias conditions, that is to say in class-AB, class-B, class-C, class-D and class-S. The model was derived from pulsed I(V), pulsed S parameters and large signals measurements. The aim is to provide to the designers a single model that can be used whatever the operating class, whatever the application referred. It should be underlined that this model is able to describe third quadrant phenomena (when driving the transistor in the negative drain voltage). The target was to make this model reliable when the transistor works in class-S operating conditions. For this purpose, the model was validated on different HEMT devices and for multi-bias conditions. [C288]

"Design of HEMT GaN power amplifiers with wideband control of 2nd harmonic impedances in S-Band"

This paper reports the design and measurement of a GaN power amplifier whose output loads are optimised at fundamental and 2ndharmonic over a wide bandwidth (20%) in S-Band to reach maximum power added efficiency (PAE). The design methodology is described in the paper. Two power amplifiers have been built. The first one is optimized at fundamental and 2ndharmonic while the other one is only optimised at fundamental. Comparisons of power measurement results demonstrate the interest of optimising load impedances at the 2ndharmonic over large bandwidths for GaN HEMTs. When loaded by the matching circuit optimised at the 2ndharmonic, the packaged GaN exhibits 23.4Watts (9.7W/mm) output power associated to 15.2dB power gain and 69% PAE at the low frequency of the bandwidth (f_{min}). The paper also proposes a new matching architecture at 2ndharmonic frequency. [C289]

"Hydrodynamic study of electronic, optical and thermal excitation of plasma waves in HEMTs"

By means of a numerical hydrodynamic model, we investigate the influence of collective plasma modes in a field-effect transistor channel under different excitation and biasing conditions. Firstly, we study the case of a device externally-excited by a harmonic optical beating or an electronic excitation and current-driven operation at the drain. The harmonic and continuous responses of the drain-source bias show sharp resonances related to the first odd plasma modes, whose frequencies and amplitudes can be modified by playing on the drain bias. Secondly, we calculate the spectral density of drain voltage fluctuations in the absence of external excitations by using the generalized impedance-field method. Also the noise spectrum exhibits peaks corresponding to the excitation by the background noise of odd plasma modes. [C290]

"Breakdown mechanism in AlGaIn/GaN HEMTs on Si substrate"

AlGaIn/GaN high electron mobility transistors (HEMTs) grown on Si substrates have attracted a great interest for power electronics applications. Despite the low cost of the Si substrate, the breakdown voltage (V_{bk}) of AlGaIn/GaN HEMTs grown on Si (less than 600 V for 2 μ m total nitride epilayer) is much lower than that grown on SiC (1.9 kV for 2 μ m total epi-layer). Although several approaches have been reported to improve V_{bk} , the breakdown mechanism in these transistors is still not well understood. This paper studies for the first time the breakdown mechanism in AlGaIn/GaN HEMTs on Si substrates. In addition, by transferring the AlGaIn/GaN HEMTs grown on Si to a glass wafer, we have achieved devices with V_{bkin} excess of 1.45 kV and specific on-resistance of 5.3 m Ω .cm². [C291]

"Preliminary reliability at 50 V of state-of-the-art RF power GaN-on-Si HEMTs"

In this paper, state-of-the-art 1 mm RF power GaN-on-Si HEMTs using thick in-situ grown SiN cap layer are presented. Output power density $POUT$ exceeding 10 W/mm is reproducibly achieved above 50 V drain voltage while still limited by thermal issues. In order to assess the device stability, the GaN-on-Si HEMTs have been tested at high channel temperature ($> 300^{\circ}\text{C}$) and under high electric field ($V_{DS} = 50$ V). The results demonstrate for the first time the possibility to combine extremely high RF output power density at $V_{DS} = 50$ V with high reliability using a cost-effective technology. [C292]

"Scalability study of In_{0.7} Ga_{0.3} As HEMTs for 22nm node and beyond logic applications"

Compound semiconductor high electron mobility transistors (HEMTs) have recently gained a lot of interest for future high-speed, low-power logic applications due to their high mobility and high effective carrier velocity. Conventional In_{0.7}Ga_{0.3}As HEMTs with 50 to 150nm gate-length (LG) have been experimentally demonstrated with excellent device performance. In this paper, (i) we use two-dimensional numerical drift-diffusion simulations [3] to model the conventional In_{0.7}Ga_{0.3}As HEMTs with different LG from 15 to 200nm and investigate its scalability for future logic applications, (ii) An accurate estimation of effective mobility (μ_{eff}) and effective carrier velocity (injection) is presented, highlighting the relevance of ballistic mobility in these short-channel HEMTs. (iii) Due to degradation in performance of the conventional scaled In_{0.7}Ga_{0.3}As HEMT at LG=15nm, three novel HEMT device architectures are studied and the design for the ultimate scaled transistor is proposed. [C293]

"Fermi level unpinning of GaSb(100) using Plasma Enhanced ALD Al₂O₃ dielectric"

This paper discusses arsenic-antimonide based MOS-HEMTs which have great potential to enable complementary logic operation at low supply voltage. The effects of various surface passivation approaches on the capacitance-voltage characteristics (C-V) and the surface chemistry of n-type and p-type GaSb(100) MOS capacitors made with ALD and Plasma Enhanced ALD (PEALD) Al₂O₃dielectrics studied in this paper. This paper also proposed for the first time unpinned Fermi level in GaSb MOS system with high- κ PEALD Al₂O₃dielectric using admittance spectroscopy and XPS analysis. [C294]

"Tellurium δ -doped 120nm AlSb/InAs HEMTs: towards sub-100mV electronics"

This paper discusses 120nm AlSb/InAs HEMTs operating at ultra low drain. HEMT is fabricated with ohmic contact evaporation and Schottky T-gates realization. A deep mesa isolation is used to remove completely the buffer leading to air-bridge gate. [C295]

"MOCVD grown normally-OFF type AlGaIn/GaN HEMTs on 4 inch Si using p-InGaIn cap layer with high breakdown"

We are reporting a p-InGaIn cap layered AlGaIn/GaN normally-OFF type HEMTs on silicon substrate with VGapplicable as high as +3.5V without gate leakage. Further we achieved a high breakdown for relatively a small gate-drain length (Lgd) of 3 μ m. Demonstrating a normally-OFF type AlGaIn/GaN HEMTs on low cost Si substrate, coupled with high breakdown is an important step forward to integrate enhancement and depletion mode devices on Si. [C296]

"Reduced self-heating in AlGaIn/GaN HEMTs using nanocrystalline diamond heat spreading films"

In this work, we present HEMTs with nanocrystalline diamond (NCD) heat spreading films, which offer a high thermal conductivity path only 50 nm away from the gate (κ_{NCD} of up to 1300 W/m-K). [C297]

"High performance E-mode InAlN/GaN HEMTs: Interface states from subthreshold slopes"

Due to the high two-dimensional electron gas (2DEG) concentration and high temperature stability, lattice matched InAlN/AlN/GaN high electron mobility transistors (HEMTs) have attracted tremendous amount of interest for high-power and high-frequency electronics. Employing the gate recess technology, a popular way to develop enhancement-mode (E-mode) devices for digital and mixed signal applications, record high performance (output current density of 2 A/mm, extrinsic transconductance of 890 mS/mm, and f_t/f_{max} of 95/135 GHz for 150-nm gate length) have been very recently reported on E-mode InAlN HEMTs. Temperature dependent characterization of the subthreshold slope (SS) can provide valuable information on the interface states and their distribution near the band edges. In this paper, we have performed the field-effect measurements on these gate-recessed E-mode InAlN HEMTs, and extracted the interface states from the temperature dependent SS from 80 to 300 K. [C298]

"T-gate technology for N-polar GaN-based self-aligned MIS-HEMTs with state-of-the-art f_{MAX} of 127 GHz: Pathway towards scaling to 30nm GaN HEMTs"

In this paper, we demonstrate a self-aligned gate-first process for fabrication of T-gates without much degradation of f_t . The device layer structure is shown. The fabrication process involves formation of W/Cr gates using a self-aligned gate-etch process similar to the InGaAs MOSFET technology reported by Rodwell et. al. [2008, 2009]. After formation of a 130 nm long gates, graded InGaIn/InN-based access regions are regrown by plasma MBE, followed by self-aligned T-gate formation. The process involves spin-coating the sample with thick layer of e-beam resist PMMA (~1 μ m) followed by height-selective etching of the resist to leave the resist everywhere except the top of the gate fingers. Any InGaIn regrown on top and protective SiO₂layer is then lifted off in hydro-fluoric acid. Ebeam lithography of 300 nm long top is done followed by deposition of Ti/Au. The schematic of the T-gate process is shown. [C299]

"Self-aligned enhancement-mode AlGaIn/GaN HEMTs using 25 keV fluorine ion implantation"

Owing to superior physical properties such as high electron saturation velocity and high electric breakdown field, GaN-based high electron mobility transistors (HEMTs) are capable of delivering superior performance in microwave amplifiers, high power switches, and high temperature integrated circuits (ICs). Compared to the conventional D-mode HEMTs with negative threshold voltages, enhancement-mode (E-mode) or normally-off HEMTs are desirable in these applications, for reduced circuit design complexity and fail-safe operation. Fluorine plasma treatment has been used to fabricate E-mode HEMTs, and is a robust process for the channel threshold voltage modulation. However, there is no standard equipment for this process and various groups have reported a wide range of process parameters. In this work, we demonstrate the self-aligned enhancement-mode AlGaIn/GaN HEMTs fabricated with a standard fluorine ion implantation. Ion implantation is widely used in semiconductor industry with well-controlled dose and precise implantation profile. [C300]

"Work-function engineering in novel high Al composition Al_{0.72}Ga_{0.28}N/AlN/GaN HEMTs"

In this paper, device performance of high Al composition Al_{0.72}Ga_{0.28}N/AlN/GaN HEMTs with ALD Al₂O₃ dielectric is reported. Employing different gate metals, the threshold voltages were shifted by -0.8 V in 0.5- μ m-long HEMTs, which indicates an unpinned Fermi level at the ALD Al₂O₃/ Al_{0.72}Ga_{0.28}N interface. With lower contact resistances, high Al AlGaIn HEMTs are well suited for further lateral and vertical scaling to push towards high frequency E/D-mode performance. [C301]

"Fast robust gate-drivers with easily adjustable voltage ranges for driving normally-on wide-bandgap power transistors"

Wide-bandgap (WBG) semiconductors, such as gallium nitride (GaN), are more and more being used in switching power devices. An AlGaIn/GaN/AlGaIn Double Heterojunction Field Effect transistor (DHFET) was developed in previous work and needed to be tested. The used test circuit was a buck converter. This type of converter, in addition with the normally-on switching behaviour of the GaN-based transistors, requires dedicated gate drive circuitry, resulting in the development of three types of gate-drivers. This paper presents the topology and performance of these drivers. Because of the type of converter, the drivers need to be galvanically isolated. Furthermore, because the experimental GaN transistors are normally-on, the drivers need to be robust so that they apply a negative gate-to-source voltage to switch off the transistor in case an error occurs in the driver. A third requirement for the drivers is that it has to be easy to adjust the voltage levels, in order to test the devices at different gate-to-source voltage conditions. A final requirement is that it has to be possible to construct the drivers with readily available electronic components. Because the drivers are galvanically isolated, there is a parasitic isolation capacitance in the DC-DC-converter of the drivers. This gives rise to a common-mode current which possibly can disturb the operation of the driver. The article also discusses this common-mode problem. [C302]

"Schrödinger-Poisson and Monte Carlo analysis of III-V MOSFETs for high frequency and low consumption applications"

III-V MOSFET (Metal Oxide Semiconductor Field Effect Transistor) with high- κ gate dielectric stack appears as a viable alternative to enhance not only microwave performance but also logic circuits with low supply voltage. This allows fulfilling high-speed and low-power specifications for intelligent applications. Indeed, combining weak gate leakage of standard MOSFETs and good RF performance of HEMTs (High Electron Mobility Transistors), they could outperform end-of-roadmap standard Si-MOSFET. Using full 2D Poisson-Schrödinger solver and a semi-classical Ensemble Monte Carlo device simulator, various 50nm MOSFET and HEMT are investigated in terms of gate charge control and both static and dynamic I-V performance. In particular, Y parameters are carefully extracted from time-varying currents. This comparative study allows us to propose an optimized III-V nano-FET architecture with high-frequency performance under low power supply. [C303]

"Analysis of plasma resonances in terahertz devices with grating gate"

Analytical model is developed and used to calculate spatial distribution of sheet electron density in the channel of grid-grating gated HEMT structure and resonant frequencies of plasma waves excited in the channel. It is shown that plasma resonances in realistic structures deviates from those predicted by ideal model. [C304]

"An In_{0.23}Ga_{0.77}As-based pHEMT-like planar Gunn diode operating at 116 GHz"

An In_{0.23}Ga_{0.77}As-based planar Gunn diode operating in its fundamental transit-time mode of oscillation at 116 GHz with output power of -24 dBm is demonstrated. The diode has a pseudomorphic HEMT-like structure grown

on a semi-insulating GaAs substrate. The layer design was carried out using a two-dimensional drift-diffusion model. The realized devices show considerable potential as a source of millimeter-wave and even terahertz radiation. [C305]

"Hydrodynamic simulation of heterodyne terahertz detection in a field effect transistor"

We propose a method for the heterodyne detection of terahertz (THz) signals. The nonlinear element is constituted by the channel of an High Electron Mobility Transistor (HEMT), while the optical beating of two laser beams exciting plasma waves in the transistor channel plays the role of the THz local oscillator. We numerically show, through an hydrodynamic modelling, the efficiency of such a mixer. [C306]

"On 10Gbps Terahertz wireless communication systems"

In order to increase the short range wireless communication to 10 Gbps, a Terahertz wireless communication system combining electro-optical technology with THz band (125 GHz) for carrier was build, which adopted 125 GHz optical THz generator, UTC-PD module, HEMT module and cassegrain antenna (CA) or Gaussian optic lens antenna (GOA) to improve system performance. It gives the researches about theoretical analysis and simulation results on output power, noisiness, relation between communication quality and antenna, data transmission feature, maximum transmission distance and so on. Experimental result shows that: the carrier to noise ratio of emission signal meets error-free transmission demand, 125 GHz waveband wireless communication supports OC-192 network interface and 10 GbE network interface. So, it's feasible to realize 10 Gbps wireless communication using electro-optical technology. [C307]

"Development of a novel HEMT-based plasmonic sensor"

In this paper, we develop a method for analyzing such a device. This implies that one must solve a multi-physics problem, one that is governed by a coupled Schrödinger-Poisson equation and is weakly perturbed by an incident electric field. This article is organized in the following manner. The next section describes all necessary physical parameters of the simulated system. Section 3 outlines the mathematical background, formulas used, and provides an outline of the self-consistent simulation routine. Finally, the results of the simulation and their importance are discussed in Section 4, along with a brief summary in Section 5. [C308]

"Temperature-dependence electrical performance of GaAs-based HEMT-embedded accelerometer"

In this paper, it is researched that how I-V characteristics and piezoresistance coefficient of GaAs-based HEMT-embedded accelerometer change when different temperatures are set. It is shown that saturation current of device would go down if the temperature goes up, which is about $3.1467\text{mA}/^\circ\text{C}$, based on the research. However, the device can work well at the temperature range of -50°C to 50°C , which indicates that it can work safely in the larger temperature range. Piezoresistance coefficient is also in down trend with the temperature rising, that it, it has negative temperature coefficient which is about $0.74\%/^\circ\text{C}$, and it's sensitivity is higher than Si. [C309]

"Viscous hydrodynamic model of non-linear plasma oscillations in two-dimensional gated conduction channels and application to the detection of terahertz signals"

We study the non-linear plasma oscillations in a semiconductor conduction channel controlled by a gate. The analysis is based on the hydrodynamic equations derived from the Boltzmann equation, and includes the effects of viscosity, finite mobility, and temperature gradients in the channel. The conduction channel of a heterostructure High Electron Mobility Transistor (HEMT) can act as a plasma wave resonator for charge density oscillations at frequencies significantly higher than the transistor cut-off frequency in a short channel device. In the Dyakonov-Shur detector a short channel HEMT is used for the resonant tunable detection of electromagnetic radiation in the low terahertz range. Within the hydrodynamic approximation we evaluated the resonant nonlinear response to a small signal, and obtained the temperature dependence of the quality factor Q of the plasma resonance. We find that in high mobility gated semiconductor conduction channels the quality of the resonance is limited by the temperature dependent viscosity of the electron fluid. [C310]

"Characteristic research on an accelerated sensor based on GaAs/AlGaAs/InGaAs PHEMT"

A novel nano electro mechanical system (NEMS) accelerated sensor which is based on a Pseudomorphic high electron mobility transistor (PHEMT) device with GaAs/AlGaAs/InGaAs is fabricated and demonstrated in this paper. The characteristics, including sensitivity and linearity of the studied device with different drain and gate bias voltage of PHEMT device, are measured and studied. Measured by the testing circuit, the accelerated

sensor has good linearity and sensitivity when the PHEMT device works in the linear region and saturation region. The impacts of drain and gate voltages on the drain current has been discussed. The relationship between sensitivity and drain, gate bias voltage is analyzed. The new structure has high sensitivity and good linearity with different bias voltages. [C311]

"Performance assessment of GaN HEMT technologies for power limiter and switching applications"

In this work, a systematic study on GaN HEMT devices for Switching and Power Limitation is presented. Various manufacturing approaches are considered, all fully compliant for monolithic integration with HPA and LNA circuits. A set of devices have been used to compare various configuration options, including different layouts, single or multiple Gate, or the adoption of Schottky or Metal-Insulator-Semiconductor (MIS) Gate junctions. Devices performances under high input power signal @3GHz have been compared, showing that MIS Gate switch devices in series configuration can handle in ON-state 80W/mm power for 1dB insertion loss compression, and for double Gate topology higher power handling can be obtained in OFF-state (>40dBm for +1dB isolation compression). GaN HEMT switches in shunt configuration have been studied for Power signal protection application, evidencing that single MIS Gate devices with $WG=900\mu m$ provides low insertion loss ($<0.1dB$) and effective power limitation ($-5dB$ @ $PIN=40dBm$), associated with 23dB ON-state isolation. [C312]

"Study of GaN HEMTs electrical degradation by means of numerical simulations"

In this paper, we investigate the effects of dc stress on GaN high-electron mobility transistors (HEMTs) by means of numerical simulations. Following stress tests showing a degradation of static characteristics (dc), the formation of an electron trap in the AlGaIn barrier layer was related to the observed degradation according to the results obtained from numerical simulations carried out by introducing a trapping region underneath the gate edge. The worsening of the device dc performance is evaluated by changing the extension of the degraded region and the trap concentration while studying the variation of parameters like the saturated drain current $IDSS$, the output conductance gO , and the device transconductance gM . An increase in the trap concentration induces a worsening of any of the above mentioned parameters; an increase in the extension of the degraded region induces a degradation of $IDSS$ and gM , but can reduce gO . [C313]

"Optimization of III-V FET architectures for high frequency and low consumption applications"

To fulfill high-speed and low-power specifications for intelligent applications, III-V FETs (Field Effect Transistor) with high-gate dielectric stack are very appealing. Indeed, combining weak gate leakage of standard MOSFETs and good RF performance of HEMTs, they could enhance device scalability. Using full 2D Poisson-Schrodinger solver and then semi-classical Ensemble Monte Carlo device simulator, MOSFET (Metal Oxide Semiconductor Field Effect Transistor) and HEMT (High Electron Mobility Transistor) structures are investigated in terms of gate charge control and both static and dynamic I-V performance. In particular, Y parameters are carefully extracted from time-varying currents. This comparative study allows us to propose optimized nanoscale III-V FET with high-frequency performance under low power supply. [C314]

"A continuous physics-based electrothermal compact model for the study of non-linearities in III-V HEMTs"

We present a newly developed continuous physics-based electrothermal I-V compact model suitable for the study intermodulation distortion in GaAs HEMTs and MESFETs. The model, which is an improvement of the standard Chalmers model, accurately includes self-heating while significantly minimizing the need for parameter fitting. The model, which is carefully calibrated using experimental data for submicrometer arsenide pHEMTs, is employed to calculate and analyze intermodulation products using the Volterra series method. [C315]

"DARPA's Nitride Electronic NeXt Generation Technology Program"

DARPA/MTO has sponsored electronics programs to exploit the unique combination of high intrinsic breakdown voltages, high electron saturation velocities, and large sheet carrier densities of the nitride material system. The NEXT program is pushing III-N-based HEMTs toward its operating frequency (size) scaling limits by simultaneously minimizing carrier transit time, maximizing electron density, reducing access resistances and optimizing parasitic capacitances with innovative epitaxial structures and dielectric heterointerfaces. The Phase I goals of the NEXT program are to demonstrate 300 GHz D-mode and 200 GHz E-mode HEMTs while maintaining the breakdown voltage and transistor cutoff frequency product of more than 5 THz·Volt. The final goal of the NEXT program is to enable a 1000-transistor, high-yield, 500 GHz E/D-mode GaN technology for mixed signal applications. [C316]

"Thermal broadening of two-dimensional electron gas mobility distribution in AlGa_N/AlN/GaN heterostructures"

Two-dimensional electron gas (2DEG) transport in Al_{0.3}Ga_{0.7}N/AlN/GaN heterostructures has been studied using magnetic-field dependent Hall-effect measurements and advanced mobility spectrum analysis techniques over the temperature range from 95 K to 300 K. It is shown that electronic transport is due to a single well-defined 2DEG species, with room-temperature sheet concentration and average mobility of $9.3 \times 10^{12} \text{ cm}^{-2}$ and $1,880 \text{ cm}^2/\text{Vs}$, respectively. No parasitic conduction through the bulk GaN layer was detected. Importantly, it is shown that the 2DEG exhibits an approximately Gaussian mobility distribution, the linewidth of which broadens with increasing temperature. This is the first reported observation of thermal broadening effects in the 2DEG mobility distribution. [C317]

"High transconductance AlGa_N/GaN HEMT with thin barrier on Si(111) substrate"

The fabrication of high transconductance AlGa_N/GaN high electron mobility transistors (HEMTs) grown on high-resistivity silicon substrate is reported with an AlGa_N barrier thickness of only 12.5 nm. A maximum DC current density of 655 mA/mm, a current gain cutoff frequency (FT) of 75 GHz and a power-gain cutoff frequency (FMAX) of 125 GHz are obtained for a 0.125 μm gate length transistor. The device provides a record peak extrinsic transconductance of 332 mS/mm and an intrinsic value of 509 mS/mm. To the authors' knowledge, the obtained transconductances are the highest reported values from AlGa_N/GaN devices grown on a Si(111) substrate. This performance demonstrates the potential of GaN transistors on silicon for low-cost microwave power applications. [C318]

"A wideband GaN Doherty amplifier with 35 % fractional bandwidth"

A wideband Doherty amplifier designed and implemented in GaN HEMT technology using simple circuitry is reported. The usefulness of the conventional quarter-wave impedance transformer at the output of the main amplifier for achieving wideband Doherty performance up to 35% fractional bandwidth is experimentally verified. This simplifies the bandwidth limitation problem of the Doherty amplifier into the wideband design of the main amplifier, peaking amplifier and the input power divider. Based on this, a wideband Doherty amplifier was designed to cover a bandwidth of 640 MHz, ranging from 1.5 GHz to 2.14 GHz. For instance, the designed Doherty amplifier achieved a 1 dB compression output power of $P_{1\text{dB}} = 43.8 \text{ dBm}$ (24.1 W), with a maximum power-added efficiency of $\text{PAE} = 69\%$ (drain efficiency of $\eta = 76\%$) at 1.9 GHz. At 6 dB output back-off from $P_{1\text{dB}}$, a PAE of 45% ($\eta = 47\%$) was measured. The designed Doherty amplifier also showed acceptable linearity when characterized with two-tone and single-carrier wideband code-division multiple access (W-CDMA) stimuli. To the best of authors' knowledge, this work introduces the most wideband Doherty amplifier published so far. [C319]

"A high efficiency and multi-band/multi-mode power amplifier using a distributed second harmonic termination"

This paper proposes a new broadband saturated power amplifier (SPA) with a distributed second harmonic termination supporting multi-band/multi-mode operation. The proposed network is composed of a fundamental matching circuit and multiple second harmonic termination circuits. Due to the multiple harmonic terminations, the proposed PA improves the frequency range where the PA can achieve a high efficiency. The proposed PA is fabricated using a 45 W Cree CGH40045 GaN HEMT. Drain efficiencies of greater than 60% (average 66%) are achieved between about 1.8 GHz and 2.3 GHz (500 MHz bandwidth). When driven with long term evolution (LTE) and two carrier wideband code division multiple access (WCDMA) signals at DCS1800, PCS1900, and WCDMA bands, the linearity specifications of the corresponding standards are satisfied using the digital predistortion linearization technique, and it attains an efficiency of greater than 30%. [C320]

"High power, fully integrated SMT amplifiers with +47dBm OIP3 at 15GHz and 6W, 38% efficiency at 30GHz using low cost, high volume PHEMT"

The system power amplifier's linearity sets the maximum bit rate and the efficiency determines the maximum output power possible given a fixed heat dissipation or DC supply. This paper demonstrates that using a GaAs PHEMT 0.15 μm gate process, industry leading performance can be attained. Shown is a 15GHz linear power amplifier capable of -52dBc IM3 at 21dBm output power (+47dBm OIP3). Also demonstrated is a 30GHz saturated power amplifier capable of making 38dBm (6W) output power at 38% peak power added efficiency. Both are fully matched to 50 Ω and have over 20dB of gain. Both are housed in a low cost laminate surface mount package. [C321]

"A voltage-mode class-S power amplifier for the 450MHz band"

This paper reports on a novel voltage-mode class-S power amplifier for the 450 MHz band, based on GaN-HEMT MMICs. It achieves a peak output power of 3.4 W for a single tone at 400 MHz, encoded in standard band-pass delta-sigma modulation with 1.6 Gbps sampling frequency. The corresponding efficiency is 38%, peaking at 52% for 0.5 W output power. In order to demonstrate the influence of coding efficiency, additional measurements using a periodic square-wave signal were performed (class-D operation), which yield a maximum output power of 6.5 W with 64% efficiency. To the authors knowledge, these are the best results in this frequency range achieved so far with the voltage-mode class-S configuration. [C322]

"GaN based power amplifiers for broadband applications from 2 GHz to 6 GHz"

A hybrid power amplifier building block and a power amplifier module from 2 GHz to 6 GHz were designed, fabricated and measured. These power amplifiers are all based on AlGaIn/GaN HEMT technology. The future applications for these types of power amplifiers are mainly electronic warfare (EW) applications. Novel communication jammers and especially active electronically scanned array EW systems have a high demand for broadband high power amplifiers. Output power levels with a peak value of 90 W at lower frequencies and more than 40 W up to 6 GHz are measured. With these power amplifiers novel EW system approaches can be investigated. [C323]

"325GHz CPW band pass filter integrated in advanced HR SOI RF CMOS technology"

Today, measurement of 65nm CMOS and 130nm-based SiGe HBTs technologies demonstrate both f_T (current gain cut-off frequency) and f_{max} (maximum oscillation frequency) higher than 200 GHz, which are clearly comparable to advanced commercially available 100nm III-V HEMT. This increase allows new millimeter wave (MMW) applications on silicon. One of the success keys is then the passive integration. In this paper, on-chip coplanar waveguides (CPWs), which have been achieved in STMicroelectronics advanced nanometric RF CMOS High Resistivity (HR) SOI ($\rho > 1\text{k}\Omega\cdot\text{cm}$) process, and characterized up to 325GHz are reported. Moreover, for the first time passive circuits working @ 325GHz have been achieved on silicon and characterized demonstrating state-of-the-art performances and good agreement with electric simulations. [C324]

"Development of 90nm InGaAs HEMTs and Benchmarking Logic Performance with Si CMOS"

We have developed 90nm In_{0.7}Ga_{0.3}As channel HEMTs, directly measured of DC and RF characteristics, and performed microwave modeling for both 90nm Si CMOS and HEMT for benchmarking logic performance for future design layout and process improvement. [C325]

"Developing GaN HEMTs for Ka-Band with 20W"

AlGaIn/GaN High Electron Mobility Transistors (HEMTs) were developed for Ka-band. The developed device showed 138 GHz of f_{max} , which depended on the thickness of the AlGaIn barrier layer and the gate length. It had a 6.4 mm gate periphery on a metal carrier plate. The output power achieved 20 W with impedance matching circuits. [C326]

"An mHEMT Q-Band Integrated LNA and Vector Modulator MMIC"

We present a Q-band high performance integrated LNA and vector modulator MMIC. The overall MMIC shows a maximum gain of 11 dB at 44 GHz. Full 360-degree phase coverage and a maximum attenuation range of over 40 dB has been achieved. With software calibration, we have demonstrated phase steps as low as 0.4 degrees and amplitude steps of 0.06 dB. An overall noise figure for the integrated MMIC of 3.5 dB has been measured. The results show the excellent performance and high integration level possible with mHEMT technology at millimeter-wave frequencies. To our knowledge, this is the first reported single-chip integration of an LNA and vector modulator at Q-band. [C327]

"A Scalable and Distributed Electro-Thermal Model of AlGaIn/GaN HEMT Dedicated to Multi-Fingers Transistors"

This paper deals with a scalable and distributed electro-thermal model of AlGaIn/GaN HEMT. This model has been especially developed for multi-fingers and large periphery transistors. Quasi isothermal measurements by means of pulsed $I(V)$ and pulsed $[S]$ have been performed at different temperatures to extract the model and its thermal dependencies. Then load-pull measurements have been performed to final validations. In terms of accuracy, the developed model has been compared to an usual compact model. Three devices with different sizes have been verified to check the validity of the scaling rules implemented. [C328]

"A Verilog-A Large-Signal GaN HEMT Model for High Power Amplifier Design"

This paper describes the high-power non-linear modeling of a GaN HEMT device using a Verilog-A-implemented and modified version of the EEHEMT model commonly found in commercial simulators. As discussed in, peculiarities of GaN device physics exposed flaws in the standard EEHEMT model such as the inability to describe trap-related phenomena such as knee walk-out, multiple voltage dependencies of conduction currents, anomalies in the saturation current/conductance, and nonlinear behavior of source resistance. Improvements were made to the standard model to accommodate GaN-specific characteristics of the knee and saturation regions of the device IV plane as well as a functional dependence of R_s on RF operating current. Additionally, temperature dependencies were implemented in the Verilog-A version using a thermal sub-circuit to account for self-heating in real-time and ambient temperature effects. Extensive pulsed and CW load-pull measurements were done at multiple source/load states and power levels and at several frequencies. Output power, gain, efficiency and load-pull contour simulations vs. measurements are presented. The improved model is shown to accurately predict actual device and scaled high-power amplifier behavior and has proven to be a useful tool in very high power product design. [C329]

"LNA Design Based on an Extracted Single Gate Finger Model"

A GaAs low-noise amplifier (LNA) is designed with first-time success using a technique for HEMT modelling which divides the device into intrinsic gate fingers embedded in an analysable metal structure. The gate finger is characterised by de-embedding metallisation from a standard test structure. The device is then re-built, with any geometry or layout that the foundry allows, and modelled by electromagnetic (EM) analysis. This allows techniques such as asymmetric inductive source feedback in an LNA to be modelled without prior fabrication of custom test structures. The 7-13 GHz, self-biased LNA has state-of-the-art noise figure (NF) of 1.25 dB at mid-band, gain of 20.5 ± 0.1 dB with 10 dB input and output matches, 10 dBm P1dB, 14 dBm Psat and 22 dBm OIP3. Excellent agreement is achieved with simulation. In a 3 Ч 3 QFN package the measured NF is 1.36 dB and the gain is 20 dB. The first-time design success achieved here validates the modelling and parameter extraction technique. [C330]

"Comparative Study of AlGaIn/GaN HEMTs on Free-Standing Diamond and Silicon Substrates for Thermal Effects"

In this work, we compare for the first time the performance results of AlGaIn/GaN HEMTs processed on a free-standing chemical vapor deposition (CVD) polycrystalline diamond substrate and a silicon substrate with nominally the same epitaxial AlGaIn/GaN layers both grown by metal-organic chemical vapor deposition (MOCVD). The objective of this work is to compare the small signal and DC trends of the transistors fabricated on the different substrates as a function of temperature. Wafer scale results were obtained from both wafers for 2 x 150 μm devices with gate lengths of 0.18 μm and 0.20 μm for the silicon and CVD diamond wafers respectively. [C331]

"A 0.1-1.8 GHz, 100 W GaN HEMT Power Amplifier Module"

We have demonstrated a 0.1-1.8 GHz, 100 W GaN HEMT power amplifier module with 11 dB gain, 94-142 W CW output power and 40.6-74.0% drain efficiency over the band. The power amplifier module uses broadband low loss coaxial baluns to combine four 30 W broadband lossy matched GaN HEMT PAs on a 2 Ч 2 inch compact PCB. The individual PAs are fully matched to 50 Ohms and obtains 23.6-30.9 W with 44.5-63.7 % drain efficiency over the band. The packaged amplifiers contain a GaN on SiC device operating at 50 V drain voltage with a GaAs integrated passive matching circuitry. These amplifiers are targeted for use in multi-band multi-standard communication systems and for instrumentation applications. [C332]

"A Metamorphic HEMT S-MMIC Amplifier with 16.1 dB Gain at 460 GHz"

In this paper, we present a four-stage submillimeter-wave monolithic integrated circuit (S-MMIC) amplifier for use in next generation radar and communication systems operating in the WR-2.2 waveguide band (325-500 GHz). The low-noise amplifier circuit (LNA) has been realized using a 35 nm InAlAs/InGaAs based metamorphic high electron mobility transistor (mHEMT) technology and demonstrates a peak gain of 16.1 dB at 460 GHz and a small-signal gain of more than 13 dB in the bandwidth from 433 to 465 GHz. The use of grounded coplanar waveguide (GCPW) topology in combination with a very compact design resulted in a die size of only 0.37 Ч 0.63 mm². [C333]

"Scaling of InP HEMT Cascode Integrated Circuits to THz Frequencies"

In this paper, we demonstrate that the cascode amplifier topology can be extended to operating frequencies

>500 GHz. Two packaged cascode amplifiers are reported, including a broadband 3 stage amplifier with ~17 dB gain and 8.3 dB packaged noise figure at 300 GHz and a narrowband amplifier with 10 dB gain at 0.55 THz measured in package. Both of these amplifiers use 30 nm InP HEMT transistors, are realized in coplanar waveguide on a 1-Mil thick InP substrate and use a monolithically integrated electromagnetic transition for coupling energy from the chip to the waveguide package. [C334]

"Single-Polarity Power Supply Bootstrapped Comparator for GaN Smart Power Technology"

A high-performance bootstrapped comparator operating with a single-polarity power supply is demonstrated for the development of GaN smart power ICs. The comparator features monolithically integrated enhancement-mode (E-mode) and depletion mode (D-mode) AlGaIn/GaN HEMTs. The tail current source uses E-mode HEMT, enabling single-polarity power supply. The input stage could be either E-mode or D-mode HEMTs to cover a wide voltage range (from 0 to 6 V), while the bootstrapped loads are implemented with D-mode HEMTs. At room temperature, the comparator delivers a voltage gain as high as 132 V/V and a unity-gain bandwidth of 270 MHz. The comparator is also capable of operating at 250 °C with temperature-compensated bias. [C335]

"E-Band 85-mW Oscillator and 1.3-W Amplifier ICs Using 0.12µm GaN HEMTs for Millimeter-Wave Transceivers"

This paper presents two oscillators (OSCs) and a high power amplifier (PA) for millimeter-wave transceivers. The circuits were designed with a grounded coplanar waveguide (GCPW) and 0.12-µm GaN HEMT technology. One OSC, which was based on a simple series source feedback topology, oscillated at a frequency of 74.5 GHz with an output power of 2.2 mW (3.38 dBm). This oscillation frequency was the highest ever reported for GaN HEMT OSCs. Another OSC with a buffer delivered a record power of 85 mW (19.28 dBm) at 70.75 GHz. In addition, a single-chip PA with a 3-stage common source scheme delivered an output power of 1.3 W (31.13 dBm) at 75 GHz with a CW source module. The 3-dB bandwidth of the PA was 13 GHz from 67 to 80 GHz. The performance of these devices is sufficient for use in E-band fixed wireless access systems and automotive radar systems. The results demonstrate that the GaN HEMTs represent a feasible means of addressing the stringent demands imposed by various millimeter-wave applications. [C336]

"Thermal and trapping phenomena assessment on AlGaIn/GaN microwave power transistor"

In this paper a systematic analysis of thermal and trapping behaviour of microwave power AlGaIn/GaN HEMTs has been carried out through pulsed current-voltage (PIV) measurements and S parameters. It is shown that the thermal resistance of the device can be accurately determined provided that some assumptions on the trapping behaviour of the device are verified. The values obtained have been checked by three dimensional finite element (3D-FE) simulations with reasonable accuracy. Kink effects in the output characteristics have been analysed at different temperatures and it has been shown that they are more pronounced at ambient temperature. Finally the microwave behaviour of the device versus temperature has been assessed. [C337]

"GaN based power amplifiers for broadband applications from 2 GHz to 6 GHz"

A hybrid power amplifier building block and a power amplifier module from 2 GHz to 6 GHz were designed, fabricated and measured. These power amplifiers are all based on AlGaIn/GaN HEMT technology. The future applications for these types of power amplifiers are mainly electronic warfare (EW) applications. Novel communication jammers and especially active electronically scanned array EW systems have a high demand for broadband high power amplifiers. Output power levels with a peak value of 90 W at lower frequencies and more than 40 W up to 6 GHz are measured. With these power amplifiers novel EW system approaches can be investigated. [C338]

"Comparison on mHEMT Q-band sub-harmonic mixers with/without delay compensation"

Q-band sub-harmonic mixers (SHMs) with and without delay compensation are demonstrated in this paper using 0.15-µm metamorphic high electron mobility transistor (mHEMT) technology. A conventional stacked-LO sub-harmonic mixing cell consists of two Gilbert cells in cascode with quadrature LO inputs. The proposed compensation core in parallel with the stacked-LO core improves the port-to-port isolation. A Marchand balun is employed at the RF port to generate wideband differential signals. As a result, SHMs w/ and w/o compensation achieve the conversion gain of 1/0.5 dB and noise figure of 23/20 dB when $2f_{LO}=39/42$ GHz. However, the compensation circuit improves the 2LO-to-RF isolation by 12 dB, 2LO-to-IF isolation by 5 dB and RF-to-IF isolation by 5 dB without additional power consumption. [C339]

"An MMIC wide-band doubly balanced resistive mixer with an active IF balun"

In this paper, we present a wideband doubly-balanced resistive mixer fabricated using a 0.5 μm GaAs p-HEMT process. Three baluns are employed in the mixer. Local oscillator (LO) and radio frequency (RF) baluns operating over an 8 to 20 GHz range were implemented with Marchand baluns. In order to reduce the chip size, the Marchand baluns were realized using a meandering multi-coupled line, and inductor lines were inserted to compensate for the meandering effect. Over a frequency range of 8 to 20 GHz, the amplitude and phase unbalances of the LO and RF baluns were less than 1 dB and 6° , respectively. A 0.3 \times 0.5 mm² IF balun was implemented through a DC-coupled differential amplifier. The measured amplitude and phase unbalances were less than 1 dB and 5° , respectively, from DC to 7 GHz. And the output third-order intercept (OIP3) and PldB, at a frequency of 1 GHz, were 18 dBm and 6 dBm, respectively. The mixer is 1.7 \times 1.8 mm² in size, has a conversion loss of 5 to 11 dB, and an OIP3 of +10 to +15 dBm at 16 dBm LO power for the operating bandwidth. [C340]

"8W 2-8GHz solid state amplifier for phased array"

A complete Tx/Rx module for phased array applications was developed. A multifunction PHEMT MMIC chip set was designed and realized with UMS foundry. A balanced HPA Assembly 2-8GHz was designed for a Tx/Rx module using two HPA and a driver. This component exhibits 35 dB of gain and 8W of output power. [C341]

"A balanced resistive 210 GHz mixer with 50 GHz IF bandwidth"

A novel balanced 210 GHz mixer MMIC with a measured IF bandwidth of more than 50 GHz and an RF bandwidth of more than 100 GHz has been successfully developed in a 50 nm mHEMT technology. The mixer achieves a measured conversion loss of 17 dB. The measured LO-to-RF isolation is better than 17 dB in the relevant frequency range. Two Lange couplers are used to balance the design. The IF signal is tapped at the isolated RF coupler port to increase the IF bandwidth. [C342]

"An all-active MMIC-based chip set for a wideband 260-304 GHz receiver"

A wideband 260 to 304 GHz (H-band) heterodyne receiver is formed by an MMIC chip set cascading a low-noise amplifier, resistive mixer with integrated frequency-doubler, LO power amplifier and frequency-multiplier-by-six. All MMICs use active circuit concepts and are realized in 100 and 50 nm gate-length metamorphic HEMT technology. The balanced active frequency-multiplier-by-six provides 0 dBm of output power in the frequency range from 110 to 152 GHz. When directly driven by the multiplier output power, the combination of frequency doubler and resistive mixer achieves a conversion loss of 20 dB. With the intermediate LO power amplifier, the conversion loss is reduced to 12 dB in the frequency range from less than 260 to 308 GHz. The LNA provides pre-amplification by 20 dB at 290 GHz with an estimated noise figure of 7.5 dB, taking the overall receiver performance to a maximum conversion gain of 8 dB and noise figure of 7.6 dB, rivaling the performance of state-of-the-art Schottky receivers. [C343]

"Determination of suitable mHEMT transistor dimensioning for power amplification at 210 GHz by comprehensive measurements"

The properties of various mHEMT technologies and their advantages for millimeter-wave (mmW) power amplification are presented. An experimental determination of the most suitable transistor technology (i.e. gate-length), transistor size (i.e. number of gate-fingers and gate-width) and transistor bias is taken. The advantages of the different technologies are pointed out. The most suitable combination of gate-length, number of fingers, gate-width and bias for obtaining maximum gain, maximum output power and maximum power added efficiency at a given frequency of 210 GHz is determined. [C344]

"High Voltage Breakdown pHEMTs for C-band HPA"

High Voltage Breakdown (HVB) HPA MMIC based on GaAs pHEMTs technology represents a useful way for high power RF application. To increase the breakdown voltage respect to conventional device, a field-plate (FP) gate structure is implemented in our standard 0.5 μm process. With this solution the off-state breakdown voltage of the device has been improved from 18V to 28V, while keeping constant the drain current. As expected, FP devices showed smaller drain current collapse than standard devices under pulsed DC measurement conditions and a significant increase in power density, i.e. 1.4 W/mm. To guaranty a full advantage for real HPA applications we have carried out numerical simulations, to optimise device thermal behaviour as a function of GaAs thickness and gate pitch. On the basis of this technology development, reliable and reproducible HPA have been fabricated with an output power of circa 30 W and power added efficiency (PAE) of circa 35% in the 4.9-6.1GHz frequency range. Therefore this proposed technological solution enables the realization of very high power T/R modules with reliable GaAs technology, waiting for more disruptive and less mature GaN HEMT one. [C345]

"Nonlinear thermal resistance characterization for compact electrothermal GaN HEMT modelling"

A new method is proposed for the empirical characterization of the nonlinear thermal resistance in GaN HEMTs. Low-Frequency dispersion due to self-heating is used as the sensing parameter of the channel temperature changes deriving from dissipated power variations. Since GaN HEMTs are also affected by LF dispersive charge-trapping phenomena, the thermal resistance description is embedded into a full electrothermal model, in order to extract the parameters by best-fitting the measured data. The method involves only multi-bias small-signal S-parameter and de I/V measurements at different base plate temperatures. It is non-invasive, does neither require special-purpose device geometries/structures nor measurements in the conduction region of the gate junction. Preliminary validation of the method is based on comparisons with measured electrothermal data, with data from the literature on similar devices and on results provided by a large-signal RF device model embedding the thermal resistance description. [C346]

"GaN power MMICs for X-Band T/R modules"

This paper presents the development of power MMICs in GaN HEMT technology for X-Band T/R modules. We will focus here specifically on the transmit path, which contains the high power amplifier and its power driver. A step by step description of the tasks in order to design this channel will be done, beginning from a short overview of the epitaxial process to the presentation of its measured and simulated power performances. [C347]

"GaN power FETs for next generation mobile communication systems"

This paper presents the RF-performance of Al-GaN/GaN high electron mobility transistors (HEMT) for applications at L-/S-band frequencies. The powerbars provide a linear gain of 20.3 dB with 90 W output power operated at 50 V drain voltage in cw-operation with a maximum drain efficiency of 59% at 2.14 GHz. This gain level is competitive to state-of-the-art LDMOS. [C348]

"Improved AlGaIn/GaN HEMTs grown on Si substrates by MOCVD"

AlGaIn/GaN high electron mobility transistors (HEMTs) were grown on Si substrates by MOCVD. In the HEMT structure, the 1 μm GaN buffer layer was partially doped with Mg in an attempt to increase the resistivity and minimize the buffer leakage current. Afterwards, an AlN spacer layer was inserted between the AlGaIn barrier layer and the GaN channel layer to effectively reduce impurity scattering and improve the mobility and sheet carrier density of two-dimensional electron gas (2DEG). Devices of AlGaIn/GaN HEMTs with 1 nm AlN spacer layer grown on undoped and partially Mg-doped GaN buffer layers were processed and characterized for comparison. For the DC characteristics, a low drain leakage current density of 55.8 nA/mm, a low gate leakage current density of 2.73 $\mu\text{A}/\text{mm}$, and a high off-state breakdown voltage of 104 V were achieved with device dimensions $L_g/W_g/L_{gs}/L_{gd} = 1/10/1/1 \mu\text{m}$, using the sample with partially Mg-doped GaN buffer layer. For the small signal RF characteristics, the device with partially Mg-doped has lower current gain cutoff frequency (f_T) and lower power gain cutoff frequency (f_{max}) than that of the device without Mg-doped, indicating that doping Mg in GaN buffer layer should introduce the potential parasitic capacitance, which is not beneficial to RF performance of HEMT devices. [C349]

"Broadband resistive-inductive compensated GaN-HEMT single-FET switch"

In this contribution an analytical approach to the design of constant-isolation microwave resistive-inductive compensated switch operating from DC to 30GHz is presented. Simulated and measured performance of a GaN HEMT single-FET switch cell topology and that of a complete SPDT using the proposed methodology are presented to demonstrate the approach feasibility and effectiveness. The single-FET switch is featured by an isolation of $5.4 \pm 0.5\text{dB}$ over the DC-30GHz band. The resulting SPDT, operating over 2-18GHz band, is featured by 2.7dB insertion loss and isolation better than 25dB all over the operating bandwidth. [C350]

"Design of a high power x-band frequency tripler using a AlGaIn/GaN HEMT device"

An active microwave frequency tripler using an AlGaIn/GaN HEMT device is developed. This is the first reported frequency tripler implemented in GaN technology. Design of the frequency tripler is performed using a high-accuracy, multi-harmonic, wideband model which predicts the effects of self-heating and charge-trapping. A method of determining the optimal load and source networks using harmonic load-/source-pull simulations and synthesizing using harmonic reflectors is described. The tripler upconverts $f_0 = 3.33\text{GHz}$ to 10GHz to achieve a maximum power of +30.0dBm (1.0W). As such, it provides multiplied powers which are approximately 50 times greater than those previously reported. [C351]

"Doherty power amplifier design employing direct input power dividing for base station applications"

For base station applications, -3 dB hybrid coupler has been used for input power dividing stage of Doherty power amplifier (PA). The input direct dividing technique has only been applied for handset applications, because the coupler occupies a large size on a chip. However, this technique provides advantages on power gain and efficiency for base station applications, also. In this paper, we have proposed a design procedure of Doherty PA applying the input direct dividing technique. Implemented Doherty PA using two Cree CGH40045 GaN HEMT achieves excellent drain efficiency of 51.2% at 41 dBm output power for long term evolution (LTE) 1FA signal at 2.14-GHz. Moreover, the Doherty PA could be linearized to -45 dBc using the digital feedback predistortion technique. [C352]

"GaN-on-Si HEMTs above 10 W/mm at 2 GHz together with high thermal stability at 325°C"

In this paper, the possibility to achieve output power density exceeding 10 W/mm at 2 GHz using 1 mm gate width GaN HEMTs on 4" large diameter Si (111) substrate is demonstrated for the first time. Additionally, storage tests at 325°C reveal the high thermal stability of these devices which we attribute to the in-situ grown SiN cap layer. These data are a first step towards a cost-effective high RF power density for high reliability GaN-on-Si HEMT technology. [C353]

"Four-channel Ku-band downconverter MMIC"

A Ku-band downconverter MMIC for satellite reception has been developed. This four channel downconverter contains four dual input LNAs, mixers and IF amplifiers and a single LO balun. The MMIC was designed in the PL15-10 pHEMT InGaAs low noise process of WIN Semiconductors. [C354]

"The effect of baseband impedance termination on the linearity of GaN HEMTs"

This paper demonstrates the significant effect of baseband impedance termination on the linearity performance of a 10W GaN HEMT device driven to deliver a peak envelope power of approximately 40dBm. The paper also proposes a further refinement to a state-of-art active IF load-pull measurement system to allow the precise independent control of all significant baseband components generated as a result of the multi-tone excitation used. The presentation of specific baseband impedances has delivered a 20dBc and 17dBc improvement in IM3 and IM5 inter-modulation products respectively, relative to the case of a classical, ideal short circuit. As expected for this device, this was achieved by emulating appropriate negative impedances lying outside of the Smith chart, and when this observation is considered alongside the Envelope Tracking PA architecture, this raises the interesting possibility of significantly improving PA linearity using the very mechanisms that are employed to improve PA efficiency. [C355]

"A novel design method of highly efficient saturated power amplifier based on self-generated harmonic currents"

A novel design method without requiring the special harmonic termination circuit for a highly efficient power amplifier (PA) is proposed. The proposed PA is driven into saturated operation, from the linear to knee region, by adjusting the only fundamental load, and the saturated operation induces self-generated harmonic currents. The current and voltage waveforms can be shaped easily by the harmonic currents, and efficiency of the PA is maximized. From the proposed design concept, a PA is implemented using 45-W GaN HEMT device at 2.655 GHz. The designed PA has a maximum drain efficiency of 71.5% at a saturated output power of 46.8 dBm for CW signal. The PA can be linearized to -46 dBc using the WDFBPD technique for a mobile WiMAX 2FA signal. [C356]

"Substrate design enabling to increase HEMTs open channel breakdown voltage"

Avalanche-injection inconsistency in a substrate of a device is responsible for the open channel breakdown in FETs. Proposed substrate construction suppresses the advancing of inconsistency in HEMTs. [C357]

"Electrothermal nonlinear FET modeling for spectral prediction"

The origin, mechanisms, and modeling of nonlinearities responsible for spectral spreading are reviewed and discussed. Intermodulation distortion, responsible for spectral spreading, is affected by slow memory effects. Pulsed IV measurements are used to obtain model current equations that have appropriate steady-state quiescent bias dependences related to channel temperature and trap occupancy. Thermal resistance can be measured in silicon devices by using ambient temperature adjustments to measure channel temperature changes due to quiescent self-heating. The presence of trap states in GaN HEMTs makes the assessment of

thermal resistance much more difficult; however, the presence of these effects can be determined by comparing two sets of IV curves taken from quiescent bias points of equal power dissipation. Results are presented showing accurate prediction of third-, fifth-, and seventh-order intermodulation products using an electrothermal model for a power Si MOSFET. [C358]

"GaN solid-state microwave power amplifiers-State-of-the-art and future trends"

The world technical achievements and tendencies in the development of GaN microwave transistors, MMICs and high power amplifiers are considered. The objective of this work is an analysis of state-of-the-art GaN microwave discrete transistors, MMICs and high power (10...100 Watt and more) amplifiers, parameters and basic tendencies in the development of GaN devices. Major properties of wideband gap semiconductors available for microwave transistors are presented in table 1. The highest energy gap, availability of high temperature and high radiation environment, an extremely high density of sheet carrier, higher electric fields and breakdown voltages result in 310 W/mm and more output power density of practical released microwave GaN transistors. Table 2 shows the main parameters of broadband (without internal matching circuits) GaN power transistors. The properties of WCDMA 120 W power transistors (Si LDMOS, GaAs MESFET and GaN HEMT) are compared in table 3. The typical density (for 1 mm gate) of various GaN and GaAs HEMT transistor parameters, including optimal load density, is presented in table 4. Many projects and MMIC topologies, designed for GaAs MMICs might be transferred with minimal corrections into the GaN MMICs based on equal or on (20...50) % wider gate of transistors with x(5-10) corresponding output power (see fig. 1). The main parameters of industrial and laboratory GaN MMIC technologies are presented in table 5, table 6 shows parameters of commercially available and lab released GaN MMICs. Fig. 2 presents the last five years of an evolution of the pulse output power of X-band GaN MMIC amplifiers for future radar systems with phased array. The parameters of the ultra-wideband GaN high power amplifiers up to 6 GHz are presented in table 7, figure 3 shows the chip sizes of the highest power of X-band GaN and GaAs MMIC amplifiers. In the decade ahead (1...50) GHz frequency range will be a topic of arguing between two power microwave technologies. One of them is a high performance and a high cost of GaN technology, the second-low cost and widely used in the industry of GaAs technology. [C359]

"Modelling and design of a wideband 6-18 GHz GaN resistive mixer"

A wideband hybrid AlGaIn/GaN resistive mixer has been designed and simulated. The cold-FET mixer is based on a $2 \times 100 \times 0.25 \mu\text{m}^2$ AlGaIn/GaN HEMT in a single-ended circuit topology. An application-specific empirical transistor model has been extracted and validated in small- and large-signal conditions, in order to carry out the mixer design and simulations. This mixer presents an IF bandwidth of 6 GHz with a conversion loss < 16 dB for each RF and LO frequency choice from 6 up to 18 GHz. [C360]

"A photonic-tunable cryogenically cooled W-band subharmonically-pumped GaAs HEMT diode mixer module"

A W-band subharmonically pumped (SHP) diode mixer module is designed, fabricated and tested for broadband astronomical applications. The packaged module performance is measured and compared under room-temperature and cryogenic environment. In summary, compared to the room-temperature performance, when the SHP diode mixer is operated under cryogenic environment, the LO power requirement is increased by 2 dB and conversion loss is reduced by 3-5 dB. Under cryogenic environment, the effect of red-light illumination to the HEMT Schottky diode is explored, the measured results indicate the existence of excess photocurrent is capable to fine-tune the conversion loss of the mixer. [C361]

"5W, 0.35-8 GHz linear power amplifier using GaN HEMT"

In this paper, a 0.35-8 GHz, 5 W, linear power amplifier based on GaN HEMT die is reported. Load pull characterization was used to optimize the power performance in the operating bandwidth. 3D-EM simulations were also performed to model the coaxial 50 Ohm connections, bond wires and matching networks resulting in an excellent agreement between simulations and measurements. Regarding the performance, the designed single stage PA has exhibited 9 ± 1 dB gain, an output power (P_{out}) of greater than 37 dBm (5 W), worst power added efficiency (PAE) of 20% over a multi-octave (0.35-8 GHz) bandwidth. The PA has been also fully characterized from the linearity point of view based on single-tone (AM/AM, AM/PM) and two-tone techniques (with 100 kHz frequency spacing). An AM/AM and AM/PM distortions of only ± 0.5 [dB/dB] and ± 2 [dB/deg] at 8 GHz have been observed. As a measure of linearity in two-tone performance an output third- and second- order intercept points (OIP3, OIP2) have been extracted over the whole bandwidth. An OIP3 of ≥ 49 dBm and OIP2 of ≥ 67 dBm can be achieved. [C362]

"X-band phase-shifting dual-output balanced amplifier MMIC"

An X-band MMIC containing two 6 bit phase shifters and 1 Watt amplifiers in balanced configuration has been developed. The device has two output ports. The balance between the output powers of the two ports can be controlled via de phase shifter settings. This MMIC could be applied in systems where variable linear polarisation control is required, such as polarimetric radar or satellite communication systems. The MMIC has been developed in the 6-inch 0.5 μm power GaAs pHEMT process (PP50-11) of WIN Semiconductors. [C363]

"An accurate package model for 60W GaN power transistors"

This paper reports on a straightforward yet highly accurate approach to determine a package model for microwave power transistors. The model is based on a lumped-element equivalent circuit for the package, into which compact models for the active transistor cells are embedded. A packaged 60 W GaN-HEMT in FBH technology is used as an example. The device is designed to operate at 2 GHz. The basis of package analysis and modeling is a full 3D emsimulation. From these results, an equivalent circuit is derived and component values are determined analytically. The extraction methodology is not limited to a certain transistor technology or dedicated type of package. The model is verified by measurements and shows very good accuracy up to the third harmonic of the target frequency, i.e., 6 GHz. [C364]

"New fabrication process to manufacture RF-MEMS and HEMT on GaN/Si substrate"

RF-MEMS represent a feasible solution to obtain very low power dissipation and insertion loss, very high isolation and linearity switch respect to solid state technologies. In this paper we demonstrate the possibility to fully integrate the process fabrication of RF-MEMS switches in the GaN-HEMT manufacturing steps to develop a RF-MEMS/MMIC prototype. MEMS RF performance reveals an insertion loss and an isolation respectively better than 0.6 dB and 25 dB in the frequency range 5-50 GHz. Moreover the coexisting HEMT devices show a f_{max} = 40 GHz and 6.5 W/mm density power, demonstrating the integration achievability. [C365]

"A new nonlinear HEMT model for AlGaIn/GaN switch applications"

We present here a new set of equations for modeling the I-V characteristics of FETs, particularly optimized for AlGaIn/GaN HEMTs. These equations describe the whole characteristics from negative to positive breakdown loci, and reproduce the current saturation at high level. Using this model allow reducing the modeling procedure duration when a same transistor topology is used for several applications in a T/R module. It can even be used for switches design, which is the most demanding application in terms of I-V swing. Moreover, a particular care was taken to model accurately the first third orders of the current derivatives, which is important for multitone applications. There are 18 parameters for the main current source (and 6 for both diodes I_{gs} and I_{gd}). This can be compared to the Tajima's equations based Model [1] (13 parameters) or to the Angelov Model (14 parameters) [2], which only fit the I-V characteristics for positive values of V_{ds} . We will detail here the model formulation, and show some measurements/modeling comparisons on both I-V and $[S]$ -parameters obtained for a $8 \times 75 \mu\text{m}$ GaN HEMT. [C366]

"A novel tuning concept for wideband VCOs based on a shunt-FET"

A novel tuning concept for wideband voltage controlled oscillators based on a shunt-FET is presented in this paper. The concept is demonstrated in a fundamental W-Band VCO, operating at 91 GHz with a relative tuning bandwidth of 10 % and an output power of 3.0 plusmn 0.5 dBm. By laser-adjustment of the resonator line length the bandwidth can be increased up to 15.4 %. In this case an output power of -1.6 to 3.3 dBm has been obtained. The phase noise varies from -45.8 to -59.4 dBc/Hz at 100 kHz offset from the carrier frequency over the full tuning range. [C367]

"Broadband AlGaIn/GaN high power amplifiers, robust LNAs, and power switches in L-band"

GaN-based HEMT's have demonstrated better power-frequency performances than other devices using smaller band gap semiconductor materials. Studies have already been realized to evaluate the impact of GaN-based devices at the system level. In this paper, we present the design and the realization of broadband power amplifiers, low noise amplifiers and power switches for future generation of TR-RX modules. These functions are based on the AlGaIn/GaN HEMT technology developed at Alcatel-Thales III-V Lab. [C368]

"GaN MMIC amplifiers for W-band transceivers"

This paper presents W-band monolithic microwave integrated circuit (MMIC) amplifiers with grounded coplanar waveguide (GCPW) in 0.12 μm GaN HEMT technology. A fabricated four-stage low-noise amplifier (LNA) exhibited a record gain of 23 dB at 76.5 GHz and a first reported noise figure (NF) of 3.8 dB at 80 GHz for any W-band GaN MMIC. Another MMIC power amplifier (PA) delivered an output power of 25.4 dBm at 76.5 GHz

with continuous wave (CW) operation. To our knowledge, this is the first demonstration of GaN LNA as well as GaN MMICs with GCPW in the W-band. In addition, a practical design technique to prevent instability of the W-band MMIC is described. [C369]

"X-Band GaN-HEMT LNA performance versus robustness trade-off"

In this paper design, fabrication and test of three X-Band robust LNA MMICs in microstrip GaN technology are presented to better understand the key aspects of performance versus robustness trade-off for said components. In particular LNAs with different number of amplification stages, input device gate peripheries and topologies have been evaluated with the objective of achieving in the 8-11 GHz frequency range a NF better than 2.5 dB, associated gain of circa 20 dB and overdrive power survivability better than 38 dBm. [C370]

"Microwave power performance on AlGaIn/GaN HEMTs on composite substrate"

In this paper, microwave power performance at 10 GHz of HEMTs fabricated on MOCVD and MBE epitaxial structures grown on composite substrates is demonstrated. These substrates, based on monocrystalline-SiC layer on a polycrystalline-SiC (SiCopSiC), are engineered using the Smart Cuttrade technology. They are based on innovative engineering in which a thin SiC single crystal layer is transferred on top of a thick polycrystalline SiC wafer with a thin SiO₂ intermediary insulating layer. The process used for the devices fabrication on SiCopSiC is quite similar to those on SiC monocrystalline bulk developed previously. High power density was measured on both epi-materials at 10 GHz. Regarding the power results for the components based on MOCVD epi-material, the best value is an output power density of 5.06 W/mm associated to a PAE of 34.7% and a linear gain of 11.8 dB at VDS= 30 V. In the frame of the MBE epilayer, the output power density is 3.58 W/mm with a maximum PAE of 25% and a linear gain around 15 dB at VDS= 40 V. [C371]

"Two-tier L-L de-embedding method for S-parameters measurements of devices mounted in test fixture"

By using an indirect method for determining the characteristic impedance of uniform transmission lines embedded in coaxial connectors, a novel two tier L-L de-embedding method is presented. The proposed de-embedding method is suitable for S parameters characterization of GaN HEMTs packaged transistors mounted on a symmetrical and reciprocal test fixture. In addition, the new technique does not presents the limitation exhibited by the Thru-Reflect-Line (TRL) in the low frequency range nor the limitation exhibited by the Thru-Reflect-Match (TRM) in the high frequency range. To validate the new two tier L-L de-embedding method, the S-parameters of a packaged GaN HEMT de-embedded with TRL are used. The good agreement between the DUT S-parameters obtained with both techniques, L-L and the TRL, validates the proposed L-L de-embedding method. [C372]

"Influence of GaN cap on robustness of AlGaIn/GaN HEMTs"

DC-Step-Stress-Tests of GaN HEMTs have been performed on wafers with and without GaN-cap. The tests consist of a step ramping of drain-source voltage VDSby 5 V every two hours at off-state. The irreversible evolution of leakage current starting at a certain drain voltage has been taken as a criterion for the onset of device degradation. It has been stated that there is a stability limit for VDSdepending on the epitaxial design. It has been found that wafers with GaN cap show much higher critical voltages as compared to non-capped epitaxial designs. Electroluminescence measurements have been performed to localize defects after DC-Step-Stress-Tests up to 80 V for wafer without GaN cap and 120 V for wafer with GaN cap. [C373]

"Study of Cl₂/BCl₃ inductively coupled plasma for selective etching of GaAs"

Inductively coupled plasma (ICP) etching has been replacing conventional reactive ion etching (RIE) for GaAs backside via etching to provide low inductance grounding in microwave devices like HEMT and MESFET. ICP tools provide higher throughput with faster etch rates in addition to better dimensional control, repeatability and reproducibility. Generally reported etch depths using ICP for via-hole etching applications in GaAs Monolithic Microwave Integrated Circuits are < 200μm using photoresist mask due to lower etch rate and poor mask selectivity. In this study, we are reporting the ICP etching of 60μm diameter via-holes for etch depth ~ 200μm, on 3-inch GaAs wafer with photoresist mask using Cl₂/BCl₃ gases. ICP process parameters like pressure and platen power were varied at a fixed ICP coil power to achieve an etch depth ~ 200μm at a relatively very high etch rate with good etch surface morphology. The etch rate, etch depth, etch profile and surface morphology of etched holes were determined using scanning electron microscope. The average etch rate decreased rapidly with time, from 7μm/min for 10 minute of etching to 3.9μm/min for 45 minutes of etching on 3-inch GaAs wafer, mainly due to increased depth. Whereas etch rate increased with the increase in process pressure due to increased density of reactive species but anisotropy is maintained, as independent ion

energy control is provided by RF biasing of the wafer platen in ICP systems. High etch rates $\sim 4.4 \mu\text{m}/\text{min}$ are obtained at 40mTorr pressure for an etch time of 45 minutes. Increasing platen power from 65W to 90W at pressure 30mTorr has resulted in reduction of etch rate from 3.9 $\mu\text{m}/\text{min}$ to 3.6 $\mu\text{m}/\text{min}$, probably due to increased physical etching component at 90W. The best mask selectivity obtained was $>12:1$. [C374]

"False surface-trap signatures induced by buffer traps in AlGaIn-GaN HEMTs"

Buffer traps can induce surface-trap signatures in AlGaIn-GaN HEMTs, namely the same type of current-mode DLTS peaks and pulse responses that are generally attributed to surface traps. Device simulations are adopted to clarify the underlying physics. Being aware of the above phenomenon is important for both reliability testing and device optimization, as it can lead to erroneous identification of the degradation mechanism, thus resulting in inappropriate correction actions on the technological process. [C375]

"Physical mechanism of buffer-related lag and current collapse in GaN-based FETs and their reduction by introducing a field plate"

Two-dimensional transient analysis of field-plate AlGaIn/GaN HEMTs and GaN MESFETs is performed, considering a deep donor and a deep acceptor in the semiinsulating GaN buffer layer. Quasi-pulsed I-V curves are derived from the transient characteristics. It is studied how the existence of a field plate affects buffer-related drain lag, gate lag and current collapse. It is shown that in both FETs, the drain lag is reduced by introducing a field plate, because electron injection into the buffer layer is weakened by it, and trapping effects are reduced. It is also shown that the buffer-related current collapse and gate lag are reduced in the field-plate structures. The dependence on SiN passivation layer thickness under the field plate is also studied, suggesting that there is an optimum thickness of the SiN layer to minimize buffer-related current collapse and drain lag in GaN HEMTs and MESFETs. [C376]

"Modeling considerations for GaN HEMT devices"

The success of simulation-based design of power amplifiers for wireless communications is limited by the accuracy of nonlinear models that are used to represent the transistors. This paper provides some considerations that should be taken into account in measurement-based modeling of GaN transistors. With GaN modeling, particular attention needs to be paid to thermal and trapping issues. The use of pulsed measurements as part of the modeling process is critical to obtaining reliable GaN models. Established models such as EEHEMT, Angelov, and CFET can be successfully used in representing GaN devices. [C377]

"Improving performance in single field plate power High Electron Mobility Transistors (HEMTs) based on AlGaIn/GaN"

In this paper we have investigated the effectiveness of employing the single field-plate (SFP) technique to enhance the breakdown voltage (BV) of AlGaIn/GaN power high electron mobility transistors (HEMTs). A systematic procedure is provided for designing the SFP device, using two dimensional (2-D) simulation to obtain the maximum improvement in the drain-source current (IDS) and to achieve maximum breakdown voltage. It is found that significantly higher breakdown voltages and IDS can be achieved by just raising the thickness of the passivation layer Si₃N₄ beneath SFP (t) and raising SFP length (L_{sfp}) between the source and drain. We demonstrate that when a single field-plate connected to the source is employed, both breakdown voltage and IDS can be enhanced by optimizing the passivation layer Si₃N₄ thickness beneath the SFP as well as the SFP geometry. [C378]

"AlGaIn/GaN HEMT temperature-dependent large-signal model thermal circuit extraction with verification through advanced thermal imaging"

Investigation has been done on procedure, development and verification of a large-signal, temperature-dependent model for aluminum-gallium-nitride/gallium-nitride (AlGaIn-GaN) high-electron-mobility transistors (HEMTs). Procedural issues have been designed to investigate model selection based on application and operation over varying bias. Theoretical and experimental analysis has been completed on device operating point selection in measurement and modeling to account for thermal coefficient extraction and RF dispersion effects. The model has been optimized for use in power amplifier design applications that apply class AB operation. Advanced thermal imaging verification has been performed to validate thermal resistance modeling parameters. [C379]

"10W GaN inverse class F PA with input/output harmonic termination for high efficiency WiMAX transmitter"

This paper presents the design of a multi-harmonic terminated inverse class F (class F-1) power amplifier (PA) using empirical load-pull technique for a 10 W GaN device operating at 2.5 GHz. The paper discusses important design parameters impacting the final PA performance. Detailed design procedures based on load-pull, impedance locations, and waveform analysis are presented. The impact of source harmonic tuning on overall power added efficiency as well as matching network design considerations are discussed. The fabricated class F-1PA achieved power added efficiency (PAE) of 73.5% with an output power of 41.04 dBm at 27 dBm input power. [C380]

"10 W Class AB power amplifier design for UMTS applications using GaN HEMT"

This paper exhibits a 10 W class AB highly linear power amplifier (PA) for a frequency of 2.14 GHz using GaN HEMT. Power and linearity measurements and simulations illustrate stupendous correspondence. An output power of 11 W (41 dBm) with maximum drain efficiency (η) of 72 % (PAE 56 %) is achieved. Linearity measurements were made with a frequency spacing of 100 KHz and output third-order and second-order intercept points (OIP3 and OIP2) were observed to be 48 dBm and 80 dBm respectively. [C381]

"An analytical expression for the I-V characteristics of AlGaIn/GaN HEMTs"

In this paper an analytical expression for the current-voltage (I-V) characteristics of AlGaIn/GaN HEMTs is presented. Two functions are suggested to model the dependence of the voltage parameter on drain voltage. The resultant I-V relationship incorporates the 2DEG sheet carrier concentration and mobility product. It also includes the effect of source and drain resistances. The obtained analytical relationship helps speeding up the I-V calculations meanwhile, keeping it simple and accurate. Due to its simplicity, it is ideally suited for circuit simulation purposes. The validity of the I-V results was tested and satisfactory results were obtained over a wide range of bias voltages. [C382]

"Design of a 2.2 GHz high efficiency GaN HEMT inverse class E transmission-line power amplifier"

This paper reports on the design and measurements of an inverse class E transmission-line power amplifier using a newly fabricated GaN HEMT device, NTPB0025. This amplifier was designed according to the inverse class E lumped prototype using load-pull optimizations. After that, the lumped amplifier was transformed to a transmission-line realization. The drain efficiency of 64%, PAE of 57.7%, and the output power of 41.5 dBm were measured at 2.2 GHz. [C383]

"Influence of the Al mole fraction on microwave noise performance of Al_xGa_{1-x}N/GaN HEMTs"

To reveal the influence of Al mole fraction on the microwave noise performance of Al_xGa_{1-x}N/GaN HEMTs, numerical analysis is performed on the intrinsic noise by reducing its value from 35% to 25% and 15% in this paper. A model based on measurement results is used and simulations are carried out by commercial TCAD soft Silvaco Atlas. The I-V curves and both of the gate and drain noise spectral density are calculated and compared at different bias. The results show that the reduction of the Al mole fraction degrades the intrinsic microwave noise behavior of HEMT's only at high bias currents due to the poor carrier confinement. The AlGaIn/GaN HEMTs with 25 % Al content has the best minimum noise figure (F_{min}) at low bias currents due to the reduction of gate noise, and it has the same F_{min} with 35% at a few higher bias current. [C384]

"A new concept of an ultra fast pulse picker for fs- and ps-pulses from GHz pulse-trains with semiconductor tapered elements"

In this paper, we present a new concept for an ultra fast pulse picker, consisting of a tapered diode amplifier and a high-speed high-current transistor switch. The transistor switch is realized using a GaN high-electron mobility transistor (HEMT), which offers low parasitic capacitances and high current capabilities together with high switching speed. Moreover, the SiC transistor substrate gives rise to an excellent thermal conductivity thus allowing for high duty cycles. The tapered diode amplifier (TDA), on the other hand, consists of a 2000μm long ridge waveguide section (RW) and a 2000μm long tapered section (TP) with a tapered angle of 4deg for the wavelength range 900-950nm. The RW section is driven by the transistor switch with short current pulses, which modulate the transparency properties. Thus, if the RW section is transparent, an injected optical pulse can pass and is amplified in the tapered section, otherwise all optical pulses will be absorbed. [C385]

"Terahertz plasmons in grating-gate AlGaIn/GaN HEMTs"

Plasma excitations in high-electron mobility transistors (HEMTs) with two-dimensional (2D) electron channels can be used for detection, mixing, and generation of terahertz (THz) radiation. Plasmon modes excited in the HEMT channel under the gate contact (gated plasmons) were considered to be more attractive for electronic

applications because their frequencies can be effectively tuned by varying the gate voltage. However, the gated plasmons are difficult to couple to THz radiation due to acoustical nature and, hence, a small net dipole moment of this plasmon mode. Hence, special antenna elements are needed to couple the gated plasmons to THz radiation. As an alternative, a grating gate in a large area (comparable with a typical cross-section area of THz beam) HEMT structure can act as an aerial matched antenna strongly coupling the plasmons to THz radiation. It was shown recently that a large-area grating-gate GaAs/AlGaAs structure can operate as an electrically tunable detector in sub-THz frequency range. A double-grating-gate HEMT structure with lateral dimensions smaller than THz wavelength was used as an effective THz photomixer and emitter. [C386]

"AlGaIn/GaN HEMT device structure optimization design"

A novel Composite-Channel Al_xGa_{1-x}N/Al_yGa_{1-y}N/ GaN HEMT is designed and optimized. The influence of two-dimensional electron gas and electric field on device structure parameter is obtained from the self-consistent solution basing on theory of semiconductor energy band and quantum well. The influence of the layer structure of the device on its performance is obtained from simulation of TCAD software. Combining with results of theory analysis and simulation results, the optimization structure Al_{0.31}Ga_{0.69}N/-Al_{0.04}Ga_{0.96}N/GaN HEMT is proposed. The simulation results show that the device with gate length of 1 μm and gate width of 100 μm has the maximum transconductance of 300 mS/mm and the little fluctuation in the gate voltage from -2V to 1V that shows the excellent linearity of the device, the maximum current density of 1300 mA/mm, the cut-off frequency of 11.5 GHz and a maximum oscillation frequency of 32.5 GHz. [C387]

"Study and design of high efficiency switch mode GaN power amplifiers at L-band frequency"

Activities have been carried out to determine the best electrical operating conditions of GaN HEMT that enable maximum power added efficiency at L-band for switch mode power amplifiers (class F, inverse class F and class E). Satellite radio navigation applications (Galileo) are targeted. Maximization of power added efficiency is of prime importance to save DC power consumption, reduce self heating effects and improve reliability of power amplifiers. At 50V drain bias, a maximum power added efficiency (PAE) of 72% and 40.3 dBm output power (P_{out}) are obtained using class-F operating conditions at 2dB gain compression while a 75% PAE and 41.0 dBm P_{out} are obtained using class E at 3dB gain compression. [C388]

"Real-time FPGA-based baseband predistortion of W-CDMA 3GPP high-efficiency power amplifiers: Comparing GaN HEMT and Si LDMOS predistorted PA performances"

We carry out a comparative design study on two high-efficiency power amplifiers (a second-harmonic tuning LD-MOS and a Doherty GaN-based amplifier) linearized through baseband digital predistortion so as to comply with the W-CDMA 3GPP standard with acceptable efficiency. Several predistortion schemes (both memoryless and with memory) were tried, having in mind the final FPGA implementation. The results, besides highlighting some interesting features of the two amplifiers considered, show that significant improvements can be achieved in the Power Added Efficiency (PAE) even starting from a highly efficient but poorly linear power stage. [C389]

"Optimum bias for highly linear and efficient doherty power amplifier with memoryless digital predistortion"

This paper investigates the optimum bias to achieve a highly efficient and linear Doherty power amplifier (DPA) with memoryless digital predistortion (DPD). The DPA is implemented using 25-W GaN HEMTs. The PAE of 54.5% is achieved at an output power of 40 dBm for a 2.14-GHz continuous wave. The bias optimization and memoryless DPD are employed to improve the linearity of the DPA. The 11th-memoryless polynomial and recursive least square algorithm are used to implement the memoryless DPD. For a one-carrier WCDMA signal at an output power of 36 dBm, the adjacent channel leakage ratio at ±5-MHz offset are below -48 dBc with the drain efficiency of 40% after the linearization with the optimum bias. [C390]

"A 7 GHz FBAR overtone-based oscillator"

Film bulk acoustic wave resonators (FBARs) prove to be good candidates for designing low-power oscillators in the low-GHz frequency region. To boost the use of FBAR resonators to higher frequencies, we demonstrate an oscillator that uses an overtone frequency of the FBAR. A 7 GHz oscillator is built on a PCB using a commercial pHEMT transistor as an active element and surface mounted passive components. The FBAR is wire bonded to the PCB. The measured phase noise of -110 dBc/Hz at 1MHz offset. To the author's knowledge this circuit is the first realized FBAR overtone-based oscillator on PCB. [C391]

"S-band discrete and MMIC GaN power amplifiers"

The use of GaN devices for microwave power amplifiers begins to be a reality in Europe. This paper describes two S-band (2.7-3.3 GHz) high power amplifier (HPA) designs; one discrete 100 W output stage and one 10 W MMIC power amplifier. The discrete power amplifier is designed using two GaN power bars with a total gate width of 19.2 mm. The GaN power bars have been developed by Selex-SI, within the European co-project Korrigan. The MMIC power amplifier was designed using a 0.25 μm GaN HEMT process supplied and processed by Chalmers. [C392]

"Systematic investigation of the impact of harmonic termination in the efficiency performance of above octave bandwidth microwave amplifiers"

The importance of harmonic terminations in achieving high-efficiency operation in narrow band (NB) amplifiers has been widely published. In Wide Bandwidth (WB) applications however, the emphasis has been on maintaining a broadband match at the fundamental frequencies with little regard to the harmonic impedances. The problem is further complicated by the fact that the harmonics of the lower frequencies often fall within the operational bandwidth of the amplifier. This paper presents an active load-pull technique for measuring and quantifying the impact of harmonic impedance on device performance, and is achieved through the characterisation of a class A biased 0.3 μm GaAs pHEMT SW device at 6, 12 and 18 GHz. [C393]

"New fabrication process to manufacture RF-MEMS and HEMT on GaN/Si substrate"

RF-MEMS represent a feasible solution to obtain very low power dissipation and insertion loss, very high isolation and linearity switch respect to "solid state" technologies. In this paper we demonstrate the possibility to fully integrate the process fabrication of RF-MEMS switches in the GaN-HEMT manufacturing steps to develop a RF-MEMS/MMIC prototype. MEMS RF performance reveals an insertion loss and an isolation respectively better than 0.6 dB and 25 dB in the frequency range 5-50 GHz. Moreover the coexisting HEMT devices show a $f_{\text{max}}=40$ GHz and 6.5 W/mm density power, demonstrating the integration achievability. [C394]

"Wide band high linearity and high isolation mixer MMIC developed on GaAs 0.25 μm power pHEMT technology"

In the frame of radar and warfare applications, a monolithic microwave integrated circuit (MMIC) mixer has been developed using a UMS GaAs 0.25 μm power pHEMT technology. The mixer presented in this document exhibits at the same time wide frequency band, high isolation and high linearity. In the 6-18 GHz frequency band, the mixer demonstrates 25 dB for the isolations, an input RF compression point higher than 16 dBm and an input IP3 of 25 dBm. To our knowledge these performances are among the highest reported on a fully integrated GaAs MMIC. [C395]

"Power amplifier memory-less pre-distortion for 3GPP LTE application"

A new and simple power amplifier (PA) linearization method is proposed and demonstrated using a very high efficiency yet inherently nonlinear inverse class-F PA. This was conducted in the presence of a generic variable envelope RF signal in order to extract its AM-AM and AM-PM characteristics. Deducing the polynomial pre-distortion parameters from the AM-AM and AM-PM characteristic has resulted in the successful linearization of the PA in the presence of 3GPP long term evolution (LTE) signals. The results obtained for the PA-a 12 W GaN HEMT inverse class-F structure designed to operate at 900 MHz-demonstrate the proof of concept and the efficiency of the proposed linearization technique with significant advantageous reduction in base-band resources for 3GPP LTE applications. [C396]

"A simplified switch-based GaN HEMT model for RF switch-mode amplifiers"

A simplified switch-based model is proposed for GaN-HEMTs, which is suitable for the design of switch-mode-type amplifiers, in both time and frequency domain. The model is validated using a current-mode class-S circuit, for signals up to 5 Gbps. This amplifier structure allows to check two important characteristics of this model: its capabilities to operate as a switch between two digital states and the broadband capabilities. Though much simpler than the conventional nonlinear HEMT models the simplified model shows very good agreement with measurements and excellent stability in time-domain simulations. [C397]

"Pulsed operation and performance of commercial GaN HEMTs"

The present study investigates the behaviour and performance of commercially available GaN HEMTs provided by Cree Inc. The gain and power variations at pulse repetition frequencies (PRFs) in the range 100-400 kHz are presented. Rise and fall times are also investigated at different PRFs and power levels. The pulsed RF waveforms are obtained by switching the gate bias of the transistor on and completely off to ensure that the

device goes through full transients for every pulse. The RF frequency at which the study is conducted is 3.5 GHz. The aim of the study is to assess the suitability of commercial GaN HEMTs to pulsed RF applications such as Radar. [C398]

"Gate technology and substrate property influence on GaN HEMT switch device performance"

This work illustrates a study on GaN HEMT switch RF performances dependence on material and fabrication technology. For said study different gate technologies has been fabricated on the same wafer and successively characterized, and for a fixed gate geometry (T-Gate) different substrate properties have been evaluated. In particular switch transistor performances in terms of off-state isolation, on-state insertion loss, and associated power handling, have been related to differences in gate technologies and material properties. The results of this study indicate that for fixed gate peripheries and device switching times, key parameters such as COFF can be appreciably improved by the adoption of an optimized GaN Fe doped buffer wafer and metal-insulator-semiconductor gate technology. The same MIS-gate device can also provide up to 1.5 dB higher input power on-state insertion loss 1 dB compression. [C399]

"RF degradation of GaN HEMTs and its correlation with DC stress and I-DLTS measurements"

The reliability of GaN HEMTs under RF stress has been evaluated and correlated with DC stress and current DLTS measurements techniques. During RF operation a degradation of output power, PAE and an increase in reverse gate current has been observed. A similar degradation has been observed by applying reverse biases to the gate terminal under DC operation, resulting in an increase in drain current-collapse as well as in the gate reverse current. DLTS measurements showed that the physical mechanisms involved in the RF- and DC-degradation are the same and that can be related to a defect which is thermally activated with an energy of 0.5 eV. The strong correlation between RF- and DC-stress results suggests that the RF degradation is related to the formation of localized defects at the gate contact. These defects degrade device performances by increasing both drain current collapse and reverse gate current. [C400]

"Wafer Scale Package construction and usage for RF through millimeter wave applications"

WSP (wafer scale packaging) has come on the market for commercial applications in 2008. But how is a WSP constructed and what are its advantages over traditional surface mount techniques? This paper explores how WSP is applied to traditional GaAs PHEMT wafer manufacture as implemented by Avago Technologies in the first volume commercial offering of WSP in 2008. The paper details the general construction and advantages of WSP over plastic, laminate, and ceramic alternate solutions. These advantages include cost, microwave performance, thermal conductance, and size. Detailed examples are shown of products on the general market today and future developments in package and component design. [C401]

"Efficiency enhancement of GaN power HEMTs by controlling gate-source voltage waveform shape"

This paper presents a technique to improve the power added efficiency (PAE) of GaN power amplifiers by an appropriate shaping of the gate source voltage waveform. The proposed technique is based on second harmonic injection at the transistor input. It is applied here to a 15 W GaN HEMT die from Cree that has been characterized using an harmonic load pull test bench at L-band. The work reported here focuses on experimental gate-source voltage waveform shaping and its impact on PAE performances. An original aspect concerns calibrated time domain waveform measurements and shaping that are performed and investigated simultaneously at both input and output ports of the transistor under test close to intrinsic accesses. Measurement results performed at 2 GHz validate optimized operating conditions derived from theoretical analysis and circuit simulations. For a fixed input bias voltage (close to pinch off voltage in our case), significant efficiency improvements are obtained when the positive half wave of the gate-source voltage is sharpened. Best and worst cases are examined respectively and show 25 point PAE difference at saturated power. [C402]

"Broadband AlGaIn/GaN high power amplifiers, robust LNAs, and power switches in L-Band"

GaN-based HEMT's have demonstrated better power-frequency performances than other devices using smaller band gap semiconductor materials. Studies have already been realized to evaluate the impact of GaN-based devices at the system level. In this paper, we present the design and the realization of broadband power amplifiers, low noise amplifiers and power switches for future generation of TR-RX modules. These functions are based on the AlGaIn/GaN HEMT technology developed at Alcatel-Thales III-V Lab. [C403]

"200W discrete GaN HEMT power device in a 747mm CMC package"

This paper presents the development of high power AlGaIn/GaN HEMTs on GaN/SiC epi-materials in MACOM Technology Solutions. Instead using state-of-the-art via-hole technology popular in the GaN HEMT industry to have the common-source on the device bottom, our source-contact is designed on the device top-surface for enhancing its surface thermal dissipation as well as achieving variable input and output inductance. The effects of various layout design and fabrication processes on the device performance as well as thermal resistance were studied. It showed that the gate-pitch was scaled up from 29 to 42 μm for optimal device performance with increasing the unit gate width from 125 to 200 μm . A similar thermal resistance of 1.38degC/W was observed for these two designs. A 25 mm total gate-periphery single chip packaged in a 7times3.5 mm CMC package showed 120 W (4.8 W/mm) P1dB and 130 W (5.2 W/mm) P2dBCW output at 2 GHz, 10.5 dB liner gain and 58% drain efficiency with a drain bias of 36 V. A single chip with a 7times7 mm larger package is in processing with an expected power of 200 W CW at 1.85 GHz and 14 dB liner gain. [C404]

"X-band GaN-HEMT LNA performance versus robustness trade-off"

In this paper design, fabrication and test of three X-Band robust LNA MMICs in microstrip GaN technology are presented to better understand the key aspects of performance versus robustness trade-off for said components. In particular LNAs with different number of amplification stages, input device gate peripheries and topologies have been evaluated with the objective of achieving in the 8-11 GHz frequency range a NF better than 2.5 dB, associated gain of circa 20 dB and overdrive power survivability better than 38 dBm. On-wafer measurements of LNA performance and robustness have been carried out in order to evaluate the incident power failure mechanisms and to individuate the best design approach for optimum performance/robustness trade-off. With one of the three LNA designs a NF < 2dB, Gassof 20 dB and P1dB > 15 dBm has been achieved in the entire 8-11 GHz bandwidth. Said MMIC can withstand a 39 dBm CW input power without any observable performance degradation. [C405]

"Device inherent IMD reproducibility issues in GaN HEMTs"

This paper stresses on critical requirements for characterizing device inherent intermodulation distortion (IMD) products in power HEMTs for 3G wideband applications. An accurate broadband RF testbench is essential for reliable nonlinearity measurements. With the optimized IMD characterization testbench, the reproducibility of sweet-spot behavior in GaAs and GaN HEMT technologies has been investigated. This involved statistical process consistency evaluation of GaAs and GaN HEMT semiconductor technologies in terms of their respective pinch-off voltages characterizing sufficient device samples. Corresponding influence on the nature of sweet-spot repeatability under two-tone and multi-carrier WCDMA stimuli revealed the importance of IF load termination. [C406]

"X-band phase-shifting dual-output balanced amplifier MMIC"

An X-band MMIC containing two 6 bit phase shifters and 1 Watt amplifiers in balanced configuration has been developed. The device has two output ports. The balance between the output powers of the two ports can be controlled via de phase shifter settings. This MMIC could be applied in systems where variable linear polarisation control is required, such as polarimetric radar or satellite communication systems. The MMIC has been developed in the 6-inch 0.5 μm power GaAs pHEMT process (PP50-11) of WIN Semiconductors. [C407]

"A 300 GHz active frequency-doubler and integrated resistive mixer MMIC"

An active frequency-doubler MMIC achieving an output frequency of 300 GHz and its monolithic integration with a 300 GHz resistive mixer is presented. The frequency-doubler provides a broadband source with an average output power of -9.5 dBm and better than 10 % conversion efficiency in the frequency range from 250 to 310 GHz. At 300 GHz, a non-saturated output power of -6.4 dBm is measured at an input power of 1 dBm. A 300 GHz down-conversion mixer MMIC, combining the frequency-doubler with a resistive mixer, achieves a conversion loss of 20 dB in the RF range from 246 to 300 GHz. Both MMICs are realized in a metamorphic HEMT technology with 50 nm gate-length. [C408]

"A 200 GHz active heterodyne receiver MMIC with low sub-harmonic LO power requirements for imaging frontends"

This paper presents the design and performance of a 200 GHz, sub-harmonically-pumped, heterodyne receiver MMIC realized in 100 nm metamorphic HEMT technology. The lownoise amplifier stage sets the receiver noise figure to 7 dB and, in combination with the resistive down-conversion mixer, allows for an overall conversion gain of 7 dB at 200 GHz RF frequency. The mixer LO port is driven by a frequency doubler and buffer amplifier stage. We use an integrated LO driver amplifier stage with two parallel cascode amplifiers to achieve the operation of the circuit with as low as -13 dBm LO power provided at 100 GHz, thus making the receiver MMIC

suitable for multichannel imaging frontends. [C409]

"A linearity improved GaAs pHEMT power amplifier using common-gate/common-source circuit topology"

A power amplifier using the common-gate (CG)/common-source (CS) circuit topology to implement the linearity improvement technique has been designed and implemented in 0.15 μm GaAs pHEMT technique for WLAN/WiMAX applications. The simulation analysis reveals that the CG circuit provides the characteristics of gain and phase compensation to improve the nonlinearity of CS circuit. Combining the CG circuit with CS amplifier can achieve the low signal distortion without consuming dc power and losing the signal gain, while operating at high output power. The power amplifier including the on-chip input/output matching networks is performed in Class-AB operation with a quiescent current of 320 mA and a linear gain of 16 dB under a 5.5 V dc supply. The amplifier also exhibits the power performances of the 1-dB compression point and the saturation power are 27.5 dBm and 29.5 dBm, containing the maximum power-added efficiency (PAE) up to 25 %. With the two-tone intermodulation distortion (IMD) testing, the measured IMD3 is close to -35 dBc under an output power of 25 dBm. [C410]

"S-band discrete and MMIC GaN power amplifiers"

The use of GaN devices for microwave power amplifiers begins to be a reality in Europe. This paper describes two S-band (2.7-3.3 GHz) high power amplifier (HPA) designs; one discrete 100 W output stage and one 10 W MMIC power amplifier. The discrete power amplifier is designed using two GaN power bars with a total gate width of 19.2 mm. The GaN power bars have been developed by Selex-SI, within the european co-project Korrigan. The MMIC power amplifier was designed using a 0.25 μm GaN HEMT process supplied and processed by Chalmers. [C411]

"Comparison of enhancement- and depletion-mode triple stacked power amplifiers in 0.5 μm AlGaAs/GaAs PHEMT technology"

This paper describes triple stacked power amplifiers using 0.5 μm enhancement- and depletion-mode (E/D-mode) AlGaAs/GaAs pseudomorphic high electron-mobility transistors (PHEMTs). Based on the optimum capacitance at the gate termination of common-gate (CG) transistor, the output 1-dB compression points (P1dB) of the E- and D-mode triple stacked power amplifiers are 22.1 and 19.3 dBm, respectively. The third-order output intercept point (OIP3) of the E- and D-mode stacked power amplifiers are higher than 32 and 25 dBm, respectively. The E-mode stacked power amplifier demonstrates better output power and linearity as compared with the D-mode stacked power amplifier due to the device characteristics. Moreover, the comparison between the E- and the D-mode stacked power amplifiers is also presented. [C412]

"Modelling and design of a wideband 6-18 GHz GaN Resistive Mixer"

A wideband hybrid AlGaIn/GaN Resistive Mixer has been designed and simulated. The cold-FET mixer is based on a $2 \times 100 \times 0.25 \mu\text{m}^2$ AlGaIn/GaN HEMT in a single-ended circuit topology. An application-specific empirical transistor model has been extracted and validated in small- and large-signal conditions, in order to carry out the mixer design and simulations. This mixer presents an IF bandwidth of 6 GHz with a conversion loss < 16 dB for each RF and LO frequency choice from 6 up to 18 GHz. [C413]

"Study of ohmic contact formation on AlGaIn/GaN HEMT with AlN spacer on silicon substrate"

This paper deals with the analyse of ohmic contact formation on GaN, AlGaIn/GaN and AlGaIn/AlN/GaN. TEM measurement was carried out on these last structures to explain the ohmic contact formation for Ti and Ti/Al contact. The difficulties to achieve an ohmic contact on AlGaIn/AlN/GaN structures leads to etch the AlGaIn barrier to obtain rapidly and easily an ohmic behaviour. At last, it is shown that TLM and TLTL are necessary to characterise the ohmic contact when an alloy is formed under the metallisation. In this case, the transport is governed by tunnel effect assisted by field effect (FE) via deep levels. [C414]

"Efficiency enhancement of GaN power HEMTs by controlling gate-source voltage waveform shape"

This paper presents a technique to improve the power added efficiency (PAE) of GaN power amplifiers by an appropriate shaping of the gate source voltage waveform. The proposed technique is based on second harmonic injection at the transistor input. It is applied here to a 15 W GaN HEMT die from Cree that has been characterized using an harmonic load pull test bench at L-band. The work reported here focuses on

experimental gate-source voltage waveform shaping and its impact on PAE performances. An original aspect concerns calibrated time domain waveform measurements and shaping that are performed and investigated simultaneously at both input and output ports of the transistor under test close to intrinsic accesses. Measurement results performed at 2 GHz validate optimized operating conditions derived from theoretical analysis and circuit simulations. For a fixed input bias voltage (close to pinch off voltage in our case), significant efficiency improvements are obtained when the positive half wave of the gate-source voltage is sharpened. Best and worst cases are examined respectively and show 25 point PAE difference at saturated power. [C415]

"Characterizing drain current dispersion in GaN HEMTs with a new trap model"

Dispersion in a GaN HEMT, including gate and drain lag, is related to a new trapping model based on SRH theory. The model is used to explain the bias- and terminal-potential dependency of the turn-on transients and their time constants. Because the time constants are extremely long they impact the measurement of true dc characteristics and contribute to knee walk-out. Temperature as a function of time is shown to be a vital consideration. The models of both drain current and trapping need to consider temperature and power dissipation versus time. The relationship between trap potentials and terminal potentials is investigated. [C416]

"High-efficiency GaN HEMT power amplifier design based on inverse class-e topology"

This paper reports a high-efficiency GaN HEMT power amplifier (PA) based on the inverse class-E topology. The parasitic inductance and large output capacitance of the packaged active device are used as the series inductance and compensated by a shunt inductor, respectively. The composite right/left-handed transmission line is used as a harmonic control network. For the experimental validation, an inverse class-E PA is designed using a GaN HEMT and tested with a continuous wave at 1 GHz. From the measured results, the power-added efficiency (PAE) of 78.8% with a gain of 19.03 dB is achieved at an output power of 41.03 dBm. [C417]

"40 to 85GHz power amplifier MMICs using an optical lithography based low cost GaAs PHEMT process"

An optical photo lithography based 0.15 μm GaAs PHEMT process and 2mil-substrate technology that enables high production throughput and low cost is described. The developed process achieved $I_{\text{max}}=575 \text{ mA/mm}$, $BV_{\text{gd}}=14 \text{ V}$, and 753 mW/mm of output power density at P-1 condition at 18 GHz. Design and test results for balanced and single-ended power amplifiers (PA) for 40 to 85 GHz applications are described as process capability verification. Balanced PA MMICs shows 18 dB of small-signal gain and 17 dBm of output power up to 85 GHz frequencies. MMIC test results verified the process capability to manufacture MMIC devices for applications up to 90 GHz. [C418]

"GaN MMIC amplifiers for W-band transceivers"

This paper presents W-band monolithic microwave integrated circuit (MMIC) amplifiers with grounded coplanar waveguide (GCPW) in 0.12 μm GaN HEMT technology. A fabricated four-stage low-noise amplifier (LNA) exhibited a record gain of 23 dB at 76.5 GHz and a first reported noise figure (NF) of 3.8 dB at 80 GHz for any W-band GaN MMIC. Another MMIC power amplifier (PA) delivered an output power of 25.4 dBm at 76.5 GHz with continuous wave (CW) operation. To our knowledge, this is the first demonstration of GaN LNA as well as GaN MMICs with GCPW in the W-band. In addition, a practical design technique to prevent instability of the W-band MMIC is described. [C419]

"Characterizing drain current dispersion in GaN HEMTs with a new trap model"

Dispersion in a GaN HEMT, including gate and drain lag, is related to a new trapping model based on SRH theory. The model is used to explain the bias- and terminal-potential dependency of the turn-on transients and their time constants. Because the time constants are extremely long they impact the measurement of true dc characteristics and contribute to knee walk-out. Temperature as a function of time is shown to be a vital consideration. The models of both drain current and trapping need to consider temperature and power dissipation versus time. The relationship between trap potentials and terminal potentials is investigated. [C420]

"InP, W-band, oscillator stabilized with a resonant cavity created by Wafer Level Packaging"

In this paper a W-band oscillator using Wafer Level Packaging (WLP) technology is reported. To the best of the authors' knowledge this is the first oscillator using a stabilizing cavity resonator created through the use of WLP. By using WLP a cavity consisting of more than one substrate can be created. Since quality factor is directly proportional to volume, a cavity of larger volume will lend itself to a better quality factor. In this work, a 2 finger 40 μm device fabricated in Northrop Grumman Aerospace Systems' (NGAS) 0.1 μm InP HEMT technology is

combined with a stabilizing resonant cavity created using WLP. With this approach, a 101 GHz oscillator has been achieved that has a measured output power of -16.6 dBm and phase noise at a 1 MHz offset of -77.4 dBc/Hz. [C421]

"Low-leakage InAs/AlSb HEMT with high FT-LG product"

Conventional InAs/AlSb HEMTs suffer high gate leakage and incomplete pinch-off issues due to instable chemical property of the AlSb and GaSb materials though their excellent performance and circuit application have already been demonstrated. Based on the concerns, we proposed a two-step passivation process for minimizing the negative effect based on developed high-quality InAs/AlSb HEMT materials by solid-source molecular beam epitaxy. Improved device performance is observed. [C422]

"Metal-oxide-HEMT on 6.1E antimonides"

We successfully demonstrated DC and RF performance of a metal-oxide-HEMT based on baseline InAs/AlSb HEMT epitaxy material. E-beam evaporated Al_{1-x}O_x was chosen for the dielectric film and its composition characterized by EDS. In a device with 2.0 μm gate length, maximum drain current is 286 mA/mm and peak transconductance is 495 mS/mm at drain voltage of 0.4 V. Microwave performance shows a fT_{0f} of 10 GHz and an f_{max} of 20 GHz. Degraded subthreshold slope but suppressed gate leakage specifically at large electric field were observed. [C423]

"Device Simulation for Future Technologies"

Simulation approaches used in Intel to evaluate the applicability of new devices and materials for future microprocessor technologies are reviewed. Examples discussed include the evaluation of highly stressed materials, III-V HEMT devices, and carbon nanoribbons. The techniques employed are similar to those used in the research community, but focused on efficient evaluation within a versatile infrastructure that works for both development and research. [C424]

"Bias Induced Strain Effects, Short-Range Electron-Electron Interactions and Quantum Effects in AlGaN/GaN HEMTs"

In this paper we present state of the art modeling of GaN HEMTs, which includes for the first time simultaneous consideration of the electromechanical coupling, short-range Coulomb and quantum mechanical size quantization effects. [C425]

"Manufacturable tri-stack AlSb/InAs HEMT low-noise amplifiers using wafer-level-packaging technology for light-weight and ultralow-power applications"

A wafer-level-packaging technology was used to integrate the 0.1 μm AlSb/InAs HEMT low-noise amplifiers with power amplifiers, switches and phase shifters to form a compact tri-stack transmit/receive module for light-weight and ultralow-power applications. The high manufacturability of AlSb/InAs HEMT receivers operating at 0.9 mW was demonstrated on a tri-stack wafer. This demonstration of manufacturable tri-stack transmit/receive modules is essential for phased-array applications requiring light weight and ultralow power. [C426]

"A 300 GHz mHEMT amplifier module"

In this paper, we present the development of an H-band (220-325 GHz) submillimeter-wave monolithic integrated circuit (S-MMIC) amplifier module for use in next generation active and passive high-resolution imaging systems operating around 300 GHz. Therefore, a variety of compact amplifier circuits has been realized by using an advanced 35 nm InAlAs/InGaAs based depletion-type metamorphic high electron mobility transistor (mHEMT) technology in combination with grounded coplanar waveguide (GCPW) circuit topology. A single-stage cascode design achieved a small-signal gain of 5.6 dB at 300 GHz and a linear gain of more than 5 dB between 258 and 308 GHz. Additionally, a four-stage amplifier S-MMIC based on conventional devices in common-source configuration was realized, demonstrating a maximum gain of 15.6 dB at 276 GHz and a linear gain of more than 12 dB over the frequency range from 264 to 300 GHz. Finally, mounting and packaging of the monolithic amplifier chips into H-band waveguide modules was accomplished with only minor reduction in circuit performance. [C427]

"DC characteristics of InAs/AlSb HEMTs at cryogenic temperatures"

The DC properties of 110-nm gate-length InAs/AlSb-based HEMTs at cryogenic (30 K) and room temperature (300 K) have been investigated. Compared to 300K, devices at 30 K exhibited lower on-resistance (RON) and

output conductance (gDS), a higher transconductance (gm) and a more distinct knee in the IDS(VDS) characteristics. The improvement in the DC performance at cryogenic temperature should mainly be attributed to the lower source-drain resistance. [C428]

"InGaAs/InAlAs/InP power hemt with an improved ohmic contact and an extremely high operating voltage"

An InGaAs/InAlAs/InP HEMT has been fabricated with 0.15 μm EBL gate, double gate recess and improved Ohmic contact. While maintaining a peak transconductance (G_{mp}) in excess of 1000 mS/mm, an onstate burnout voltage exceeding 8 V and an operating drain voltage of 5 V have been achieved. A loadpull measurement at 40 GHz was conducted. An output power density of 471 mW/mm, a power-added efficiency of 38% and a power gain of 8 dB were demonstrated, making this technology attractive for power applications at millimeter wave frequencies. [C429]

"Title page"

The following topics are dealt with: power semiconductor technology; high voltage IC technology; power MOSFET; IGBT; low voltage devices; DMOS technology; SOI power devices; HEMT; high voltage diodes; smart power technologies; JFET; wide band gap semiconductor devices; superjunction; and BJT. [C430]

"Multi-decade GaN HEMT Cascode-distributed power amplifier with baseband performance"

This paper reports on multi-decade bandwidth GaN HEMT cascode-distributed power amplifier designs which achieve performance from base-band to over 20 GHz. The GaN MMICs are based on a 0.2 μm AlGaIn/GaN low noise T-gate HEMT technology with an $f_T \sim 75$ GHz. To increase the MMIC power capability of this low noise GaN technology, a cascode DA design approach was employed which can operate at twice the recommended V_{ds} voltage. The resulting amplifiers achieve 1-4 Watts of saturated CW power from 100 MHz to over 20 GHz at an operating voltage of 30 V. Typical OIP3 > 40 dBm and NF of 3 dB were also achieved. Compared to equivalent designs in a similar 0.15 μm GaAs PHEMT low noise technology fabricated in the same foundry, these multi-decade GaN HEMT MMIC DAs obtain 6 dB higher output power and 5.8-6.6 dB higher OIP3 while achieving comparable gain, noise figure, and bandwidth. These are believed to be the first multi-decade GaN power distributed amplifiers that have been demonstrated and can enable future ultra-wideband frequency agile and software defined radio systems that require baseband to microwave frequency operation. [C431]

"GaAs pseudomorphic HEMTs for low voltage high frequency DC-DC converters"

Efficient power conversion at high switching frequencies requires switching transistors with a low gate charge to limit the switching losses in addition to low specific ON resistance. We report two integrable GaAs switching PHEMTs, 14 V enhancement mode and 7 V depletion mode transistors that show much superior switching figure of merit (Rontimes QG) than that of state-of-the-art silicon MOSFETs. These transistors can achieve highly efficient DC-DC power conversion at 100 MHz and beyond. [C432]

"Integrated voltage reference and comparator circuits for GaN smart power chip technology"

GaN smart power chip technology has been realized using GaN-on-Si HEMT platform, featuring monolithically integrated high-voltage power devices and low-voltage peripheral devices for mixed-signal functional blocks. Two imperative functional blocks for smart power applications with wide-temperature-range stability are demonstrated. The first one is a voltage reference generator, and the second one is a temperature-compensated comparator. These circuits are capable of proper functions within a wide temperature range from room temperature up to 250degC, illustrating the unique advantage of the wide-bandgap GaN. The voltage reference generator was designed with an AlGaIn/GaN HEMT and Schottky diodes, and the devices were operated in the subthreshold regime to obtain low power consumption. The voltage reference generator achieved an average drift of less than 70 ppm/degC and can be used as a reference voltage in various biasing and sensing circuits. The temperature-dependent performance of a conventional comparator is characterized and a new temperature-compensated comparator circuit is proposed. The positive limiting level of the temperature-compensated comparator is less than 450 ppm/degC drift compared to 1350 ppm/degC in the conventional comparator. [C433]

"Quantum Transport Simulations of InGaAs HEMTs: Influence of Mass Variations on the Device Performance"

This paper presents a simulation work of In_{0.7}Ga_{0.3}As HEMT devices for logic applications using a quantum ballistic 2D simulator based on the non-equilibrium Green's function (NEGF) approach coupled to a 2D Poisson

for the electrostatics. In a previous study, we showed that In_{0.7}Ga_{0.3}As short channel HEMT devices operates close to the ballistic limit and can be modeled as a ballistic channel attached to two series resistances. Since the electronic structure of the quantized channel is not known precisely, or can be altered by strain fields, in this work, we quantify our results, by investigating the variation in device performance due to variations in the effective mass values. We conclude that for these devices, variations in the electronic structure do not impact the device performance significantly. The results also provide insight into the expected effect of strain on the performance due to mass variations. [C434]

"Numerical Simulation of Plasma Waves in High-Electron-Mobility Transistors Using Kinetic Transport Model"

We study plasma waves in a high-electron-mobility transistor (HEMT) structure by numerical simulation using the kinetic electron transport model. We find that the plasma waves in the gated section of the channel can damp even without the electron collisions with impurities and phonons. The damping is related to the thermal spread of the electron velocity. We also show that the ungated sections of the channel play an important role in determining the plasma frequency and the damping rate because the plasma waves spread over the entire channel. [C435]

"Wi-Fi/WiMAX dual mode RF MMIC front-end module"

A dual-mode RF front-end module is designed and implemented for Wi-Fi/WiMAX applications. It consists of a front-end MMIC and a dual-band power amplifier MMIC, both fabricated by 0.5 μm E/D-mode p-HEMT process. The front-end MMIC integrates a single-pole triple-throw antenna switch, two low noise amplifiers, a low pass filter and a diplexer in single chip. Overall module size is compact 7 mm times 10 mm, well tested with Wi-Fi/WiMAX OFDM signals. [C436]

"Parameter extraction of HEMT models from multibias s-parameters"

The aim of the paper is to show how to identify the parameters of various nonlinear circuit models of a high electron mobility transistor from the multibias S-parameter dataset measured on a pHEMT device. A three-step identification procedure is described that uses tested optimization methods. Two original model modifications are suggested based on empirical relations for the transconductance dependence on gate-source voltage. Various models including the modified ones are compared in terms of the root-mean-square errors of multibias S-parameters. [C437]

"Metamorphic HEMT technology for low-noise applications"

Different noise sources in HEMTs are discussed, and state-of-the-art low-noise amplifiers based on the Fraunhofer IAF 100 nm and 50 nm gate length metamorphic HEMT (mHEMT) process are presented. These mHEMT technology feature an extrinsic f_T of 220 / 375 GHz and an extrinsic transconductance g_{m,max} of 1300 / 1800 mS/mm. By using the 50 nm technology several low-noise amplifier MMICs were realized. A small signal gain of 21 dB and a noise figure of 1.9 dB was measured in the frequency range between 80 and 100 GHz at ambient temperature. To investigate the low temperature behaviour of the 100 nm technology, single 4 * 40 μm mHEMTs were integrated in hybrid 4-8 GHz (Chalmers) and 16-26 GHz (Yebes) amplifiers. At cryogenic temperatures noise temperatures of 3 K at 5 GHz and 12 K at 22 GHz were achieved. [C438]

"Monte Carlo analysis of thermal effects in GaN HEMTs"

By means of a semi-classical Monte Carlo simulator with a consistent self-heating model we have analyzed how the static DC characteristics of GaN HEMTs are modified with respect to the constant room temperature model. The main consequence of the heating of the devices is a decrease of the drain conductance, mainly when the dissipated power is high (high V_{DS} and V_{GS}). Regarding the dynamic SSEC parameters, both C_{gs} and g_m decrease when increasing T, thus reducing the intrinsic cutoff frequency of the transistors. [C439]

"Electrical and Microstructural Characteristics of Ohmic Contacts formation on AlGaIn/GaN HEMT"

Electrical and microstructural characterization of Ti/Al/Ti/Au ohmic contact scheme for AlGaIn/GaN heterostructures is presented. It has been found that the Al/Ti thickness ratio influences the Ga-Au phase formation, which is linked to the contact resistivity, and that an Al excess content leads to a rough surface. The thickness of the barrier layer (Ti) was found to play an important role to achieve simultaneously low ohmic contact resistance and good line edge definition, although it does not act as an effective diffusion barrier. The role of the thermal annealing cycles is also discussed. [C440]

"Design and Realization of an Output Network for a GaN-HEMT Current-Mode Class-S Power Amplifier at 450MHz"

This paper describes the design and realization of a hybrid lumped output network for a current-mode class-S power amplifier. It consists of a band pass filter, a balun and a broad-band constant current supply. The filter achieves a bandwidth of 300 MHz and 0.5 dB insertion loss. As a demonstrator for the class-S concept, the developed network together with a GaN MMIC switching stage and GaAs Schottky-diodes demonstrates a complete class-S power amplifier for a data rate of 1.8 Gbps for an analog signal frequency of 450 MHz. An output power of 2.7 W at 450 MHz with an efficiency of 19% and a very high power gain of 37 dB has been achieved. This is the first demonstration of class-S operation at these power levels for this frequency range.

[C441]

"High Power, High Linearity and Low-Noise Hybrid RF Amplifiers Based on GaN HEMTs"

This paper details the potential of GaN HEMT technology for RF high power amplifiers (HPA), low noise amplifiers (LNA) and high linearity amplifiers with practical application examples. Large GaN HEMT powerbars are measured in a 50-ohm system at 2 GHz. Measurements show excellent characteristics in terms of power, linearity and noise. This combination of high power and low noise performance allows the realization of highly linear LNAs, which could significantly reduce protection and filter efforts at receiver inputs.

[C442]

"Parameters Extraction for Pseudomorphic HEMTs Using Genetic Algorithms"

A proposed small-signal model parameters for a pseudomorphic high electron mobility transistor (PHEMT) is presented. Both extrinsic and intrinsic circuit elements of a small-signal model are determined using genetic algorithm (GA) as a stochastic global search and optimization tool. The parameters extraction of the small-signal model is performed on 200-nm gate width AlGaAs/InGaAs PHEMT. The equivalent circuit elements for a proposed 18 elements model are determined directly from the measured S-parameters. The GA is used to extract the parameters of the proposed small-signal model from 0.5 up to 18 GHz.

[C443]

"An Introduced Neural Network-Differential Evolution Model for Small Signal Modeling of PHEMTs"

Since neural network algorithms are able to model nonlinear relations between different data sets, an introduced neural network model (INN) based on a generalized differential evolution training algorithm (INN-DE) is presented for pseudomorphic high electron mobility transistor (PHEMT). This global optimization algorithm is applied to avoid the local minima problem in the gradient descent-training algorithm and to achieve acceptable solution. The main advantage of this technique is its validation in wide range of frequencies and high accuracy for the small signal characteristics. The proposed (INN-DE) model is used to predict the scattering parameter values for various bias values different from the ones in the data set used for training. This model has been verified by comparing predicted and measured values of a PHEMT for a certain data set of S-parameters at different frequencies and bias points.

[C444]

"Monte Carlo Simulation of Sb-based Heterostructures"

Narrow band gap semiconductors have become a great option to increase mobility and operation frequency in high electron mobility transistors (HEMTs). In this work, two different narrow band gap semiconductors, InAs and InSb, and their associated heterostructures, AlSb/InAs and AlInSb/InSb, have been studied by means of Monte Carlo simulations.

[C445]

"Monte Carlo Study of an InAlAs/InGaAs Velocity Modulation Transistor"

We report a Monte Carlo study of an InP-based InAlAs/InGaAs velocity modulation transistor (VMT) based on the double-gate high electron mobility transistor (DG-HEMT), a HEMT with two opposite gates controlling the carrier flow through the conducting channel. In the VMT the source and drain electrodes are connected by two channels with different mobility, and electrons are transferred between the channels by changing the gate voltages in differential mode. As a result, the drain current is modulated while keeping the total carrier density constant, thus in principle avoiding capacitance charging/ discharging delays. The numerical analysis of the carrier density and velocity variations with the gate bias in differential mode demonstrates the actual velocity modulation operation of the proposed VMT transistors.

[C446]

"A 40-nm-Gate InAs/In_{0.7}Ga_{0.3}As Composite-Channel HEMT with 2200 mS/mm and 500-GHz f_T"

A 40-nm T-gate high-electron-mobility-transistor with InAs/In_{0.7}Ga_{0.3}As composite-channel has been

fabricated. The device exhibits a transconductance (g_m) of 2200 mS/mm, a cutoff frequency f_{To} of 506 GHz and a minimum noise figure of 1.21 dB at a frequency of 58 GHz. These performances make the device well-suited for millimeter-wave or sub-millimeter-wave applications. [C447]

"High performance InP HEMT technology with multiple interconnect layers for advanced RF and mixed signal circuits"

We report the development of high performance InP high electron mobility transistors (HEMTs) supported with three interconnect metal layers suitable for advanced RF and mixed signal integrated circuits. Depletion and enhancement mode devices with 35 nm gate-lengths are available with f_T / f_{max} of 536/307 GHz and f_T/f_{max} of 550/346 GHz, respectively. The process shows excellent device uniformity, yield, and reliability. The technology was used to demonstrate broadband feedback-linearized amplifiers with 20 dB S_{21} gain and an OIP3 of 37 dBm at 2 GHz operation, where PDC is only 313 mW. [C448]

"Sub-MMW active integrated circuits based on 35 nm InP HEMT technology"

In this paper, we present the latest advancements of active sub-MMW integrated circuits (S-MMIC) based on 35 nm InP HEMT technology. The current state-of-the-art results include the first demonstrated LNA, PA and fundamental oscillator modules above 300 GHz. [C449]

"Hetero-epitaxy of III-V compounds lattice-matched to InP by MOCVD for device applications"

Device quality Al_{0.49}In_{0.51}As/Ga_{0.47}In_{0.53}As MHEMT structures have been grown by MOCVD on GaAs substrates, with 2-DEG mobility over 8700 cm²/V-s and sheet carrier density at around 4 times 10¹² cm⁻². A 150 nm T-gate transistor demonstrated unity current gain cutoff frequency (f_T) and maximum oscillation frequency (f_{max}) of 279 and 231 GHz, respectively. [C450]

"Intrinsic Mechanism of Drain-Lag and Current Collapse in GaN-Based HEMTs"

The intrinsic mechanism of drain-lag and current collapse in GaN-based high-electron-mobility-transistors are studied by using two-dimensional transient simulations. The simulated drain-lag characteristics are in good agreement with the reported experimental data. Dynamic pictures of trapping of hot electron under drain-pulse voltages are discussed in detail. The trapped charges may accumulate at gate edge drain side, where the electric field significantly changes, causing a notable current collapse. Quantum-well HEMT structures have been proposed and demonstrated to obtain the optimized performance. [C451]

"Design of Class F-1 Power Amplifier Using GaN pHEMT for Industrial Applications"

This work presents a Class F-1 power amplifier (PA) operating at 2.35 GHz. An output power of 40 W (46 dBm) was achieved with 10 dB gain. The maximum drain efficiency was measured to be 60.8% (PAE = 55.7 %). The power amplifier was implemented using GaN pHEMT. The realization of the optimum load resonator was designed by a microstrip resonator, for the first four harmonics. The resonator achieves an optimum load for the transistor at the fundamental frequency. [C452]

"Committee"

The following topics are dealt with: indium phosphide; HBT devices; HBT circuits; photonic crystals; long wavelength lasers; epitaxy; hetero-integration; quantum dots; nanostructured lasers; substrate technology; HEMT devices; photodetectors; photonic integration technology; HEMT circuits; quantum cascade devices; semiconductor nanowires; semiconductor heterostructures; and high speed laser sources. [C453]

"Advanced design of an extended GaN HEMT Doherty amplifier using uneven saturation power for WiMAX applications"

This paper reports the advanced design of an extended GaN HEMT Doherty power amplifier (DPA). For high efficiency over a wide output power range, the DPA is designed using two cells with uneven saturation power (P_{sat}). A cell with lower P_{sat} is used as the carrier cell. For experimental validations, the carrier and peaking cells are designed and implemented with 25-W GaN HEMTs at world interpretability for microwave access (WiMAX) band of 2.6 GHz, and then show the P_{sat} of 40.9 dBm and 43.8 dBm, respectively. For the proposed DPA, the continuous wave results show the power-added efficiency (PAE) of 37.5% at an output power of 36 dBm (10-dB back-off power from P_{sat}). For a WiMAX signal, the PAE of 36.9% with an relative constellation error (RCE) of -31 dB is obtained at 36 dBm, which is 7.8% improvement compared to the conventional DPA. [C454]

"Enhanced terahertz detection using multiple GaAs HEMTs connected in series"

We report here, for the first time, on enhanced nonresonant detection of terahertz radiation using multiple InGaAs/GaAs high-electron-mobility transistors (HEMTs) connected in series and biased by a direct drain current. A 1.63 THz (184 μm) response is proportional to the number of detecting transistors operating in saturation region at the same gate-source bias voltage. The experimental data are in agreement with the detection mechanism based on the rectification of overdamped plasma waves excited by radiation in channels of devices. [C455]

"High efficiency Class-E tuned Doherty amplifier using GaN HEMT"

This paper describes the design and fabrication of a highly efficient switching-mode class-E Doherty power amplifier using gallium nitride (GaN) high-electron mobility transistor (HEMT) for S-band radar applications. Measured results of the Doherty amplifier show power-added efficiency (PAE) and drain efficiency of 62.6% and 73.1% at 37 dBm of 6 dB output back-off point from saturated output power at 2.85 GHz, compared with PAE and drain efficiency of 42.9% and 44.7% for the case of balanced amplifier. It was found that PAE was improved by 19.7% by adopting the Doherty efficiency enhancement technique. [C456]

"On-wafer integration of nitrides and Si devices: Bringing the power of polarization to Si"

The seamless integration of AlGaIn/GaN transistors and Si CMOS electronics on the same chip will revolutionize digital and mixed signal electronics. In this talk we describe our group's effort on demonstrating this integration. Si-GaN-Si virtual substrates have been recently fabricated through substrate removal and wafer bonding processes. The very high thermal stability of nitrides allows for the fabrication of Si CMOS electronics on these substrates without degrading the performance of the embedded nitride layer. In addition, GaN transistors on Si (001) have been fabricated on these substrates for the first time. Some of the many new circuits and devices that this integration allows include high power analog-to-digital converters, high speed differential amplifiers, normally-off power transistors, and highly-compact power regulator circuits. [C457]

"Lumped element thermal modeling of GaN-Based HEMTs"

This paper shows a practical approach to GaN-based HEMT self-consistent electro-thermal simulation for circuit modeling and reliability estimation. A physical-level lumped element dynamic thermal network able to describe the two-dimensional device geometry is self-consistently coupled with an electro-thermal compact large-signal model. The results obtained with the lumped-element thermal network are compared with finite-element simulations and shown to provide valuable estimates of the thermal behavior of very large 2D structures. [C458]

"A straightforward method to determine the parasitic gate resistance of GaN FET"

In this paper a straightforward method to determine the parasitic gate resistance (R_g) of GaN FET is introduced. The method uses a simple linear regression to directly determine the value of R_g without prior knowledge of the Schottky diode resistance R_0 and capacitance C_0 . Furthermore, the method requires only a single bias point with low DC current at the gate. In addition to this straightforward method, a reliable procedure for extracting the parasitic source inductance L_s is also introduced. This procedure for extracting the source inductance is useful for GaN FET when the imaginary part of Z_{12} is negative. The new method has been used successfully in the parasitic element characterization of power AlGaIn/GaN HFETs. [C459]

"Temperature dependent microwave noise parameters and modeling of AlGaIn/GaN HEMTs on Si substrate"

In this paper, we present the temperature dependent microwave noise measurements and modeling of AlGaIn/GaN HEMTs on Si substrate over a wide temperature range from -50 to 200 degC. The typical noise parameters including minimum noise figure (NF_{min}), noise equivalent resistance (R_n), optimum source reflection coefficient (Γ_{opt}) and associated gain (G_a) at different temperatures were measured and their dependencies on temperature were modeled by a linear or a quadratic approximation. The internal noise source coefficients and small signal equivalent circuit parameters (ECPs) were extracted and their variations over temperature were also modeled and discussed. The degradation rate of the noise parameters and internal noise source coefficients of the AlGaIn/GaN HEMT on Si with temperature are found to be comparable with the GaN HEMT on SiC and sapphire substrates and also comparable with the GaAs- and InP-based HEMTs. The results demonstrate the great potential of AlGaIn/GaN HEMTs on Si for low noise amplifier applications at high temperature. [C460]

"Thermal analysis and its application to high power GaN HEMT amplifiers"

A systematic and consistent approach to the thermal modeling and measurement of GaN on SiC HEMT power transistors is described. Since the power density of such multilayered wide bandgap structures and assemblies can be very high compared with other transistor technologies, the application of such an approach to the prediction of operating channel temperatures (and hence product lifetime) is important. Both CW and transient (i.e. pulsed and digitally modulated) thermal resistances are calculated for a range of transistor structures and sizes as a function of power density, pulse length and duty factor and compared with measured channel temperatures and RF parameters. The resulting thermal resistance values have then been imported into new self-heating large signal models so that transistor channel temperatures and the resulting effects on RF performance such as gain, output power and efficiency can be determined during the amplifier design phase. Some practical examples are included in the paper including the temperature rises in the carrier and peaking transistors of a high power Doherty amplifier. [C461]

"The dependence of GaN HEMT's frequency figure of merit on temperature"

This study presents extensive thermal characterization of GaN/SiC devices from five US sources across temperature (-25degC to +125degC). The changes with temperature for: cutoff frequency (f_t), maximum oscillation frequency (f_{max}), saturated current (I_{dss}), transconductance (g_m) are measured, statistics studied, and correlations investigated. Temperature-coefficients are established for f_t , f_{max} , I_{dss} , and g_{min} GaN technology. The results obtained provide MMIC designers with key information required for meeting temperature specifications. [C462]

"Design of a Ka-band bandpass filter with asymmetrical compact resonator"

This paper presents the realization of millimeter-wave bandpass filter consisting of asymmetrical compact resonator structure (ACRS) by using 0.15- μm pHEMT process. The filter utilizes two series resonators, which are resonated at different frequencies and connected in parallel on GaAs substrate, to achieve the desired coupling impedance in passband for the wanted filter characteristics. The filter is not only very compact in size, but it also can demonstrate low insertion loss in passband and achieve two controllable transmission zeros at lower and upper stopbands, respectively. A prototype operated at 34 GHz was designed and fabricated. The measurements of the prototype agree very well with the EM simulations, which exhibits less than 3.2dB insertion loss in the passband and greater than 25 and 50 dB attenuations at the frequencies of the zeros, respectively. [C463]

"Hybrid EER transmitter using highly efficient saturated power amplifier for 802.16e mobile WiMAX application"

We have demonstrated a highly efficient Hybrid Envelope Elimination and Restoration transmitter for IEEE 802.16e Mobile WiMAX application using a highly efficient saturated Power amplifier (PA). For the optimum H-EER operation, the PA has been designed to have a maximum PAE at the average V_{ds} region by using 10 W (P3dB) GaN High Electron Mobility Transistor. The maximum Power-added efficiency (PAE) is a 74.07 % at the 14 V V_{ds} . The bias modulator designed using a Hybrid Switching Amplifier (HSA) has a 73.3 % of efficiency. In the interlock experiment, the transmitter has shown an excellent PAE performance of 45.9 % at an average output power of 33.07 dBm with drain efficiency (DE) of 48.86 %. By using digital predistortion technique, the Relative Constellation Error (RCE) has been satisfied the specification of -30 dB with -36.88 dB. When considering the saturated PA with constant drain bias, the average PAE of the proposed transmitter has been hugely improved, about 13.64 %. These results clearly show that the H-EER transmitter using the saturated PA can deliver the excellent PAE performance. [C464]

"Reliability of GaN HEMTs: current status and future technology"

In this paper, we describe highly reliable GaN high electron mobility transistors (HEMTs) for high-power and high-efficiency amplifiers. First, we present the reliability mechanisms and progress on the previously reported GaN HEMTs. Next, we introduce our specific device structure for GaN HEMTs for improving reliability. An n-GaN cap and optimized buffer layer are used to realize high efficiency and high reliability by suppressing current collapse and quiescent current (I_{dsq})-drift. Finally, we propose a new device process around the gate electrode for further improvement of reliability. Preventing gate edge silicidation leads to reduced gate leakage current and suppression of initial degradation in a DC-stress test under high-temperature and high-voltage conditions. Gate edge engineering plays a key role in reducing the gate leakage current and improving reliability. [C465]

"Bias dependent and scalable small-signal modeling of pseudomorphic HEMTs"

Results of small-signal modeling of 0.5 μm gate length pseudomorphic HEMTs are presented here. Modeling

included scalability with respect to number of gate fingers, gate width and gate bias dependence of Equivalent Circuit Parameters (E.C.Ps). p-HEMTs with gate widths of 100 μm and 150 μm , each with varying number of gate fingers (2, 4, 6) keeping all other structural parameters constant were fabricated for this study. To find small-signal E.C.Ps we used method proposed by Dambrine et.al. and White-Healy. On-wafer measurement of S-parameters for all devices was done from 100 MHz to 40 GHz under different bias-conditions. Using this data, all the E.C.Ps were then extracted for each device, at various gate-biases and $V_{ds} = 3 \text{ V}$. Finally we have a model that can give the E.C.Ps of any device we fabricated, given the gate-bias, number of gate-fingers and gate-width. This equivalent circuit can be used to generate S-parameters of devices with good accuracy in the whole frequency range of measurement. [C466]

"Characterization of traps in AlGaIn/GaN HEMTs with a combined large signal network analyzer/deep level optical spectrometer system"

A study of the effects of traps on the RF characteristics of AlGaIn/GaN HEMTs is conducted using small and large-signal microwave measurements with deep-level optical spectroscopy. Different variations of the drain current swing are observed for illuminations of different photon energies. The time evolution of the current swing in transient measurements enabled to determine the optical transient time-constant and the equilibrium relaxation time-constant. The dependence of the S-parameters upon the illumination yielded results consistent with the variation of the drain current swing under illumination. A variation in the small signal transconductance and drain conductance was extracted at 2 GHz which presumably arises from the variation of the drain resistance under illumination. In addition, it was verified that the SiN passivation greatly helps in mitigating the RF performance degradation arising from deep trapping centers. [C467]

"Broadband time-domain measurement system applied to the characterization of cross-modulation in nonlinear microwave devices"

This paper presents a calibrated 4 channel broadband time-domain measurement system for the characterization of nonlinear microwave devices. The hardware architecture of the proposed measurement system is described with particular emphasis on the samplers and intermediate frequency (IF) circuit configuration. The sampling heads are working at a high strobe signal repetition frequency that can be tuned between 357 MHz and 536 MHz. 40 GHz RF frequency bandwidth is achieved. The calibration procedure of this system is also described. This instrument is then used for cross-modulation characterization of a 15W GaN HEMT CREE power amplifier at S Band. Cross-modulation measurements between a double side band amplitude modulation and a single tone signal at a 60 MHz offset frequency are performed to illustrate the capabilities of the proposed system. Time-domain waveforms are measured and variations of amplitude and phase modulation indices versus input power are recorded. [C468]

"A 33W GaN HEMT Doherty amplifier with 55% drain efficiency for 2.6GHz base stations"

A 33 W average output power Doherty power amplifier (PA) for 2.6 GHz band was developed using compact package advanced GaN HEMTs which have C_{ds} reduced 20%. A small-footprint Doherty network was successfully designed with plain small signal analysis, and the method was very practical. The Doherty PA exhibited a saturation output power of 52.5 dBm (178 W) and a saturated drain efficiency of 65.6%. The Doherty PA also achieved a drain efficiency of 55%, an ACLR of -52.8 dBc and a power gain of 13.8 dB at the average output power of 45.2 dBm (33 W) with 4-carrier W-CDMA signal at 2.6 GHz using commercially available digital pre-distortion system. These excellent performances show good suitability for 2.6 GHz band base stations (BTS), for example, W-CDMA, LTE and WiMAX, and small-sized circuit structure contributes to realize compact remote radio head type of BTS. [C469]

"C-band 340-W and X-band 100-W GaN power amplifiers with over 50-% PAE"

In this paper, we report a C-band power amplifier with over 340-W output power using 0.8- μm GaN-HEMTs and an X-band power amplifier with over 100-W output power using 0.25- μm GaN-HEMTs. We used two-chip configurations and the three-stage impedance transformers to extend the bandwidth for both circuits. The input and output lines adjacent to each chip are divided by four to suppress the non-uniform heat distribution in a chip at high frequencies. As a result, we obtained 343-W output power and 53-% power added efficiency (PAE) at 4.8 GHz. This is the highest output power ever reported C-band power amplifiers. We also obtained 101-W output power and 53-% PAE at 9.8 GHz. This is also the highest PAE ever reported X-band power amplifiers with over 50-W output power. [C470]

"Broadband GaN switch mode class E power amplifier for UHF applications"

In this work a broad-band class E power amplifier (PA) is designed, manufactured and measured. 400 MHz bandwidth with a center frequency of 800 MHz was realized using a GaN HEMT device. A novel and easy circuit topology is proposed for broad-band bandpass filter with integrated output matching network. Different filter types are discussed, suitable topology is chosen and design equations are shown. A maximum drain efficiency of 87.8 % (PAE = 80.6 %) is observed. Maximum output power of 49 W is measured with 16.3 dB power gain at the 1 dB compression point. [C471]

"DC-2 GHz low loss cryogenic InAs/AlSb HEMT switch"

A DC-2 GHz InAs/AlSb HEMT MMIC single pole double throw (SPDT) switch designed for cryogenic temperature has been fabricated and characterized. This switch is suitable for low RF power applications that require low insertion loss and high isolation. At 2 GHz, the SPDT switch demonstrated a typical low insertion loss of 0.7 dB at 300 K and 0.3 dB at 90 K. The isolation is greater than 40 dB for both temperatures. These results demonstrate the outstanding potential of ABCS HEMT technology for low loss SPDT switches for cryogenic temperature. [C472]

"Novel RF devices with multiple capacitively-coupled electrodes"

We present operation concepts and performance characteristics of novel microwave devices and structures using Oxide-AlGaIn/GaN Heterostructures with multiple capacitively-coupled contacts (C3). The C3 electrodes do not require annealing and, hence, such devices with tight electrode spacing can be fabricated using a self-aligned process. To illustrate the advantages of C3- technology, we demonstrate multi-gate C3- RF switches, RF switches with side control electrodes and novel RF-TLM test structures for layer and contact parameter extraction. [C473]

"Wideband medium power amplifiers using a short gate-length GaAs MMIC process"

We present the design of several wideband, millimeter-wave, MMIC, medium power amplifiers using a newly developed high-power, high-yield, 70 nm gate-length GaAs MMIC pHEMT process. These amplifiers cover a range of about 65-125 GHz, and were designed for the purpose of driving sub-millimeter wave multipliers in the local oscillator subsystem of the Atacama Large Millimeter Array (ALMA) radio telescope. The highest-frequency amplifiers in this chipset have average output power density over wide bandwidth of 200 mW/mm, representing the best performance to date for GaAs pHEMTs above W-Band. [C474]

"Ku-band AlGaIn/GaN-HEMT with over 30% of PAE"

AlGaIn/GaN high electron mobility transistors (HEMTs) were improved for X-band and Ku-band applications. The power added efficiency (PAE) was achieved over 40% for X-band and over 30% for Ku-band. The developed devices combined two AlGaIn/GaN HEMTs of 12 mm gate periphery and exhibited the output power of over 50 W. An AlGaIn/GaN HEMT with four dies of 12 mm gate periphery was developed and exhibited the output power of over 120 W. [C475]

"Design of compact-sized class-F PA for wireless handset applications"

In this paper, a highly efficient and compact 840 MHz class-F amplifier using E-pHEMT FET is implemented with the minimal footprints, where only the 2nd and 3rd harmonics is controlled to obtain the high efficiency within the harmonic control circuit. Compared to the transmission line, the discrete LC network is a more suitable solution to the small-sized implementation when it is carefully designed for the maximum performance. As such, this paper shows that the small-sized class-F PA can equally perform the ones with transmission lines for the harmonic control, and is more suitable for compact sized wireless terminal applications. The implemented power amplifiers have the peak efficiency of 81.2% with output power of 24.4 dBm. [C476]

"Enhancement-mode GaN hybrid MOS-HEMTs with breakdown voltage of 1300V"

We have studied and optimized the breakdown voltage of enhancement-mode n-channel GaN hybrid MOS-HEMTs on sapphire substrate. These MOS-gated transistors, with different Mg doped p-type GaN layer underneath the unintentional doped AlGaIn/GaN layer, have breakdown voltage as high as 1300 V using a dielectric isolation (DI) RESURF approach. [C477]

"A broadband 60-to-120 GHz single-chip MMIC multiplier chain"

This paper presents a single-chip 60 GHz to 120 GHz frequency multiplier chain based on 0.1 μm GaAs mHEMT. The MMIC can deliver 3 to 5 dBm of output power from 110 GHz to 130 GHz with 2 dBm input power

and consumes only 65 mW of DC power. The signal at the fundamental frequency is suppressed more than 20 dB over the band of interest. The impedance matching networks are realized using coupled transmission lines. [C478]

"A 144 GHz power amplifier MMIC with 11 dBm output power, 10 dB associated gain and 10 % power-added efficiency"

A millimeter-wave monolithic integrated circuit power amplifier operating in the frequency range between 135 and 155 GHz is presented. The D-band power amplifier, realized in a 100 nm gate length metamorphic high electron mobility transistor technology, employs a three-stage design with four parallel transistors in the output stage. At 144 GHz and under 1-dB gain compression, the amplifier achieves an output power of more than 11 dBm with an associated gain of 10 dB and a high power-added efficiency of 10%. A comparison to state-of-the-art power amplifiers at high millimeter-wave frequencies is given. [C479]

"V-band 8th harmonic push-push oscillator using microstrip ring resonator"

In this paper, the 8th harmonic push-push oscillator is firstly presented. A push-push principle is applied in this oscillator. The proposed push-push oscillator consists of two sub-circuits, a microstrip ring resonator, and an output circuit. A simplified circuit configuration is adopted in the proposed oscillator. The microstrip ring resonator plays two roles of a resonator and a power combiner circuit. This kind of push-push oscillator has the advantages of the easy circuit design, the simple circuit configuration and the miniaturization of the circuit size. Using the effective circuit configuration of the output circuit, a desired 8th harmonic signal is successfully enhanced. This push-push oscillator achieves high quality V-band millimeter wave oscillation using inexpensively available X-band HEMTs. The measured output power of -12 dBm at the frequency of 51 GHz is obtained with the phase noise of -94 dBc/Hz at the offset frequency of 1 MHz. [C480]

"A W-band low-noise amplifier with 22K noise temperature"

A W-band MMIC low-noise amplifier (LNA) was designed and fabricated using NGST's 35 nm InP HEMT process. It was packaged in a WR-12 module and tested at 297K and 17.5K ambient temperatures. At room temperature, the WR-12 LNA module has 26-30 dB gain from 70 to 92 GHz and less than 300K noise temperature from 65-86 GHz. At 17.5K ambient temperature, the WR-12 LNA module has a minimum noise temperature of 22K at 85 GHz and less than 40K noise temperature from 70-96 GHz (below 30K noise temperature from 78-95 GHz). Gain at 17.5K is 27-31 dB from 70 to 94 GHz. Power dissipation cold is 2.1 mW. Analysis is also included to investigate the observed frequency shift with ambient temperature. It is believed that these are the lowest noise temperature measured for a packaged W-band amplifier at both room and cryogenic temperatures. [C481]

"An improved empirical large-signal model for high-power GaN HEMTs including self-heating and charge-trapping effects"

A new empirical large-signal model for high-power GaN HEMTs utilizing an improved drain current (I_{ds}) model is presented. The new I_{ds} formulation accurately predicts the asymmetric bell-shaped transconductance (g_m) over a large drain-source bias range which is crucial in modeling high-power GaN HEMTs. A method of utilizing a combination of pulsed-gate (PGIV) and pulsed-gate-and-drain (PIV) IV measurements to characterize the dispersive behavior of GaN HEMT nonlinear I_{ds} characteristics is developed. Dispersion due to self heating is modeled by modifying I_{ds} parameters as a function of the temperature change and drain-source bias. Dispersion due to trapping is modeled using an effective gate-source voltage model. Accurate predictions of the RF small-signal and large-signal performance are demonstrated for two quiescent biases. [C482]

"Electrothermal large-signal model of III-V FETs accounting for frequency dispersion and charge conservation"

A comprehensive electrothermal model of III-V FETs is presented which accounts for gate/drain trapping effects and charge conservation. Two improved drain current models with and without transconductance compression mechanism, respectively, along with a consistent charge-conservative gate charge model have been developed. The channel current modeling parameters are extracted from DC and Pulsed I-V measurements at different ambient temperatures and quiescent biasing points. And the validity of the complete large-signal model is demonstrated by comparing the predicted I-V, C-V as well as power characteristics with the measured ones by employing GaAs pHEMTs. [C483]

"An efficient, linear, broadband class-J-mode PA realised using RF waveform engineering"

Results from a fully implemented class-J RFPA (RF power amplifier) are presented for the first time, which demonstrate this mode's high efficiency potential across a substantial bandwidth. Using a commercially available 10W GaN (gallium nitride) HEMT device, and the high power waveform measurement and active load-pull capability at Cardiff University, class-J operation has demonstrated drain efficiencies between 60-70% across a 1.35-2.25 GHz (50%) bandwidth whilst delivering 10 Watts of power at the 2dB compression point. Realisation of the design has confirmed that the optimum harmonic load impedances of the class-J amplifier are more practically realisable than conventional class-AB modes, with better compromise between power and efficiency tradeoffs over a substantial RF bandwidth. [C484]

"W-band transmitter and receiver modules for 10-Gb/s impulse radio"

Using InP HEMT technologies, we developed transmitter and receiver modules based on impulse radio (IR) architecture that are capable of 10-Gb/s data transmission in W-band frequencies. The new modules achieve ON/OFF keying modulation without using local oscillators, mixers, or other components that had been needed in previous millimeter-band modules. The transmitter, consisting of a 6.5-ps pulse modulator and a band-pass filter with 5-stage microstrip coupled lines, emits wavelets, or RF pulses, with a full width at half maximum of less than 80 ps and a voltage amplitude of 76 mVpp, occupying frequencies between 78-93 GHz. The receiver is composed of a low-noise amplifier (LNA), an envelope detector, and a limiting amplifier. The group delay property of the LNA, opposite to that of a waveguide to microstrip line transition in the module, makes the received signal distortion smaller, resulting in a reduction in intersymbol interference (ISI). As results of a back-to-back test, error free transmission/reception (BER < 10⁻¹²) was confirmed with a test pattern of PRBS 231-1 at the OC-192 compliant data rate of 9.95328 Gb/s. These results established the basic technologies for simple and compact IR-based systems, which could be used as an alternative to fiber optic cables. [C485]

"Design and analysis of ultra wideband GaN dual-gate HEMT low noise amplifiers"

This paper presents two ultra wide bandwidth low noise amplifiers utilizing 0.18- μ m AlGaIn/GaN HEMT technology. The single-stage, resistive feedback microstrip amplifiers target two different frequency bands, 0.3-4 GHz and 1.2-18 GHz, capable of better than 13:1 bandwidth. Both amplifiers use dual-gate HEMT devices with an on-chip drain bias network. The low frequency amplifier achieves 17.7 dB flat gain between 300 MHz-3 GHz, and 1.2 dB minimum noise figure around 1.3 GHz. The high frequency LNA shows an average of 13 dB gain and between 2 to 3 dB noise figure across the band. The robust LNAs can be operated under various bias voltages while similar gain and noise figure performance are maintained. [C486]

"A compact 12-watt high-efficiency 2.1-2.7 GHz class-E GaN HEMT power amplifier for base stations"

A compact broadband class-E power amplifier design is presented. High broadband power efficiency is observed from 2.0-2.5 GHz, where drain efficiency > 74% and PAE > 71%, when using 2nd-harmonic input tuning. The highest in-band efficiency performance is observed at 2.14 GHz from a 40 V supply with peak drain-efficiency of 77.3% and peak PAE of 74.0% at 12 W output power and 14 dB gain. The best broadband output power performance is observed from 2.1-2.7 GHz without 2nd-harmonic input tuning, where the output power variation is within 1.5 dB and power efficiency is between 53% and 66%. [C487]

"A compact low DC consumption 24-GHz Cascode HEMT VGA"

This paper presents a 24-GHz high gain and wide gain control range in cascode device technique. The VGA is implemented in 0.15- μ m GaAs PHEMT process. This VGA has 15.7 dB gain and 18.5% 3-dB bandwidth and over 20 dB gain control range at 24 GHz, with a low dc power of 13.5 mW. These results indicate that cascode technique is suitable for low power consumption and small chip size for high frequency amplifiers using GaAs PHEMT process. [C488]

"Analysis and optimum design of impedance matching for Ka-Band cryogenic low noise amplifiers"

High electron mobility transistors (HEMTs) and cryogenic cooling are widely employed in high gain and low noise millimeter-wave amplifiers. By using the temperature dependant model of HEMT, this paper further investigated the optimum impedance matching for low noise amplifiers (LNAs) to exhibit a significant improvement in noise and gain performance under cryogenic temperatures. One MMIC LNA covering 26-40 GHz frequency band has been developed on GaAs substrate with 0.15 μ m PHEMT devices, and it was measured on-wafer and in-module at the operating temperatures of 300 K and 77 K. [C489]

"New analytical expressions for the design of linear power amplifier using GaN HEMTs"

This paper provides new analytic expressions for prediction of the large signal gain of GaN high electron mobility transistors (HEMTs). Using the concept of load line resistance, optimum matching impedances and power gain are demonstrated for commercial GaN HEMT from a 14 lumped elements model. The source impedance is more accurately determined by this model. [C490]

"A novel metamorphic high electron mobility transistors with $(\text{In}_x\text{Ga}_{1-x}\text{As})_m/(\text{InAs})_n$ superlattice channel layer for millimeter-wave applications"

High performance MHEMTs using $(\text{In}_x\text{Ga}_{1-x}\text{As})_m/(\text{InAs})_n$ superlattice structure as a channel layer have been fabricated successfully. These HEMTs with 80 nm gate length exhibit high drain current density of 392 mA/mm at drain bias 1.0 V and transconductance of 991 mS/mm at drain bias 1.2 V. Comparison with regular $\text{In}_x\text{Ga}_{1-x}\text{As}$ channel, the superlattice channel HEMTs show an outstanding performance because of high electron mobility, and better carrier confinement in the $(\text{In}_x\text{Ga}_{1-x}\text{As})_m/(\text{InAs})_n$ channel layer. The current gain cutoff frequency (f_T) and maximum oscillation frequency (f_{max}) were extracted to be 304 GHz and 162 GHz, respectively. The device demonstrated a 0.75 dB noise figure with an associated gain 9.6 dB at 16 GHz. The excellent device performance shows that the superlattice channel can be practically used for high-frequency and millimeter-wave application. [C491]

"A 29dBm linear power amplifier module for IEEE 802.16e (Wimax) and LTE applications using E-mode pHEMT technology"

This paper describes, for the first time, the design and realization of a 5V supply 29dBm linear power amplifier for the IEEE 802.16e (WiMax) and LTE applications in the (2.5-2.7)GHz band. When tested using a 10MHz bandwidth OFDMA signal with 64-QAM modulation, the amplifier consumes 950mA of total current. Nominal gain is 35dB, and a 20dB gain attenuator that is activated by a CMOS-compatible voltage pin is included on-chip. Output power detection is achieved by the use of an on-chip power detector and a bias shutdown voltage shuts down the complete amplifier. Low power operation is also possible with 26dBm of linear output power at less than 2.5% EVM. The amplifier is fabricated using a proprietary 0.25μm enhancement-mode pHEMT (EpHEMT) technology. The complete module is packaged in a multilayer chip-on-board (MCOB) 5 mm Γ B—5 mm module. [C492]

"RF characterization of planar dipole antenna for on-chip integration with GaAs-based schottky diode"

The design and RF characteristics of planar dipole antenna facilitated with coplanar waveguide structure was presented. The dipole antennas were fabricated on semi-insulated GaAs substrates by using standard photolithography and lift-off process. As expected, it can be seen that the fundamental resonant frequency shift to higher frequency when the length of antenna decreases. Interestingly, the resonant frequencies of antenna are almost unchanged with the variation of antenna width and metal thickness. The width of dipole antenna and metal thickness only has an effect on the magnitude of return loss where the magnitude increases to more negative value with the increase of width and decrease of metal thickness. One of the most promising applications of our proposed dipole antenna is the capability to be integrated directly with AlGaAs/GaAs Schottky diode without any insertion of matching circuit between them. [C493]

"C-Ku band 120% relative bandwidth high efficiency high power amplifier using GaN HEMT"

This paper reports on a GaN HEMT (gallium nitride high electron mobility transistor) HIC (hybrid integrated circuit) high power amplifier, which features high efficiency over C-Ku band 120% relative bandwidth. It was found that the output impedance of a transistor under high efficiency operation can be modeled by parallel circuit of R and C. In the circuit design, BPF (band pass filter) configuration is employed, where parasitic capacitance of the transistor is utilized as a part of BPF matching circuit. Hence broadband matching was successfully obtained. A C-Ku band GaN HEMT HIC amplifier was manufactured and measured at 30 V drain voltage. More than 4 W output power and 18% PAE (Power Added Efficiency) were obtained over 120% relative bandwidth. This result is state-of-the-art high efficiency for GaN HEMT HIC amplifier with more than 100% relative bandwidth. [C494]

"A GaN HEMT Doherty amplifier with a series connected load"

Doherty introduced two types of concepts for high-efficiency amplifiers in 1936. One involved a shunt connected load and the other involved a series connected load. The first one is well known. We propose a microwave Doherty power amplifier with a series connected load using baluns. A 1.9 GHz GaN HEMT Doherty power amplifier was designed and fabricated. At 24 dBm middle and 31 dBm saturated output powers, the amplifier realized improved power efficiencies of 31% and 56%, respectively, compared to power efficiencies of 15% at 24

dBm output power and 57% at 34 dBm saturated power, respectively, obtained with a reference push-pull amplifier. [C495]

"Tunable pulse generator for ultra-wideband applications"

For the first time, an ultra-wideband pulse generator is fabricated in GaAs HBT IC technology. The generator includes delay and differential circuits to convert a TTL input into an impulse signal and a Class-C amplifier to increase the pulse amplitude while compressing the pulse width. By adjusting the bias of the Class-C amplifier, the pulse amplitude can be varied linearly between 3.5 V and 11.5 V while maintaining the pulse width at 0.3Г,В ±0.1 ns. Alternatively, the pulse width can be varied linearly between 0.25 ns and 0.65 ns, while maintaining the pulse amplitude at 10Г,В±1 V. Finally, the amplified impulse signal can be shaped into a monocycle signal by an L-C derivative circuit. These results compare well with that of pulse generators fabricated in GaAs HEMT, Si CMOS or Si discrete technologies. [C496]

"Trading-off stability for efficiency in designing switching-mode GaN PAs for WiMAX applications"

This paper presents a 10 W, 2.4 GHz switching-mode power with a GaN HEMT transistor for WiMAX applications. By trading the stability for the efficiency, the overall power efficiency of the designed PA can be increased. It is shown in this paper that the parasitic effect introduced by the stability circuit affects the waveform shaping at large-signal drive level in switching mode PAs and consequently degrades its maximum peak efficiency. Hence, by using a potentially instable design, the efficiency and gain performance of a given transistor can be increased compared to an unconditionally stable design. To validate this approach an inverse class F PA was manufactured and tested. The power added efficiency and gain performance increased by 3.5% and 0.25 dB to reach 72% and 14.5 dB, respectively, when using a potentially instable design. [C497]

"On the large-signal modeling of AlGaIn/GaN HEMTs for RF switching-mode power amplifiers design"

A large-signal model for GaN HEMT transistor suitable for designing switching-mode power amplifiers (SMPAs) is presented along with its parameters extraction procedure. This model is relatively easy to construct and implement in CAD software since it requires only DC and S-parameter measurements. The modeling procedure was applied to a 4-W packaged GaN-on-Si HEMT and the developed model is validated by comparing its small- and large-signal simulation to measured data. The model has been employed for designing a switching-mode inverse class-F power amplifier. Very good agreement between the amplifier simulation and measurement shows the validity of the model. [C498]

"Intrinsic capacitances effects on the accuracy of the large-signal switch-based GaN device model"

This paper assesses the impact of two modelling approaches for the nonlinear drain-source and gate-drain capacitances in a switch-based GaN HEMT model on predicting large-signal and switching-mode device performance. The extracted values for these intrinsic capacitors, derived from measured S-parameters in deliberate bias points, are modelled by a zeroth and first order approximation. Using these approximations in an in-house developed large-signal switch-based device model for GaN HEMTs, their effects on modelling accuracy of switching-mode operation at microwave frequencies are shown by comparing simulation and load-pull measurement results for inverse class-F operation. Whereas a zeroth order approximation is confirmed to provide good accuracy for both output power and efficiency prediction in saturation, the study shows that modelling the gate-drain capacitance with a linear equation instead of constant values extends the application range of the switch-based model to the linear region. Good agreement between large-signal simulation results and load-pull measurements in this operation mode has been obtained. [C499]

"High-efficiency transmission-line GaN HEMT inverse class F power amplifier for active antenna arrays"

In this paper, a novel load-network solution to implement the transmission-line inverse Class F power amplifier for WCDMA active antenna array applications is presented. The theoretical analysis is based on an analytical derivation of the optimum load-network parameters to control the second and third harmonic at the device output including the device output parasitic shunt capacitance and series inductance. For an inverse Class F power amplifier based on a Nitronex GaN HEMT NPTB00004 with hybrid microstrip implementation, the simulated output power of 37 dBm and power-added efficiency of more than 70% are achieved at a supply voltage of 25 V in a frequency bandwidth of 2.11 to 2.17 GHz. The test board with implemented inverse Class F GaN HEMT power amplifier has been measured and high-performance results with drain efficiencies of about 80% and higher were achieved across the wide ranges of bias supply voltages and operating frequencies. [C500]

"Electromagnetic only HEMT model for switch design"

Electromagnetic (EM) only HEMT model has been proposed and realized with commercial available EM simulator. EM analysis has been applied, for the first time, to the intrinsic part of HEMT device. The small signal behaviors of HEMT can be accurately predicted based directly on the layout and process information. After introducing two EM HEMT models for HEMTs in both on and off states, entire switch circuit, as a whole, can be EM simulated. The prediction accuracy for switch performance can be remarkably improved by taking into account all of the distributed and coupling effects inside the circuit. [C501]

"A predistortion linearizer for a class-F GaN HEMT power amplifier using two independently controlled diodes"

A novel pre-distortion technique using two independently bias-controlled Schottky diodes is proposed to compensate the complicated nonlinear characteristics of the AlGaIn/GaN HEMT microwave class-F amplifier, in which inferior intermodulation distortions are often observed for an output power range of large back-off. The newly developed technique has made it possible to achieve both high drain efficiency and low intermodulation distortion simultaneously. The developed linearizer was fabricated in MMIC form and applied to a one watt AlGaIn/GaN HEMT class-F amplifier operating at 1.9 GHz, where harmonic frequencies up to the fifth higher order were controlled. With the diode predistortion linearizer, the third-order intermodulation distortion ratio (IMD3) of the 1.9-GHz class-F GaN HEMT power amplifier was improved over power output from 0 to 18 dBm. The IMD3 was under -40 dBc at output powers lower than 10 dBm. The amplifier had a maximum drain efficiency of 70.6 % at output power of 27 dBm. [C502]

"Thermal management for flip-chip high power amplifiers utilizing carbon nanotube bumps"

Carbon nanotubes (CNTs) have been successfully used as source bumps for flip-chip high power amplifiers (HPAs). We have fabricated fine pitch CNT bumps with metal coating, which have been connected to electrodes close to the active areas of AlGaIn/GaN HEMTs. A flip-chip AlGaIn/GaN HEMT HPA with a gate width of 28.8 mm utilizing CNT bumps and an operating voltage of 50 V exhibits an output power of 49.3 dBm at a frequency of 2.4 GHz. [C503]

"Modeling the small signal characteristics of an ALD Al₂O₃ insulated-gate AlN/GaN high electron mobility transistor"

In this work the authors show the employment of an atomic layer deposited (ALD) high-K Al₂O₃ gate oxide in an AlN/GaN HEMT that suppresses the unwanted gate current and simultaneously enhances parasitic influence on frequency performance. Small signal modeling of the Al₂O₃/AlN/GaN HEMT has allowed the accurate extraction of this detrimental influence on device RF performance. It was shown that both intrinsic f_{tand} and f_{max} are notably higher when parasitic elements are removed from S-parameter data, as expected. These results provide a more accurate understanding of the intrinsic functionality of the AlN/GaN HEMT and serve as a guide for further refinements of the device. [C504]

"Analysis of physics based model of AlGaIn/GaN power HEMT with temperature compensation"

An AlGaIn/GaN high electron mobility transistor (HEMT) model with temperature compensation is proposed. The simulation and experimental data are in close agreement within the measured temperature range. Despite of drain current degradation, the characteristics exhibit high temperature compatibility of AlGaIn/GaN HEMTs. [C505]

"High-temperature modeling of AlGaIn/GaN HEMTs"

Wide bandgap, high saturation velocity, and high thermal stability are some of the properties of GaN, which make it an excellent material for high-power, high frequency, and high temperature applications. Given the predicted wide-spread use, reliable models are needed for simulation based optimization. As several application areas require the devices to operate at elevated temperatures, a proper modeling of the temperature dependences of the band structure and transport parameters is highly important. We present two-dimensional hydrodynamic simulations of AlGaIn/GaN high electron mobility transistors (HEMTs) supported by measured data at high temperatures. [C506]

"Self-aligned ALD AlO_x T-gate footprint insulator for gate leakage current suppression in SiN_x passivated AlGaIn/GaN HEMTs"

The devices in this study demonstrate a novel process methodology that allows for a self-aligned ALD AlO_x/Bi

gate insulator to be placed directly under the T-gate footprint and not in the access regions. After gate contact formation, standard PECVD SiN_x/Bi passivation can be applied just as in a conventional HEMT process. Preliminary devices show promising results that this technique can be used to achieve high power mm-wave performance. [C507]

"Investigation of breakdown behavior for AlGa_N HEMTs"

The ability to accurately determine the breakdown voltage of microwave transistors is critical to the design of high power microwave amplifiers. The optimal bias point and output impedance should be selected to ensure that the load line of the device during peak output power does not intersect the portion of the IV curve where the device breaks down. This paper presents a technique to determine a drain-source breakdown voltage measurement that is useful for the design of high power microwave amplifiers. This measurement has been performed on GaN HEMTs from several different domestic foundries. Using the results of this experiment, an optimal bias point that makes use of the entire load line while at the same time avoiding the destructive effects of breakdown, can be selected. [C508]

"Fabrication of open gate structure on GaN-based HEMT for pH sensing"

In recent years, there has been demonstrated a rapid progress of the AlGa_N/GaN system applications in optical and electronic device research due to its unique features. One of unique features of AlGa_N/GaN system includes chemically stable where stability of surface is essentially important for liquid-phase sensor applications. Besides, AlGa_N/GaN also allows highly sensitive detection of surface phenomena with the presence of a high-density two-dimensional electron gas (2DEG) in the high electron mobility transistor (HEMT) structure. Furthermore, the GaN material allows sensing operations at high temperatures due to large bandgap energies. This paper presents the design and fabrication of an open-gate structure on undoped AlGa_N/GaN and n-AlGa_N/GaN HEMT structure for sensing the pH level of certain electrolyte solutions. It is found that the drain-source current decreases with the pH level as expected. [C509]

"Enhancement mode AlN/ultrathin AlGa_N/GaN HEMTs using selective wet etching"

The demonstration of device structure incorporating an ultrathin AlGa_N barrier capped with a thin AlN layer in the source-drain access region to maintain high 2DEG charge, with a gate opening formed by selective wet etching of the AlN using heated photoresist is reported. AlN/AlGa_N/GaN layer structures are grown on a-plane Al₂O₃ substrates by metalorganic chemical vapour deposition. In conclusion, the process is employed using 4 nm AlGa_N barrier to demonstrate HEMTs with a threshold voltage of +0.21 V while maintaining a high mobility (>700 cm²/V-s) and with little loss in current density relative to an unetched device. [C510]

"Optimization of power AlGa_N/GaN vertical HEMT devices with low on-state resistance and high breakdown voltage"

Recently we have developed a numerical technique for the optimization of parameters in semiconductor devices. This technique allows the computation ("redesign") of the doping profiles of most semiconductor devices such as MOSFETs and SOI transistors, in order to decrease (or increase) the values of given parameters of the device. In this presentation we show how to adjust this optimization technique to the minimization of the on-state resistance (Ron) in AlGa_N/GaN vertical HEMT devices with high breakdown voltage (BV). The technique is based on the computation of doping sensitivity functions of Ron and BV and the minimization of Ron, in which the optimization variables are the values of the doping concentrations at each location inside the device. Constraints are taken into consideration by using the method of Lagrange multipliers. [C511]

"A compact X-band balanced frequency doubler on GaAs pHEMT 3D MMIC"

A compact GaAs pHEMT monolithic microwave integrated circuit balanced frequency doubler is presented. It is composed of a common-source/common-gate active balun, a balanced frequency doubler, and a band pass filter. Excellent miniaturization is achieved by using double- and triple-layer stacked inductors and a miniaturized stub as a band-pass filter with a thin-film microstrip line. The chip size is only 0.95 mm × 1.05 mm and power consumption is 63 mW. The measured conversion gain is -4 dB, and the fundamental and 3rd order frequency leakage to the 2nd order harmonic signal are less than -25 dB and -35 dB respectively. [C512]

"Analytical modeling of the temperature dependent microwave noise in AlGa_N/GaN HEMTs"

In this paper, we present the analytical modeling on the temperature dependent microwave noise in AlGa_N/GaN HEMTs on Si substrate over a wide temperature range from -50 to 200 °C. The noise source coefficients and small signal equivalent circuit parameters (ECPs) were extracted and their variations over temperature were

fitted using a simple quadratic relationship. An analytical model for the overall noise parameters including temperature dependence is proposed based on the Pucel's PRC model and verified with the measured temperature-dependent noise parameters. The feedback capacitance C_{gd} was found to be important to accurately simulate all the measured noise parameters over temperature. [C513]

"Integration of RF MEMS switch with MMIC pHEMT and passive devices on GaAs"

Process integration of RF MEMS switches with MMIC pHEMT devices and passive components on GaAs has been developed. Measurement results of the RF MEMS switches showed a C_{down}/C_{up} ratio of approximately 20:1, pHEMT devices with gate periphery of 1.2 mm show an I_{max} of 400 mA/mm, with f_T and f_{max} of 60 GHz and 100 GHz, respectively. TaN resistors were measured at 65 Ω , B_i/Γ , B_i sheet resistance, the MIM capacitors have a capacitance of 550 pF/mm² and the 5 turn spiral inductors have approximately 4.3 nH inductance. [C514]

"Multifunctional frequency converter MMIC for 38GHz band 600Mbps multi-level QAM wireless system"

The highly integrated up and down converter MMICs which uses the GaAs_HEMT process with three-dimensional MMIC technology is presented. These frequency converters consist of a balanced mixer, RF band amplifiers, an IF band amplifier, a step attenuator, an active band pass filter and a local quadrupler. A smaller surface mount package of 5 mm Γ_B — 5 mm Γ_B — 1.65 mm has also been developed and the MMIC chips are mounted in it, respectively. The 38 GHz broadband wireless system as the ultra compact and very light weight has been realized by using these developed MMICs. [C515]

"TCAD analysis of self heating in AlGaIn/GaN HEMTs under pulsed conditions"

The purpose of this work was to develop a TCAD device model to study the electrical and thermal characteristics of the AlGaIn/GaN HEMT in the time domain in contrast to a DC thermal equilibrium analysis. We first examined a channel temperature technique that utilizes temperature dependence of gate voltage on gate current to predict channel temperature. The predicted channel temperature of Method 3104 of MIL-STD 750D is then compared to the simulated temperature profile to determine the corresponding temperature location in the HEMT structure. Second, we investigated the performance of single and multiple pulses effects on heating of the HEMT. Third, we studied and compared the heating between the DC analysis and a RF transient (multiple pulses) analysis with the same average device power. Finally, we observed large temperature gradients in the device in initial device heating not capable of being observed with conventional DC TCAD analysis. [C516]

"Extraction of intrinsic AC parameters of mm wavelength GaAs HEMTs from measured DC characteristics"

This paper discusses the estimation of intrinsic small signal parameters of GaAs high electron mobility transistors (HEMTs). In the proposed technique observed DC characteristics of submicron GaAs HEMTs are first simulated by using a four-parameter non-linear model. Intrinsic AC small signal parameters of the device are then estimated by using DC experimental data. The study showed that intrinsic small signal parameters of an HEMT can only be estimated, to an acceptable accuracy, if the device Schottky barrier conditions are taken into account. The effects of non-ideal Schottky barrier response and the parasitic FET on the device transconductance, output conductance, channel resistance and Miller capacitances have been evaluated. In general, it has been shown that the technique is accurate as well as efficient in estimating AC parameters of GaAs HEMTs by using their DC characteristics, and could be employed in device simulation software. [C517]

"Integrated receivers up to 220 GHz utilizing GaAs-mHEMT technology"

The status of integrated receivers for remote sensing and communication applications from 60 GHz to higher frequencies is reviewed. Recent receiver results for silicon and III-V technologies are compared with Schottky diode receivers. [C518]

"A 40 GHz power amplifier using a low cost high volume 0.15 μ m optical lithography pHEMT process"

A 40 GHz power amplifier is realized with a new 0.15 μ m optical lithography pHEMT process developed for low-cost microwave and millimeter wave circuits. Several Ka and V band market requirements have driven demand for higher bandwidth, low-cost, integrated circuits. A 40 GHz power amplifier is used to demonstrate the process capabilities, starting from the initial design phase and culminating with the fabrication and measurement of the solid state power amplifier. [C519]

"Performance analysis of ultra-scaled InAs HEMTs"

The scaling behavior of ultra-scaled InAs HEMTs is investigated using a 2-dimensional real-space effective mass ballistic quantum transport simulator. The simulation methodology is first benchmarked against experimental I_d - V_{gs} data obtained from devices with gate lengths ranging from 30 to 50 nm, where a good quantitative match is obtained. It is then applied to optimize the logic performance of not-yet-fabricated 20 nm InAs HEMT. It is demonstrated that the best performance is achieved in thin InAs channel devices by reducing the insulator thickness to improve the gate control while increasing the gate work function to suppress the gate leakage. [C520]

"30 nm In_{0.7}Ga_{0.3}As Inverted-Type HEMTs with reduced gate leakage current for logic applications"

We have fabricated 30 nm In_{0.7}Ga_{0.3}As Inverted-Type HEMTs with outstanding logic performance, scalability and high frequency characteristics. The motivation for this work is the demonstration of reduced gate leakage current in the Inverted HEMT structure. The fabricated devices show excellent I_g scalability down to 30 nm. I_g = 30 nm devices have been fabricated with exhibit g_m = 1.27 mS/ Γ , B_{im} , S = 83 mV/dec, DIBL = 118 mV/V, I_{ON}/I_{OFF} = 4 Γ B— 104, all at 0.5 V. More significantly, the removal of dopants from the barrier suppresses forward gate leakage current by over 100X when compared with equivalent normal HEMTs. The I_g = 30 nm devices also feature record high-frequency characteristics for an inverted-type HEMT design with f_T = 500 GHz and f_{max} = 550 GHz. [C521]

"Correlation between DC and rf degradation due to deep levels in AlGaIn/GaN HEMTs"

We investigate the role of the 0.5 eV traps in determining GaN HEMT degradation by means of DC and rf testing, and 2D numerical simulation. We demonstrate that generation of deep levels, having an activation energy of 0.5 eV, is responsible for the degradation observed during rf aging; we show that the occurrence of trap-induced degradation depends on rf driving conditions. We also show that degradation can be explained by the generation of a damaged region within the AlGaIn layer at the gate-drain edge, and that the DC and pulsed device degradation effects have a different dependence on the width and depth of the damaged region. [C522]

"N-polar GaN-based highly scaled self-aligned MIS-HEMTs with state-of-the-art f_T .LG product of 16.8 GHz- μ m"

In this paper, we describe a gate-first self-aligned MBE InGaIn regrowth methodology for fabricating N-polar GaN-based MIS-HEMTs which exhibit ultra-low contact resistances of 23 Ω - μ m, which is comparable to the lower band-gap technologies. These devices, not only show state-of-the-art f_T .LG product values of 16.8 GHz- μ m for 130 nm gate length for GaN, but also show exceptional performance at low supply voltages (V_D s = 500 mV), thereby making GaN competitive not only to wide band-gap materials like SiC but also to low band-gap technologies by InGaAs HEMTs and InSb by having low knee voltages, high drive currents while still demonstrating relatively large breakdown voltages for unipolar (non-CMOS like) operation. [C523]

"High efficiency GaN class E amplifier for polar transmitter"

This paper focuses on the design of a high efficiency 10 Watt Class E power amplifier (PA) suitable for polar radio transmitters. The PA prototype, designed using GaN HEMT devices to operate at 2.5 GHz, revealed a Power Added Efficiency (PAE) and an output power of 74% and 38.3 dBm, respectively, for a supply voltage equal to 28 V. It also demonstrated an excellent suppression of the second and third harmonics in excess of -50 dBc. The measurement of the Class E performance over large range of drain supply voltages confirmed its appropriateness for polar transmitter as a good efficiency was maintained at large output power back-off, i.e. PAE equal to 48% was measured at 11 dB back off. [C524]

"Study of field plate effects on AlGaIn/GaN HEMTs"

In this paper we carry out study of the Field Plate (FP) effects on AlGaIn/GaN HEMTs (high electron mobility transistors) by modeling the electric field in the structure FP-HEMT (with Field Plate). It consist to analyze the maximum of the electric field according to the gate voltage and drain voltage taking into account several technological parameters of the Field Plate such as the passivation layer thickness, the FP length and the distance gate-drain. We have shown that, the main functions of the field plate are to reshape the electric field distribution in the channel and to reduce its peak value on the drain side of the gate edge. The benefit is an increase of the breakdown voltage and a reduced high-field trapping effect. [C525]

"Quantum capacitance in scaled down III-V FETs"

We have built a physical gate capacitance model for III-V FETs that incorporates quantum capacitance and centroid capacitance in the channel. We verified its validity with simulations (Nextnano) and experimental measurements on High Electron Mobility Transistors (HEMTs) with InAs and InGaAs channels down to 30 nm in gate length. Our model confirms that in the operational range of these devices, the quantum capacitance significantly lowers the overall gate capacitance. In addition, the channel centroid capacitance is also found to have a significant impact on gate capacitance. Our model provides a number of suggestions for capacitance scaling in future III-V FETs. [C526]

"Normally-off 5A/1100V GaN-on-silicon device for high voltage applications"

We report the DC and switching performance of a normally-off 5 A/1100 V GaN-on-Si device. The device had a breakdown field of 95 V/ Γ ,B μ m and a $V_{B2}/R_{on,spof}$ 272 MW/cm². A 360 V/180 W boost converter was operated at 200 KHz, with an efficiency >92%. Respectively, these values are the highest for a normally-off GaN-on-Si device. [C527]

"Improved mathematical model for the investigation of deep traps into semiconductor devices: application to Metamorphic HEMT"

Several parasitic effects that penalize III-V IC and RF transistors performances are directly linked to deep level trapping mechanisms into the structure. The analysis of these phenomena is correlated to the presence of traps signature related to intrinsic and/or process dependent defects. We propose in this paper a survey of a non-linear measurement method namely the isothermal relaxation method used to extract trap signatures. We improve the effectiveness of the mathematical part of the method to obtain more precise results in a more efficient way. An application of our software to Metamorphic HEMTs and a comparison to results obtained with the DLTS method is proposed. [C528]

"Additive phase noise measurements of AlGaIn/GaN HEMTs using a large signal network analyzer and a tunable monochromatic light source"

An additive phase noise measurement system is integrated with a large signal network analyzer (LSNA) and a tunable monochromatic light source. This system is used to measure the additive phase noise characteristics of an unpassivated AlGaIn/GaN high electron mobility transistor (HEMT) at 2 GHz under various operating conditions. Illumination with different photon energies, below the AlGaIn bandgap, is applied to probe the dependence of the RF additive phase noise on the trap and 2DEG population. Different drain voltages are also used to investigate the bias dependence of the phase noise. From 1 Hz to 10 KHz, an 1/f region is identified in the additive phase noise at 2 GHz, which is indicative of the presence of uniformly distributed traps. Further a decrease in additive phase noise is clearly observed with increasing photon energies below the GaN bandgap. This is due to the decrease of the trap population induced by photon assisted emission of electrons from the trap levels to the conduction band. Further it is found that the additive phase noise at 2 GHz increases at higher drain voltages. Various RF load impedances are also used to further characterize the noise performance of both passivated and unpassivated AlGaIn/GaN HEMTs. The larger the drain voltage swing introduced, the more additive phase noise is observed. A degradation of additive phase noise is also observed with the unpassivated device compared to the passivated device. Some preliminary results from a physical cyclostationary model are also presented. The observed 1/f noise increase at RF occurring at large bias or in large signal RF operation are attributed to the increase efficiency of the RF upconversion of the trap 1/f occupation fluctuation when the drain resistance increases. This work also demonstrates that the new combined additive phase noise/LSNA testbed developed is a useful tool for characterizing the additive phase noise in transistors/amplifiers under large signal operation. [C529]

"Effect of variation of topological changes on the Equivalent Circuit Parameters of pseudomorphic HEMTs"

This paper describes the study of effect of variation of topological changes on parameters of pseudomorphic HEMTs. Devices with 2 gate fingers, having gate width of 150 Γ ,B μ m, source-drain spacing of 4 Γ ,B μ m and 3 Γ ,B μ m, and with two different gate structures, viz., Γ ,Bi and T types were fabricated. On-wafer measurement of S-parameters for different devices was done from 100 MHz to 40 GHz under different bias conditions. Using this data, all the Equivalent Circuit Parameters (ECPs) were then extracted for each device. This method was then used for the calculation of the ECPs of 4 Γ ,B μ m and 3 Γ ,B μ m spacings, and trends of various parameters were analyzed. [C530]

"SUMATRA, a W-band SAR for UAV application"

Based upon most recent advances in millimeterwave technology, especially monolithic integrated low noise or medium power HEMT amplifiers and an integrated receiver containing an LNA, Mixer and IF Amplifier, a miniaturized experimental radar at 94 GHz was designed with the aim to be used on board of a remotely piloted model aircraft. This highly advanced front-end technique was combined with of-the-shelf model aircraft hardware and miniaturized GPS and data transmission equipment which is readily available. Goal of the project is to demonstrate, that using modern 94-GHz front-end technique combined with achievable back-end components it is possible to set up a versatile SAR system usable for a wide range of remote sensing applications at medium range. The paper describes the current state of the research project SUMATRA-94 and gives some perspectives for future applications. [C531]

"GaN monolithic inverter IC using normally-off gate injection transistors with planar isolation on Si substrate"

We present a GaN monolithic inverter IC on Si substrate and successful motor-drive by it for the first time. Taking advantages of the bi-directional operation free from the forward voltage off-set, the inverter can be operated just by the integrated six GaN-based normally-off gate injection transistors (GITs) without any external fast recovery diodes (FRDs) to flow the fly-wheel current. The IC enables the efficiency as high as 93% at low power operation where so far that of conventional Si-based inverters has remained lower value owing to the forward voltage off-set. The key processing technology is the newly introduced planar isolation using Fe ion implantation which fully isolates the GaN-based lateral devices each other. [C532]

"Copyright"

The following topics are dealt with: CMOS junctions, annealing, metrology, CMOS devices, semiconductor device modelling and simulation, PRAM, RRAM, Fermi level pinning, NexFET, power semiconductor devices, displays, sensors, MEMS, TFTs, solid-state and nanoelectronic devices, graphene, FinFET, nanowire devices, thin film circuits, ESD, reliability, HEMT, MOSFET, CMOS process modelling and simulation, carbon nanotube transistors, medical electronics and bioelectronics, stackable cross point phase change memory, SoC, random telegraph noise, microresonators, flash memory, quantum well field effect transistors, interconnections, and solid electrolyte switches. [C533]

"The effect of multiple gate for P1dB and PAE of AlGaAs/InGaAs HEMT"

The impacts of numbers of gate fingers on large signal of High Electron Mobility Transistor (HEMT) were studied in this paper. The analysis was carried out measurement using Maury Automated Tuner System (ATS) at frequency of 2.4 GHz and 5.8 GHz. The measurement results shows that the transistor that has higher number of gate fingers is less preferred for high P1dB compression and Power Added Efficiency (PAE) performance. This is due to the parasitic existed in larger transistors that cause P1dB and PAE to drop significantly. Moreover, higher input impedance of the transistors further contributions to the degradation of these performance indicators. Finally, the optimum transistors is proposed. [C534]

"Generic Power Amplifier linearization"

Classic linearization of a radiofrequency (RF) Power Amplifier (PA) is based on measuring its response to a representative test signal in order to extract pre-distortion parameters. Characterizing an RF PA under 3GPP Long Term Evolution (LTE) RF signals requires high speed data acquisition instruments and customized algorithms to estimate its response. In this work, a PA linearization method using a generic probing signal to extract pre-distortion parameters is proposed. A GaN HEMT Class-AB structure is tested to demonstrate the effectiveness of the proposed linearization method. [C535]

"Characteristics analysis of gate dielectrics in AlGaIn/GaN MIS-HEMT"

Compared with the conventional high electron mobility transistor (HEMT), the metal-insulator-semiconductor (MIS)-HEMT has several advantages such as lower gate leakage current, higher maximum saturation drain current and the better restrain of current collapse. This paper studied the effects of temperature and the thickness of dielectric on the characteristics of Al₂O₃MIS-HEMT. The device characteristics degrade with the increase of temperature. The thicker dielectric can decrease the gate leakage current. However, it can not provide larger transconductance because the permittivity of Al₂O₃ isn't very high. Several promising alternatives of gate dielectrics (HfSiON, HfAlON, LT-GaN) are presented in this paper. [C536]

"Effect of high temperature AlN interlayer on the performance of AlGaIn/GaN properties"

A novel structure of AlGaIn/GaN heterostructure which has a high temperature AlN interlayer (HT-AlN) in GaN buffer grown by metal organic chemical vapor deposition (MOCVD) on c-plane sapphire substrate has been researched. It is found that both electron mobility and sheet carrier concentration are increased by the HT-AlN interlayer compared to AlGaIn/GaN heterostructure without HT-AlN interlayer. The sheet carrier concentration and Hall mobility measured by Hall increased from $1.446 \times 10^{13} \text{ cm}^{-2}$ and $1019 \text{ cm}^2/\text{V}\cdot\text{s}$ to $1.605 \times 10^{13} \text{ cm}^{-2}$ and $1036 \text{ cm}^2/\text{V}\cdot\text{s}$, respectively, hence the sheet resistance decreased from $424 \Omega/\square$ to $376 \Omega/\square$. [C537]

"GaN smart power chip technology"

Wide-bandgap GaN-based semiconductor materials are attracting considerable attention as the preferred material for power electronics applications, owing to their superior properties including high breakdown electric-field, high carrier density, high electron mobility and high saturation velocity. In this paper, the technologies for implementing GaN smart power ICs will be introduced based on the large-size, low-cost and highly scalable GaN-on-Si platform. High-voltage power components (normally-off power transistors and HEMT-compatible rectifiers) and low-voltage periphery devices for digital/analog mixed-signal circuits are successfully integrated with the same fabrication process. In particular, key analog functional blocks such as voltage reference generators and comparators are demonstrated using GaN-based technology for the first time. The optimized voltage reference generator achieved less than $70 \text{ ppm}/\text{V}\cdot^\circ\text{C}$ drift and can be used as a reference voltage in various biasing and sensing circuits. The temperature-dependent performance of a conventional comparator is characterized and a new temperature-compensated comparator circuit is also demonstrated. The positive limiting level of the temperature-compensated comparator is less than $450 \text{ ppm}/\text{V}\cdot^\circ\text{C}$ drift compared to $1400 \text{ ppm}/\text{V}\cdot^\circ\text{C}$ in the conventional comparator. [C538]

"RF-DC power conversion of Schottky diode fabricated on AlGaAs/GaAs heterostructure for on-chip rectenna device application in nanosystem"

The Schottky diodes enjoined with coplanar waveguides are investigated for applications in on-chip rectenna device application without insertion of a matching circuit. The design, fabrication, DC characteristics and RF-to-DC conversion of the AlGaAs/GaAs HEMT Schottky diode is presented. The RF signals are well converted by the fabricated Schottky diodes with cut-off frequency up to 20 GHz estimated in direct injection experiments. The outcomes of these results provide conduit for breakthrough designs for ultra-low power on-chip rectenna device technology to be integrated in nanosystems. [C539]

"Terahertz resonant frequencies of grating-bicoupled plasma wave devices"

Resonant frequencies of plasma oscillations in the grating-bicoupled HEMT-like structures with interdigitated gates are evaluated in the presence of non-saturated source-drain current for different combinations of gate bias voltages. [C540]

"Multi-cantilever HEMT-based resonant sensor"

In this paper resonant sensor based on micro-machined high-electron mobility transistor (HEMT) in which multiple suspended resonant cantilevers serve as floating gates is proposed and its analytical and lumped equivalent circuit models are developed. The proposed HEMT-based multi-cantilever resonant sensor enables electrostatic actuation and electrical readout. Mass absorption by a cantilever results in the change in its mechanical resonant frequency. Mechanical oscillations of such a cantilever excited electrically control the source-drain current. Thus, its resonant frequency shift can be detected as a frequency shift in the resonant peak of the source-drain current. Mechanical oscillations of each cantilever and electromechanical transducer are represented by relevant circuit components. The developed equivalent circuit of multi-cantilever resonant sensor was used to simulate its frequency response using Is-Spice software. The simulation reveals an enhanced source-drain current with a peak at a single frequency for the array of the identical cantilevers. In the case of multiple different cantilevers the simulated source-drain current reveals peaks at frequencies corresponding to mechanical resonances of the cantilevers, as expected. [C541]

"Low-cost high-efficient 10-Watt X-band high-power amplifier"

A high power X-band amplifier with an output power over 10 Watts and a Power Added Efficiency (PAE) in excess of 40 percent has been developed. The design was fabricated in a $0.25 \mu\text{m}$ pHEMT GaAs process (WIN Semiconductor PP25-01). The small die area in combination with a 6-inch wafer technology provides the possibility for low cost production of a high performance X-band T/R chipset. [C542]

"GaN lattice matched ZnO/Pr₂O₃ film as gate dielectric oxide layer for AlGaIn/GaN HEMT"

In this work, we perform AlGaIn/GaN MOS-HEMT by using ZnO/Pr₂O₃ as gate dielectric. After 600 °C annealing, the XRD analysis shows ZnO thin films with highly crystalline characteristics, which exhibit a lattice constant ($a = 3.2498$, $c = 5.2066$) matched to GaN ($a = 3.1890$, $c = 5.1855$). The gate leakage current can be improved significantly by inserting ZnO/Pr₂O₃ dielectric layer; meanwhile, ZnO/Pr₂O₃ MOS-HEMT shows superior breakdown voltage performance toward ZnO MOS-HEMT and conventional Ni/Au HEMT. From these results, ZnO/Pr₂O₃ dielectric is promising for low leakage current of AlGaIn/GaN based MOS-HEMT. [C543]

"Microwave characteristics of Al_xGa_{1-x}N/In_xGa_{1-x}N/GaN-based HEMT using propagation delay model"

A new GaN-based high electron mobility transistor (HEMT) structure is proposed to study DC, RF and microwave characteristics using TCAD tool and propagation delay model. The proposed device is embedded into the circuit and its circuit characteristics are also studied and presented in this paper. Apart from DC and small-signal characteristics, we have investigated various microwave parameters such as maximum allowable gain (MAG), maximum stable gain (MSG), Rollet stability factor (K), Mason's unilateral gain (MUG), cutoff frequency (f_T), maximum frequency of oscillation (f_{max}), two port network parameters such as input/output reflection parameters (S_{11} , S_{22}) followed by Smith chart. We have determined the range of frequency where proposed HEMT will be used as stable amplifier/oscillator. The cut-off frequency of such structure is found to be 32 GHz and noteworthy. [C544]

"An 18GHz LNA Ga FET high gain amplifier for WLAN"

In this article we design a novel Ka band low noise amplifier with high stability. In this design Ga FET is used to high gain and low noise figure and conditional and unconditional stability. We applied a low noise cost solution for various Ka band receivers such as P-to-P radio, WLAN and UWB sensors. Finally circuit layout with ADS software is presented and very low noise figure about 1.3 dB and about 16 dB gain was taken. [C545]

"Modeling of AlGaIn/GaN HEMTs using field-plate technology"

An analytical approach for calculating the electric field and designing field plates (FP) for reducing the peak electric field in the channel and at the surface of high electron mobility transistors (HEMTs) for a given gate and drain voltage is presented in this paper. The difference caused by the field plate is better demonstrated by the electrical field distribution in the channel. A 50% reduction of the maximum electric field, located at the drain side of the gate edge, is achieved by the introduction of the field plate, thus increasing the breakdown voltage. [C546]

"Satellite-receiving-system overlay with WDM RoF on 10Gb/s link"

Received signal from weather satellite is overlaid with WDM RoF technique on 10.7Gb/s (OTU2) data stream. For extending the signal transmission distance between the antenna and the receiver, a low noise amplifier is designed by using an EP-HEMT to achieve lower noise and higher gain so that the received signal level is as low as -130dBm. The received signal is amplified by using a laser driver which is also designed by using the EP-HEMT. A low noise and linear 1550nm DFB laser is modulated by the laser driver. The converted optical signal is overlaid on a 10.7Gb/s (OTU2) data streams by using a 1310/1550nm WDM. A clear image from the weather satellite is received after 40km SMF. There was no degradation in the eye diagram and total jitter of the 10.7Gb/s data signal. [C547]

"Subwavelength detection of terahertz radiation using GaAs HEMTs"

We have designed and fabricated THz detectors based on excitation and rectification of radiation induced overdamped THz plasmons in InGaAs/GaAs HEMT structures. These plasma wave detectors were used to image the beam profile of THz gas laser operating at 1.63 THz with FWHM of 140 GHz. The images were recorded with deep sub-wavelength spatial resolution. This allowed to resolve a sub-wavelength shifts in the detected THz responses from adjacent transistors with equivalent separation distances of 12 GHz and 30 GHz. Our results motivate the utilization of plasma wave detectors for near-field terahertz imaging and suggest the possibility of designing focal plane arrays with subwavelength pixel pitch. [C548]

"A high performance plastic air-cavity QFN solution for future potential microwave package large scale application"

A potential large scale QFN package solution-plastic air-cavity QFN package, compatible with SMD assembly lines, for future low cost, miniature size and attractive performance microwave package application is proposed

in this paper. A 6 GHz~18 GHz LNA MMIC (2 ГрВ— 1mm²) is developed using a commercial GaAs pHEMT process and integrated into this novel and cost effective package solution. The measured results (not de-embedded with test fixture) show that noise figure is less than 2.75 dB, and input return loss is below 10dB, moreover small signal gain is more than 19.3 dB and gain flatness is $\Gamma_{B\pm 1.75dB}$ with 4 ГрВ— 4 mm² packaged area and DC power dissipation 120 mW across 6 GHz to 18 GHz. [C549]

"High-dynamic-range zero-bias microwave detector using AlGaIn/GaN-based lateral field-effect diode"

A zero-bias microwave detector using AlGaIn/GaN-based lateral field-effect diode is demonstrated. The diode is compatible with AlGaIn/GaN HEMT in fabrication process. Taking advantage of threshold-voltage modulation of fluorine plasma treatment technique, the diode features low turn-on voltage and strong nonlinearity at zero bias thus eliminating DC supplies for the application of zero-bias microwave detection. The diode exhibits good sensitivity from room temperature to 250Г,B°C. The peak on-wafer measured sensitivity ($\Gamma_{B\mu V}$) of 1027 mV/mW is achieved at 5 GHz at 50Г,B°C. The maximum conjugately-matched sensitivity ($\Gamma_{B\mu V,opt}$) of 9030 mV/mW is obtained at 2 GHz at 50Г,B°C and decreases to 1227 mV/mW at 250Г,B°C. At room temperature, the dynamic range as high as 53 and 54 dB at 2 and 5 GHz is observed, respectively, which are the highest values reported so far. [C550]

"Critical voltage for electrical reliability of GaN high electron mobility transistors on Si substrate"

We have evaluated the electrical reliability of GaN HEMTs on Si by carrying out VDS= 0 V step-stress experiments. We have found that these devices show a degradation pattern that is very similar to that of devices on SiC with a critical voltage at which a sudden degradation of the gate current takes place. In general, devices on Si have a relatively high critical voltage although its distribution on a wafer is fairly broad even on a short-range scale. [C551]

"Reliability of AlGaIn/GaN HEMTs under DC- and RF-operation"

In this work, device reliability under DC- and RF-operation at high temperatures ranging from 140degC to 200degC and at high drain voltage of 50 V has been achieved by improving the gate metal processing technology. It will be shown by long term stress tests that the gate processing technology is the key to improve the stability of the gate leakage current. The short term drain voltage robustness under off state condition has been examined by a DC-voltage-step-stress test. At the maximum drain voltage of 130 V the gate and drain current densities remain below 0.1 mA/mm. First RF stress test of a 2.4 mm power FETs at 2 GHz also shows little degradation. [C552]

"Reliability of AlGaIn/GaN HEMT: Impact of acceleration condition on dominant degradation mechanism"

Reliability issue for AlGaIn/GaN HEMT is in focus of today's research, especially for high voltage operation. RF overload tests at various channel temperatures and drain bias were performed using on-probes reliability testing allowing quick feedback to technology. Two degradation mechanisms: inverse piezoelectric effect and electron trapping were recognized. Unambiguous identification of degradation mechanism by gate current evolution was proposed. Mapping of dominant degradation mechanism as a function of channel temperature and drain bias was performed for given technology. Both electron trapping and inverse piezoelectric effect depend on electric field and on channel temperature, which are controlled by operational biases and base plate temperature consequently. [C553]

"Self heating of AlGaIn/GaN HEMTs in pulsed operation"

The purpose of this work was to develop a TCAD device model to study the electrical and thermal characteristics of the AlGaIn/GaN HEMT in the time domain in contrast to a DC thermal equilibrium analysis. We first examined a channel temperature technique Method 3104 of MIL-STD 750D to determine the corresponding location in the HEMT structure that the gate voltage measurement predicts the temperature. Second, we investigated the performance of single and multiple pulses effects on heating of the HEMT. Third, we studied and compared the heating between the DC analysis and a RF transient (multiple pulses) analysis with the same average device power. Finally, we observe large temperature gradients in the device in initial device heating not capable of being observed in a DC TCAD device analysis. [C554]

"Reliability evaluation of hermetic GaAs HEMT MMICs using wafer-scale-assembly technology for compact and light-weight applications"

Wafer-scale-assembly (WSA) technology has been developed for compact and light-weight applications at the Northrop Grumman Corporation. To insure successful insertion of WSA hermetic MMICs for military and space applications, high-reliability demonstration is essential. In this study, we performed two-temperature lifetesting to evaluate the reliability performance of WSA hermetic GaAs HEMT MMICs. It was observed that gate sinking is still the primary degradation mechanism. In addition, finite-element thermal analysis was performed on the hermetic HEMT MMICs. The results showed an increase in channel temperature over similar non-hermetic GaAs HEMTs of approximately 8degC. The median-time-to-failure (MTF) of approximately 5.6 times 10⁶ hours at T_{channel} of 125degC was obtained based on reliability analysis with lower bound activation energy (E_a) of 1 eV. This promising result suggests that WSA technology could deliver reliable compact and light-weight HEMT MMICs for military and space applications. [C555]

"Recent advances on the understanding of the physics of failure of GaN on SiC FET technology"

GaN on SiC high electron mobility transistor (HEMT) is the most promising III-V semiconductor technology to deliver large RF power densities (5 W/mm and beyond) at high frequency (~10 GHz and beyond). This performance can be achieved because of the large bandgap of GaN that allows for high critical fields and thus high voltage operation and high RF power densities at small drain-source spacing, because of the existence of an even higher heterobarrier (AlGa_N) with a reasonable lattice mismatch, capable of providing the conduction band discontinuity required for effective carrier confinement, and because of the existence of a semi insulating substrate (SiC) with excellent thermal and insulating properties on which GaN of reasonable quality can be grown. [C556]

"Comparison of DC measurement methods to determine GaN HEMT reliability"

In this paper we compare methods to determine the life-time of AlGa_N/GaN HEMTs by accelerated DC life-tests. They all base on monitoring of both, IDSS and IDQ during the life-test, either at room temperature or at the elevated ambient temperature. The goal is to investigate whether interruptions of the life test to measure IDSS at room temperature can be prevented and replaced by screening this parameter during the life test at higher temperature. The investigation shows that the so called intrinsic IDSS measurement is a quite interesting and helpful tool, but too often measurement of this parameter adds additional stress to the device. In addition we saw that intermediate measurements did not stress the devices as suspected. We also observed that for stress tests at constant P_D the drift of the gate voltage can be used as failure criterion, although it has no linear relationship to IDSS and therefore the gate voltage drifts more than IDSS and leads to more conservative life-time. [C557]

"MMIC LNAs for Radioastronomy Applications Using Advanced Industrial 70 nm Metamorphic Technology"

A set of monolithic low-noise amplifiers have been designed and realised making use of an advanced industrial GaAs 70 nm metamorphic technology with high indium content. Operating frequencies of the realised amplifiers span from C-to W-band, with resulting performance in line with the requirements of many advanced radioastronomy applications. As an example, 2.7 dB NF from 75 to 90 GHz associated to 25 dB gain and 1.3 typical NF from 30 to 50 GHz with 30 dB gain have been achieved. [C558]

"0.5-2.5 GHz, 10W MMIC Power Amplifier in GaN HEMT Technology"

We report a broadband lossy matched GaN on SiC HEMT power amplifier MMIC with 15 dB gain, 0.5-2.5 GHz bandwidth, 9-13.6 W CW output power and 44.9-63.6% drain efficiency over the band. The amplifier operates from a 48 V drain supply and is packaged in a ceramic S08 package. These amplifiers are intended for use in wideband digital communication applications. [C559]

"High Linearity AlGaAs/InGaAs Pseudomorphic HEMT Driver Amplifier Using Tunable Field-Plate Voltage Technology"

A high-linearity AlGaAs/InGaAs pseudomorphic HEMT RF driver amplifier was developed using a tunable field-plate (FP) bias voltage technology in this study. In order to improve the circuit linearity performance, an FP device was employed at the output stage to provide an additional mechanism to suppress the power of the second and third-order harmonics in a two stage 5.2 GHz driver amplifier. A standard Class AB driver amplifier without using FP technology was also implemented for comparison under the identical power consumption. The circuit with an FP device biased at V_{FP} = -4 V in the output stage demonstrated at least 2 dB improvement on the third-order intercept point at input (IIP₃) performance over the standard one within the useful power range in two tone measurement. [C560]

"A Fully Integrated, Compound Transceiver MIMIC Utilizing Six Antenna Ports for 60 GHz Wireless Applications"

A fully integrated transceiver MIMIC (millimeter wave monolithic integrated circuit) with six antenna port functionality for 55 to 65 GHz wireless applications has been developed. The chip has been realized using 100 nm gatelength metamorphic InAlAs / InGaAs HEMT (high electron mobility transistor) technology on GaAs substrates together with CPW (coplanar waveguide) technology. The novel transceiver topology consists of switches, amplifiers, mixers, a voltage controlled oscillator and a frequency divider. The receiver chain shows noise figure < 2.6 dB on the low noise amplifier level and smaller than 7 dB including the antenna switching network. The medium output power amplifier delivers the saturated power level of + 14 dB m. This is the highest integration level for a 60 GHz compound semiconductor transceiver chip reported to-date. [C561]

"Design Method for UHF Class-E Power Amplifiers"

This paper describes a method for designing single-ended high-efficiency switched-mode class-E UHF power amplifiers. The design procedure consists of a modified load pull transistor characterization from which a power/efficiency metric is calculated. Results for four prototypes using different device technologies are presented in detail. Amplifiers with Si-LDMOS, SiC-MESFET, GaN-HEMT on a Si substrate, and GaN-HEMT on a SiC substrate produce power over 40W with power-added efficiency greater than 75% and gain between 13 dB and 17 dB. [C562]

"Accurate HEMT Switch Large-Signal Device Model Derived from Pulsed-Bias Capacitance and Current Characteristics"

Large-signal operation of HEMT (High Electron Mobility Transistor) switch device is found to be much affected by trap-induced slow dynamic effects. Off-state gate and drain capacitances derived from pulsed S-parameter measurements with a large negative gate quiescent voltage are less voltage-dependent than capacitances measured by a continuous bias. Two-dimensional device simulation suggests that surface traps near the gate edge are responsible for the observed dynamic effect. A new large-signal device model is developed that takes both C-V and I-V pulsed dynamic behavior into account. The new model is shown to accurately predict harmonics generated from off-and on-state switches. [C563]

"Sub-mW Operation of InP HEMT X-Band Low-Noise Amplifiers for Low Power Applications"

For the first time, the sub-mW operation of InP HEMT X-band low-noise amplifiers on 4-inch InP wafer was demonstrated. With optimized non-alloyed ohmic contact, gate recess profile and epitaxial layer design, the InP HEMT achieves average peak transconductance of 1150 mS/mm at $V_{DS} = 0.3$ V. The mean current cut off frequency is above 150 GHz at $V_{DS} = 0.3$ V and $I_{DS} = 150$ mA/mm. The developed low power InP HEMTs enables the manufacturing of low-noise amplifiers for low power applications. The superior performance of X-band low-noise amplifiers was also demonstrated. Operating at a supply voltage of 0.25 V and drain current of 3.75 mA with DC power of 0.937 mW, the low noise amplifier exhibits noise figure of 1.6 dB and gain of 11 dB at frequencies from 6 to 12 GHz. [C564]

"High Efficiency Digital GaN MMIC Power Amplifiers for Future Switch-Mode Based Mobile Communication Systems"

A high efficiency digital MMIC amplifier for mobile communication switch-mode concepts was designed by utilizing a 0.25 μ m GaN HEMT technology with f_{tau} of 32 GHz. A comparative investigation of two different driver concepts for a 1.2 mm GaN HEMT PA is shown. The MMICs were on-wafer evaluated for class-D and class-S operation. A drain efficiency of 70% for an output power of 4.4 W for a band pass delta-sigma (BPDS) class-S input signal at a bit rate of 3.6 Gbps equivalent to a 0.9 GHz fundamental was obtained. For the first time the operating mode up to 8 Gbps (2 GHz) is shown with an efficiency of 62%, demonstrating the prospect of future use of GaN HEMTs for switch mode amplifier concepts. [C565]

"Broadband CPW-fed active monopole antenna for WLAN applications"

A coplanar waveguide (CPW)-fed monopole as a radiating element of an active antenna amplifier is proposed for chip size realization. A monopole antenna, which is integrated with a high electron mobility transistor (HEMT), demonstrates stable oscillations at a frequency of around 5.8 GHz within a 10% bandwidth of 580 MHz (from 5.58 to 6.16 GHz). The active antenna has dimensions of 9 mm times 8 mm times 1.3 mm. The measurement results show that the antenna effective isotropic radiated power (EIRP) is +10.5 dBm, power added efficiency (PAE) 30.3%, and the phase noise at 100 kHz offset -88.3 dBc/Hz. [C566]

"A 24-48 GHz cascode HEMT mixer with DC to 15 GHz IF bandwidth for astronomy radio telescope"

This paper presents a wide IF bandwidth (dc15 GHz) mixer with 27 to 48 GHz RF bandwidth using cascode device technique. The mixer is implemented in 0.15- μ m GaAs PHEMT process. The measured 3-dB IF bandwidth is from dc to 15 GHz and RF bandwidth is from 27 to 48 GHz. This mixer achieves a measured conversion gain of 0 dB and isolation of 23 dB. This is the first demonstration of wide IF bandwidth mixers using GaAs cascode HEMT devices. [C567]

"A highly efficient Doherty power amplifier employing optimized carrier cell"

We have proposed a novel design of the Doherty power amplifier (PA) to improve the efficiency at a back-off output power level. It is shown that the carrier PA having 100 Ω load impedance is not an optimum for maximizing the efficiency at the back-off level due to the knee voltage effect. Thus, we introduce a Doherty PA having a load impedance larger than 100 Ω when the peaking PA is turned off. For experimental demonstration, we have implemented and tested the Doherty PA using Cree GaN HEMT CGH40045 devices at 2.655 GHz. The measured results clearly show that the proposed Doherty PA delivers better efficiency at the back-off output power level than the conventional PA due to the better load condition for improving efficiency. [C568]

"Critical analysis of results for a european GaN power amplifier after first iteration"

This paper presents the results of the development of 2-6 GHz broadband high-power amplifiers (HPA) within the 1st iteration of the European Korrigan project. The HPAs were fabricated using AlGaIn/GaN high electronic mobility transistors (HEMT) and monolithic microwave integrated circuit (MMIC) technology. Two microstrip HPAs with output-stage active periphery of 4 mm and 8 mm are reported. The two-stage amplifiers were designed to be fully matched to 50 Ω input and output impedances. Based on a 0.5 μ m gate-length microstrip HEMT technology, the MMICs were fabricated on a 70 μ m thick SiC substrate. Under a 25 V DC bias condition the broadband amplifiers have exhibited about 18 dB small-signal gain. The 4mm-HPA delivers 10 W output power and 25% power added efficiency (PAE) in the 2-6 GHz frequency band, in continuous wave operation (CW) at $V_{ds}=25V$. On the other hand, the 8mm-HPA delivers 16 W and 20% PAE in CW. In pulsed-mode, the output powers are 14 W and 25 W for the 4 mm and the 8 mm HPAs, respectively. [C569]

"Wide band high linearity and high isolation mixer MMIC developed on GaAs 0.25 μ m Power pHEMT technology"

In the frame of radar and warfare applications, a Monolithic Microwave Integrated Circuit (MMIC) Mixer has been developed using a UMS GaAs 0.25 μ m Power pHEMT Technology. The mixer presented in this document exhibits at the same time wide frequency band, high isolation and high linearity. In the 6-18 GHz frequency band, the mixer demonstrates 25 dB for the isolations, an input RF compression point higher than 16 dBm and an Input IP3 of 25 dBm. To our knowledge these performances are among the highest reported on a fully integrated GaAs MMIC. [C570]

"Sub-harmonic self-oscillating mixer design using dual-mode substrate integrated waveguide cavity"

This paper presents a novel sub-harmonic self-oscillating mixer (SOM) topology that makes use of the orthogonality of two operating modes in a substrate integrated waveguide (SIW) cavity. The SOM circuit consists of a dual-mode SIW band-pass filter (BPF), a common source hetero-junction FET (HJFET) and a low-pass filter. The fundamental mode (H101) of the SIW cavity is used for RF mode operation while the H202 mode is used for local oscillation. A Ka-band experimental prototype has been designed to demonstrate and validate our circuit concept. Measurement results show good performances of our proposed circuitry. [C571]

"A complete 38 GHz transmit and receive chip set in low cost surface mount package"

While most Point-to-Point radio systems migrate to SMT (Surface Mount Technology) over chip-and-wire, the 38 GHz band has provided the largest challenge. This paper demonstrates a commercially viable complete SMT solution to receive LNA-down-converter and transmit up-converter, VGA, power amp and directional power detector. The receive chain provides 10 dB conversion gain with 4.5 dB NF. The transmit chain provides 26 dB maximum total gain with 24 dB gain control and 30 dBm maximum power out at 1 dB compression. The amplifiers are housed in 5times5 mm packages while the detector uses a chip scale 1times0.5 mm package. All cover the 37 to 42 GHz radio bands. This is the only known complete SMT Tx/Rx solution to be published or

demonstrated. [C572]

"Design of X-Band GaN MMICs using field plates"

Two field plate variants of AlGaIn/GaN-HEMTs with and without source-connected field plate (Idquoshieldrdquo) were analyzed for the design of efficient High-Power-Amplifier MMICs operating at X-Band frequencies. This paper presents the design and realization of three dual-stage microstrip MMICs using different device variants for narrowband and broadband applications. Two narrowband HPAs, using GaN HEMTs with and without shield, achieve a maximum output power and PAE of 20 W and >39 %, respectively. A broadband amplifier containing GaN HEMTs without shield reaches a simulated output power beyond 12 W with >30 % PAE over 9-11 GHz. [C573]

"A novel size reduction of a MMIC I/Q direct down converter in uniplanar technology at 20 GHz using CPW and ACPS stubs loading for an EHF satcom terminal phased array size"

This paper proposes a novel compact uniplanar 20 GHz/baseband I/Q direct downconverter GaAs MMIC. It uses previously developed ACPS and CPW structures for capacitive and inductive loading techniques to drastically reduce its size. The proposed I/Q down converter uses direct analog extraction of the baseband in-phase and quadrature (I and Q) signals from the 20 GHz RF signal. Two pairs of antiparallel diodes achieve frequency translation by mixing the RF signal with the fundamental local oscillator (LO) pump while novel ACPS reduced size magic T, provide high local oscillator (LO)-to-RF isolation and good spurious suppression. The circuit was fabricated using OMMIC's ED02AH foundry process and contains two pairs of 0.18 μm PHEMT based diodes, each having two 15- μm cathode fingers. This 3.15 times 4.1 mm²chip uses a previously developed, reduced size Wilkinson divider as an RF divider and a previously developed, reduced size 90deg coupler. The I/Q down converter conversion gain was measured to be -15.5dB plusmn1 dB over the RF frequency range of 20.2 to 21.2 GHz with the IF fixed at 1 MHz. The amplitude imbalance between the I&Q channels was under 0.8dB and the quadrature phase error was less than 4degover the frequency range. The circuit also does not require any dc bias. Compared to the conventional microstrip I/Q direct down converter a 40% reduction in circuit area was achieved with better performance. [C574]

"An inverse class-F GaN HEMT power amplifier with 78% PAE at 3.5 GHz"

This paper presents the design and implementation of an inverse class F power amplifier (PA) using a high power GaN HEMT transistor. For a 3.5 GHz continuous wave (CW) signal, the measurement results show state-of-the-art power-added efficiency (PAE) of 78%, a drain efficiency of 82%, a gain of 12 dB, and an output power of 11 W. Moreover, drain efficiency is maintained over 60% and the output power level is higher than 10 W over 300 MHz bandwidth. To our knowledge, the presented power amplifier represents the highest efficiency for all switching mode PAs that have been reported for high power applications at frequencies above 2 GHz. [C575]

"A highly efficient Doherty power amplifier employing optimized carrier cell"

We have proposed a novel design of the Doherty power amplifier (PA) to improve the efficiency at a back-off output power level. It is shown that the carrier PA having 100 Ω load impedance is not an optimum for maximizing the efficiency at the back-off level due to the knee voltage effect. Thus, we introduce a Doherty PA having a load impedance larger than 100 Ω when the peaking PA is turned off. For experimental demonstration, we have implemented and tested the Doherty PA using Cree GaN HEMT CGH40045 devices at 2.655 GHz. The measured results clearly show that the proposed Doherty PA delivers better efficiency at the back-off output power level than the conventional PA due to the better load condition for improving efficiency. [C576]

"X-band T/R module in state-of-the-art GaN technology"

In this paper a first iteration X-band T/R module based on a GaN-HEMT MMIC Front-End chip-set, comprising a power amplifier, robust low-noise amplifier and power switch will be presented. Even though ultimate T/R module performance cannot be achieved with current GaN-HEMT technological maturity the impact that this technology can have at systems level in terms of performance/cost trade-off will be illustrated by means of a preliminary innovative module architecture which foresees the elimination of more traditional T/R module components such as ferrite circulator and limiter for front-end signal routing and protection. [C577]

"A 5GHz WLAN amplifier with novel on-chip positive voltage switchable bias implemented in a D-pHEMT process"

This paper presents the RF characterization of a 4.9-5.9 GHz microwave amplifier for WLAN applications with a novel on-chip positive voltage switchable bias implemented in a depletion p-HEMT process. In order to assess

the impact of the novel bias network on the amplifier's RF performance, a second amplifier without DC switch has also been designed and tested. Both amplifiers are biased at the same collector current value. Full characterization of both designs has been carried out vs. frequency, bias conditions and control voltage V_{Cfor} for the DC switchable amplifier at room temperature. The results demonstrate that the DC switch does not degrade the linear gain and return loss. The switch impact on the linearity performance is limited and still allows for a highly linear design. To the authors' knowledge, DC switching capability driven by a positive voltage has never been reported in normally on, D-FET based, monolithic microwave integrated circuits. [C578]

"Long-term stability of Gallium Nitride High Electron Mobility Transistors: a reliability physics approach"

Several groups have demonstrated nitride-based High Electron Mobility Transistors with excellent rf output power, with a constant increase in performances. However, despite the large efforts spent in the last few years, and the progress in MTTF (Mean Time To Failure) values, reliability of GaN HEMTs (High Electron Mobility Transistors) and MMICs (Millimeter Microwave Integrated Circuits) still has to be fully demonstrated, due to the continuous evolution of adopted processes and technologies, and to the lack of information concerning failure modes and mechanisms. The role of temperature in promoting GaN HEMT failure is controversial, and the factors accelerating degradation are largely unknown. This paper proposes a methodology for the analysis of failure modes and mechanisms of GaN HEMTs, based on the extensive characterization of deep levels using Deep Level Transient Spectroscopy (DLTS) and pulsed measurements, on the detailed analysis of electrical characteristics, and on comparison with two-dimensional device simulations. Results of failure analysis using various microscopy and spectroscopy techniques are presented and failure mechanisms observed at the high electric field values typical of the operation of these devices are reviewed. [C579]

"An ultra-low power OOK RF transceiver for wireless sensor networks"

An ultra-low power On-Off Keying (OOK) RF transceiver using a quasi-Monolithic Microwave Integrated Circuits (quasi-MMICs) method has been designed and fabricated on GaAs substrate for wireless sensor networks. To minimize power consumption, the transceiver was implemented using commercial $0.25\ \mu\text{m}$ \times $200\ \mu\text{m}$ Pseudomorphic High Electron Mobility Transistors (PHEMTs), with a switched oscillator for transmitter and direct detection architecture for receiver. The transceiver successfully operates at the center frequency of 10 GHz for compact antenna and with ultra-low power consumption and shows an output power of -15 dBm for the transmitter, an output voltage of 35 mV_P at an input power of -40 dBm for the receiver and a total power consumption of less than 0.9 mW. [C580]

"A 3.5 GHz 2nd harmonic tuned PA design"

The efficiency of microwave PAs is limited by the active device parameters and operating conditions. High efficiency can be obtained by a proper selection of bias point and harmonic terminations or, from a different point of view, by a proper output voltage and/or current waveform shaping. This work describes the design of a high efficient 3.5 GHz GaN HEMT power amplifier which may be used in WiMAX applications. The PA is designed by using a 2nd harmonic tuned (HT) approach and has been realized and measured. Its measured performances confirm the improvement obtained by means of harmonic manipulation over class AB (TL PA). An output power of 35.3 dBm has been measured for the maximum power added efficiency of 57.7%, drains efficiency of 69.18% and measured C/I₃ of 19.1 dB. [C581]

"A 140 GHz Heterodyne Receiver Chipset for Passive Millimeter Wave Imaging Applications"

A heterodyne receiver chipset for 140 GHz passive millimeter wave imaging applications is presented in this paper. The chipset consists of two different millimeter wave monolithic integrated circuits (MIMICs): a voltage controlled oscillator (VCO) working in the 35 GHz frequency range and a receiver chip hosting a low noise amplifier, a down-conversion mixer, a frequency multiplier and a local oscillator buffer amplifier together with a local oscillator distribution network. Both chips presented are realized using latest 100 nm gate length metamorphic InAlAs / InGaAs HEMT (high electron mobility transistor) technology on 50 μm thick and 4 inch diameter GaAs substrates. The chips are utilizing grounded coplanar waveguide (GCPW) technology. Within the frequency band of operation from 120 to 145 GHz the receiver is showing a noise figure of ~ 5 dB and a conversion gain between -1 and 2 dB. The voltage controlled oscillator can be tuned from 31 to 37 GHz with associated output power levels from -2 to +2 dBSm. All building blocks are explained in detail and measured results are presented. Finally the overall receiver performance is given. [C582]

"Modeling and performance analysis of high-speed, high-power GaN nanowire FETs"

We present the first analysis of the transport properties of deeply scaled (2 nm and 4 nm diameter) GaN NW

FETs. Even for the ultra-small diameter (~ 2 nm) GaN NW FET, the geometric gate capacitance C_G is smaller than the quantum capacitance C_Q , and thus the NW FETs operate in the classical capacitance limit (CCL) instead of operating in the quantum capacitance limit (QCL). This is a result of the high electron effective mass (0.19 m_0 and 0.16 m_0 for the lowest conduction band, respectively, for the 2 and 4 nm diameter NWs) and consequent high density of states. For the NW FETs with source Fermi levels such that $(E_{FEC}) = 0.2$ eV, the current density is 8.5, and 5 A/mm, respectively for the 2 and 4 nm diameter, which is 2–4 times higher than the experimental value of 2.3 A/mm for an AlN/GaN HEMT with a 3.5 nm AlN barrier. The off-current for these NW FETs is insignificant as a result of the wide bandgaps. The bandgaps for the 2 nm and 4 nm wires are 3.4 eV and 3.3 eV, respectively. The confinement has little effect on both the bandgap and conduction band effective mass. The output power is 0.06 mW and 0.07 mW for the 2 and 4 nm devices, respectively. [C583]

"A high-power Ka-band power amplifier design based on GaAs P-HEMT technology for VSAT ODU applications"

In this paper, a Ka-band GaAs pseudomorphic high electron mobility transistor (P-HEMT) monolithic microwave integrated circuit (MMIC) power amplifier for very small aperture terminal (VSAT) outdoor unit (ODU) transmitter applications is demonstrated. This three-stage power amplifier is designed to fully match the 50 Ω input and output impedances. With 6 V and -0.75 V DC bias, a small signal gain of 11 dB, a 1 dB compression power (P_{1dB}) of 29.5 dBm, a power added efficiency (PAE) of 31%, and a better than -15 dB input return loss are achieved from 28.5 to 31.5 GHz. The proposed Ka-band power amplifier is designed within a die size of about 3.344 Γ B— 1.964 mm² on GaAs substrate. [C584]

"An Overview of Semiconductor Technologies and Circuits for Terahertz Communication Applications"

An overview of the current status of the semiconductor device technologies and circuits for terahertz applications, especially for the broadband wireless communication systems, is provided in this work. Comparison between various semiconductor device technologies such as III-V HEMTs and HBTs, SiGe HBTs, and Si MOSFETs is presented and the current record performances of each technology are described. In addition, the best performing amplifiers, oscillators, and mixers as of today for possible terahertz communication system applications are presented and related issues are discussed. [C585]

"Small-signal and 30-GHz power performance of AlGaIn/GaN HFETs without back barriers"

Recently, back barrier structures using AlGaIn or InGaIn have commonly been employed for GaN heterostructure field-effect transistors (HFETs) with a goal of developing high-power amplifiers in the mm-wave frequency range. However, the back barrier possibly causes some disadvantages such as decreases in electron density (n_s) and thermal conductivity in exchange for an improvement on output conductance due to its strong carrier confinement. In this work, we characterized capabilities of AlGaIn/GaN HFETs without a back barrier for the mm-wave high-power applications. To enhance charge control, the device relied solely on a high gate aspect ratio design by using an extremely thin AlGaIn top barrier instead of the back barrier. The decrease in n_s caused by the thin AlGaIn barrier can be compensated by SiNx deposition. Similar device structures with a gate length (L_g) of 60 nm have demonstrated record RF small-signal characteristics in previous work; therefore, we studied the applicability of this concept to large-signal applications. [C586]

"High performance monolithic InP HBT-HEMT integration"

In this paper, we report the successful integration of high performance 0.5 Γ B μ m heterojunction bipolar transistors (HBTs) and 35 nm high electron mobility transistors (HEMT) on an indium phosphide (InP) substrate. Both transistors demonstrate power gain cutoff frequencies (f_{max}) in excess of 300 GHz, a $\sim 2\times$ improvement over previously reported results from integrated InP devices. The device epitaxy is grown in a single growth with the HEMT beneath the HBT sub-collector. Optimization of the device epitaxy and the HEMT lithography processes allow for HEMT-to-HBT separation of $<10 \Gamma$ B μ m. [C587]

"High current operation of enhancement-mode GaN MIS-HEMTs with triple cap structure using atomic layer deposited Al₂O₃ gate insulator"

In summary, we demonstrated AlGaIn/GaN enhancement-mode MIS-HEMTs that exhibited a high maximum drain current of 860 mA/mm and high off-state breakdown voltage of 320 V with threshold voltage of 3 V by introducing a piezoelectric-induced cap and a recessed ALD-MIS-gate structure. This is the highest $I_{d,on}/I_{d,off}$ with the breakdown voltage of over 300 V for enhancement-mode HEMTs. The 1 mm gate width device showed the output power of 4.8 W/mm and high drain efficiency of 61% at the $V_{gs} = 3.8$ V. These results suggest that the

recessed AlGaIn/GaN MIS-HEMT with the triple layer cap could be a promising technique for the Enhancement-mode transistors with a high breakdown voltage. [C588]

"60-nm GaN/AlGaIn DH-HEMTs with 1.0 Ω -mm Ron, 2.0 A/mm Idmax, and 153 GHz fT"

GaN-based HEMTs offer a unique combination of high electron velocity and high breakdown field making them the prime candidate for the highest performance millimeter-wave solid-state power amplifiers (PAs). Recently, we have demonstrated GaN MMIC PAs with an output power of 500 mW at W-band frequency range. The device high frequency performance has been significantly improved during the past years through vertical epitaxial scaling with double-hetero (DH) HEMT structures using an AlGaIn back barrier and reduction of gate length (Lg) down to 30 nm. One of technical challenges for further device scaling is reduction of parasitic resistances. Various approaches including alloyed contact to an n+-GaN cap layer, ion implantation, and a multichannel structure were attempted. However, a resulting on-resistance (Ron) is typically larger than 1.6 Ω ,Bi-mm. In this paper, we report on 60-nm gate GaN/Al0.3Ga0.7N DH-HEMTs with non-alloyed ohmic contacts and a very short gate recess of 100 nm in length, demonstrating an extremely low Ron of 1.0 Ω ,Bi-mm, a very high maximum drain current (Id,Bi)max of 2.0 A/mm, and a cutoff frequency (fT,Bi) of 153 GHz. [C589]

"The application analysis of GaN power devices in Radar transmitter"

Radar and electronic warfare (EW) system designers continually seek more affordable, lower weight, lower volume, and higher performance electronics that will support improved system effectiveness. Wide bandgap semiconductors are extremely attractive for the gamut of power electronics applications from power conditioning to microwave transmitters for Radar. Of the various materials and device technologies, the GaN HEMT seems the most promising. Compared with Si power device, it has remarkable advantages in output power, power density, operating frequency, operating bandwidth, environment adaptability and total efficiency and so on. It is shown that the superior physical attributes of GaN wide bandgap power devices lead to microwave transistors that are extremely well suited for high power applications. The performance characteristics and advantages of the GaN wide bandgap semiconductor are analyzed in detail. An L band 40W power amplifier was developed with the GaN wide bandgap semiconductor power devices. The performance test was carried out, which showed that compared with Si power device, the performance of Radar transmitter can be improved with the application of GaN wide band gap power devices. The superior properties of GaN wide band gap power devices make GaN technology a prime candidate for use in transmitters for radar systems. [C590]

"MBE-grown buffer with high breakdown voltage for nitride HEMTs on GaN template"

The paper presents a molecular beam epitaxial (MBE) grown buffer for nitride HEMT. The samples were grown at the same thermocouple temperature of 660 $^{\circ}$ C. GaN buffer layer was directly grown on the GaN template. In the secondary ion mass spectrometry (SIMS) measurements, unexpected silicon and oxygen impurity atoms at the template surface that caused the buffer leakage were identified. [C591]

"Effect of GaN buffer thickness on the electrical properties of RF-MBE grown AlGaIn/GaN HEMTs on free-standing GaN substrates"

In this work we investigated the effect of varying the thickness of the UID GaN buffer, dUID, on the electrical properties of AlGaIn/GaN heterostructures and HEMTs. Seven heterostructures with 50 nm < dUID < 500 nm were grown by RF-MBE on free-standing, semi-insulating HVPE-grown GaN substrates. Hall patterns, isolation test patterns, and HEMTs have been fabricated on these structures. We find that when dUID < 200 nm, a wide range of electrical properties, including Hall mobility, sheet resistance, gate leakage, interdevice isolation, and output conductance degrade as the UID GaN buffer thickness is decreased. [C592]

"Modeling of floating gate AlGaIn/GaN heterostructure-transistor based sensor"

This paper presents an analytical model for the estimation of charge concentration in liquid or gas analyte or of the charges induced by biomolecules detected by an AlGaIn/GaN high electron mobility transistor (HEMT) based sensor. The adsorbed molecules on the gate surface change the electrostatic potential of the surface. The change in electrostatic condition has been combined with the threshold and drift current equations to calculate the output current of the sensor. The model predicts the change in sensor current with the changes in the density of target analyte and calculates the concentration for which the output saturates at a certain drain-to-source potential. [C593]

"Ultra-scaled AlN/GaN enhancement- & depletion-mode nanoribbon HEMTs"

Due to its high electron density (> 1 $\times 10^{13}$ cm⁻²) and high electron mobility (> 1000 cm²/V.s), AlN/GaN

high-electron mobility transistors (HEMTs) present themselves as attractive candidates for high power and high speed applications. In order to continue increasing their high frequency performance, gate length (L_g) needs to be scaled down below 30 nm. For ultrascaled HEMTs, the barrier thickness includes the thickness of Al(GaN)N and a possible gate dielectric. To maintain the aspect ratio of L_g to barrier thickness (t_g) with a reasonable two-dimensional electron gas (2DEG) channel and low gate leakage, the gate length will be limited to be ~ 75 nm assuming a 2 nm AlN and a 3 nm gate dielectric. In this paper, a 3-dimensional nano-ribbon AlN/GaN HEMT structure is studied by simulations in comparison with experiments as a candidate for mitigating the short channel effects. By reducing the ribbon width, the device threshold voltage can also be continuously tuned from depletion mode to enhancement mode. [C594]

"Asymmetric condition computed from the four tone input GaN HEMT"

Asymmetric condition among the IMD components with respect to gate to source voltage (V_{gs}) of four tone input GaN HEMT is determined which is based on the carrier frequency (f_{B10}). In addition to that, the critical operating frequency interval is established. [C595]

"An MMIC receiver front-end design for 2.4GHz frequency band applications in 0.2 μ m GaAs pseudomorphic HEMT process"

A 2.4-GHz radio receiver front-end for ISM-band applications incorporating the superheterodyne architecture is designed and simulated in 0.2 μ m GaAs pseudomorphic HEMT technology. It features an ultra low-noise cascode-topology highly-integrated amplifier followed by an external image-rejection band-pass filter and an active half-Gilbert-cell down-conversion mixer with an IF frequency of 340 MHz. The receiver chain showed a gain, noise figure and input-referred third-order intercept-point equal to 17.9 dB, 1.8 dB and -18 dBm, respectively. Operating in 3-volt DC supply, it draws a 33-mA current. Finally, the characteristics of this front-end are compared in brief with those of a front-end of the same topology, but in a different process. [C596]

"Study on the Impact of Operating Point on Transmission Efficiency and Harmonic Suppression of T/R Module Based on Wide Bandgap Semiconductor"

Focusing on the impact of operating point to transmission efficiency and harmonic suppression of T/R module based on wide bandgap semiconductor, this paper theoretically analyzes the relation between operating point and transmission efficiency and linearity. Experiment of GaN T/R module based on GaN HEMT NPTB0004 shows that with optimal static current of 50mA, transmission PAE is up to 45.5% and suppression of second harmony is better than -21dBc, and suppression of third harmony is better than -15dBc. This can supply engineering value of active phase array radar for SAR application. [C597]

"High performance MBE-grown N-face microwave GaN HEMTs with >70% PAE"

In summary, MBE-grown N-face HEMTs deliver outstanding large signal performance in the C-band, comparable to well-developed Ga-face devices. It was demonstrated that back-barrier engineering could effectively enhance device performance, and hence should be identified as an important design consideration when scaling N-face HEMTs for millimeter-wave operations. [C598]

"X-band GaN HEMT advanced power amplifier unit for compact active phased array antennas"

A compact power amplifier unit for X-band solid-state Active Phased Array Antennas (APAAs) has been developed. Its major features are, (1) high power GaN (Gallium Nitride) HEMT is employed, (2) 16 transmit MIC modules are arrayed in line on a thin flat printed wiring board (PWB), (3) output power is 30 W (pulse) at each transmit-output port of the unit, hence 480 W in total, and (4) other necessary functions for phased array antennas, such as digital phase-shifters and RF dividers, are all included in this PWB. Resulting electrical measured data are presented in detail in the paper, proving that further power and frequency range increase for APAAs would become feasible by the concepts employed in this unit design. [C599]

"Hybrid PKI empirical-neural bias dependent noise model of microwave transistors"

In this paper a novel type of bias-dependent hybrid empirical-neural noise model of microwave transistors is proposed. It consists of an empirical noise model based on equivalent circuit representation and a PKI artificial neural network that produces values of the four noise parameters for an arbitrary bias point and frequency on the basis of the noise parameter values obtained by the empirical noise model. As it is shown by the numerical example of pHEMT device, this model provides results that agree well with the device measured characteristics. [C600]

"Combined empirical and look-up table approach for non-quasi-static modelling of GaN HEMTs"

In this paper the empirical and the look-up table approaches are combined to accurately model a gallium nitride based HEMT on silicon carbide. That solution allows to exploit the advantages of both approaches. The validity of the extracted model is verified by comparing model simulations with DC and microwave measurements.

[C601]

"Evaluation of commercial GaN HEMTs for pulsed power applications"

The present study investigates the behaviour and performance of commercially available GaN HEMTs provided by Cree Inc. The output power variation at pulse repetition frequencies (PRFs) in the range 100-450 kHz is presented. Rise and fall times are also investigated at different PRFs and power levels. The pulsed RF waveforms are obtained by switching the gate bias of the transistor on and completely off to ensure that the device goes through full transients for every pulse. The RF frequency at which the study is conducted is 3.5 GHz. The aim of the study is to assess the suitability of commercial GaN HEMTs to pulsed RF applications such as Radar. [C602]

"Device performance of AlGaIn/GaN MOS-HEMTs using La₂O₃ high-k oxide gate insulator"

AlGaIn/GaN metal-oxide-semiconductor high electron mobility transistors (MOS-HEMTs) using La₂O₃ as gate oxide by electron-beam evaporated have been investigated and compared with the regular HEMTs [1]. The La₂O₃ thin film achieved a good thermal stability after 200degC, 400degC and 600degC post-deposition annealing due to its high binding energy (835.7 eV) characteristics. Our measurements have shown that La₂O₃ MOS-HEMTs exhibiting the best characteristics, including the lowest gate leakage current, the largest gate voltage swing, and pulsed-mode operation. In addition, a negligible hysteresis voltage shift in the C-V curve can be improved significantly after high temperatures annealing. [C603]

"Comparison of Cu-gate and Ni/Au-gate GaN HEMTs large signal characteristics"

In this paper a complete comparison between Copper (Cu) gate and Nickel-Gold (Ni/Au) gate passivated AlGaIn/GaN High Electron Mobility Transistors (HEMTs) is presented. DC and Radio Frequency (RF) performance was compared in order to evaluate the behaviour of the two Schottky contacts in the standard HEMT structure. From the obtained data a critical drain current collapse was observed in the Cu-gate devices, with detrimental effects on the RF performance, while the Ni/Au-gate performed nicely both during pulsed I-V and RF measurements. An investigation on the drain current transients and on ID-VGS characteristics, obtained by pulsed signals showed that an acceptor trap at the Cu/AlGaIn interface, with activation energy of about 0.43 eV, could be responsible for the Cu-gate HEMT poorer performance. The results suggest that a detailed investigation on surface treatments, gate metal quality and deposition methods is needed in order to fabricate Cu-gate GaN HEMTs. [C604]

"Si ICL based Si₃N₄ passivation on InAlAs surface of InP-HEMT by RPECVD system"

As a promising device for high speed communication, HEMT has got many attention. But, it is long way to field-application of HEMT because of instability of the device. Especially, surface of InP-HEMT (InAlAs) is very unstable and bandgap of InP is narrower than conventional GaAs-HEMT, so kink effect is very severe consequently. Si ICL (Inter Control Layer) based SiN passivation for GaAs-HEMT has been suggested before, and I applied it to the InP-HEMT passivation process. It showed that Si ICL based passivation was more effective for reducing surface state. [C605]

"Seamless on-wafer integration of GaN HEMTs and Si(100) MOSFETs"

The integration of III-V compound semiconductors and silicon (100) CMOS technologies has been a long pursued goal. A robust low-cost heterogeneous integration technology would make the outstanding analog and mixed-signal performance of compound semiconductor electronics available on an as-needed basis to realize key functions on VLSI chips that are difficult to implement in Si technology. In this paper, we demonstrate the first on-wafer integration of AlGaIn/GaN high electron mobility transistors (HEMTs) with Si(100) MOSFETs.

[C606]

"Al_xSi_yN_z passivated AlGaIn/GaN high electron mobility transistors"

The performance of AlGaIn/GaN high electron mobility transistors (HEMTs) with an Al_xSi_yN_z passivation is reported for the first time. Thin films (30 nm) of Al_xSi_yN_z and Si_yN_z were used to passivate devices (fabricated side-by-side) and their performance was compared in both small signal and large signal

measurement environments. Examination of MIS structures with each dielectric by capacitance-voltage measurements revealed the $\text{Al}_x\text{Si}_{1-x}\text{N}_z$ provides a net negative fixed charge density allowing controlled depletion of the two dimensional electron gas (2DEG) in ungated regions of the channel. This is in contrast to Si_3N_4 passivation where the surface depletion of the 2DEG is almost completely removed, which results in the full channel charge existing in the ungated portions of the channel. Reducing the charge in the ungated portions of the channel can be used to reduce the electric field at high drain bias with small increases in source and drain access resistance. Reduction of channel charge using a MIS gate extension (field plate) is now commonly used to increase the device performance at large drain bias. The charged dielectric approach described in this study allows for the elimination of the field plate (and its associated parasitic capacitances) while maintaining state-of-the-art performance at drain biases up to 55 V for a device with a 0.2 micron gate length. [C607]

"Enhancing the breakdown voltage by growing 9 μm thick AlGaIn/GaN HEMTs on 4 inch silicon"

We have designed a high breakdown yielding AlGaIn/GaN HEMTs on 4 inch silicon wafer without using a field plate or increasing the gate-drain length (L_{gd}). Our approach is based on improving the total thickness ($\Gamma_{\text{B}}^{\text{tot}}$) of the AlGaIn/GaN epi-layers as high as 9 $\Gamma_{\text{B}}^{\text{im}}$ which improves the quality of i-GaN. Growing i-GaN on thick buffer reduces the dislocation density, increases the resistance between the surface electrode and Si substrate which considerably suppresses the leakage through buffer (Γ_{but}) and substrate (Γ_{sub}) to enhance the breakdown. For a small gate-drain spacing of $L_{gd} = 3 \Gamma_{\text{B}}^{\text{im}}$ we achieved a high three terminal off breakdown (3TBV) of 403 V. A very high breakdown of 1813 V was achieved across 10 $\Gamma_{\text{B}}^{\text{im}}$ electrode spacing on 2 $\Gamma_{\text{B}}^{\text{im}}$ i-GaN grown on 7 $\Gamma_{\text{B}}^{\text{im}}$ thick buffer. Further, we have identified the leakage path which triggers the breakdown of AlGaIn/GaN HEMTs. [C608]

"Above 500 °C operation of InAlN/GaN HEMTs"

Due to their ceramic-like thermal/chemical stability GaN-based HEMTs are expected to be of high robustness and may also be a prime candidate for reliable high temperature operation. In gas sensing AlGaIn/GaN heterostructures have been investigated up to 800 $\Gamma_{\text{B}}^{\text{C}}$. In a simple proof-of-concept experiment InAlN/GaN HEMTs have been operated at 1000 $\Gamma_{\text{B}}^{\text{C}}$ for a short period of time in vacuum. However in respect to continuous operation most tests have been limited to a temperature range below 500 $\Gamma_{\text{B}}^{\text{C}}$. Here a continuous test is described operating devices under 1 MHz large signal conditions for 250 hrs at a given temperature increased in steps of 100 $\Gamma_{\text{B}}^{\text{C}}$ (in vacuum), concentrating on the temperature range above 500 $\Gamma_{\text{B}}^{\text{C}}$, until failure. [C609]

"Terahertz CMOS circuit design and applications for ultra-high data rate (> 100Gbps) communication"

Wedged between traditional microwave and optics, the term $\Gamma_{\text{B}}^{\text{Terahertz}}$ was first named by Fleming to designate EM spectrum range from 300 GHz to 3 THz. It remains one of the least tapped spectra over time. Terahertz image and spectroscopic systems have drawn substantial attention recently due to their unique capabilities in detecting and/or analyzing concealed objects through fog and fabrics. The generation of practical Terahertz signals is nevertheless nontrivial and can only be accomplished by using Free-Electron Radiation, Optical Lasers, Gunn Diodes and sometimes oscillators made of III-V compound based HBT/HEMTs. However, these prior arts suffer major disadvantages of size, cost, complexity, efficiency and/or even cryogenic cooling to produce meaningful signals in the notorious $\Gamma_{\text{B}}^{\text{Terahertz}}$ Gap $\Gamma_{\text{B}}^{\text{I}}$. [C610]

"Top-down AlN/GaN enhancement- & depletion-mode nanoribbon HEMTs"

III-V nitride HEMTs are currently being intensively investigated for both depletion and enhancement mode operation at high powers and high frequencies. Among the various methods that can render the polarization-doped HEMTs enhancement-mode, the least investigated are those that exploit 3-D nanoscale geometrical electrostatic effects. Recently, bottom-up grown GaN nanowire MISFETs have shown respectable depletion-mode device performance. However, the handling of isolated nanowires is technologically challenging. This paper demonstrates that by combining conventional epitaxially grown AlN/GaN HEMT structures with top-down nanoribbon fabrication, both E-mode and D-mode HEMTs with high performance can be realized in a facile manner, and allow integration on the same substrates. In addition to the ease of realizing E-mode and D-mode devices, these top-down nanoribbon HEMTs also take advantage of the superior electrostatics of wrap-gates and quasi-1D charge transport for high performance. [C611]

"Enhancement-mode AlGaIn/GaN HEMTs with high linearity fabricated by hydrogen plasma treatment"

Enhancement-mode (E-mode) AlGaIn/GaN high electron mobility transistors (HEMTs) are highly desirable for power and digital electronic circuits. Several technologies have been demonstrated in the last few years to fabricate E-mode devices. For example, gate recess can be applied to conventional AlGaIn/GaN HEMTs to achieve E-mode operation. However, these devices have very low threshold voltage and large gate leakage. Alternatively, the use of CF₄ plasma treatment in the gate region prior to gate metallization results in E-mode AlGaIn/GaN HEMTs with higher threshold voltage. In this paper, we demonstrate E-mode AlGaIn/GaN HEMTs by hydrogen plasma treatment. The results are compared to the F-treated HEMTs and depletion-mode (D-mode) HEMTs and important differences have been found in the linearity of these transistors. [C612]

"X-Band Microstrip AlGaIn/GaN HEMT Power MMICs"

X-Band AlGaIn/GaN HEMT power MMIC on Si-SiC designed in microstrip technology is presented in this paper. Recessed-gate and field-plate are used in the device process to improve the AlGaIn/GaN HEMTs performances. S-parameter measurements show a strong dependence of the frequency performances of the AlGaIn/GaN HEMTs on the operating voltage. Higher operating voltage is key to get higher power gain for the AlGaIn/GaN HEMTs. The developed 2-stage power MMIC delivers a pulsed output power in excess of 10 W at a drain bias of 30 V with a power gain of more than 12 dB over the band of 9-11 GHz. Peak output power inside the band reaches 14.7W with a power gain of 13.7dB and a power-added- efficiency (PAE) of 23%. The MMIC chip size is only 2.0 mm times 1.1 mm. This work shows superiority over reported results of X-band AlGaIn/GaN HEMT power MMICs up to date in output power per millimeter gate width and output power per unit chip size. [C613]

"A CW 7-12 GHz GaN Hybrid Power Amplifier IC with High PAE Using the Load-Impedance Change Compensation Technique"

In this paper, we demonstrated a broadband GaN power amplifier hybrid IC with high power added efficiency (PAE) under CW operation using load-impedance change compensation technique. The external output matching circuit is composed of a transmission line, an open stub and a short stub with chip capacitors to realize both wide bandwidth and high voltage operation. As a result, we developed 7-12 GHz broadband medium power amplifier and demonstrated a CW output power of 6.5 W with the PAE of 40% using 0.5- μ m GaN-HEMT technology at 7 GHz. The output power also exceeded 4.9 W with PAE of over 31% up to 11 GHz. At 12 GHz, the output power was 4.1 W with PAE of 26%. [C614]

"77GHz Low-Cost Single-Chip Radar Sensor for Automotive Ground Speed Detection"

A new 77 GHz single-chip radar sensor has been developed, which encapsulates a GaAs p-HEMT transceiver MMIC with an on-chip patch antenna in a resin-molded package integrated with a resin collimating lens on the top to achieve an EIRP of 13.5 dBm and a receiving gain of 8 dB. The packaged sensor, measuring 6.5times4.4times6.0 mm³ with only DC and baseband- frequency leads, offers ease of handling with an extreme low-cost potential for a variety of applications. When adopted to an automotive ground speedometer integrated with an signal processing unit, the sensor demonstrated accurate and reliable detections of vehicle speed with a standard deviation of 1.5% under normal driving conditions. [C615]

"A Metamorphic 220-320 GHz HEMT Amplifier MMIC"

In this paper, we present the development of a compact H-band (220-325 GHz) submillimeter-wave monolithic integrated circuit (S-MMIC) amplifier for use in next generation active and passive high-resolution imaging systems. The low- noise amplifier (LNA) circuit has been realized using an advanced 35 nm InAlAs/InGaAs based metamorphic high electron mobility transistor (mHEMT) technology and achieves a small-signal gain of 13.5 dB at 300 GHz and a linear gain of more than 10.5 dB over the bandwidth from 220 to 320 GHz. The use of grounded coplanar waveguide (GCPW) topology in combination with cascode transistors resulted in a very compact die size of only 0.43 times 0.82 mm². [C616]

"Improved Drain-Source Current Model for HEMT's with Accurate Gm Fitting in All Regions"

In this paper, we present an improved drain-source current (I-V) model for HEMT's which is simple and easy to extract, suitable for implementation in simulation tools. A single modeling equation is developed, allowing accurate prediction of both static and dynamic I-V characteristics. The model parameters can be extracted to match the measured data closely for a wide bias range without sacrificing accuracy. It is validated through DC as well as power measurements compared to simulations using GaAs HEMT transistors. [C617]

"State of the Art 58W, 38% PAE X-Band AlGaIn/GaN HEMTs Microstrip MMIC Amplifiers"

This paper presents the results obtained on X-Band GaN MMICs developed in the frame of the Kerrigan project

launched by the European Defense Agency. A new step was achieved, 58 W of output power with 38% PAE in X-Band were obtained using an 18 mm 22-stages amplifier. To our knowledge, these results present a new state-of-the-art of X-Band MMIC power amplifiers. [C618]

"A Wideband Power Amplifier MMIC Utilizing GaN on SiC HEMT Technology"

The design and performance of a wideband power amplifier MMIC suitable for electronic warfare (EW) systems and other wide bandwidth applications is presented. The amplifier utilizes dual field plate 0.25- μm GaN on SiC device technology integrated into the three metal interconnect (3MI) process flow. Experimental results for the MMIC at 30V power supply operation demonstrate greater than 10 dB of small signal gain, 9 W to 15 W saturated output power and 20% to 38% peak power added efficiency over a 1.5 GHz to 17 GHz bandwidth. [C619]

"A Cool, Sub-0.2 dB, Ultra-Low Noise Gallium Nitride Multi-Octave MMIC LNA-PA with 2-Watt Output Power"

This paper reports on a S-,C-band LNA-PA which achieves a sub-0.2 dB noise figure over a multi-octave band and a P_{sat} of 2 Watts at a cooled temperature of -30degC. The GaN MMIC is based on a 0.2 μm AlGaIn/GaN-SiC HEMT technology with an $f_T \sim 75$ GHz. At a cool temperature of -30degC and a power bias of 15 V-400 mA, the MMIC obtains 0.25-0.45 dB NF over a 2- 8 GHz band and a linear PIdB of 32.8 dBm (~2 Watts) with 25% PAE. At a medium bias of 12 V-200 mA, the amplifier obtains 0.1- 0.2 dB NF across the same band and a PIdB of 32.2 dBm (1.66 Watts) with 35% PAE. The corresponding PSAT is better than 2 Watts. At a low-noise bias of 5 V-200 mA, 0.05-0.15 dB NF is achieved with a PIdB > 24 dBm and PAE~33%. These results are believed to be the lowest NF ever reported for a multi-octave fully matched MMIC amplifier capable of > 2 Watts of output power. The ultra-low noise, wide band, and high power obtained at modestly low temperature operation makes this an attractive and practical low-cost solution for applications such as WiMAX, CATV, base-stations, and broadband communication systems. [C620]

"C-Band GaN-HEMT Power Amplifier with Over 300-W Output Power and Over 50-% Efficiency"

In this paper, we report a C-band power amplifier with over 300-W output power using 0.8- μm GaN-HEMTs. We used two-chip configuration and the three-stage impedance transformer to extend the bandwidth. The input and output lines adjacent to each chip are divided by four to suppress the non-uniform heat distribution in a chip at high frequencies. We confirmed that the uniform heat distribution in each chip under RF operation at 4.8 GHz. As a result, we obtained over 320-W output power and 57 % drain efficiency at 4.8 GHz. This is the highest output power of the one-package power amplifiers at C-band. We also obtained over 250-W output power and over 44-% drain efficiency between 4.7 GHz and 5.3 GHz. [C621]

"AlGaIn/GaN MOS-HEMT with Stack Gate HfO₂/Al₂O₃ Structure Grown by Atomic Layer Deposition"

We have developed a novel AlGaIn/GaN metal-oxide-semiconductor high electron mobility transistor (MOS-HEMT) using stack gate IHD₂/Al₂O₃ structure grown by atomic layer deposition (ALD). The stack gate consists of a thin HfO₂(30Å) gate dielectric and a thin Al₂O₃(20Å) interfacial passivation layer (IPL). For the 50Å stack gate, no measurable C-V hysteresis and smaller threshold voltage shift were observed, indicating that a high quality interface can be achieved using a Al₂O₃IPL on AlGaIn substrate. Good surface passivation effects of the Al₂O₃IPL have also been confirmed by pulsed gate measurements. Devices with 1- μm gate lengths exhibit a cutoff frequency (f_T) of 12 GHz and a maximum frequency of oscillation (f_{MAX}) of 34 GHz. The gate leakage current is at least six orders of magnitude lower than that of the reference HEMTs at positive gate bias. [C622]

"AlGaIn/GaN-on-SiC HEMT Technology Status"

GaN-based devices offer significant advantages for next generation military and commercial systems. Military systems benefit from high power densities of 4 to 7 W/mm depending on bias conditions along with efficiencies over 60% at frequencies through X-band, and commercial systems take advantage of excellent linearity as well. In this paper, we will review a number of commercial products that only GaN technology can achieve. In addition to narrow-band circuits for highly linear commercial applications, results will be shown for two commercial GaN MMIC products that have been developed for general-purpose applications in the 2.5-6.0 GHz and DC-6.0 GHz bands. Additionally, results are shown for a 2-stage high efficiency S-band switch mode amplifier operating from 3.1-3.5 GHz. Significant progress has also been made in the development of 100-mm SiC substrates. Micropipe densities as low as 2.5 cm^{-2} have been demonstrated for 100-mm HPSI substrates. [C623]

"A comparison of polar transmitter architectures using a GaN HEMT power amplifier"

In this paper three transmitter architectures are compared, that each use the low-frequency envelope and high-frequency phase component of an RF signal. A power amplifier (PA) with Pulse Width Modulation by Variable Gate Bias (PWMVGB) is compared to an Envelope Elimination and Restoration (EER) and Envelope Tracking (ET) configuration. The test circuit is implemented using a discrete GaN HEMT power amplifier and discrete surface-mount passive components assembled on a PCB. Measurements show that the EER architecture maintains a drain efficiency of 56 to 69% for a wide output power range, while the PA with variable gate bias shows a significant drop in efficiency for lower output powers (from 59 to 6%). Other comparison issues are modulation of the supply voltage and transmitter complexity. [C624]

"A balanced sub-millimeter wave power amplifier"

In this paper, a new balanced sub-millimeter wave power amplifiers is presented. The amplifier uses CPW-grounded MIM capacitors to form low-loss, lumped element matching networks and uses a branchline coupler to achieve requisite quadrature phase shifts. The balanced amplifier achieves 12-dB small signal gain and 6.1-mW output power (not saturated) at a center frequency of 270-GHz. The high gain allows the amplifier to reach a moderate Power Added Efficiency (PAE) of 5.25% at the highest drive power. The results in this paper are the highest reported output powers achieved from a solid state amplifier at these frequencies, and were achieved with a high fMAXInP HEMT process. [C625]

"A 12.5-Gb/s Pulse Modulator with 6.5-ps FWHM Using 0.1- μ m InP HEMTs for Ultra-Wideband Impulse Radio Communications"

We developed an ON/OFF pulse modulator IC using 0.1- μ m-gate-length InP HEMTs for ultra-wideband impulse radio (UWB-IR) communications systems. The IC generated extremely short pulses whose full width at half maximum (FWHM) were 6.5 ps. Furthermore, our new circuit architecture that retimes output pulses at both rising and falling edges made the IC robust against timing fluctuations or jitter. The output pulses had very small jitters of 256 fs rms and 1.3 ps p-p and thus had little degradation from intersymbol interference (ISI) when a 231-1 length pseudo random bit stream (PRBS) at a bit rate of 12.5 Gb/s was input. The pulse modulator can be used to construct an ON/OFF keying transmitter based on UWB-IR architecture that sends more than 10 Gb/s of data in the W-band (75-110 GHz) and above. [C626]

"RLC Matched GaN HEMT Power Amplifier with 2 GHz Bandwidth"

We have demonstrated a RLC matched GaN HEMT power amplifier with 12 dB gain, 0.05-2.0 GHz bandwidth, 8 W CW output power and 36.7-65.4% drain efficiency over the band. The amplifier is packaged in a ceramic S08 package and contains a GaN on SiC device operating at 28 V drain voltage, alongside GaAs integrated passive matching circuitry. A second circuit designed for 48 V operation and 15 W CW power over the same band, obtains over 20 W under pulsed condition with 10% duty cycle and 100 μ s pulse width. CW measurements are pending after assembly in an alternate high power package. These amplifiers are suitable for use in wideband digital cellular infrastructure, handheld radios, and jamming applications. [C627]

"High power on-wafer capabilities of a time domain load-pull setup"

High power LSNA on-wafer measurements up to 20 Watts at 2 GHz have been performed on a 3.2 mm gate width AlGaIn/GaN HEMT. Time domain slopes in pulsed mode are given for different pulsed drain voltages, showing the importance to monitor the drain voltage and current slopes, as they are directly linked to the transistor reliability. At such power range, the LSNA on-wafer load-pull setup with two dasiawave probespsila couplers demonstrates its capabilities to handle up-to-date power transistors in the S band, and to provide the time domain information usually missing with classical load-pull setups. [C628]

"An efficient technique for designing balanced vector modulators with low insertion loss"

This paper describes and analyses an improved technique for the realization of balanced vector modulators. The analysis focuses on the effect of the Lange coupler characteristic impedance on the modulator minimum insertion loss. A method of adjusting the impedance to a calculated optimum value is used to reduce the loss and achieve a more symmetrical constellation. Based on this technique, a balanced vector modulator MMIC for millimeter-wave communication applications is fabricated on a 100 μ m thick GaAs substrate with 0.15 μ m pHEMT devices. This circuit is operating at 40GHz and has a chip size of 1.9 \times 1.5mm². The static constellation has been obtained with swept bias voltage control, and shows good agreement with the analysis. [C629]

"First-principles calculations for effects of Fluorine impurity in GaN"

Fluoride-based plasma treatment has been approved to be an effective technique to make E-Mode GaN-based HEMT by experiments. However, the detailed effect of Fluorine doping in GaN and AlGaN is still unclear and has never been studied theoretically. In this paper, F impurity in GaN material is firstly studied by First Principle Calculations. Sound explanations for the experimental phenomenon are derived from the results and further discuss is presented. [C630]

"New Technologies for Improving the High Frequency Performance of AlGaN/GaN High Electron Mobility Transistors"

In this paper, we have used a combination of physical analysis, numerical simulation and experimental work to overcome some of the main challenges in AlGaN/GaN high electron mobility transistors (HEMTs) for high frequency applications. In spite of their excellent material properties, GaN-based HEMTs are still below the theoretical predictions in their high frequency performance. If the frequency performance could be improved, the superior breakdown characteristics of nitride semiconductors would make these devices the best option for power amplifiers at Ka and even W band frequencies. To achieve this goal, we have first identified some of the critical parameters that limit the high frequency performance of AlGaN/GaN HEMTs and we have demonstrated several technologies to increase the performance. Some of these technologies include deep-submicron T-gate technology, thin-body GaN HEMTs, and advanced drain delay engineering. [C631]

"Highly efficient operation modes in GaN power transistors delivering upwards of 81% efficiency and 12W output power"

This paper investigates the development of an inverse class-F design procedure for obtaining very high efficiency performance at high power levels. RF waveform engineering was used to obtain high efficiency inverse class-F waveforms at the device current-generator plane. Drain efficiencies above 81% have been achieved at 0.9 and 2.1 GHz for a wide band-gap gallium nitride (GaN) HEMT transistor and 12 W fundamental output power. Investigations into improvements in drain efficiency through increases in drain bias voltage have yielded drain efficiencies of up to 84% at 2.1 GHz. To the author's knowledge, the efficiencies presented in this study are the highest published, measured efficiencies of a high power GaN HEMT at these frequencies. [C632]

"Low noise amplifier for 180 GHz frequency band"

Measurement of the humidity profile of the atmosphere is highly important for atmospheric science and weather forecasting. This sounding measurement is obtained at frequencies close to the resonance frequency of water molecules (183 GHz). We have designed and characterized a MMIC low noise amplifier that will increase the sensitivity of sounding instruments at these frequencies. This study demonstrated a factor of two improvement in MMIC LNA noise temperature at this frequency band. The measured packaged InP monolithic millimeter-wave integrated circuit (MMIC) amplifier had a noise temperature of $NT=390$ K ($NF=3.7$ dB). The circuit was fabricated in 35 nm InP high electron mobility transistor (HEMT) process. [C633]

"Linearity-optimized power tracking GaN HEMT Doherty amplifier using derivative superposition technique for repeater systems"

This paper presents the linearity-optimized power tracking Gallium Nitride (GaN) high electron mobility transistor (HEMT) Doherty power amplifier (DPA) for wide-band code division multiple access (WCDMA) repeater systems. Also, we analyze effects of the drain bias of the carrier amplifier on the linearity and efficiency of the DPA. To improve linearity of the DPA without extra linearization techniques, the derivative superposition technique (DST) is employed by using higher drain bias of carrier amplifier than that of peaking amplifier and the optimization of the gate bias of peaking amplifier. The optimum drain and gate biases are adaptively controlled by the power tracking bias supply circuit. For experimental validation, the DPA is designed and implemented with 25-W peak envelope power (PEP) GaN HEMT and tested with a 1-carrier WCDMA signal of 2.14 GHz. At an adjacent channel leakage ratio (ACLR) of -45 dBc, a P_{out} of 39.4 dBm (7.6-dB back-off power from P_{sat}) and a power-added efficiency (PAE) of 31.8% is achieved for the power tracking DPA. For the conventional DPA, a P_{out} of 32.7 dBm with a PAE of 21.4% is achieved at an ACLR of -45 dBc. [C634]

"Broadband hybrid flip-chip 6-18 GHz AlGaN/GaN HEMT amplifiers"

GaN Based HEMT's have shown superior power-frequency performances than lower band-gap materials. In this paper, we present the design of broadband hybrid 6-18 GHz amplifiers based on AlGaN/GaN HEMT technology with a flip chip approach. Measurements of a single ended amplifier based on a 0.6mm gate width device allow us to achieve more than 1.8W in the [6.5-16] GHz bandwidth corresponding to a power density of 3W/mm. A

Maximum output power is obtained at 8 GHz at 2.7W corresponding to 4.5W/mm. Average typical PAE values higher than 17% in the bandwidth with a maximum of 39% were obtained. A balanced amplifier based on two single ended amplifiers was also realized. The output power is above 2.8W in the [7-17] GHz bandwidth corresponding to a power density of 2.4W/mm. Maximum output power is obtained at 7.5 GHz at 4.5W corresponding to 3.8W/mm. [C635]

"Thermal characterization of the intrinsic noise parameters for AlGaIn/GaN HEMTs"

The noise parameters of AlGaIn/GaN-HEMTs are measured between 298 K and 423 K. The temperature dependent access resistances are de-embedded and the intrinsic noise parameters are studied as a function of temperature. It is shown that the parasitic access resistances are limiting the high-frequency noise performance of the AlGaIn/GaN-HEMT. The intrinsic noise sources are extracted and a noise model is derived and verified for a MMIC amplifier. [C636]

"Distributed amplifier using enhancement-mode AlGaIn/GaN HEMTs"

Distributed amplifiers (DAs) using 1mm-gate enhancement-mode AlGaIn/GaN HEMT were designed and fabricated. Design process and simulation results of the DA are given. Simulation results show the input and output VSWR (voltage standing wave ratio) of less than 2, associated gain of more than 8.5dB and gain ripple of less than 1dB at frequency from 2GHz to 6GHz. [C637]

"Room temperature terahertz imaging by a GaAs-HEMT transistor associated with a THz time domain spectrometer"

We demonstrated a room-temperature detection of terahertz radiation with a plasma wave nanometric transistor. The detection is resonant and can be efficient for terahertz time-resolved imaging. [C638]

"Low noise radiometers for passive millimeter wave imaging"

W-band passive millimeter wave imaging cameras for concealed weapons detection are being developed and commercialized for security screening and rotorcraft applications. The direct detection chipset from HRL Laboratories has become the standard for the front end because of the low noise of its Sb-based backward tunnel diode detectors and InP HEMT low noise amplifiers. Here we review recent results demonstrating that an NETD < 0.5 K can be achieved without the use of Dicke switching or optical chopping using a two-MMIC chipset consisting of a low noise amplifier and matched detector. Recent results for an 8times8 imaging array with no RF amplification will also be presented, indicating an NETD of < 3 K for a 30 Hz video rate. [C639]

"The DARPA FLARE Program: Recent Advances in Ultra High Linearity RF Amplifiers"

The DARPA Feedback Linearized Amplifier for RF Electronics (FLARE) Program has demonstrated the world's first microwave operational amplifier with record linearity through the use of strong negative feedback made possible by the large available gain-bandwidth product in state-of-the-art Indium Phosphide (InP) transistor technologies. The output third-order intercept point (OIP3) near 2 GHz is measured to be +51.4 dBm while consuming only 899 mW of power (PDC), leading to a record Linearity Figure of Merit (OIP3/PDC) of 154 which is roughly 5X higher than that of any RF amplifiers in use at these frequencies today. This amplifier design is enabled by 400 GHz InP Hetero-junction Bipolar Transistor (HBT) technology with multi-level interconnect technology and novel feedback circuit design to efficiently eliminate the nonlinearity while maintaining loop stability at high frequency. This successful demonstration shows a clear path toward power-efficient low-noise ultra-high-linearity (OIP3 > +60 dBm) RF amplifiers for future military systems. [C640]

"GaN MMIC PAs for E-Band (71 GHz-95 GHz) Radio"

High data rate E-band (71 GHz- 76 GHz, 81 GHz-86 GHz, 92 GHz-95 GHz) communication systems will benefit from power amplifiers that are more than twice as powerful than commercially available GaAs pHEMT MMICs. We report development of three stage GaN MMIC power amplifiers for E-band radio applications that produce 500 mW of saturated output power in CW mode and have > 12 dB of associated power gain. The output power density from 300 μ m output gate width GaN MMICs is seven times higher than the power density of commercially available GaAs pHEMT MMICs in this frequency range. [C641]

"Homodyne mixing at 150 GHz in a high electron mobility transistor"

We explore the possibility of using an AlGaIn/GaN high electron mobility transistor (HEMT) as a free-space coupled homodyne mixer. We used 150 GHz radiation from a Free Electron Laser, hence 5 times higher than

the HEMT nominal band center at 30 GHz. The homodyne mixing provides a quasi-dc output signal, which makes the HEMT a detector of the radiation at 150 GHz. [C642]

"Room temperature generation of terahertz radiation from dual grating gate HEMT's"

We report on room temperature generation of the terahertz radiation from dual grating gate high electron mobility transistor. The emission spectra were measured using Fast Fourier Spectroscopy. Both coherent and incoherent excitation of the plasmons can give rise to the broadband emission in the present device. [C643]

"Equivalent circuit model for GaN-HEMTs in a switching simulation"

An equivalent circuit model for gallium nitride-based high electron mobility transistors (GaN-HEMTs) in an exact circuit simulation is proposed. The equivalent circuit contains inherent GaN device properties, such as current-collapse and shot-channel effects. Based on the equivalent model, a power loss simulator was developed. The simulation accuracy was more than 93%. A converter optimum design method is discussed using the power loss simulator. [C644]

"A G-Band multi-chip MMIC T/R module for radar applications"

In this paper, we describe the design and measurements of a MMIC amplifier-based multi-chip transmit/receive (T/R) Module for radar applications in G-band (140-220 GHz). The module is designed with InP HEMT MMIC power amplifiers for the transmit channel and InP MMIC low noise amplifiers for the receive channel. Arrays of these 150 GHz T/R modules could be used for applications such as automotive radar and landing radar. [C645]

"Tunable InGaAs/InAlAs/InP far-IR detector based on plasmon resonance"

An InGaAs/InP based HEMT with grating gate is investigated as a THz detector. Resonant THz absorption by two-dimensional plasmons is tunable with a gate bias. [C646]

"Elimination of parasitic generation in power X-band internally matched transistors with high associated gain"

Stability problems for X-band internally matched HEMT pHEMTs with output power higher than 10 W, associated gain higher than 13 dB are discussed. Several variants of schematic design for parasitic generation elimination are proposed. [C647]

"InP-HEMT MMICs for passive millimeter-wave imaging sensors"

This paper describes InP-HEMT MMICs for 94 GHz band passive millimeter-wave (PMMW) imaging sensors. In order to obtain high sensitivity with a single MMIC, we developed a new structure in MMIC to suppress unwanted feedback power that causes amplifier instability. The structure is also suited for flip chip bonding (FCB). The measured sensitivity of the MMIC was over 500,000 V/W at the frequency of 94 GHz. We also developed the RF front-end of the PMMW imager by mounting the MMIC on an antenna substrate by FCB assembly. In addition, we demonstrated examples of a millimeter-wave image acquired by the PMMW imager. [C648]

"Fabrication of InP HEMT devices with extremely high Fmax"

In this paper, we present the latest advancements of short gate length InGaAs/InAlAs/InP high electron mobility transistor (InP HEMT) devices that have achieved extremely high extrapolated Fmax above 1 THz. The high Fmax is validated through the first demonstrations of sub-MMW MMICs (s-MMICs) based on these devices including the highest fundamental transistor oscillator MMIC at 347 GHz and the highest gain greater than 15 dB (greater than 5 dB per stage) at 340 GHz. [C649]

"Computer simulation of low-noise SHF amplifier using field effect transistor"

In the work the results of computer simulation of low-noise amplifier using HEMT NE3210S01 at frequency 4 GHz with the help of Microwave Office are presented. The diagrams of amplification and noise, the comparison of results of modeling with experiment are submitted. [C650]

"DC-40-GHz SP4T switch IC using high-breakdown-voltage InGaAs/InP composite-channel HEMTs with an InAlP etch stopper"

This paper presents a wideband and high power-handling single-pole four-throw (SP4T) switch IC using

InGaAs/InP composite-channel (CC) HEMTs. Owing to the CC structure with an InAlP barrier, the input power for P1dB of 19.4 dBm is 6 dB higher than that of our conventional InGaAs single-channel HEMT switch, with identical wideband performance of ~40 GHz. [C651]

"AlSb/InAs HEMTs on InP substrate using wet and dry etching for mesa isolation"

In this paper, we present experimental results on AlSb/InAs HEMTs with deep and shallow mesa using wet and dry etching techniques respectively. Similar electrical results have been obtained using both techniques. [C652]

"Simultaneous achievement of high-speed and low-noise performance of pseudomorphic InGaAs/InAlAs HEMTs"

We achieved a minimum noise figure (NF_{min}) of 1.0 dB at a frequency of 90 GHz, a current gain cutoff frequency (f_T) of 520 GHz and a maximum oscillation frequency (f_{max}) of 425 GHz for a 35-nm-gate pseudomorphic In_{0.7}Ga_{0.3}As/In_{0.52}Al_{0.48}As high electron mobility transistor (HEMT) biased at a drain-source voltage (V_{ds}) of 0.8 V and a gate-source voltage (V_{gs}) of 0.0 V. The simultaneous achievement of high f_T, high f_{max} and low NF_{min} is the first demonstration for InGaAs/InAlAs HEMTs with over 500-GHz-f_T. Furthermore, an NF_{min} of 0.8 dB at 90 GHz was also obtained at V_{ds}= 0.8 V and V_{gs}= -0.1 V, which is one of the lowest values ever reported. [C653]

"Optical control of InP-based HEMT millimeter-wave oscillators"

Optical control of a 60 GHz millimeter-wave oscillator using InP-based HEMTs is studied. Oscillation frequency tuning by using focused CW laser beam illumination and modulation of a frequency-locked 60 GHz millimeter-wave signal by using modulated laser beam illumination are presented. [C654]

"The effect of gate metals on manufacturability of 0.1 μm metamorphic AlSb/InAs HEMTs for ultralow-power applications"

Four types of gate metallization were investigated to evaluate the manufacturability of 0.1 μm AlSb/InAs HEMTs. It has been found that device performance strongly depends on the gate metallization. This information is essential for the manufacturability of 0.1 μm AlSb/InAs HEMTs for ultralow-power applications. [C655]

"High performance future hybrid transceiver module using GaN power devices for seeker applications"

A solid-state transceiver module for use in millimeter waves has been developed using HEMT GaAs technology. This module shown to have good performances in order to be used in active missile seekers. Despite the very good performances achieved, we show that it's possible to increase them using GaN devices. This technology allows the realisation of high power, high efficiency power amplifiers, very good switches and LNA. We show that taking in account the actual trend of GaN research, it's possible to foresee the development of a such device in two or three years. [C656]

"Present and future prospects of GaN-based power electronics"

GaN/AlGaN device technologies are reviewed aiming at the applications to power switching systems. SL (Super Lattice) capping and QA (Quaternary Alloy) over-layer techniques have been developed to reduce the on-resistance of GaN/ AlGaN HFET. Further, we achieved GaN on Silicon epitaxial growth technology with almost the same mobility keeping the same 2DEG density, which will make the cost comparable to conventional Si one. The experimentally obtained R_{onA} of the FET is 1.9 mΩ·cm², which is 14 times lower than that of Si ones. Additionally, a novel approach to realize enhancement mode operation of GaN/AlGaN FET is proposed using minority carrier injection by the gate. [C657]

"Fluorine plasma ion implantation technology: a new dimension in GaN device processing"

The recent discovery of the potential and charge modulation by fluorine ions incorporated in III-nitride heterojunction FETs has opened up numerous new opportunities of realizing desired device performance and fabricating integrated circuits with desirable circuit configurations. The most significant development based on the fluorine plasma ion implantation technology is the demonstration of self-aligned enhancement-mode (E-mode) AlGaN/GaN HEMT (high electron mobility transistors) that exhibits low on-resistance and low knee-voltage. In this paper, a comprehensive overview of the fluorine plasma ion implantation technology is presented. The discussions will focus on: 1) underlying physical mechanisms; 2) detailed DC and RF device characteristics; 3) circuit applications in wireless communication, high temperature electronics and power electronics and; and 4)

reliability of fluorine ions in III-nitride semiconductors. [C658]

"Evidence of mobile holes on GaN HFET barrier layer surface-root cause of high power transistor amplifier current collapse"

Evidence of mobile, positive charges (holes) on the top surface of GaN HFET is found by conducting C-V measurement of a MIS HEMT diode. Significantly improved understanding of the effects of built-in electric polarization and doping on III-nitride heterojunction device structure electrical properties has been made. The result also confirms that removal of surface mobile holes is the root cause for high power GaN HEFT current collapse. [C659]

"The comprehensive study of liquid phase oxidation on GaAs-based transistor applications"

The GaAs-based HEMTs with gate oxide and HBTs with surface passivation prepared by liquid phase oxidation (LPO) will be demonstrated. As compared to the Schottky-gate HEMTs, the lower gate leakage currents, higher breakdown voltages, and improved RF performances make the proposed technique suitable for high-power and high-speed applications. Moreover, the HBTs with oxide passivation possess the characteristics of lower surface recombination currents, higher breakdown voltage, and improved higher dc current gain. [C660]

"Road-blocks to Tera-level nanoelectronics"

The national program for Tera-level Nanodevices (TND) serves as a frontier research resource to a broad range of nanoscale electronics areas. Outstanding nanoscale devices have been achieved and are being further developed using core technologies such as fast nanoscale molecular assembly, damage-free nano-etch process with a neutral beam and nano-rod and particle formation technology. Sub-30 nm scale nonvolatile memory arrays have been demonstrated by changing structures and materials. Using high quality heterojunction epitaxial growth technology, ultra high speed HEMT devices have been demonstrated with cut-off frequencies of approximately 610 GHz corresponding to gate length of 15 nm. Additionally, single electron transistor logic circuits have been extended to multi-valued static random access memory applications. [C661]

"Innovative T/R module in state-of-the-art GaN technology"

In this paper a first iteration X-band T/R module based on a GaN-HEMT MMIC front-end chip-set, comprising a power amplifier, robust low-noise amplifier and power switch will be presented. Even though ultimate T/R module performance cannot be achieved with current GaN-HEMT technological maturity the impact that this technology can have at systems level in terms of performance/cost trade-off will be illustrated by means of a preliminary innovative module architecture which foresees the elimination of more traditional T/R module components such as ferrite circulator and limiter for front-end signal routing and protection. [C662]

"AlGaIn/AlN/GaN/InGaIn/GaN DH-HEMTs with improved mobility grown by MOCVD"

AlGaIn/AlN/GaN/InGaIn/GaN double heterojunction high electron mobility transistors (DH-HEMTs) structures with improved buffer isolation have been investigated. The structures were grown by MOCVD on sapphire substrate. AFM result of this structure shows a good surface morphology with the root-mean-square roughness (RMS) of 0.196 nm for a scan area of 5 $\mu\text{m} \times 5 \mu\text{m}$. A mobility as high as 1950 cm^2/Vs with the sheet carrier density of $9.89 \times 10^{12} \text{ cm}^{-2}$ was obtained, which was about 50% higher than other results of similar structures which have been reported. Average sheet resistance of 327 Ω/sq was achieved. The HEMTs device using the materials was fabricated, and a maximum drain current density of 718.5 mA/mm , an extrinsic transconductance of 248 mS/mm , a current gain cutoff frequency of 16 GHz and a maximum frequency of oscillation 35 GHz were achieved. [C663]

"Investigations on $\text{In}_{0.2}\text{Ga}_{0.8}\text{AsSb}/\text{GaAs}$ high electron mobility transistors with gate passivations"

This work reports, high electron mobility transistors (HEMTs) using a dilute antimony $\text{In}_{0.2}\text{Ga}_{0.8}\text{AsSb}$ channel, grown by molecular beam epitaxy (MBE) system. Introducing the surfactant-like Sb atoms during growth of the $\text{InGaAs}/\text{GaAs}$ quantum well (QW) was devised to effectively improve the channel confinement capability and the interfacial quality within the $\text{InGaAsSb}/\text{GaAs}$ QW heterostructure, resulting in enhanced carrier transport property and superior device performances. In comparison, the proposed devices with employing sulfur (NH_4) $_2\text{S}$ passivation (sample A), silicon nitride (SiN_x) surface passivation (sample B), or without passivation (sample C) have been investigated. Sample A (B/C) has demonstrated superiorly the maximum extrinsic transconductance ($g_{m,\text{max}}$) of 221 (205/183) mS/mm , the drain saturation current density (I_{DSS}) of 205 (190/174) mA/mm , the gate-voltage swing (GVS) of 1.105 (1.28/1.482) V, and the P.A.E. characteristic 30.4 (21.4/13) % at 300 K, with the gate dimensions of 1 $\mu\text{m} \times 200 \mu\text{m}$. [C664]

"Liquid phase oxidation on InAlAs and application to gate insulator of InAlAs/InGaAs HEMT lattice-matched to InP substrate"

The selective oxidation on InAlAs by liquid phase oxidation using photoresist or metal as a mask is proposed. Further application to gate insulator of InAlAs/InGaAs HEMT lattice-matched to InP substrate is also conducted. The high mobility electrons are constrained in 2DEG instead of traditional oxide-semiconductor interface. Also, this oxidation provides new opportunities to explore many alternative dielectrics for use as gate oxides and as passivation layers on III-V compound semiconductor devices. [C665]

"Fabrication of In_{0.52}Al_{0.48}As/In_{0.53}Ga_{0.47}As p-HEMT utilizing Ne-based atomic layer etching"

The characteristics of 0.15 μm In_{0.52}Al_{0.48}As/In_{0.53}Ga_{0.47}As pseudomorphic high electron mobility transistors (p-HEMTs) fabricated using the Ne-based atomic layer etching (ALET) technology and the Ar-based conventional reactive ion etching (RIE) technology are reported. Compared to the p-HEMTs fabricated using the Ar-based RIE, the p-HEMTs fabricated using the ALET exhibited improved device performance including transconductance ($G_m = 1.38 \text{ S/mm}$), I_{ON}/I_{OFF} ratio (1.18 times 10⁴), and cutoff frequency ($f_T = 233 \text{ GHz}$), mainly due to the extremely low plasma-induced damage of the ALET to the Schottky gate area. [C666]

"Fabrication technology and device performances of ultra-short 30-nm-gate pseudomorphic In_{0.52}Al_{0.48}As/In_{0.75}Ga_{0.25}As HEMTs"

In this paper, we succeed in fabricating ultra short 30 nm gate pseudomorphic high electron mobility transistors (HEMT) with excellent cutoff frequencies. Devices with smaller Schottky barrier layer exhibited a current gain cutoff frequency f_{T0} of 450 GHz and a simultaneous maximum oscillation frequency f_{MAX} of 500 GHz. This performance can be attributed to the use of the two-step-recessed gate technology and the maintaining of high aspect ratio in our HEMTs. [C667]

"35 nm metamorphic HEMT MMIC technology"

A metamorphic high electron mobility transistor (mHEMT) technology featuring 35 nm gate length has been developed. The optimized MBE grown layer sequence has a channel mobility and a channel electron density as high as 9800 cm^2/Vs and $6.1 \times 10^{12} \text{ cm}^{-2}$, respectively. To enable a maximum extrinsic transconductance g_m , m_{max} of 2500 mS/mm the source resistance has been reduced to 0.1 Ω/mm . An f_{TOF} of 515 GHz was achieved for a 2 times 10 μm device. Based on this advanced 35 nm mHEMT technology very compact single-stage H-band amplifiers circuits have been realized demonstrating a high small-signal gain of more than 7 dB at 270 GHz. [C668]

"CH029"

Interest in the integration of wide bandgap oxides, such as the rocksalts MgO and CaO, lies in the possibility of optimizing High Electron Mobility Transistor (HEMT) structures, as well as the potential for combining the polar semiconductor GaN with ferroic materials, in which the interaction between GaN's polar axis and the reorientable polarizations found in such materials as ferroelectrics can be leveraged. In either case, the epitaxial growth of rocksalt oxides on GaN is of interest, because of the need for passivation layers in the case of HEMT structures, and because of the need for tunneling barriers in the GaN/ferroelectric structures (due to the expected small band offsets between such materials). Here we report on spectroscopic studies of the MgO/GaN and CaO/GaN systems, focusing on growth mode determination, band alignment, and phase stability (particularly as it relates to water uptake under atmospheric exposure). [C669]

"AlInGaN/GaN heterostructures with 2D electron gas and quantum wells for transistors and light emitting diodes"

AlInGaN/GaN heterostructures with 2D electron gas and quantum wells were grown on Si substrates. Optical and electrical properties of the heterostructure were investigated; high electron mobility transistors (HEMT) and light emitting diodes (LED) were fabricated. [C670]

"CH029"

Interest in the integration of wide bandgap oxides, such as the rocksalts MgO and CaO, lies in the possibility of optimizing High Electron Mobility Transistor (HEMT) structures, as well as the potential for combining the polar semiconductor GaN with ferroic materials, in which the interaction between GaN's polar axis and the reorientable polarizations found in such materials as ferroelectrics can be leveraged. In either case, the epitaxial

growth of rocksalt oxides on GaN is of interest, because of the need for passivation layers in the case of HEMT structures, and because of the need for tunneling barriers in the GaN/ferroelectric structures (due to the expected small band offsets between such materials). Here we report on spectroscopic studies of the MgO/GaN and CaO/GaN systems, focusing on growth mode determination, band alignment, and phase stability (particularly as it relates to water uptake under atmospheric exposure). [C671]

"Adsorption-controlled growth of BiFeO₃ by MBE and integration with wide band gap semiconductors"

BiFeO₃ thin films have been deposited on (101) DyScO₃, (0001) AlGa_{0.3}N/GaN, and (0001) SiC single crystal substrates by reactive molecular-beam epitaxy in an adsorption-controlled growth regime. This is achieved by supplying a bismuth over-pressure and utilizing the differential vapor pressures between bismuth oxides and BiFeO₃ to control stoichiometry. Four-circle x-ray diffraction reveals phase-pure, epitaxial films with rocking curve full width at half maximum values as narrow as 7.2 arc seconds (0.002°). Epitaxial growth of (0001)-oriented BiFeO₃ thin films on (0001) GaN, including AlGa_{0.3}N HEMT structures, and (0001) SiC has been realized utilizing intervening epitaxial (111) SrTiO₃ / (100) TiO₂ buffer layers. The epitaxial BiFeO₃ thin films have two in-plane orientations: [112]BiO BiFeO₃ [112]BiO GaN (SiC) plus a twin variant related by a 180° in-plane rotation. This epitaxial integration of the ferroelectric with the highest known polarization, BiFeO₃, with wide band gap semiconductors is an important step toward novel field-effect devices. [C672]

"The upper limits of cut-off frequency in ultra-short gate length InP-based p-HEMTs"

Ultrashort gate length pseudomorphic high-electron-mobility transistors (p-HEMTs) based on an InP substrate have been modeled using a full-band cellular Monte Carlo simulator. The RF response has been obtained for lithographic gate lengths ranging from 10 nm to 50 nm and for channel thicknesses of 18 and 10 nm. These results in turn have been used in a transit time analysis to determine the effective gate length in each case. By interpolation, one can make an estimate of the absolute upper limit for the cut-off frequency, f_T , which we find to be 2.9 THz in 18 nm device and 3.1 THz in the 10 nm device. [C673]

"W-band low-noise amplifier with 50 nm In_{0.8}GaP/In_{0.4}AlAs/In_{0.35}GaAs metamorphic HEMT"

W-band low-noise amplifier (LNA) has been successfully demonstrated with 50 nm metamorphic HEMT (MHEMT) technologies. 50 nm MHEMT showed a g_m of 760 mS/mm, a f_T of 216 GHz, and a f_{max} of 400 GHz in spite of indium content of 35 % in the channel. W-band LNA with three-stage showed the small signal gain of 9.4 dB from 40 GHz to 110 GHz. These results are well suited for high frequency applications. [C674]

"Investigation of impact ionization from In_xGa_{1-x}As to InAs Channel HEMTs for high speed and low power applications"

80-nm high electron mobility transistors (HEMTs) with different indium content in In_xGa_{1-x}As channel from 52%, 70% to 100% have been fabricated. Device performance degradation were observed on the DC measurement and RF characteristics caused by impact ionization at different drain bias, >0.8 V (InAs/In_{0.7}Ga_{0.3}As), >1 V (In_{0.7}Ga_{0.3}As) and >1.5 V (In_{0.52}Ga_{0.48}As), respectively. The impact ionization phenomenon should be avoided for high speed, low power application because it limits the highest drain bias of the device which in turn limits the drift velocity under specific applied electric field. [C675]

"Improvement in high frequency and noise characteristics of InP-based HEMTs by reducing parasitic capacitance"

We improved the high frequency and noise characteristics of InP-based high electron mobility transistors (HEMTs) by reducing parasitic capacitance in the gate region and achieved a cutoff frequency (f_T) of 517 GHz and minimum noise figure (NF_{min}) of 0.71 dB at 94 GHz even after the interconnection process. Scaling of the gate-recess length is effective for enhancing transconductance (g_m). Furthermore, the cavity structure successfully reduced the parasitic capacitance originating from interlayer dielectric films. [C676]

"Channel noise in InGaAs/InP composite channel high electron mobility transistors (HEMTs)"

High frequency channel noise in InP HEMTs with an InGaAs/InP composite channel has been characterized and analyzed to gain a better understanding on the high frequency noise originating from a more complicated channel structure. The channel noise in the composite channel HEMT shows different drain voltage dependence as compared to the conventional HEMT using a single InGaAs layer as the channel. A reduction of the channel noise at high drain voltage is observed in composite channel. This can be attributed to the suppression of the

frequency dependent channel noise component, which is related to the impact ionization in the narrow bandgap InGaAs channel, due to the carrier transfer from InGaAs channel to InP subchannel at high V_d . [C677]

"A W-band InGaAs/InAlAs/InP HEMT Low-Noise Amplifier MMIC with 2.5dB noise figure and 19.4 dB gain at 94GHz"

A three-stage W-band InGaAs/InAlAs/InP HEMT Low-Noise Amplifier (LNA) has been fabricated with 0.1μm EBL gate and improved Ohmic contact. A noise figure of 2.5 dB with an associated gain of 19.4 dB is demonstrated at 94 GHz. To our knowledge, it is the best noise/gain performance in a W-band LNA ever reported. A noise figure of 2.7 dB and an associated gain of 14.6 dB is also demonstrated with a dc power of 3.6 mW, making it a viable alternative to the ABCS technology for low dc power LNA applications. [C678]

"Preliminary investigations on the Te-doped AlInSb/GaInSb heterostructures for High Electron Mobility Transistor (HEMT) applications"

This work reports on the Te delta-doping of high electron mobility AlInSb/GaInSb heterostructures grown on InP(001). We show a significant increase of the electron sheet density when the delta-doping plane is incorporated in a thin AlSb layer introduced in the barrier. For the first time, AlInSb/GaInSb heterostructures with an electron mobility of 18,000 cm²/V.s and sheet density of 2.2×10¹² cm⁻² at room temperature are demonstrated. [C679]

"DC and RF characteristics of InAlAs/In_{0.7}Ga_{0.3}As HEMTs at 16 K"

DC and RF characteristics at 300 and 16 K of In_{0.52}Al_{0.48}As/In_{0.7}Ga_{0.3}As high electron mobility transistors (HEMTs) were measured in the gate length L_{gr} range of 50 to 700 nm. The maximum drain-source current I_{ds} and the maximum transconductance g_m increased at 16 K as expected. We observed an increase of 21 to 36% in the value of the cutoff frequency f_T at 16 K over that at 300 K. Furthermore, we measured f_T values at 16 K of a 30-nm-gate HEMT that had a multi-layer cap structure to reduce source and drain resistances under various bias conditions. The maximum f_T exceeded 600 GHz at 16 K. Even at a drain-source voltage V_{ds} of 0.4 V, we obtained an f_T of 500 GHz at 16 K. [C680]

"InAs/InGaAs composite-channel HEMT on InP: Tailoring InGaAs thickness for performance"

Maximizing In composition in the channel structures of high-electron-mobility transistors on InP is one important aspect of achieving devices capable of operating beyond 300 GHz. In this article, we compare dc and rf performance results from two variations of one such device design, incorporating a composite-channel structure comprised of InAs clad by InP-lattice-matched InGaAs. The only difference between these two variations is the thickness of the bottom InGaAs cladding layer. The thicker gave extremely high performance, with current-gain-cutoff frequency (f_T) exceeding 500 GHz, enabled by room-temperature channel-electron Hall mobility (μ_{he}) as high as 15,400 cm²/V.s and dc transconductance (g_m) exceeding 2700 mS/mm; but it also incurred significant impact ionization. The thinner incurred less of this short-channel effect and yet gave very high performance, with f_T exceeding 440 GHz, enabled by μ_{he} as high as 14,800 cm²/V.s and g_m exceeding 2200 mS/mm, initially indicating that such a tradeoff might be the more overall beneficial. However, from a subsequent process iteration, in which the gate-recess etch was deepened for reduced short-channel effects, both of these same composite-channel design variations gave even better performance results. In that process iteration, the thicker variation not only achieved f_T exceeding 500 GHz, but also achieved the recently-published new record maximum frequency of oscillation (f_{MAX}) exceeding 1 THz. Therefore, the thicker bottom InGaAs cladding layer has indeed proven to be the more optimal composite-channel design variation for performance beyond 300 GHz. [C681]

"An 18-40 GHz ultra broadband low noise amplifier MMIC"

A monolithic 18-40 GHz low noise amplifier (LNA) has been developed using 0.25 μm gate length GaAs/InGaAs/AlGaAs pseudomorphic HEMT technology. This MMIC amplifier achieved 1.4-2.3 dB noise figure with more than 10 dB associate gain from 18-40 GHz. This result rivals some 0.15 μm GaAs PHEMT process. [C682]

"High-efficiency doherty amplifier using GaN HEMT class-F cells for WCDMA applications"

This paper presents a high-efficiency GaN high electron mobility transistor (HEMT) class-F Doherty amplifier (CFDA) for wide-band code division multiple access (WCDMA) applications. The class-F power amplifiers (PAs) with significant harmonic suppression are used as the carrier and peaking cells. For validations, the class-F PA is designed and implemented with 25-W GaN HEMT at 2.14 GHz. From the measured results for a single tone,

the implemented class-F PA shows the peak power-added efficiency (PAE) and drain efficiency of 72.2% and 75.8% with a gain of 13.2 dB at an output power of 43.2 dBm by suppressing harmonic power levels below -55 dBc. For the proposed CFDA, the PAE and drain efficiency of 56.3% and 60.1% is achieved at 39.5 dBm (6-dB back-off power from P_{sat}) for a single tone. For a one-carrier WCDMA signal, the CFDA shows the PAE of 44.9% with an adjacent channel leakage ratio (ACLR) of -22.1 dBc (plusmn2.5 MHz offset) at 36.5 dBm, while an ACLR of -35.4 dBc with the PAE of 39.7% is achieved for the CEDA after linearity optimization. [C683]

"A charge-pump based 0.35-um CMOS RF switch driver for multi-standard operations"

A novel RF switch driver for high-power wireless applications is presented. The switch driver employs a novel structure of a charge pump to generate up-converted voltage to ensure linearity of an antenna switch made of GaAs p-HEMT technology. The novel charge pump can generate up-converted voltage that is higher than that of conventional charge pumps by using a parallel structure and PMOS body bias technique. The proposed switch driver was fabricated using a 0.35-um standard CMOS technology. The up-converted voltage reaches up to 8.6 V with 3 V-supply voltage and less than 30 mV of ripple. The size of the chip is less than 0.12 mm . [C684]

"Analysis of pulsed I-V curves and power slump in field-plate GaN-based FETs"

Two-dimensional transient analyses of GaN MESFETs and AlGaIn/GaN HEMTs are performed in which a deep donor and a deep acceptor are considered in a buffer layer, and pulsed I-V curves are derived from them. It is studied how the existence of field plate affects buffer-related lag phenomena and power slump. It is shown that in both FETs, the power slump could be reduced by introducing a field plate, because electron injection into the buffer layer is weakened by it. The dependence on insulator-thickness under the field plate is also studied, suggesting that there is an optimum thickness of insulator to minimize the power slump. [C685]

"Improved formal passivations of pseudomorphic high electron mobility transistors"

Temperature-dependent characteristics of high electron mobility transistors (HEMTs) with sulfur and SiNxpassivations are comprehensively studied and demonstrated. Experimentally, for the studied device with formal passivations, better DC and microwave characteristics are obtained over wide operating temperature range. In particular, as compared with the device only with sulfur passivation, the slightly degradations of device performance are caused by the temperature stress during the deposition of SiNxlayer and presence of surface traps at the SiNx/AlGaAs interface. Based on these good results, the formal-passivated HEMT is expected to exhibit relatively better long-term operation stability and reliable device characteristics. [C686]

"Enhancement-mode gan hybrid mos-hemts with ron,sp of 20 mΩ-cm²"

We report on the experimental demonstration of a novel n-channel GaN hybrid MOS-HEMT realized on AlGaIn/GaN heterostructure on sapphire substrate. This enhancement-mode MOS-gated heterojunction transistor, with 3 μm channel length and 20 μm RESURF length, exhibited a specific on-resistance as low as 20 mΩ-cm². Simulations indicated the strong dependence of device breakdown voltage on the doping and concentration of the bottom p-GaN layer and its important role in reducing the surface electric field to suppress oxide breakdown. [C687]

"Characterization of the noise performance of a cryogenically-cooled HEMT Low-Noise Amplifier"

In this paper three methods are employed to characterize the equivalent input noise temperature of a cryogenically-cooled IF HEMT LNA. They are the conventional Y- factor method, variable-temperature method and shot-noise method. Through the measurements, their merits and drawbacks are compared. [C688]

"Performance of capless self-aligned gate D- and QE-mode p-HEMTs"

Characteristics of 0.2 μm depletion mode (D) and quasi-enhancement mode (QE) capless InAlAs/InGaAs p-HEMTs having a self-aligned gate (SAG) are reported. The QE SAG capless p-HEMT showed improved output conductance and subthreshold characteristics due to the increased gate-to-channel aspect ratio implemented by using a buried Pt technology. The maximum gm, ION/IOFF, sub-threshold slope, ftau, and fmaxof the QE SAG capless p-HEMT were 1.22 S/mm, 2.11 times 10⁵, 65 mV/dec, 210 GHz, and 250 GHz and those of the D SAG capless p-HEMT were 1.12 S/mm, 1.27 times 10⁴, 78 mV/dec, 185 GHz, and 225 GHz, respectively. The QE SAG capless p-HEMT also exhibited a shorter drain delay time than the D SAG capless p-HEMT by about 46%. [C689]

"Highly linear broadband GaN power amplifier design"

In this paper, a 1 MHz to 3.4 GHz, 5 W, highly linear power amplifier based on GaN HEMT is reported. Load-pull technique has been applied to introduce a compromising solution for the PA performance trade-off problem. Over the whole bandwidth a small signal gain of 14 plusmn 0.7 dB and an output return loss of better than -10 dB have been achieved. The input return loss was better than -10 dB up to 3 GHz. Power and linearity performances have been measured and compared to simulations resulting in a very good agreement. At a frequency spacing of 100 kHz, minimum values of output IP3 and output IP2 have been evaluated and found to be 48.5 dBm and 59.3 dBm. At 1 dB power compression point, minimum Pout and Gp were found to be 37.3 dBm and 13.3 dB, respectively within the whole frequency band. [C690]

"The role of Ti/Al ratio in nanolayered ohmic contacts for GaN/AlGaIn HEMTs"

The role of the former-Ti/Al ratio in the nanolayered ohmic contacts to GaN/AlGaIn HEMT structures has been studied for three ratios: (30/70) wt.%, (50/50) wt.% and (70/30) wt.%. The dependence of the electrical properties and surface morphology on the initial contact composition and annealing conditions has been investigated. Lowest contact resistivity of $4.22 \times 10^{-5} \Omega \text{cm}^2$ has been achieved for Ti/Al (30/70 wt.%) and Ti/Al (50/50 wt.%) contacts to semi-insulating GaN/AlGaIn heterostructures. Smoothest contact surface and most narrow contact periphery have been obtained with a Ti/Al (70/30 wt.%) contact indicating that increase of the Ti/Al ratio improves the contact morphology. The contact composition with former-Ti/Al ratio of (50/50) wt.% has been found to fulfill the best both requirements for low resistivity and a smooth surface of the contact. [C691]

"Effects of hot hole trapping in GaN HEMTs"

Hot hole trapping was mechanism was reported for GaN HEMTs from observations of electroluminescence changes and threshold voltage shifts. Passivation effect was studied through EL on the surface traps or surface states and proved to be effective in real-time monitoring of HEMT operation. Hole trapping leading to an increase in the drain to source current, and a decrease in the threshold voltage have also been shown. [C692]

"Efficient three-state WCDMA PA integrated with high-performance BiHEMT HBT / E-D pHEMT process"

Power amplifiers for WCDMA applications must provide competitive power efficiency at low power levels as well as at full power. This paper presents a novel approach to obtain high PAE performance over a wide power band from three power states. It uses a novel BiHEMT process to co-integrate InGaP/GaAs HBT technology with InGaAs/AlGaAs E/D-Mode pHEMT into a single process. No bias reference voltage is required. Typical ultra-low power mode quiescent current is 5 mA. [C693]

"Modeling of nanoscale GaN FET in a compact 2-D model with gate stack effects"

We report a compact 2D model for AlGaIn/GaN HEMT with different gate stack configurations. A two dimensional analysis is done which also includes the various polarization effects. The output characteristics, device transconductance and cut-off frequency (f_T) for 120 nm gate length device are obtained. Peak transconductance of 320 mS/mm and a cut-off frequency (f_T) of 120 GHz has been obtained. It is also demonstrated that the gate metal pattern largely affect the device characteristics and the small signal parameters. The results show excellent agreement when compared with experimental data thereby proving the validity of the model. [C694]

"X-Band GaN FET reliability"

Over the last 3 years under the Wide Band Gap Semiconductor (WBGs) DARPA program, TriQuint and their partners, II-VI, IQE, BAE, MIT, RPI and UTD, have performed multiple multi-structure, multi-wafer, multi-technology reliability experiments and failure analysis studies on its GaN on SiC HEMT technology for X-band applications. This manuscript summarizes the main results of this effort. [C695]

"Reliability and improved performance of AlGaIn/GaN high electron mobility transistor structures"

We present a systematic study of the impact of layer structure design on the channel temperature of AlGaIn/GaN high electron mobility transistor (HEMT) structures. Device layer structures have been optimized to obtain minimum overheating temperature at high dissipated power in channel of HEMTs grown on different substrates. It is shown that temperature increase has opposite dependence on buffer thickness for sapphire and SiC substrates. Noise spectroscopy is also used to monitor the self-heating effect. Moreover, it is shown that the room temperature spectra can be used to determine the activation energy of the traps. An irreversible improvement in mobility is registered after irradiation of AlGaIn/GaN heterostructures at a total dose $1 \times 10^6 \text{ rad}$ of ^{60}Co gamma rays. [C696]

"Reliability assessment of AlGaIn/GaN HEMT technology on SiC for 48V applications"

We present wearout reliability assessment of GaN HEMTs fabricated on SiC. Based on 3 temperature 48 V dc stress tests and using a failure criterion of 10% reduction in I_{dss} , the 60% confidence interval on estimate of E_{awas} [2.00,2.94] eV and the predicted 60% confidence interval on estimate of MTTF at $T_j=200$ degC was [1.0×10^6 , 3.0×10^7] hours. To compare the impact of dc and RF stress, additional experiments were conducted on a smaller sample set and the results indicate that the impact of dc and RF stress is not significantly different.

[C697]

"Degradation mechanisms of 0.1 μm AlSb/InAs HEMTs for ultralow-power applications"

The degradation mechanisms of 0.1 μm AlSb/InAs HEMTs subjected to elevated-temperature lifetesting at three temperatures in N_2 atmosphere were investigated. Device degradation exhibits the increase of non-pinch-off drain current (I_{DS}), the decrease of transconductance (g_m) and the gate current (I_G) increase. The I_G increase was found to correlate with material degradation on the gate-recess and Al_{0.7}Ga_{0.3}Sb-mesa-floor surfaces. Higher oxygen content was detected on these surfaces, indicating that they were modified by oxidation, which resulted in the I_G increase. Despite the degradation observed in 0.1 μm AlSb/InAs HEMTs, the three-temperature lifetesting shows that the activation energy (E_a) is approximately 1.5 eV and demonstrates a median time to failure (MTF) of 2 times 10^6 hours at T_{junction} of 85 degC. This reliability result is essential for successful insertion of AlSb/InAs HEMTs into systems with ultralow-power requirements. Moreover, ohmic-metal lateral diffusion of Pd and Au elements was observed. To avoid potential ohmic-metal-lateral-diffusion induced device failure, lifetesting temperatures were kept below 190 degC in this investigation. [C698]

"High power RF switch MMICs development in GaN-on-Si HFET technology"

The development of a high power RF SP4T MMIC switch using AlGaIn/GaN HFETs on Si substrate is reported for applications up to 2 GHz. The off-state capacitance (C_{off}) of a single-gate GaN based HFET is 250 fF and the on-state resistance (R_{on}) is 4.1 Ω at a gate length of 0.7 μm and a width of 1 mm. The MMIC SP4T switch with a size of 1.2 x 1.6 mm² is implemented for system applications of three transmit paths and a receiver, of which each was configured with a series-shunt self-biased configuration. The switch has achieved an insertion loss of -0.95 dB with power handling of $P(-0.1\text{dB})=45$ dBm at 1 GHz at the transmitter paths and an optimized isolation of better than 28 dB at the receiver path of up to 2.5 GHz. In addition, a high voltage switch driver using the GaN power HFET technology was designed with an input control voltage of 0/2.3 V to provide an output voltage of 0/28 V. This development provides a baseline design for our first generation MMIC switches in GaN technology. [C699]

"Design and implementation of an inverse class-F power amplifier with 79 % efficiency by using a switch-based active device model"

This paper presents the design and implementation of an inverse class-F power amplifier using a commercially available GaN 2 W power transistor. A switch-based model for this transistor was implemented in ADS and used to design this high efficiency amplifier. Simulation results with the developed model show drain efficiency of 79%, more than 19 dB of large-signal gain for an output power of greater than 5 W at 1 GHz. These values are confirmed by measurements, showing the usefulness of the switch-based active device model for this type of switching-mode power amplifiers. [C700]

"Device Modeling using Neural Network Techniques for Solid State Power Amplifier Applications"

In this paper, the integration of an advanced device model for solid state power amplifiers is proposed. The model accounts for both the static and dynamic response of HEMT devices very accurately. This large signal model utilizes a feed-forward neural network using the back-propagation method with the Levenberg-Marquardt (LM) algorithm. The model presented was used on a 3 MI 0.15 μm power pHEMT process developed by Triquint. Excellent agreement is observed between the advance model and measured DC, AC and load pull data. [C701]

"Phase Control in Small Linear Antenna Arrays Based on LNA's Parasitic Phase Shifts"

We have in this paper, reported on the investigation and validation of the existence of parasitic phase shifts. The cases of HEMT FHX35LG in [4] and E-pHEMT MGA53543 were used for validation, where in both cases; similar phase shifting behaviour was exhibited. This behaviour was exploited for a pre-liminary design of a small linear antenna array. Future work will involve array structures with more than 2 elements. The limitations of using our approach in highly populated arrays will be investigated. Miniaturization of the designed parasitic phase shifter to chip level shall remain a challenge for the industry. [C702]

"An X-band 250W solid-state power amplifier using GaN power HEMTs"

More than 250 W of peak output power (pulse width 64 μ s, duty cycle 7%) is achieved with newly developed X-band solid-state power amplifier. The final stage of the SSPA consists of four 80 W class GaN power HEMTs and a low loss 4-way combiner. Compared with the conventional klystron tubes, our newly developed SSPAs are smaller, more reliable and require less amounts of occupied frequency bandwidth. [C703]

"High-power and high-efficiency GaN HEMT amplifiers"

We report a current status of high-power GaN HEMTs for high-power and high-efficiency amplifiers with higher efficiency by 5% especially at a backed-off region than the conventional GaN HEMTs. First, we introduce our specific device structure GaN HEMT with dispersion-free I-V characteristics, low I_{dsq} -drift and high reliability. Record average drain efficiency of over 50% and linear gain of 17.2 dB were obtained at an output power of 45 dBm and 2.5 GHz. Next, we discuss their reliability with high-temperature life tests resulting in their estimated life of over 1 times 106hours at T_j of 200degC. Finally, we describe the next generation GaN HEMTs for millimeter-wave applications. [C704]

"60 GHz flip-chip mounted frequency doubler/PA chain MMIC with low input power and high output power"

An active single-ended 30 to 60 GHz doubler/power amplifier chain MMIC based on a commercial 0.15 μ m GaAs pHEMT process has been developed that requires low input drive power and produces high output power with high fundamental suppression without external filter. The maximum conversion gain is 17 dB with -25 dB fundamental signal suppression and saturated output power is 19 dBm at 59 GHz output frequency. Packaging and interconnects are discussed and as an alternative to wire bonding, flip-chip mounting test with SNU's MCM-D (multi-chip module) substrate are presented. These test indicate that the presented MMIC and this flip-chip technologies are especially well suited for the 60 GHz wireless communication systems. [C705]

"Optimization of broadband drain modulation in GaN HEMT devices"

This paper focuses on the optimization of broadband envelope termination for reliable device characterization for future UMTS-LTE systems. Drain bias modulation is suppressed in 8times500 μ m GaN HEMT using compensation network overcoming the parasitic effects of the DC feed, generally ignored during broadband measurements. Drain modulation index (DMI) metric is defined for quantifying the extent of drain voltage modulation as a function of carrier spacing and up to 80% reduction in DMI is achieved after drain bias compensation. Further, based on the experimental analysis, a simple bias tee is designed which can overcome improper DC feed conditions. Under 2-carrier CW and W-CDMA excitation, maximum of 19 dB and 18 dB IMD3 suppression together with the minimization of IMD asymmetry, were achieved using in-house bias tee, emphasizing the importance of broadband bias network design. [C706]

"Design of High Performance HEMT Switch for S-band MSM of Satellite Transponder"

A SPST switch MMIC which used for microwave switch matrix (MSM) of communications satellite payload with multi-beam function has been designed and fabricated. New RF FET switch configuration has been devised to improve power characteristics and isolation. Input and output return losses are better than another switches reported previously for both on and off states. The MMIC chips were fabricated in 0.15 μ m GaAs pHEMT process and measured insertion loss less than 2.0 dB and isolation more than 63 dB in the frequency range of 3 GHz ~ 4 GHz. Output 3rd order interceptpoint above 32 dBm has been recorded and the value is very high even though the unit pHEMT has gate width of 0.2 mm and only four pHEMT are used in the MMIC. [C707]

"Two-Stage 94 GHz drive Amplifiers Using 0.1- μ m Metamorphic HEMT Technology"

In this paper, millimeter-wave 94 GHz drive amplifiers based on metamorphic high electron mobility transistors (MHEMTs) were designed and fabricated. The fabricated 100 nm gate length MHEMT devices exhibit DC characteristics with a drain current density of 690 mA/mm and an extrinsic transconductance of 770mS/mm. The current gain cutoff frequency (f_T) and the maximum oscillation frequency (f_{max}) are 185 GHz and 230 GHz, respectively. The matching circuit of amplifier was designed using CPW (coplanar wave-guide) transmission line. The fabricated amplifier shows a good S_{21} gain of 7.79 dB, an input return loss (S_{11}) of -16.5 dB and an output return loss (S_{22}) of -15.9 dB. [C708]

"Studies on Modification of Channel Material and Gate Recess Structures in Metamorphic HEMT"

In this study, we have performed both the channel modification of the conventional MHEMT (Metamorphic High Electron Mobility Transistor) and the variation of gate recess. The modified channel consists of the $\text{In}_{0.53}\text{Ga}_{0.47}\text{As}$ and the InP layers. Since InP has lower impact ionization coefficient than $\text{In}_{0.53}\text{Ga}_{0.47}\text{As}$, we have adopted the InP -composite channel in the MHEMT. Also, the gate recess width is both functions of breakdown and RF characteristic of a HEMT structure. Therefore, we have studied the breakdown and RF characteristic for various gate recess widths of MHEMT's. We have compared breakdown characteristic of the InP -composite channel with that of conventional MHEMT's. It is shown that on and off state breakdown voltages of the InP -composite channel MHEMT were increased by about 20 and 27 %, respectively, compared with the conventional structure. Also, breakdown voltage of the InP -composite channel MHEMT was increased with increasing gate recess width. The f_{max} was increased with decreasing the gate recess width, whereas f_{max} was increased with increasing the gate recess width. Also, we extracted small-signal parameters. It was shown that G_{dof} of the InP -composite channel MHEMT is decreased about by 30 % compared with the conventional MHEMT. Therefore, the suppression of the impact ionization in the InP -composite channel increases the breakdown voltage and decreases the output conductance. [C709]

"High Breakdown Voltage AlGaIn/GaN HEMTs by Employing Proton Implantation"

The breakdown voltage of AlGaIn/GaN high electron mobility transistors (HEMTs) was increased considerably without sacrificing any other electrical characteristics by proton implantation. The breakdown voltage increased from 416 V of conventional device to 719 V by proton implantation with 150 KeV, $1 \times 10^{14} \text{cm}^{-2}$ fluence after a thermal annealing at 400degC for 5 min under N_2 ambient. The increase of breakdown voltage is attributed to the expansion of depletion region under the 2-dimensional electron gas (2-DEG) channel. The depletion region expanded downwards to the GaN buffer layer because implanted protons act as positive ions and attract the electrons in the 2-DEG channel. Proton implantation successfully reduced the electric field concentration so that the breakdown voltage increased. [C710]

"Millimeter-wave Broadband Amplifier using MHEMT"

In this paper, millimeter-wave broadband cascode amplifiers were designed and fabricated. The 0.1 μm $\text{InGaAs/InAlAs/GaAs}$ MHEMT (metamorphic high electron mobility transistor) was fabricated for the cascode amplifier. The DC characteristics of MHEMT are 670 mA/mm of drain current density, 688 mS/mm of maximum transconductance. The current gain cut-off frequency (f_T) is 139 GHz and the maximum oscillation frequency (f_{max}) is 266 GHz. To prevent oscillation of the designed cascode amplifiers, a parallel resistor and capacitor were connected to the drain of common gate device. By using the CPW (coplanar wave guide) transmission line, the cascode amplifier was designed and matched for the broadband characteristics. The designed amplifier was fabricated by the standard MHEMT MMIC (millimeter-wave monolithic IC) process that was developed through this research. As the results of measurement, the amplifier was obtained 3 dB bandwidth of 50.37 GHz from 20.76 to 71.13 GHz. Also, the amplifier represents the S_{21} gain with the average 7.07 dB in bandwidth and the maximum gain of 10.3 dB at 30 GHz. [C711]

"The Sensing Performance of Undoped-AlGaIn/GaN/Sapphire HEMT Hydrogen Gas Sensor"

The hydrogen sensing characteristics of undoped- AlGaIn/GaN/sapphire circular Schottky diodes are systematically studied and compared over wide hydrogen concentration and temperature ranges. High purity hydrogen gas was exposed to the sample together with the ambient gas of either air or pure nitrogen or without ambient gas (vacuum) at pressure in the range of 50 Torr to 200 Torr was used for both types of ambient gases. The sensing characteristics at different hydrogen concentration are investigated. The sensitivity to hydrogen gas was also investigated in dependence of various catalytic metals thickness and operating temperatures. [C712]

"Broadband Characterization of a 100 to 180 GHz Amplifier"

Atmospheric science and weather forecasting require measurements of the temperature and humidity vs. altitude. These sounding measurements are obtained at frequencies close to the resonance frequencies of oxygen (118 GHz) and water (183 GHz) molecules. We have characterized a broadband amplifier that will increase the sensitivity of sounding and other instruments at these frequencies. This study demonstrated for the first time continuous low noise amplification from 100 to 180 GHz. The measured InP monolithic millimeter-wave integrated circuit (MMIC) amplifier had more than 18 dB of gain from 100 to 180 GHz and 15 dB of gain up to 220 GHz. This is the widest bandwidth low noise amplifier result at these frequencies to date. The circuit was fabricated in Northrop Grumman Corporation 35 nm InP high electron mobility transistor (HEMT) process. [C713]

"Modeling and Characterization of Capacitively Coupled Interdigital-Gated HEMT Plasma Device for Terahertz Wave Amplification"

A capacitively coupled interdigital-gated HEMT structure was used to investigate the occurrence of uniformity of electric field distribution along the structure. The structure was designed and simulated using Commercial Electromagnetic Sonnet Suites software. The return loss characteristics were analyzed and evaluated. The comparison of the admittance characteristics from simulation between dc connected structure and capacitively coupled structure is carried out in order to evaluate electromagnetic wave propagation. This structure kept uniform electric field in the channel when the dc biased is applied to the interdigital gate, which modulates the potential in the channel. [C714]

"Modeling and Characterization of Schottky Diode on AlGaAs/GaAs HEMT Structure for Rectenna Device"

The modeling and characterization of Schottky diode on AlGaAs/GaAs HEMT structure for rectenna device is presented. The rectenna device can be used as a wireless power supply where it can capture microwave power and convert to the dc power to generate the others devices or circuits on a chip. Design and simulation of Schottky diode on AlGaAs/GaAs HEMT structure was carried out. From the simulated results, it was found that the operating frequency of the Schottky diode is tunable based on the length of coplanar waveguide. [C715]

"High power GaN-HEMT microwave switches for X-Band and wideband applications"

In this article the design, fabrication and test of X-band and 2-18 GHz wideband high power SPDT MMIC switches in GaN technology are presented. Said switches have demonstrated state-of-the-art performance and RF fabrication yields better than 65%. In particular the X-band switch exhibits an on-state power handling capability of better than 37 dBm at the 1 dB insertion loss compression point and the wideband switch shows an insertion loss compression of 1 dB for input power higher than 34.3 dBm in the entire bandwidth. [C716]

"A mixed HEMT-HBT MMIC technology using MBE regrowth"

Current microwave systems are constructed by integrating a large number of single technology components into a final product due to the limitations of any single transistor technology across all functions and metrics, thereby increasing cost and size of a given system. In this paper, we present a fabrication process using Molecular Beam Epitaxy (MBE) regrowth which allows the combination of High Electron Mobility Transistors (HEMT) with Heterostructure Bipolar Transistors (HBT) on a single GaAs chip without compromising the performance of either the HBT or HEMT. HBT f_T/f_{max} of 40/85 GHz and Beta of 170 for a collector current of 1 mA; and HEMT f_T/f_{max} of 115/160 GHz with a g_m -peak of 755 mS/mm has been achieved. Circuit performance demonstrates the potential of performance advances over HEMT-only circuit embodiments. [C717]

"Monolithic millimeter-wave distributed amplifiers using AlGaIn/GaN HEMTs"

Two monolithic broadband distributed amplifiers have been designed and fabricated using AlGaIn/GaN HEMTs. One of them uses a standard HEMT for the unit cell and shows a measured S_{21} of 5.2 dB from 1-50 GHz. The second distributed amplifier uses dual-gate HEMTs for the unit cell and achieves a measured S_{21} of 12 dB from 2-32 GHz. The process consists of 200 nm gate-length HEMTs, CPW transmission lines, MIM capacitors and thin-film resistors. The dual-gate distributed amplifier achieves a CW peak output power of 1 W and a PAE of about 16% at 4 GHz. [C718]

"High power AlGaIn/GaN Ku-band MMIC SPDT switch and design consideration"

An AlGaIn/GaN HEMT Ku-band MMIC single pole double throw (SPDT) switch has been fabricated and characterized. Due to the high breakdown voltage and the high electron mobility of the AlGaIn/GaN HEMT, this switch has high power handling capability and low insertion loss. It does not require DC power consumption, unlike the PIN diode switch, and it has higher power handling than the GaAs FET switch. The reported SPDT switch has 1.4 dB insertion loss, 35 dB isolation, and 36 dBm input RF power at the 1 dB compression point (P_{1dB}) at 18 GHz. Additionally, design considerations that are unique to the AlGaIn/GaN switch will be presented. We performed multiple design variations of a single pole single throw (SPST) switch and we report on the effect of these variations on the performance. [C719]

"A new method for determining the gate resistance and inductance of GaN HEMTs based on the extrema points of Z_{11} curves"

This paper presents a new method for calculating the gate resistance R_g and inductance L_g , of GaN HEMTs. The method consists in forward biasing the gate with low I_g currents ($I_g > 0$; $0 < V_{gs} < V_{bi}$; drain open) and is based on the extrema of Z_{11} curves. R_g and L_g are determined from the extrema of Z_{11} curves measured (after conversion of S to Z parameters) at single DC gate forward current. This new method differs from those

previously published in that it avoids the use of the resonance frequency in the imaginary part of Z_{11} and the large DC gate forward current. The good agreement between experimental and model data confirms the validity of the proposed method. [C720]

"GaAs C-band 4-bit phase shifter MMIC"

This paper describes design and performance of a C-band monolithic phase shifter made in 0.18 μm PHEMT technology for the phased array radar application. This compact 3 mm² MMIC features extremely low phase error, fine VSWR and adequate insertion loss. [C721]

"0.8-4 GHz high efficiency power amplifier in GaN technology"

In this contribution, the design and full characterisation of a high efficiency ultra-wide-band power amplifier are presented. The amplifier, based on GaN technology device, has been designed using a CAD oriented broad band matching approach for both input and output networks. The continuous wave measurements results in an average drain efficiency around 50% from 0.8 GHz to 4 GHz with an output power higher than 32 dBm in the overall bandwidth. [C722]

"35 dBm, 35 GHz power amplifier MMICs using 6-inch GaAs pHEMT commercial technology"

A 3.5 watt, 35 GHz power amplifier MMIC has been developed. The amplifier exhibits high performance at low processing cost, through the use of a commercially available 6-inch, 0.15- μm pHEMT process with 100 μm thick substrate. The single-ended four stage amplifier MMIC has 22 dB of gain at 35 GHz, 3.5 watts saturated output power (35.5 dBm), and power added efficiency of more than 25%, within a chip size of 12.75 mm². In terms of power density, this is 740 mW/mm, which is to the authors' knowledge the best reported for fully matched GaAs pHEMT MMICs on 100- μm substrates at millimetre-wave frequencies. [C723]

"Switch-mode amplifier ICs with over 90% efficiency for Class-S PAs using GaAs-HBTs and GaN-HEMTs"

This paper reports on design and realization of monolithic switch-mode amplifiers for data rates up to 1.8 Gbps, suitable for Class-S and inverse class-D PA modules. GaN HEMT as well as high-voltage GaAs-HBT technologies are employed and compared. For digital signal transmission without output filtering, the chips achieve efficiencies of more than 90% at an output power of 5.4 W and 6.5 W with PAE values including the on-chip drivers, of 75% and 80% for GaAs-HBT and GaN-HEMT ICs respectively. These high efficiencies values are very promising since such PA chips represent the key building block for future class S systems. [C724]

"Characterization of switched mode LDMOS and GaN power amplifiers for optimal use in polar transmitter architectures"

In this paper, switched mode power amplifiers classes of operation and device technologies are characterized versus input power and output supply voltage. The results are used to identify optimal control schemes for use in polar transmitter architectures. Then the effects of different control schemes on the requirements for the power amplifier, and the envelope amplifier, as the main building blocks of this architecture, are investigated. [C725]

"A high efficiency broadband monolithic gallium nitride distributed power amplifier"

A 50-ohm 100-2200 MHz distributed power amplifier (DPA) MMIC has been developed using Nitronex's proprietary GaN-on-Si NRE1 process. The DPA MMIC exhibits -10dB minimum input/output return loss, 39.4 dBm average output power, and a power added efficiencies of 30 to 66% over the entire bandwidth. [C726]

"Wideband 400 W pulsed power GaN HEMT amplifiers"

We have developed 400 W pulsed output power GaN HEMT amplifiers with 2.9-3.5 GHz bandwidth. Operating the amplifier from a 65 V drain supply under pulsed operation with 10% duty cycle and 100 μs pulse width obtains an output power in the range of 401-446 W over the band with a drain efficiency of 48-55%. The amplifier uses AlGaIn/GaN HEMTs with a total device periphery of 44.4 mm and advanced source connected field plates for high breakdown voltage. These wideband high power amplifiers are suitable for use in pulsed radar applications. [C727]

"A 330-GHz MMIC oscillator module"

In this paper, a 0.27 mW fundamental oscillator module operating at 330 GHz is presented. The MMIC in the module contains both the oscillator circuit and waveguide probes integrated on the same InP substrate. The oscillator is implemented in coplanar waveguide (CPW) technology and uses advanced high f_{MAX} 35 nm InP HEMT transistor in a common gate configuration. The integrated radial E-plane probe has been designed to operate over a frequency range of 300-350 GHz, using WR2.2 for the input and output waveguide. A free-running frequency of 330.5 GHz has been measured by down-converting the signal to an IF frequency observable on a spectrum analyzer. This is the first oscillator module above 300 GHz and demonstrates that fundamental signal generation at submillimeter wave frequencies can be simply and reliably generated. [C728]

"Over 57% efficiency C-band GaN HEMT high power amplifier with internal harmonic manipulation circuits"

In this paper, a high efficiency C-band GaN HEMT high power amplifier with internal harmonic manipulation circuits is presented. We employed a new circuit topology for simultaneous high efficiency matching at both fundamental and 2nd-harmonic frequencies. The developed GaN HEMT amplifier has achieved over 57% drain efficiency (50% power-added-efficiency) with 100 W output power at C-band. This is the state-of-the-art efficiency of GaN HEMT high power amplifier at C-band to the best of our knowledge. [C729]

"An AlGaIn/GaN class-S amplifier for RF-communication signals"

A Gallium-Nitride (GaN) current switched class-S amplifier for 450 MHz RF-signals is presented. A FPGA board is used to generate a band-pass delta sigma sequence with 1800 Mbit/s. This quasi digital signal is amplified to the required gate voltage swing for the HEMTs using a commercial available preamplifier. The AlGaIn/GaN-HEMTs are driven in a high efficient switch mode. Linearity is preserved using the class-S architecture. Limits of this classical amplifier architecture are shown and discussed. Simulation results are presented and the realized class-S demonstrator is shown. [C730]

"A 65-W high-efficiency UHF GaN power amplifier"

This paper presents a high-efficiency UHF power amplifier (PA) using a GaN HEMT on a SiC substrate transistor as the active device. The PA delivers 65 W with 82% power added efficiency (PAE), and 45 W with 84% PAE at 370 MHz, with supply voltages of 35 V and 28 V, respectively. Load pull techniques under Class-E conditions are used for device characterization and matching network design. The PA is implemented in a hybrid circuit with mixed lumped-element and transmission-line matching networks. A weighted Euclidean distance is defined to enable tradeoff studies between output power (POUT) and efficiency, in order to find the final optimal amplifier design. [C731]

"A Q-Band MHEMT 100-mW MMIC power amplifier with 46 % power-added efficiency"

A Q-band MMIC power amplifier has been designed, processed, and measured with first pass success. Design parameters include 20 dBm power, 25 dB gain, 40% PAE, input return loss of 10 dB and output return loss of 6 dB across 43.5 to 45.5 GHz. The MMIC design is based on the BAE Systems 0.1 μm MHEMT device, which has high gain and excellent PAE. The two-stage amplifier uses a 2-finger, 75 μm unit gate width, 0.1 μm gate length MHEMT device for the first stage and two 4-finger, 75 μm unit gate width, 0.1 μm gate length MHEMT devices for the output stage. Complete stabilization for both the even and odd mode is provided using feedback and resistors in critical locations of the circuit. The first stage is optimized for gain while the output stage is optimized for power and power-added efficiency (PAE). The complete MMIC amplifier measures 3.5 mm times 1.7 mm complete with dc blocks and dc biasing elements. Measured performance includes record high PAE of 46% at 44.5 GHz, 24 dB small-signal gain, 1 dB compressed power of 18 dBm, and 3-dB compressed power of 20.5 dBm across the 43.5 to 45.5 GHz frequency band. [C732]

"A W-band wavelet generator using 0.13-μm InP HEMTs for multi-gigabit communications based on ultra-wideband impulse radio"

A wavelet generator (WG) based on simple ultra-wideband impulse radio (UWB-IR) architecture has been developed to use for multi-gigabit communications systems that utilize the W-band millimeter wave (75-110 GHz). The W-band WG radiates a pulse signal, or a wavelet, whose full width at half maximum is less than 80 ps, which makes it possible to realize a 12.5-Gb/s ON/OFF keying transmitter. The WG consists of only two components: a pulse generator (PG) and a band pass filter (BPF). The digital-based PG was fabricated by using 0.13-μm InP HEMTs and created a record short pulse of 7.6 ps and 0.8 V_{pp}. The BPF was designed to be a five-stage microstrip coupled line filter on an alumina substrate. The 3-dB pass band of the BPF was 78-93 GHz and its insertion loss was 1.5±0.1 dB. The group delay was 100±10 ps in the pass band. To the

best of our knowledge, the WG is the first UWB-IR-based signal source that generates more than 10-Gb/s wavelets in the W-band. [C733]

"Microwave Characterization and Properties of 2 μ m Gate Length AlGaIn/GaN HEMT Structures"

The paper reports the properties of AlGaIn/GaN HEMT fabricated on sapphire substrate. Using 2 μ m length of gate electrode 6.67 GHz transition frequency as well as 24.5 GHz maximum frequency of oscillation was achieved. Small-signal model was identified. The transistor transconductance is in the range of 170 mS/mm. However the transistor was intended for structure and technology verification, it could be used in RF circuits. To improve HEMT's microwave properties, gate length and source-drain distance shortening are in progress. [C734]

"High performance 1.5W pHEMT Distributed Power Amplifier with Adjustable Inter-Stage Cascaded Network for 10-2000 MHz"

A new topology of high performance pHEMT distributed power amplifier is presented. An adjustable inter-stage cascaded matching network between two non-identical transistors is proposed. The superiority of the topology as indicated by the theoretical discussion is verified through simulation. Gain and PAE of 24 dB and 45+56%, respectively while output power of 32 dBm (plusmn2 dB) for frequency ranges (10-2000 MHz) are achieved. Moreover, stability analysis through pole-zero identification indicated, for this topology, and acceptable stability margin even under large-signal operation. [C735]

"Genetic algorithm for optimization of HEMT model parasitic parameters"

In this paper, we present a new approach to extract parasitic elements of high electron mobility transistors (HEMTs). By using genetic algorithm (GA), the values of biased-independent parasitic elements will be determined by minimizing the error between calculated and measured S-parameters. Some optimization examples are given for an HEMT from 1 up to 25 GHz. The results show that the proposed method is suitable to determine exactly many parasitic parameters of HEMT model with the excellent fit between measured and calculated S- parameters. [C736]

"GaN Power Transistors in Narrow and Wide Bandwidth Applications"

An active load-pull based investigation was conducted into the achievable performance of a 10 W gallium nitride (GaN) HEMT whilst operating in both narrow and wide bandwidth applications. It was found that a minimum efficiency of 40% was obtained over a broad bandwidth whilst delivering a constant output power of 10 W with the device biased in a class-AB mode. Conversely, in a narrow-band, high efficiency inverse class-F mode very high performance in terms of output power (12 W) and efficiency (81% PAE) has been measured. This has demonstrated the significant benefits in terms of the versatility of GaN devices for current and future PA applications. [C737]

"Optical stepper based 150mm GaAs PHEMT for microwave and millimeter-wave MMIC applications"

The gate geometry of PHEMT determines the upper limit in microwave and millimeter-wave frequencies at which the transistor can be optimally useful as amplifiers. In addition to production of 0.5 μ m and 0.15 μ m feature gate length PHEMT on 150 mm GaAs wafer substrate, WIN has recently developed the 0.25 μ m variety targeting mmic solutions covering from below X-band to frequency as high as 60 GHz. This presentation reports on device amplification performance achieved by various gate length from 0.5 μ m to 0.25 μ m that are created with optical I-line stepper based photolithography. At 10 GHz, both the 0.5 μ m and 0.25 μ m devices achieved 60% power-added efficiency while the later is able to provide higher output power of 900 mW/mm at 7 volt operation. This report also looks at how the higher fabrication throughput, stepper-based device approaches RF performance of the 0.15 μ m device made with electron-beam based lithography. Our stepper-based device has a lower capacitance CGD than our E-beam based 0.15 μ m device due to optimization of gate formation. This provides a higher gain upto 60 GHz inspite of its slightly lower unity current gain cutoff frequency f_T , which is a result of the longer gate length. Leveraging the high gain available, it is possible to realize multi-function millimeter-wave MMIC with this stepper-base technology where the PHEMT needs to have good performance in gain, RF output power, and efficiency; and it also needs to have good low noise characteristics for LNA circuit, and low on resistance and high isolation when working as a switching device. From characterization data, we are showing here that this can be simultaneously achieved. Additionally, in order to aid versatility in circuit design, both the depletion-mode device and the enhancement mode device are fabricated. This will enable low supply power consumption, and the integration of logic and control circuits in the monolithic multi-function chip. [C738]

"Experimental evidence of surface mobile holes on GaN HEMT structure"

In this paper, Hall measurement with an unconventional test vehicle was employed to verify the existence of these surface holes. The result represents a major breakthrough in understanding the effect of polarization induced electron-hole pairs on transistor electrical characteristics and reliability. [C739]

"GaN Device Technology: Manufacturing, Characterization, Modelling and Verification"

Gallium Nitride's superior physical properties, in comparison with other semiconductors, make GaNHEMT active devices a prime candidate in the implementation of next generation transmitters for radar systems, 3G/4G base stations and WiMAX. In this contribution, the characterization, modelling and verification of different families of high efficiency, high- power devices manufactured at SELEX Sistemi Integrati are reported. Process, characterization and modelling phases are analyzed to improve and refine the technology's fabrication techniques, thermal degradation issues and dispersion phenomena. [C740]

"Design of power amplifiers using high breakdown GaN HEMT devices"

Some applications of the new GaN HEMT technology have been demonstrated. Class AB allows either very wide bandwidth or very high power. Doherty produces very good efficiency that is correctable for acceptable linearity at high efficiency. [C741]

"Ultra low-loss high power AlGaIn/GaN HFET switches"

Novel design concepts and cutting edge results are presented for high-power AlGaIn/GaN Heterostructure Field-Effect Transistor switches for power converters, control and radio-frequency applications. For power switching, the HFET design has to be different from that of power amplifiers in order to minimize the contact resistance and avoid current crowding in the metal electrodes of large-periphery devices. Developed high-power III-Nitride HFET switches have the ON-resistance less than 1.25 Ω for a 3-mm wide multi-finger device, equivalent to less than 0.4 m Ω /cm² specific ON-resistance. New design and technology allows for low-loss power switching with above 1kV operating voltages, sub-nanosecond switching times, operating temperatures ranging from cryogenic up to 300degC and even higher. [C742]

"A novel high effective envelope-tracking amplifier for OFDM systems"

OFDM (orthogonal frequency division multiplex) mobile communication system is so popular in recent because it has so many virtues as effective frequency spectrum, wide-band, high speed rate, etc. But it has so many challenges in technical field, such as the high efficiency of PA (power amplifier) and linearity. RF (radio frequency) amplifier with ET (envelop-tracking) structure is described for OFDM systems in this paper. The first study the ET amplifier model, and then a high-efficiency OFDM amplifier is presented with GaN HEMT (heterostructure field-effect transistors), and includes the theoretic analysis and circuit design. Finally, the design circuit is simulated by ADS (advanced design systems) software, and gets the average DE (drains efficiency) of the amplifier is as high as 50% for an OFDM (Wimax) modulated signal with EVM of 2.94% at an average output power of 50 W and gain of 13.0 dB from simulating result. The design has good efficiency and linearity. All of these performances are satisfied with the OFDM systems requirement of RF. This design may be applied for the OFDM systems compare with the standard of OFDM. [C743]

"Predict the characteristics of a terahertz photomixer based on HEMT with the cap region from the analytical theory"

The characteristics of a terahertz photomixer using the excitation of plasma oscillation in the channel of a high-electron mobility transistor (HEMT) with the cap region are predicted in this paper from the developed analytic model. In the proposed model, the photo beam is inputted to the absorption layer of HEMT through the ungated area. Starting from the Euler equation and continuity equation, we obtained a response expression depicting the terahertz characteristics of that HEMT photomixer. As a result, the response as a function of the signal frequency is analyzed and the dependence of resonant frequency and amplitude on different length of cap region, voltage, and physical parameters are demonstrated. [C744]

"Towards fully integrated high temperature wireless sensors using GaN-based HEMT devices"

Wireless sensors that are capable of working in extreme environments can significantly improve the efficiency and performance of industrial processes by facilitating better monitoring and control. Gallium nitride (GaN), a widely researched wide bandgap material, can potentially be used to fabricate components for sensing and actuation for high temperature integrated wireless sensors. In this paper we are presenting an experimental

study on the performance of AlGaIn/GaN HEMT at high temperatures (up to 300degC). From test results, DC and microwave parameters at different temperatures were extracted. [C745]

"Central frequency tuning considerations for Gm-C resonators in GaAs technology"

The ability of adjustment of the central frequency of a Gm-C resonator in GaAs technology is discussed. First, it is shown that whatever the technology, the desired quality factor can be reached through an appropriate sizing of the transconductance values, by adding an external feedback capacitor in the transconductance amplifiers. Then, it is demonstrated that the adjustment of the central frequency must be made preferentially by a specific transconductance. Finally, because in GaAs technologies varying the transconductance values leads to current offsets which could be detrimental to the performances, the maximal allowed current offsets are determined. To illustrate these considerations, transistor-level simulation of a proposed structure in GaAs P-HEMT 0.2 μm with integrated feedback capacitors is presented and demonstrates a tunable central frequency from 750 to 810 MHz. [C746]

"Channel modulated AlGaIn/GaN HEMTs employing fluoride plasma treatment"

We proposed channel modulated AlGaIn/GaN high electron mobility transistors (HEMTs) employing fluoride plasma treatment and carried out the detailed numerical simulation of device operation using ISE-TCAD. The reduction of peak electric field is required to achieve the high breakdown voltage of AlGaIn/GaN HEMTs. Proposed channel modulated AlGaIn/GaN HEMTs created the fluoride plasma treated region between the gate and the drain. The fluoride plasma treated region modulated the two-dimensional electron gas (2-DEG) channel concentration, and effectively reduced the peak electric field without any field plates. The reduction of peak electric field in the gate-to-drain region made the breakdown voltage increased by 206 %. DC characteristics of channel modulated AlGaIn/GaN HEMTs remained practically the same as those of the conventional AlGaIn/GaN HEMTs. The breakdown voltage could be increased without a significant degradation of DC characteristics due to the SiO₂ passivation layer. The deposition of SiO₂ passivation layer combining with fluoride plasma treatment is a powerful process for channel modulated AlGaIn/GaN HEMTs. [C747]

"1.4 kV AlGaIn/GaN HEMTs employing As⁺ ion implantation on SiO₂ passivation layer"

We proposed As⁺ ion implantation on SiO₂ passivation layer of AlGaIn/GaN HEMTs to improve the forward and reverse electric characteristics of AlGaIn/GaN HEMTs. SiO₂ passivation layer which was applied in this work suppressed the electron hopping from gate to the surface states of gate-drain region so that the virtual gate formation was suppressed and the electric field concentration was terminated. As⁺ ions which were implanted on SiO₂ passivation layer changed the depletion region curvature so that the electric field distribution became moderate. To verify that As⁺ ions exist as positively charged after ion implantation, we measured electric force microscopy (EFM) with EFM test sample. After ion implantation, 2DEG concentration was slightly increased due to the induced electrons in channel which is the countercharge of positive ions in SiO₂ layer generated by As⁺ ion implantation. Therefore, forward electric characteristics were slightly improved after ion implantation. Reverse characteristics were improved significantly after As⁺ ion implantation. The leakage current when VGD is -100 V and the breakdown voltage of the conventional device was 51.36 $\mu\text{A}/\text{mm}$ and 523 V. The leakage current and the breakdown voltage under the same condition were improved to 38.82 $\mu\text{A}/\text{mm}$ and 1380 V after As⁺ ion implantation under the condition of 80 keV energy and 1 times 10¹⁴/cm² dose. After annealing (400degC, 10 min and N₂ SLPM), most of positive charge was removed, which was observed by EFM measurement. The breakdown voltage was decreased and the leakage current was increased. These results showed that the improvement of electric characteristics of AlGaIn/GaN HEMT is due to implanted As⁺ ions. [C748]

"Demonstration of resonant inverter circuit for electrodeless fluorescent lamps using high voltage GaN-HEMT"

This paper reports the demonstration of the resonant inverter circuit for electrodeless fluorescent lamps using a high-voltage GaN-HEMT as a main switching device. A 620-V/1.4-A GaN-HEMT was designed and fabricated for power electronic applications. The dynamic on-resistance increased with current collapse phenomena was suppressed by the dual-FP structure and the switching operation could be realized under high applied voltage of over 350 V. As a high-voltage and high-frequency power supply application, a 13.56-MHz resonant inverter circuit for electrodeless fluorescent lamps was demonstrated using the fabricated device. The demonstrated circuit achieved high-voltage operation of 380 V, high-speed gate-switching of 4.5-7 ns, and lighting of the electrodeless lamp with an input power of 7-10 W. High-voltage operation realized a simple circuit composition for high-power efficiency and the discharge ignition of the lamp without the starting circuit. The power efficiency of the inverter circuit was over 90% with an input power of 9 W. These results show that high-voltage GaN devices are suitable for high-frequency switching applications under high-input voltages of several hundred volts.

[C749]

"AlGaIn/GaN high-electron-mobility transistor(HEMT) employing Schottky contact on the unetched region and the silicon dioxide passivation"

AlGaIn/GaN high-electron-mobility transistors (HEMTs) which have the Schottky contact only formed on the unetched region and the SiO₂ passivation using an inductively coupled chemical vapor deposition (ICP-CVD) was proposed. The proposed device does not have any Schottky contact on the dry-etched region because the Schottky contact formation is performed prior to the mesa isolation, which suppresses problems induced by the poor interface between the etched region and Schottky metal. The SiO₂ passivation using ICP-CVD suppresses the electron trapping in surface states so that improves the reverse characteristics of the passivated device. We have fabricated the AlGaIn/GaN HEMT without Schottky contact on the dry-etched region employing the SiO₂ passivation using an ICP-CVD and measured the electrical characteristics of the proposed device. The proposed device achieved the on resistance of 3.06 mΩcm² (at LG=3 μm, LGD=20 μm) and improves the breakdown voltage from 363.0 V to 815.0 V (at LG=3 μm, LGD=20 μm). The figure-of-merit (VB/RON) is 217.07 MW/cm². The proposed device removes the poor Schottky contact interface and suppresses the electron trapping at surface states, which results in high breakdown voltage. [C750]

"Molecular dynamics simulation study on fluorine plasma ion implantation in AlGaIn/GaN heterostructures"

Fluorine plasma ion implantation is a robust technique that enables shallow implantation of fluorine ions into group III-nitride epitaxial structures. This technique has been used to achieve robust threshold control of the AlGaIn/GaN high electron mobility transistors (HEMTs) and led to the realization of self-aligned enhancement-mode devices. To reveal the atomic scale interactions and provide a modeling tool for process design and optimization, a molecular dynamics (MD) simulation is conducted for carbon tetrafluoride (CF₄) plasma implantation. Specific potential functions are applied to calculate the interactions among atoms and simulate the dynamics process of fluorine ions' penetration and stopping in III-nitride materials. The MD simulation provides accurate information on dopant profiles that are verified by secondary ion mass spectrum (SIMS) measurements. Defect formation and distributions, that are critical in process development, are also investigated. The MD simulation tool is capable of providing 2-dimensional fluorine dopant profiles. [C751]

"Source injection induced off-state breakdown and its improvement by enhanced back barrier with fluorine ion implantation in AlGaIn/GaN HEMTs"

The mechanisms of AlGaIn/GaN HEMT's off-state breakdown are investigated. Both the source- and gate-injection induced impact ionizations are identified with the former leading to premature three-terminal breakdown. A 35% improvement of the breakdown voltage could be achieved in an enhanced back barrier HEMT by implanting fluorine ions under the channel region and effectively block the source injection through the buffer layer. [C752]

"Monolithic integration of lateral field-effect rectifier with normally-off HEMT for GaN-on-Si switch-mode power supply converters"

A lateral field-effect rectifier (L-FER) that can be fabricated with normally-off transistor on the same AlGaIn/GaN HEMT with the same fabrication process has been demonstrated. The L-FER exhibits low turn-on voltage, low specific on-resistance and high reverse breakdown. A prototype of switch-mode dc-dc boost converter that features monolithically integrated L-FER and normally-off HEMT is demonstrated for the first time using industry-standard GaN-on-Si epitaxial wafers to prove the feasibility of GaN power integrated technology. [C753]

"Full-band and atomistic simulation of realistic 40 nm InAs HEMT"

A realistic 40 nm InAs high electron mobility transistor is studied using a two-dimensional, full-band, and atomistic Schrodinger-Poisson solver based on the sp³d⁵s* tight-binding model. Bandstructure non-parabolicity effects, strain, alloy disorder in the InGaAs and InAlAs barriers, as well as band-to-band tunneling in the transistor OFF-state are automatically included through the full-band atomistic model. The source and drain contact extensions are taken into account a posteriori by adding two series resistances to the device channel. The simulated current characteristics are compared to measured data and show a good quantitative agreement. [C754]

"Session 30: Quantum, power, and compound semiconductors devices-heterostructure high-speed devices"

This session highlights the recent world record breaking high speed performance achieved with heterostructure FETs and bipolar devices. In the first paper, Massachusetts Institute of Technology presents 30nm gate length enhancement mode InAs HEMTs with world record performance combination of f_T (601 GHz) and f_{max} (609) coupled with low power operation at 0.5 supply voltage. An invited paper from Hong Kong University of Science and Technology presents their pioneering work in the metamorphic growth of high performance InAlAs/InGaAs HEMTs on silicon substrate using MOCVD, suitable for high volume manufacturing. Intel and QinetiQ jointly demonstrate a high performance p-channel HEMT with 40nm physical gate length exploiting record hole mobility with strain engineered quantum well and remote modulation doping, thereby providing a promising option for high-speed complementary III-V logic. In another record setting paper, IHIP Technologies showcases the fastest SiGe HBT based ring-oscillator circuit with 2.5 picosecond delay. Newcastle University achieves extremely high DC current gain of 3,700 incorporating 30% Ge mole fraction in the base in a strained Si/SiGe HBT grown on a virtual substrate. Rochester Institute of Technology in collaboration with Amberwave Systems and University of Notre Dame demonstrates heterogeneous integration of high PVCR InGaAs/GaAs resonant tunnel diodes on silicon using aspect ratio trapping (ART) and Ge buffer layer. [C755]

"Low Noise Amplifier for front end transceiver at 5.8 GHz"

This paper presents the design of 5.8 GHz front end low noise amplifier application for IEEE standard 802.11 systems for WLAN application. Revolution and demand of WLAN technology have urged development of low cost, low power and small size transceiver by using microstrip technology. This paper is present design and simulation of single stage LNA circuits. This paper is focusing on development of low noise amplifier operating at 5.75-5.85 GHz (5 GHz upper U-NII band) for WLAN application. The amplifier design used FHX76LP low noise superHEMT from Eudyna device USA Inc. The design circuit uses lumped elements to implement the matching networks. The purpose single stage of input and output matching network is to produces 50. impedance at the input and output port of the LNA. The matching network is used at both sides of the transistor. The target simulation are gain (S_{21}) with >10 dB, noise figure with <10 dB and input and output return loss <-10 dB at 5.8 GHz. A single stage LNA has successfully designed with 15.924 dB forward gain, 0.552 dB noise figure, -11.182 dB output return loss(S_{22}) and -13.246 dB input return loss(S_{11}) by using ADS software. [C756]

"15 GHz SPDT switch design using 0.15 μ m GaAs technology for microwave applications"

In this paper, very low loss and high isolation single pole double throw (SPDT) switch design for microwave applications using pseudomorphic high-electron mobility transistor (pHEMT) is presented. The MMIC switch design is developed using a commercially available 0.15 μ m GaAs pHEMT technology. At the operating frequency of 15 GHz, the SPDT switch has 1.89 dB insertion loss and 26.66 dB of isolation. It also demonstrates 28.8 dBm of input P1dB gain compression point (P1dB) and 25.9 dBm of output P1dB. [C757]

"Physical degradation of GaN HEMT device observed in TEM during reliability test"

HRTEM observation was conducted to find evidence of physical degradation in AlGaIn/GaN heterostructure HEMT devices after life time testing. A strong relationship between electrical degradation and defects formation near the gate edge was observed. Detailed features of physical damages correlated with the degradation mechanism were discussed. [C758]

"Reliability evaluation of wafer-level-packaging AlSb/InAs HEMT receivers for light-weight and ultralow-power applications"

Wafer-level-packaging (WLP) AlSb/InAs HEMT receivers have been developed for lightweight and ultralow-power applications. To warrant successful insertion of WLP AlSb/InAs HEMT receivers for military and space applications, highreliability demonstration is essential. In this study, we performed three-temperature lifetesting to evaluate the reliability performance of WLP AlSb/InAs HEMT receivers. For the first time, the high-reliability performance of WLP AlSb/InAs HEMT receivers was demonstrated. The results show a median time to failure (MTF) of approximately 1.98×10^6 hours at $T_{junction}$ of 85 °C with activation energy (E_a) of approximately 1.87 eV. High-reliability performance is essential for successful insertion of WLP AlSb/InAs HEMT receivers for military and space applications with light-weight and ultralow-power requirements. [C759]

"Reliability and degradation mechanism of AlGaIn/GaN HEMTs for next generation mobile communication systems"

Excellent reliability performance of AlGaIn/GaN HEMTs on SiC substrates for next generation mobile communication systems has been demonstrated using DC and RF stress tests on $8 \times 60 \mu$ m wide and 0.5 μ m long AlGaIn/GaN HEMTs at a drain voltage of $V_d=50$ V. Drain current recovery measurements after stress

indicate that the degradation is partly caused by slow traps generated in the SiN passivation or in the HEMT epitaxial layers. The traps in the SiN passivation layer were characterized using high and low frequency capacitance voltage (CV) measurements of MIS test structures on thick lightly doped GaN layers. [C760]

"N-face GaN/AlGaN Transistors Through Substrate Removal"

In this paper, we present a new method to fabricate N-face GaN/AlGaN HEMTs based on the substrate removal of a Ga-face AlGaN/GaN layer grown on Si. A new substrate removal and transfer technology with no degradation to the GaN active layer. This technology has allowed the fabrication of N-face GaN transistors with record sheet resistance values. The Ga-face surface was bonded to a Si carrier wafer by using a hydrogen silsesquioxane (HSQ) interlayer. HSQ is a flowable oxide with excellent thermal stability. [C761]

"High-efficiency, high-breakdown AlGaN/GaN HEMTs with lifetimes beyond 20 years"

AlGaN/GaN HEMTs on various substrates have raised a lot of interest for the application in future high-efficiency base station systems for next generation mobile communication, currently dominated by LDMOS technology. Using GaN technology in a transmitter, infrastructure equipment manufacturers will benefit from major improvements in system performance and flexibility. AlGaN/GaN HEMTs enable innovative circuit concepts and transceiver architecture (e.g. switch mode power amplifiers, SMPA) with high efficiency and high operating bias. However, besides performance it will be crucial to match or even exceed the device reliability of other technologies in order to be competitive. To meet this goal, it is vital to optimize epitaxial growth as well as process technology. [C762]

"Origin of the Increasing Access Resistance in AlGaN/GaN HEMTs"

We have studied the origin of the increasing source access resistance in GaN HEMTs through a combination of theoretical modeling, simulations and experimental approaches. The reduction of the differential mobility as the electric field in the source region increases to 30 KV/cm in open channel conditions has been identified as the main cause of the increasing access resistance. Although excellent qualitative agreement between our modeling/simulations and the experimental results has been found, the quantitative results are very sensitive to the actual transport model in nitrides. From our results, the electron transport in the 10-30 kV/cm range is better described by a Trofimenkoff model than by the different Monte Carlo simulations reported in the literature, which indicates that current Monte Carlo techniques are overestimating the mobility at moderate electric fields (10-30 KV/cm). The design of new transistor structures with more constant access resistances is critical to improve the frequency performance and linearity of these devices and several new structures will be proposed at the meeting. [C763]

"Power performance of MBE-grown N-face high electron mobility transistors with AlN back barrier"

In summary, an N-face HEMT with good DC and RF properties was demonstrated. The use of AlN for electron confinement eliminates alloy scattering and offers a strong back barrier to mitigate short channel effects for highly scaled submicron devices. N-face devices are therefore expected to deliver excellent power density and efficiency with low leakage at microwave and mm-wave frequencies. [C764]

"Electrical and thermal modeling of AlGaN/GaN HEMTs on diamond silicon substrates"

The following work modeled an AlGaN/GaN HEMT on a silicon/polydiamond/polycrystalline silicon substrate to predict the self heating aspects of the FETs current and voltage characteristics. Various thermal conductivity substrate structure combinations were investigated. Simulation and measured data are compared for DC IV curves. The 2D modeling was used to examine self heating in the DC IV by mobility and thermal conductivity parameters. Removal in the simulation of the bottom polysilicon handle was used to predict improved HEMT DC performance. Results are shown that suggest that a 20 Г,Вm diamond substrate layer improves the DC IV characteristics and lowers channel temperatures. [C765]

"Finite-element thermal modeling of N-based HEMT structures"

The aim of this paper is to show and discuss results of 3D finite-element thermal simulation of GaN HEMT structures. HEMTs differing by geometry, substrate material, passivation, and heat removal strategy are simulated and compared in order to give a picture of the complex interplay of factors that must be reckoned with for proper thermal management. [C766]

"High-Performance E-Mode AlGaN/GaN HEMTs with LT-GaN Cap Layer Using Gate Recess

Techniques"

We have fabricated an E-mode LT-GaN/AlGaIn/GaN HEMT by using a gate recess technique to reduce leakage. The gate recess process consisted of SiCl₄ plasma etching, a N₂ plasma treatment, and a BHF treatment. The fabricated device with 0.6 μm -long gate exhibited a V_{thof} +0.51 V, a g_{mof} 236 mS/mm, and a BV_{off} 131 V. [C767]

"Temperature-dependent microwave noise characteristics of AlGaIn/GaN HEMTs on silicon substrate"

In this work, we report for the first time the detailed temperature dependent microwave noise characteristics of AlGaIn/GaN HEMTs on Si substrate from -50degC to 175degC (223 K to 448 K). The AlGaIn/GaN HEMT layer structures and fabrication details were published. The fabricated HEMTs have also gone through post gate annealing at 400degC for 5 minutes. However, it is interesting to note that at high temperature the degree of noise degradation of AlGaIn/GaN HEMT on Si substrate is lower than that on sapphire substrate and close to that on SiC substrate. [C768]

"Full W-Band High-Gain LNA in mHEMT MMIC Technology"

In this contribution the possible applications, technology, design and measurements of a W-Band high gain LNA are given. The main features of the four stage LNA can be summarised as following: a 25 dB average gain with plusmn2 dB ripple from 70 to 105 GHz, where gain is higher than 21 dB on the entire 70-110 GHz range. LNA predicted noise figure is 2.7 dB between 80 and 95GHz and less than 3.2 dB up to 108 GHz while the chip's power consumption is 35 mW. The technology used is a 70 nm GaAs mHEMT process from OMMIC. [C769]

"A Low-voltage, Fully-integrated (1.5-6) GHz Low-Noise Amplifier in E-mode pHEMT Technology for Multiband, Multimode Applications"

This paper describes the design and implementation of a fully-integrated MMIC low-voltage, low-noise amplifier (LNA) for use in multimode, multiband receivers using 0.25 μm enhancement-mode GaAs pHEMT technology. The LNA has two cascaded gain stages and is fully usable down to 0.8 V supply voltage and 5 mA total current drain. Power supply inductors, bypass capacitor and interstage matching are integrated on the die. An external inductor can be added to improve input match and gain. At 1.4 V supply, it achieves broadband (1.5-6)GHz gain of 17.5 dB and typical noise figure of 1.5 dB while consuming 18 mA of total current. Gain variation is typically less than 1.5 dB. Input IP₃ is better than -4 dBm across the band. The complete chip occupies an area of 1.1 mm². [C770]

"A Reflection-Type Biphase Modulator with Balanced Loads"

In this contribution a new balanced biphase modulator topology is presented. The new biphase modulator allows the reduction of the resulting chip area occupation by using 3 couplers only, in contrast with traditional reflection-type balanced biphase modulators with 4 couplers, and exhibiting comparable performances. A 45-65 GHz test vehicle adopting the proposed topology has been designed and realised in monolithic form in 70 nm mHEMT technology, resulting in a 1.8 times 1 mm²die size. The novel topology and the resulting measured performances of the test vehicle are described in the following. [C771]

"Performance of Unstuck-Gate AlGaIn/GaN HEMTs on (001) Silicon Substrate at 10 GHz"

This paper shows the capability of AlGaIn/GaN high electron mobility transistors (HEMTs) on (001) oriented silicon substrate with 300 nm gate length using unstuck Gamma gate for low cost device microwave power applications. The total gate periphery of 300 μm , exhibits a maximum DC drain current density of 600 mA/mm at V_{DS} =7V with an extrinsic transconductance (g_{mmax}) around 200 mS/mm. An extrinsic current gain cutoff frequency (f_{T}) of 37 GHz and a maximum oscillation frequency (f_{max}) of 55 GHz are deduced from Sij-parameters measurements. At 10 GHz, an output power density of 2.9 W/mm associated to a power added efficiency (PAE) of 20% and a linear gain of 7 dB are obtained at V_{DS} =30 V and V_{GS} =-2 V. [C772]

"GaIn MMIC based T/R-Module Front-End for X-Band Applications"

Amplifiers for a next generation of T/R-modules in future active array antennas are realized as monolithically integrated circuits (MMIC) on the bases of novel AlGaIn/GaN HEMT structures. Both, low noise and power amplifiers are designed for X-band frequencies. The MMICs are designed, simulated and fabricated using a novel via-hole microstrip technology. Output power levels of 6.8 W (38 dBm) for the driver amplifier (DA) and 20 W (43 dBm) for the high power amplifier (HPA) are measured. The measured noise figure of the low noise

amplifier (LNA) is in the range of 1.5 dB. A T/R-module front-end with mounted GaN MMICs is designed based on a multilayer LTCC technology. [C773]

"Advanced Components for Applications in S-Band and X-Band Radars"

Performance issues in S-Band and X-Band radar applications, have been investigated in parallel paths. The first approach continued with the basic GaAs based MESFET and pHEMT devices with the addition of field plate structures to enhance the transistor source-to-drain breakdown, enabling operation at higher voltages and producing significant improvements in device operation. The second direction questioned the basic material properties underlying the device structures. This methodology has led to the investigation of a number of pHEMT and HEMT designs based on SiC, GaN on SiC, and GaN on silicon devices for both S-Band and X-Band radar applications. [C774]

"Accurate Nonlinear Electron Device Modelling for Cold FET Mixer Design"

A nonlinear empirical model is here adopted to model the cold-FET behaviour of a GaAs pHEMT, in the framework of a resistive mixer application. The model, purely mathematical and technology independent, is suitably identified in the device operative region of interest and is validated in large-signal conditions by exploiting a measurements setup based on LS-VNA. [C775]

"A Nonlinear Drain Resistance pHEMT model for Millimeter-wave High Power Amplifiers"

A high power pHEMT with longer drain-gate separation can operate at higher voltage. However, it shows large output power loss at millimeter-wave in addition to the conventional parasitic power dissipation. The nonlinear drain resistance R_d of the pHEMT is found to cause the large power loss, although it behaves as a conventional resistor at low frequency. The nonlinearity of the R_d is modeled and shows good agreement with the measurement. Comparisons of pHEMTs with different nonlinear R_d also support the model. [C776]

"A Highly Linear (40.5-43.5) GHz MMIC Single Balanced pHEMT Resistive Up-Converter Mixer for LMDS Applications"

This paper presents the design and performance of a highly linear (40.5-43.5)GHz MMIC single balanced pHEMT resistive up-converter mixer dedicated to LMDS applications. The mixer achieves good performance in terms of conversion loss which is about 6 -7 dB and LO/RF isolation that is better than 30 dB under LO power equal to 14 dBm. The main feature of the mixer is its high linearity since it presents an RF output power@1 dB compression point ($P_{out@1\text{ dB}}$) superior to 5 dBm in the (39.5-43.5)GHz frequency range. The measured OIP3 is equal to 20.2 dBm at 40.5 GHz and 12.2 dBm at 42 GHz. The 2 mmx1.5 mm circuit was fabricated using the D01PH (0.13 μm GaAs depletion mode pHEMT) process provided by the OMMIC foundry. To the best of our knowledge, this is the most linear up-converter mixer reported to date in this frequency range associated with as low conversion loss. [C777]

"10 Watt High Efficiency GaAs MMIC Power Amplifier for Space Applications"

This paper describes the design of a GaAs monolithic high power amplifier at Ku band. The chip delivers about 40 dBm of saturated output power, in CW operating conditions, at 11.7 GHz central frequency, with 17% of bandwidth. The saturated power gain is 12.4 dB with 2 dB gain flatness across the application bandwidth while the chip power added efficiency is estimated between 33% to 47%. The amplifier is designed to be used as final stage of a downlink satellite transmitter for Tracking Telemetry & Command system. A commercial power pHEMT process capable of handling a power density higher than 1 W/mm has been selected for the MMIC design. Due to the space application, special attention must be put on the process and MMIC reliability: to this aim performances must be guaranteed in de-rated conditions respect to the process maximum ratings and, in addition, the channel temperature of the active devices must be kept within the value established by Space Requirements and carefully controlled. This makes the design objective very tight. The MMIC power amplifier design and some measurement results are presented in the paper. [C778]

"A Four-Antenna Transceiver MIMIC for 60 GHz Wireless Multimedia Applications"

A transceiver MIMIC (millimeter wave monolithic integrated circuit) with four antenna ports functionality for 55 to 65 GHz wireless multimedia applications has been developed. The chip has been realized using 100 nm gatelength metamorphic InAlAs / InGaAs HEMT (high electron mobility transistor) technology on GaAs substrate together with GCPW (grounded coplanar waveguide) technology. The novel transceiver topology for the MIMIC is described. The different building blocks, namely the 2:4-switch design, sub-harmonic IQ-resistive mixer and variable gain amplifiers, are explained in details. Simulated and measured results are compared. Finally, the

overall performance for the integrated transceiver chip is presented. [C779]

"A Compact 20-35 GHz Quadrature Coupler using 0.15 μ m pHEMT Coplanar Waveguide Technology"

A coplanar waveguide (CPW) mode 20-35 GHz quadrature coupler has been demonstrated in this study. Good microwave performance and compact size can be achieved simultaneously. The measured return loss is better than 16.6 dB and insertion loss of S₂₁ and S₃₁ are 3.6 \pm 0.2 dB. The measured phase difference is 88 \pm 2 deg from 20 to 35 GHz. Total chip size including RF pads is 0.72 times 0.48 cm². Comparing the performance and chip-size between a non-bending and a bending couplers, the bending one shows 0.4 dB worse in simulated insertion loss than the other but the chip-size is 50 percent in reduction. This circuit is adaptable for the applications in wideband double balanced mixers and power amplifiers. [C780]

"High Linearity 5.2 GHz Power Amplifier MMIC Using the Linearizer Circuit"

This paper aimed to study the linearity in the 5.2 GHz power amplifier microwave monolithic integrated circuit (MMIC), which was performed with a 0.15 μ m AlGaAs/InGaAs D-mode pHEMT technology. The power amplifier (PA) was studied taking into account the linearizer circuit and the coplanar waveguide (CPW). Based on those technologies, the power amplifier obtained the output power of 13.3 dBm and the power gain of more than 15 dB. The input third-order intercept point (IIP₃) of 1.4 dBm and the output third-order intercept point (OIP₃) of 22.5 dBm and power added efficiency (PAE) of 21% were attained, respectively. Finally, the overall power characterization exhibited high gain and linearity, which illustrated that power amplifier had the circuit compact size and exhibited favorable RF characteristics. [C781]

"120-GHz-band Low-noise Amplifier with 14-ps Group-delay Variation for 10-Gbit/s Data Transmission"

This paper presents a 120-GHz-band low-noise amplifier (LNA) for a receiver microwave monolithic integrated circuit (MMIC), which is used for a 10-Gbit/s wireless link. The LNA was designed for low-noise performance, a high gain, and low group-delay variation. To achieve enough stability with low-noise performance and low group-delay variation, we introduce a new stabilizing circuit consisting of two coplanar-waveguide stubs. The LNA MMIC was fabricated using 0.1- μ m-gate InP high-electron-mobility transistors (HEMTs). We integrated the LNA into a WR-8 (90-140 GHz) waveguide module and evaluated it. The LNA module achieved an averaged noise figure of 5.6 dB, a gain of >19.5 dB, and group-delay variation of <14 ps from 117.5 to 132.5 GHz. [C782]

"Multiple-Throw Millimeter-Wave FET Switches for Frequencies from 60 up to 120 GHz"

This paper presents the design and performance of various millimeter-wave FET switches realized in a metamorphic HEMT technology. The single-pole multi-throw switch configurations are targeting wireless communication frontends and imaging radiometers at 60, 94 and 120 GHz. In SPDT switches, state-of-the-art insertion loss of 1.4 and 1.8 dB is achieved at 60 and 94 GHz, respectively. Rivalled only by PIN diode switches, an insertion loss of <2 dB is demonstrated up to 120 GHz. Shorted stubs are used to compensate for parasitic FET capacitance and allow for matching. Linearity data is presented for 60 and 94 GHz SPDT switches. A comprehensive comparison with state-of-the-art planar SPDT switches is included. A 2:6 switch network for multi-antenna transceivers achieves <4 dB insertion loss at 60 GHz. [C783]

"24 GHz LTCC Amplifier Using Packaged HEMTs"

The design of an LTCC self-packaged amplifier for the 24 GHz ISM band using packaged transistors is described. The amplifier utilizes to a full extent the benefits of the multilayer environment as all matching networks are realized by employing multilayer impedance transformers. Advantages of using such transformers are the elimination of dedicated DC blocks, flexible layout routing and a milder discontinuity in the vertical transitions towards the PCB connection. A combination of on-tile and off-tile distributed matching has been implemented allowing for the amplifier to be used on various PCB substrate materials. The amplifier can be used in both the receiver and transmitter chains, in various application scenarios. Examples of the measured amplifier characteristics designed on two different substrate materials are shown, illustrating the trade-off between the cost and the performance of the materials used. [C784]

"24 GHz LTCC I/Q Mixer Using Packaged HEMTs"

An I/Q active mixer in LTCC technology using packaged HEMTs as mixing devices is described. A mixer is designed for use in the 24 GHz automotive radar application. An on-tile buffer amplifier was added to compensate for the limited power available from the system oscillator. Careful choice of the type or topology for

each of the passive circuits implemented resulted in an optimal mixer layout, so a very small size for a ceramic tile of 15times15times0.8 mm³ was achieved. The measured conversion gain of the mixer for a 0 dBm LO level was -6.7 dB for I and -5.2 dB for Q. The amplitude imbalance between I and Q signals resulting from the aggressive miniaturization of the quadrature coupler could be compensated in the DSP stages of the system at no additional cost. The measured I-Q phase imbalance was around 3 degrees. The measured return losses at mixer ports and LO-RF isolations are also very good. [C785]

"V-Gate GaN HEMTs with 12.2 W/mm and 65% PAE at X-Band"

In this paper, we present our development of a novel HEMT which uses V-shaped gate geometry to reduce the field crowding at the gate edge, and pushes the high power performance of the deeply recessed HEMTs toward higher operating voltages. The V-gate GaN HEMTs were fabricated by using a highly manufacturable approach, and demonstrated X-band power performance superior to devices made by other technologies. [C786]

"A study of switchable dual-frequency oscillator for 60 GHz FSK modulation"

This paper reports on practical study of a switchable dual-frequency oscillator for 60-GHz binary FSK modulation, using a 0.15 μm commercial GaAs p-HEMT technology. The oscillator obtained an output power of 1.8 dBm at 61.43 GHz with a phase noise of -65dBc/Hz at 100 kHz offset and -87dBc/Hz at 1MHz offset to the carrier at the free-run state. A 500 Mbit/s FSK modulation was confirmed with the developed oscillator. This type of oscillator is feasible for of multi-gigabit data rate FSK modulation. [C787]

"AIN SAW structures for GHz applications"

SAW type structures for an operating frequency of about 2.8 GHz and 3.2 GHz have been successfully developed on a thin A1N layer sputtered on high resistivity silicon. Nanolithography was used to manufacture the interdigitated transducer. Fingers and interdigits 300nm and 150nm have been manufactured. A thinner metalization on the IDT will contribute to improve the frequency performances of the devices. We are now developing SAW structures with nanometric IDTs on thin GaN layers. These structures have the advantage in the possibility of monolithic integration with other circuit elements, like HEMT transistors. Future development of WBG semiconductors and nanolithography based techniques will permit the developing of a new generation of SAW devices, operating over 5 GHz, able to be used in 4G mobile phones and in 5.2 GHz WLAN applications. [C788]

"A wideband GaN HEMT distributed power amplifier for WiMAX applications"

In this paper, we propose a high power and wideband dual-fed GaN HEMT DP A for 2.6 GHz WiMAX applications, which is implemented a push-pull GaN HEMT with the P1dB of 20 W to avoid circuit complexity and large size. From the measured results for a continuous wave (CW) and a WiMAX signal, the dual-fed GaN HEMT DPA shows wideband performances. [C789]

"Capacitance modeling of 120nm AlGaIn/GaN HEMT for microwave and high speed circuit applications"

The capacitance-voltage(C-V) and switching characteristics of AlGaIn/GaN HEMT has been calculated analytically. The device capacitances and switching parameters, which have been calculated, depends on the basic device parameters and terminal voltages which determine the microwave behavior of a device. The nonvariant nature of this device with drain voltage leads to better device choice for high power microwave frequency. [C790]

"A ultrawideband low noise amplifier using metamorphic HEMT on organic substrate"

The U.S. Federal Communications Commission (FCC) approved the unlicensed use of ultra- wideband (UWB) (range of 3.1-10.6 GHz) for commercial purposes in 2002 [1]. The chip-set for lowband (range 3.1-4.8 GHz) application has already been developed and UWB system for lowband has been evaluated by many companies. But the chip-set for full-band (range of 3.1-10.6 GHz) is on its developing stage. Therefore, various researches on the active devices like LNA, PA and the passives like filter, balun, antenna for full-band application are being performed vigorously [2], [3]. High electron mobility transistors(HEMTs) have played an important role in applications at millimeter wave ranges due to its high speed, low noise characteristics. Focusing on the low noise and high gain characteristics of the devices, applications at 3.1-10.6 GHz, utilizing pseudomorphic HEMT(pHEMT) has reported with excellent performance [4]. Motivated by this we have fabricated balanced low noise amplifier for UWB application utilizing metamorphic InAlAs/InGaAs HEMTs(MHEMT) on GaAs substrate. For the wideband amplifier evaluation, the balanced amplifier with the broadband coupler was designed and

realized using multilayer organic substrate based on the ceramic- polymer composite materials developed in this work. [C791]

"Linearity-optimized class-E GaN HEMT Doherty amplifier"

In this paper, we have proposed a linearity-optimized class-E GaN HEMT DPA. To improve linearity without extra linearization techniques, not only the gate biases but also matching circuits of the carrier and peaking cells were optimized. For verification, a class-E DPA was designed and implemented using GaN HEMTs with 25-W PEP and tested using a two-tone signal with 1-MHz tone spacing and a 1-carrier WCDMA signal. The measured two-tone results showed that the class-E DPA optimized at an average output power of 38 dBm delivered the IMD3 of -58 dBc with a PAE of 45.4%. For a 1-carrier WCDMA signal, the class-E DPA produced an ACLR of -32.9 dBc with a PAE of 46.7%. The measured results prove that the proposed class-E GaN HEMT DPA can be a promising solution for high- performance PA. [C792]

"DMG AlGaIn/GaN HEMT: A solution to RF and wireless applications for reduced distortion performance"

The study thus proves that DMG AlGaIn/GaN HEMT is a potential candidate for growing requirement of high linearity and low distortion in the telecommunication industry due to reduced SCEs and a more uniform electric field distribution. The study also shows that the linearity performance improves further on using lower doping and thickness of the barrier layer and increased metal gate workfunction difference; thus presenting DMG AlGaIn/GaN HEMT as a promising solution for high performance RF applications. [C793]

"A high-efficiency class-F GaN HEMT power amplifier with a diode predistortion linearizer"

The class-F amplifier has high-efficiency, but shows specific distortion behavior. AM/AM and AM/PM characteristics of the series diode linearizer have been designed to cancel those of the class-F power amplifier by controlling the bias voltage and the bias feed resistance of the diode. With the diode predistortion linearizer, the IMD3 of the 1-watt 1.9-GHz class-F GaN HEMT power amplifier is improved by 4 dB over power outputs 6 to 23 dBm. The drain efficiency of the amplifier with the linearizer is not reduced that much. The diode linearizer has IMD3 asymmetry, and the effect of this on the linearization of the amplifier is discussed. [C794]

"Quarter-micron optical gate 6" power pHEMT technology"

A production ready pseudomorphic high electron mobility transistor (pHEMT) using i-line 0.25 μm optical gate lithography has been developed for both Ka- and Ku-band power applications. These 0.25 μm Ka- and Ku-version pHEMT devices demonstrate state-of-the-art power performance at 29 and 10 GHz, respectively. Excellent reliability has been achieved at channel temperature exceeding 275degC. Yield exceeding 95% is demonstrated for devices with 1.875 mm gate width across a 6-inch GaAs wafer. These results indicate that the 0.25 μm pHEMT technology is ready for high volume production with low cost at WIN Semiconductors. [C795]

"D-band amplifier using metamorphic HEMT technology"

In this paper, we successfully demonstrated the D-band MMIC amplifiers based on 0.1 μm InGaAs/InAlAs/GaAs MHEMT which has two fingers of 30 μm gate width. The device exhibited a cut-off frequency (f_T) of 189 GHz, and a maximum oscillation frequency (f_{max}) of 334 GHz. The D-band MMIC amplifier exhibited a good RF gains of 7.8 dB at a frequency of 110 GHz. Actually, the D-band MMIC amplifiers exhibited the S21gains of at 140 GHz in Momentum simulation. We try to measure a frequency range of 110-140 GHz because our measurement equipment can measure in a frequency range of 0.1-110 GHz. Proceeding from these results, we expect satisfactory results in S21gain performance at 140 GHz. [C796]

"Influence of gate width and gate finger towards noise figure of p-HEMT"

This study will try to get the percentage of noise figure improvement on specific HEMT layout within a region. The measurement result obtained will be analyzed according to the related theories and observations which are commonly occur in GaAs-based HEMT. [C797]

"Steady-state and transient temperature distribution in GaAs microwave circuits"

This work models and simulates the electrothermal properties of GaAs pHEMT based Monolithic Microwave Integrated Circuits (MMIC). The temperature increase of each component due to the self heating of the power devices in the packages was simulated coupled with the static electromagnetic analysis. A linear RC thermal macromodel was developed for the die, and the temperatures are solved by using nodal equations numerically.

Stead-state and transient simulations of temperature distribution of the MMIC structures were performed. The need for thermal vias was demonstrated as essential parts of the package for thermal cooling purposes. [C798]

"Low-phase-noise, phase-locked tunable millimeter-wave signal source for calibration of W-band low-noise astronomical heterodyne receivers"

One of the solutions to overcome the problem introduced by larger characteristic parameter variation is to calibrate the characteristics of the system by a known weak signal periodically. The calibration signal can be either a signal from known celestial objects or an artificial signal source built in the telescope system. The disadvantage of the celestial calibration sources is that their orientations may be far from the observing area, which takes longer time on the pointing and alignment before and after calibration. The system built-in calibration signal source can omit such kind of inconvenience. The system considered in this paper is the Array of Microwave Background Anisotropy (AMiBA), which is with 13-element millimeter-wave telescope array with HEMT based heterodyne receivers operated in 85-104 GHz band. In this paper, a frequency selectable CW source for AMiBA system calibration is presented. [C799]

"High power X-band internally-matched AlGaIn/GaN HEMT"

High-performance internally-matched GaN HEMT with 0.3 μm gate length and 4times2.5 mm of the total gate width was successfully fabricated. The large signal RF characteristics of the internally-matched device were measured at 8 GHz. A maximum output power of 64.5 W, a gain of 7.2 dB and a peak power-added efficiency (PAE) of 40% was obtained, respectively. [C800]

"A 3.7GHz GaN HEMT Doherty power amplifier using digital predistortion linearization"

In this study, we implemented a 3.7 GHz band Doherty amplifier based on GaN HEMTs which was linearized using a digital predistortion method. The forward and reverse models of the predistortion consist of simple polynomials whose coefficients are extracted using a conventional LMSE algorithm. Using two carrier signals based on IEEE 802.16e, whose PAR is 9.44 dB, an ACLR improvement of 10.74 dB was achieved to give an ACLR level of 41.74 dBc at an offset of 4.79 MHz. The overall efficiency of the Doherty power amplifier is 13.74% which represents a 2.44% improvement compared to that of a balanced class-AB power amplifier at an average power of 36 dBm. [C801]

"Evaluation of RF and logic performance for 40 nm InAs/InGaAs composite channel HEMTs for high-speed and low-voltage applications"

The DC and RF performances of 40 nm high electron mobility transistors (HEMTs) with composite channel of InAs channel and In_{0.53}Ga_{0.47}As sub-channel were demonstrated. The drain current was 870 mA/mm ($V_{ds}=0.4\text{V}$, $V_{gs}=0\text{V}$) and maximum gm_{max} 1750 mS/mm ($V_{ds}=0.5\text{V}$, $V_{gs}=-0.65\text{V}$). The devices showed high current gain cutoff frequency (f_T) of 420 GHz and low gate delay time of 0.77 ps owing to the nanometer gate length and extremely high electron mobility of the InAs channel. Under low DC power consumption; these InAs HEMTs still exhibited excellent RF and logic performance which indicates these devices have great potential for future high-speed and low-voltage applications. [C802]

"A low-power subharmonic injection-locked oscillator using E/D-mode GaAs PHEMTs for Ka-band applications"

A subharmonic injection-locked oscillator (SILO) implemented by using 0.5 μm E/D-mode PHEMT process is demonstrated to achieve a Ka-band low-power and low phase noise source in this paper. Based on a 15 GHz cross-coupled oscillator, a signal having the frequency around 30 GHz can be generated in this SILO circuit through the push-push technique. A cascode amplifier is also arranged to be the output buffer for gaining the output amplitude of 30 GHz signal. The total power consumption of SILO is 24.5 mW under 2.5 V supply voltage. The measured free-running phase noise is -101 dBc/Hz at 1 MHz offset. With injecting a 2nd-order subharmonic signal (7.5 GHz) into this ILO, the output phase noise can be further improved to -127 dBc/Hz. The overall frequency multiplication factor is 4. [C803]

"Improved robustness of AlGaIn/GaN HEMTs using Deuterium to passivate the structural defects"

GaN related devices have demonstrated excellent performances for high power, high temperature up to X-band applications. However, even if the reliability studies on AlGaIn/GaN high electron mobility transistors (HEMT) have led to higher mean time to failure (MTTF), physical mechanisms induced by stresses are still not well known. This paper proposes an original solution to improve the robustness of the devices by passivating the traps that are supposed to be related to the degradation process. Based on the experience of previous works,

we use Deuterium H⁺ to block the traps located at the AlGa_N/Ga_N interface above the gated zone of the device, and the traps in the bulk of the conducting channel (2 dimensions electron gas: 2DEG). 2 batches of devices are processed with and without deuterium, and submitted to temperature stresses at 500degC. Low frequency noise (LFN) measurements are performed to track the evolution of the spectral current density of the drain current, which is known to be related to the structural evolution of the traps and of the crystal structure perfection. Devices with deuterium feature stable LFN spectra, while LFN spectra of the devices without deuterium evolve during the different stress steps. Thus, deuterium can offer an interesting alternative to enhance the robustness of AlGa_N/Ga_N devices operating under stringent temperature conditions. [C804]

"High-Performance AlGa_N/Ga_N HEMT-Compatible Lateral Field-Effect Rectifiers"

In conclusion, an AlGa_N/Ga_N HEMT-compatible lateral field-effect rectifier is demonstrated by utilizing the threshold-voltage controlling capability of the fluorine plasma treatment technique. The rectifier features low on-resistance, low turn-on voltage, high temperature operation and high reverse breakdown voltage. The rectifier is expected to exhibit fast reverse recovery time because of its unipolar nature. In addition, the rectifiers are fabricated with the same process as the normally-off AlGa_N/Ga_N HEMTs, indicating a robust low-cost approach of realizing Ga_N-based power integrated circuits. [C805]

"5-6 GHz Front End Low Noise Amplifier"

This paper presents 5-6 GHz front end low noise amplifier application for IEEE standard 802.11 system for WLAN application. This amplifier uses FHX76LP low noise SuperHEMT device designed for DBS application from Eudyna Device USA Inc. This paper is present design and simulation of single stage LNA circuits. A single stage LNA has successfully designed with 26.92 dB forward gain and 1.32 dB noise figure, which stable along the UNII frequency band. [C806]

"Reliability of Ga_N-Based HEMT devices"

This paper reviews the main problems characterizing the past and present of Ga_N-based HEMT reliability. Some general considerations on the maturity of this technology and published lifetesting extrapolations are followed by a review of physical degradation mechanisms, subdivided between temperature-activated and electrical ones, the latter generally linked with the much-debated I_{d} current collapse. The paper ends with some conclusive remarks on what has been achieved and what still lies ahead. [C807]

"Broadband Terahertz Emission from Dual-Grating Gate HEMT's-Mechanism and Emission Spectral Profile"

We observed and characterized broadband terahertz emission from our original plasmon-resonant emitter structured by dual-grating gate high electron mobility transistors (HEMT's). The samples are fabricated in two structures: a standard single-heterostructure HEMT with metallic grating gates and a double-decked (DD) HEMT with semiconducting 2-dimensional electron gas (2DEG) grating gates. The mechanism of the broadband emission originated from multi modes of incoherent/coherent plasmon excitations is revealed. [C808]

"Enhancement-mode 130 nm InAs p-HEMTs having f_T of 403 GHz and f_{max} of 470 GHz fabricated using atomic-layer-etching technology"

High-performance 130 nm E-mode InAs p-HEMTs is fabricated using the Ne-based ALET and the buried Pt gate technology. Results from the combination of the improved gate-to-channel aspect ratio achieved by the buried Pt gate technology show that performance of the device is remarkable and the improved carrier transport property is achieved using the ALET technology. [C809]

"Surface control of AlGa_N for the stability improvement of AlGa_N/Ga_N HEMTs"

Highly stable and reliable operation is absolutely required for Ga_N-based high-efficiency power switching devices and high-power RF AlGa_N/Ga_N HEMTs. For the improvement of operation stability in such devices, in this paper, the surface control technologies will be addressed by introducing an ultrathin-Al-layer process and a multi-mesa-channel structure with relevant technologies. [C810]

"Simulating Pseudomorphic HEMTs: Optimizing Performance to Achieve Multi-terahertz Operating Frequencies"

In summary, we show that properly scaled HEMT devices can operate will into the THz regime, and provide a viable device option in this spectral region. These results are also important for logic devices desired for

operation in the Tbs regime, as the cutoff frequency f_T is intimately related to the logic delay time in a switching transistor. [C811]

"A GaN HEMT Class-F amplifier for UMTS/WCDMA applications"

In this work, the authors present a highly efficient GaN HEMT Class-F amplifier designed for Universal Mobile Telecommunications Systems using Wideband Code Division Multiple Access (UMTS/WCDMA). The amplifier has a peak PAE of 76% with an output power of 10.5 W. A comparison between class-F and inverse Class-F was also made. [C812]

"A compact size Ka band pHEMT MMIC frequency tripler using lump element balun"

This work presented a compact size Ka band pHEMT MMIC frequency tripler that incorporates a simple LC-lumped balun. The configuration not only can provide a flexible way to control the phases but also can reduce the chip size of the MMIC. As compared to the third harmonic frequency, the fundamental and second harmonic frequency can be suppressed more than 24 dB. [C813]

"A 40-80-GHz mHEMT single-pole-double-throw switch using traveling-wave concept"

This paper presents a 40-80-GHz SPDT switch fabricated in mHEMT process. The SPDT switch accomplished insertion loss lower than 2.4 dB and isolation better than 23 dB. Via holes were shared to compact the layout and the chip size of 1 x 1 mm² is obtained. Table 1 summarizes recently reported performance of SPDT switches in GaAs HEMT process. [C814]

"GaN X-band 43% internally-matched FET with 60W output power"

An X-band high efficiency GaN internally-matched FET has been developed. Asymmetric matching circuit layout is employed to avoid decrease of efficiency caused by impedance mismatch and unbalance power dividing in matching circuits. The designed asymmetric input and output matching circuits have achieved equal dividing characteristics. A power added efficiency (PAE) of 43.4% and an output power of 47.8 dBm (60.3 W) have been achieved with the developed GaN internally-matched FET. [C815]

"On the noise performance of 80nm InAs/In_{0.7}Ga_{0.3}As HEMTs using gate sinking technology"

80nm InAs/In_{0.7}Ga_{0.3}As HEMTs using Pt gate sinking were characterized for ultra-low power low noise applications. While the epitaxial structure of the device was optimized, the reduction of gate-to-channel distance was achieved from gate sinking process. The device exhibited very high drain current density of 1066 mA/mm and maximum gm of 1900 mS/mm at V_{ds} = 0.5 V. Excellent $f_T(f_{max})$ up to 113 GHz (110 GHz) at V_{DS} = 0.1 V was achieved with very low NF_{min} of 1.05dB and associated gain of 8.6dB at 17 GHz were achieved at 0.1V V_{DS}. These results demonstrated the outstanding potential for state-of-art ultra-low power and low noise applications. [C816]

"Ku-band MMIC power amplifier with on-chip compensation gate bias circuit"

Recently, Ku-band PHEMT MMIC power amplifiers have been demonstrated for LMDS, point-to-point wireless communications systems and VSAT applications with high gain, low cost and single-supply characteristics. These MMICs operate without any compensation mechanism such as process and temperature variations. However, PHEMT MMICs are sensitive to the threshold voltage and temperature variations. The threshold voltage of the transistor determines the yield of a MMIC amplifier. And HEMT amplifiers are seriously affected by temperature variation. In this work, we propose compensation gate bias circuit for threshold voltage and temperature variations, and its application to the Ku-band MMIC power amplifier. [C817]

"High efficiency 600-mW pHEMT balance amplifier design with load pull technique"

This paper provides suitable design method to achieve high efficiency of single balanced amplifier based on load pull technique. The device technology is using pseudomorphic High Mobility Electron Transistor (pHEMT) having gate-width of 6400-μm. Power-added-efficiency (PAE) of 60-70 %, output power of 1 W and gain of 14 dB for the entire range 1-1.5 GHz is achieved at simulation level. Degradation of 30 % of PAE, 4 mW of output power and 5 dB of gain have been experienced at measurement level. [C818]

"Accurate modeling noise characteristic of microwave field-effect transistor"

In this paper, a new method based support vector regression (SVR) is introduced for modeling noise parameters

of FETs. Support vector machines (SVMs), which are based on the structural risk minimization (SRM) principle, have powerful generalization ability, and can handle problems with finite samples. By using the proposed method, the effect of the measurement errors can be excellently treated. As a result, the noise characteristics of FETs can be accurately predicted with a few measurements. The SVR based modeling method about bias and frequency dependences of noise parameters is developed. An AlGaIn/GaN HEMT is used as an example to demonstrate this method. Experimental results are given out to validate the proposed methods. [C819]

"A low noise figure high linearity balanced amplifier module for cellular band base station's tower mounted amplifier application using E-mode pHEMT technology"

This paper describes the design and realization of a low noise high linearity balanced amplifier module for cellular band tower mounted amplifier application using a proprietary 0.25 μ m enhancement mode pseudomorphic high electron mobility transistor (EpHEMT) technology. The low noise balanced amplifier module exhibits a noise figure of 0.8dB across cellular band (0.8-1GHz) with gain (S21) of 31dB on a single 5V supply and 2.8V control voltage while consuming 520mA of total current. 1 watt output power can be achieved in the balanced configuration with output third order intermodulation distortion (OIP3) of 46dBm. The two-stage balanced amplifier MMIC is designed in a chip size of 1.6 x 2.0 mm² and is housed in a miniature 5.0 x 6.0 x 1.1 mm³ 22-lead multiple-chip-on-board (MCOB) module. [C820]

"High-Efficiency GaN-HEMT Class-F Amplifier Operating at 5.7 GHz"

We report on the design, fabrication, and measurement results of a high-efficiency class-F amplifier using an AlGaIn/GaN HEMT at 5.7 GHz. Because of their higher operating voltage, GaN devices are expected to have higher operating efficiency as compared to GaAs devices. The fabricated amplifier using a low-loss resin microstrip substrate validated high efficiency expectations with a maximum drain efficiency of 77.1%, maximum power added efficiency of 68.7%, and output power of up to 34.5 dBm at 5.69 GHz. [C821]

"The frequency limits of field-effect transistors: MOSFET vs. HEMT"

An overview on the current understanding of the frequency limits (in terms of the cutoff frequency f_T) of FETs is provided. Main factors affecting f_T in MOSFETs and HEMTs are discussed and the effects of material properties and FET design on f_T are examined. In particular, the role of channel mobility, density of states, and of the design of the gate-channel barrier is discussed. We show that the MOSFET concept has some inherent advantages regarding the f_T limits compared to HEMTs. [C822]

"Pulse Profiling for AlGaIn/GaN HEMTs Large Signal Characterizations"

This paper deals with pulsed LSNA measurements of high power AlGaIn/GaN transistors performed in a multi-harmonic passive load-pull environment. Time domain waveforms are acquired during a 150 ns window. This measurement window is moved across the 20 μ s duration of pulses, the period is 1 ms. Phase and gain drifts of transistor characteristics versus time during the pulses are obtained and discussed. [C823]

"Designing, Fabrication and Characterization of Power Amplifiers Based on 10-Watt SiC MESFET & GaN HEMT at Microwave Frequencies"

This paper describes the design, fabrication and measurement of two single-stage class-AB power amplifiers covering the frequency band from 0.7-1.8 GHz using a SiC MESFET and a GaN HEMT. The measured maximum output power for the SiC amplifier at $V_d = 48$ V was 41.3 dBm (~ 13.7 W), with a PAE of 32% and a power gain above 10 dB. At a drain bias of $V_d = 66$ V at 700 MHz the P_{max} was 42.2 dBm (~ 16.6 W) with a PAE of 34.4%. The measured results for GaN amplifier are; maximum output power at $V_d = 48$ V is 40 dBm (~ 10 W), with a PAE of 34% and a power gain above 10 dB. The results for SiC amplifier are better than for GaN amplifier for the same 10-W transistor. [C824]

"Transient leakage current technique for MIS HEMT (Al₂O₃/AlGaIn/GaN) dielectric semiconductor interface property characterization"

We report the successful assessment of both dielectric semiconductor interface, and transistor channel sheet charge densities through the device leakage current characteristics of a MIS GaN HEMT structure. The unconventional test vehicle and procedure described here provide ferroelectric hetero-junction device properties not obtainable using traditional characterization tools. [C825]

"A High-Efficiency GaN HEMT Hybrid Class-E Power Amplifier for 3.5 GHz WiMAX Applications"

This paper represents a high-efficiency class-E power amplifier (PA) using a 10-W GaN HEMT for WiMAX applications of 3.5 GHz. The compensation elements to cancel parasitic components of a packaged device are used for an ideal class-E operation. The harmonic-suppression network using open-stub transmission lines is employed to obtain high output power level and high efficiency. For a 3.5 GHz continuous wave, the measured results show that a peak power-added efficiency (PAE) of 72.1% with a gain of 10.5 dB is achieved at an output power of 40.5 dBm, which delivers a drain efficiency of 79.2%. All harmonic components are suppressed below -57.1 dBc over a whole output power range. The PAE over 60% and the output power level over 40 dBm are maintained in 200 MHz bandwidth. [C826]

"High-Efficiency Class-E-Cells-Based GaN HEMT Doherty Amplifier for WCDMA Applications"

This paper represents a high-efficiency GaN high electron mobility transistor (HEMT) class-E Doherty amplifier (CEDA) for wide-band code division multiple access (WCDMA) applications. The class-E power amplifiers (PAs) with significant harmonic suppression are used as the carrier and peaking cells. To further improve the efficiency, the asymmetrical drain biases are applied to the CEDA. For validations, the class-E PA is designed and implemented with 25-W GaN HEMT at 2.14 GHz. From the measured results for a single tone, the peak power-added efficiency (PAE) and drain efficiency of 73.5% and 76.5% are achieved with a gain of 14.1 dB at an output power of 43.1 dBm by suppressing harmonic power levels below -60 dBc. For the proposed CEDA, the PAE and drain efficiency of 56.1% and 61.2% is achieved at 40 dBm (6-dB back-off power from P_{sat}) for a single tone. For a 1-carrier WCDMA signal, the PAE of 57.2% is obtained with an adjacent channel leakage ratio (ACLR) of -27.2 dBc at 40 dBm, which is 9.6% improvement over the conventional Doherty amplifier with an ACLR of -29.5 dBc. [C827]

"Enhanced device performance of AlGaIn/GaN HEMTs using thermal oxidation of electron-beam deposited aluminum for gate oxide"

We report on an AlGaIn/GaN metal-oxide-semiconductor high-electron-mobility transistor (MOS-HEMT) using thermal oxidation of electron-beam deposited aluminum as the gate dielectric. This novel dielectric deposition process is simple, and less expensive than electron cyclotron resonance (ECR) plasma oxidation of Al or atomic layer deposited (ALD) Al_2O_3 . The X-ray Photoelectron Spectroscopy (XPS) O1s spectrum showed that the Al_2O_3 with a bandgap of 7.8 eV was obtained in this specimen. The resulted MOS-HEMT exhibits several orders of magnitude lower gate leakage, larger drain saturation current and larger gate voltage swing compared to a conventional AlGaIn/GaN high-electron-mobility transistor (HEMT) of similar design. The MOS-HEMT is therefore a viable alternative to regular HEMTs for high-power, high-frequency and high-temperature applications. [C828]

"A design of Ka-band GaAs PHEMT power amplifier MMIC"

The design of a Ka-band power amplifier is presented. The three-stage amplifier exhibits an output power of 0.5 watt with small signal gain above 16 dB across the 32 GHz to 34 GHz band. The amplifier is characterized using linear and nonlinear methods. The stability, especially odd mode stability, is carefully considered. Both schematic and EM simulation results are shown. [C829]

"A 20 Watt Micro-strip X-Band AlGaIn/GaN HPA MMIC for Advanced Radar Applications"

In this paper a first iteration design, fabrication and test of a two-stage X-Band MMIC HPA in micro-strip AlGaIn/GaN technology is reported. With 20 V drain voltage operating bias point, at 3 dB compression point, the HPA delivers a pulsed output power ranging from 21 to 28.5 W, an associated gain from 12.9 to 16.5 dB and an associated PAE from circa 30% to 40%, over the 8-10.5 GHz frequency bandwidth. In the best performance frequency points (8.5 and 9 GHz) the HPA exhibits a saturated output power of 30 W with an associated PAE of 40%. [C830]

"10 Watt High Efficiency GaAs MMIC Power Amplifier for Space Applications"

This paper describes the design of a GaAs monolithic high power amplifier at Ku band. The chip delivers about 40 dBm of saturated output power, in CW operating conditions, at 11.7 GHz central frequency, with 17% of bandwidth. The saturated power gain is 12.4 dB with 2 dB gain flatness across the application bandwidth while the chip power added efficiency is estimated between 33% to 47%. The amplifier is designed to be used as final stage of a downlink satellite transmitter for Tracking Telemetry & Command system. A commercial power p-HEMT process capable of handling a power density higher than 1 W/mm has been selected for the MMIC design. Due to the space application, special attention must be put on the process and MMIC reliability: to this aim performances must be guaranteed in de-rated conditions respect to the process maximum ratings and, in addition, the channel temperature of the active devices must be kept within the value established by Space Requirements and carefully controlled. This makes the design objective very tight. The MMIC power amplifier

design and some measurement results are presented in the paper. [C831]

"Multiple-Throw Millimeter-Wave FET Switches for Frequencies from 60 up to 120 GHz"

This paper presents the design and performance of various millimeter-wave FET switches realized in a metamorphic HEMT technology. The single-pole multi-throw switch configurations are targeting wireless communication frontends and imaging radiometers at 60, 94 and 120 GHz. In SPDT switches, state-of-the-art insertion loss of 1.4 and 1.8 dB is achieved at 60 and 94 GHz, respectively. Rivalled only by PIN diode switches, an insertion loss of 1.2 dB is demonstrated up to 120 GHz. Shorted stubs are used to compensate for parasitic FET capacitance and allow for matching. Linearity data is presented for 60 and 94 GHz SPDT switches. A comprehensive comparison with state-of-the-art planar SPDT switches is included. A 2:6 switch network for multi-antenna transceivers achieves 1.4 dB insertion loss at 60 GHz. [C832]

"A Highly Linear (40.5-43.5) GHz MMIC Single Balanced pHEMT Resistive Up-Converter Mixer for LMDS Applications"

This paper presents the design and performance of a highly linear (40.5- 43.5) GHz MMIC single balanced pHEMT resistive up-converter mixer dedicated to LMDS applications. The mixer achieves good performance in terms of conversion loss which is about 6-7 dB and LO/RF isolation that is better than 30 dB under LO power equal to 14 dBm. The main feature of the mixer is its high linearity since it presents an RF output power @1 dB compression point ($P_{out@1dB}$) superior to 5 dBm in the (39.5-43.5) GHz frequency range. The measured OIP3 is equal to 20.2 dBm at 40.5 GHz and 12.2 dBm at 42 GHz. The 2 mmx1.5 mm circuit was fabricated using the D01PH (0.13 μ m GaAs depletion mode pHEMT) process provided by the OMMIC foundry. To the best of our knowledge, this is the most linear up-converter mixer reported to date in this frequency range associated with as low conversion loss. [C833]

"Power Amplifier Design for E-band Wireless System Communications"

E-band wireless communications will become important as the microwave backhaul for high-speed data transmission. One of the most critical components is the front-end power amplifier in this system. The paper analyzes different technologies with potential in the E-band frequency range and present a power amplifier design satisfying the E-band system specifications. The designed power amplifier achieves a maximum output power of 20 dBm with a state-of-the-art power-added efficiency of 15%. The power is realized using InP DHBT technology. To the best of our knowledge it is the highest output power and efficiency reported for an InP HBT power amplifier in this frequency range. The predicted power-added efficiency is higher than that of power amplifiers based on SiGe HBT and GaAs pHEMT technologies. The design shows the capabilities of InP DHBT for power amplifier applications as an alternative to HEMT based technologies in the millimeter-wave frequency range. [C834]

"Design of GaN HEMT Transistor Based Amplifiers for 5-6 GHz WiMAX Applications"

2.5 and 5 Watt average power (15 and 30 Watt peak power) GaN HEMT amplifiers for WiMAX signal protocols have been designed and fabricated for use in the 5.5 to 5.8 GHz band. The 2.5 Watt PA produces 11 dB of gain and the 5 Watt PA produces 10 dB of gain with EVMs less than 2.5% at the respective average power with drain efficiencies greater than 26% at average power. A design methodology for optimizing linear performance is described for these two transistors and resultant amplifiers. [C835]

"Alignment Verification of the PLANCK Reflector Configuration by RCS Measurements at 320 GHz"

In the Flight Model (FM) of the PLANCK telescope, the feed horns are connected to either HEMTs or bolometers operating at cryogenic temperatures to detect the Cosmic Microwave Background radiometric signal. For the purpose of an overall alignment verification at ambient temperature, RCS measurements have been performed using an auxiliary feed horn that is terminated with a switching diode. This verification test has been conducted at 320 GHz, to benefit from the narrow beam and a high sensitivity to misalignment. To perform the RCS measurements, an additional "circulator" with low propagation loss and high isolation from transmit to return channel had to be developed. Besides that, the circulator also co-locates the phase centres of both Tx and Rx range antennas on the focal point of the CATR, which allows mono-static RCS measurements. Quasi-optical techniques have been used to design a circulator that meets these requirements. To test the feasibility of determining the feed location from the RCS measurements with an uncertainty of plusmn1 mm, a test campaign was conducted with the so called RF Qualification Model (RFQM). In this campaign, 9 feed locations with 1 mm separation were tested. With the Flight Model, the test was on the critical path of the planning and only one test

could be conducted to verify the overall alignment. [C836]

"Design of a Ka-band MMIC Filtering LNA with a Metamorphic HEMT Technology for a Space Application"

This paper presents a new approach to design MMIC LNAs. The proposed method allows to filter the out-of-band LNA gain and ensures the best compromise between input and noise matching in the Ka band (27-31 GHz) example. Because of these very strong constraints a rigorous method has been planned for selecting the best transistor whatever the MMIC technology. Then, in order to relax front-end selective filter specifications, out-of-band gain is eliminated thanks to different matching filtering circuits designed with a new filters synthesis tool (GENESYN). [C837]

"Pulse Operation of an Inverse Class-F GaN Power Amplifier"

This paper presents an inverse class-F power amplifier (PA) based on gallium nitride (GaN) high electron mobility transistor (HEMT) at 1 GHz. The implemented PA has a peak power-added-efficiency (PAE) of 74.1%, drain efficiency (DE) of 77.36%, and a gain of 13.76 dB at an output power of 39.58 dBm with a continuous wave operation at 28 volts. We have carried out the experiments with various pulsed operating conditions. A RF performance peak PAE of 74.28% with drain efficiency of 77.57% and a gain of 13.73 dB, at an output power of 39.66 dBm, was obtained at a pulse width of 100 mus with a duty of 10%. To evaluate the linearity of the inverse class-F amplifier, two-tone measurements have been tested. At a tone spacing of 100 kHz, the measured third-order intermodulation distortion (IMD3) was 13.2 dBc at peak PAE. [C838]

"High Frequency Characterization and Properties of AlGaIn/GaN HEMT Structures"

The paper reports microwave properties of AlGaIn/GaN HEMT fabricated on sapphire substrate. The measured transition frequency as well as maximum frequency of oscillation was taken as a figure of merit for comparison of influence of different treatment. Using 2 mum length of gate electrode 7.425 GHz transition frequency as well as 23.437 GHz maximum frequency of oscillation was achieved. Significant influence of surface plasma treatment on HEMT microwave properties was found. [C839]

"Surface Acoustic Wave Excitation on SF6 Plasma Treated AlGaIn/GaN Heterostructure"

We present a new modified approach in the forming of interdigital transducers (IDTs) on AlGaIn/GaN heterostructure fully compatible with the process technology of HEMTs. The modified approach uses a shallow recess-gate plasma etching of AlGaIn barrier layer in combination with "in-situ" SF6surface plasma treatment under Schottky gate fingers of IDTs. It enables to excite surface acoustic wave (SAW) in the AlGaIn/GaN heterostructure without any high external bias voltages needed to apply to the IDTs. The initial results in the process technology and characterization are presented. [C840]

"Sub-0.5 dB NF broadband low-noise amplifier using a novel InGaAs/InAlAs/InP pHEMT"

Linear and non-linear modelling of a novel ultra-low noise InGaAs/InAlAs pHEMTs have been used to design a low noise amplifier operating from 0.3 to 2 GHz. The LNA has ~ 0.4 dB NF across the whole frequency band, power gain of 26 dB at 1.4 GHz and IP3 of 14 dBm, making it a good candidate for the aperture array concept of the Square Kilometre Array (SKA) telescope, GSM, GPS, civil and military DAB. [C841]

"Impact of SF6 Plasma on DC and Microwave Performance of AlGaIn/GaN HEMT Structures"

The improved dc and microwave properties of 2 mum gate length AlGaIn/GaN based HEMT structures were observed after applying of a novel approach in the forming of the Schottky gate interface. The new approach uses a shallow recess-gate plasma etching of AlGaIn barrier layer in combination with "in-situ" SF6surface plasma treatment under Schottky gate. A significant improvement in both the current gain cut-off frequency (ft) and maximum oscillation frequency (fmax) were demonstrated. The exact mechanism to explain the improved performance of the SF6plasma treated HEMTs is in progress. A great potential of the approach for sub-micrometer gate length technology of HEMTs is also emphasized. [C842]

"Reliability aspects of GaN-HEMTs on composite substrates"

This paper shows electrical characterizations and reliability analysis performed on AlGaIn/GaN HEMTs processed on epitaxial layers grown on composite substrates. The results are very promising for the fabrication of low cost high power microwave transistors for wireless communication systems. The composite substrates constitute a valuable alternative to the silicon since better thermal properties are expected. [C843]

"A 2.469 2.69GHz AlGa_N/Ga_N HEMT power amplifier for IEEE 802.16e WiMAX applications"

This paper presents a 2.469~2.69 GHz AlGa_N/Ga_N HEMT power amplifier for IEEE 802.16e WiMAX applications operating at E mode under a single supply of +6v. At the central frequency point, the power added efficiency (PAE) can achieve 96.37%, the small signal gain is 20.81dB, and the output power is 25.39dBm. The paper describes the circuit design in detail, then shows the simulation results and discusses about the simulation results. In the end, the paper concludes the design. [C844]

"Frequency performance of plasmawave devices for THZ applications and the role of fringing effects"

Paper is focused on the model in which reduction of resonant frequency of plasma oscillations in the HEMT channel experimentally observed is associated with the gate contact fringing effects. Sheet electron density distribution in the fringed ungated channel region and expression for the resonant plasma frequency are obtained. Cascaded transmission line equivalent circuit model accounting for both gated and fringed ungated channel regions has been developed and used for simulation of HEMT frequency performance with IsSpice software. [C845]

"2-D Physical Modelling of 6-doped GaAs/AlGaAs HEMT"

GaAs/AlGaAs is one the most prevalent material systems for high electron mobility transistors (HEMTs) especially at very low temperatures because of its very high mobility under these conditions. In this work, full physical modelling of a GaAs/AlGaAs HEMT with 1 μm gate length geometry is presented. The model is developed using 2-D ATLAS SILVACO[f] simulator and compared with measurements obtained from a similar HEMT fabricated at the University of Manchester using molecular beam epitaxy (MBE). Models taking into account the effect of transverse and lateral electric fields on mobility, deep-level traps, Fermi-level pinning, carrier generation/recombination and tunnelling have been included and these have led to excellent agreements between modelled and experimental values. The mobility model used has the largest effect on simulated I-V curves and inclusion of deep-level traps in the AlGaAs buffer layer improved the model considerably by raising carrier confinement in the channel. [C846]

"Surface control structures for high-performance AlGa_N/Ga_N HEMTs"

Highly stable and reliable operation is absolutely required for GaN-based high-efficiency power switching devices and high-power RF AlGa_N/Ga_N HEMTs. For the improvement of operation stability in such devices, in this paper, the surface control technologies will be addressed by introducing an ultrathin-Al-layer process, an electrochemical oxidation and a multi-mesa-channel structure with relevant technologies. [C847]

"Analysis of trap states effects on the frequency-dependent capacitance and conductance of an AlGa_N/Ga_N heterostructure"

The work presented in this paper consists of trap characterization of an Al_{0.25}Ga_{0.75}N/GaN heterostructure field effect transistors. Measurements of the gate-source capacitance and conductance of the High Electron Mobility Transistors HEMT Al_{0.25}Ga_{0.75}N/GaN were performed in order to study the frequency dependent characteristics induced by the effect of the interface states. By varying the frequency measurement and the bias applied to the gate, the density and the time-constant of the trap states have been determined. The analysis of the measured data was performed assuming models in which the traps are present at the interface of the heterojunction. A time-constant on the order of 4 μs and a density of about 10¹²cm⁻²eV⁻¹ were calculated. [C848]

"Modelling of temperature and dispersion effects in MESFET and HEMT transistors"

In this paper, an accurate technique to model temperature, bias, and frequency dispersion effects in MESFET and HEMT transistors is presented. The approach is based on a single drain to source current source Idsnonlinear model. Pulsed I/V characteristics measurements are used to model bias and frequency dispersion effects while temperature is directly implemented in the Idsequation. Model parameters extraction strategy is simple, being based just on a few measurements. The approach validity is verified by comparing the simulated and measured I/V characteristics of the device tested under continuous and pulsed excitation. Large-signal simulation results show that the model can efficiently predict the output power under different bias and temperature conditions. [C849]

"A 28-dBm pHEMT Power Amplifier Using Voltage Combiner for K-Band Applications"

A K-band power amplifier was implemented using a 0.25- μm pHEMT process. A tournament-shaped voltage combiner that combines power by combining voltage was used in the output matching network. The voltage combining method alleviates the drain voltage swing requirement of the power transistor, whose junction breakdown voltage becomes quite low especially for high frequency applications. The chip size of the designed power amplifier is only 2.52 mm². The amplifier achieved a P1dB of 28.0 dBm. The measured linear gain was 25 dB at 23.1 GHz. These demonstrate the operation of the tournament-shaped voltage combiner at K-band.

[C850]

"A 8W High efficiency X-band Power pHEMT amplifier"

A monolithic two-stage high power, high efficiency and high robustness amplifier was developed for X-band applications. The combination of the improvement of the UMS Power PHEMT technology called PPH25X in term of breakdown, and the adapted design regarding output mismatch and overdrive explain the performances of this device. The MMIC HPA, with a surface of 14.6 mm², provides 8 W output power in pulsed mode associated to a PAE of about 45% at ambient temperature and can operate at 6 dB compression in a wide frequency bandwidth (35% of frequency band). The good level of performance, the low sensitivity to the environment make this amplifier an excellent candidate for X band applications such as phased array active antennas. [C851]

"The versatility of verilog-A based models on commercial microwave simulators"

Verilog-A Hardware Description Language (VHDL) is a behavioral description language for analog systems. It is derived from the IEEE 1364 Verilog HDL specification and it is intended to let designers of analog and integrated circuits to create and use modules described mathematically in terms of its terminals and external parameters applied to the module. This paper shows the simplicity and versatility technique of modeling active microwave devices using Verilog-A language. We have made several comparisons under two different commercial simulators: Agilent ADS and GENESYS. [C852]

"Characterization of the temperature dependent access resistances in AlGaIn/GaN HEMTs"

The temperature dependence of the access resistances for AlGaIn/GaN HEMTs is investigated. The self-heating is measured using infrared microscopy and the access resistances are extracted at different ambient temperatures. Their influence on the intrinsic small signal parameters is studied versus bias and ambient temperature. [C853]

"InAlN/GaN MOSHEMT with Al₂O₃ insulating film"

In this article, we investigate the effect of a rapid thermal annealing (RTA) on electrical properties InAlN/GaN MOSHEMT with Al₂O₃ insulating film. On samples, we measured input, output and pulse characteristics. Consequently, a threshold voltage and an extrinsic transconductance was determined. A more dramatic influence of RTA was observed after annealing at 700degC. In this case, a reduction of the leakage current was about 7 orders of magnitude compared with HEMT structures without the insulating film. [C854]

"Power and thermal design criteria of AlGaIn/GaN cascode cell for wideband distributed power amplifier"

This paper deals with non-linear modeling of power GaN HEMT and design of power balanced cascode cell for wideband distributed power amplifiers. The active device is a 8times50 μm AlGaIn/GaN HEMT grown on SiC substrate. The cascode die is flip-chipped onto an AlN substrate via electrical and mechanical bumps. This GaN-based cascode cell is dedicated to act as the unit power device within a broad-band capacitively-coupled 4-18 GHz distributed amplifier. [C855]

"Impact of Ron (VDD) dependence on polar transmitter residual distortion"

In this paper, the particular impact of switching device ON resistance variation with drain supply voltage, Ron(VDD), on polar transmitter distortion is considered. Pulsed I/V measurement results over a GaN HEMT are used to predict the deviation in the Vdd-to-AM modulation profile. System-level calculations, in the presence of other nonidealities, allow the evaluation of the relative contribution of this frequency dispersion related effect.

[C856]

"InN-based dual channel high electron mobility transistor"

This paper describes the theoretical design and predicts the performances using Monte Carlo simulation of InN-based dual channel high electron mobility transistor (HEMT). A high sheet carrier concentration and strong

electron confinement at specific interfaces of the InN-based heterostructures are predicted as a consequence of piezoelectric and spontaneous polarization effects. The calculated sheet carrier concentration reaches as high as $1.64 \times 10^{14} \text{ cm}^{-2}$ for dual channel HEMT. The sheet carriers generated in InN-based double channel are found to be higher than the reported values for the conventional single channel HEMTs. The 2DEGs mobility is found to be $11.76 \times 10^4 \text{ cm}^2 \text{ V}^{-1} \text{ s}^{-1}$ at sheet carrier concentration, $n_s = 1.2 \times 10^{13} \text{ cm}^{-2}$ for 100 K. At room temperature, the drain current of the proposed InN-based dual channel HEMTs is 1.2 A/mm at gate voltage $V_G = 2 \text{ V}$. The drain current capabilities are found to be substantially superior to the conventional single channel HEMTs. [C857]

"Design of 2-stage medium power amplifier using 0.5 μm GaAs PHEMT for wireless LAN applications"

This paper presents the design and fabrication of two-stage medium power amplifier (MPA) using 0.5 μm GaAs PHEMT technology for the wireless LAN applications. The die size of this amplifier is only 1.7 mm times 0.85 mm. At a supply voltage of 5.0 V and 5.8 GHz operating frequency, a 2-stage MPA achieves a linear gain (S₂₁) of 16.39 dB, P₁ dB of 20.18 dBm, power gain of 15.15 dB and the PAE of 25.29%. [C858]

"Parasitic effects of spiral inductors on the performance of GaAs-based MMIC low noise amplifier"

This paper discusses about parasitic effect of spiral inductors on 5.8 GHz low noise amplifier (LNA) performances based on 0.5 μm GaAs pHEMT technology. Using S-parameter simulation, performance of the LNA between lump and distributed circuit are compared at 5.8 GHz. Electrical performance of the LNA performances by placing ideal components with non-ideal components shows that noise figure is increased by 2.31 dB, gain is decreased by 11.38 dB and input and output return loss is increased by 0.31 dB and 4.31 dB respectively. By using non-ideal components in the lump circuit analysis, it is shown that the spiral inductor has a noticeable impact on the LNA performance. The parasitic effects including self resonance on spiral inductors is discussed. This analysis is essential to ensure the simulation results yield realistic measured results for the fabricated LNA. Therefore the designer will have a good estimation on the performance of the LNA performance during the design stage prior to the testing stage. [C859]

"2-6 GHz GaN MMIC Power Amplifiers for Electronic Warfare Applications"

This paper presents two MMIC broadband high power amplifiers of 4 mm of periphery at the output stage in the frequency band 2-6 GHz. The amplifiers are based on Al-GaN/GaN high electron mobility transistor (HEMT) technology on SiC substrate. They have been fabricated in two different european foundries: SELEX Sistemi Integrati and QINETIQ. SELEX has a gate process technology of 0.5 μm , and devices of $10 \times 100 \text{ mm}$ periphery in microstrip technology and QINETIQ has a gate-length of 0.25 μm , and devices of $8 \times 125 \text{ mm}$ in coplanar technology. The coplanar amplifier from QINETIQ has demonstrated an output power of 8 W in continuous wave at $V_{ds} = 20 \text{ V}$ which confirm model predictions. On the other hand, SELEX microstrip amplifier has a saturation power of 10 W CW at $V_{ds} = 25 \text{ V}$ and 4 GHz. This amplifier measured on-wafer in pulsed conditions exhibits a maximum power of 17 W at $V_{ds} = 30 \text{ V}$. [C860]

"HEMT Transistor Noise modeling using generalized radial basis function"

In this paper, one important architecture of neural networks named a generalized radial basis function (GRBF) is applied in order to model HEMT transistor noise parameters dependence on bias conditions such as DC drain-to-source voltage, DC drain-to-source current, frequency and S-parameters that can accurately predict transistor noise parameters in a wide frequency ranges for all bias points from the operating range including transistor S-parameters. [C861]

"A 18-40GHz Monolithic GaAs pHEMT low noise amplifier"

This paper describes the design and measured performance of 18-40 GHz MMIC low noise amplifier developed for mm-wave point to point, SATCOM, LMDS, VSAT and EW applications. A two stage amplifier has been designed and developed on 4-mil thick InGaAs pHEMT with a mature gate length of 0.15 μm low noise process from the foundry, namely, WIN Semiconductor Corp., Taiwan. Two range couplers were incorporated at the RF input & output of the two stage amplifier. This balanced topology enhanced the electrical specifications like stability, return losses and the output power. Rigorous sensitivity checks and electromagnetic simulations were carried at the design stage to ensure proper design centering. The measured data shows better than 3.6 dB of noise figure with an associated gain of 11 plusmn 0.5 dB gain flatness. Excellent input/output return losses better than 15 dB and 1 dB compression more than 6 dBm has been achieved over the entire frequency band of 18-40 GHz. The chip features a size of 2.4 mm times 2.1 mm. [C862]

"Thermal model for AlGaIn/GaN HEMTs including self-heating effect and non-linear polarization"

A unified thermal model based on polynomial relationship of n_{sat} and E_{F} is presented for AlGaIn/GaN high electron mobility transistors (HEMTs). Self heating and polarization effects are included in the calculations of I_{d} - V_{d} characteristics. The model is based on closed form expressions and does not require elaborate computation. Our results agree with published experimental data. [C863]

"High temperature alloyed Ag based ohmic contacts to pseudomorphic high electron mobility transistor (p-HEMT)"

The quality of ohmic contacts in pseudomorphic high electron mobility transistors (p-HEMTs) formed by sequential e-beam evaporation of Ni/Ge/Au/Ag/Au was investigated as a function of alloying cycles in the range from 390degC to 460degC for duration of 30 sec. The contact resistance (R_{c}) and the specific transfer resistance (ohm-mm) values of ohmic contacts so formed were measured by Transmission line method (TLM) and compared with the contacts formed without Ag interlayer. XRD technique revealed the presence of Au-Ga phase at alloying temperatures 420degC and 440degC indicative of the formation of good quality and low R_{ohmic} contacts. The Ag based contacts showed improved specific transfer resistance values and smooth surface morphology at wider alloying temperatures compared to the contacts formed without using Ag as a barrier layer. This factor is beneficial in the fabrication of lower resistance ohmic contacts in HEMTs, where a deeper penetration of ohmic metal up to the 2DEG channel is desirable. [C864]

"Comparative subthreshold analysis for channel thickness variation on sub-100 nm Double Gate with Single-Gate HEMT"

In recent years, double gate high electron mobility transistor (DGHEMT) have been introduced to provide better immunity to short channel effects which are inescapable with downscaling of the single gate devices due to fundamental limit on gate-to-channel thickness. Furthermore, in sub 100 nm regime, for lower device aspect ratio, channel thickness also becomes an important parameter affecting the device performance due to oncoming of short channel effects. In this paper, the effect of channel thickness in sub 100 nm DGHEMT and SGHEMT devices under OFF conditions has been studied using ATLAS device simulator. The analysis provides a valuable insight into the subthreshold behavior and presents a comparative picture of the two types of devices. [C865]

"Investigation of temperature dependent microwave performance of AlGaIn/GaN MISHFETs for high power wireless applications"

The objective of this paper is to investigate and explore the potential of AlGaIn/GaN based metal insulator semiconductor heterostructure field effect transistor (MISHFET) device for high temperature applications. A temperature dependent analytical model is proposed taking into account the effect of various temperature dependent material properties. The electrical characteristics like drain current, transconductance, cut-off frequency and saturation output power are evaluated for temperature range up to 573 K and a relative comparison is done with conventional HFET structures. [C866]

"High Power Microstrip GaN-HEMT Switches for Microwave Applications"

In this paper the design, fabrication and test of X-band and 2-18 GHz wideband high power SPDT MMIC switches in microstrip GaN technology are presented. Such switches have demonstrated state-of-the-art performances. In particular the X-band switch exhibits 1 dB insertion loss, better than 37 dB isolation and a power handling capability at 9 GHz of better than 39 dBm at 1 dB insertion loss compression point; the wideband switch has an insertion loss lower than 2.2 dB, better than 25 dB isolation and a power handling capability of better than 38 dBm in the entire bandwidth. [C867]

"Increased reliability of AlGaIn/GaN HEMTs versus temperature using deuterium"

Low frequency noise (LFN) is a reliable diagnostic tool to evaluate and locate the defects of a technology. In this study, LFN is used to assess effects of deuterium (H^+ ions) in diffusion condition on the robustness of $0.25 \times 0.75 \text{ } \mu\text{m}^2$ gate area AlGaIn/GaN high electron mobility transistors (HEMT) grown on Si substrate. H^+ ions are diffused from the above AlGaIn/GaN layer through the AlGaIn/GaN interface and GaN layer, notably under the gated channel where the defects are located. Two batches of devices are stressed under high temperature condition at 400degC during 5 minutes (step 1) and 500degC during 15 minutes (step 2). The first batch is composed with 8 deuterated transistors while the second batch is composed with 8 non deuterated transistors. Static measurements and low frequency noise spectral density measurements of the drain current (SID) are examined after each step of temperature. The first step does not reveal any degradation, while the second step highlights

significant differences between the deuterated and non deuterated devices: LFN of deuterated devices remains constant, whereas LFN of non deuterated devices increases (GR superimposed with 1/f flicker noise). The deuteration of the devices can open the way to robust temperature devices, as AlGaIn/GaN HEMT are dedicated to applications at high power and high temperature. [C868]

"Metamorphic MMICs for Operation Beyond 200 GHz"

In this paper, we present the development of advanced millimeter-wave and submillimeter-wave monolithic integrated circuits for use in active and passive high-resolution imaging systems operating beyond 200 GHz. A 210 GHz subharmonically pumped dual-gate field-effect transistor (FET) mixer has been successfully realized using our 100 nm InAlAs/InGaAs based depletion-type metamorphic high electron mobility transistor (mHEMT) technology in combination with grounded coplanar circuit topology (GCPW). Furthermore, a G-band low-noise amplifier MMIC demonstrating a linear gain of more than 16 dB between 180 and 220 GHz and a state-of-the-art noise figure of 4.8 dB was fabricated using a gate length of 50 nm. Finally, a submillimeter-wave monolithic integrated circuit (S-MMIC) could be realized based on an advanced 35 nm mHEMT technology, offering a small-signal gain of more than 15 dB between 270 and 310 GHz. [C869]

"6-24 GHz Mixer Using 0.25 μ m Enhancement Mode PHEMT Technology in a Low Cost Chip Scale Package"

This paper discusses development of a 6-24 GHz mixer in a novel chip scale package. The mixer and package was fabricated together using Avago's enhancement mode (E-mode) PHEMT technology. This chip scale package is high performance, low cost and it totally eliminates all the assembly steps (such as die attach, bond wire etc) required to package a singulated die in a package. The mixer has been tested at two different stages of fabrication, first Un-Capped (like without top-lid in case of conventional package) and after final GaAs-Capped (with top-lid on). The measured conversion loss of un-capped mixer is ~9 dB upto 22 GHz @LO=+16 dBm. Conversion loss of capped wafer is marginally lower than uncapped mixer upto 22 GHz. The IIP3 of uncapped mixer is about +19 dBm and capped mixer IIP3 is about 1-2 dB lower than Capped mixer in most of the band. Rest of the performances of (Capped and Un-capped) mixers are very similar. L-R Isolation ~35 dB, L-I Isolation ~40 dB. IF test frequency is 2 GHz. To the best of author's knowledge this is the first reported chip scale packaged Mixer. [C870]

"Thermal Model Extraction of GaN HEMTs for Large-Signal Modeling"

Self-heating has a large effect on electrical performance of RF power devices. In the past, several methods were developed to estimate the average channel temperature of FETs. Some of these are based on approximate closed form expressions. These techniques give acceptable results under limited conditions and only for specific device layouts. In this proposed work, we present an accurate method for the extraction of the thermal profile of large-size AlGaIn/GaN HEMTs using both Finite Element Method (FEM) simulation and measurement techniques. The thermal investigation of the complete structure of the device permits an accurate calculation of the distributed device temperature taking into account the temperature dependence of the thermal conductivities. This analysis also helps device designers tuning physical and geometrical parameters of the structure. The thermal resistances and the thermal time constants under each finger and of the whole FET structure are calculated from static and transient FEM thermal simulations, respectively. Alternatively, the thermal time constant is also determined from drain current transient measurements. Using this procedure, we obtained detailed thermal profile for AlGaIn/GaN HEMT and implemented the resulting thermal sub-circuit in the large-signal model of GaN HEMTs. The simulated static and transient I(V) characteristics of the large-signal model are in good agreement with the measured data. [C871]

"AlGaIn/GaN HEMT with over 110 W Output Power for X-Band"

AlGaIn/GaN HEMT using field plate and recessed gate for X-band application was developed on SiC substrate. Internal matching circuits were designed to achieve high gain at 8 GHz for the developed device with single chip and four chips combining, respectively. The internally matched 5.52 mm single chip AlGaIn/GaN HEMT exhibited 36.5 W CW output power with a power added efficiency (PAE) of 40.1% and power density of 6.6 W/mm at 35 V drain bias voltage (Vds). The device with four chips combining demonstrated a CW over 100 W across the band of 7.7-8.2 GHz, and an maximum CW output power of 119.1 W with PAE of 38.2% at Vds =31.5 V. This is the highest output power for AlGaIn/GaN HEMT operated at X-band to the best of our knowledge. [C872]

"Efficient AlGaIn/GaN HEMT Power Amplifiers"

This paper describes efficient GaN/AlGaIn HEMTs and MMICs for L/S-band (1-4 GHz) and X-band frequencies (8-12 GHz) on three-inch s.i. SiC substrates. Dual-stage MMICs in microstrip transmission-line technology yield

a power-added efficiency of 61.40% at 8.56 GHz for a power level of 11 W. A single-stage MMIC yields a PAE of 55% with 6 W of output power at $V_{DS} = 20$ V. The related mobile communication power HEMT process yields an average power density of 10 W/mm at 2 GHz and $V_{DS} = 50$ V. The average PAE is 61.3% with an average linear gain 24.4 dB and low standard deviation of all parameters. The devices yield more than 25 W/mm of output power at 2 GHz when operated in cw at $V_{DS} = 100$ V with an associated PAE of 60%. The GaN HEMT process with 0.5 μm gate-length yields an extrapolated lifetime of 105h when operated at $V_{DS} = 50$ V at a channel temperature of 90°C. When operated at 2 GHz devices with 480 μm gate-width yield a change of the RF power-gain of less than 0.2 dB under high gain-compression at $V_{DS} = 50$ V and a channel temperature of 250°C. [C873]

"Balanced Microstrip AlGaIn/GaN HEMT Power Amplifier MMIC for X-Band Applications"

This paper describes a balanced AlGaIn/GaN HEMT single-stage power amplifier demonstrator for X-band frequencies in microstrip line technology on thinned s.i. SiC substrates. The design features a modular circuit concept and microstrip MMIC directional couplers with low impedance levels. These 3 dB-couplers designed for a center frequency of 10 GHz show a coupling factor of 3.5 dB plusmn 0.4 dB and a low net insertion loss of 0.3 dB. The balanced amplifier reaches 11 W pulsed output power at 3 dB compression level and a maximum gain of 10 dB at 8.56 GHz with an input and output match of better than 14 dB from 8.3 to 13 GHz. This 0deg/90deg balanced microstrip AlGaIn/GaN HEMT power amplifier MMIC demonstrator may be an interesting alternative to existing hybrid solutions. [C874]

"Decrease in Slow Current Transients and Current Collapse in GaN-based FETs with a Field Plate"

Two-dimensional transient analyses of AlGaIn/GaN HEMTs and GaN MESFETs are performed in which a deep donor and a deep acceptor are considered in a semi-insulating buffer layer. Quasi-pulsed I-V curves are derived from the transient characteristics. It is studied how the existence of field plate affects buffer-related lag phenomena and current collapse. It is shown that in both FETs, the lag phenomena and current collapse could be reduced by introducing a field plate, because electron injection into the buffer layer is weakened by it, and trapping effects are reduced. The dependence on insulator-thickness under the field plate is also studied, suggesting that there is an optimum thickness of insulator to minimize the current collapse and drain lag. [C875]

"Advanced Modeling of MISHFET Devices and their Performance in Current-Mode Class-D Power Amplifiers"

GaN HFETs and MISHFETs are promising power devices for RF and microwave power applications. However, the performance of devices can be compromised under some operating conditions. From the device development point of view, device optimization is necessary to obtain the best possible performance. For device modeling and design purposes, the device needs to be characterized and modeled accurately in order to foresee how the device will behave under realistic operating conditions. In this paper, an improved EEHEMT1-based model for GaN MISHFETs, will be introduced. This model is capable of describing the knee region of the device's output characteristics, dispersion effects as well as gate diode behavior accurately. The models will be incorporated in a switched-mode amplifier topology and evaluations will be made to determine the suitability of MISHFETs in these amplifiers. [C876]

"Structural and electrical characteristics of lanthanum oxide gate dielectric film on GaAs pHEMT technology"

In this study, a high dielectric constant lanthanum oxide thin film (La_2O_3) was fabricated as a gate dielectric on GaAs pHEMTs to reduce the effect of the gate leakage caused by continuing the constant field-scaling trend of MOS technology. The chemical compositions and the crystalline structure at different annealing temperatures were observed by X-ray photoelectron spectroscopy (XPS) and x-ray diffraction (XRD) respectively, and the results reveal its significant thermal stability. By fabricating the capacitor, the dielectric constant of La_2O_3 with annealing at 400°C was calculated to be 21.6 which is higher than the sample without annealing. In addition, transistors with two different gate materials were successfully fabricated, Pt/ La_2O_3 /Ti/Au gate and the conventional Pt/Ti/Au gate. The DC results shown the oxide-device performed higher turn-on and breakdown voltage, exhibited better RF characteristic, and the gate leakage current was at least one order lower than the conventional device. Therefore, La_2O_3 is a potential candidate high-k material as the gate dielectric which can enhance the performance while scaling down the device dimension and overcome the thermal effect applied for high power applications. [C877]

"A low insertion loss GaAs pHEMT switch utilizing highly n+ -doping AlAs etching stop layer"

design"

This study reports, for the first time, AlGaAs/InGaAs/AlGaAs high-electron mobility transistors (HEMTs) devices and single-pole-single-throw (SPST) switches with utilizing n+-type doping on etching stop AlAs layer (M-HEMTs) designs were fabricated and investigated. We doping on etching stop AlAs layer to reduce parasitic resistances and enhance device DC and RF power performance. These modified M-HEMTs(HEMTs) demonstrated an Sheet resistance (R_{sh}) is 65.9 Ohms/sq(71.9 Ohms/sq), maximum I_{dsis} 317.8 mA/mm(290.3 mA/mm), transconductance(g_m) is 259.3 mS/mm(252.1 mS/mm), cut-off frequency(f_T) and maximum frequency(f_{max}) are 19.4 GHz(18.1 GHz) and 58.6 GHz(45.9 GHz), a power-added efficiency of 33.4 %(30.6 %), and a linear power gain of 13.1 dB(10.3 dB) for an 1.0 μ m gate-long device under a 2.4 GHz operation. In addition, both off-state capacitance and the specific on-resistance (R_{on}) of HEMT are dominated factors which are sensitive to doping n+-type on etching stop layer for RF switch applications. The SPST switches on-state an insertion loss of 1.42 dB(1.68 dB), the off-state an isolation of 13.02 dB(11.42 dB). These characteristics suggest that utilizing n+-type doping on etching stop AlAs layer provide a better device and switches performances improvement. [C878]

"Analytical approach for high temperature analysis of AlGaIn/GaN HEMT"

An analytical thermal model of AlGaIn/GaN high electron mobility transistor (HEMTs) has been developed. This temperature dependent model incorporates the polarization effects at heterointerface. The model also accounts for the mobility degradation with increase in temperature, which is one of the major causes in deteriorating the driving current. By using the variation of band gap with temperature, the temperature dependence on threshold voltage, sheet carrier concentration and drain current is studied. Further, the temperature variation shows the applicability of the device in a variable thermal environment. The results show excellent agreement when compared with experimental data thereby proving the validity of the model. [C879]

"Temperature dependence of AlGaIn/GaN HEMT-compatible lateral field effect rectifier"

The lateral field effect rectifier (L-FER) on AlGaIn/GaN heterostructure on silicon substrate compatible with the HEMT process has been characterized for high temperature operation (up to 250 degC). The proposed rectifier takes advantage of adjusting the forward-on voltage to a slightly positive value by fluorine plasma treatment. The temperature dependences of the forward-on voltage and the on-resistance of the rectifiers with different drift lengths were measured. The knee voltage of the rectifier exhibits very little temperature dependence as the temperature raised to 250 degC. These results indicate that L-FER is promising for operation over a wide range of ambient temperatures. [C880]

"High sensitivity pH sensor using Al_{0.3}Ga_{0.7}N/GaN HEMT heterostructure design"

Gateless AlGaIn/GaN high electron mobility transistors (HEMTs) has some advantages include rapid response, low noise, and superior sensitivity. In different Al content, the Al_{0.3}Ga_{0.7}N has the excellent performance among Al_{0.17}Ga_{0.83}N and Al_{0.25}Ga_{0.75}N, and the performance can be achieved about -0.923 mA/mm-pH during pH 4-10, and -2.24 mA/mm-pH during pH 7-8. The result indicates that the better performance of Al_{0.3}Ga_{0.7}N can be applied in high sensitivity pH sensor. Using the characteristic and modifying by different gate oxide, there are many application in the technology of medical for detecting the disease. [C881]

"24 GHz LTCC Amplifier Using Packaged HEMTs"

The design of an LTCC self-packaged amplifier for the 24 GHz ISM band using packaged transistors is described. The amplifier utilizes to a full extent the benefits of the multilayer environment as all matching networks are realized by employing multilayer impedance transformers. Advantages of using such transformers are the elimination of dedicated DC blocks, flexible layout routing and a milder discontinuity in the vertical transitions towards the PCB connection. A combination of on-tile and off-tile distributed matching has been implemented allowing for the amplifier to be used on various PCB substrate materials. The amplifier can be used in both the receiver and transmitter chains, in various application scenarios. Examples of the measured amplifier characteristics designed on two different substrate materials are shown, illustrating the trade-off between the cost and the performance of the materials used. [C882]

"120-GHz-band Low-noise Amplifier with 14-ps Group-delay Variation for 10-Gbit/s Data Transmission"

This paper presents a 120-GHz-band low-noise amplifier (LNA) for a receiver microwave monolithic integrated circuit (MMIC), which is used for a 10-Gbit/s wireless link. The LNA was designed for low-noise performance, a high gain, and low group-delay variation. To achieve enough stability with low-noise performance and low group-

delay variation, we introduce a new stabilizing circuit consisting of two coplanar-waveguide stubs. The LNA MMIC was fabricated using 0.1- μm -gate InP high-electron-mobility transistors (HEMTs). We integrated the LNA into a WR-8 (90-140 GHz) waveguide module and evaluated it. The LNA module achieved an averaged noise figure of 5.6 dB, a gain of > 19.5 dB, and group-delay variation of < 14 ps from 117.5 to 132.5 GHz.

[C883]

"10 Watt high efficiency GaAs MMIC power amplifier for space applications"

This paper describes the design of a GaAs monolithic high power amplifier at Ku band. The chip delivers about 40 dBm of saturated output power, in CW operating conditions, at 11.7 GHz central frequency, with 17% of bandwidth. The saturated power gain is 12.4 dB with 2 dB gain flatness across the application bandwidth while the chip power added efficiency is estimated between 33% to 47%. The amplifier is designed to be used as final stage of a downlink satellite transmitter for Tracking Telemetry & Command system. A commercial power p-HEMT process capable of handling a power density higher than 1 W/mm has been selected for the MMIC design. Due to the space application, special attention must be put on the process and MMIC reliability: to this aim performances must be guaranteed in de-rated conditions respect to the process maximum ratings and, in addition, the channel temperature of the active devices must be kept within the value established by Space Requirements and carefully controlled. This makes the design objective very tight. The MMIC power amplifier design and some measurement results are presented in the paper. [C884]

"A Four-Antenna Transceiver MIMIC for 60 GHz Wireless Multimedia Applications"

A transceiver MIMIC (millimeter wave monolithic integrated circuit) with four antenna ports functionality for 55 to 65 GHz wireless multimedia applications has been developed. The chip has been realized using 100 nm gatelength metamorphic InAlAs / InGaAs HEMT (high electron mobility transistor) technology on GaAs substrate together with GCPW (grounded coplanar waveguide) technology. The novel transceiver topology for the MIMIC is described. The different building blocks, namely the 2:4-switch design, sub-harmonic IQ-resistive mixer and variable gain amplifiers, are explained in details. Simulated and measured results are compared. Finally, the overall performance for the integrated transceiver chip is presented. [C885]

"RF performance investigation of DMG AlGaIn/GaN high electron mobility transistor"

In this paper, the RF performance of dual material gate (DMG) AlGaIn/GaN HEMT is investigated using ATLAS device simulator and presented as a high performance RF solution to microwave applications. Simulations result reveal improved RF characteristics of DMG AlGaIn/GaN HEMT in comparison to Single Material Gate (SMG) AlGaIn/GaN HEMT in terms of higher cut-off frequency, current gain and reduced parasitic capacitances strengthening the idea of using it for HF wireless and RF applications. [C886]

"A novel on-chip protection circuit for RFICs implemented in D-mode pHEMT technology"

This paper presents development of novel circuitry that protects circuits developed in pHEMT technology with minimal impact on RF performance. Reduced on-state resistance, low parasitic capacitance, variable trigger voltage, and small physical size allow the protection circuit to be an attractive solution for ESD protection. Implementation of the circuit in a wideband low noise amplifier (LNA) is presented. [C887]

"Reliability Evaluation of 0.1 μm AISb/InAs HEMT Low Noise Amplifiers for Ultralow-Power Applications"

Three-temperature lifetesting was performed to evaluate the reliability performance of 0.1 μm AISb/InAs HEMT low noise amplifiers (LNAs) for ultralow-power applications. For the first time, the reliability performance of 0.1 μm AISb/InAs HEMT LNAs was demonstrated. The results show a median time to failure of approximately 2×10^6 hours at T_{junction} of 85°C with activation energy of 1.5 eV. High-reliability performance is essential for successful insertion of 0.1 μm AISb/InAs HEMT LNAs for military and space applications with ultralow-power requirements. [C888]

"Reliability Study of 0.15 μm MHEMT with V_{ds} 3V Bias for Amplifier Application"

MHEMT technology using metamorphic buffer layers growing on GaAs substrate can overcome InP substrate issues. Several researchers have demonstrated reliable MHEMT devices, mainly with the drain bias at 1 V. This work, however, demonstrated for the first time MHEMT devices operated at drain voltage greater than 3 V for the amplifier application. We have demonstrated the power MHEMT at 3.5V drain bias with E_a of 1.53eV and MTTF of 2.32×10^6 hours at T_{eh} of 125degC on WIN Semiconductors'1 technology. We also found that stressed voltage bias plays a more important role than the current density in short-term reliability evaluation. [C889]

"A Fully On-Chip, Single-Ended S-Band Image Reject Mixer for High Dynamic Range Applications"

An S-band image reject downconversion mixer with high intercept point and fully integrated single-ended ports, including a UHF output, is demonstrated using GaAs pHEMT technology. The image rejection is better than 20 dB across a wide IF bandwidth ranging from 400 MHz to beyond 1 GHz with a high input IP3 of 20 dBm. On-chip passive baluns are used to provide the single-ended to differential conversion in the RF and IF paths necessary for the resistive FET mixer core. A polyphase filter is used to generate the quadrature local oscillator (LO) components, while an integrated UHF lumped element quadrature hybrid combines the intermediate frequency (IF) components to achieve image rejection fully on-chip without the need for external components.

[C890]

"A Support Vector Machine Method for Electrothermal Modeling of Power FETs"

An accurate electrothermal modeling method for power FETs is presented. The thermal models are setup by using Support Vector Machine Regression (SVR) approach, which is like artificial neural network (ANN) method leading a knowledge-based model. Unlike traditional ANNs, Support Vector Machine (SVM) method requires fewer samples in statistical learning and is free of local minima in optimization. A comparison among the SVM model, the empirical model and the measurement data of a GaAs power pHEMT are given out to validate the proposed approach. [C891]

"Plasma effects in HEMT-like structures: Equivalent circuit model and simulation"

An electric equivalent circuit is developed to study the manifestation of the plasma oscillations excited in the two-dimensional electron (2DE) channel of high-electron mobility transistor (HEMT)-like structure implementing IsSpice simulation. The components of the equivalent circuit model are related to physical and geometrical parameters of the structure. The distinctive feature of the developed model is the distributed circuit representation of the gated portion of the 2DEG channel with gate voltage dependent resistance and inductance. The simulated HEMT frequency performance reveals resonant behavior. The effect of "load" impedance mismatch is also discussed. The reported equivalent circuit approach invoking IsSpice simulation can be used for the evaluation and optimization of the performance of HEMT-like structures which operation is based on plasma wave excitation. [C892]

"Linearity and Efficiency Optimisation in Microwave Power Amplifier Design"

In this contribution the minimisation of asymmetry between lower and upper side band intermodulation products will be discussed, starting from a Volterra analysis approach. Base-band and harmonic device terminations effects will be analysed, identifying novel conditions minimising IMD asymmetry and IM3 power levels. Such conditions, not relying on base-band terminations, are the basis for IM3 products minimisation via second harmonic load selection. The proposed criterion is then verified by harmonic load-pull measurements on a GaN HEMT under two-tone excitation. Measurements agree with the analysis, demonstrating a null IMD asymmetry and 6 dBc increase in C/I3, without affecting output power (34 dBm @ 1 dB compression) and power added efficiency performance (65% @ 1 dB compression). [C893]

"0.5 W High Linearity Power Amplifier for Broadband Wireless (3.3 ~ 3.9 GHz)"

This paper presents a 0.5 Watt amplifier that operates over the 3.3 ~ 3.9 GHz range. The target applications are pre-driver in base-stations and power amplifier in subscriber units. The design marries good Third Order Output Intercept Point (OIP3) and exceptional Power Added Efficiency (PAE) at 1 dB gain compression point (P1dB). The performances are: -G = 11.8 dB, IRL & ORL < -8 dB, P1dB = 28.5 dBm and OIP3 = 42.6 dBm. The superior performance is achieved through the use of Avago Technologies' proprietary 0.25 μm GaAs Enhancement mode pHEMT process. The device requires simple matching components to achieve wide bandwidth because of the built-in input pre-match. From the reliability standpoint, pHEMT devices are eminently suited to PA use -the drain to source resistance (RDSon) will inherently rise to counteract the thermal runaway that blights bipolar and HBT PAs. The internal bias circuit is temperature compensated and can be adjusted for either class A or class AB operation. The device is housed inside a standard 16 pin LPCC 3X3 package. [C894]

"ESD robustness of AlGaIn/GaN HEMT devices"

We have investigated the robustness of GaN-HEMT devices submitted to ESD events in different configurations. A good scaling of the failure current with the device width has been observed for both drain and gate TLP stresses. We have identified two failure mechanisms, related to the gate-source diode degradation and drain to gate filaments formation. Filaments formation was identified by means of emission microscopy, both while

applying DC bias and during the TLP measurement itself. We have also found that the traditional TLP leakage measurement can not be used as a valid failure criterion. On the contrary, the gate-source diode measurement can provide interesting information on the device life-state. [C895]

"Low level and high linearity amplifiers in integrated technologies for satellite receivers: Technical issues of linearization techniques"

Based on carrier to third intermodulation ratio (C/I3), reverse engineering of a two stages low level amplifier has been made in order to access the current transistor nonlinear models. Comparisons between two models of HEMT have been performed in order to choose the one which represent accurately weak nonlinearities at low level power dynamic range. By judicious choice of bias point, 12 dB improvement of linearity has been achieved. Other issues of linearization techniques have been studied so that to be suitable for MMIC implementation. [C896]

"Demonstration of a 3-D GaAs HEMT Phase Shifter MMIC Utilizing a Five Layer BCB Process with Seven Metal Layers"

In this paper, we demonstrate a vertically integrated 3-D MMIC phase shifter at 8 GHz that utilizes a 5-layer benzocyclobutene (BCB) process providing a total of 7 metal layers. This multi-layer technology is fully compatible with Northrop Grumman's 0.15 μm GaAs HEMT technology and enables a high level of MMIC compaction which will substantially reduce the size and cost of MMICs. A key feature of this technology is the ability to isolate vertically integrated components of a MMIC' with separate ground planes allowing circuit compaction while maintaining high isolation. [C897]

"Detection of Photosystem I Reaction Centers using Chemically Derivatized High Electron Mobility Transistor"

This paper presents for the first time a micro-sensor for detecting Photosystem I (PS I) reaction centers. In oxygenic plants, photons are captured with high quantum efficiency by two specialized reaction centers, Photosystems I and II (PS I and PS II). Photon capture triggers rapid charge separation and the conversion of light energy into an electric voltage across the nanometer-scale (~ 6 nm) reaction centers. AlGaIn/GaN based high electron mobility transistors (HEMTs) show high current throughputs and greater sensitivity to surface charges. PS I molecules were chemically immobilized on the HEMT device and significant changes in the transistor characteristics were noticed. With zero gate bias and 5 V at drain terminal, drain current changes by about 5 mA for 6 μL drop of PS I solution. The difference between light and dark measurements is ~ 0.8 mA. Test results demonstrate that this approach is a potential candidate for detection and characterization of biomolecular photodiodes -PS I reaction centers. [C898]

"Ultra-Wideband Ultra-Low-DC-Power High Gain Differential-Input Low Noise Amplifier MMIC Using InAs/AlSb HEMT"

This paper reports an ultra-wideband ultra-low-DC power high gain MMIC low noise amplifier (LNA) with differential RF input using 0.1- μm gate length InAs/AlSb metamorphic HEMTs, fabricated and characterized on a GaAs substrate. For testing purpose and for generating a differential RF input, a 3-12 GHz wideband on-chip MMIC balun is connected to the differential input. Even with the loss of the balun included, the differential amplifier demonstrated 4 dB typical noise figure with associated gain of 22 dB from 3-12 GHz at a low DC dissipation of 23 mW. Additionally, a single-ended LNA, which the differential LNA is based on, is also fabricated for evaluation. The single-ended LNA demonstrated 1.5 dB typical noise figure with associated gain of 25 dB from 1-16 GHz at a low DC dissipation of 16 mW [C899]

"Tunable plasma wave resonant detection of optical beating in high electron mobility transistor"

This paper presents the recent, experimental studies on the plasma resonant detection in high electron mobility transistors (HEMTs). Experiments were performed using an AlGaAs/InGaAs/InP HEMT with gate-length $L_g = 800$ nm. The whole HEMT structure is transparent to the incident radiation excepted the InGaAs-channel where the interband photoexcitation occurs. By using a tunable optical beating this photoexcitation is modulated over a large frequency range. Their mixing produces a tunable optical beating from 0 up to 600 GHz. The photoconductivity response, due to the difference frequency generation, is obtained by monitoring the modulation of the dc drain-to-source potential. [C900]

"Metamorphic HEMT Amplifier Circuits for Use in a High Resolution 210 GHz Radar"

In this paper, we present the development of a W-band power amplifier (PA) circuit and a G-band low-noise amplifier (LNA) MMIC for use in a high-resolution radar system operating at 210 GHz. The power amplifier circuit has been realized using a 0.1 μm InAlAs/InGaAs based depletion-type metamorphic high electron mobility transistor (MHEMT) technology in combination with grounded coplanar circuit topology and cascode transistors, thus leading to a small-signal gain of 12 dB and a saturated output power of 20.5 dBm at 105 GHz. The low-noise amplifier MMIC was fabricated using an advanced 0.05 μm MHEMT technology and achieved a small-signal gain of more than 16 dB over the frequency band from 180 to 220 GHz together with a state-of-the-art room temperature noise figure of only 4.8 dB. Both amplifier circuits were successfully packaged into millimeter-wave waveguide modules and used to realize a 210 GHz radar, which delivers an instantaneous bandwidth of 8 GHz and an outstanding spatial resolution of 1.8 cm. [C901]

"2007 ROCS Workshop"

The following topics are dealt with: accelerated lifetest techniques; reliability studies of advanced HEMTs; reliability and failure analysis tools. [C902]

"A Classic Nonlinear FET Model for GaN HEMT Devices"

This paper shows the effective modeling of GaN HEMT devices using Agilent EEHEMT, a commercially available model in Agilent ADS, Microwave Office, etc. Using a series of pulsed IV, DC, S-parameter and Load-pull measurements, a nonlinear large-signal model is extracted to fit the circuit behavior of the device in a real application. Detailed steps are shown in extracting extrinsic and intrinsic parameters in addition to peculiarities of GaN HEMTs in challenging the conventional FET modeling practices. Simulation capabilities of the model are demonstrated through prediction of experimental output power, PAE and input reflection characteristics of a practical amplifier. [C903]

"Investigation of AlGaIn/GaN metal-oxide-semiconductor high electron mobility transistors using Photoelectrochemical Oxidation Method"

A photoelectrochemical (PEC) oxidation method was used to directly grow oxide films on AlGaIn surface as gate insulator for AlGaIn/GaN metal-oxide-semiconductor high electron mobility transistors (MOS-HEMTs). The threshold voltage of MOS-HEMT devices is -5 V. The gate leakage current is 50 pA and 20 pA at forward gate bias of $V_{gs}=10$ V and reverse gate bias of $V_{gs}=-10$ V, respectively. Maximum value of g_{mis} 50 ms/mm of V_{gs} biased at -2.09 V. [C904]

"Broadband GaN Dual-Gate HEMT Low Noise Amplifier"

This paper presents a broadband low noise amplifier MMIC utilizing 0.2 μm AlGaIn/GaN HEMT technology. The single-stage, resistive feedback amplifier is designed in co-planar waveguide (CPW) topology. It uses dual-gate devices with on-chip drain bias network to achieve 18 dB flat gain between 300 MHz -4 GHz. Measured noise figure is around 1.5 dB between 2 and 5 GHz, and better than 2 dB between 1 and 2 GHz. The amplifier is capable of 25 dBm saturated output power with 1 dB compression point around 20 dBm across the band. Due to high breakdown voltage of GaN devices, the LNA can withstand high input power and shows no sign of degradation. [C905]

"Wafer-level Accelerated Lifetesting of Individual Devices"

The thermal activation energies of TriQuint Semiconductor's TQPED devices are evaluated with an innovative wafer-level technique for accelerated life testing. The method was used to determine the activation energy for both the depletion-mode and enhancement-mode pHEMT devices. An on-wafer heating element around individual devices allowed stressing at various temperatures on the same wafer. Temperatures above 275degC were easily achieved without the need to self-heat the transistors. The technique allows for the separation of thermally activated mechanisms from any influence of bias. The wafer-level aspect of stressing provides a spatial map of reliability for a wafer. A single wafer provides adequate samples to evaluate lifetime distributions. Without the need for hundreds of devices and long-term life testing at lower temperatures, this method allows for a rapid and efficient evaluation of device reliability. By doing lifetime aging studies on wafer, packaging considerations are eliminated. The wafer form factor makes it easier to observe physical device degradation and subsequently perform root cause analysis of the failure mechanism. [C906]

"0.1 μm n+-InAs-AISb-InAs HEMT MMIC Technology for Phased-Array Applications"

-A 0.1 μm n+-InAs-AISb-InAs MMIC technology was developed for phased-array applications requiring ultralow power consumption. An n doped cap layer was utilized to provide lower access resistance and to reduce

detrimental effects of cap layer etching during the process. As a result, the performance and manufacturability can be enhanced. In this work, we have demonstrated excellent DC and RF uniformity on both devices and low-noise amplifiers (LNA) using 0.1 μm n+-InAs-AlSb-InAs HEMTs on 3-inch GaAs substrates. In addition, the LNAs also demonstrate excellent RF performance while operating at ultralow power (~ 1 mW). This accomplishment is crucial for phased-array applications requiring ultralow power dissipation. [C907]

"High-efficiency GaN class-E power amplifier with ecompact harmonic-suppression network"

This paper presents a high efficiency class-E power amplifier (PA) suitable for wireless transmitters operating at 2 GHz. Compact impedance transformation network is designed, using micro-strip transmission lines, so that it simultaneously achieves fundamental load transformation and harmonic impedance control using only two open-circuit stubs ($2f_0$, $3f_0$). The dimensions of the network's elements were determined in order to concurrently attain a high harmonic suppression, minimum loss and high power added efficiency. The measurement results of the PA prototype, which is designed using a 10 W gallium nitride (GaN) HEMT transistor, showed state-of-the-art drain and power added efficiency (PAE). The achieved PAE, power gain and output power, when the drain is biased at 50 V, were equal to 74%, 12.6 dB and 11.4 W respectively. In addition, a second and third harmonic suppression in excess of -40 dBc and -75 dBc, respectively, is achieved without extra circuit tuning or additional filtering. [C908]

"Characterization of insulated-gate versus schottky-gate InAs/AlSb HEMTs"

Fabrication and characterization of 225 nm gate-length InAs/AlSb HEMTs with excellent RF performance are reported. We show the importance of an insulating layer between the gate and the semiconductor to improve g_m , f_T and f_{max} , and most important from a noise perspective, the gate-leakage current I_G . By using an insulated-gate, I_G was reduced by two orders of magnitude. The insulated-gate HEMTs exhibited extrinsic f_T and f_{max} of 155 GHz and 115 GHz, respectively, at $V_{DS}=0.5$ V. [C909]

"Large-Signal modeling of power GaN HEMTs including thermal effects"

In this paper a procedure to extract temperature dependent equivalent circuits for modeling the small and large signal behavior of GaN HEMTs is presented. The technique explained in this work uses pulsed I-V measurements to obtain the temperature dependence of the parameters describing the nonlinear drain current source behavior. The equivalent circuits extracted are capable of correctly modeling the DC, small signal and large signal characteristics of GaN HEMTs devices. Simulations and measurements carried out on three transistors developed by SELEX-SI are compared over a wide range of frequencies, bias and load conditions. [C910]

"Investigation of IMD3 in GaN HEMT based on extended volterra series analysis"

This paper mainly focuses on providing theoretical justification for possible GaN device linearity improvement, interpreting key physical origins of IMD3. Based on bias dependent S-parameter measurement data of field-plate-free 8×125 μm GaN HEMT, IMD3 is modelled using classical Volterra series theory. Device diagnosis is hence carried out, by means of this technique, for efficiently localizing the distortion behaviour. Further, device linearity is shown to improve by appropriately tuning gate-drain feedback capacitance by taking advantage of field-plate technology proving the analysis to be a powerful tool for developing GaN HEMT technology. Further, with the intension of understanding IMD nulling, Volterra analysis is extended to 5th-degree nonlinearity through which an insight into the distortion cancellation mechanism is obtained. [C911]

"Optically controllable millimeter-wave oscillator using InP-based HEMTs"

Optical response in InP-based HEMT by focusing a laser beam onto a surface was studied in detail. The changes in Drain current, gain, and capacitance were observed clearly. We propose an optically controllable millimeter-wave oscillator. [C912]

"Driver amplifier for 60 GHz communication systems"

A driver amplifier for the ISM band around 60 GHz has been designed and tested. The amplifier has been designed in conjunction with other transceiver sub-systems in the 0.15 μm GaAs pHEMT process of UMS (PH15). The measurements show behaviour very well matched with the extensive circuit and field simulations. The amplifier is approx. 3 times 1.8 mm, consumes 910 mW, has a gain of 22 dB, a P-1dBat the output of +14 dBm, and is well matched in the band 60-65 GHz. [C913]

"Benchmarking of low band gap III-V based-HEMTs and sub-100nm CMOS under low drain voltage regime"

this works reports on speed and high performance benchmarking of low band gap III-V based-HEMTs versus advanced n-MOSFET in low drain voltage regime (few kT/q). In this low bias condition, figure of merits such as, fT_{are} higher and intrinsic gate delay and energy are almost one order of magnitude lower in the case of III-V based-devices (two orders of magnitude for the delay-energy product). [C914]

"Scalable equivalent circuit PHEMT modelling using an EM-based parasitic network description"

Electron device modelling requires the accurate identification of a suitable parasitic network accounting for the passive structures which connect the intrinsic electron device to the external world. In conventional approaches, the parasitic network is described by a proper topology of lumped elements. As an alternative, a distributed description of the parasitic network can be conveniently adopted. In particular, the latter solution is the better choice when dealing with device scaling and very high operating frequencies. In this paper the parasitic network is described by means of a suitable distributed network identified through electromagnetic simulations of the device layout. It is shown how the adoption of a distributed instead of a lumped description leads to a more accurate equivalent-circuit-based electron device model. The good scalability properties of the approach are also presented through experimental results. [C915]

"AlGaIn/GaN HEMTs on epitaxies grown on composite substrate"

In this paper, are presented the first results obtained from AlGaIn/GaN HEMTs devices processed on both MBE and MOCVD epitaxial structures grown on "composite" substrates. These substrates are based on innovative structures in which a thin Si or SiC single crystal layer is transferred on top of a thick polycrystalline SiC wafer with a thin SiO₂ intermediary insulating layer. The fabrication of the transistors is based on the process flow developed by "TIGER" for HEMT epitaxy on SiC bulk substrates. The obtained results show the capabilities of such composite devices, providing HEMT device electrical and small signal microwave performance similar to those obtained currently on bulk single crystal SiC substrates. The composite substrate approach appears as very promising for applications requiring low cost microwave power devices, such as mobile communications. [C916]

"Simultaneous dual-band high efficiency harmonic tuned power amplifier in GaN technology"

In this contribution for the first time the design of a simultaneous dual band high efficiency harmonic tuned power amplifier is presented. The active device used is a GaN HEMT with 1 mm of gate periphery. The realised amplifier operates at 2.45 GHz and 3.3 GHz, and the measured results shown a drain efficiency of 53% and 46%, with an output power of 33 dBm and 32.5 dBm at the two hard widths. A zero transmission condition has been obtained, resulting in a measured value of S₂₁ lower than -15 dB at 2.8 GHz. [C917]

"Design of GaN-based balanced cascode cells for wide-band distributed power amplifier"

This paper reports on the design of a cascode GaN HEMT cell dedicated to 4-18 GHz flip-chip distributed power amplifier. The active device is a 8x50 μm AlGaIn/GaN HEMT grown on SiC substrate. The GaN-based die which integrates the active cascode cell and its matching elements is flip-chipped via electrical bumps onto an AlN substrate. The matching elements of the balanced cascode cell are composed of series capacitances on the gate of both transistors with additional resistances to insure stability and bias path. The series capacitor on the gate of the 1st transistor is added for the distributed amplifier optimisation while the series capacitor on the gate of the 2nd transistor is dedicated [C918]

"Characterization and modeling of substrate trapping in HEMTs"

We present a novel and simple model of FET trapping based on a study of HEMTs using pulse techniques. This model accounts for the observed variation of extent of gate lag with bias and step potentials, and the variation of gate-lag time constant with drain potential. Because both charge capture and emission are accounted for, the model is appropriate for the simulation of both large-signal and small-signal dynamics. The model is verified by comparison with large-signal transient measurements and is consistent with small-signal gain measurements. [C919]

"Low-frequency dynamic drain current modeling in AlGaIn-GaN HEMTs"

Low-frequency dispersive effects in AlGaIn/GaN HEMTs are here modeled above their cutoff frequencies by adopting a modeling approach developed for GaAs PHEMTs. To this aim, a new identification procedure is

proposed, which allows to obtain very accurate predictions of the pulsed drain currents, even in the presence of strong kink effects in the DC characteristics. In addition, a dedicated algorithm of data extrapolation is used, in order to make the model more computationally efficient. [C920]

"AlGaIn/GaN HEMTs on (001) oriented silicon substrate based on 100nm SiN recessed gate technology for low cost device fabrication"

This paper shows the capability of AlGaIn/GaN high electron mobility transistors (HEMTs) with 0.1 μm gamma shaped gate length on (001) oriented silicon substrate for microwave power applications. The gate technology is based on silicon nitride thin film and uses a digital etching to perform the recess through the SiN mask. Output current densities of 420 mA/mm, extrinsic cut-off frequencies (f_T) of 28 GHz and maximum oscillations frequencies (f_{max}) of 46 GHz are measured on 300 μm gate periphery device. At 2.15 GHz, an output power density of 1 W/mm associated to a power added efficiency of 17% and a linear gain of 24 dB are achieved at $V_{\text{DS}} = 30\text{ V}$ and $V_{\text{GS}} = -1.2\text{ V}$. [C921]

"Compact front-end filter banks for wideband multi-role AESA systems"

This paper presents design and measurements of filter banks for T/R-modules in potential wideband multi-role two-dimensional active phased array (AESA) systems. Two different technologies of implementation have been evaluated in this context. Firstly, a multilayer printed circuit boards (PCB) approach; using distributed filters, microstrip and stripline filter, is evaluated in terms of size and performance. Especially, the performance in terms of isolation between adjacent filters has been evaluated. Furthermore, 3D-stacked filter banks are demonstrated, showing a drastic reduction of expended circuit area. Secondly, design and measurements of a 3-channel semi-lumped filter bank in GaAs MMIC is presented, showing the feasibility of an "on-chip" integrated implementation. The study shows that both implementation are compatible, assuming a 10 GHz lattice, for T/R-modules. The MMIC solution offers 50-100 times smaller circuit area, but PCB filters on the other hand offer lower loss and improved selectivity. [C922]

"Linearity and efficiency optimisation in microwave power amplifier design"

In this contribution the minimisation of asymmetry between lower and upper side band intermodulation products will be discussed, starting from a Volterra analysis approach. Base-band and harmonic device terminations effects will be analysed, identifying novel conditions minimising IMD asymmetry and IM3 power levels. Such conditions, not relying on base-band terminations, are the basis for IM3 products minimisation via second harmonic load selection. The proposed criterion is then verified by harmonic load-pull measurements on a GaN HEMT under two-tone excitation. Measurements agree with the analysis, demonstrating a null IMD asymmetry and 6 dBc increase in C/I3, without affecting output power (34 dBm @ 1 dB compression) and power added efficiency performance (65% @ 1 dB compression). [C923]

"High-efficiency GaN class-E power amplifier with compact harmonic-suppression network"

This paper presents a high efficiency class-E power amplifier (PA) suitable for wireless transmitters operating at 2 GHz. Compact impedance transformation network is designed, using micro-strip transmission lines, so that it simultaneously achieves fundamental load transformation and harmonic impedance control using only two open-circuit stubs (2fo, 3fo). The dimensions of the network's elements were determined in order to concurrently attain a high harmonic suppression, minimum loss and high power added efficiency. The measurement results of the PA prototype, which is designed using a 10 W gallium nitride (GaN) HEMT transistor, showed state-of-the-art drain and power added efficiency (PAE). The achieved PAE, power gain and output power, when the drain is biased at 50 V, were equal to 74%, 12.6 dB and 11.4 W respectively. In addition, a second and third harmonic suppression in excess of -40 dBc and -75 dBc, respectively, is achieved without extra circuit tuning or additional filtering. [C924]

"GaN HEMT Based Doherty Amplifier for 3.5-GHz WiMAX Applications"

We have implemented a Doherty amplifier for 3.5-GHz World Interoperability for Microwave Access (WiMAX) applications using Eudyna 90-W (P3dB) Gallium-Nitride (GaN) High Electron Mobility Transistor (HEMT) because of the poor efficiency of a standard class AB amplifier when the linearity performance is good. The load modulation performance of the GaN HEMT device for the Doherty operation is rather moderate but workable. The linearity is improved using the in-band error cancellation technique of the Doherty amplifier. The implemented Doherty amplifier has been designed at an average output power of 43 dBm, backed-off about 8 dB from the 51 dBm (P3dB). For WiMAX signal with 28 MHz signal bandwidth, the measured drain efficiency of the amplifier is 27.8%, and the measured Relative Constellation Error (RCE) is -33.17 dB, while those of the comparable class AB amplifier are 19.42% and -24.26 dB, respectively, at the same average output power level.

[C925]

"2-GHz Band Cryogenically-Cooled GaN HEMT Amplifier for Mobile Base Station Receivers"

This paper presents a 2-GHz band gallium nitride (GaN) high electron mobility transistor (HEMT) amplifier cryogenically cooled to 60 K as a part of the cryogenic receiver front-end (CRFE) for mobile base station receivers. The GaN HEMT amplifier attains the output power of 3 W and the maximum power added efficiency of 62% with a 50 V drain bias for class-AB operation. The results reported herein are the first on the performance of a cryogenically cooled GaN HEMT amplifier aiming at use in a 2-GHz band CRFE. [C926]

"GaAs monocycle pulse generator for UWB applications"

This paper reports the design and test of a wavelet generator circuit which provides ultra short monocycle pulses of about 300 ps width alternately in phase and out of phase. This generator circuit is based on the representation of the pulse as a mathematical function which is a combination of four hyperbolic tangents. The final circuit of the generator was designed and realized on a monolithic microwave integrated circuit (MMIC) GaAs technology based on a pseudomorphic heterojunction FET (PHEMT) having a gate length of 0.25 μm (PH25 of UMS foundry). [C927]

"GaN HEMT based Doherty amplifier for 3.5-GHz WiMAX applications"

We have implemented a Doherty amplifier for 3.5- GHz world interoperability for microwave access (WiMAX) applications using Eudyna 90-W (P3dB) gallium-nitride (GaN) high electron mobility transistor (HEMT) because of the poor efficiency of a standard class AB amplifier when the linearity performance is good. The load modulation performance of the GaN HEMT device for the Doherty operation is rather moderate but workable. The linearity is improved using the in-band error cancellation technique of the Doherty amplifier. The implemented Doherty amplifier has been designed at an average output power of 43 dBm, backed-off about 8 dB from the 51 dBm (P3dB). For WiMAX signal with 28 MHz signal bandwidth, the measured drain efficiency of the amplifier is 27.8%, and the measured relative constellation error (RCE) is -33.17 dB, while those of the comparable class AB amplifier are 19.42% and -24.26 dB, respectively, at the same average output power level. [C928]

"5W highly linear GaN power amplifier with 3.4 GHz bandwidth"

In this paper, a 1 MHz to 3.4 GHz, 5 W, highly linear power amplifier based on GaN HEMT is reported. Load-pull technique has been applied to introduce a compromising solution for the PA performance trade-off problem. Over the whole bandwidth a measured small signal gain of 14 plusmn 0.7 dB and an output return loss of better than -10 dB have been achieved. The input return loss was better than -10 dB up to 3 GHz. Power and linearity performances have been measured and compared to simulations resulting in a very good agreement. At a frequency spacing of 100 kHz, minimum values of output IP3 and output IP2 have been evaluated and found to be 48.5 dBm and 59.3 dBm. At 1 dB power compression point, minimum Pout and Gp were found to be 37.3 dBm and 13.3 dB, respectively within the whole frequency band. [C929]

"Improved design methodology for a 2 GHz class-E hybrid power amplifier using packaged GaN-HEMTs"

This paper reports on design methodology and realization of a class-E power amplifier (PA) for 2 GHz using a packaged GaN-HEMT. The circuit achieves 36 dBm output power and 57% PAE, with drain efficiency as high as 62%. In addition to the large-signal simulation considerations, we discuss particularly the problem of input matching of the amplifier under class-E operation. [C930]

"P5I-1 Multiple States Switching Operation of AlGaIn /GaN Layer Mode Device"

In this paper, we have experimentally studied DC bias depending frequency characteristics of SAW and layer mode and their higher frequency mode, on the hetero epitaxially grown AlGaIn/GaN film on Sapphire substrate which is used for HEMT IC. By applying DC bias signal surface and layer waves are generated by depleting 2DEG, which is shortening the surface area of the substrate. In this operation, the size of 2DEG distributed near at finger electrodes are modulated by the DC bias and provides the variable size electrodes, which causes the efficient generation of space harmonics. It also provides variable filter including selective switching of frequency pass band. [C931]

"2-GHz band cryogenically-cooled GaN HEMT amplifier for mobile base station receivers"

This paper presents a 2-GHz band gallium nitride (GaN) high electron mobility transistor (HEMT) amplifier cryogenically cooled to 60 K as a part of the cryogenic receiver front-end (CRFE) for mobile base station receivers. The GaN HEMT amplifier attains the output power of 3 W and the maximum power added efficiency of 62% with a 50 V drain bias for class-AB operation. The results reported herein are the first on the performance of a cryogenically cooled GaN HEMT amplifier aiming at use in a 2-GHz band CRFE. [C932]

"X-band phase shifting power amplifier MMIC for phased array transmit modules"

An X-band phase shifting power amplifier with six-bit phase control and 5 Watt output power has been developed and tested. The aim of the development is cost reduction for transmit and receive components for phased array systems. The device has been developed in the 6-inch 0.5 μm power pHEMT process (PP50-11) of WIN semiconductors. The use of this process results in cost effective devices with a high power capability. [C933]

"A cost-effective high-power s-band 6-bit phase shifter with integrated LVCMOS control logic"

In this paper the design and performance of a high- power S-band 6-bit phase shifter is discussed. It is shown that excellent results have been obtained in the low cost high volume PP50-11 0.5 μm PHEMT process of WIN Semiconductors. The obtained results demonstrate that realization of a single chip transmit chip consisting of a phase shifter and a high-power amplifier is feasible. [C934]

"Statistical Large-Signal Model Enabling Yield Optimization in High-Power Amplifier Design"

A statistical large-signal model is presented that allows for optimizing yield of high-power amplifier MMICs. The modeling technique is based on the transformation of process control data into modeling parameters of an empirical, compact large-signal device model, followed by a multi-variant statistical analysis, resulting in a full set of principal components for both the current and the charge model. The model component has been implemented into ADS (Agilent) and an automated software periodically updates the statistical model parameters. [C935]

"High Power Pseudomorphic HEMTs' with Doped Channel"

The design principles and technology of growth of pseudomorphic AlGaAs/InGaAs heterostructure with silicon-doped canal for high frequency high power transistors as well as fabrication technology of the transistors were developed. Special attention has been paid to growth of the Al-GaAs/InGaAs heterojunction. PHEMTs' with the specific output power of 1.1 W/mm, PAE of 45.6 % and power gain of 6.8 dB at 17.7 GHz have been fabricated. [C936]

"New IR Photodetector Based on GaN QWs' or QDs' Located in Barrier of AlGaIn/GaN HEMT Structure"

The design principles and technology of fabricating novel quantum-dot (QD) infrared (IR) detectors based on AlGaIn/GaN high-electron-mobility transistors (HEMTs) with GaN QDs inserted into the AlGaIn barrier of HEMT (QDIP-HEMT) are proposed. Computation of electron energy levels in GaN/AlGaIn QWs' and QDs' is carried out and technology of its growth is developed. [C937]

"Radiation Effects in Heterostructures on Gallium Arsenide"

The radiation effects in GaAs Pseudomorphic High Electron Mobility Transistors (pHEMT) and Resonant Tunneling Diodes (RTD) have been experimentally investigated. [C938]

"X-band MMIC Low-Noise Amplifier Based on 0.15 μm GaAs PHEMT Technology"

The design and fabrication of X-band MMIC low-noise amplifier (LNA) based on 0.15 μm GaAs pHEMT technology is presented. The design and fabrication of X-band MMIC LNA is presented. MMIC is implemented with 0.15 μm pHEMT GaAs technology developed in the Institute of Microwave Semiconductor Electronics (Russia). Two-stage LNA is designed with using "visual" design CAD tools. In 7-10 GHz, it provides power gain $G = 15.5 - 17$ dB, noise figure from 2.1 to 2.9 dB, input and output return losses from -8 to -12 dB, and linear output power of +6 dBm. [C939]

"Visual" Design of X-Band Two-Stage MMIC Low-Noise Amplifier"

An application of a new "visual" technique to design multistage low-noise amplifiers (LNA's) is presented. As an

example, the design of X-band two-stage MMIC LNA is demonstrated basing on 0.15 μm GaAs p-HEMT technology. The design of multistage microwave LNA's is cumbersome and time-consuming process. In this paper we demonstrate an application of a new interactive "visual" technique to design X-band two-stage MMIC LNA. The design procedure consists in the sequential implementation of two main operations for each compensation (CN) and matching (MN) network: (1) determination of acceptable regions (AR's) of CN's and MN's impedances at sample frequencies based on amplifier stage requirements; (2) synthesis of CN's and MN's from AR's. The procedure is implemented in our "visual" CAD tools, AMP, REGION and LOCUS, providing the fast and convenient amplifier design. The amplifier designed is implemented based on 0.15 μm GaAs p-HEMT technology. [C940]

"Heat Generation in High Power hemt's Size Estimashion"

A simple model for the heat generation area size depending on HEMT topology and active layers properties is developed. It is shown that real heat generation area size is much less than transistor structure period and the gate drain distance. [C941]

"AlGaIn/GaN HEMTs with Large Angle Implanted Nonalloyed Ohmic Contacts"

In this work we report AlGaIn/GaN HEMTs with nonalloyed ohmic contacts by large angle ion implantation with a contact resistance to the channel of 0.2 Ωmm . [C942]

"Self-Aligned AlGaIn/GaN High Electron Mobility Transistors"

In this paper, we present high performance 0.25 μm gate-length self-aligned AlGaIn/GaN HEMTs on 6H-SiC substrates using a single ohmic step. Our recently developed Mo/Al/Mo/Au-based ohmic contact requiring annealing temperatures between annealing temperatures 500 and 600degC was utilized. Ohmic contact resistances between 0.3-0.5 Ωmm have been achieved. [C943]

"Analysis of lateral surface leakage in the vicinity of Schottky gates in AlGaIn/GaN HEMTs"

In this paper, we systematically characterize surface leakage current in the vicinity of Schottky gates on the AlGaIn/GaN heterostructure, separating it from the normal leakage current through the Schottky interface. [C944]

"AlGaIn/GaN HEMTs on Diamond Substrate"

In this paper AlGaIn/GaN high electron mobility transistor (HEMT) fabricated on diamond substrate is presented. Epitaxial AlGaIn/GaN layers were first grown on high resistivity Si (111) substrate and transferred to polycrystalline diamond substrate, which was separately grown by chemical vapor deposition (CVD). It is concluded that these are the best-reported results for a transistor using GaN on diamond material. [C945]

"Analysis of the impact of intrinsic parameter fluctuations in a 50 nm InP HEMT"

Intrinsic parameter fluctuations associated with the discreteness of charge and matter become an important factor when the semiconductor devices are scaled to nanometre dimensions. These effects have a considerable effect on the overall device performance. In this work, we have employed a 3D parallel drift-diffusion device simulator to study the impact of intrinsic parameter fluctuations in a 50 nm gate length InP HEMT with an In_{0.7}Ga_{0.3}As channel. After careful calibration of the I-V characteristics obtained from the device simulator against experimental data we carry out a statistical study considering the fluctuations in the delta-doping layer and interface charges as well as Indium content variation in the channel. We have found that the presence of random discrete dopants in the delta-doping layer are the major factor introducing the variations in the drive current. [C946]

"10 W/mm and High PAE Field-plated AlGaIn/GaN HEMTs at Ka-band with n+GaIn Source Contact Ledge"

The paper reports small-signal and large-signal performance of 140 nm gatelength field-plated AlGaIn/GaN HEMTs at Ka-band frequencies, in which the AlGaIn/GaN HEMTs were fabricated with n+ GaIn source ledge to reduce source access resistance such that the gate-to-drain feedback capacitance and breakdown voltage is not impacted. [C947]

"Low-Noise Microwave Devices: AlGaIn/GaN High Electron Mobility Transistors and Oscillators"

Noise and transport properties of state-of-the-art AlGaIn/GaN high electron mobility transistor (HEMT)

heterostructures are analyzed with respect to high-frequency oscillator applications for different dissipated powers. The phase noise of a monolithic microwave integrated circuit oscillator based on the best choice AlGaIn/GaN HEMT amplifier was investigated. A low level of the phase noise of the oscillator was registered. The up-conversion factor was found to be as low as 15 MHz/V for a frequency offset of 100 KHz, demonstrating that AlGaIn/GaN HEMTs offer an excellent potential for a wide range of microwave applications. [C948]

"Low-Noise pHEMT Amplifier Operating at Extra-Low Supply Voltage and Power"

We report on the successful development of an extra-low supply single-drain-operated amplifier intended for use as a general-purpose LNA for the practical frequency band over 1.5 to 2.5 GHz. It is a two-stage amplifier based on cost-effective commercial pHEMTs. The amplifier design and performance is discussed. [C949]

"Discrete and Half Bridge Module using GaN HFETs for High Temperature Applications more than 200°C"

AlGaIn/GaN HFETs are expected to be a good candidates for power switching application at high temperatures. We optimized the fabrication process of the AlGaIn/GaN HFET. A low specific on-state resistance of 6.3 mΩcm² and a large breakdown voltage of 600 V were achieved at 225°C. We also designed and fabricated a half bridge module using the AlGaIn/GaN HFETs and SiC SBDs. Switching characteristics of the AlGaIn/GaN HFET were investigated. The small turn-on delay of 7.2 nsec, which is 1/10 of Si MOSFET, was observed. The switching characteristics of the HFET showed no significant degradation up to 225°C. [C950]

"InAlAs/InGaAs heterostructures for THz generation"

We present a microscopic analysis of current fluctuations in InAlAs/InGaAs slot diodes (base of HEMT devices). An ensemble Monte Carlo simulation is used for the calculations. We analyze the origin of the strong THz oscillations appearing when the bias surpasses 0.5 V. This effect is apparently caused by the presence of Gunn-like oscillations whose dynamics is controlled by ballistic Gamma-valley electrons in the channel. These carriers are capable to reach extremely high velocities due to (i) the influence of degeneracy effects, which significantly reduces the rate of scattering mechanisms, and (ii) the presence of the recess, which strongly accelerate the electrons, launching them into the drain region. The influence of the effective distance travelled by the domain and the recess length are analyzed in order to improve the control of the frequency and magnitude of the oscillations. [C951]

"2-DEG Characteristics Improvement by N₂-plasma exposure in GaN HEMT heterostructures"

The lack of maturity in GaN HEMT processing is strongly limiting transistor expected performances. RF-DC dispersion, known as current collapse, seems to be related with carriers being trapped at the AlGaIn surface. The use of a preprocessing N₂-plasma treatment of the surface seems to have no effective improvement, in comparison with that of the pre-passivation processing step. A set of three AlGaIn/GaN heterostructures, subject to various surface treatment and cleaning procedures, have been studied. A reduction of ΔV_{th} = (1.3 ± 0.4) V for the pinch off voltage and of Δn_s = (-2.4 ± 0.3) cm⁻² for the 2DEG charge density were found, for the three samples. The N₂-plasma treated samples showed a modification on the surface states and consequently a worsening of the initial characteristics of the surface. On the other side, an annealing post-processing shows a layer oxidation that modifies the electron distance to the surface ΔW_B = (-5 ± 2) nm, and increases the 2DEG charge density, Δn_s = (1.4 ± 0.3) cm⁻². Finally from XPS results, a contamination of oxygen, carbon and fluorine was found. The stronger cleaning power of the N₂-plasma, aside from the RTA, is used as a great carbon surface cleaner, reducing carbon concentration up to a (70 ± 6) %. [C952]

"Analysis of Drain Lag and Current Slump in GaN-Based HEMTs and MESFETs"

Two-dimensional transient analyses of AlGaIn/GaN HEMTs are performed in which a deep donor and a deep acceptor are considered in a semi-insulating buffer layer. Quasi-pulsed I-V curves are derived from the transient characteristics. It is shown that the deep levels affect the results essentially in a similar way as for GaN MESFETs. It is shown that so-called current slump is more pronounced when the deep-acceptor density in the buffer layer is higher and when an off-state drain voltage is higher, because trapping effects become more significant. It is suggested that to minimize current slump in GaN-based FETs, an acceptor density in a semi-insulating GaN layer should be made low. [C953]

"1.8 kV AlGaIn/GaN HEMTs with High-k/Oxide/SiN MIS Structure"

We report the fabrication of AlGaIn/GaN high electron mobility transistors (HEMTs) having metal-insulator-

semiconductor (MIS) gate structure with the high-A/SiN and high-k/oxide/SiN insulator structures. The SiO₂ and Al₂O₃ were used as the oxide, and the HfO₂, ZrO₂ and TiO₂ were used as the high-k materials. Both high-k/SiN and high-k/oxide/SiN MIS-gate HEMTs showed good DC operating characteristics. However, there was significant difference in the breakdown voltage characteristics. In the case of the high-k/oxide/SiN MIS-HEMT, the off-state drain current was significantly reduced due to the presence of the SiO₂ or Al₂O₃ layer, and the breakdown voltage characteristics were improved. The breakdown voltage of HfO₂/SiO₂/SiN and ZrO₂/SiO₂/SiN MIS-HEMT for the gate-drain distance $L_{gd} = 28 \text{ }\mu\text{m}$ were 1.8 kV and 1.7 kV, respectively. [C954]

"Hydrogen Sensing Characteristics of a Pd/GaAs Semiconductor Transistor-Type Sensor"

An interesting Pd-GaAs high electron mobility transistor (HEMT) hydrogen sensor is fabricated and studied. For the studied device, a 5 nm-thick undoped GaAs cap layer is grown to suppress the oxidation of the underneath AlGaAs layer. Comprehensive analysis on the electrical properties including transconductance (g_m), channel conductance (g_D), and gate-source voltage shift (ΔV_{GS}) is presented. Experimentally, the maximum variation of transconductance (Δg_m) is about 46.8 mS/mm while the maximum transconductance ($g_{m,max}$) is still maintained at about 176 mS/mm. A high channel conductance variation (Δg_D) of 25.1 mS/mm is obtained in 9970 ppm H₂/air gas at 50 degC. This indicates that, in hydrogen-containing ambience, the channel resistance reduces in the linear region of transistor operation. The negative ΔV_{GS} value in hydrogen-containing ambience means that a lower V_{GS} value is sufficient to maintain the same drain current (I_D) value than that in air. [C955]

"Studies on Uniformity of MOVPE-Grown AlGaIn/GaN HEMT Structures by Spectroscopic Ellipsometry"

The uniformities of AlGaIn/GaN HEMT structures grown by MOVPE have been studied by using spectroscopic ellipsometry. The results show that the total flow rate is the most critical growth parameter for the uniformity. [C956]

"Hot-Carrier-Stress-Induced Degradation of 1 kV AlGaIn/GaN HEMTs by Employing SiO₂ Passivation"

High-voltage AlGaIn/GaN HEMTs (high-electron-mobility transistors) are fabricated by employing SiO₂ passivation and the degradation due to the hot carrier stress has been investigated. Our experimental result shows that the SiO₂ passivation of AlGaIn/GaN HEMT successfully achieves the breakdown voltage of 1 kV without any field plate design. The pulsed I-V measurement for AlGaIn/GaN HEMT shows that the SiO₂ passivation suppresses the frequency dispersion and decreases the on-resistance from 2.46 to 1.38 m Ω -cm². The hot carrier stress degrades the electric characteristics of AlGaIn/GaN HEMT because the high field increases the trapping at the surface and the interface. However, the SiO₂ passivation of AlGaIn/GaN HEMT decreases the surface trapping and 2DEG depletion during the hot carrier stress, so that a passivated device exhibits less degradation than an unpassivated one. After the hot carrier stress with $V_{DS} = 30 \text{ V}$ and $V_{GS} = 10 \text{ V}$ is applied to the device for 5 times 10⁴ sec, the SiO₂ passivation decreases the stress-induced degradation of forward drain current from 30.4 to 24.5 %. [C957]

"Induction heating system operation by soft switching GaN heterojunction field effect transistors"

The induction heating (IH) system with a soft switching was fabricated using AlGaIn/GaN heterojunction field effect transistors (HFETs). The operation current and breakdown voltage of an AlGaIn/GaN HFET were over 50 A and 800 V, respectively. The specific on-resistance was 10 m Ω -cm². The turn-on and turn-off time were less than 20 ns, respectively. We fabricated the IH system with a soft switching circuit which can be driven using normally-on AlGaIn/GaN HFETs. The IH system with a soft switching using normally-on AlGaIn/GaN HFETs was demonstrated for the first time. Then output power was 3.2 kVA. [C958]

"Normally-off AlGaIn/GaN Low-Density-Drain HEMTs (LDD-HEMT) with Enhanced Breakdown Voltage and Suppressed Current Collapse"

We report a low-density drain HEMT (LDD-HEMT) that exhibits enhanced breakdown voltage and reduced current collapse. The LDD region is created by introducing negatively charged fluorine ions in the region between the gate and drain electrodes, effectively modifying the surface field distribution on the drain side of the HEMT without using field plate electrodes. Without changing the device physical dimensions, the breakdown voltage can be improved by 50% in LDD-HEMT and the current collapse can be reduced. No degradation of current cutoff frequency (f_t) and slight improvement in power gain cutoff frequency (f_{max}) are achieved in the LDD-HEMT, owing to the absence of any additional field plate electrode. [C959]

"DC Characterization and Validation of the Improved Analytical Model of AlGaIn/GaN HEMT"

Research is being conducted for a high-performance building block for high frequency applications that combine lower costs with improved performance and manufacturability. Researchers have focused their attention on wide band gap (WBG) semiconductor materials for use in device technology to address system improvements. Of the contenders, silicon carbide (SiC), gallium nitride (GaN), and diamond are emerging as the front-runners. The objective of this paper is to demonstrate the DC characterization of high electron mobility transistor (HEMTs) with a focus on gallium nitride process in relevant high frequency applications. The transfer properties of the HEMTs in gallium nitride process are studied by characterizing the two dimensional electron gas (2DEG) and spontaneous and piezoelectric polarization induced charges. The research involves test, characterization and validation of the improved analytical model for the AlGaIn/GaN HEMT. The DC characterization includes the measurement of device output characteristics (I_{ds} vs V_{ds}) and transfer characteristics (I_{ds} vs V_{gs}). These GaN HEMTs demonstrate excellent DC capabilities and can cause electric fields up to 3 MV/cm in group III-nitride crystal. For achieving design success it is very important to develop an accurate empirical and analytical model of the device. A custom DC measurement system is used to facilitate the DC characterization of the unpackaged GaN HEMT test device. The experimental results are in close agreement with the simulation results. The experimental results measured in this research will not only help the GaN device researchers in the device behavioral study but will also provide valuable information for wide band gap (WBG) semiconductor researchers as well as circuit designer. [C960]

"High F_{max} GaN-HEMT with High Breakdown Voltage for Millimeter-Wave Applications"

First Page of the Article [C961]

"Recent Advances in GaN-on-SiC HEMT Reliability and Microwave Performance within the DARPA WBGs-RF Program"

The Wide Band Gap Semiconductor for RF Applications (WBGs-RF) program, supported by the Defense Advanced Research Projects Agency (DARPA), is developing microwave and millimeter-wave gallium nitride-based devices on silicon carbide substrates. Recent advances within Phase II of the Program include excellent results for both performance and reliability. Significant progress has been made towards developing manufacturable wide-bandgap devices that provide outstanding performance at reliability levels that will allow their use in a wide variety of high frequency, high power applications. [C962]

"Monte Carlo Comparison Between InAlAs/InGaAs Double-Gate and Standard HEMTs"

An ensemble 2D Monte Carlo simulator is employed to analyze the static and dynamic performance of InAlAs/InGaAs double-gate high electron mobility transistors (DG-HEMTs) by comparing them with standard single-gate (SG) ones. Different gate length devices are analyzed in order to check the attenuation of short-channel effects expected in the DG-structures. The transconductance g_m and the output conductance g_d are confirmed to be improved by the DG-geometry. As well, the higher values of the figure of merit g_m/g_d jointly with the lower value of the gate resistance $R_{g,lead}$ lead to an improvement of the extrinsic frequency performance (f_{max} and ft). [C963]

"Novel Plasmon-Resonant Terahertz-Wave Emitter Using a Double-Decked HEMT Structure"

A new plasmon-resonant THz-wave emitter is fabricated and characterized. The heterostructure of the device consists of double-decked high electron mobility transistor (HEMT) and the upper-deck HEMT works as a grating antenna to convert the non-radiative plasmonic wave in the lower-deck HEMT channel to radiative THz electromagnetic wave. This conversion can be done more efficiently than a metal grating antenna. The experimental observed clear evidence of the THz-wave emission from the double-decked HEMT device. [C964]

"InGaAs CMOS: a "Beyond-the-Roadmap" Logic Technology?"

This talk will discuss the general issues associated with III-V CMOS that are enunciated above. It will also describe the authors' research activities in the area of InGaAs HEMTs for logic. In particular, we will summarize the findings of a recent scaling study of InGaAs HEMTs down to 60 nm in gate length [1]. In this work, we fabricated HEMTs with a 70% InAs composition in the channel and with varying gate lengths and InAlAs barrier thicknesses (from 11 to 3 nm). This study resulted in devices that have substantially more current drive than state-of-the-art 65 nm CMOS at a voltage of 0.5 V. It also showed that InGaAs HEMTs scale according to a simple electrostatics law similar to fully-depleted SOI MOSFETs. Our research reveals that HEMTs are excellent test vehicles to study topics of great relevance to future III-V MISFETs, such as self-aligned device architectures, scaling limit of planar devices, impact of strain on transport physics, and the consequences of a low density of

states on current drive of deeply scaled devices.. [C965]

"Demonstration of a S-MMIC LNA with 16-dB Gain at 340-GHz"

In this paper, an amplifier with a significant amount of gain is demonstrated at sub-millimeter wave frequencies ($f > 300$ -GHz) for the first time. The three stage amplifier uses advanced InP HEMT transistors to realize 16-dB gain at 340-GHz and > 20 dB gain at 280-GHz. The amplifier demonstrates > 100 GHz of bandwidth with gain > 10 dB. This paper demonstrates that full WR-3 waveguide band (220-325 GHz) InP HEMT amplifiers are currently possible and that current device capabilities enable operation well into the sub-millimeter wave regime. [C966]

"A W-Band 4-Bit Phase Shifter in Multilayer Scalable Array Systems"

This paper presents an ultra-compact W-band 4-bit phase shifter integrated in a 5-layer wafer-scale assembly phased array system. The phase shifter was implemented using a reflective-type circuit topology, consisting of a 3 dB Lange coupler and a pair of reflective loads. GaAs HEMT switches were used for switching the loads to achieve the desired phase shifts. On-wafer measurements of the single-bit test cells show phase deviations of 2.5deg from the target phase shifts and an insertion loss of 1.5 plusmn 0.7 dB at 91.5 GHz, while the measured 4-bit phase shifter data shows an insertion loss of 6.9 plusmn 1.1 dB and better than 10 dB return loss at 94 GHz. With its ultra-compact size, two 4-bit phase shifters can be fit into a 1.6 mm times 1.6 mm array-cell. This phase shifter combines state-of-the-art performance and size. To our knowledge, this is the first reported W-band phase shifter fabricated for multilayer wafer-scale assembly in a phased array system. [C967]

"GaAs PHEMT Power Amplifier MMIC with Integrated ESD Protection for Full SMD 38-GHz Radio Chipset"

The performance of a compact 38-GHz linear power amplifier MMIC' designed for use in SMD package is presented. The amplifier is fabricated with a 6-inch 0.15 mum GaAs low-noise PHEMT technology, and features on-chip ESD protection with input short-circuit stub, robust capacitors at RF ports and high current diode arrays. While occupying a chip area of only 3.5 mm², at 5 V and 600 mA, this 4-stage amplifier achieves a small signal gain of more than 26 dB over the 35-to 42 GHz frequency band, 26-dBm output power in saturation, and excellent intermodulation performance with up to 37-dBm OIP3when backed-off. Finally, the PA MMIC exhibits excellent performance in packaged form as well, with 25-dB linear gain in the 35-42 GHz band and output referred intercept point of more than to 35 dBm. [C968]

"A 250W S-Band GaN HEMT Amplifier"

We report an efficient 250 W GaN HEMT power amplifier with 2.1 -2.5 GHz bandwidth. The amplifier employs AlGaN/GaN HEMTs with advanced source connected field plates, which are suitable for 48 V operation. The package combines two 22.2 mm periphery devices to obtain 54.0 dBm output power at 2.14 GHz and 54.6 dBm at 2.5 GHz, under pulsed condition with 10% duty cycle and 20mus pulse width. To our knowledge this is one of the widest bandwidth reported at this power level and frequency. These amplifiers are targeted for wideband digital cellular infrastructure; satellite communication, avionics and ISM band applications. [C969]

"A 40W GaN HEMT Doherty Power Amplifier with 48% Efficiency for WiMAX Applications"

A 40W GaN HEMT Doherty power amplifier (PA) for 2.5GHz band was developed. The Doherty PA was designed using large signal GaN HEMT models, and demonstrated a saturation output power of 54dBm (250W) and a drain efficiency of more than 60%. The measurement result shows good agreement with the large signal simulation result. We also investigated the Doherty PA linearity with digital pre-distortion (DPD) system, and obtained a drain efficiency of 48%, an ACLR of -53dBc and a power gain of 13.4dB at the average output power of 46dBm (40W) with 64QAM modulation signal. These superior performances show good suitability for 2.5GHz band WiMAX base stations. [C970]

"A 210 GHz, Subharmonically-Pumped Active FET Mixer MMIC for Radar Imaging Applications"

A conversion loss of 8.5 dB is achieved for down-conversion of a 210 GHz RF signal in a sub-harmonically pumped mixer MMIC. The active FET mixer, realized in a 100 nm gate length metamorphic HEMT process, employs a dual-gate topology. The mixer achieves a 3-dB RF bandwidth from 188 to more than 210 GHz and is driven by a 10 dBm subharmonic LO signal. The combination with an integrated source follower stage results in a 2 GHz IF bandwidth. The mixer is dedicated to active imaging systems for concealed weapon detection operating in the atmospheric window around 220 GHz. [C971]

"AlGaIn/GaN Bidirectional Power Switch"

This paper presents a novel approach to achieving BPS functionality using AlGaIn/GaN HFETs and for the first time presents experimental data showing the power bidirectional capability of the devices. We present the first detailed study of the bidirectional power switching capability of single and dual gate AlGaIn/GaN BPS. One approach to achieve a symmetrical voltage blocking capability in AlGaIn/GaN HFET is to place the gate electrode in the middle of the source-drain spacing. [C972]

"Schottky Drain AlGaIn/GaN HEMTs for mm-wave Applications"

AlGaIn/GaN high electron mobility transistors (HEMTs) are some of the most promising devices for power amplification. Important efforts have been taken to expand the operating frequency of these devices to mm-waves. As shown by Tasker et al., the drain parasitic resistance is one of the main factors limiting the current gain cut-off frequency (f_T) and the power gain cut-off frequency (f_{max}) in high performance devices. The drain parasitic resistance consists of two components: the contact resistance between the metal and the channel and the access resistance due to the distance between the gate edge and drain contact. In this paper, we demonstrate a new drain contact technology based on the use of a Schottky metallization in the drain contact. This new technology has the potential to significantly reduce the contact resistance and at the same time minimize the access resistance. [C973]

"Barrier layer downscaling of InAlN/GaN HEMTs"

In this study we have investigated heterojunctions on sapphire with barrier thicknesses between 13 nm and 5 nm maintaining a high output current. The results indicate that InAlN/GaN HEMT device structures can be reliably designed and fabricated with barrier layer thicknesses approaching the tunnelling thickness and approaching enhancement mode characteristics. Using Al₂O₃ as high-k gate dielectric also high aspect ratio MOSHEMTs could be designed with comparable characteristics to MESHEMTs of the same barrier thickness. This is an ongoing study and results on further barrier downscaling experiments will be presented. [C974]

"Drain-to-Gate Field Engineering for Improved Frequency Response of GaN-based HEMTs"

This paper reports a novel approach in designing high frequency AlGaIn/GaN HEMTs based on gate-drain field engineering utilizing a drain-connected field controlling electrode. The absence of frequency behavior degradation with drain bias as well as record high electron velocity values were obtained using gate-to-FCE separation of 0.5-0.7 μm . Thus, we demonstrated that the FCE is a powerful way to improving the high frequency, high power performance of GaN HEMTs at high drain biases. [C975]

"Effects of Source Access Resistance on Gate lag in AlGaIn/GaN HEMTs and Current Slump Behavior"

In summary, two-dimensional transient simulations of AlGaIn/GaN HEMTs have been made in which a deep donor and a deep acceptor are considered in the buffer layer. The lag phenomena and current slump could be reproduced. Particularly, it has been shown that the gate lag is correlated with relatively high source access resistance of AlGaIn/GaN HEMTs, and that the drain lag could be a major cause of current slump. It is concluded that an acceptor density in the buffer layer should be made low to minimize current slump, although current cutoff behavior may be degraded when the gate length becomes short. [C976]

"Microwave Noise Characterization of Enhancement-Mode AlGaIn/GaN/InGaIn/GaN Double-Heterojunction HEMTs"

In this work, we report the microwave noise characterization of E-mode double-heterojunction HEMT (DH-HEMT). The E-mode DH-HEMT shows reduced noise figure compared to its D-mode counterpart, mainly owing to the lower gate leakage current achieved by the Schottky barrier enhancement in fluorine-plasma treated gate region and the favorable bias conditions for the E-mode HEMT. [C977]

"Electric-Field Dependence of Junction Temperature in GaN HEMTs"

Here we report junction temperature and thermal spreading in GaN HEMTs using a transient measurement technique that utilizes the thermionic Schottky gate characteristics to obtain temperatures. Our technique first calibrates the gate-to-source forward I-V characteristics of the device under test as a function of temperature by mounting on a chuck at a known temperature and under vacuum to eliminate heat loss effects. Thermal spreading measurements indicate a thermal resistance of $\sim 25^\circ\text{C/W}$ per mm between the two sensors located at $-450\mu\text{m}$ and $-225\mu\text{m}$ from the heater device. [C978]

"Advanced InP and GaAs HEMT MMIC technologies for MMW commercial products"

NGST is developing advanced high frequency HEMT device and MMIC technologies to address imminent applications at MMW frequencies above 80 GHz through 300 GHz. The improved device transport characteristics, high transconductance, and gain at very high frequencies will benefit next generation communications, radar, imaging and radiometer systems. In this paper, we status the development and production of 0.1 μm GaAs HEMT, 0.1 μm InP HEMT and sub 0.1 μm InP HEMT technologies for high frequency mmW circuits. [C979]

"Ultra-Low Resistance Ohmic Contacts to InGaAs/InP"

An extremely low in situ metal contacts can be formed to (In,Ga)As on InP. it is also possible to form ultra low resistance ex situ contacts by improved surface treatment. However, unlike in situ contacts, ex situ contacts are very sensitive to surface preparation. Similar contact resistivities to InAs on GaAs were reported by Nittono et al. This is the first time such low metal-semiconductor contacts have been demonstrated in In_{0.53}Ga_{0.47}As system that does not deteriorate at least upto 500 degC. These thermally stable, extremely low resistances, ohmic contacts are an enabling technology for THz bandwidth InGaAs/InP HBTs, mm wave InGaAs HEMT technologies, and the evolving III-V MOSFET technologies. [C980]

"Estimation of Trap Density in AlGaIn/GaN HEMTs from Subthreshold Slope Study"

In this paper, we first demonstrate effects of thermal annealing on subthreshold slope in AlGaIn/GaN HEMTs. Then, based on the temperature dependence of subthreshold slope, we introduce a new method to estimate interface trap density in these devices. The understanding of this interface trap is critical to optimize the gate modulation efficiency of these transistors and maximize their high frequency performance. [C981]

"Surface Treatment for Leakage Reduction in AlGaIn/GaN HEMTs"

Development of AlGaIn/GaN HEMTs has been largely advanced in recent years, leading to record microwave power performance from solid-state devices. With the AlGaIn/GaN HEMTs emerging as a viable technology for high frequency low noise amplifiers and power amplifiers, there are still several problems to be solved. One key problem is the relatively high gate leakage current, which may cause extra noise and reliability problems. In this report, we present a technology which reproducibly reduces gate leakage by two orders without introducing any negative effect on the device performance. [C982]

"AlGaIn/GaNHEMT with High PAE and Breakdown Voltage Grown by Ammonia MBE"

In this paper, a report on high PAE, high breakdown-voltage HEMTs grown by ammonia MBE is discussed. First, an AlN nucleation layer was grown by plasma-assisted MBE on SiC. Then GaN buffer was grown by ammonia MBE, followed by 30 nm ammonia Al_{0.3}Ga_{0.7}N. A sheet charge of $1 \times 10^{13} \text{ cm}^{-2}$ with a mobility of $1500 \text{ cm}^2 \text{ V}^{-1} \text{ s}^{-1}$ was obtained from Hall measurements. [C983]

"Silicon nitride films for passivation of pHEMT based MMIC"

Passivation of pseudomorphic high electron mobility transistor (pHEMT) based MMIC's by silicon nitride films deposited by PECVD is reported here. These films were first optimized for passivation of MESFET's to get desired performance. No degradation in pHEMT/MESFET characteristics like I_{dss} , g_m/V_p and C_{gs} were observed while only nominal degradation was found in Schottky diode ideality factor η and its breakdown voltage V_B . The refractive index of the films was 1.92 with 1200 Å thickness. The films have high dielectric strength $> 5 \text{ E}6 \text{ V/cm}$, low tensile stress $< 5 \text{ E}9 \text{ dynes/cm}^2$ and dielectric constant 6.9 - 7.1. The etch rate of the film is $\sim 900 \text{ Å/min}$ in BHF and fine patterns can be etched with 1-2 minutes etch time in BHF. The film composition was analyzed by FTIR and SIMS studies. [C984]

"Study of selective gate recess etching of InGaAs/InAlAs/InGaAs metamorphic HEMT structures using succinic acid based etchant"

Metamorphic HEMTs on GaAs substrates are promising devices of today as they are operated at even higher frequencies for microwave applications compared to pseudomorphic HEMTs. The selective removal of n⁺InGaAs ohmic contact layer from the top of the device structure poses a major challenge during fabrication. We have studied the influence of temperature on the selectivity of etch rate between the n⁺InGaAs and underlying InAlAs layers using succinic acid based etchant. The etchant was composed of succinic acid solution mixed with hydrogen peroxide and deionized water. The pH of the solution was adjusted to 5 by adding NH₄OH. The etch

rates at different temperatures between 14degC to 30degC were estimated by profiling the etched pattern using atomic force microscopy (AFM). Surface roughness of the etched area also was studied using AFM. It was found that the selectivity has improved with temperature. This is possibly due to simultaneous occurrence of low etch rates of InAlAs due to presence of aluminum oxide and high etch rates of InGaAs due to increased temperature. It was also found that the surface roughness was higher at lower temperatures contrary to the observations made in the case of pseudomorphic HEMTs. [C985]

"Modeling of a radio frequency transimpedance amplifier based on a δ -doped AlInAs-GaNAs HEMT and its performance optimization"

A simple approach has been proposed for the optimization of performance parameters such as transimpedance-bandwidth product, transition frequency f_T and maximum frequency of oscillations f_{max} of high electron mobility transistors (HEMTs). The radio frequency (RF) small-signal equivalent circuit model has been employed to represent the ac behavior of T-shape gate AlInAs-GaNAs delta-doped HEMTs. All the circuit parameters pertaining to the model have been determined as a function of the width W of the device and surface density of charge δ in the channel. Then PSpice has been used to simulate the device. Good agreement between experimental and simulation results of $|h_{fe}|^2$ for different frequencies is obtained. The same model is then employed to optimize performance parameters of the HEMT and the MSM-HEMT amplifier with reference to width and surface density of charge δ in the channel. [C986]

"InAlN-A new barrier material for GaN-based HEMTs"

The InAlN/GaN heterojunction is a new alternative to the common AlGaIn/GaN configuration with high sheet charge density and high thermal stability, promising very high power and temperature performance as well as robustness. The status, focussing on the lattice matched materials configuration is reviewed. [C987]

"Surface passivation effects in AlGaIn/GaN HEMTs on high-resistivity Si substrate"

AlGaIn/GaN high-electron-mobility transistors (HEMTs) were successfully fabricated on high-resistivity (HR) Silicon substrate. Surface passivation effects on AlGaIn/GaN HEMTs were studied using Si₃N₄ dielectric layer grown by plasma enhanced chemical vapor deposition. The device direct-current current-voltage (IDS-VDS) characteristics, pulsed IDS-VDS characteristics, microwave small-signal and large-signal characteristics were studied before and after passivation. An enhancement of drain current (ID) density and the extrinsic transconductance was observed for the devices with full Si₃N₄ passivation. An improvement of f_T , f_{max} and device output power (P_{out}) was also observed after surface passivation. A new evaluation method implemented to identify the ID collapse related traps from AlGaIn/GaN HEMTs. More than 80% of ID collapse suppression and 80% of increase in P_{out} were observed in AlGaIn/GaN HEMTs by Si₃N₄ passivation. The P_{out} increase in AlGaIn/GaN HEMTs by surface passivation is in good agreement with the ID collapse suppression in AlGaIn/GaN HEMTs by surface passivation. [C988]

"3-dimensional analytical modeling and simulation of fully depleted AlGaIn/GaN modulation doped field effect transistor"

We propose a simple and accurate three-dimensional (3-D) analytical model for the threshold voltage of AlGaIn/GaN modulation doped field effect transistor (MODFET) taking into account the short channel effects (SCEs) and the narrow width effects (NWEs) present simultaneously in a small geometry device. The model includes the effect of vital parameters such as doping and thickness of the barrier layer on the threshold voltage. The accuracy of the proposed analytical model is verified by comparing the model results with 3-D device simulations. It has been demonstrated that the proposed model correctly predicts the potential, the electric field distribution along the channel and the threshold voltage. [C989]

"Superconducting microresonators for detection and multiplexing"

Superconducting microresonators are drawing increasing attention for use in sensitive THz detection, especially for astronomical applications. These are relatively simple thin-film lithographically produced devices that are amenable to large-scale microwave frequency multiplexing. Indeed, such resonators have very high quality factors, in the range 10^4 to 10^6 , potentially allowing 10^3 to 10^4 resonators to be multiplexed using a single cryogenic low-noise amplifier (HEMT). The resonators may themselves serve as detectors given appropriate coupling of the signal energy, or the resonators may be used to multiplex a broad range of other devices such as SIN or SIS tunnel junction detectors, SQUID preamplifiers for TES bolometers, etc. One of the major advantages of microwave frequency multiplexing is that much of the complexity of the readout system is transferred to room temperature, where it is now feasible to produce readouts with very high channel counts

using FPGA digital signal processing along with fast, high-resolution ADCs and DACs. This presentation will give an overview of the topics described above, including an introduction to the basic physics of superconducting microresonators and their noise mechanisms, and as a concrete example will describe the development of a 2.5 kilopixel millimeter-wave multicolor camera system for the Caltech Submillimeter Observatory. [C990]

"Emission of terahertz radiation from an interdigitated grating gates high electron-mobility transistors"

New doubly interdigitated grating gate high- electron mobility transistor (HEMT) was illuminated at room temperature by a 1.5- μm CW laser. A clear emission of the terahertz radiation has been detected using a Silicon bolometer cooled down to 4.2 K and placed in the front of the sample. The observed signal was related to the self oscillation of the plasma waves in our new HEMT device. [C991]

"Room temperature amplification of optical-beating photoresponse in HEMTs"

The authors report on tunable terahertz resonant detection of two 1.55 μm cw-lasers beating by plasma waves in AlGaAs/InGaAs/InP high-electron-mobility transistor. The fundamental plasma resonant frequency and its odd harmonics can be tuned with the applied gate-voltage in the range 0-600 GHz. Amplification of photoresponse under applied DC drain-source current is demonstrated. [C992]

"Gallium Nitride power HEMT for high switching frequency power electronics"

Very large number of power semiconductor devices (semiconductor power switches) are used in power electronics systems such as AC-DC converter for PCs, DC-DC converters for CPU, motor driver systems and induction heating systems for home appliances, and GaN device is one of a promising candidate for future power devices thanks to the wide band gap semiconductor material property. In GaN base device research, the GaN-HEMT structure is widely investigated than the other device structures specially in RF technology field. This structure also suits to high switching frequency power electronics applications because of the high breakdown voltage and the inherent high speed characteristics of HEMT device. This paper describes the possibility of GaN-HEMT for power electronics applications specially focused on high switching frequency applications comparing the limit of silicon devices such as MOSFETs and IGBTs, and also describes latest research result including demonstration of high switching frequency power electronics circuit. [C993]

"A GaN HEMT power amplifier with variable gate bias for envelope and phase signals"

This paper describes the design, simulation and measurement of a GaN power amplifier suitable for envelope and phase signal combination. The low-frequency envelope signal is used to vary the gate (bias) voltage of the device, resulting in a pulse width modulated drain voltage, while modulation of supply voltage or current is avoided. The test circuit is implemented using a discrete GaN HEMT power amplifier and discrete surface-mount passive components assembled on a PCB. Measurements showed a maximum drain efficiency of 59% at 360 MHz, at an output power of 29 dBm. The output power as a function of the gate bias voltage varied between 3 and 29 dBm, with the drain efficiency varying between 6 and 59%. [C994]

"Cosmic Microwave Background experiments-past, present and future"

The cosmic microwave background (CMB) is the oldest electromagnetic radiation to reach the earth. Measurements of this radiation play a central role in modern Cosmology. In this presentation, I will describe the information that can be obtained from measurements of the CMB. The importance of these measurements is such that there have been two rounds of Nobel Prizes. The field has been advanced by small ground- and balloon-based measurements followed by space missions including COBE and WMAP. The Planck mission will be launched next year. A new generation of ground-based observations is now beginning, which may lead to yet another space mission. The requirements for such measurements have strongly driven the development of direct detection systems at millimeter and submillimeter wavelengths. The physical and practical issues that generally favor the use of coherent receivers (now based on HEMT amplifiers) at frequencies below -90 GHz and bolometric detectors at higher frequencies will be discussed. The development of this field will be illustrated by describing generic types of technology developments and of experiments. [C995]

"Optical fibre CDMA for access and optical networks"

A new design technique for circuits capable of encoding and decoding 40 GChip/s CDMA signals is proposed. We report the concept and circuit design of two novel structures, based on the distributed amplifier/filter topology, to operate at speeds close to the cut-off frequency of the transistors employed. The main application is for generation and detection of signals in optical CDMA systems. Theoretical analysis and potential implementation

using an MMIC-HEMT foundry process are presented, with predicted results based on full MMIC simulation. [C996]

"Advances in Gallium Nitride-based Electronics"

The III-nitrides AlN, GaN, InN and their alloys are a novel family of semiconductor materials for optoelectronics as well as for electronics. GaN-based high electron mobility transistors (HEMTs) have shown superior power density and operating temperatures at frequency ranges that are beyond the limits of devices fabricated from Si and other III-V materials. This paper presents the advances in the GaN HEMT technology. [C997]

"A Novel Parameter Extraction Method for HEMT Models by Using Generic Algorithms"

This work reports an accurate, reliable, and systematic method to extract the small-signal equivalent-circuit elements of the high electron mobility transistor (HEMT) models by integrating the generic algorithm (GA) analyses. Superior extraction accuracy of 95% over the entire operation frequency range has been achieved. Different from the strong dependence on the starting value of parameter search by the conventional techniques, the proposed method sets the respective searching range with physical meanings by referring to the initial values. The proposed methodology can be applied to extracting different high-speed devices and is promisingly useful for the RFIC design technologies. [C998]

"MMIC technologies for MW and MMW applications"

This paper covers two recent progresses on MW and MMW MMIC technologies. One is the high efficiency and high power density pHEMT technology for power amplifier MMICs. The nonlinear drain resistance is found to be the cause of large power loss at millimeter-wave, although it acts like the conventional resistor at low frequency. A new device structure is proposed to overcome this problem, and results in excellent performance of 0.65 W/mm output power and 35% PAE at Ka band. The other topic is the InGaP HBT oscillator enhancing the output power without any reduction of the phase noise. At 40 GHz, 6 dBm output power and -113 dBc/Hz phase noise has been demonstrated. The 2nd harmonic matching is the key to achieve high output power and low phase noise simultaneously. Results are supported by both simulations and measurements. [C999]

"Modeling of 0.15 μm InGaAs pHEMT up to 60 GHz"

In this paper, a small-signal model for a two finger 0.15 μm gate width InGaAs pHEMT up till 60 GHz is presented. Measured methods are explored to obtain accurate S-parameters of the pHEMT. The modeling results have shown good agreement with the experimentally extracted S-parameters. [C1000]

"Design and simulation of high gain PHEMT low noise amplifier (LNA)"

This paper presents a 5.8 GHz low voltage, low power, and wide band LNA design using PHEMT transistor. The simulated LNA is a single stage with pi input and output matching circuits. The noise canceling principle and sensitivity analysis is performed for the simulated low noise amplifiers. The simulated results are compared with identical LNA published and give a significant increase in the gain by more than 23 % at the same noise figure, input and output return loss. Another LNA is optimized in the design to achieve a maximum gain with low noise figure and input, output return loss which gives a maximum gain of 16 dB at 3GHz frequency with 0.65 Noise figure. [C1001]

"Development of GaN HEMT based High Power High Efficiency Distributed Power Amplifier for Military Applications"

Implementing wide bandgap GaN HEMT device into broadband distributed power amplifier creates a tremendous opportunity for RF designers to develop high power high efficiency very broadband power amplifiers for military applications. Several prototypes of 10-40 W GaN based distributed power amplifiers, including MMIC distributed PA, are currently under the development at Rockwell Collins, Inc. In this paper, we will discuss the results of a 10 W distributed power amplifier with the maximum power output of more than 40 dBm and a power-added efficiency of 30-70% over the bandwidth of 20-2000 MHz. [C1002]

"Electrostatic mechanisms responsible for device degradation in AlGaIn/AlN/GaN HEMTs"

Displacement-damage induced degradation in AlGaIn/AlN/GaN HEMTs with polarization charge induced 2DEGs is examined using simulations and experiments. Carrier removal in the unintentionally doped AlGaIn layer changes the space charge in the structure and this changes the band bending. The band bending decreases the 2DEG density, which in turn reduces the drain current in the device. The effect of the defect energy levels on

the 2DEG density is also studied. The interplay between carrier removal, mobility degradation, and the charged defects is analyzed and quantified. [C1003]

"MMIC technology at Gallium Arsenide Enabling Technology Centre"

An overview of the activities at Gallium Arsenide Enabling TEchnology Centre (GAETEC) at Hyderabad, India is being presented here. GAETEC is a vertically integrated foundry with design, fabrication, assembly, testing, packaging and module-making facilities. The technologies available for production would be described in detail, and mention would be made of those being implemented. Examples of products developed and delivered, and those under development would also be given. [C1004]

"Evaluation of RF and Logic Performance for 80 nm InAs/InGaAs Composite Channel HEMTs Using Gate Sinking Technology"

80-nm-gate In_{0.7}Ga_{0.3}As/InAs/In_{0.7}Ga_{0.3}As composite channel high-electron mobility transistors (HEMTs) fabricated using platinum (Pt) buried gate as the Schottky contact metal were evaluated for RF and logic application. After gate sinking at the 250degC for 3 minutes, the device exhibited a high gmvalue of 1590 mS/mm at V_d= 0.5 V and the current gain cutoff frequency f_T was measured to be 494 GHz. The intrinsic gate delay time was calculated to be 0.78 psec at supply voltage of 0.6 V. This is the highest f_T achieved for 80 nm gate length HEMT devices. These superior performances are attributed to the reduction of distance between gate and channel, and the reduction of parasitic gate capacitances during gate-sinking process. [C1005]

"Analytical Study of the DC Characteristics on the InAlAs/InGaAs Metamorphic HEMT with Oxidized InGaAs Gate"

The analytical model is developed to calculate the sheet carrier densities of InAlAs/InGaAs metal-oxide-semiconductor metamorphic high electron mobility transistor (MOS-MHEMT) with a thin InGaAs native oxide layer and conventional MHEMT structures. The electric field, potential, and sheet carrier density versus different position within the gate length are investigated for both structures. [C1006]

"Generation of terahertz radiation from a new InGaP/InGaAs/GaAs Double Grating Gate HEMT Device"

We observed a generation of terahertz radiation from different grating gate devices. The devices are subjected to the CW laser and then to the impulsive laser at room temperature. [C1007]

"A High Power, High Efficiency Amplifier using GaN HEMT"

A class B and a class F power amplifier are described using a GaN HEMT device. They both were designed to operate at a frequency of 1.7 GHz with the same bias conditions. The performances of each amplifier were successfully simulated and compared. A class B amplifier was physically implemented and achieved a high power-added-efficiency of 69.2%, 39.9 dBm output power and associated gain of 14.9 dB. The experimental results were in close agreement to the simulation results. [C1008]

"Negative input resistance and real-time active load-pull measurements of a 2.5GHz oscillator using a LSNA"

A large-signal measurement-based methodology to design oscillators using the Kurokawa theory is presented in this paper. Measurements of the negative input resistance and device line of a 2.5 GHz HEMT oscillator versus frequency and power, and its optimization using real-time active load-pull (RTALP) for the 2nd and 3rd harmonics are performed with a large signal network analyzer (LSNA). As a result, the maximum output power of the oscillator is increased from 31.0 mW to 38.8 mW. Finally self-oscillation is verified using a load tuner to yield an output power and frequency of oscillation in reasonable agreement with the Kurokawa analysis. [C1009]

"Monte Carlo simulation of GaN n+nn+ diode including intercarrier interactions"

Gallium nitride (GaN) is becoming increasingly more attractive for a wide range of applications, such as optoelectronics, wireless communication, automotive and power electronics. Switching GaN diodes are becoming indispensable for power electronics due to their low on-resistance and capacity to withstand high voltages. A great deal of research has been done on GaN diodes over the decades but a major issue with previous studies is the lack of explicit inclusion of electron-electron interaction, which can be quite important for high carrier densities encountered. Here we consider this electron-electron interaction, within a non-parabolic band scheme, as the first attempt at including such effects when modeling nitride devices. Electron-electron scattering is

treated using a real space molecular dynamics approach, which exactly models this interaction within a semi-classical framework. Results in particular focus on the strong effect of carrier-carrier scattering on the drain side of the gate, where rapid carrier relaxation occurs. [C1010]

"A High Isolation 0.15 μ m Depletion-Mode pHEMT SPDT Switch Using Field-Plate Technology"

A high isolation GaAs microwave switch has been successfully developed using field-plate technology, which is effective to improve the isolation. The developed wideband SPDT switch shows a greater than 40 dB isolation before 10 GHz and also achieves good performance at higher frequency. A GaAs-based pseudomorphic high electron mobility transistors (pHEMTs) in which the field-plate (FP) metal is supplied with various biases was developed and evaluated experimentally to determine their dc and rf performance. Owing to the depth modulation of the field-plate-induced depletion region at various field-plate biases, the intrinsic devices were influenced by the tunable VFP. This technique is easy to apply, based on standard p HEMT fabrication. [C1011]

"Influence of Gate Head Dimensions on the Device performance of 0.12 μ m PHEMT"

In this paper, the fabrication technology of SiN- assisted 0.12 μ m double deck T-gate AlGaAs/InGaAs p-HEMT and 60 GHz-band MMICs for high rate personal area network (WPAN) systems is described. The effect of the gate head dimension, such as the 1st-deck and the 2nd-deck gate head size, on the DC and RF characteristics of the p-HEMT device and the device performance at the optimum gate head size are also presented. At the optimum gate head size, the p-HEMT device with two finger gates of 0.12 μ m length and 50 μ m width showed an extrinsic transconductance of 511 mS/mm and a drain current of 20.6 mA at 1.5 V of drain voltage. The cut-off frequency and the maximum frequency of oscillation were 96.8 GHz and 192.6 GHz, respectively. Gate head dimensions of the p-HEMT device are correlated to parasitic capacitances, including Cgs, which effect the RF performance including a cut-off frequency (ft) and a maximum frequency of oscillation (fmax). [C1012]

"High Performance InAs-Channel HEMT for Low Voltage Millimeter Wave Applications"

An 80-nm InP HEMT with InAs channel and InGaAs sub-channels has been fabricated. The high current gain cutoff frequency (ft) of 350 GHz and maximum oscillation frequency (fmax) of 360 GHz were obtained at VDS = 0.7 V due to the high electron mobility in the InAs channel. DC and RF characterizations on the device have been performed and the on- state breakdown voltage of the device was measured to be 1.75 V. A 2-stage MMIC gain block was designed using such device. A simulated gain of better than 12 dB from 54 GHz to 71 GHz with only 14 mW DC power consumption was achieved. Such high performance HEMTs demonstrated in this study shows great potential for very low power millimeter wave applications. [C1013]

"A MMIC control chipset for T/R modules-A SiP approach"

This paper describes the design and development of S-band GaAs MMIC chipset consisting of a digital phase shifter, a digital attenuator, and a SPDT switch. The MMICs have been designed using a mature 0.5 μ m InGaAs pHEMT technology. To offer an attractive solution for phased array systems, the chipset has been integrated in a small form factor hermetically sealed metal package with plug and play features. The package design has been carried out in-house and reflects a System in Package (SiP) approach suited for high volume production. The integrated control component offers typically 9dB of insertion loss, a RMS phase error of 1.5 deg and a RMS attenuation error of 0.1 dB. The module features a high isolation of 55 dB between transmit and receive ports. The developed control module has been tested successfully in beam forming systems. The design of the constituent MMICs are presented in the initial sections followed by the description of the SiP module and the performance of the integrated entity. [C1014]

"Large-Signal Model for AlGaIn/GaN HEMT for Designing High Power Amplifiers of Next Generation Wireless Communication Systems"

In this paper, an accurate table-based large-signal model for AlGaIn/GaN HEMT accounting for trapping and self-heating induced current dispersion is presented. This model will be used for designing of high power amplifiers for next generation communication systems. The B-spline approximation technique is used for the model element derivation, which improves the intermodulation distortion simulation. The model implementation takes in to account the dynamic behavior of the trapping and self-heating processes. The model validity is verified through simulated and measured outputs of the device under pulsed and continuous large-signal excitations for 1-mm gate width devices. Single and two-tone simulation results show that the model can efficiently predict the output power and its harmonics and the associated intermodulation distortion under different input power and bias conditions. [C1015]

"Analysis of a radio frequency transimpedance amplifier based on a δ -doped AlInAs-GaInAs HEMT and its performance optimization"

A simple approach has been proposed for the optimization of performance parameters such as transimpedance-bandwidth product, transition frequency f_T and maximum frequency of oscillation f_{max} of high electron mobility transistors (HEMTs). The radio frequency (RF) small-signal equivalent circuit model has been employed to represent the ac behavior of T-shape gate AlInAs-GaInAs δ -doped HEMTs. All the circuit parameters pertaining to the model have been determined as a function of the width W of the device and surface density of charge d in the channel. Then PSpice has been used to simulate the device. Good agreement between experimental and simulated values of $|h_{fe}|^2$ versus frequency is obtained. The same model is then employed to optimize performance parameters of the HEMT and the MSM-HEMT amplifier with reference to width and surface density of charge δ in the channel. [C1016]

"Novel sloped etch process for 15nm InAlAs/InGaAs metamorphic HEMTs"

We developed a new technology that reduces gate length with modified sloped etch process to fabricate nanometer scale high-electron mobility transistors (HEMTs). The polymer deposition and Si₃N₄ etching with positive slope make this technology realizable. A HEMT with this technology has merits of both fine length definition beyond the limit of an electron beam (E-beam) lithography system and overcoming the metal filling problem caused by a high aspect ratio. Using this technology, we could get 15 nm gate length from initial 40 nm line pattern. The fabricated 15 nm InAlAs/InGaAs metamorphic HEMTs (MHEMTs) have high DC and RF performance characteristics, a transconductance of 1.6 S/mm, a cutoff frequency f_T of 580 GHz. [C1017]

"New NRZ-mode resonant tunneling bistable-to-monostable-to-bistable transition logic element operating up to 36 Gb/s"

In this paper, we present new resonant tunneling bistable-to-monostable-to-bistable transition logic element with non-return-to-zero (NRZ) mode output. The proposed circuit is composed of resonant tunneling diode (RTD)/high electron mobility transistor (HEMT) series connection (RHS) and RTD/HEMT parallel connection (RHP). Novel high-speed and low-power NRZ delayed flip-flop (D-F/F) operation has been successfully achieved using RTD/HEMT integration technology on an InP substrate. The operation of the fabricated circuit was confirmed up to 36 Gb/s with a very low power dissipation of about 3 mW at a power supply voltage of 0.9 V. [C1018]

"Gain and cut-off frequency analysis of multiple-gated AlGaAs/InGaAs HEMTs"

A small signal analysis was performed on a specific 0.2 μ m HEMT device to study the impact of multiple-gated layout towards the gain and cut-off frequency performance. The characterization process was using on-wafer measurement technique to AlGaAs/InGaAs HEMT devices which consisted of three types of layouts of various gate finger numbers and widths. The devices were biased at the optimum biasing voltage obtained from DC characterization performed previously. From the result, it was observed that the device with higher number of gates exhibited higher gain only at low frequency, while at higher frequency the gain dropped significantly. This significant drop in gain was due to the increase of the gate-source capacitance in the device, thus leading to a reduction of the device cut-off frequency. The experimental findings were strongly supported by simulation which was based on related theory on the layout dimension contribution. [C1019]

"A design of multi-GHz continuous-time bandpass filters using 0.1- μ m HEMT technology"

A multi-GHz continuous-time bandpass filter based on 0.1- μ m InP-based high-electron mobility transistor (HEMT) technology is designed. Since p-channel devices are not commonly used in HEMT technology, bootstrap current sources consisting of n-channel depletion-type HEMTs are used in the Gm-C circuit to obtain high-frequency high-gain operation. By transistor-level simulations, center frequencies of more than 10 GHz are predicted. [C1020]

"Accurate Performance Evaluation of HEMT Devices for High-Speed Logic Applications through Rigorous Device Modelling Technique"

Tremendous progress has been made recently in the research of novel nanotechnology for future nano-electronic applications. Among all the possible technologies, III-V FETs particularly the heterostructure high electron mobility transistors (HEMT) have demonstrated promising results to be the future device technology for high-speed logic applications. Precise evaluation of the delay performance for HEMT requires highly accurate intrinsic device models extracted from available measurements. In this paper, a rigorous device modelling technique based on 3-D full wave electromagnetic analysis of the device structure is presented. This technique is efficient and accurate, and the determined equivalent circuit model fits the measured S-parameter very well

within the frequency range of interest. [C1021]

"Modification of EEHEMT1 Model for Accurate Description of GaN HEMT Output Characteristics"

GaN HEMTs are promising power devices for RF and microwave power applications. However, the performance of devices can be compromised under some operating conditions by charge carrier trapping. From the device development point of view, device optimization is necessary to obtain the best possible performance. For device modeling and design purposes, the device needs to be characterized and modeled accurately in order to foresee how the device behaves under realistic operating conditions. The prediction of the device performance is also significant for the decision, whether the device is able to satisfy the requirements of the application of interest. In this paper, a modified EEHEMT1 model describing GaN HEMTs, which is capable to describe the knee region of the device's output characteristic more accurate than before, will be introduced. [C1022]

"Detector of modulated terahertz radiation based on HEMT with mechanically floating gate"

We consider a concept of a resonant detector of modulated terahertz radiation based on a micromachined high-electron-mobility transistor with a microcantilever serving as the mechanically floating gate. The device can exhibit both the plasma (in terahertz range) and mechanical (in megahertz or gigahertz range) resonances. [C1023]

"Compact Load-Coupling Network for Microwave Current Mode Class-D Power Amplifiers"

This paper presents the design and implementation of a highly efficient current-mode class D (CMCD) power amplifier (PA) using a 2W GaN HEMT device. A switched-based model was developed in-house for the commercially available GaN power device and used extensively for the analysis and the design of the CMCD PA. The compact load coupling network, comprising a load transformation network, a higher harmonic impedance termination tank and a balun, used for the 1 GHz power amplifier measures only 37 mm times 76 mm while providing suitable means for tuning the performance of the amplifier. The fabricated CMCD PA achieves a drain efficiency of 65% for an output power of around 36 dBm with more than 7.4 dB of power gain at 1 GHz. [C1024]

"Ensemble Monte Carlo Simulation of a Pseudomorphic HEMT Structure"

The paper presents an analysis of a pseudomorphic HEMT structure through an ensemble Monte Carlo simulation. The effect of velocity overshoot and real-space transfer on the device performance is investigated. The electron drift velocity drops due to the intervalley transfer in the bulk InGaAs, and real-space transfer into the surrounding lower mobility GaAs and AlGaAs layers. Depending on the gate bias, the velocity near the drain is limited by either k-space or real-space transfer. At low gate bias real-space transfer occurs, while at high gate bias intervalley transfer within the bulk InGaAs limits the carrier speeds. [C1025]

"Analytical Modeling and Simulation of Potential and Electric Field Distribution in Dual Material Gate HEMT For Suppressed Short Channel Effects"

In this paper, we present a simple 2- dimensional analytical model for exploring the novel features of the dual material gate (DMG) high electron mobility transistor (HEMT) for reduced short channel effects (SCE). The model accurately predicts the channel potential and electric field for single material gate (SMG) and DMG structures. It is seen that the work function difference of the two metal gates leads to a screening effect of the drain potential variation, by the gate near the drain resulting in suppressed drain induced barrier lowering (DIBL) and hot carrier effect. Moreover, carrier transport efficiency improves due to a more uniform electric field along the channel. The model takes into account the effects of the lengths of the two metal gates and their work function difference. The results predicted by the model are compared with those obtained using ATLAS device simulator to verify the accuracy of the proposed model. [C1026]

"PHEMT SP6T ICs for Quadband GSM Handset Applications"

An integrated circuit of quad-band GSM single pole six thru (SP6T) switch is designed with an InGaAs/GaAs PHEMT technology. It had successfully demonstrated as play for all quad-band operations (GSM850, EGSM900, DCS1800, PCS1900). Both requirements of low insertion loss (less than 1 dB) and high isolation are achieved at the same time. Some of termination methods were used to improve the isolation between Tx and Rx. [C1027]

"Kink Effect Phenomenon in I-V Characteristic of Multiple-Gated AlGaAs/InGaAs HEMTs Device"

The electrical measurement to obtain output current characteristic of 0.2 μm AlGaAs / InGaAs HEMTs device

has been performed within specific drain and gate bias voltages. The samples which consist a few layouts were designed based on different number of gate fingers to observe the effect towards the output characteristic performance. From the I_{ds} - V_{ds} characteristic, a sudden change in output current magnitude or kink effect is observed when the gate was biased at < 0.5 V. This kink effect condition was common for all layouts with different gate finger. However, the kink was so significant for device with higher gate finger. The phenomenon is due to the impact ionization in the GaAs buffer or substrate layer that allows electron trapped suddenly jump to the channel layer thus affecting the electron density magnitude in the channel. This sudden change in electron density in the channel cause the output current fluctuated and caused the kink phenomenon. The detail explanation of this phenomenon will be further discussed. [C1028]

"A Low Current Fully Integrated Front End Module On GaAs E/D p-HEMT For 2.4 GHz Applications"

The wireless world is shrinking and so is the size of all electronic wireless devices which is aggressively pushing the chip manufacturers to reduce the size and power consumption of their IC's. This work presents a similar case wherein all the blocks of a FEM are tightly integrated on a single die measuring 1500 times 1350 μm^2 using GaAs E/D p-HEMT process and packaged in 3 times 3 times 0.7 mm³ 16 lead QFN package. We have developed a compact Front End Module (FEM) for a range of wireless applications such as ZigBee, Wireless Audio Streaming and bluetooth. The FEM contains a PA, LNA and SPDT Switch which is fully integrated and matched to a 50 ohm system. In transmit chain FEM has a gain of 26.5 dB, output power 21.5 dBm at 3.3 V with 124 mA peak current and input-output return loss better than 10 dB for 24 mA of quiescent current. The receive chain has a noise figure 2 dB, gain of 15 dB, IIP3 better than 6 dBm for 8 mA of quiescent current. This integrated FEM solves the issue of integrating discrete RF components on RF board and also reduces size, cost and time to market for wireless product vendors. [C1029]

"Characterization of Electrical Memory Effects in Power Amplifier using Multi-tone Measurement"

In this paper, an efficient method to characterize electrical memory effects arising from the interaction between the static nonlinearity and the frequency response is proposed using a multi-tone measurement. A transmitter system with nonlinear power amplifier (PA) is modeled with two box Wiener structure that consists of a static Saleh model and a linear filter. A nonlinear least square method with a multi-tone measurement is used to extract frequency response and nonlinear characteristics. The proposed method is verified with a simulation and experiment with a 10W class AB gallium-nitride (GaN) HEMT PA. [C1030]

"Preamplifier for fiber-optic Millimeter wave Wireless LAN"

A preamplifier for fiber-optic millimeter-wave wireless system is presented based on a fully stabilized 0.12 μm PHEMT technology and is realized in a LTCC technology. The preamplifier is designed with parallel feedback and is minimized using inter-stage and T-section matching for chip size. The preamplifier module, in corporation of three amplifying stages, is used in microstrip line type, and shows measured transimpedance gain of 59 dB Ω and return loss of less than -5 dB with a 1 dB Ω ripple around the center frequency. [C1031]

"Newly developed chip sets for 60 GHz radio communication systems"

In order to reduce the manufacturing cost for future 60 GHz products, a high integration level is necessary. Recent results on mHEMT and pHEMT multifunctional receiver/transmitters realized at Chalmers University are reported. Multifunctional MMICs utilizing single ended, subharmonically pumped, balanced and single sideband mixers are reported. Other chipsets for additional applications such as radiometers are reported as well. Most recently, a 220 GHz integrated receiver utilizing mHEMT technology was demonstrated. [C1032]

"Improved design methodology for a 2 GHz class-E hybrid power amplifier using packaged GaN-HEMTs"

This paper reports on design methodology and realization of a class-E power amplifier (PA) for 2 GHz using a packaged GaN-HEMT. The circuit achieves 36 dBm output power and 57% PAE, with drain efficiency as high as 62%. In addition to the large-signal simulation considerations, we discuss particularly the problem of input matching of the amplifier under class-E operation. [C1033]

"Reliability of Enhancement-mode AlGaIn/GaN HEMTs Fabricated by Fluorine Plasma Treatment"

The reliability of enhancement-mode AlGaIn/GaN HEMTs fabricated by the fluorine plasma treatment technique was investigated by applying OFF-state and ON-state long-term high-electric-field stress. A moderate negative shift (-0.25 V) was observed in the threshold voltage after 288 hours of stress. This shift, however, can be

eliminated with an enhancement/depletion dual-gate configuration which effectively prevents high electric field from influencing the fluorine plasma treated area. [C1034]

"Drain Corrosion in RF Power GaAs PHEMTs"

We have investigated drain degradation in a set of experimental RF power GaAs PHEMTs. Drain degradation was observed in the form of an increase in R_{D} and a reduction in I_{max} in a variety of conditions. We found that both forms of degradation arise from surface corrosion that takes place on different locations on the drain and dominate in different regimes of operation. Specifically, the increase in R_{D} was prominent in the ON-state and was found to be associated with corrosion on the drain n-GaAs ledge. The reduction in I_{max} , in contrast, was prominent in the OFF-state and was associated with corrosion on the exposed AlGaAs barrier close to the gate. A significant finding is that in both cases, the drain-to-gate voltage emerges as a significant accelerating factor of drain corrosion. [C1035]

"Single-chip RF Front-end MMIC using InGaAs E/DpHEMT for 3.5 GHz WiMAX applications"

A single chip RF front-end MMIC is designed, developed and measured for 3.5 GHz WiMax application. The proposed MMIC integrated PA, LNA and SPDT switch by utilizing the cost-effective 0.5 μm InGaAs E/D-pHEMT process of WINs Corp.. In this paper, D-pHEMT are applied for switch designed and E-pHEMT are applied for LNA and PA design. The LNA exhibits 1.8 dB of noise figure, 16.7 dB of gain, -10 dBm of input P_{1dB} and 3 dBm of IIP3. The SPDT switch shows 0.8 dB of insertion loss, 20 dB of isolation and 27.4 dBm of input P_{1dB}. The PA demonstrates the 29dBm of output P_{1dB}, 2.7% of EVM at 24.4 dBm with 25.6 dB of gain and over 15% of PAE. To the best of our knowledge, this is the first solution on 3.5 GHz WiMax PA, LNA and SPDT switch integrated in a single chip with InGaAs E/D-pHEMT. [C1036]

"Integrated 48 GHz LO chain for 60 GHz communication systems"

A frequency doubler with pre-amplifier and driver amplifier for the LO chain of a 60 GHz communication system has been designed and tested. The circuit has been designed in conjunction with other transceiver sub-systems in the 0.15 μm GaAs pHEMT process of UMS (PH15). The measurements show good fundamental suppression of 35 dBc and an output power that can drive the co-designed mixer circuit. The doubler chain with amplifiers is approx. 3times1.3 mm, has a gain of 11 dB and a P-1dB at the output of +11 dBm. [C1037]

"5W Highly Linear GaN power amplifier with 3.4 GHz bandwidth"

In this paper, a 1 MHz to 3.4 GHz, 5 W, highly linear power amplifier based on GaN HEMT is reported. Load-pull technique has been applied to introduce a compromising solution for the PA performance trade-off problem. Over the whole bandwidth a measured small signal gain of 14 plusmn 0.7 dB and an output return loss of better than -10 dB have been achieved. The input return loss was better than -10 dB up to 3 GHz. Power and linearity performances have been measured and compared to simulations resulting in a very good agreement. At a frequency spacing of 100 kHz, minimum values of output IP3 and output IP2 have been evaluated and found to be 48.5 dBm and 59.3 dBm. At 1 dB power compression point, minimum P_{out}, and G_p were found to be 37.3 dBm and 13.3 dB, respectively within the whole frequency band. [C1038]

"Sub 50 nm InP HEMT Device with F_{max} Greater than 1 THz"

In this paper, we present the latest advancements of sub 50 nm InGaAs/InAlAs/InP high electron mobility transistor (InP HEMT) devices that have achieved extrapolated F_{max} above 1 THz. This extrapolation is both based on unilateral gain (1.2 THz) and maximum stable gain/maximum available gain (1.1 THz) extrapolations, with an associated f_T of 385 GHz. This extrapolation is validated by the demonstration of a 3-stage common source low noise MMIC amplifier which exhibits greater than 18 dB gain at 300 GHz and 15 dB gain at 340 GHz. [C1039]

"610 GHz InAlAs/In_{0.75} GaAs Metamorphic HEMTs with an Ultra-Short 15-nm-Gate"

Ultra-short-gate InAlAs/InGaAs high electron mobility transistors (HEMTs) have been successfully fabricated with nano-gate fabrication technology and epitaxial optimization. We obtained an extrinsic maximum transconductance (G_{m,max}) of 1.65 S/mm and a current gain cutoff frequency (f_T) of 610 GHz for 15-nm-gate HEMTs on GaAs substrates. Through a delay time analysis, the ultrahigh f_T of this work is explained by an enhanced average electron velocity under the gate (V_{ave}) of 4.3 x 10⁷ cm/s, which was a result of reduction of gate length (L_g) and epitaxial engineering. This report is the first experimental demonstration of 15 nm InAlAs/TnGaAs metamorphic HEMTs (MHEMTs) with an extremely high f_T of 610 GHz. [C1040]

"0.1 μm In_{0.2}Al_{0.8}Sb-InAs HEMT low-noise amplifiers for ultralow-power applications"

A 0.1 μm In_{0.2}Al_{0.8}Sb-InAs HEMT MMIC technology was developed for phased-array applications with ultralow-power and oxidation-free requirements. An In_{0.2}Al_{0.8}Sb layer was utilized to replace the upper AlSb layer in the conventional AlSb-InAs HEMT in order to mitigate the oxidation incurred by the AlSb layer. In this work, we have demonstrated excellent dc and rf performance on both devices and low-noise amplifiers (LNAs) using 0.1 μm In_{0.2}Al_{0.8}Sb-InAs HEMTs on 3-inch GaAs substrates. This accomplishment is crucial for phased-array applications with ultralow-power and oxidation-free requirements. [C1041]

"Remarkable Breakdown Voltage Enhancement in AlGa_N Channel HEMTs"

We demonstrated a remarkable breakdown voltage enhancement in a new high-electron-mobility transistor (HEMT) with a wider bandgap AlGa_N channel layer. A Si ion implantation doping technique was utilized to achieve sufficiently low resistive source/drain contacts. The obtained maximum breakdown voltage was 1650 V with a gate-drain distance of 10 μm . This result is very promising for the further higher-power operation of high-frequency HEMTs. [C1042]

"Characterisation of AlGa_N/Ga_N HEMT epitaxy and devices on composite substrates"

This paper shows results obtained on AlGa_N/Ga_N FJEMTs processed on epitaxy grown on composite substrates. The results are very promising for the fabrication of low cost high power microwave transistors for wireless communication systems. The composite substrates constitute a valuable alternative to the silicon since better thermal properties are expected. [C1043]

"High-voltage Millimeter-Wave Ga_N HEMTs with 13.7 W/mm Power Density"

Short-gate-length Ga_N HEMTs with advanced features including a field plate and an InGa_N back-confinement barrier showed excellent I-V characteristics at high voltages. A 0.4-mm wide device with 0.15- μm gate and 0.25- μm field plate operated up to 60 V and achieved 13.7 W/mm power density at 30 GHz, the highest for a FET at millimeter-wave frequencies. [C1044]

"A 9.5-10.5GHz 60W AlGa_N/Ga_N HEMT for X-band high power application"

In this paper, we report our result of a 60W AlGa_N/Ga_N HEMT with the operating frequency in X-band. The device technology is extension of well-established Eudyna commercial L-/S-band AlGa_N/Ga_N HEMT technology. The device shows output power of over 60W and a high linear gain of 9.6dB in wide frequency range of 9.5-10.5GHz, operating at 40 V drain bias voltage with the pulsed conditions at a duty of 10% with a pulse width of 100 μs . The results show the developed 60W AlGa_N/Ga_N HEMT has high power capability covering practical frequency range for X-band high power applications with proven device technology. [C1045]

"A kW-class AlGa_N/Ga_N HEMT pallet amplifier for S-band high power application"

We developed a kW-class AlGa_N/Ga_N HEMT pallet amplifier operating at S-band. The pallet amplifier consists of an internally partial-matched AlGa_N/Ga_N HEMT optimized for S-band on a copper base with soft PC boards. The developed pallet amplifier showed excellent performance, which is output power of over 800 W, high linear gain of 13.6dB and high efficiency of 52% over the wide frequency range of 2.9-3.3 GHz, operating at 65 V drain voltage with the pulsed condition at a duty of 10% and a pulse width of 200 μs . With 80 V drain voltage operation the peak power reached to 1 kW with 49.5% drain efficiency and 14.1 dB linear gain at 3.2 GHz. To the best of our knowledge, this is the highest power pallet amplifier ever reported for S-band. [C1046]

"Linearity and efficiency optimisation in microwave power amplifier design"

In this contribution the minimisation of asymmetry between lower and upper side band intermodulation products will be discussed, starting from a Volterra analysis approach. Base-band and harmonic device terminations effects will be analysed, identifying novel conditions minimising IMD asymmetry and IM3, power levels. Such conditions, not relying on base-band terminations, are the basis for IM3, products minimisation via second harmonic load selection. The proposed criterion is then verified by harmonic load-pull measurements on a Ga_N HEMT under two-tone excitation. Measurements agree with the analysis, demonstrating a null IMD asymmetry and 6 dBc increase in C/I₂, without affecting output power (34 dBm @ 1dB compression) and power added efficiency performance (65% @ 1 dB compression). [C1047]

"X-Band 11W AlGa_N/Ga_N HEMT power MMICs"

AlGaIn/GaN HEMT power MMIC which is designed in microstrip technology on Si-SiC substrate is presented in this work. The chip size is only 2.0 mm×1.1 mm×0.08 mm. The developed two-stage power MMIC operates at frequency between 9.4-10.6 GHz and delivers a pulsed output power of 11.1 W at 9.7 GHz under a drain bias of 30 V. The linear gain of the MMIC is about 10 dB which is much lower than the simulated value of 15 dB. Further optimization of the MMIC processing and circuit design is necessary to improve the performances of the MMIC. [C1048]

"Optimising AlGaIn/GaN HFET designs for high efficiency"

This paper uses measured waveforms to demonstrate how to optimise GaN HFET PA designs in order to achieve high power and high efficiency. Efficiency values of 80% were achieved at a power density of 3 W/mm². The design procedure shows how waveform engineering, i.e. a combination of RF current and voltage waveform measurements, bias control and active harmonic load-pull, allow maximum performance to be achieved. The significant role of the device output capacitance in GaN designs that utilise large voltage swings is also explained, and a simple method for limiting the effect of C_{ds} is presented. [C1049]

"Ku-band AlGaIn/GaN HEMT with over 30W"

AlGaIn/GaN high electron mobility transistors (HEMTs) were developed for Ku-band applications. The operating voltage characteristics in CW operating conditions were investigated. The developed AlGaIn/GaN HEMT with combined two dies of 12 mm gate periphery exhibits output power of over 30 W with a power added efficiency (PAE) of 12% under V_{DS} = 30 V, CW operating condition at 14.25 GHz, and a gain compression level of 3 dB. [C1050]

"2-GHz band cryogenically-cooled GaN HEMT amplifier for mobile base station receivers"

This paper presents a 2-GHz band gallium nitride (GaN) high electron mobility transistor (HEMT) amplifier cryogenically cooled to 60 K as a part of the cryogenic receiver front-end (CRFE) for mobile base station receivers. The GaN HEMT amplifier attains the output power of 3 W and the maximum power added efficiency of 62% with a 50 V drain bias for class-AB operation. The results reported herein are the first on the performance of a cryogenically cooled GaN HEMT amplifier aiming at use in a 2-GHz. band CRFE. [C1051]

"X-band Phase Shifting Power Amplifier MMIC for phased array transmit modules"

An X-band Phase Shifting Power Amplifier with six-bit phase control and 5 Watt output power has been developed and tested. The aim of the development is cost reduction for Transmit and Receive components for phased array systems. The device has been developed in the 6-inch 0.5 μm power pHEMT process (PP50-11) of WIN Semiconductors. The use of this process results in cost effective devices with a high power capability. [C1052]

"30 GHz (Ka-band) VSAT DVB-RCS Mixer-Driver multifunction MMIC"

This paper presents the design and performance of a Ka-band VSAT DVB-RCS (Digital Video Broadcast -Return Channel Satellite) Mixer Driver multifunction MMIC developed on a 0.25 μm GaAs pHEMT process. The MMIC up-converts an IF signal at 1-1.5 GHz to a +16 dBm RF output at 29.5 -30 GHz with an LO at 14.275 GHz. It is intended to be used in conjunction with an SSPA to deliver 2 Watts into the return channel VSAT antenna. A second output frequency band at 28.15 -28.65 GHz is accommodated in the MMIC. [C1053]

"High efficiency distributed amplifier using optimum transmission line"

In this paper, we performed numerical analysis on reversed current of distributed amplifier (DA) based on transmission line theory and proposed optimum transmission line (OTL) to cancel reversed currents. This OTL has improved electrical performances of DA. The distributed amplifier using optimum transmission line (DAOTL) has been implemented with pHEMT transistor. Due to high capacitance of pHEMT, cutoff frequency is decided to 3.6 GHz. As a result of measurement, we could obtain maximum gain of 14.5 dB and minimum gain of 12.8 dB in operation band. Moreover, we could PAE of 25.6% which is higher about 7.6% than the conventional DA (CDA) at 3GHz. The output power was obtained 10.9 dBm which is higher about 1.7 dB than the conventional at 3GHz. [C1054]

"High-efficiency GaN class-E power amplifier with compact harmonic-suppression network"

This paper presents a high efficiency class-E power amplifier (PA) suitable for wireless transmitters operating at 2 GHz. Compact impedance transformation network is designed, using micro-strip transmission lines, so that it

simultaneously achieves fundamental load transformation and harmonic impedance control using only two open-circuit stubs ($2f_0$, $3f_0$). The dimensions of the network's elements were determined in order to concurrently attain a high harmonic suppression, minimum loss and high power added efficiency. The measurement results of the PA prototype, which is designed using a 10 W Gallium Nitride (GaN) HEMT transistor, showed state-of-the-art drain and power added efficiency (PAE). The achieved PAE, power gain and output power, when the drain is biased at 50 V, were equal to 74%, 12.6 dB and 11.4 W respectively. In addition, a second and third harmonic suppression in excess of -40 dBc and -75 dBc, respectively, is achieved without extra circuit tuning or additional filtering. [C1055]

"GaN HEMT based Doherty amplifier for 3.5-GHz WiMAX Applications"

We have implemented a Doherty amplifier for 3.5-GHz World Interoperability for Microwave Access (WiMAX) applications using Eudyna 90-W (P3dB) Gallium-Nitride (GaN) High Electron Mobility Transistor (HEMT) because of the poor efficiency of a standard class AB amplifier when the linearity performance is good. The load modulation performance of the GaN HEMT device for the Doherty operation is rather moderate but workable. The linearity is improved using the in-band error cancellation technique of the Doherty amplifier. The implemented Doherty amplifier has been designed at an average output power of 43 dBm, backed-off about 8 dB from the 51 dBm (P3dB). For WiMAX signal with 28 MHz signal bandwidth, the measured drain efficiency of the amplifier is 27.8%, and the measured Relative Constellation Error (RCE) is -33.17 dB, while those of the comparable class AB amplifier are 19.42% and -24.26 dB, respectively, at the same average output power level. [C1056]

"Extraction of effective trap density and gate length in AlGaIn/GaN HEMTs based on pulsed I-V characteristics"

Reliability issues such as degradation of DC, transient, and RF characteristics have been intensively investigated in AlGaIn/GaN HEMT applications. The instability of AlGaIn/GaN HEMT operations is attributed to modification in electrical behavior of trapping centers induced during the material growth and device fabrication, and/or introduction of new traps, caused by electrical/thermal stress. However, it has been difficult to analyze accurate trapping density and effective gate length under device operation since electron capture and emission are varied depending on bias condition and trap position/energy level. Thus, precise monitoring methodology for trapping effects is required. In this paper, we report a simple method to extract effective trap density based on pulsed I-V measurements under different quiescent bias (QB) conditions with a very short pulse width. [C1057]

"Current collapse and reliability mechanisms in GaN HEMTs"

Current collapse and performance degradation effects remain the most serious problem in short channel GaN HEMTs with operating frequencies above 20 GHz and aggressive designs for achieving highest power levels (exceeding 6-8 W/mm). Although for lower frequency operation, significant progress in mitigating these effects has been achieved, this approach is not applicable for ultra high frequency, higher performance devices. To facilitate the development of such advanced devices, the authors propose novel model applicable to short (down to sub-100 nm) channel devices operating in high power regime. This novel model accounts for three different degradation mechanisms related to (a) current collapse, (b) gate leakage current degradation and (c) structural damage caused by high electric fields. [C1058]

"80nm In_{0.52}Al_{0.48}As/In_{0.53}Ga_{0.47}As/InAs_{0.3}P_{0.7} Composite channel HEMT with an fT of 280GHz"

We have demonstrated a high performance 80nm gate In_{0.52}Al_{0.48}As/In_{0.53}Ga_{0.47}As/InAs_{0.3}P_{0.7} composite channel HEMT. The device has a g_{mas} high as 1 S/mm and an f_T 280 GHz. To complete this study, the noise and power performance of such device will be further studied and compared with conventional InGaAs channel devices in near future. [C1059]

"Analysis of AlGaIn/GaN HEMT modulated by photosystem I reaction centers"

This paper presents for the first time a practical substitute to the laboratory (KFM) techniques for electrical characterization of PS I reaction centers which is necessary precondition to eventual commercial realization of molecular photovoltaic devices. The experimental study and an analytical model have been presented to investigate the charge effects of PS I reaction centers on the characteristics of AlGaIn/GaN high electron mobility transistor (HEMT). [C1060]

"The coming revolution in RF electronics"

This paper is about the biography of Dr. Mark J. Rosker. He joined the Rockwell Scientific Co. (RSC) in 1989. This group is well known for its pioneering development of millimeter wave quasi-optics, GaAs PHEMT and InP HEMT MMICs, photonic bandgap-based millimeter wave waveguides, and electronically scanned antenna technologies. [C1061]

"Gate I-V characteristics degradation in AlGaIn/AlN/GaN HEMTs"

AlGaIn/AlN/GaN high electron mobility transistor (HEMT) is one of the most promising device structures for high frequency power applications. Although high power density was demonstrated by number of groups [1], several unresolved issues remain. One of them is the gate breakdown under forward bias. Figure 1 shows the typical gate I-V characteristics of the devices obtained by applying voltage (V_g) between gate and drain with source floating. At certain voltage (4.5-6 V), the gate current (I_g) increases instantaneously. The change is permanent with current in both forward and reverse direction increased by several orders of magnitude. [C1062]

"Investigation of AlGaIn/GaN/AlGaIn metal -oxide-semiconductor high electron mobility transistors"

A photoelectrochemical (PEC) oxidation method was used to grow oxide films on AlGaIn surface directly as gate insulator for AlGaIn/GaN/AlGaIn metal-oxide-semiconductor high electron mobility transistors (MOS-HEMTs). The threshold voltage of AlGaIn/GaN/AlGaIn MOS-HEMT devices is -3.5 V. The gate leakage current is 1.8 times 10^{-5} A at reverse gate bias of $V_{GS} = -10$ V. Maximum value of g_{m1} is 53.8 mS/mm biased at $V_{GS} = -0.87$ V. The current collapse is not obvious in the MOS-HEMT devices. [C1063]

"A High-Sensitive Pd/InGaP transistor hydrogen sensor"

In this work, the electroless plated (EP) Pd/InGaP high electron mobility transistor (HEMT) was firstly employed for hydrogen sensing. The current-voltage (I-V) characteristics under hydrogen concentrations of 5 ppm-1% and temperatures of 303-503 K were investigated. Experimentally, the Pd gate of three-terminal devices were successfully fabricated by the electroless plating method, and the studied devices exhibited excellent current-voltage characteristics with superior current control ability. For hydrogen sensing performances, the studied EP device demonstrated low detection limit, high sensitivity, and fast response. As compared with the thermal evaporated (TE) device, larger current variations can be achieved by the EP device. Even at extremely low hydrogen concentration, e.g., 4.3 ppm H_2 /air, obvious current modulation was found. The maximum relative sensitivity reaches up to 428 % at a optimal gate voltage of -0.75 V. Furthermore, the transient detections showed that the sensing response was fairly fast, especially at high concentrations and high temperatures. At detection temperature of 403 K, the time for 90% response at 1 % H_2 /air was within 4 seconds. These excellent sensing performances of the EP device indeed made it promising and competitive in future developments of smart hydrogen sensors integrated microelectronic systems. [C1064]

"High-resolution alpha-particle spectroscopy with an hybrid SiC/GaN detector/front-end detection system"

An alpha-particle spectrometer has been assembled, consisting of an epitaxial 50 μ m thick 4H silicon carbide detector connected to a gallium nitride HEMT used as input transistor of the front-end electronics. The depleted layer of the SiC diode detector was sufficient to stop all alpha particles of the used emitter in the 4.8-MeV to 5.8-MeV energy range. An excellent energy resolution of $\sim 0.9\%$ has been obtained in this energy range at a temperature of 55degC, which is comparable to that of single-crystal diamond detectors. The energy-resolution limiting factor is found to be the dispersion of the energy loss in the gold Schottky contact, which acts as entrance window to the detector. We used a gallium nitride (GaN) front-end transistor because this material offers two important advantages against silicon: (i) it can be grown on SiC substrates so as to realize SiC/GaN integrated systems, (ii) it is a wide band-gap semiconductor and therefore is intrinsically more adequate for room and above-room temperature operation. SiC-detector spectrometers are interesting in many nuclear application where the operation environment is hostile, both in terms of ionising radiation contamination and of high temperatures. Such applications include monitoring of ionising radiations in nuclear power plants and beam diagnostic in fundamental nuclear physics experiments. [C1065]

"Impact of lateral engineering on the logic performance of sub-50 nm InGaAs HEMTs"

We have studied the combined impact of side-recess length and the gate length on the logic performance of sub-100 nm InGaAs HEMTs. We have found that increasing L_{side} significantly improves the short-channel effects and the logic performance of the device. Our experimental work confirms that lateral engineering at the drain side is essential for improving the electrostatic integrity of sub-100 nm gate length InGaAs HEMTs. The trade-off of widening L_{side} is the increase of R_s . With further device optimization in the form of reduced gate leakage current, self-aligned ohmic contacts and the development of a high performance p-channel device InGaAs-based

FETs could well be the technology of choice when the Si CMOS roadmap comes to end. [C1066]

"Application of linearization modeling technology for nonlinear RF power devices"

Based on nonlinear large-signal scattering functions theory and harmonic superposition principle, we describe a novel method to linearize the scattering function in a form that is similar with classical scatter parameter when considering the influence of the conjugate term of incident signal. Moreover, in case of weakly nonlinear device, combining phase normalization and linearization technique, we analyze the expression of linearized scattering function in polar coordinates and predict the characters of the track of reflected waves. Further examination of these characters, we prove that they are derived from the emergence of conjugate term. To testify the linearization model, we apply this linearization model technique for modeling high electron mobility transistor (HEMT) on large signal network analyzer platform. Finally, after contrasting the linearization model with classical scatter parameter model for the measurements data, we conclude with the efficiency of the model for modeling RF devices. [C1067]

"A single chip dual-band low noise amplifier"

This paper describes a dual-bands low noise amplifier design for WCDMA and WiMAX applications. The low-noise amplifier (LNA) is implemented with the proposed dual-band matching network that consists of a high-pass and low-pass ladder. The LNA is fabricated in 0.5 μm enhancement-mode pHEMT (E-mode pHEMT) technology for high linearity and low noise application. The measured noise figures (NF) and insertion gains (S21) are 1.2 dB and 16.1 dB at WCDMA band, 1.45 dB and 15.1 dB at WiMAX band. With 3-V supply voltage and 28.8-mW power consumption, the input third order intercept points (IIP3) are 6.5 dBm and 8.9 dBm for WCDMA and WiMAX, respectively. [C1068]

"Current Collapseless High-Voltage GaN-HEMT and its 50-W Boost Converter Operation"

Suppression of the on-resistance modulation caused by the current collapse phenomena in the high-voltage GaN-HEMT was successful by using dual-field plate (FP) structure and back-side FP. A 480-V/2A GaN-HEMT was designed and fabricated for power electronic applications. In this device, the on-resistance modulation was negligible as low as 5% even under an applied voltage of 300 V. Boost converter circuit was demonstrated using the fabricated device with an output power of 54 W, high power efficiency of 92.7% and high switching frequency of 1 MHz. [C1069]

"Redesign and optimization of semiconductor devices"

Recently, we have developed an automated technique for the design of random fluctuation resistant structures of semiconductor devices. This technique allowed us to recompute ("redesign") the doping profile of any general semiconductor device such as MOSFET, HEMT, SOI, etc. in order to decrease the fluctuations of device parameters induced by random doping fluctuations. In this oral presentation we present a similar optimization technique for the maximization of device performance under various constraints. The technique is based on the computation of doping sensitivity functions and the multidimensional minimization of device parameters, in which the variables are the values of the doping concentrations at each location inside the device. Constraints are taken into consideration by using the Lagrange multipliers technique. [C1070]

"2-Dimensional simulation and characterization of deep-submicron AlGaIn/GaN HEMTs for high frequency applications"

This paper presents the characterization of deep-submicron AlGaIn/GaN HEMTs for high performance applications, using ATLAS device simulator. The simulations reported in this work involve optimization of the investigated structure. The high RF performance of the device is attributed to the high quality of material and also to optimized device processing. The results are in good agreement with the experimental data as well as with the simulated data. [C1071]

"Logic Performance of 40 nm InAs HEMTs"

We have experimentally evaluated the logic performance of 40 nm InAs HEMTs. For a barrier thickness of 4 nm, we find that 40 nm InAs HEMTs exhibit excellent logic figures of merit and scalability at $V_{DS} = 0.5$ V, such as $DIBL = 80$ mV/V, $S = 70$ mV/dec, and $fT = 475$ GHz. These remarkable results arise from the combination of the outstanding transport properties of InAs channel, and the use of a thin insulator and a thin channel. In addition, these devices exhibit I_{ON}/I_{OFF} ratios in excess of 104, revealing that band-to-band tunneling is not a significant concern in our device design. Our InAs HEMTs exhibit an injection velocity at the virtual source point that is a factor of 1.6X higher than state-of-the-art Si n-MOSFETs, in spite of the significantly lower supply voltage.

[C1072]

"90 nm Self-aligned Enhancement-mode InGaAs HEMT for Logic Applications"

We have demonstrated 90 nm self-aligned enhancement mode InGaAs HEMTs with outstanding logic figures of merit. The gate-source ohmic separation was reduced to 60 nm, a 20times reduction over conventional designs. Devices in which the barrier was thinned to 5 nm by means of a dry etch had a VT of 60 mV, gm of 1.3 mS/mum, DIBL of 55 mV/V and a SS of 70 m V/dec. [C1073]

"8300V Blocking Voltage AlGaIn/GaN Power HFET with Thick Poly-AlN Passivation"

We report ultra high voltage AlGaIn/GaN heterojunction transistors (HFETs) on sapphire with thick poly-AlN passivation. Extremely high blocking voltage of 8300 V is achieved while maintaining relative low specific on-state resistance ($R_{on} \cdot A$) of 186 m Ω cm². Via-holes through sapphire at the drain electrodes enable very efficient layout of the lateral HFET array as well as better heat dissipation. [C1074]

"Normally-off AlGaIn/GaN HEMTs with InGaIn cap layer: A theoretical study"

AlGaIn/GaN high electron mobility transistors (HEMTs) are favored for the use in high-power and high-frequency applications. However, in order to successfully apply them in circuit design normally-off HEMTs are needed. Conventional normally-off HEMTs are plagued by several production and performance issues. Recently, a new approach was proposed by Mizutani et al.: a thin InGaIn cap layer introduces a polarization field, which raises the conduction band of the AlGaIn/GaN interface. As a result a threshold voltage shift to the positive direction is observed. Relying on the experimental work of Mizutani et al. we conduct a theoretical study of the proposed devices. We calibrate our simulation tool against the measured DC characteristics. Using this setup, we can further explore the device specific effects and conduct a predictive analysis of the AC characteristics. The presented methodology is a valuable tool for the design and optimization of novel devices. [C1075]

"Thermal stability of 5 nm barrier InAlN/GaN HEMTs"

In this paper, the properties of 5 nm barrier HEMT devices has been investigated in a temperature ramping experiment as used for AlGaIn/GaN devices. The pinch-off voltage remains identical and the Schottky diode leakage only marginally increased. The ohmic contacts, which have been alloyed at 850 degC by RTA show also exceptional stability. The initial alloying cycle still kept the alloy front just out of reach for high tunnelling probability. It has been moved within this distance in a very controlled way, however without degrading the contact resistance by the 1000 degC post alloying cycle. In conclusion, the InAlN/GaN heterojunction is exceptionally stable even for barrier thicknesses below 10 nm. Experiments for barrier thicknesses of approx. 2.5 nm (verified by a pinch-off voltage of -0.8 V) are presently performed and results will be reported. [C1076]

"Ultrathin MBE-Grown AlN/GaN HEMTs with record high current densities"

III-V nitride-based HEMT technology has made rapid progress over the last decade. Benefiting from the extremely high polarization charge, in this work, we demonstrate record high DC current density (2.9 A/mm) and very high extrinsic transconductance (~430 mS/mm) AlN/GaN HEMTs. [C1077]

"Two-dimensional analytical sub-threshold modeling and simulation of Gate Material Engineered HEMT for enhanced carrier transport Efficiency"

A 2- dimensional analytical sub-threshold model for exploring the novel features of AlGaIn/GaN gate material engineered (GME) high electron mobility transistor (HEMT) for reduced short channel effects (SCE) and enhanced carrier transport efficiency (CTE) is proposed. The model accurately predicts the channel potential and electric field (EF) of the conventional and GME HEMT structures. In GME HEMT, the gate is made up of two materials and the work function (WF) difference between the two gate materials results in (1) improved CTE (due to a more uniform electric field along the channel) leading to rapid acceleration of charge carriers and (2) diminished SCEs due to a step in the channel potential. The analytical results have been validated by the device simulator ATLAS. [C1078]

"Effect of the aspect ratio in AlGaIn/GaN HEMT's DC and small signal parameters"

In this work the effects of the aspect ratio (gate width/ channel length, W/L) in DC and small signal parameters of AlGaIn/GaN HEMTs are studied. An analytical model has been developed for theoretical calculation of the device DC performance at different aspect ratios. Experimental results of the fabricated AlGaIn/GaN HEMT devices are used to validate the analytical model. Numerical simulations are performed to observe the effects of

the aspect ratio on gate capacitance, transconductance and unity gain cut-off frequency. [C1079]

"AlGaIn/GaN HEMT without Schottky contact on the dry-etched region for high breakdown voltage"

The purpose of our work is to propose and fabricate a new AlGaIn/GaN HEMT without Schottky contact on the dry-etched region to decrease leakage current and to improve high breakdown voltage. The proposed device does not have any Schottky contact on the mesa etched region because the Schottky contact formation is performed prior to the mesa isolation. The measured breakdown voltage of the proposed device was 302.0 V while that of the conventional device was 70.4 V. These results show that the proposed device decrease the leakage current through the Schottky contact on the mesa-etched region. [C1080]

"A PLL-Stabilized W-Band MHEMT Push-Push VCO with Integrated Frequency Divider Circuit"

In this paper, a PLL-based stabilization technique for monolithic integrated W-band voltage controlled oscillators (VCOs) is presented. A 92 GHz push-push oscillator in coplanar waveguide technology and a frequency divider by eight were developed and integrated on a single MMIC using our established 100 nm metamorphic HEMT technology. The oscillator achieves a tuning range of 3.4 GHz around the center frequency of 92 GHz and an output power of more than 5.5 dBm. By applying this concept, the VCO was synchronized to a low frequency reference signal at 180 MHz using a commercially available PLL circuit. Compared to the free running oscillator, the phase-noise was improved by 24 dB to -77 dBc/Hz at 100 kHz offset from the carrier. [C1081]

"Degradation-Mode Analysis for Highly Reliable GaN-HEMT"

We analyzed the degradation mode of GaN-HEMTs. We observed the sudden degradation to make serious influence on the reliability. In this paper, we proposed a new approach to eliminate sudden-degradation devices. By measuring the gate leakage current before stress test, we can predict the sudden degradation. We also discussed the gate leakage current factor, for example, the surface hexagonal pits. Using this eliminating method, we could select the reliable devices with a life of over 1 times 106hours at high-temperature of 200degC. [C1082]

"Robust Extraction of Access Elements for Broadband Small-signal FET Models"

A small-signal transistor model extraction technique is proposed. It partitions access and intrinsic elements with a more accurate network for the intrinsic section. This resolves problems of nonphysical parameters and inconsistencies across bias. The technique uses low gate and zero drain bias measurements to directly determine an access network. There is no need to apply electrical stress to the device during measurement. The procedure is deterministic. [C1083]

"A New and Better Method for Extracting the Parasitic Elements of On-Wafer GaN Transistors"

By biasing the AlGaIn/GaN HEMTs with low DC gate forward current and floating drain, a new method for extracting parasitic resistances and parasitic inductances is introduced. The originality of the proposed method lies in the low DC gate forward current used for extracting R_{gnd} and L_g . While the classical method for extracting R_{gnd} and L_g uses a set of S-parameters measured under different large DC gate forward current, the proposed method uses a data set of S-parameters measured at a single low DC gate forward current. The excellent agreement between model and experimental data verify the validity of the proposed method. [C1084]

"A new physics-based compact model for AlGaIn/GaN HFETs"

A physics-based analytic model with no fitting parameters is introduced for the AlGaIn/GaN HFET. For unsaturated operation, non-linear analytic models for the I-V characteristics in the two access regions and beneath the gate are developed. The resulting equations are linked together by voltage and current continuity at the boundaries. Good agreement between the model and corresponding simulations with ATLAS, a commercial simulator, is demonstrated. In addition, the proposed model is shown to compare favorably with popular curve-fitting models of HFET operation. [C1085]

"A 2 Watt, Sub-dB Noise Figure GaN MMIC LNA-PA Amplifier with Multi-octave Bandwidth from 0.2-8 GHz"

This paper reports on a 0.2-8 GHz high dynamic range GaN MMIC LNA-PA which achieves sub-dB noise figure and a P_{1dB} of 2 watts. The GaN MMIC utilizes a 0.2 μ m AlGaIn/GaN-SiC HEMT technology with an f_T ~75 GHz. At high power bias (15 V/400 mA), the MMIC amplifier achieves sub-dB NF ~0.7-0.9 dB over a 2-8 GHz band. At low bias(12 V, 200 mA), the amplifier achieves ~0.5dB over the same band. This is believe to be the

lowest NF reported for a multi-octave MMIC amplifier in the S-and C-band frequency range. In addition, the amplifier obtains ultra high linearity with an OIP3 of 43.2-46.5 dBm and P1 dB of 32.8-33.2 dBm (2 watts) over a 2-6 GHz bandwidth. The PAE at P1 dB is ~28.6-31%. The Psat is 34.2 dBm with 39% PAE @ 2 GHz. To our knowledge, this is the first report of a multi-octave MMIC amplifier with sub-dB NF and a pout >2 Watt. [C1086]

"A Drain-Lag Model for AlGaIn/GaN Power HEMTs"

A circuit modeling drain-lag effects has been added in a non-linear electrothermal model for AlGaIn/GaN HEMTs. Modeling these trapping effects allows a better description of the I-V characteristics of measured devices as well as their large-signal characteristics. This drain-lag model is well suited to preserve the convergence capabilities and the simulation times of the non linear models of these devices. This paper presents our drain-lag modeling approach, the implementation of the model in CAD software, its operating mode, and also the parameters extraction from measurements. Then, significant comparison results will be reported on pulsed IV and large signal measurements with an AlGaIn/GaN HEMT transistor. [C1087]

"Deep-recessed GaN HEMTs using selective etch technology exhibiting high microwave performance without surface passivation"

A selective dry etch technology of GaN over AlGaIn using BCl₃/SF₆ has been applied to passivation-free deep-recessed GaN HEMTs, significantly reducing the effects of growth and process variations on the device performance, improving reproducibility and manufacturability. The effects of Si delta-doping density on the gate leakage, breakdown voltage and dispersion were investigated. Excellent microwave power performances were achieved without SiNx passivation. 6 W/mm with PAE of 72% at VD= 30 V and 11.6 W/mm with PAE of 63% at VD=50 V were demonstrated at 4 GHz, while 5 W/mm with PAE of 63% at VD= 28 V and 10.5 W/mm with PAE of 53% at VD=48 V were obtained at 10 GHz. [C1088]

"Multi-Watt Wideband MMICs in GaN and GaAs"

A comparison is presented of 4 to 18 GHz MMIC power amplifiers implemented in AlGaIn-GaN HEMT and GaAs PHEMT with common circuit design technology. Both GaN and GaAs MMICs were designed as non-uniform distributed power amplifiers and achieved approximately 4 Watts over the band. The circuit complexity of the GaAs circuit is much greater than for GaN, as shown by the relative transistor output peripheries of 14.4 mm and 2 mm. The authors believe that both the GaN and GaAs MMICs have higher power than any published result of comparable bandwidth. [C1089]

"AlGaIn/GaN HEMTs with PAE of 53% at 35 GHz for HPA and Multi-Function MMIC Applications"

We would like to report on AlGaIn/GaN HEMTs on SiC substrate with state-of-the-art power performance at Ka-band. Power gains of 5.6, 6.3 and 6.7 dB and peak PAE of 53, 53 and 51% were measured at 35 GHz when 200-μm GaN HEMTs were biased at 10, 15 and 20 volts, respectively. At 10 GHz, 400-μm GaN HEMTs exhibited maximum PAE of 67%, power gain of 11.3 dB and power density of 5.6 W/mm when devices were biased at 30 volts. Furthermore, we have also achieved 36 to 38.7 iBm TOI at a wide range of 10 to 26 dBm total output power for a 400-μm GaN HEMT. Very low noise figures of 1.4 dB at 26 GHz were measured on 100, 200 and 300-μm wide GaN HEMTs as well. In this work, we have demonstrated that GaN HEMTs on SiC substrate is a much superior device technology to GaAs-based pHEMT for microwave applications up through Ka-band. [C1090]

"Switch-based GaN HEMT model suitable for highly-efficient RF power amplifier design"

A new approach to accurately model the transistor performance in radio frequency (RF) switching-mode operation is proposed. The purpose of the presented switch-based model is to facilitate and speed up considerably extraction and implementation of large-signal device models for computer aided design (CAD). Only a small number of DC and low-frequency small-signal S-parameter measurements are required for the extraction of the complete set of element parameters of the model. Accuracy and efficacy of the nonlinear model in predicting the performance of a single-ended RF power amplifier (PA) is demonstrated by experimental results. For a PA based on a commercial GaN HEMT, measured output power and efficiency match with simulations over a broad frequency range. Moreover, robustness of the developed switch-based model is demonstrated by the design of a voltage-mode class-D PA. [C1091]

"A 2.5 Watt 3.3-3.9 GHz Power Amplifier for WiMAX Applications using a GaN HEMT in a Small Surface-Mount Package"

A 2.5 watt average power (15 watt peak power) amplifier for application with WiMAX signal protocols has been

constructed using small surface-mount GaN HEMT transistors. The GaN HEMT characteristics are uniquely suitable for producing high peak power in very small (3times3 mm) surface-mount packages. The PA produces 12.5 dB of gain over 3.3-3.9 GHz, with EVM under 2.5% with 2.5 watts average output. A design methodology for optimizing performance for the WiMAX protocol is presented. [C1092]

"Applications of GaN HEMTs and SiC MESFETs in High Efficiency Class-E Power Amplifier Design for WCDMA Applications"

This paper presents high efficiency class-E power amplifiers using wide-bandgap devices such as GaN HEMT and SiC MESFET, which are designed at WCDMA band of 2.14 GHz. The output network using transmission lines is implemented to suppress harmonics and minimize losses. Measured results of the class-E power amplifier using wide-bandgap devices for a single tone have been compared to that of the class-E Si LDMOS power amplifier. For GaN HEMT and SiC MESFET cases, the power-added efficiency (PAE) of 70% with a gain of 13.0 dB and 72.3% with a gain of 10.3 dB are achieved at an output power of 43.0 dBm and 40.3 dBm, respectively, through significant reduction of harmonic power levels. [C1093]

"An Analogue, 4:2 MUX/DEMUX Front-End MIMIC for Wireless 60 GHz Multiple Antenna Transceivers"

A front-end MIMIC (millimeter wave monolithic integrated circuit) with a 4:2 MUX/DEMUX (multiplexer / demultiplexer) functionality for 60 GHz transceiver with multiple antennas has been developed. The chip has been realized using 100 nm gatelength metamorphic InAlAs / InGaAs HEMT (high electron mobility transistor) technology on GaAs substrate together with CPW (coplanar waveguide) technology. The chip has been designed for functionality over the frequency range of 55-65 GHz. The novel topology for the MIMIC will be described. The single building blocks and details for the DPDT (double pole double throw) switch design will be explained, simulated and measured results will be compared. Finally, the overall performance for the integrated chip will be presented. [C1094]

"High Efficiency GaN HEMT Power Amplifier optimized for OFDM EER Transmitter"

We have proposed a highly efficient power amplifier (PA) for the envelope elimination and restoration (EER) transmitter using gallium nitride (GaN) HEMT. The class AB, B, C and F mode PAs have been implemented with EUDYNA's 10 watts GaN HEMT and compared the bias modulation performances in order to investigate the optimum PA structure. The proposed class F mode PA has been biased at class C and adopted a new output matching topology that improves the overall transmitter efficiency. For the WiMAX OFDM signal, the calculated overall drain efficiencies of the optimized EER amplifier, which are based on the measured bias dependent efficiencies, are about 73 % at an average power of 31 dBm at 2.14 GHz. The proposed highly efficient bias modulation PA for the EER transmitter provides a superior overall efficiency than that of any conventional switching or saturation mode PAs. [C1095]

"A Miniature 38-48 GHz MMIC Sub-Harmonic Transmitter With Post-Distortion Linearization"

This paper presents a miniature 38-48 GHz sub-harmonic transmitter with post-distortion linearization using a 0.15-μm GaAs HEMT process. The transmitter, which integrates a sub-harmonic mixer, a band-pass driver amplifier, and a linearizer, has a compact chip size of 2.5 mm² with conversion gain of 7 plusmn 1.5 dB from 38 to 48 GHz. With the features of the sub-harmonic mixer and band-pass driver amplifier, the 2fLO leakage rejection of the transmitter is 47 dB. For the linearity of the transmitter, a post-distortion linearizer is added. After linearization, the output spectrum re-growth can be suppressed by 8 dB at 40 GHz. To keep ACPR below -35 dBc, the output power has been increased from -2 to 1 dBm, which means the linear output power has been doubled after linearization. [C1096]

"A K-band low cost plastic packaged high linearity Power Amplifier with integrated ESD protection for Multi-band Telecom applications"

The design and performance of cost effective packaged linear power amplifier in K-band is reported in this paper. Based on a specific characterizations and model developments done on a standard 6-inch 0.15-μm GaAs power pHEMT technology, a high linearity-oriented design has been done and is described. Thanks to this work, excellent linearity performances have been achieved. This power amplifier exhibits 19 dB linear gain in the 17 to 27 GHz frequency band with 28.5 dBm CW output power at 1 dB gain compression and 29.5 dBm in saturated mode. The output referred third-order intercept point (OIP3) exceeds 38 dBm over the whole frequency band. As this amplifier was developed and was proposed in SMD package (standard 32L-QFN5X5 plastic molded package), it integrates an on-chip ESD protection. This makes this component easy to use in

standard SMT assembly lines and significantly contributes to the reduction of the overall module cost. [C1097]

"A High Power and High Breakdown Voltage Millimeter-Wave GaAs pHEMT with Low Nonlinear Drain Resistance"

A new GaAs pHEMT structure, which has achieved both high power density and high breakdown voltage for millimeter-wave amplifiers, is presented. According to the nonlinear drain resistance model previously proposed, we have adopted a "Stepped Recess" structure, which includes a GaAs buried layer 150 nm thick to reduce the nonlinear drain resistance and a recessed area at the gate side to control the gate leakage current. Consequently, even at the 2.0 μm width of the gate-to-drain separation, the developed pHEMT has showed a high power density of 0.65 W/mm in the Ka band, and high on-state breakdown voltage of over 30 V at once. In addition, the proposed nonlinear drain resistance model effectively explains this power performance. [C1098]

"Advances in Microwave Technology for the MESSENGER Mission to Mercury"

The MESSENGER spacecraft, designed to orbit the planet Mercury, uses the first electronically scanned phased-array antenna for a deep-space telecommunication application. Two lightweight phased arrays, mounted on opposite sides of the spacecraft, provide the high-gain downlink coverage. Medium-gain antennas are used for uplink and downlink during cruise phase. The invention of a method for achieving circular polarization in a high-temperature (+300degC) environment has doubled the science return of the mission relative to the inherent linear polarization from a slotted waveguide array. Monolithic microwave integrated circuits and discrete heterostructure field effect transistors are integrated to provide the high-efficiency X-band solid-state power amplifier. [C1099]

"Overcoming pHEMT Linearity Dependence on Fundamental Input Tuning by Digital Pre-Distortion"

In order to achieve highest possible gain and lowest input reflection coefficient, a conjugate match at the input of power transistors is desired. Unfortunately, as will be shown in this paper, such an input termination is not adequate for best linear performance of pHEMT power transistors operated in class AB. Therefore, these parameters need to be traded off against each other, if the device is used as a stand alone amplification stage. The use of digital pre-distortion allows operation of the transistor at best gain, input return loss, and linearity simultaneously. [C1100]

"High Gain, High Efficiency 12V pHEMT Power Transistors for WiMAX Applications"

The combination of Freescale's production pHEMT process with a self-aligned field plate, creates a device technology that delivers high gain and efficiency while meeting WiMAX linearity requirements. Compared to the standard production process, field plate devices show gain improvement of about 3 dB while other important device parameters such as power density, linearity, and efficiency are maintained. To demonstrate the improved performance of the field plate technology, three devices with total gate width of 7.2 mm, 14.4 mm, and 25.2 mm were designed and evaluated using a 64 QAM OFDM signal at 3.55 GHz. The devices delivered power of 28.5 dBm, 31.2 dBm, and 33 dBm, respectively, while meeting an EVM linearity requirement of 3%. [C1101]

"A new nonlinear HEMT model allowing accurate simulation of very low IM3 levels for high-frequency highly linear amplifiers design"

Today, confident design of highly linear MMICs is of primary concern for high-frequency applications. Unfortunately, at high frequencies and low output powers, accurate prediction of intermodulation distortions fails with most of the available HEMT models due to nonlinearity extractions based on CW S-parameter measurements at DC bias points or low RF frequency measurements. In this paper, we propose a suitable HEMT model, extracted from pulsed I/V and pulsed S-parameter measurements over a wide frequency range, which allows accurate prediction of intermodulation distortions at both high frequencies and large output power range. [C1102]

"A Bandpass $\Delta\Sigma$ DDFS-Driven 19GHz Frequency Synthesizer for FMCW Automotive Radar"

A 19GHz frequency-modulated continuous-wave TX based on a bandpass $\Delta\Sigma$ DDFS-driven RF frequency synthesizer is presented. Implemented in a 0.25 μm SiGe process, the synthesizer draws 63mA from a 2.5V supply while achieving a 512MHz FM deviation with a 200Hz FM rate at a center frequency of 19GHz. The measured phase noise of the frequency synthesizer is -113.68dBc/Hz at 1MHz offset frequency from a 19GHz carrier [C1103]

"Vertical device operation of AlGaIn/GaN HEMTs on free-standing n-GaN substrates"

We report on the demonstration of normally off and normally on vertical AlGaIn/GaN high electron mobility transistors (HEMTs). The normally off device shows the threshold voltage of 1.6 V. The normally on device shows the normalized on resistance of 1.48 m Ω -cm² and the maximum drain current density of 3.9 kA/cm². Before then, the dependence of threshold voltage on the thickness of n-GaN in the structure of AlGaIn/n-GaN/p-GaN was studied experimentally. [C1104]

"Advanced MMIC for Passive Millimeter and Submillimeter Wave Imaging"

Passive millimeter wave imaging systems above 100GHz have traditionally relied on mixer front-ends. InP HEMT low-noise amplifiers are reported for considerably higher frequencies, including a 70nm gate cascode amplifier with gain well into the 100GHz range, and two 35nm gate amplifiers operating at ~300GHz. [C1105]

"Accurate Modeling of Drain Current Derivatives of MESFET/HEMT Devices for Intermodulation Analysis"

An alternative technique for modeling MESFET's for calculation of intermodulation responses is presented. This algorithm not only characterizes the I/V characteristics of the device, but also the derivatives are accurately modeled. The method proposed utilizes a feed-forward neural network using the back-propagation method with the Levenberg-Marquardt (LM) algorithm. The advantage of this technique is that it can be used for both MESFET and HEMT devices. Furthermore, the need to extract fitting parameters is not required. This approach is truly independent of device process and technology, and can therefore be applicable to FET devices from SiC, GaN, GaAs and InP. Excellent agreement is observed between the neural network model and measured I/V data and I/V derivatives up to the 8th order. The I/V derivative evaluation was performed in Agilent's Advance Design Systems. [C1106]

"A Four-Resonant-Tunneling-Diode (4RTD) NAND/NOR Logic Gate"

A NAND/NOR logic gate using four resonant-tunneling diodes (RTD's), which is introduced by the analogy of RTD current-voltage characteristics to those of superconducting Josephson junctions (JJ's), has been investigated. The NAND/NOR function is obtained by a simple configuration consisting of four RTD's without using any conventional transistors, such as HEMT's or HBT's. The operation principle is analyzed by a graphical method, and a condition required for a normal logic operation is clarified. A NAND/NOR circuit was fabricated by using an InP technology. The experimental result agrees well with our circuit simulation [C1107]

"Temperature and Voltage Dependent RF Degradation Study in Algan/gan HEMTs"

The reaction-diffusion limited trap generation model used to explain MOSFET degradation has been applied to GaN HEMT degradation. An analytical expression to describe the time dependence of RF output power has been derived based on this model. In addition, the voltage and temperature dependence of the fitting parameters have been determined. [C1108]

"60 GHz Amplifier MMICs and Module for 60 GHz WPAN System"

This paper introduces the design and the implementation of the 60 GHz amplifier MMICs and the module for the 60 GHz WPAN system with a RoF (radio-over-fiber) link. The MMICs were designed using ETRI's 0.12 μ m GaAs PHEMT 4-inch process. The MCLFs (microstrip coupled line filters) compared with the MIM (metal-insulator-metal) capacitors have greater stability and less effect by the variation of fabrication. The 60 GHz drive amplifier MMIC and the 60 GHz power amplifier MMIC were designed by 4-stage structures using the MCLFs instead of the MIM capacitors for unconditional stability of the amplifiers and yields enhancement. The fabricated 60 GHz drive amplifier (DA) MMIC achieves a small signal gain (S₂₁) of 22 dB, a gain flatness of 0.8 dB, an input reflection coefficient (S₁₁) of -12 ~ -9 dB and an output reflection coefficient (S₂₂) of -10 ~ -7 dB for 59.5 to 60.5 GHz. The fabricated 60 GHz power amplifier (PA) MMIC achieves an S₂₁ of 15 dB, a gain flatness of 0.04 dB, an S₁₁ of -12 dB, an S₂₂ of -12 ~ -11 dB and an output P_{1dB} of more than 14 dBm for 59.5 to 60.5 GHz. The chip sizes of the DA and the PA are 3.8 times 1.6 mm² and 3.7 times 1.6 mm², respectively. The waveguide-typed module was implemented with a DA MMIC and a PA MMIC. And it performed an S₂₁ of 38 ~ 39 dB, a gain flatness of 1.2 dB, an S₁₁ of -29 ~ -26 dB, an S₂₂ of -16 ~ -14 dB and an output P_{1dB} of 12.3 ~ 14.3 dBm for 59.5 to 60.5 GHz. And the size of the module is 8.0 times 6.0 times 2.3 cm³ [C1109]

"Novel IR Photodetectors Based on GaN/AlGaIn HEMT with QWs or QDs in the Barrier"

We present results of computation of electron energy levels in GaN/AlGaIn QWs and QDs embedded in the

barrier of HEMT structures. Wurtzite materials and, in addition 3-d confinement for QDs, cancel polarization limitations regarding the light absorption. Computations are performed with the help of envelope functions for the QWs and of a pseudopotential method for the QDs. Very small dots are considered (with a height of 5 Ga layers) that can be achieved using Volmer-Weber formation mechanism. Electron intersubband optical transitions reach middle- and near-infra-red regions. [C1110]

"Restrictions in Using Large Signal and Small Signal Models of FET Transistors"

A frequency doubler from 8.5 to 17 GHz was used to study reliability and accuracy of large signal Curtis Cubic model of HEMT transistor. Excelics EPA018A-70 was used for the tests. Two large signal designs and realizations for working points in class B and open state (near I_{dss}) were made. Another design based on measured small signal s-parameters only was done for comparison, too. AWR Microwave Office was used for simulations. All designs were realized and measured. Significant discrepancies between simulated and measured parameters for Curtis Cubic model operated in class B were observed. [C1111]

"Broadband Medium-Power Transistor Amplifier 12-18 GHz"

A medium-power two-stage transistor microwave amplifier for frequency band of 12 to 18 GHz using eight packaged HEMTs has been designed and developed. Gain over 16 dB, output power $P_{1db} > 22$ dBm and return loss better than 10 dB both on the input and output has been achieved in the whole band. The input and output are DC grounded to protect the amplifier from electrostatic discharge (ESD). Mutually linked AWR microwave office circuit simulator, 3D EM field simulator CST microwave studio and precise small-signal s-parameters vector measurements were used for the design. [C1112]

"Non Linear RF Device Characterization in Time Domain using an Active Loadpull Large Signal Network Analyzer"

Over the last years, there is an increasing need to know and characterize the non linear behaviour of most high frequency semiconductor devices. For that, a new and original automatic active load-pull system based on a large signal network analyzer is presented which allows to carry out an accurate non linear characterization with very high load reflection coefficient (more than 0.96) under microwaves probes. After describing the setup and the calibration procedure, a dedicated study has been performed in order to validate the active load-pull system and to know and evaluate the good accuracy of non linear measurements. At non linear model of AlGaIn/GaN HEMT device has been established in order to compare measurements and simulations. [C1113]

"1.8 dB insertion loss 200 GHz CPW band pass filter integrated in HR SOI CMOS Technology"

Today, measurement of 65 nm CMOS [Dambrine, G., et al., 2005] and 130 nm-based SiGe HBTs [Chevalier, p. et al., 2004] technologies demonstrate both f_T (current gain cut-off frequency) and f_{max} (maximum oscillation frequency) higher than 200 GHz, which are clearly comparable to advanced commercially available 100nm III-V HEMT. This increase allows new millimeter wave (MMW) applications on silicon. One of the success keys is then the passive integration. In this paper, on-chip coplanar waveguides (CPWs), which have been achieved in STMicroelectronics advanced nanometric RF CMOS High Resistivity (HR) SOI ($\rho > 1$ k Ω cm) process, and characterized up to 220 GHz are reported. Moreover, for the first time passive circuits working @ 220 GHz have been achieved and characterized demonstrating state-of-the-art performances and good agreement with electric simulations using developed models. [C1114]

"WE2A: Low Noise CMOS and Low Power HEMT Technologies"

First Page of the Article [C1115]

"High-power III-Nitride Integrated Microwave Switch with capacitively-coupled contacts"

We fabricated novel monolithically integrated microwave switch using AlGaIn/GaN heterojunction field-effect transistors (HFET) without ohmic contacts. All three electrodes: source, gate and drain, formed by capacitively coupled contacts (C3) to the 2D channel. The C3HFETs do not require annealed contacts and hence can be fabricated using alignment-free technology. This makes them ideally suitable for microwave ICs. C3HFETs have much higher RF switching powers. In the frequency range 1...10 GHz the switch IC shows -1 dB insertion loss, the isolation -30 dB and the switching powers +39 dBm (limited by the available RF power source). [C1116]

"A 40-GHz MMIC SPDT Bandpass Filter Integrated Switch"

Stepped-impedance resonators (SIR) with HEMTs loaded at one end are used to develop a 40 GHz MMIC

SPDT filter integrated switch. The HEMTs are used to switch the resonant frequencies of the loaded stepped-impedance resonators. At on-state, the resonators resonate at the same center frequency to pass the RF signal. With the coupled-resonator filter theory, the filter response could be easily designed and synthesized. At off-state, the resonant frequencies of the resonators between input and output ports are staggered to block the RF signal. In this paper, a compact 40-GHz MMIC single-pole-double-throw (SPDT) switch with integrated a third-order bandpass filter is demonstrated. At thru-port, a bandpass filter response with measured insertion loss of 3.1 dB at the center frequency is obtained. At the isolated-port, an isolation of higher than 30 dB is also obtained. The proposed circuit successfully combines an SPDT switch and a bandpass filter into a single circuit component, and makes a high level of MMIC integration become possible. [C1117]

"Manufacturable and Reliable 0.1 μm AISb/InAs HEMT MMIC Technology for Ultra-Low Power Applications"

This paper describes a manufacturable and reliable 0.1 μm AISb/InAs MMIC technology for ultra-low power applications. AISb/InAs HEMTs have been demonstrated with only one-tenth power dissipation of conventional InAlAs/InGaAs/InP HEMTs. The uniform DC and RF performance of AISb/InAs HEMTs have been demonstrated on 3-inch GaAs substrates. The further demonstration of reliable AISb/InAs HEMT technology warrants the successful insertion of AISb/InAs HEMT MMICs for military and space applications with ultra-low power requirements. [C1118]

"Voltage Dependent Characteristics of 48V AlGaIn/GaN High Electron Mobility Transistor Technology on Silicon Carbide"

Gallium nitride based HEMTs are a promising technology for high voltage, high power, high frequency applications. In addition to the potential for high operating voltage, this technology may also be suited for applications that utilize modulation of the drain voltage to improve overall amplifier efficiency. RFMD has developed a GaN HEMT technology platform on semi-insulating SiC substrates. This technology includes a 0.5 μm gate process and advanced field plate designs to maximize device performance. We report on devices from this technology, operated over a range of drain bias conditions. Performance and reliability results illustrate the compatibility of this device technology for high voltage and variable voltage applications. [C1119]

"Single-chip Dual-Mode Power Amplifier MMIC using GaAs E-pHEMT for WiMAX/WLAN Applications"

A single-chip dual-mode power amplifier monolithic microwave integrated circuit (MMIC) operating at 5 V single supply has been developed for both WLAN 2.45 GHz IEEE 802.11b/g and WiMAX 3.5 GHz IEEE 802.16d WiMAX standards applications. The PA MMIC utilizes the GaAs E-pHEMT process (enhancement-mode pseudomorphic high electron-mobility transistor) of WINs Corp.. The PldB of dual-mode power amplifier are 30 dBm at 3.5 GHz and 27 dBm at 2.45 GHz. In WiMAX mode, under WiMAX IEEE 802.16-2004 OFDM modulation the EVM(error vector magnitude) is 2.7% at 24.4 dBm Pout with 25.6 dB of gain and over 15% of PAE (power added efficiency). In WLAN IEEE 802.11g mode, under OFDM 64 QAM/54 Mbps modulated signal the PA is 2.5% of EVM at 19 dBm Pout with 21 dB of gain. The dual-mode PA chip is implemented as a two-stage structure integrated with broad-band input-matching and inter-stage matching networks and external dual-band output-matching network. [C1120]

"Survivability of AlGaIn/GaN HEMT"

Using harmonic balance simulations, we have examined the survivability limiting mechanisms of a 0.2 μm T-gate AlGaIn/GaN HEMT device under RF overdrive. Simulations are performed using a 4-finger 200 μm AlGaIn/GaN HEMT device model. Two catastrophic failure mechanisms are identified. At low quiescent drain-source voltages (<10 V), the forward turn-on of the gate diode may exceed the burnout limit, resulting in a sudden failure. Increasing the quiescent drain-source voltage increases the peak drain-gate voltage and changes the failure mechanism to gate-drain reverse breakdown. The model is consistent with experimental measurements. [C1121]

"Metamorphic H-Band Low-Noise Amplifier MMICs"

In this paper, we present the development of H-band (220 -325 GHz) low-noise amplifier MMICs for use in next generation high-resolution imaging systems. The amplifier circuits have been realized using an advanced 70-nm InAlAs/InGaAs based metamorphic high electron mobility transistor (MHEMT) technology. Furthermore, airbridge type transmission lines (ABTL) and conductor-backed coplanar circuit topology (CBCPW) were applied, leading to a compact chip size and excellent gain performance at high millimeter-wave frequencies. A realized four-stage

ABTL low-noise amplifier circuit exhibited a small-signal gain of more than 18 dB between 216 and 238 GHz, while a four-stage coplanar LNA MMIC achieved a linear gain of 15 dB at 225 GHz and more than 12 dB over the bandwidth from 217 to 245 GHz. [C1122]

"A 245-GHz MMIC Amplifier with 80- μ m Output Periphery and 12-dB Gain"

In this paper we present a MMIC amplifier which demonstrates ~12-dB gain at a center frequency of 245-GHz. The MMIC is intended to demonstrate the potential of power amplification at short-millimeter wave frequencies. Each stage of the three stage amplifier utilizes a 1:2 output split to reach a total output periphery of 80- μ m. The combination of high realized gain per stage and output periphery indicate the potential generating output powers on the order of several mW at short mm-wave frequencies using MMIC amplifiers for the first time. The amplifier is implemented in coplanar waveguide and uses an InP HEMT process with a 35-nm gate. [C1123]

"An Analytical Model and Measurement on the InAlAs/InGaAs High-Electron-Mobility Transistor with Oxidized InAlAs Gate"

The analytical model and measurement of InAlAs/InGaAs metal-oxide-semiconductor high-electron-mobility transistor (MOS-HEMT) lattice-matched to InP substrate with a thin InAlAs native oxide layer are compared and achieved a good agreement, which show the validity of the proposed MOS-HEMT model. [C1124]

"Characteristics of 80 nm T-Gate Metamorphic HEMTx with 60 % Indium Channel"

The 80 nm T-gate metamorphic high electron mobility transistors (MHEMTs) with 60% indium channel have been fabricated and the DC, microwave, and uniformity of the device were characterized. The MHEMT device showed the DC characteristics having an extrinsic transconductance of 1150 mS/mm and a gate breakdown voltage of -6.2 V. The fT and f_{max} obtained for the 80 nm times 100 μ m MHEMT device are 235 GHz and 290 GHz, respectively. The MHEMT exhibited uniform threshold voltage of -0.47 V with a standard deviation of 0.045 V across the wafer. [C1125]

"(Cl₂:Ar) ICP/RIE Dry Etching of Al(Ga) Sb FOR AlSb/InAs HEMTs"

Dry etching of AlSb and Al_{0.80}Ga_{0.20}Sb has been performed by inductively coupled plasma/reactive ion etching based on a (Cl₂:Ar) gas mixture without addition of BCl₃. The dry etch process has been used to fabricate AlSb/InAs high electron mobility transistors isolated by a shallow mesa. Good DC/RF results, with extrinsic fT/f_{max} = 135/105 GHz, have been measured for a 2times50 μ m HEMT with a gate length of 295 nm. [C1126]

"Evidence of Existence of Different Surface States in INP-Based High Electron Mobility Transistors (HEMTs)"

-We have provided direct evidence of the existence of two different kinds of surface traps in InAlAs/InGaAs high electron mobility transistors through measurement of the device transient drain current. The mechanisms that were responsible for the observed drain current transient at different gate voltages have been proposed. In addition, two different kinds of interface traps with distinct time constants have been measured. [C1127]

"DC and RF Performance of 0.2-0.4 μ m Gate Length InAs/AlSb HEMTs"

InAs/AlSb HEMTs with gate lengths in the range 225-335 nm processed on the same wafer have been investigated with respect to DC and RF performance. While the magnitude of the transconductance g_m was similar for all gate lengths, the shortest gate length HEMT exhibited the highest extrinsic maximum frequency of oscillation f_{max} and extrinsic current gain cut-off frequency fT of 115 GHz and 165 GHz, respectively. [C1128]

"High Performance and High Reliability of 0.1 μ m InP HEMT MMIC Technology on 100 mm InP Substrates"

Uniform millimeter wave 0.1 μ m InP HEMT MMICs (Ka-band, Q-band, W-band, and distributed amplifiers) on 100 mm InP substrates have been demonstrated. Moreover, high performance and high reliability have been achieved. The results indicate that the readiness of 100 mm InP HEMT technology for insertion to support military/space applications. [C1129]

"InP-HEMT-TIA with Differential Optical Input Using Vertical High Topology Pin-Diodes"

A monolithically integrated combination of high electron mobility transistors and high responsivity (1.0 A/W) vertical pin-diodes have been used in optical synchronous quadrature phase-shift keying transimpedance

amplifier design for 40 Gbit/s transmission. [C1130]

"Optical Response of InP-based High-Electron Mobility Transistor and its Applications to High-Speed Photo-Detectors and Signal Converters"

The increases of drain current, small signal gain, and gate capacitance in InP-based HEMTs were observed clearly by irradiating a 1550 nm focused laser beam onto their surface. They lead to high-speed photo-detectors and signal converters. [C1131]

"Self Oscillation of the Plasma Waves in a Dual Grating Gates HEMT Device"

We report on the photoresponse and emission measurements of the dual grating gates HEMT. An emission of terahertz radiation at room temperature has been detected by a Silicon bolometer. The signal was attributed to the self oscillation of the plasma waves. [C1132]

"65 nm HR SOI CMOS Technology: emergence of Millimeter-Wave SoC"

Today, measurement of 65 nm CMOS and 130 nm-based SiGe HBTs technologies demonstrate both f_{tau} (current gain cut-off frequency) and f_{max} (maximum oscillation frequency) higher than 200 GHz, which are clearly comparable to advanced commercially available 100 nm III-V HEMT. Consequently, the integration of full transceiver at 60 GHz has been achieved both in SiGe bipolar and CMOS technology. In the same time passive circuits working at 220 GHz have been achieved and characterized on high resistivity SOI demonstrating state-of-the-art performances and good agreement with electrical simulations using developed models. Moreover, HR SOI has also demonstrated some advantages concerning the performances of integrated antennas and a first fully integrated prototype with amplifier, filter and antenna has already been achieved using STMicroelectronics 130 nm CMOS HR SOI technology. This paper will review the MMW performances of STMicroelectronics 65 nm CMOS HR SOI technology from device up to circuit level and discuss the opportunities of MMW SoC integrated on CMOS HR SOI technology. [C1133]

"A Single Chip 802.11abgn Enhancement Mode PHEMT MMIC with dual LNAs, Switches, and Distortion Compensation Power Amplifiers"

An enhancement mode PHEMT MMIC with integrated dual low noise amplifiers, dual switches, and dual distortion compensation power amplifiers is presented. It is used in an 802.11abgn FEM (front end module) which further integrates the antenna diplexer, LNA post filters, PA pre-filters, and baluns. The LNAs provide less than 1.2 dB noise figure in the 2.4/5-6 GHz receive chains at 16 dB gain and 10 mA. The switches can handle up to 30 dBm peak power with less than 1.4 dB loss and with 25 dB isolation. The power amplifier section provides fully matched 26 dB gain with 25 dBm of saturated power. In the 802.11g 2.4GHz transmit mode the MMIC gives over 20 Bm linear power out under 54 Mbps OFDM, at 4% EVM, while drawing only 123 mA of peak current. In the 802.11 a 5-6 GHz transmit mode the MMIC gives over 20 dBm linear power out under 54 Mbps OFDM at 6% EVM while drawing 149 mA of peak current. The MMIC has integrated all control functions for power down and mode select; while the power amplifiers have integrated directional couplers and temperature compensated power detection. This is the highest integration and performance level combination known to be published for 802.11abgn application specific integrated circuits. [C1134]

"1-Watt Conventional and Cascoded GaN-SiC Darlington MMIC Amplifiers to 18 GHz"

A 0.2 μm T-gate GaN-SiC HEMT technology with f_T -70 GHz are used to achieve GaN Darlington MMIC Amplifiers with bandwidths up to 18 GHz. Both conventional Darlington and Cascoded-Darlington feedback designs were fabricated and measured. The Darlington Cascode obtains 14.7 dB gain and a bandwidth of 0.05-12.3 GHz. The conventional Darlington obtains 11 dB gain and a record 0.05-18.7 GHz multi-decade bandwidth for a GaN Darlington. These are the highest BWs reported for GaN Darlington MMIC amplifiers. In addition, $P_{1\text{dB}} \sim 1$ Watt and > 40 dBm OIP3 was obtained beyond 4 GHz. To our knowledge, these results represent the widest bandwidths so far demonstrated for fully monolithic GaN Darlington MMICs. [C1135]

"A Spectrally pure 5.0 W, High PAE, (6-12 GHz) GaN Monolithic Class E Power Amplifier for Advanced T/R Modules"

This paper introduces a new highly efficient broadband monolithic class-E power amplifier utilizing a single 0.25 μm times 800 μm AlGaIn/GaN field-plated HEMT producing 8 W/mm of power at 10.0 GHz. The HPA utilizes a novel distributed broadband class-E load topology to maintain a simultaneous high PAE and output Power over (6-12 GHz). The HPA's peak PAE and output power performance measured under three pulsed drain voltages at 7.5 GHz are: (67%, 36.8 dBm @ 20 V), (64%, 37.8 dBm @ 25 V) and (58%, 38.3 dBm @ 30 V). The new

broadband load also provides a spectrally pure output power response under CW and pulsed modulated RF input conditions. The HPA spurious free performance is evident from its low AM and PM noise figures of <-125 dBc at 10 KHz from carrier and <-130 dBc at 15 KHz from 10 GHz respectively. To the best of our knowledge, this is the highest ever reported performance for a high power, 6-12 GHz GaN class-E power amplifier. [C1136]

"A new Linearization technique of Power Amplifier"

The linearity of the wireless communication circuits became more important with the progress of the communication technology. The nonlinearity of the power amplifier (PA) in the wireless communication circuits can directly lead to nonlinearity of circuit system, so it is important to use linear modulation techniques to improve the nonlinear distortion of PA. This paper describes a novel approach of using a diode as an active linearizer to minimize nonlinear distortion. In case of pHEMT, this technique reduces the effect of nonlinearities in power amplifiers due to voltage variable input capacitance. [C1137]

"0-80GHz 0.15 μ m GaAs PHEMT Distributed Amplifier for Optic-Fiber Transmission Systems"

In this paper, the available gain of 7.7 dB with bandwidth over 80 GHz distributed amplifier based on OMMIC 0.15 μ m GaAs PHEMT is presented. The cascode structure is adopted to enhance the bandwidth and to keep the circuit stability. The circuit includes four cascode cells, and the area of chip is 2.240.7 mm². [C1138]

"Direct Extraction Techniques for Thermal Resistance of MESFET and HEMT Devices"

A simple technique for direct extraction of junction temperature and thermal resistance for MESFET and HEMT FET is proposed and experimentally evaluated. The techniques were applied for thermal resistance extraction of the mHEMT devices in a microstrip three-stage amplifier before and after flip chip assembly. [C1139]

"The Present State of the Art of Wide-Bandgap Semiconductors and Their Future"

This paper summarizes recent improvements in the performance and reliability of microwave and millimeter-wave wide-bandgap gallium nitride on silicon carbide devices and their promise for future integrated circuits. Many recent advances have been made as a result of the on-going Phase II wide band gap semiconductor for RF applications (WBGs-RF) program funded by the Defense Advanced Research Projects Agency (DARPA). During Phase II of the program, significant progress has been made toward realizing wide-bandgap devices that provide outstanding performance at reliability levels that will allow their use in a wide variety of high power applications. [C1140]

"Planar Two-dimensional Electron Gas (2DEG) IDT SAW Filter on AlGaIn/GaN Heterostructure"

Surface acoustic wave (SAW) filters using two-dimensional electron gas (2DEG) as interdigital transducers (IDT) on AlGaIn/GaN heterostructure has been demonstrated for the first time using a fluoride-based (CF₄) plasma treatment technique. The CF₄ plasma treatment is used to pattern 2DEG IDT on a planar surface without removing the top AlGaIn layer. The RF characteristics of the SAW filters with planar 2DEG IDTs are compared with metal IDT SAW filters. It is shown that the massloading effects and the triple-transit-interference (TTI) are suppressed in the 2DEG IDT SAW devices owing to the removal of the metal IDTs. It is capable of reducing not only the passband ripple, but also the size of devices because 2DEG IDTs can be placed closer. In addition, the detection part of the SAW sensor can be performed on the top of the planar 2DEG IDTs rather than in the SAW propagation path. This novel SAW device can be integrated with high-electron mobility transistors (HEMTs) on AlGaIn/GaN heterostructure to deliver a viable approach for single chip GaN wireless sensors. [C1141]

"Technology for Submillimeter Astronomy"

Despite about three decades of progress, the field of submillimeter astronomy remains quite challenging, because the detection technology is still under development and the transmission of the atmosphere is poor. The latter problem has been overcome by constructing submillimeter telescopes at excellent sites, first on Mauna Kea and later in Chile and Antarctica, and also by using airborne and space telescopes. Meanwhile, the improvements in technology over the past several decades have been remarkable. While considerable opportunities for improvement remain, existing detector and receiver technologies now often approach fundamental limits. This technological revolution has brought submillimeter astronomy from the fringes to the forefront of modern astrophysics and has stimulated major investments such as the 50-element ALMA interferometer and the ESA/NASA Herschel Space Observatory. [C1142]

"A Broadband Frequency Sixtupler MIMIC for the W-Band with >7 dBm Output Power and >6 dB

Conversion Gain"

We demonstrate the circuit concept and performance of a broadband six-fold frequency multiplier for the W-band. The MIMIC, realized in a 100 μm metamorphic HEMT technology, combines an active single-ended to differential converter with balanced tripler and doubler stages. The novel doubler stage design employs a cascode topology. The sextupler achieves a saturated output power of over 7 dBm and a conversion gain of more than 6 dB in a 3-dB-bandwidth of 78 to 104 GHz, with in-band contributions of unwanted harmonics staying below -25 dBc to ensure spectral purity. [C1143]

"AlInN/GaN a suitable HEMT device for extremely high power high frequency applications"

AlInN/GaN unpassivated high electron mobility transistor (HEMT) on sapphire substrate has yielded a maximum drain current density close to 2 A/mm in steady state. Superior gate length downscaling than AlGaIn/GaN devices has been observed owing to the possibility of the use of ultra thin barrier layer while keeping extremely high sheet carrier density. We reached an extrinsic current gain cut-off frequency of 70 GHz for a 0.08 μm gate length device. Large signal measurements reveal a relatively low RF power dispersion. Indeed, at 10 GHz we performed for the first time power measurements on such a HEMT structure. We achieved 1.5 W/mm output power density at low bias condition ($V_{DS}=15\text{V}$) in agreement with the expected power in spite of a strong thermal effect due to the sapphire substrate, a large leakage current in the Schottky diode characteristic and a low buffer layer resistivity. These results demonstrate the great potential of this structure for extremely high power high frequency applications. [C1144]

"94-GHz Band High-Gain and Low-Noise Amplifier Using InP-HEMTs for Passive Millimeter Wave Imager"

This paper describes 94-GHz band low-noise and high-gain amplifier MMICs using InP HEMTs, which have been developed for passive millimeter-wave (PMMW) imaging. To achieve a high gain with low noise performance, we propose a new stabilizing technique for the amplifier. The measured noise figure was 3.2 dB and the gain was 33 dB. In addition, we developed a PMMW imager using this amplifier. We also demonstrated an example of a millimeter-wave image acquired by the PMMW imager. [C1145]

"GaN HEMT 60W Output Power Amplifier with Over 50% Efficiency at C-Band 15% Relative Bandwidth Using Combined Short and Open Circuited Stubs"

In this paper, a broadband high efficiency amplifier is proposed, which uses both short and open circuited stubs for simultaneous broadband impedance matching for fundamental frequency and 2nd-harmonic. The developed GaN HEMT amplifier with 16 mm gate periphery has achieved over 60 W output power with over 50% drain efficiency (over 45% power-added-efficiency) across 15% relative bandwidth at C-Band. This is the state-of-the-art efficiency of GaN HEMT high power amplifier with over 50 W output power at C-band to the best of our knowledge. [C1146]

"C-band GaN HEMT Power Amplifier with 220W Output Power"

In this paper, GaN HEMT high power amplifiers operating at C-band are presented. Improvement of device performance and reduction of thermal resistance with larger gate pitch enabled 1.4 times power density compared with the previous work [1]-[2]. 167 W output power was extracted from a single chip GaN HEMT with 7 W/mm power density. 2-chip amplifier have recorded 220 W output power at C-band, which is the highest output power ever reported for GaN HEMT amplifiers at C-band and higher bands. [C1147]

"50% Drain Efficiency Doherty Amplifier with Optimized Power Range for W-CDMA Signal"

A novel high-efficiency Doherty amplifier is presented. A carrier amplifier and a peak amplifier in the Doherty amplifier are set to asymmetrical drain voltages to extend the power range where a high drain efficiency of the Doherty amplifier is maintained. Matching circuits of the carrier amplifier and the peak amplifier are designed for each drain voltage so that the drain efficiency and signal linearity of the Doherty amplifier at a 9 dB backoff point from its saturated output power (P_{sat}) become higher than those of a conventional Doherty amplifier. These simple steps optimize the power range of the Doherty amplifier for a wideband code-division multiple-access (W-CDMA) signal that has a peak-to-average power ratio (PAR) of 9 dB. A Doherty amplifier containing gallium nitride (GaN) high-electron-mobility transistors (HEMTs) achieves an adjacent channel leakage power ratio (ACLR) of -38 dBc and a drain efficiency of 50% at an output power of 45 dBm. This is the highest drain efficiency of a Doherty amplifier for a W-CDMA signal to the best of the authors' knowledge. [C1148]

"A 80W 2-stage GaN HEMT Doherty Amplifier with 50dBc ACLR, 42% Efficiency 32dB Gain with

DPD for W-CDMA Base station"

A 2-stage 80 W amplifier, which consists of a 450 W saturated power GaN HEMT Doherty amplifier and a 30 W driver, was developed. At first we developed the 450 W GaN HEMT Doherty amplifier and obtained saturation power of 56.5 dBm(450 W) and drain efficiency of 55% at 6 dB back-off power showing typical Doherty amplifier behavior. Then we built the 2-stage amplifier up with the 30 W driver stage amplifier. With this amplifier we obtained 42% efficiency (including 30 W driver amplifier) and -50 dBc ACLR at the average power of 49 dBm(80 W) with saturation power of 56.5 dBm and Gain of 32 dB. [C1149]

"Frequency Limits of InP-based Integrated Circuits"

We examine the limits in scaling of InP-based bipolar and field effect transistors for increased device bandwidth. With InP-based HBTs, emitter and base contact resistivities and IC thermal resistance are the major limits to increased device bandwidth; devices with 1-1.5 THz simultaneous f_{tau} and f_{max} are feasible. Major challenges faced in developing either InGaAs HEMTs having THz cutoff frequencies or InGaAs-channel MOSFETs having drive current consistent with the 22 nm ITRS objectives include the low two-dimensional effective density of states and the high bound state energies in narrow quantum wells. [C1150]

"Beyond CMOS: Logic Suitability of InGaAs HEMTs"

For over 30 years, Si CMOS scaling has brought along exponential improvements in chip density, speed and power consumption. With CMOS rapidly approaching fundamental limits, the "microelectronics revolution" is threatened. A way to reinvigorate logic technology is to introduce new channel materials with improved transport properties. In this, III-V compound semiconductors and, in particular, InGaAs with high InAs compositions are very promising. This paper reviews the merits and challenges of III-V's for logic applications. It also summarizes recent work of the authors in investigating the logic suitability of InGaAs HEMTs. [C1151]

"35-nm-Gate In_{0.7}Ga_{0.3}As/In_{0.52}Al_{0.48}As HEMT with 520-GHz f_T "

We fabricated a 35-nm-gate In_{0.7}Ga_{0.3}As/In_{0.52}Al_{0.48}As high electron mobility transistor by using a simple, self-aligned one-step-recessed gate procedure. An extrinsic maximum transconductance (g_{m_max}) of 1.7 S/mm and a current gain cutoff frequency (f_T) of 520 GHz were achieved at room temperature. This significantly high f_T was obtained by reducing the gate length to 35 nm and using an epitaxial structure with a 3-nm-thick InAlAs spacer layer, a 6-nm-thick InAlAs Schottky barrier layer and a 2-nm-thick InP etching stopper layer to decrease the gate-to-channel distance to 8 nm, and form simultaneously 50-nm-long side-recess structures and T-shaped gates stacked on the InAlAs Schottky barrier layer. These results are the first experimental achievement of f_T as high as 520 GHz by using the one-step-recessed gate procedure. [C1152]

"35nm InP HEMT for Millimeter and Sub-Millimeter Wave Applications"

A new InP HEMT process has been developed with 35nm gate length and improved Ohmic contact. A gate-source capacitance of 0.4pF/mm is achieved with the reduced gate length, a 30% improvement over our baseline 70nm device. The contact resistance is successfully reduced to 0.07 with the newly designed contact layer combined with an alloyed Au/Ge/Ni/Au Ohmic metal. Good device characteristics has been demonstrated with a transconductance as high as 2 S/mm and a cutoff frequency f_{rof} of 420GHz. A single-stage common-source amplifier was fabricated with this new process. A peak gain of 5dB is measured at 265GHz. A MAG/MSG of 3dB at 300GHz was achieved, making the device suitable for applications at frequencies well into the millimeter-wave and even sub-millimeter-wave band. [C1153]

"InAlAs/InGaAs HEMTs with Minimum Noise Figure of 1.0 dB AT 94 GHz"

The authors achieved a minimum noise figure (NF_{min}) of 1.0 dB at 94 GHz using 110 nm-gate InAlAs/InGaAs HEMTs with a thin Schottky barrier layer. The obtained NF_{min} is one of the lowest values ever reported for HEMTs. This low-noise property is promising for applications involving millimeter-wave communications and image sensors. [C1154]

"50 nm MHEMT Technology for G- and H-Band MMICs"

A metamorphic HEMT (MHEMT) MMIC technology including circuit applications is presented. The MHEMT layers are MBE grown on 4-inch GaAs wafers. The technology is based on a 50 nm gate length MHEMT and includes a 50 μm substrate backside process with dry etched through-substrate vias. For the electron confinement an In_{0.8}Ga_{0.2}As/In_{0.53}Ga_{0.47}As composite channel was used. The devices are passivated with BCB and SiN to achieve a median time-to-failure of 2.7 times 10⁶h in air. Cut-off frequencies f_{T} and f_{max} of 375 GHz were

extrapolated for a 2 times 15 μm gate width device. Low-noise amplifiers with more than 15 dB gain in the frequency range from 192 GHz to 235 GHz were realized. [C1155]

"Extremely High $g_m > 2.2 \text{ S/mm}$ and $f_T > 550 \text{ GHz}$ in 30-nm Enhancement-Mode InP-HEMTs with Pt/Mo/Ti/Pt/Au Buried Gate"

We have successfully developed 30-nm enhancement-mode (E-mode) InGaAs/InAlAs high electron mobility transistors (HEMTs) with an extremely high transconductance (g_m) of 2.22 S/mm, a current gain cutoff frequency (f_T) of 554 GHz, and a maximum oscillation frequency (f_{max}) of 358 GHz. The excellent high-speed performance was obtained by using a Pt/Mo/ Ti/Pt/Au buried gate technology, which enabled E-mode operation for very short 30-nm HEMTs while maintaining a low access resistance as well as a low gate leakage current. The effectively short gate-to-channel distance suppressed the short channel effect, resulting in a very high g_m independent of the gate length (L_g) and a greatly reduced output conductance (g_d). [C1156]

"High Gain G-Band MMIC Amplifiers Based on Sub-50 nm Gate Length InP HEMT"

We have recently developed a sub-50nm gate length InP HEMT (high electron mobility transistor) process with a peak transconductance of 2000 mS/mm at 1V. A 3-stage single-ended common source 150-220 GHz MMIC LNA demonstrates greater than 20 dB gain at 200 GHz ($> 7 \text{ dB gain per stage}$) and is $> 5 \text{ dB}$ higher LNA gain compared to the same MMIC design fabricated on our baselined 70 nm gate length InP HEMT MMIC process. To our knowledge, this is the highest amplifier gain per stage achieved at this frequency range. [C1157]

СПИСОК ЛИТЕРАТУРЫ

- C1. Guerra D. Terahertz-capability nanoscale InGaAs HEMT design guidelines by means of full-band Monte Carlo device simulations. / Guerra D., Marino F.A., Akis R., Ferry D.K., Goodnick S.M., Saraniti M. // 2011 IEEE 11th Topical Meeting on Silicon Monolithic Integrated Circuits in RF Systems (SiRF). - Phoenix, AZ, 17-19 Jan. 2011. - P. 193-196. ↑
- C2. Giovannelli Niccolo. A concurrent dual band 870 and 1970 MHz 10 W envelope tracking PA designed by a WCDMA probability distribution conscious approach. / Giovannelli Niccolo, Cidronali Alessandro, Manes Gianfranco. // 2011 IEEE Topical Conference on Power Amplifiers for Wireless and Radio Applications (PAWR). - Phoenix, AZ, USA, 16-19 Jan. 2011. - P. 1-4. ↑
- C3. Mimis K. A 2GHz GaN Class-J power amplifier for base station applications. / Mimis K., Morris K.A., McGeehan J.P. // 2011 IEEE Topical Conference on Power Amplifiers for Wireless and Radio Applications (PAWR). - Phoenix, AZ, USA, 16-19 Jan. 2011. - P. 5-8. ↑
- C4. Xie Chenggang. Characterization of broadband Monolithic Gallium Nitride distributed power amplifier using thermal imaging technique. 2011 IEEE Topical Conference on Power Amplifiers for Wireless and Radio Applications (PAWR). - Phoenix, AZ, USA, 16-19 Jan. 2011. - P. 77-80. ↑
- C5. Mercanti Massimiliano. HEMT GaAs/GaN power amplifiers architecture with discrete dynamic voltage bias control in envelope tracking RF transmitter for W-CDMA signals. / Mercanti Massimiliano, Cidronali Alessandro, Maurri Stefano, Manes Gianfranco. // 2011 IEEE Topical Conference on Power Amplifiers for Wireless and Radio Applications (PAWR). - Phoenix, AZ, USA, 16-19 Jan. 2011. - P. 9-12. ↑
- C6. Lv J.N. Characterization of GaN cantilevers fabricated with GaN-on-silicon platform. / Lv J.N., Yang Z.C., Yan G.Z., Cai Y., Zhang B.S., Chen K.J. // 2011 IEEE 24th International Conference on Micro Electro Mechanical Systems (MEMS). - Cancun, Mexico, 23-27 Jan. 2011. - P. 388-391. ↑
- C7. Faucher M. Gallium nitride approach for MEMS resonators with highly tunable piezo-amplified transducers. / Faucher M., Cordier Y., Semond F., Brandli V., Grimbert B., Amar A. B., Werquin M., Boyaval C., Gaquiere C., Theron D., Buchaillat L. // 2011 IEEE 24th International Conference on Micro Electro Mechanical Systems (MEMS). - Cancun, Mexico, 23-27 Jan. 2011. - P. 581-584. ↑
- C8. Nishikawa K. Broadband and compact 3-dB MMIC directional coupler with lumped element. / Nishikawa K., Kawashima M., Seki T., Hiraga K. // 2010 IEEE MTT-S International Microwave Symposium Digest (MTT). -

Anaheim, CA, 23-28 May 2010. - P. 728-731. ↑

C9. Marante Reinel. Nonlinear characterization techniques for improving accuracy of GaN HEMT model predictions in RF power amplifiers. / Marante Reinel, Garcia Jose A., Cabria Lorena, Aballo Theophile, Cabral Pedro M., Pedro Jose C. // 2010 IEEE MTT-S International Microwave Symposium Digest (MTT). - Anaheim, CA, USA, 23-28 May 2010. - P. 1680-1683. ↑

C10. Yuk K. High power, high conversion gain frequency doublers using SiC MESFETs and AlGaIn/GaN HEMTs. / Yuk K., Branner G.R., Wong C. // 2010 IEEE MTT-S International Microwave Symposium Digest (MTT). - Anaheim, CA, 23-28 May 2010. - P. 1008-1011. ↑

C11. Santarelli A. Empirical modeling of GaN FETs for nonlinear microwave circuit applications. / Santarelli A., Di Giacomo V. // 2010 IEEE MTT-S International Microwave Symposium Digest (MTT). - Anaheim, CA, 23-28 May 2010. - P. 1198-1201. ↑

C12. Lai R. HEMT MMW MMICS for radiometer sensor applications. 2010 IEEE MTT-S International Microwave Symposium Digest (MTT). - Anaheim, CA, USA, 23-28 May 2010. - P. 1. ↑

C13. Bergeras F. Novel MMIC architectures for tunable microwave wideband active filters. / Bergeras F., Dueme P., Plaze J.-P., Darcel L., Jarry B., Campovecchio M. // 2010 IEEE MTT-S International Microwave Symposium Digest (MTT). - Anaheim, CA, 23-28 May 2010. - P. 1356-1359. ↑

C14. Krishnamurthy K. 100 W GaN HEMT power amplifier module with > 60% efficiency over 100-1000 MHz bandwidth. / Krishnamurthy K., Driver T., Vetury R., Martin J. // 2010 IEEE MTT-S International Microwave Symposium Digest (MTT). - Anaheim, CA, USA, 23-28 May 2010. - P. 940-943. ↑

C15. Ben Heying. Reliable GaN HEMTs for high frequency applications. / Ben Heying, Wen-Ben Luo, Smorchkova I., Din S., Wojtowicz M. // 2010 IEEE MTT-S International Microwave Symposium Digest (MTT). - Anaheim, CA, 23-28 May 2010. - P. 1218-1221. ↑

C16. Piotrowicz S. 43W, 52% PAE X-Band AlGaIn/GaN HEMTs MMIC amplifiers. / Piotrowicz S., Ouarch Z., Chartier E., Aubry R., Callet G., Floriot D., Jacquet J.C., Jardel O., Morvan E., Reveyrand T., Sarazin N., Delage S.L. // 2010 IEEE MTT-S International Microwave Symposium Digest (MTT). - Anaheim, CA, 23-28 May 2010. - P. 505-508. ↑

C17. Shin S. Frequency-tunable high-efficiency power oscillator using GaN HEMT. / Shin S., Choi G., Kim H., Lee S., Kim S., Choi J. // 2010 IEEE MTT-S International Microwave Symposium Digest (MTT). - Anaheim, CA, USA, 23-28 May 2010. - P. 1. ↑

C18. Moon J. Doherty amplifier with envelope tracking for high efficiency. / Moon J., Son J., Kim J., Kim I., Jee S., Woo Y. Y., Kim B. // 2010 IEEE MTT-S International Microwave Symposium Digest (MTT). - Anaheim, CA, USA, 23-28 May 2010. - P. 1. ↑

C19. Mishra U. K. N-polar GaN-based MIS-HEMTs for Mixed Signal Applications. / Mishra U. K., Wong M., Nidhi N., Dasgupta S., Brown D. F., Swenson B. L., Keller S., Speck J. S. // 2010 IEEE MTT-S International Microwave Symposium Digest (MTT). - Anaheim, CA, USA, 23-28 May 2010. - P. 1. ↑

C20. Jong-Gon Heo. Fabrication of AlGaIn/GaN HEMT with the improved ohmic contact by encapsulation of silicon dioxide thin film. / Jong-Gon Heo, Ho-Kun Sung, Jong-Won Lim, Shin-Keun Kim, Won-Kyu Park, Chul-Gi Ko. // 2010 IEEE MTT-S International Microwave Symposium Digest (MTT). - Anaheim, CA, 23-28 May 2010. - P. 308-311. ↑

C21. Mishra U.K. N-polar GaN-based MIS-HEMTs for mixed signal applications. / Mishra U.K., Man Hoi Wong, Nidhi, Dasgupta S., Brown D.F., Swenson B.L., Keller S., Speck J.S. // 2010 IEEE MTT-S International Microwave Symposium Digest (MTT). - Anaheim, CA, 23-28 May 2010. - P. 1130-1133. ↑

C22. Masuda S. Over 10W C-Ku band GaN MMIC non-uniform distributed power amplifier with broadband couplers. / Masuda S., Akasegawa A., Ohki T., Makiyama K., Okamoto N., Imanishi K., Kikkawa T., Shigematsu H. // 2010 IEEE MTT-S International Microwave Symposium Digest (MTT). - Anaheim, CA, 23-28 May 2010. - P. 1388-1391. ↑

C23. Seelmann-Eggebert M. A versatile and cryogenic mHEMT-model including noise. / Seelmann-Eggebert

M., Schajfer F., Leuther A., Massler H. // 2010 IEEE MTT-S International Microwave Symposium Digest (MTT). - Anaheim, CA, 23-28 May 2010. - P. 501-504. ↑

C24. Nemati H.M. Evaluation of a GaN HEMT transistor for load- and supply-modulation applications using intrinsic waveform measurements. / Nemati H.M., Clarke A.L., Cripps S.C., Benedikt J., Tasker P.J., Fager C., Grahn J., Zirath H. // 2010 IEEE MTT-S International Microwave Symposium Digest (MTT). - Anaheim, CA, 23-28 May 2010. - P. 509-512. ↑

C25. Wei-Hung Liao. Single-chip integration of electronically switchable bandpass filter for 3.5GHz WiMAX application. / Wei-Hung Liao, Chang-Sheng Chen, Yo-Shen Lin. // 2010 IEEE MTT-S International Microwave Symposium Digest (MTT). - Anaheim, CA, 23-28 May 2010. - P. 1368-1371. ↑

C26. Liero A. Laser driver switching 20 A with 2 ns pulse width using GaN. / Liero A., Klehr A., Schwertfeger S., Hoffmann T., Heinrich W. // 2010 IEEE MTT-S International Microwave Symposium Digest (MTT). - Anaheim, CA, USA, 23-28 May 2010. - P. 1. ↑

C27. Liero A. Laser driver switching 20 A with 2 ns pulse width using GaN. / Liero A., Klehr A., Schwertfeger S., Hoffmann T., Heinrich W. // 2010 IEEE MTT-S International Microwave Symposium Digest (MTT). - Anaheim, CA, 23-28 May 2010. - P. 1110-1113. ↑

C28. Wen C.P. Current collapse, memory effect free GaN HEMT. / Wen C.P., Jinyan Wang, Yilong Hao. // 2010 IEEE MTT-S International Microwave Symposium Digest (MTT). - Anaheim, CA, 23-28 May 2010. - P. 149-152. ↑

C29. Wentzel A. RF class-S power amplifiers: State-of-the-art results and potential. / Wentzel A., Meliani C., Heinrich W. // 2010 IEEE MTT-S International Microwave Symposium Digest (MTT). - Anaheim, CA, USA, 23-28 May 2010. - P. 1. ↑

C30. Saguatti D. TCAD optimization of field-plated InAlAs-InGaAs HEMTs. / Saguatti D., Chini A., Verzellesi G., Isa M.M., Ian K.W., Missous M. // 2010 International Conference on Indium Phosphide & Related Materials (IPRM). - Kagawa, May 31 2010-June 4 2010. - P. 1-3. ↑

C31. Mateos J. Plasma-resonant THz detection with HEMTs. / Mateos J., Marinchio H., Palermo C., Varani L., Gonzalez T. // 2010 International Conference on Indium Phosphide & Related Materials (IPRM). - Kagawa, May 31 2010-June 4 2010. - P. 1-4. ↑

C32. Che-Kai Lin. An optoelectronic mixer based on composite transparent gate InAlAs/InGaAs metamorphic HEMT. / Che-Kai Lin, Chao-Wei Lin, Yi-Chun Wu, Hsien-Chin Chiu. // 2010 International Conference on Indium Phosphide & Related Materials (IPRM). - Kagawa, May 31 2010-June 4 2010. - P. 1-4. ↑

C33. Wen C. P. Current collapse, memory effect free GaN HEMT. / Wen C. P., Wang J., Hao Y. // 2010 IEEE MTT-S International Microwave Symposium Digest (MTT). - Anaheim, CA, USA, 23-28 May 2010. - P. 1. ↑

C34. Rodilla H. Isolated-gate InAs/AlSb HEMTs: A Monte Carlo study. / Rodilla H., Gonzalez T., Malmkvist M., Lefebvre E., Moschetti G., Grahn J., Mateos J. // 2010 International Conference on Indium Phosphide & Related Materials (IPRM). - Kagawa, May 31 2010-June 4 2010. - P. 1-4. ↑

C35. Tae-Woo Kim. Logic characteristics of 40 nm thin-channel InAs HEMTs. / Tae-Woo Kim, Dae-Hyun Kim, del Alamo J.A. // 2010 International Conference on Indium Phosphide & Related Materials (IPRM). - Kagawa, May 31 2010-June 4 2010. - P. 1-4. ↑

C36. Yamasaki T. A 68% efficiency, C-band 100W GaN power amplifier for space applications. / Yamasaki T., Kittaka Y., Minamide H., Yamauchi K., Miwa S., Goto S., Nakayama M., Kono M., Yoshida N. // 2010 IEEE MTT-S International Microwave Symposium Digest (MTT). - Anaheim, CA, USA, 23-28 May 2010. - P. 1. ↑

C37. Ostinelli O. Semi-insulating iron-doped InP buffer layers for Al-free GaInP/GaInAs pHEMTs. / Ostinelli O., Alt A.R., Lovblom R., Bolognesi C.R. // 2010 International Conference on Indium Phosphide & Related Materials (IPRM). - Kagawa, May 31 2010-June 4 2010. - P. 1-4. ↑

C38. {no data available}. Front cover. 2010 International Conference on Indium Phosphide & Related Materials (IPRM). - Kagawa, May 31 2010-June 4 2010. - P. 1. ↑

- C39.** Moschetti G. DC and RF cryogenic behaviour of InAs/AlSb HEMTs. / Moschetti G., Nilsson P.-A., Desplanque L., Wallart X., Rodilla H., Mateos J., Grahn J. // 2010 International Conference on Indium Phosphide & Related Materials (IPRM). - Kagawa, May 31 2010-June 4 2010. - P. 1-4. ↑
- C40.** Suk Woo Shin. Frequency-tunable high-efficiency power oscillator using GaN HEMT. / Suk Woo Shin, Gil Wong Choi, Hyoung Jong Kim, Su Hyun Lee, Sang Hoon Kim, Jin Joo Choi. // 2010 IEEE MTT-S International Microwave Symposium Digest (MTT). - Anaheim, CA, 23-28 May 2010. - P. 1000-1003. ↑
- C41.** Lai R. HEMT MMW MMICs for radiometer sensor applications. / Lai R., Sarkozy S. // 2010 IEEE MTT-S International Microwave Symposium Digest (MTT). - Anaheim, CA, 23-28 May 2010. - P. 832-835. ↑
- C42.** Yamasaki T. A 68% efficiency, C-band 100W GaN power amplifier for space applications. / Yamasaki T., Kittaka Y., Minamide H., Yamauchi K., Miwa S., Goto S., Nakayama M., Kohno M., Yoshida N. // 2010 IEEE MTT-S International Microwave Symposium Digest (MTT). - Anaheim, CA, 23-28 May 2010. - P. 1384-1387. ↑
- C43.** Albahrani S. A. Characterization of trapping and thermal dispersion in GaN HEMTs. / Albahrani S. A., Parker A. E. // 2010 IEEE MTT-S International Microwave Symposium Digest (MTT). - Anaheim, CA, USA, 23-28 May 2010. - P. 1. ↑
- C44.** Wentzel A. RF class-S power amplifiers: State-of-the-art results and potential. / Wentzel A., Meliani C., Heinrich W. // 2010 IEEE MTT-S International Microwave Symposium Digest (MTT). - Anaheim, CA, 23-28 May 2010. - P. 812-815. ↑
- C45.** Woodington S. Behavioral model analysis of active harmonic load-pull measurements. / Woodington S., Saini R., Williams D., Lees J., Benedikt J., Tasker P.J. // 2010 IEEE MTT-S International Microwave Symposium Digest (MTT). - Anaheim, CA, 23-28 May 2010. - P. 1688-1691. ↑
- C46.** Lin-Sheng Liu. Nonlinear HEMT model direct formulated from the second-order derivative of the I-V/ Q-V characteristics. / Lin-Sheng Liu, Jian-Guo Ma, Hai-Feng Wu, Geok-Ing Ng, Qi-Jun Zhang. // 2010 IEEE MTT-S International Microwave Symposium Digest (MTT). - Anaheim, CA, 23-28 May 2010. - P. 1676-1679. ↑
- C47.** Micovic M. W-Band GaN MMIC with 842 mW output power at 88 GHz. / Micovic M., Kurdoghlian A., Shinohara K., Burnham S., Milosavljevic I., Hu M., Corrión A., Fung A., Lin R., Samoska L., Kangaslahti P., Lambrigtsen B., Goldsmith P., Wong W.S., Schmitz A., Hashimoto P., Willadsen P.J., Chow D.H. // 2010 IEEE MTT-S International Microwave Symposium Digest (MTT). - Anaheim, CA, 23-28 May 2010. - P. 237-239. ↑
- C48.** Micovic M. W-band GaN MMIC with 842 mW output power at 88 GHz. / Micovic M., Kurdoghlian A., Shinohara K., Milosavljevic I., Burnham S. D., Hu M., Corrión A. L., Wong W. S., Schmitz A., Hashimoto P. B., Willadsen P. J., Chow D. H., Fung A., Lin R. H., Samoska L., Kangaslahti P. P., Lambrigtsen B. H., Goldsmith P. F. // 2010 IEEE MTT-S International Microwave Symposium Digest (MTT). - Anaheim, CA, USA, 23-28 May 2010. - P. 1. ↑
- C49.** Curtice W.R. Nonlinear modeling of compound semiconductor HEMTs state of the art. 2010 IEEE MTT-S International Microwave Symposium Digest (MTT). - Anaheim, CA, 23-28 May 2010. - P. 1194-1197. ↑
- C50.** Heo Jong-Gon. Fabrication of AlGaIn/GaN HEMT with the improved ohmic contact by encapsulation of silicon dioxide thin film. / Heo Jong-Gon, Sung Ho-Kun, Lim Jong-Won, Kim Shin-Keun, Park Won-Kyu, Ko Chul-Gi. // 2010 IEEE MTT-S International Microwave Symposium Digest (MTT). - Anaheim, CA, USA, 23-28 May 2010. - P. 1. ↑
- C51.** Heying B. Reliable GaN HEMTs for high frequency applications. / Heying B., Luo W., Smorchkova I., Din S., Wojtowicz M. // 2010 IEEE MTT-S International Microwave Symposium Digest (MTT). - Anaheim, CA, USA, 23-28 May 2010. - P. 1. ↑
- C52.** Li Z. Experimental study on current collapse of GaN MOSFETs, HEMTs and MOS-HEMTs. / Li Z., Marron T., Naik H., Huang W., Chow T.P. // 2010 22nd International Symposium on Power Semiconductor Devices & IC's (ISPSD). - Hiroshima, 6-10 June 2010. - P. 225-228. ↑
- C53.** Zhongda Li. Channel scaling of hybrid GaN MOS-HEMTs. / Zhongda Li, Chow T.P. // 2010 22nd International Symposium on Power Semiconductor Devices & IC's (ISPSD). - Hiroshima, 6-10 June 2010. - P. 221-224. ↑

- C54.** Young-Hwan Choi. High voltage AlGaIn/GaN High-Electron-Mobility Transistors (HEMTs) employing oxygen annealing. / Young-Hwan Choi, Jiyong Lim, Young-Shil Kim, Ogyun Seok, Min-Ki Kim, Min-Koo Han. // 2010 22nd International Symposium on Power Semiconductor Devices & IC's (ISPSD). - Hiroshima, 6-10 June 2010. - P. 233-236. ↑
- C55.** Vitusevich S.A. AlGaIn/GaN microwave transistors for wireless communication systems and advanced nanostructures for high-speed sensor applications. 2010 International Kharkov Symposium on Physics and Engineering of Microwaves, Millimeter and Submillimeter Waves (MSMW). - Kharkiv, 21-26 June 2010. - P. 1-6. ↑
- C56.** Gang Xie. Breakdown voltage enhancement for GaN high electron mobility transistors. / Gang Xie, Bo Zhang, Fu F.Y., Ng W.T. // 2010 22nd International Symposium on Power Semiconductor Devices & IC's (ISPSD). - Hiroshima, 6-10 June 2010. - P. 237-240. ↑
- C57.** Imada T. Enhancement-mode GaN MIS-HEMTs for power supplies. / Imada T., Kanamura M., Kikkawa T. // 2010 International Power Electronics Conference (IPEC). - Sapporo, 21-24 June 2010. - P. 1027-1033. ↑
- C58.** Delage Sylvain L. Achievement and perspective of GaN technology for microwave applications. / Delage Sylvain L., Morvan Erwan, Sarazin Nicolas, Aubry Raphael, Chartier Eric, Jardel Olivier, diForte-Poisson Marie-Antoinette, Dua Christian, Jacquet Jean-Claude, Piotrowicz Stephane, Piotrowska Anna., Kaminska Eliana., De Jaeger Jean-Claude, Gaquiere Christophe, Heinlen Ulrich, Kohn Ehrard, Alomari Mohammed, Maier David, Kuzmik Jan, Pogany Dionyz. // 2010 18th International Conference on Microwave Radar and Wireless Communications (MIKON). - Vilnius, Lithuania, 14-16 June 2010. - P. 1-5. ↑
- C59.** Hilt O. Normally-off AlGaIn/GaN HFET with p-type Ga Gate and AlGaIn buffer. / Hilt O., Knauer A., Brunner F., Bahat-Treidel E., Wujrl J. // 2010 22nd International Symposium on Power Semiconductor Devices & IC's (ISPSD). - Hiroshima, 6-10 June 2010. - P. 347-350. ↑
- C60.** Saito W. Influence of electric field upon current collapse phenomena and reliability in high voltage GaN-HEMTs. / Saito W., Nitta T., Kakiuchi Y., Saito Y., Noda T., Fujimoto H., Yoshioka A., Ohno T. // 2010 22nd International Symposium on Power Semiconductor Devices & IC's (ISPSD). - Hiroshima, 6-10 June 2010. - P. 339-342. ↑
- C61.** Chunhua Zhou. Self-protected GaN power devices with reverse drain blocking and forward current limiting capabilities. / Chunhua Zhou, WanJun Chen, Piner E.L., Chen K.J. // 2010 22nd International Symposium on Power Semiconductor Devices & IC's (ISPSD). - Hiroshima, 6-10 June 2010. - P. 343-346. ↑
- C62.** But D.B. Current sensivity of Si mosfet to terahertz irradiation. / But D.B., Golenkov O.G. // 2010 International Kharkov Symposium on Physics and Engineering of Microwaves, Millimeter and Submillimeter Waves (MSMW). - Kharkiv, 21-26 June 2010. - P. 1. ↑
- C63.** Jarndal A. Large-signal modeling of AlGaIn/GaN HEMTs based on DC IV and S-parameter measurements. / Jarndal A., Aflaki P., Ghannouchi F.M. // 2010 IEEE International Conference on Semiconductor Electronics (ICSE). - Melaka, 28-30 June 2010. - P. 34-37. ↑
- C64.** Jarnda A. Genetic algorithm based extraction method for distributed small-signal model of GaN HEMTs. 2010 IEEE International Conference on Semiconductor Electronics (ICSE). - Melaka, 28-30 June 2010. - P. 41-44. ↑
- C65.** Turowski M. Analysis of transient radiation effects in III-V compound high electron mobility transistors using mixed-mode 3D simulations. / Turowski M., Raman A., Fedoseyev A., McMorow D., Boos J.B. // 2010 Proceedings of the 17th International Conference Mixed Design of Integrated Circuits and Systems (MIXDES). - Warsaw, 24-26 June 2010. - P. 391-396. ↑
- C66.** Feng Gao. Self-consistent electro-thermal simulation of AlGaIn/GaN HEMTs for reliability prediction. / Feng Gao, Hsin-Yi Lo, Ram R., Palacios T. // 2010 Device Research Conference (DRC). - South Bend, IN, 21-23 June 2010. - P. 127-128. ↑
- C67.** Schreurs D. Capabilities and limitations of equivalent circuit models for modeling advanced Si FET devices. / Schreurs D., Homayouni M., Avolio G., Crupi G., Caddemi A. // 2010 Proceedings of the 17th International Conference Mixed Design of Integrated Circuits and Systems (MIXDES). - Warsaw, 24-26 June 2010. - P. 70-74. ↑

- C68.** Timofeyev V.I. Small-signal and noise parameters of heterotransistor with quantum dots. / Timofeyev V.I., Faleyeva E.M. // 2010 33rd International Spring Seminar on Electronics Technology (ISSE). - Warsaw, 12-16 May 2010. - P. 417-420. ↑
- C69.** Semenenko V.L. Parametric instability of mobile elastic gate in tera- and nano- high electron mobility transistor. / Semenenko V.L., Leiman V.G., Arsenin A.V., Gladun A.D., Ryzhii V.I. // 2010 International Kharkov Symposium on Physics and Engineering of Microwaves, Millimeter and Submillimeter Waves (MSMW). - Kharkiv, 21-26 June 2010. - P. 1-3. ↑
- C70.** Dobes. Selecting an optimal structure of artificial neural networks for characterizing RF semiconductor devices. / Dobes, J., Posil L., Pan,ko V. // 2010 53rd IEEE International Midwest Symposium on Circuits and Systems (MWSCAS). - Seattle, WA, 1-4 Aug. 2010. - P. 1206-1209. ↑
- C71.** Abidin M.S.Z. Gateless-FET undoped AlGaIn/GaN HEMT structure for liquid-phase sensor. / Abidin M.S.Z., Sharifabad M.E., Hashim A.M., Rahman S.F.A., Rahman A.R.A., Qindeel R., Omar N.A., Aziz A.A., Hashim M.R., Mohamed M.H.M. // 2010 IEEE International Conference on Semiconductor Electronics (ICSE). - Melaka, 28-30 June 2010. - P. 309-312. ↑
- C72.** Mohamad M. The sensing performance of hydrogen gas sensor utilizing undoped-AlGaIn/GaN HEMT. / Mohamad M., Mustafa F., Abidin M.S.Z., Rahman S.F.A., Al-Obaidi N.K.A., Hashim A.M., Aziz A.A., Hashim M.R. // 2010 IEEE International Conference on Semiconductor Electronics (ICSE). - Melaka, 28-30 June 2010. - P. 301-304. ↑
- C73.** Maier D. High temperature stability of nitride-based power HEMTs. / Maier D., Alomari M., Kohn E., Diforte-Poisson M.-A., Dua C., Delage S. L., Grandjean N., Carlin J.-F., Chuvilin A., Kaiser U., Troadec David, Gaquiere Christophe. // 2010 18th International Conference on Microwave Radar and Wireless Communications (MIKON). - Vilnius, Lithuania, 14-16 June 2010. - P. 1-4. ↑
- C74.** Yongbo Chen. The microwave noise characteristics of InAlN/GaN HEMTs. / Yongbo Chen, Yunchuan Guo, Wen Huang, Ruimin Xu. // 2010 International Conference on Microwave and Millimeter Wave Technology (ICMMT). - Chengdu, 8-11 May 2010. - P. 1710-1714. ↑
- C75.** Palmour J. W. 100 mm GaN-on-SiC RF MMIC technology. / Palmour J. W., Hallin C., Burk A., Radulescu F., Namishia D., Hagleitner H., Duc J., Pribble B., Sheppard S. T., Barner J. B., Milligan J. // 2010 IEEE MTT-S International Microwave Symposium Digest (MTT). - Anaheim, CA, USA, 23-28 May 2010. - P. 1. ↑
- C76.** Ni Feng. Design of an X-band high power solid state power amplifier based on GaN HEMT. / Ni Feng, Fang Jianhong, Feng Hao, Wang Chaoyang, Liu Jianwei. // 2010 International Conference on Microwave and Millimeter Wave Technology (ICMMT). - Chengdu, 8-11 May 2010. - P. 1916-1918. ↑
- C77.** Yuehang Xu. Characterization of high-frequency noise performance of GaN double heterojunction HEMT. / Yuehang Xu, Yunchuan Guo, Yunqiu Wu, Ruimin Xu, Bo Yan. // 2010 International Conference on Microwave and Millimeter Wave Technology (ICMMT). - Chengdu, 8-11 May 2010. - P. 1606-1609. ↑
- C78.** Bo Chen. A broadband low noise amplifier MMIC in 0.15μm GaAs pHEMT technology. / Bo Chen, Wen Huang, Guang Yang, Yunchuan Guo. // 2010 International Conference on Microwave and Millimeter Wave Technology (ICMMT). - Chengdu, 8-11 May 2010. - P. 1941-1943. ↑
- C79.** Krishnamurthy K. 100 W GaN HEMT power amplifier module with 60% efficiency over 100-1000 MHz bandwidth. / Krishnamurthy K., Driver T., Vetury R., Martin J. // 2010 IEEE MTT-S International Microwave Symposium Digest (MTT). - Anaheim, CA, 23-28 May 2010. - P. 1. ↑
- C80.** Junghwan Moon. Doherty amplifier with envelope tracking for high efficiency. / Junghwan Moon, Junghwan Son, Jungjoon Kim, Ildu Kim, Seunghoon Jee, Young Yun Woo, Bumman Kim. // 2010 IEEE MTT-S International Microwave Symposium Digest (MTT). - Anaheim, CA, 23-28 May 2010. - P. 1086-1089. ↑
- C81.** Ciccognani W. An ultra-broadband robust LNA for defence applications in AlGaIn/GaN technology. / Ciccognani W., Limiti E., Longhi P.E., Mitrano C., Nanni A., Peroni M. // 2010 IEEE MTT-S International Microwave Symposium Digest (MTT). - Anaheim, CA, 23-28 May 2010. - P. 493-496. ↑
- C82.** Santarelli A. Empirical modeling of GaN FETs for nonlinear microwave circuit applications. / Santarelli A., Di Giacomo V. // 2010 IEEE MTT-S International Microwave Symposium Digest (MTT). - Anaheim, CA, USA, 23-

28 May 2010. - P. 1. ↑

C83. Yuk K. S. High power, high conversion gain frequency doublers using SiC MESFETs and AlGaIn/GaN HEMTs. / Yuk K. S., Branner G. R., Wong C. // 2010 IEEE MTT-S International Microwave Symposium Digest (MTT). - Anaheim, CA, USA, 23-28 May 2010. - P. 1. ↑

C84. Zhou J.J. The performance of thin barrier InAlN/AlN/GaN MIS HEMT with high dielectric insulators. / Zhou J.J., Dong X., Liu H.Q., Chen T.S., Chen C. // 2010 International Conference on Microwave and Millimeter Wave Technology (ICMMT). - Chengdu, 8-11 May 2010. - P. 643-645. ↑

C85. Colantonio Paolo. Design of a dual-band GaN Doherty amplifier. / Colantonio Paolo, Feudo Fabio, Giannini Franco, Giofre Rocco, Piazzon Luca. // 2010 18th International Conference on Microwave Radar and Wireless Communications (MIKON). - Vilnius, Lithuania, 14-16 June 2010. - P. 1-4. ↑

C86. Ebata T. Enhancement of comparator operation speed by using negative-differential-resistance devices. / Ebata T., Omae U., Machida K., Hoshi K., Waho T. // Proceedings of 2010 IEEE International Symposium on Circuits and Systems (ISCAS). - Paris, May 30 2010-June 2 2010. - P. 3020-3023. ↑

C87. Colantonio P. Doherty power amplifier and GaN technology. / Colantonio P., Giannini F., Giofre R., Piazzon L. // 2010 18th International Conference on Microwave Radar and Wireless Communications (MIKON). - Vilnius, Lithuania, 14-16 June 2010. - P. 1-4. ↑

C88. Samulak Andrzej. Design and simulation GaN based class-S PA at 900MHz. / Samulak Andrzej, Fischer Georg, Weigel Robert. // 2010 18th International Conference on Microwave Radar and Wireless Communications (MIKON). - Vilnius, Lithuania, 14-16 June 2010. - P. 1-4. ↑

C89. Fang Jie. Development strategy for GaN-based high-efficiency hybrid medium-power RF amplifiers through low-cost substrate prototyping. / Fang Jie, Moreno J., Quaglia R., Tinivella R., Camarchia V., Pirola M., Ghione G. // 2010 18th International Conference on Microwave Radar and Wireless Communications (MIKON). - Vilnius, Lithuania, 14-16 June 2010. - P. 1-4. ↑

C90. Jen-Yi Su. Quadrature regenerative frequency dividers using HEMT technology. / Jen-Yi Su, Chinchun Meng, Kuan-Chang Tsung, Guo-Wei Huang. // 2010 International Conference on Microwave and Millimeter Wave Technology (ICMMT). - Chengdu, 8-11 May 2010. - P. 1944-1947. ↑

C91. Yanjun Peng. A 5.25GHz GaAs PHEMT power amplifier for 802.11a application. / Yanjun Peng, Tsang K.F., Ling Sun, Huaxiang Lu, Yanjin Li, Weiping Jing. // 2010 International Conference on Microwave and Millimeter Wave Technology (ICMMT). - Chengdu, 8-11 May 2010. - P. 693-695. ↑

C92. Liu H.Q. InAlN/AlN/GaN HEMTs on sapphire substrate. / Liu H.Q., Zhou J.J., Dong X., Chen T.S., Chen C. // 2010 International Conference on Microwave and Millimeter Wave Technology (ICMMT). - Chengdu, 8-11 May 2010. - P. 2059-2062. ↑

C93. Wang Xiao-mei. Design of X-band low-noise amplifier for optimum matching between noise and power. / Wang Xiao-mei, Sun Zhengwen, Chen Yong, Wang Sixiu. // 2010 2nd International Conference on Education Technology and Computer (ICETC). - Shanghai, 22-24 June 2010. - Vol. 5. - P. V5-184-V5-188-184. ↑

C94. Wen Tang. High conversion gain broadband frequency doubler design. / Wen Tang, Song Tang, Qiuyang He, Zhen-hai Shao. // 2010 International Conference on Microwave and Millimeter Wave Technology (ICMMT). - Chengdu, 8-11 May 2010. - P. 536-538. ↑

C95. Chou Y.C. Progressive Schottky junction reaction induced degradation in Pt-sunken gate InP HEMT MMICs for high reliability applications. / Chou Y.C., Leung D.L., Biedenbender M., Buttari D., Eng D.C., Tsai R.S., Lin C.H., Lee L.S., Mei X.B., Wojtowicz M., Barsky M.E., Lai R., Oki A.K., Block T.R. // 2010 IEEE International Reliability Physics Symposium (IRPS). - Anaheim, CA, 2-6 May 2010. - P. 807-812. ↑

C96. Mosbahi H. Investigation of deep levels in AlGaIn/GaN HEMTs on silicon substrate by conductance deep level transient spectroscopy. / Mosbahi H., Gassoumi M., Charfeddine M., Gaquiere C., Zaidi M.A., Maaref H. // 2010 5th International Conference on Design and Technology of Integrated Systems in Nanoscale Era (DTIS). - Hammamet, 23-25 March 2010. - P. 1-3. ↑

C97. DasGupta S. Electrical stress induced degradation in InAs-AlSb HEMTs. / DasGupta S., Reed R.A.,

Schrimpf R.D., Fleetwood D.M., Shen X., Pantelides S.T., Bergman J., Brar B. // 2010 IEEE International Reliability Physics Symposium (IRPS). - Anaheim, CA, 2-6 May 2010. - P. 813-817. ↑

C98. Marino F.A. Reliability assessment of state-of-the-art GaN HEMT by means of cellular Monte Carlo Simulation. / Marino F.A., Guerra D., Goodnick S.M., Saraniti M. // 2010 IEEE International Reliability Physics Symposium (IRPS). - Anaheim, CA, 2-6 May 2010. - P. 516-521. ↑

C99. Killat N. Temperature assessment of AlGaIn/GaN HEMTs: A comparative study by Raman, electrical and IR thermography. / Killat N., Kuball M., Chou T., Chowdhury U., Jimenez J. // 2010 IEEE International Reliability Physics Symposium (IRPS). - Anaheim, CA, 2-6 May 2010. - P. 528-531. ↑

C100. Ghione G. Compact GaAs HEMT D flip-flop for the integration of a SAR MMIC core-chip digital control logic. / Ghione G., Pirola M., Quaglia R., Ciccognani W., Limiti E., Cavanna T. // 2010 Workshop on Integrated Nonlinear Microwave and Millimeter-Wave Circuits (INMMIC). - Goteborg, 26-27 April 2010. - P. 62-65. ↑

C101. Marante R. Temperature dependent memory effects on a drain modulated GaN HEMT power amplifier. / Marante R., Cabria L., Cabral P., Pedro J.C., Garcia J.A. // 2010 Workshop on Integrated Nonlinear Microwave and Millimeter-Wave Circuits (INMMIC). - Goteborg, 26-27 April 2010. - P. 75-78. ↑

C102. Rui Liu. A very compact power amplifier using GaN HEMTs in multilayer thin-film technology. / Rui Liu, Schreurs D., De Raedt W., Vanaverbeke F., Das J., Germain M., Mertens R. // 2010 Workshop on Integrated Nonlinear Microwave and Millimeter-Wave Circuits (INMMIC). - Goteborg, 26-27 April 2010. - P. 37-40. ↑

C103. Avolio G. Experimental investigation of LF dispersion and IMD asymmetry within GaN based HEMT technology. / Avolio G., Raffo A., Schreurs D., Vadala V., Di Falco S., Lorenz A., de Raedt W., Nauwelaers B., Vannini G. // 2010 Workshop on Integrated Nonlinear Microwave and Millimeter-Wave Circuits (INMMIC). - Goteborg, 26-27 April 2010. - P. 24-27. ↑

C104. Oishi T. Semi-physical nonlinear model for HEMTs with simple equations. / Oishi T., Otsuka H., Yamanaka K., Inoue A., Hirano Y., Angelov I. // 2010 Workshop on Integrated Nonlinear Microwave and Millimeter-Wave Circuits (INMMIC). - Goteborg, 26-27 April 2010. - P. 20-23. ↑

C105. Marcon D. High temperature on- and off-state stress of GaN-on-Si HEMTs with in-situ Si₃N₄ cap layer. / Marcon D., Medjdoub F., Visalli D., Van Hove M., Derluyn J., Das J., Degroote S., Leys M., Kai Cheng, Decoutere S., Mertens R., Germain M., Borghs G. // 2010 IEEE International Reliability Physics Symposium (IRPS). - Anaheim, CA, 2-6 May 2010. - P. 146-151. ↑

C106. Fathallah O. Effects of the drain width on the electrical behavior of deep defect in AlGaIn/GaN/SiC HEMTs. / Fathallah O., Gassoumi M., Saadaoui S., Grimbert B., Gaquiere C., Maaref H. // 2010 27th International Conference on Microelectronics Proceedings (MIEL). - Nis, 16-19 May 2010. - P. 479-481. ↑

C107. Ok I. Reducing Rext in laser annealed enhancement-mode In_{0.53}Ga_{0.47}As surface channel n-MOSFET. / Ok I., Veksler D., Hung P.Y., Oh J., Moore R.L., McDonough C., Geer R.E., Gaspe C.K., Santos M.B., Wong G., Kirsch P., Tseng H.H., Bersuker G., Hobbs C., Jammy R. // 2010 International Symposium on VLSI Technology Systems and Applications (VLSI-TSA). - Hsinchu, 26-28 April 2010. - P. 38-39. ↑

C108. Yahyazadeh R. Effect of temperature on the electronic current of two dimensional quantum well in AlGaIn/GaN high electron mobility transistors (HEMT). / Yahyazadeh R., Hashempour Z. // 2010 27th International Conference on Microelectronics Proceedings (MIEL). - Nis, 16-19 May 2010. - P. 189-193. ↑

C109. Monprasert G. 2.45 GHz GaN HEMT Class-AB RF power amplifier design for wireless communication systems. / Monprasert G., Suebsombut P., Pongthavornkamol T., Chalermwisutkul S. // 2010 International Conference on Electrical Engineering/Electronics Computer Telecommunications and Information Technology (ECTI-CON). - Chaing Mai, 19-21 May 2010. - P. 566-569. ↑

C110. Yahyazadeh R. The effect of depletion layer on the cut off frequency of AlGaIn/GaN high electron mobility transistors. / Yahyazadeh R., Hashempour Z. // 2010 27th International Conference on Microelectronics Proceedings (MIEL). - Nis, 16-19 May 2010. - P. 165-168. ↑

C111. Demirtas S. Effect of trapping on the critical voltage for degradation in GaN high electron mobility transistors. / Demirtas S., del Alamo J.A. // 2010 IEEE International Reliability Physics Symposium (IRPS). - Anaheim, CA, 2-6 May 2010. - P. 134-138. ↑

- C112.** Tapajna M. Identification of electronic traps in AlGaIn/GaN HEMTs using UV light-assisted trapping analysis. / Tapajna M., Simms R.J.T., Faqir M., Kuball M., Pei Y., Mishra U.K. // 2010 IEEE International Reliability Physics Symposium (IRPS). - Anaheim, CA, 2-6 May 2010. - P. 152-155. ↑
- C113.** Malbert N. Reliability assessment in different HTO test conditions of AlGaIn/GaN HEMTs. / Malbert N., Labat N., Curutchet A., Sury C., Hoel V., de Jaeger J.-C., Defrance N., Douvry Y., Dua C., Oualli M., Piazza M., Bru-Chevallier C., Bluet J.-M., Chikhaoui W. // 2010 IEEE International Reliability Physics Symposium (IRPS). - Anaheim, CA, 2-6 May 2010. - P. 139-145. ↑
- C114.** Germain M. GaN-on-Si power field effect transistors. / Germain M., Derluyn J., Van Hove M., Medjdoub F., Das J., Cheng S.D.K., Leys M., Visalli D., Marcon D., Geens K., Viaene J., Sijmus B., Decoutere S., Cartuyvels R., Borghs G. // 2010 International Symposium on VLSI Technology Systems and Applications (VLSI-TSA). - Hsinchu, 26-28 April 2010. - P. 171-172. ↑
- C115.** Dammann M. Reliability status of GaN transistors and MMICs in Europe. / Dammann M., Cajsar M., Konstanzer H., Waltereit P., Quay R., Bronner W., Kiefer R., Mujller S., Mikulla M., van der Wel P.J., Rojdl T., Bourgeois F., Riepe K. // 2010 IEEE International Reliability Physics Symposium (IRPS). - Anaheim, CA, 2-6 May 2010. - P. 129-133. ↑
- C116.** Santarelli A. Large-signal characterization of GaN-based transistors for accurate nonlinear modelling of dispersive effects. / Santarelli A., Cignani R., Di Giacomo V., D'Angelo S., Niessen D., Filicori F. // 2010 Workshop on Integrated Nonlinear Microwave and Millimeter-Wave Circuits (INMMIC). - Goteborg, 26-27 April 2010. - P. 115-118. ↑
- C117.** Gilabert P.L. FPGA-based set-up for RF power amplifier dynamic supply with real-time digital adaptive predistortion. / Gilabert P.L., Montoro G., Bertran E., Garcia J.A. // 2010 IEEE Radio and Wireless Symposium (RWS). - New Orleans, LA, 10-14 Jan. 2010. - P. 248-251. ↑
- C118.** Mercanti M. A 2.14 GHz GaN power amplifier with 1-bit discrete power control. / Mercanti M., Cidronali A., Magrini I., Manes G. // 2010 IEEE Radio and Wireless Symposium (RWS). - New Orleans, LA, 10-14 Jan. 2010. - P. 240-243. ↑
- C119.** Hale C. A 1mm² flip-chip SP3T switch and low noise amplifier RFIC FEM for 802.11b/g applications. / Hale C., Baeten R. // 2010 IEEE Radio and Wireless Symposium (RWS). - New Orleans, LA, 10-14 Jan. 2010. - P. 208-211. ↑
- C120.** Cabria L. A class E power amplifier design for drain modulation under a high PAPR WiMAX signal. / Cabria L., Cabral P.M., Pedro J.C., Garcia J.A. // 2010 IEEE International Microwave Workshop Series on RF Front-ends for Software Defined and Cognitive Radio Solutions (IMWS). - Aveiro, 22-23 Feb. 2010. - P. 1-4. ↑
- C121.** Song Lin. Ultra wideband high gain GaN power amplifier. / Song Lin, Eron M. // 2010 IEEE Radio and Wireless Symposium (RWS). - New Orleans, LA, 10-14 Jan. 2010. - P. 264-267. ↑
- C122.** Ubostad M. Linearity performance of an RF power amplifier under different bias-and load conditions with and without DPD. / Ubostad M., Olavsbraten M. // 2010 IEEE Radio and Wireless Symposium (RWS). - New Orleans, LA, 10-14 Jan. 2010. - P. 232-235. ↑
- C123.** Tingting Hou. Research on mechanical-electrical coupling characteristics of GaAs HEMT build-in cantilevers-mass. / Tingting Hou, Chenyang Xue, Guowen Liu, Zhenxin Tan, Binzhen Zhang, Jun Liu, Wendong Zhang. // 2010 3rd International Nanoelectronics Conference (INEC). - Hong Kong, 3-8 Jan. 2010. - P. 1008-1009. ↑
- C124.** Raab F.H. Kahn-technique transmitter for L-band communication/radar. / Raab F.H., Poppe M.C. // 2010 IEEE Radio and Wireless Symposium (RWS). - New Orleans, LA, 10-14 Jan. 2010. - P. 100-103. ↑
- C125.** Toriyama Y. Multi-level QAM single-carrier high-efficiency broadband wireless system for millimeter-wave applications. / Toriyama Y., Kojima K., Taniguchi T., Miao Zhang, Hirokawa J. // 2010 IEEE Radio and Wireless Symposium (RWS). - New Orleans, LA, 10-14 Jan. 2010. - P. 677-680. ↑
- C126.** Yong-Sub Lee. Advanced design of high-linearity analog predistortion Doherty amplifiers using spectrum analysis for WCDMA applications. / Yong-Sub Lee, Mun-Woo Lee, Sang-Ho Kam, Yoon-Ha Jeong. // 2010 IEEE Radio and Wireless Symposium (RWS). - New Orleans, LA, 10-14 Jan. 2010. - P. 140-143. ↑

- C127.** Cidronali A. Power amplifier architectures with discrete power control for high average efficiency. / Cidronali A., Magrini I., Mercanti M., Fagotti R., Manes G. // 2010 IEEE International Microwave Workshop Series on RF Front-ends for Software Defined and Cognitive Radio Solutions (IMWS). - Aveiro, 22-23 Feb. 2010. - P. 1-4. ↑
- C128.** Marani R. Thermal and electrical layout optimisation of multilayer structure solid-state devices based on the 2-D Fourier series. / Marani R., Perri A.G. // MELECON 2010-2010 15th IEEE Mediterranean Electrotechnical Conference. - Valletta, 26-28 April 2010. - P. 755-758. ↑
- C129.** Khmyrova I. Equivalent circuit modeling of terahertz devices and resonant MEMS with two-dimensional electron gas system. MELECON 2010-2010 15th IEEE Mediterranean Electrotechnical Conference. - Valletta, 26-28 April 2010. - P. 1027-1032. ↑
- C130.** Han Peng. A 150MHz, 84% efficiency, two phase interleaved DC-DC converter in AlGaAs/GaAs P-HEMT technology for integrated power amplifier modules. / Han Peng, Pala V., Chow T.P., Hella M. // 2010 IEEE Radio Frequency Integrated Circuits Symposium (RFIC). - Anaheim, CA, 23-25 May 2010. - P. 259-262. ↑
- C131.** Akmal M. The impact of baseband electrical memory effects on the dynamic transfer characteristics of microwave power transistors. / Akmal M., Lees J., Bensmida S., Woodington S., Benedikt J., Morris K., Beach M., McGeehan J., Tasker P.J. // 2010 Workshop on Integrated Nonlinear Microwave and Millimeter-Wave Circuits (INMMIC). - Goteborg, 26-27 April 2010. - P. 148-151. ↑
- C132.** Jihoon Kim. 60 GHz broadband image rejection receiver using varactor tuning. / Jihoon Kim, Wooyeol Choi, Youngrak Park, Youngwoo Kwon. // 2010 IEEE Radio Frequency Integrated Circuits Symposium (RFIC). - Anaheim, CA, 23-25 May 2010. - P. 381-384. ↑
- C133.** Rudolph M. Modeling GaN power transistors. 2010 IEEE 11th Annual Wireless and Microwave Technology Conference (WAMICON). - Melbourne, FL, 12-13 April 2010. - P. 1-4. ↑
- C134.** Shiwei Feng. Determination of channel temperature of AlGaIn/GaN HEMT by electrical method. / Shiwei Feng, Peifeng Hu, Guangchen Zhang, Chunsheng Guo, Xuesong Xie, Tangsheng Chen. // 2010. SEMI-THERM 2010. 26th Annual IEEE Semiconductor Thermal Measurement and Management Symposium. - Santa Clara, CA, 21-25 Feb. 2010. - P. 165-169. ↑
- C135.** Markos A.Z. Design of GaN HEMT based Doherty amplifiers. / Markos A.Z., Bathich K., Boeck G. // 2010 IEEE 11th Annual Wireless and Microwave Technology Conference (WAMICON). - Melbourne, FL, 12-13 April 2010. - P. 1-5. ↑
- C136.** Wang Xiao-mei. Design and Analysis of an X-band Low Noise Amplifier. / Wang Xiao-mei, Sun Zhengwen, Chen Yong, Wang Si-xiu. // 2010 Second International Conference on Multimedia and Information Technology (MMIT). - Kaifeng, 24-25 April 2010. - Vol. 1. - P. 278-282. ↑
- C137.** Ekpo S. 4-8 GHz LNA design for a highly adaptive small satellite transponder using InGaAs pHEMT technology. / Ekpo S., George D. // 2010 IEEE 11th Annual Wireless and Microwave Technology Conference (WAMICON). - Melbourne, FL, 12-13 April 2010. - P. 1-4. ↑
- C138.** Khansalee E. Design of 140-170 MHz class E power amplifier with parallel circuit on GaN HEMT. / Khansalee E., Puangngernmak N., Chalermwisutkul S. // 2010 International Conference on Electrical Engineering/Electronics Computer Telecommunications and Information Technology (ECTI-CON). - Chaing Mai, 19-21 May 2010. - P. 570-574. ↑
- C139.** Marante R. Nonlinear characterization techniques for improving accuracy of GaN HEMT model predictions in RF power amplifiers. / Marante R., Garcia J. A., Cabria L., Aballo T., Cabral P., Pedro J. C. // 2010 IEEE MTT-S International Microwave Symposium Digest (MTT). - Anaheim, CA, USA, 23-28 May 2010. - P. 1. ↑
- C140.** Takahashi H. 10-Gbit/s QPSK modulator and demodulator for a 120-GHz-band wireless link. / Takahashi H., Kosugi T., Hirata A., Murata K., Kukutsu N. // 2010 IEEE MTT-S International Microwave Symposium Digest (MTT). - Anaheim, CA, 23-28 May 2010. - P. 632-635. ↑
- C141.** Woodington S. P. Behavioral model analysis of active harmonic load-pull measurements. / Woodington S. P., Saini R. S., Willams D., Lees J., Benedikt J., Tasker P. J. // 2010 IEEE MTT-S International Microwave

Symposium Digest (MTT). - Anaheim, CA, USA, 23-28 May 2010. - P. 1. ↑

C142. Liu L. Nonlinear HEMT model direct formulated from the second-order derivative of the I-V/ Q-V characteristics. / Liu L., Ma J., Wu H., Ng G., Zhang Q. // 2010 IEEE MTT-S International Microwave Symposium Digest (MTT). - Anaheim, CA, 23-28 May 2010. - P. 1. ↑

C143. Jarndal A. Improved parameter extraction method for GaN HEMT on Si substrate. / Jarndal A., Markos A. Z., Kompa G. // 2010 IEEE MTT-S International Microwave Symposium Digest (MTT). - Anaheim, CA, USA, 23-28 May 2010. - P. 1. ↑

C144. Florian C. A C-band GaAs-pHEMT MMIC low phase noise VCO for space applications using a new cyclostationary nonlinear noise model. / Florian C., Traverso P.A., Feudale M., Filicori F. // 2010 IEEE MTT-S International Microwave Symposium Digest (MTT). - Anaheim, CA, 23-28 May 2010. - P. 284-287. ↑

C145. Albahrani S.A. Characterization of trapping and thermal dispersion in GaN HEMTs. / Albahrani S.A., Parker A.E. // 2010 IEEE MTT-S International Microwave Symposium Digest (MTT). - Anaheim, CA, 23-28 May 2010. - P. 413-416. ↑

C146. Radisic V. A 50 mW 220 GHz power amplifier module. / Radisic V., Leong K.M.K.H., Xiaobing Mei, Sarkozy S., Yoshida W., Po-Hsin Liu, Uyeda J., Lai R., Deal W.R. // 2010 IEEE MTT-S International Microwave Symposium Digest (MTT). - Anaheim, CA, 23-28 May 2010. - P. 45-48. ↑

C147. Griffith Z. A 206-294GHz 3-stage amplifier in 35nm InP mHEMT, using a thin-film microstrip environment. / Griffith Z., Ha W., Chen P., Kim D., Brar B. // 2010 IEEE MTT-S International Microwave Symposium Digest (MTT). - Anaheim, CA, USA, 23-28 May 2010. - P. 1. ↑

C148. Radisic V. A 50 mW 220 GHz power amplifier module. / Radisic V., Leong K. M., Mei X., Sarkozy S., Yoshida W., Liu P., Uyeda J., Lai R., Deal W. R. // 2010 IEEE MTT-S International Microwave Symposium Digest (MTT). - Anaheim, CA, USA, 23-28 May 2010. - P. 1. ↑

C149. Darwish A.M. Multi-octave GaN MMIC amplifier. / Darwish A.M., Hung H.A., Viveiros E., Ming-Yih Kao. // 2010 IEEE MTT-S International Microwave Symposium Digest (MTT). - Anaheim, CA, 23-28 May 2010. - P. 141-144. ↑

C150. Alt A.R. Aluminum-free GaInP/GaInAs pHEMTs for low-noise applications with peak $f_T = 256$ GHz and peak $f_{MAX} = 360$ GHz. / Alt A.R., Ostinelli O., Bolognesi C.R. // 2010 International Conference on Indium Phosphide & Related Materials (IPRM). - Kagawa, May 31 2010-June 4 2010. - P. 1-3. ↑

C151. Chou Y.C. High reliability performance of 0.1- μ m Pt-sunken gate InP HEMT low-noise amplifiers on 100 mm InP substrates. / Chou Y.C., Leung D.L., Biedenbender M., Eng D.C., Buttari D., Mei X.B., Lin C.H., Tsai R.S., Lai R., Barsky M.E., Wojtowicz M., Oki A.K., Block T.R. // 2010 International Conference on Indium Phosphide & Related Materials (IPRM). - Kagawa, May 31 2010-June 4 2010. - P. 1-4. ↑

C152. Mei X.B. Sub-50NM InGaAs/InAlAs/InP HEMT for sub-millimeter wave power amplifier applications. / Mei X.B., Radisic V., Deal W., Yoshida W., Lee J., Dang L., Liu P.H., Liu W., Lange M., Zhou J., Uyeda J., Leong K., Lai R. // 2010 International Conference on Indium Phosphide & Related Materials (IPRM). - Kagawa, May 31 2010-June 4 2010. - P. 1-3. ↑

C153. Leuther A. Metamorphic HEMT technology for submillimeter-wave MMIC applications. / Leuther A., Tessmann A., Kallfass I., Massler H., Loesch R., Schlechtweg M., Mikulla M., Ambacher O. // 2010 International Conference on Indium Phosphide & Related Materials (IPRM). - Kagawa, May 31 2010-June 4 2010. - P. 1-6. ↑

C154. Takahashi T. Improvement in noise figure of wide-gate-head InP-based HEMTs with cavity structure. / Takahashi T., Sato M., Nakasha Y., Hirose T., Hara N. // 2010 International Conference on Indium Phosphide & Related Materials (IPRM). - Kagawa, May 31 2010-June 4 2010. - P. 1-4. ↑

C155. Palmour J.W. 100 mm GaN-on-SiC RF MMIC technology. / Palmour J.W., Hallin C., Burk A., Radulescu F., Namishia D., Hagleitner H., Duc J., Pribble B., Sheppard S.T., Barner J.B., Milligan J. // 2010 IEEE MTT-S International Microwave Symposium Digest (MTT). - Anaheim, CA, 23-28 May 2010. - P. 1226-1229. ↑

C156. Kukutsu N. Toward practical applications over 100 GHz. / Kukutsu N., Hirata A., Yaita M., Ajito K., Takahashi H., Kosugi T., Song H.-J., Wakatsuki A., Muramoto Y., Nagatsuma T., Kado Y. // 2010 IEEE MTT-S

International Microwave Symposium Digest (MTT). - Anaheim, CA, 23-28 May 2010. - P. 1134-1137. ↑

C157. Griffith Z. A 206-294GHz 3-stage amplifier in 35nm InP mHEMT, using a thin-film microstrip environment. / Griffith Z., Wonill Ha, Chen P., Dae-Hyun Kim, Brar B. // 2010 IEEE MTT-S International Microwave Symposium Digest (MTT). - Anaheim, CA, 23-28 May 2010. - P. 57-60. ↑

C158. Murata H. Optical control of InP-based HEMT 60GHz oscillators with sub-harmonic injection locking. / Murata H., Nishi-oka T., Okamura Y., Kosugi T., Enoki T. // 2010 International Conference on Indium Phosphide & Related Materials (IPRM). - Kagawa, May 31 2010-June 4 2010. - P. 1-2. ↑

C159. Lai R. Sub 50 nm InP HEMT with $f_T = 586$ GHz and amplifier circuit gain at 390 GHz for sub-millimeter wave applications. / Lai R., Mei X.B., Sarkozy S., Yoshida W., Liu P.H., Lee J., Lange M., Radisic V., Leong K., Deal W. // 2010 International Conference on Indium Phosphide & Related Materials (IPRM). - Kagawa, May 31 2010-June 4 2010. - P. 1-3. ↑

C160. Limiti E. An ultra-broadband robust LNA for defence applications in AlGaIn/GaN technology. / Limiti E., Ciccognani W., Longhi P.E., Mitrano C., Nanni A., Peroni M. // 2010 IEEE MTT-S International Microwave Symposium Digest (MTT). - Anaheim, CA, 23-28 May 2010. - P. 1. ↑

C161. Kuhn S. GaN large-signal oscillator design using Auxiliary Generator measurements. / Kuhn S., Heinrich W. // 2010 German Microwave Conference. - Berlin, 15-17 March 2010. - P. 110-113. ↑

C162. Sayed A. Comparative analysis of RF wide bandgap technologies for UMTS applications. / Sayed A., Sajjad A., Al Tanany A., Bengtsson O., Boeck G. // 2010 German Microwave Conference. - Berlin, 15-17 March 2010. - P. 126-129. ↑

C163. Markos A.Z. A 4W GaN power amplifier for C-band application. / Markos A.Z., Bathich K., Gruner D., Bengtsson O., Boeck G. // 2010 German Microwave Conference. - Berlin, 15-17 March 2010. - P. 118-121. ↑

C164. Bathich K. A 2 W GaAs Doherty power amplifier for WiMAX applications. / Bathich K., Markos A.Z., Bengtsson O., Boeck G. // 2010 German Microwave Conference. - Berlin, 15-17 March 2010. - P. 170-173. ↑

C165. Kallfass I. A W-band active frequency-multiplier-by-six in waveguide package. / Kallfass I., Tessmann A., Massler H., Kuri M., Riessle M., Zink M., Leuther A. // 2010 German Microwave Conference. - Berlin, 15-17 March 2010. - P. 74-77. ↑

C166. Saini R.S. An intelligence driven active loadpull system. / Saini R.S., Woodington S., Lees J., Benedikt J., Tasker P.J. // 2010 75th ARFTG Microwave Measurements Conference (ARFTG). - Anaheim, CA, 28-28 May 2010. - P. 1-4. ↑

C167. Suebsombut P. Development of a GaN HEMT class-AB power amplifier for an envelope tracking system at 2.45 GHz. / Suebsombut P., Koch O., Chalermwisutkul S. // 2010 International Conference on Electrical Engineering/Electronics Computer Telecommunications and Information Technology (ECTI-CON). - Chaing Mai, 19-21 May 2010. - P. 561-565. ↑

C168. Albahrani S.A. Impact of the pulse-amplifier slew-rate on the pulsed-IV measurement of GaN HEMTs. / Albahrani S.A., Parker A.E. // 2010 75th ARFTG Microwave Measurements Conference (ARFTG). - Anaheim, CA, 28-28 May 2010. - P. 1-7. ↑

C169. Kujhn J. Harmonic termination of AlGaIn/GaN/(Al)GaIn-single-and double-heterojunction HEMTs. / Kujhn J., Waltereit P., van Raay F., Aidam R., Quay R., Ambacher O., Thumm M. // 2010 German Microwave Conference. - Berlin, 15-17 March 2010. - P. 122-125. ↑

C170. Jian Xu. Design of 50MHz-1GHz low noise and high linearity MMIC amplifier. / Jian Xu, Gong-Zhi Wang, Ying Zhang, Jing Huang. // 2010 2nd International Conference on Future Computer and Communication (ICFCC). - Wuhan, 21-24 May 2010. - Vol. 3. - P. V3-489-V3-491-489. ↑

C171. Ching-Sung Lee. Optical Sensing Characteristics in a Transparent Al-Doped Zinc Oxide-Gated Al_{0.2}Ga_{0.8}As/In_{0.2}Ga_{0.8}As High Electron Mobility Transistor. / Ching-Sung Lee, Bo-Yi Chou, Wei-Chou Hsu, Sheng-Yuan Chu, Der-Yu Lin, Chiu-Sheng Ho, Yin-Lai Lai, Shen-Han Yang, Wei-Ting Chien. // 2010 Symposium on Photonics and Optoelectronic (SOPO). - Chengdu, 19-21 June 2010. - P. 1-3. ↑

- C172.** Rosker M.J. DARPA's GaN technology thrust. / Rosker M.J., Albrecht J.D., Cohen E., Hodiak J., Chang T.-H. // 2010 IEEE MTT-S International Microwave Symposium Digest (MTT). - Anaheim, CA, 23-28 May 2010. - P. 1214-1217. ↑
- C173.** Zomorrodian V. High-efficiency class E MMIC power amplifiers at 4.0 GHz using AlGaIn/GaN HEMT technology. / Zomorrodian V., Yi Pei, Mishra U.K., York R.A. // 2010 IEEE MTT-S International Microwave Symposium Digest (MTT). - Anaheim, CA, 23-28 May 2010. - P. 513-516. ↑
- C174.** Deal W.R. Solid-state amplifiers for terahertz electronics. 2010 IEEE MTT-S International Microwave Symposium Digest (MTT). - Anaheim, CA, 23-28 May 2010. - P. 1122-1125. ↑
- C175.** Zomorrodian V. High-efficiency class E MMIC power amplifiers at 4.0 GHz using AlGaIn/GaN HEMT technology. / Zomorrodian V., Pei Y., Mishra U. K., York R. A. // 2010 IEEE MTT-S International Microwave Symposium Digest (MTT). - Anaheim, CA, USA, 23-28 May 2010. - P. 1. ↑
- C176.** Mashad Nemati H. Evaluation of a GaN HEMT transistor for load- and supply-modulation applications using intrinsic waveform measurements. / Mashad Nemati H., Clarke A. L., Cripps S. C., Benedikt J., Tasker P. J., Fager C., Grahn J., Zirath H. // 2010 IEEE MTT-S International Microwave Symposium Digest (MTT). - Anaheim, CA, USA, 23-28 May 2010. - P. 1. ↑
- C177.** Liang Pang. Large-Periphery ALGaIn/GaN High Electron Mobility Transistors for High-Power Operation. / Liang Pang, Zhi Zheng, Hui-Chan Seo, Chapman P., Krein P., Jung-Hee Lee, Ki-Won Kim, Kyekyoon Kim. // 2010 18th Biennial University/Government/Industry Micro/Nano Symposium (UGIM). - West Lafayette, IN, June 28 2010-July 1 2010. - P. 1-5. ↑
- C178.** Valkonen Risto. Frequency-reconfigurable mobile terminal antenna with MEMS switches. / Valkonen Risto, Luxey Cyril, Holopainen Jari, Icheln Clemens, Vainikainen Pertti. // 2010 Proceedings of the Fourth European Conference on Antennas and Propagation (EuCAP). - Barcelona, Spain, 12-16 April 2010. - P. 1-5. ↑
- C179.** Tack M. Energy efficient power MOSFETs. 2010 IEEE International Conference on IC Design and Technology (ICICDT). - Grenoble, 2-4 June 2010. - P. 159-163. ↑
- C180.** Lee Y. Advanced design of double Doherty power amplifier with a flat efficiency range. / Lee Y., Lee M., Kam S., Jeong Y. // 2010 IEEE MTT-S International Microwave Symposium Digest (MTT). - Anaheim, CA, 23-28 May 2010. - P. 1. ↑
- C181.** Jarndal A. Improved parameter extraction method for GaN HEMT on Si substrate. / Jarndal A., Markos A.Z., Kompa G. // 2010 IEEE MTT-S International Microwave Symposium Digest (MTT). - Anaheim, CA, 23-28 May 2010. - P. 1668-1671. ↑
- C182.** Peifeng Hu. Reliability evaluation of Schottky contact of AlGaIn/GaN HEMT, based on two AC voltages with different frequencies. / Peifeng Hu, Shiwei Feng, Chunsheng Guo, Guangchen Zhang, Yanbin Qiao. // 2010 10th IEEE International Conference on Solid-State and Integrated Circuit Technology (ICSICT). - Shanghai, 1-4 Nov. 2010. - P. 1710-1712. ↑
- C183.** Dawn Wang. High performance SOI RF switches for wireless applications. / Dawn Wang, Wolf R., Joseph A., Botula A., Rabbeni P., Boenke M., Hameed D., Dunn J. // 2010 10th IEEE International Conference on Solid-State and Integrated Circuit Technology (ICSICT). - Shanghai, 1-4 Nov. 2010. - P. 611-614. ↑
- C184.** Hai-Ou Li. 0.3- μ m gate-length metamorphic AlInAs/GaInAs HEMTs on Silicon substrates by MOCVD. / Hai-Ou Li, Ming Li, Chak Wah Tang, Zhen Yu Zhong, Kei May Lau. // 2010 10th IEEE International Conference on Solid-State and Integrated Circuit Technology (ICSICT). - Shanghai, 1-4 Nov. 2010. - P. 1374-1376. ↑
- C185.** Minglan Zhang. Effect of field plate length on DC characteristics of high breakdown voltage GaN HEMTs for power switching application. / Minglan Zhang, Xiaoliang Wang, Mingzeng Peng, Xinyu Liu, Ru Wang. // 2010 10th IEEE International Conference on Solid-State and Integrated Circuit Technology (ICSICT). - Shanghai, 1-4 Nov. 2010. - P. 1356-1358. ↑
- C186.** Chen K.J. GaN Smart Discrete power devices. / Chen K.J., Chunhua Zhou. // 2010 10th IEEE International Conference on Solid-State and Integrated Circuit Technology (ICSICT). - Shanghai, 1-4 Nov. 2010. - P. 1303-1306. ↑

- C187.** Vincze A. SIMS depth profile characterisation of InAlN/GaN structures. / Vincze A., Kovac J., Behmenburg H., Srnanek R., Uherek F., Donoval D., Heuken M. // 2010 8th International Conference on Advanced Semiconductor Devices & Microsystems (ASDAM). - Smolenice, 25-27 Oct. 2010. - P. 309-312. ↑
- C188.** Paszkiewicz B. Inter-digitated AlGaIn/GaN Schottky diode for monolithic integration. / Paszkiewicz B., Paszkiewicz R., Wosko M., Tlaczala M. // 2010 8th International Conference on Advanced Semiconductor Devices & Microsystems (ASDAM). - Smolenice, 25-27 Oct. 2010. - P. 57-60. ↑
- C189.** Noudeviwa A. 100mV noise performances of Te-doped Sb-HEMT. / Noudeviwa A., Olivier A., Roelens Y., Danneville F., Wichmann N., Waldhoff N., Desplanque L., Wallart X., Bollaert S. // 2010 8th International Conference on Advanced Semiconductor Devices & Microsystems (ASDAM). - Smolenice, 25-27 Oct. 2010. - P. 25-28. ↑
- C190.** Andrei P. Breakdown voltage enhancement in lateral AlGaIn/GaN heterojunction FETs with multiple field plates. 2010 10th IEEE International Conference on Solid-State and Integrated Circuit Technology (ICSICT). - Shanghai, 1-4 Nov. 2010. - P. 1344-1346. ↑
- C191.** Gang Xie. GaN high electron mobility transistors with localized Mg doping and Drain Metal Extension. / Gang Xie, Bo Zhang, Fu F.Y., Ng W.T. // 2010 10th IEEE International Conference on Solid-State and Integrated Circuit Technology (ICSICT). - Shanghai, 1-4 Nov. 2010. - P. 1341-1343. ↑
- C192.** Wei Huang. High-breakdown voltage field-plated normally-off AlGaIn/GaN HEMTs for power management. / Wei Huang, Shudan Zhang, Juyan Xu. // 2010 10th IEEE International Conference on Solid-State and Integrated Circuit Technology (ICSICT). - Shanghai, 1-4 Nov. 2010. - P. 1335-1337. ↑
- C193.** Bhattacharya M. Impact of doping concentration and donor-layer thickness on the dc characterization of symmetric double-gate and single-gate InAlAs/InGaAs/InP HEMT for nanometer gate dimension-A comparison. / Bhattacharya M., Jogi J., Gupta R.S., Gupta M. // TENCON 2010-2010 IEEE Region 10 Conference. - Fukuoka, 21-24 Nov. 2010. - P. 134-139. ↑
- C194.** Guerra D. Cellular Monte Carlo study of RF short-channel effects, effective gate length, and aspect ratio in GaN and InGaAs HEMTs. / Guerra D., Akis R., Ferry D.K., Goodnick S.M., Saraniti M., Marino F.A. // 2010 14th International Workshop on Computational Electronics (IWCE). - Pisa, 26-29 Oct. 2010. - P. 1-4. ↑
- C195.** Uchiyama H. Consideration of impact of GaN HEMT for class E amplifier. / Uchiyama H., Yamamoto R., Ishikawa Y., Suetsugu T. // TENCON 2010-2010 IEEE Region 10 Conference. - Fukuoka, 21-24 Nov. 2010. - P. 1780-1783. ↑
- C196.** Kuznetsov S.S. High-speed driver for pin diode microwave switch. / Kuznetsov S.S., Yushenko A.Y., Bozhkov V.G. // 2010 IEEE 2nd Russia School and Seminar on Fundamental Problems of Micro/Nanosystems Technologies (MNST). - Novosibirsk, 9-11 Dec. 2010. - P. 41-42. ↑
- C197.** Ya-Lan Chiou. AlGaIn/GaN MOS-HEMTs with ZnO gate insulator and chlorine surface treatment. / Ya-Lan Chiou, Ching-Ting Lee. // TENCON 2010-2010 IEEE Region 10 Conference. - Fukuoka, 21-24 Nov. 2010. - P. 1222-1224. ↑
- C198.** Hartin O. AlGaIn/GaN HEMT TCAD simulation and model extraction for RF applications. / Hartin O., Green B. // 2010 IEEE Bipolar/BiCMOS Circuits and Technology Meeting (BCTM). - Austin, TX, 4-6 Oct. 2010. - P. 232-236. ↑
- C199.** Andrei P. Analytical models of the transition layer in HEMTs on silicon substrate for device simulation. 2010 10th IEEE International Conference on Solid-State and Integrated Circuit Technology (ICSICT). - Shanghai, 1-4 Nov. 2010. - P. 1931-1933. ↑
- C200.** Lee C.S. Double δ -doped AlGaAs/InGaAs MOS-pHEMTs by using ozone water oxidation treatment. / Lee C.S., Yang S.H., Hung J.T., Chien W.T., Lin M.Y., Liao Y.H., Tseng L.Y., Hsu W.C., Ho C.S., Chou B.Y., Lai Y.N. // 2010 International Symposium on Next-Generation Electronics (ISNE). - Kaohsiung, 18-19 Nov. 2010. - P. 178-181. ↑
- C201.** Romano G. Handshaking multiscale thermal model of nanostructured devices. / Romano G., Auf der Maur M., Di Carlo A., Pecchia A. // 2010 14th International Workshop on Computational Electronics (IWCE). - Pisa, 26-29 Oct. 2010. - P. 1-4. ↑

- C202.** Typpo J. A 900 MHz 10 mW monolithically integrated inverse class E power amplifier. / Typpo J., Hietakangas S., Rahkonen T. // 2010 NORCHIP. - Tampere, 15-16 Nov. 2010. - P. 1-4. ↑
- C203.** Rendek K. Noise in the InAlN/GaN HEMT transistors. / Rendek K., S,atka A., Kova,c, J., Donoval D. // 2010 8th International Conference on Advanced Semiconductor Devices & Microsystems (ASDAM). - Smolenice, 25-27 Oct. 2010. - P. 53-56. ↑
- C204.** Sommet R. Thermal modeling and measurements of AlGaIn/GaN HEMTs including Thermal Boundary Resistance. / Sommet R., Mougnot G., Que, re, R., Ouarch Z., Heckmann S., Camiade M. // 2010 16th International Workshop on Thermal Investigations of ICs and Systems (THERMINIC). - Barcelona, 6-8 Oct. 2010. - P. 1-5. ↑
- C205.** Anichenko E.V. Production of 150 NM T-gate on basis of Ti/Mo/Cu for p-HEMT. / Anichenko E.V., Erofeev E.V., Ishutkin S.V., Kagadei V.A., Nosaeva K.S. // 2010 20th International Crimean Conference Microwave and Telecommunication Technology (CriMiCo). - Sevastopol, 13-17 Sept. 2010. - P. 754-755. ↑
- C206.** Bazzano G. 2D Thermal propagation analysis of discrete power devices based on an innovative distributed model technique and CAD framework. / Bazzano G., Cavallaro D.G., Greco G., Grimaldi A., Rinaudo S. // 2010 16th International Workshop on Thermal Investigations of ICs and Systems (THERMINIC). - Barcelona, 6-8 Oct. 2010. - P. 1-6. ↑
- C207.** Kumar M. Active UWB antenna. / Kumar M., Basu A., Koul S.K. // 2010 URSI International Symposium on Electromagnetic Theory (EMTS). - Berlin, 16-19 Aug. 2010. - P. 497-500. ↑
- C208.** Kumar M. Electromagnetic short pulse generation techniques. / Kumar M., Basu A., Koul S.K. // 2010 URSI International Symposium on Electromagnetic Theory (EMTS). - Berlin, 16-19 Aug. 2010. - P. 299-302. ↑
- C209.** Torkhov N.A. Fractal nature of resistance of the drain-doped channel of the gan-based heterostructure of the field effect transistor with bidimensional electron gas. / Torkhov N.A., Bozhkov V.G. // 2010 20th International Crimean Conference Microwave and Telecommunication Technology (CriMiCo). - Sevastopol, 13-17 Sept. 2010. - P. 729-730. ↑
- C210.** Wei Huang. A novel AlGaIn/GaN HEMTs technology for intelligent electric network application. / Wei Huang, Sheng Wang, Qing Wan, Nanzhong Hu, Guangjian Wang, Shudan Zhang. // 2010 International Conference on Computer Application and System Modeling (ICCA SM). - Taiyuan, 22-24 Oct. 2010. - Vol. 7. - P. V7-323-V7-327-323. ↑
- C211.** Krutov A.V. An experimental recovery of GaAs and GaN PHEMT linear equivalent circuits and noise models. / Krutov A.V., Rebrov A.S. // 2010 20th International Crimean Conference Microwave and Telecommunication Technology (CriMiCo). - Sevastopol, 13-17 Sept. 2010. - P. 214-215. ↑
- C212.** Rakov Yu.N. Nitride gallium high power integrated heterostructure FETs. / Rakov Yu.N., Monchares N.V., Bobrova T.P., Schepina L.V., Uzelmann G.F., Mjakishev Yu.B., Bondareva T.K., Zazulnikov A.F., Sveshnikov Yu.N. // 2010 20th International Crimean Conference Microwave and Telecommunication Technology (CriMiCo). - Sevastopol, 13-17 Sept. 2010. - P. 101-102. ↑
- C213.** Salnikov A.S. Approach to formation of cell libraries of MMIC and automatic layout generation for electromagnetic simulation. / Salnikov A.S., Kokolov A.A., Sheyerman F.I. // 2010 20th International Crimean Conference Microwave and Telecommunication Technology (CriMiCo). - Sevastopol, 13-17 Sept. 2010. - P. 196-197. ↑
- C214.** Zhytnytska R. Thermal optimisation of GaN flip chip power transistors. / Zhytnytska R., Hilt O., Sidorov V., Wujrfl J., Trajnkle G. // 2010 3rd Electronic System-Integration Technology Conference (ESTC). - Berlin, 13-16 Sept. 2010. - P. 1-3. ↑
- C215.** Edwards M.J. Modelling and optimisation of a sapphire/GaN-based diaphragm structure for pressure sensing in harsh environments. / Edwards M.J., Vittoz S., Amen R., Rufer L., Johander P., Bowen C.R., Allsopp D.W.E. // 2010 8th International Conference on Advanced Semiconductor Devices & Microsystems (ASDAM). - Smolenice, 25-27 Oct. 2010. - P. 127-130. ↑
- C216.** T. On the identification of trap location in AlGaIn/GaN HEMTs during electrical stress. / T,apajna M., Simms R.J.T., Pei Y., Mishra U.K., Kuball M. // 2010 8th International Conference on Advanced Semiconductor

Devices & Microsystems (ASDAM). - Smolenice, 25-27 Oct. 2010. - P. 119-122. ↑

C217. Marek J. Analysis of structure geometry and interface charge on electrical characteristics of InAlN/GaN HEMTs. / Marek J., Donoval D., Kova,c, J., Molna,r M., Chvala A., Kordos P. // 2010 8th International Conference on Advanced Semiconductor Devices & Microsystems (ASDAM). - Smolenice, 25-27 Oct. 2010. - P. 143-146. ↑

C218. Kuzmik J. Role of the gate-to-drain distance in the performance of the normally-off InAlN/GaN HEMTs. / Kuzmik J., Ostermaier O., Pozzovivo G., Basnar B., Schrenk W., Carlin J., Gonschorek M., Feltin E., Grandjean N., Douvry Y., Gaquiere C., De Jaeger J., Strasser G., Pogany D., Gornik E. // 2010 8th International Conference on Advanced Semiconductor Devices & Microsystems (ASDAM). - Smolenice, 25-27 Oct. 2010. - P. 163-166. ↑

C219. Khmyrova I. Model for evaluation of terahertz plasma resonances in HEMT-based devices with grating gate. / Khmyrova I., Yamase R., Watanabe N. // 2010 8th International Conference on Advanced Semiconductor Devices & Microsystems (ASDAM). - Smolenice, 25-27 Oct. 2010. - P. 13-16. ↑

C220. Chvala A. Characterisation of electrical properties of AlGaIn/GaN Schottky diode at very high temperature. / Chvala A., Donoval D., Sramaty R., Marek J., Kovac J., Kordos P., Skrinjarova J. // 2010 8th International Conference on Advanced Semiconductor Devices & Microsystems (ASDAM). - Smolenice, 25-27 Oct. 2010. - P. 115-118. ↑

C221. Hoque M.E. Scalable HEMT model for small signal operations. / Hoque M.E., Heimlich M., Tarazi J., Parker A., Mahon S. // 2010 International Conference on Electromagnetics in Advanced Applications (ICEAA). - Sydney, NSW, 20-24 Sept. 2010. - P. 309-312. ↑

C222. Kova. Study of temperature distribution in the channels of AlGaIn/GaN HEMT devices by μ - Raman characterization techniques. / Kova,c, J., Jha S.K., Jelenkovic, E.V., Kutsay O., Pejovic, M., Surya C., Zapien J.A., Bello I., Srna,nek R., Kova,c, J., Flickyngerova, S. // 2010 8th International Conference on Advanced Semiconductor Devices & Microsystems (ASDAM). - Smolenice, 25-27 Oct. 2010. - P. 123-126. ↑

C223. Ry. HEMT-SAW structures for chemical gas sensors in harsh environment. / Ry,ger I., Lalinsky, T., Vanko G., Toma,s,ka M., Kostic, I., Has,c,ik S., Vallo M. // 2010 8th International Conference on Advanced Semiconductor Devices & Microsystems (ASDAM). - Smolenice, 25-27 Oct. 2010. - P. 131-134. ↑

C224. Bouzid S. AlGaIn/GaN HEMT on Si (111) substrate for millimeter microwave power applications. / Bouzid S., Hoel V., Defrance N., Maher H., Lecourt F., Renvoise M., Smith D., De Jaeger J.C. // 2010 8th International Conference on Advanced Semiconductor Devices & Microsystems (ASDAM). - Smolenice, 25-27 Oct. 2010. - P. 111-114. ↑

C225. Chi Ming Lee. GaN-based lamb-wave mass-sensors on silicon substrates. / Chi Ming Lee, Ka Ming Wong, Peng Chen, Lau K.M. // 2010 IEEE Sensors. - Kona, HI, 1-4 Nov. 2010. - P. 2008-2011. ↑

C226. Zhu Yu. Complete electromagnetic simulation of HEMT switch circuit. / Zhu Yu, Wei Cejun, Nohra George, Zhang Cindy, Klimashov Oleksiy, Yin Hong, Bartle Dylan. // 2010 Asia-Pacific Microwave Conference Proceedings (APMC). - Yokohama, Japan, 7-10 Dec. 2010. - P. 2315-2318. ↑

C227. Huang Chun-Yen. Novel designs for high-efficiency millimeter-wave zero-bias detectors. / Huang Chun-Yen, Nien Chin-Chung, Li Chen-Ming, Yu Ya-Chung, Chang Li-Yuan, Tarnng Jenn-Hwan. // 2010 17th IEEE International Conference on Electronics, Circuits, and Systems (ICECS). - Athens, Greece, 12-15 Dec. 2010. - P. 507-510. ↑

C228. Kawai Satoshi. Distortion reduction of a GaN HEMT Doherty power amplifier with a series connected load. / Kawai Satoshi, Takayama Yoichiro, Ishikawa Ryo, Honjo Kazuhiko. // 2010 Asia-Pacific Microwave Conference Proceedings (APMC). - Yokohama, Japan, 7-10 Dec. 2010. - P. 658-661. ↑

C229. Suzuki Yasunori. Experimental investigation on wideband intermodulation distortion compensation characteristics of 3.5-GHz band 140-W class feed-forward power amplifier employing GaN HEMTs. / Suzuki Yasunori, Ohkawara Junya, Narahashi Shoichi. // 2010 Asia-Pacific Microwave Conference Proceedings (APMC). - Yokohama, Japan, 7-10 Dec. 2010. - P. 1-4. ↑

C230. Huang Fan-Hsiu. A Dual-gate subharmonic injection-locked oscillator using 0.5 μ m GaAs pHEMT

technology. / Huang Fan-Hsiu, Tsai Meng-Hsiu, Chang Hong-Yeh, Hsin Yue-Ming. // 2010 Asia-Pacific Microwave Conference Proceedings (APMC). - Yokohama, Japan, 7-10 Dec. 2010. - P. 940-943. ↑

C231. Giri S.K. Design and development of an S-band Low Noise Amplifier. / Giri S.K., Bose C. // 2010 Annual IEEE India Conference (INDICON). - Kolkata, 17-19 Dec. 2010. - P. 1-4. ↑

C232. Douglas E.A. Degradation of sub-micron gate AlGaIn/GaN HEMTs due to reverse gate bias. / Douglas E.A., Chih-Yang Chang, Anderson T., Hite J., Liu Lu, Chien-Fong Lo, Byung-Hwan Chu, Cheney D.J., Gila B.P., Ren F., Via G.D., Whiting P., Holzworth R., Jones K.S., Soohwan Jang, Pearton S.J. // 2010 IEEE International Integrated Reliability Workshop Final Report (IRW). - Stanford Sierra, CA, 17-21 Oct. 2010. - P. 125-128. ↑

C233. Hong Yin. Progress on distributed resistance model for pHEMT. / Hong Yin, Cejun Wei, Yu Zhu, Klimashov A., Zhang C., Bartle D. // 2010 IEEE International Conference of Electron Devices and Solid-State Circuits (EDSSC). - Hong Kong, 15-17 Dec. 2010. - P. 1-4. ↑

C234. Rasmi A. 2.4 GHz medium power amplifier for wireless LAN applications using GaAs PHEMT. / Rasmi A., Rose M.R.C., Rahim A.I.A., Marzuki A. // 2010 IEEE Asia-Pacific Conference on Applied Electromagnetics (APACE). - Port Dickson, 9-11 Nov. 2010. - P. 1-4. ↑

C235. Rasidah S. 3-stage 15 GHz p-HEMT power amplifier design for MMIC applications. / Rasidah S., Rasmi A., Siti Maisurah M.H., Rahim A.I.A., Yahya M.R. // 2010 IEEE International Conference of Electron Devices and Solid-State Circuits (EDSSC). - Hong Kong, 15-17 Dec. 2010. - P. 1-4. ↑

C236. Akmal M. Minimization of baseband electrical memory effects in GaN HEMTs using active IF load-pull. / Akmal M., Lees J., Carrubba V., Bensmida S., Woodington S., Benedikt J., Morris K., Beach M., McGeehan J., Tasker P.J. // 2010 Asia-Pacific Microwave Conference Proceedings (APMC). - Yokohama, Japan, 7-10 Dec. 2010. - P. 5-8. ↑

C237. Xu Yingjie. Analysis and implementation of inverse class-F power amplifier for 3.5GHz transmitters. / Xu Yingjie, Wang Jingqi, Zhu Xiaowei. // 2010 Asia-Pacific Microwave Conference Proceedings (APMC). - Yokohama, Japan, 7-10 Dec. 2010. - P. 410-413. ↑

C238. Albahrani Sayed A. Analysis of dispersion in intermodulation distortion in GaN HEMT devices. / Albahrani Sayed A., Parker Anthony E., Gutta Venkata. // 2010 Asia-Pacific Microwave Conference Proceedings (APMC). - Yokohama, Japan, 7-10 Dec. 2010. - P. 398-401. ↑

C239. Khansalee Ekkaphol. A high efficiency VHF GaN HEMT class E power amplifier for public and homeland security applications. / Khansalee Ekkaphol, Puangngernmak Nutdechatorn, Chalermwisutkul Suramate. // 2010 Asia-Pacific Microwave Conference Proceedings (APMC). - Yokohama, Japan, 7-10 Dec. 2010. - P. 437-440. ↑

C240. Shin O.C. Implementation of new SP6T switch achieving high quality and small size at same time. / Shin O.C., Kim Y.S., Jeong I.H. // 2010 Asia-Pacific Microwave Conference Proceedings (APMC). - Yokohama, Japan, 7-10 Dec. 2010. - P. 473-476. ↑

C241. Taking S. DC and RF performance of AlN/GaN MOS-HEMTs. / Taking S., MacFarlane D., Khokhar A.Z., Dabiran A.M., Wasige E. // 2010 Asia-Pacific Microwave Conference Proceedings (APMC). - Yokohama, Japan, 7-10 Dec. 2010. - P. 445-448. ↑

C242. Mizuno Shinya. A 5.9 GHz-8.5 GHz 20 Watts GaN HEMT. / Mizuno Shinya, Yamamoto Hiroshi, Yamamoto Takashi, Nishihara Makoto, Sano Seigo. // 2010 Asia-Pacific Microwave Conference Proceedings (APMC). - Yokohama, Japan, 7-10 Dec. 2010. - P. 123-126. ↑

C243. Yamanaka K. Internally-matched GaN HEMT high efficiency power amplifier for Space Solar Power Stations. / Yamanaka K., Tuyama Y., Ohtsuka H., Chaki S., Nakayama M., Hirano Y. // 2010 Asia-Pacific Microwave Conference Proceedings (APMC). - Yokohama, Japan, 7-10 Dec. 2010. - P. 119-122. ↑

C244. Nakade K. Development of 150W S-band GaN solid state power amplifier for satellite use. / Nakade K., Seino K., Tsuchiko A., Kanaya J. // 2010 Asia-Pacific Microwave Conference Proceedings (APMC). - Yokohama, Japan, 7-10 Dec. 2010. - P. 127-130. ↑

C245. Hangai Masatake. An X-band 50% bandwidth high-power GaN HEMT T/R switch. / Hangai Masatake,

Komaru Ryota, Tarui Yukinobu, Kamo Yoshitaka, Hieda Morishige, Nakayama Masatoshi. // 2010 Asia-Pacific Microwave Conference Proceedings (APMC). - Yokohama, Japan, 7-10 Dec. 2010. - P. 135-138. ↑

C246. Boles Timothy. Cost effective, high performance GaN technology. / Boles Timothy, Carlson Douglas, Varmazis Costas, Barrett Jason. // 2010 Asia-Pacific Microwave Conference Proceedings (APMC). - Yokohama, Japan, 7-10 Dec. 2010. - P. 131-134. ↑

C247. Wenzheng Liu. Class-E Doherty power amplifier based on harmonic tuning. / Wenzheng Liu, Shouzhao Jing. // 2010 International Symposium on Intelligent Signal Processing and Communication Systems (ISPACS). - Chengdu, 6-8 Dec. 2010. - P. 1-4. ↑

C248. Tulip F.S. GaN-AlGaIn high electron mobility transistors for multiple biomolecule detection such as photosystem I and human MIG. / Tulip F.S., Mostafa S., Islam S.K., Eteshola E., Eliza S.A., Lee I., Greenbaum E., Evans B.R. // 2010 International Conference on Electrical and Computer Engineering (ICECE). - Dhaka, 18-20 Dec. 2010. - P. 310-313. ↑

C249. Eliza S.A. Modeling of AlGaIn/GaN HEMT based stress sensors. / Eliza S.A., Islam S.K., Mostafa S., Tulip F.S. // 2010 International Conference on Electrical and Computer Engineering (ICECE). - Dhaka, 18-20 Dec. 2010. - P. 306-309. ↑

C250. Eliza S.A. Ultra-high sensitivity gas sensors based on GaN HEMT structures. / Eliza S.A., Dutta A.K. // 2010 International Conference on Electrical and Computer Engineering (ICECE). - Dhaka, 18-20 Dec. 2010. - P. 431-433. ↑

C251. Abidin M.S.Z. Characterization of liquid-phase sensor utilizing GaN-based two-terminal device. / Abidin M.S.Z., Wang Soo Jeat, Hashim A.M., Abdul Rahman S.F., Sharifabad M.E. // 2010 International Conference on Enabling Science and Nanotechnology (ESciNano). - Kuala Lumpur, 1-3 Dec. 2010. - P. 1-2. ↑

C252. Aizad F. Logic performance of 40 nm InAs/In_xGa_{1-x}As composite channel HEMTs. / Aizad F., Heng-Tung Hsu, Chien-I Kuo, Li-Han Hsu, Chien-Ying Wu, Chang E.Y., Guo-Wei Huang, Szu-ping Tsai. // 2010 International Conference on Enabling Science and Nanotechnology (ESciNano). - Kuala Lumpur, 1-3 Dec. 2010. - P. 1-2. ↑

C253. Jongwook Kim. SiO₂/Si₃N₄ bilayer sloped etching for 20nm InAlAs/InGaAs metamorphic HEMTs. / Jongwook Kim, Minseong Lee, Kwangseok Seo. // 2010 10th IEEE Conference on Nanotechnology (IEEE-NANO). - Seoul, 17-20 Aug. 2010. - P. 246-249. ↑

C254. Kundu S. Reduction of negative differential conductivity effect of AlGaIn/GaN HEMTs using gate scaling. / Kundu S., Das P., Pathak S., Mukhopadhyay P., Reddy J., Chang E.Y., Biswas D. // 2010 10th IEEE Conference on Nanotechnology (IEEE-NANO). - Seoul, 17-20 Aug. 2010. - P. 794-797. ↑

C255. Rout S. Embedded HEMT/metamaterial composite devices for active terahertz modulation. / Rout S., Shrekenhamer D., Sonkusale S., Padilla W. // 2010 23rd Annual Meeting of the IEEE Photonics Society. - Denver, CO, 7-11 Nov. 2010. - P. 437-438. ↑

C256. Hasan M.T. Effects of cap layer on 2DEGs in InN-based heterostructures. / Hasan M.T., Hossain M.A., Haque M.M., Bhuiyan A.G., Yamamoto A. // 2010 International Conference on Electrical and Computer Engineering (ICECE). - Dhaka, 18-20 Dec. 2010. - P. 120-122. ↑

C257. Avolio G. A de-embedding procedure oriented to the determination of FET intrinsic I-V characteristics from high-frequency large-signal measurements. / Avolio G., Schreurs D., Raffo A., Crupi G., Vannini G., Nauwelaers B. // 2010 76th ARFTG Microwave Measurement Symposium (ARFTG). - Clearwater Beach, FL, Nov. 30 2010-Dec. 3 2010. - P. 1-6. ↑

C258. Nainani A. Development of high-k dielectric for antimonides and a sub 350°C III-V pMOSFET outperforming Germanium. / Nainani A., Irisawa T., Ze Yuan, Yun Sun, Krishnamohan T., Reason M., Bennett B.R., Boos J.B., Ancona M.G., Nishi Y., Saraswat K.C. // 2010 IEEE International Electron Devices Meeting (IEDM). - San Francisco, CA, 6-8 Dec. 2010. - P. 6.4.1-6.4.4. ↑

C259. Shinohara K. 220GHz f_T and 400GHz f_{max} in 40-nm GaN DH-HEMTs with re-grown ohmic. / Shinohara K., Corrion A., Regan D., Milosavljevic I., Brown D., Burnham S., Willadsen P.J., Butler C., Schmitz A., Wheeler D., Fung A., Micovic M. // 2010 IEEE International Electron Devices Meeting (IEDM). - San Francisco,

CA, 6-8 Dec. 2010. - P. 30.1.1-30.1.4. ↑

C260. Chenyue Ma. Reliability of enhancement-mode AlGaIn/GaN HEMTs under ON-state gate overdrive. / Chenyue Ma, Hongwei Chen, Chunhua Zhou, Sen Huang, Li Yuan, Roberts J., Chen K.J. // 2010 IEEE International Electron Devices Meeting (IEDM). - San Francisco, CA, 6-8 Dec. 2010. - P. 20.4.1-20.4.4. ↑

C261. Chung J.W. Advanced gate technologies for state-of-the-art fT in AlGaIn/GaN HEMTs. / Chung J.W., Tae-Woo Kim, Palacios T. // 2010 IEEE International Electron Devices Meeting (IEDM). - San Francisco, CA, 6-8 Dec. 2010. - P. 30.2.1-30.2.4. ↑

C262. Tae-Woo Kim. 60 nm self-aligned-gate InGaAs HEMTs with record high-frequency characteristics. / Tae-Woo Kim, Dae-Hyun Kim, del Alamo J.A. // 2010 IEEE International Electron Devices Meeting (IEDM). - San Francisco, CA, 6-8 Dec. 2010. - P. 30.7.1-30.7.4. ↑

C263. Yong Tang. High-performance monolithically-integrated E/D mode InAlN/AlN/GaN HEMTs for mixed-signal applications. / Yong Tang, Saunier P., Ronghua Wang, Ketterson A., Xiang Gao, Shiping Guo, Snider G., Jena D., Huili Xing, Fay P. // 2010 IEEE International Electron Devices Meeting (IEDM). - San Francisco, CA, 6-8 Dec. 2010. - P. 30.4.1-30.4.4. ↑

C264. Xinke Liu. Diamond-like carbon (DLC) liner with highly compressive stress formed on AlGaIn/GaN MOS-HEMTs with in situ silane surface passivation for performance enhancement. / Xinke Liu, Bin Liu, Low E.K.F., Hock-Chun Chin C., Wei Liu, Mingchu Yang, Leng Seow Tan, Yee-Chia Yeo. // 2010 IEEE International Electron Devices Meeting (IEDM). - San Francisco, CA, 6-8 Dec. 2010. - P. 11.3.1-11.3.4. ↑

C265. John D.L. A surface-potential based model for GaN HEMTs in RF power amplifier applications. / John D.L., Allerstam F., Rodle T., Murad S.K., Smit G.D.J. // 2010 IEEE International Electron Devices Meeting (IEDM). - San Francisco, CA, 6-8 Dec. 2010. - P. 8.3.1-8.3.4. ↑

C266. Mishra U.K. AlGaIn/GaN transistors for power electronics. 2010 IEEE International Electron Devices Meeting (IEDM). - San Francisco, CA, 6-8 Dec. 2010. - P. 13.2.1-13.2.4. ↑

C267. Marcon D. A comprehensive reliability investigation of the voltage-, temperature- and device geometry-dependence of the gate degradation on state-of-the-art GaN-on-Si HEMTs. / Marcon D., Kauerauf T., Medjdoub F., Das J., Van Hove M., Srivastava P., Cheng K., Leys M., Mertens R., Decoutere S., Meneghesso G., Zanoni E., Borghs G. // 2010 IEEE International Electron Devices Meeting (IEDM). - San Francisco, CA, 6-8 Dec. 2010. - P. 20.3.1-20.3.4. ↑

C268. Arehart A.R. Spatially-discriminating trap characterization methods for HEMTs and their application to RF-stressed AlGaIn/GaN HEMTs. / Arehart A.R., Sasikumar A., Via G.D., Winningham B., Poling B., Heller E., Ringel S.A. // 2010 IEEE International Electron Devices Meeting (IEDM). - San Francisco, CA, 6-8 Dec. 2010. - P. 20.1.1-20.1.4. ↑

C269. Zirath H. Power detectors and envelope detectors in mHEMT MMIC-technology for millimeterwave applications. / Zirath H., Zhongxia He. // 2010 European Microwave Integrated Circuits Conference (EuMIC). - Paris, 27-28 Sept. 2010. - P. 353-356. ↑

C270. Marinkovic. Development of a neural approach for bias-dependent scalable small-signal equivalent circuit modeling of GaAs HEMTs. / Marinkovic, Z., Crupi G., Caddemi A., Markovic V. // 2010 European Microwave Integrated Circuits Conference (EuMIC). - Paris, 27-28 Sept. 2010. - P. 182-185. ↑

C271. Darwish A.M. Dependence of FET/HEMT reliability on substrate thickness and gate length. / Darwish A.M., Hung H.A. // 2010 European Microwave Integrated Circuits Conference (EuMIC). - Paris, 27-28 Sept. 2010. - P. 262-265. ↑

C272. Ross T. Current density dependence of minimum noise figure for gallium nitride HEMTs. / Ross T., Cormier G., Hettak K., Amaya R.E. // 2010 European Microwave Integrated Circuits Conference (EuMIC). - Paris, 27-28 Sept. 2010. - P. 278-281. ↑

C273. Zamudio-Flores J.A. Improved measurement-based extraction algorithm of a comprehensive extrinsic element network for large-size GaN HEMTs. / Zamudio-Flores J.A., Kompa G. // 2010 European Microwave Integrated Circuits Conference (EuMIC). - Paris, 27-28 Sept. 2010. - P. 250-253. ↑

- C274.** Blount P. Low noise, low power dissipation mHEMT-based amplifiers for phased array application. / Blount P., Trantanell C.J., Coryell L., Lau R. // 2010 IEEE International Symposium on Phased Array Systems and Technology (ARRAY). - Waltham, MA, 12-15 Oct. 2010. - P. 233-237. ↑
- C275.** Klimenko O.A. Terahertz detection by InGaAs HEMTs in quantizing magnetic fields: Relation between magnetoresistance and photovoltaic response. / Klimenko O.A., Mityagin Y.A., Videlier H., Boubanga-Tombet S., Teppe F., Dyakonova N.V., Nadar S.H., Savinov S.A., Consejo C., Murzin V.N., Knap W. // 2010 35th International Conference on Infrared Millimeter and Terahertz Waves (IRMMW-THz). - Rome, 5-10 Sept. 2010. - P. 1-2. ↑
- C276.** Noude. Potentiality of commercial metamorphic HEMT at cryogenic temperature and low voltage operation. / Noude,viwa A., Roelens Y., Danneville F., Olivier A., Wichmann N., Waldhoff N., Lepilliet S., Dambrine G., Desplanque L., Wallart X., Bellaiche J., Smith D., Maher H., Bollaert S. // 2010 European Microwave Integrated Circuits Conference (EuMIC). - Paris, 27-28 Sept. 2010. - P. 286-289. ↑
- C277.** Banerjee A. Development of enhancement mode AlGaIn/GaN MOS-HEMTs using localized gate-foot oxidation. / Banerjee A., Taking S., MacFarlane D., Dabiran A., Wasige E. // 2010 European Microwave Integrated Circuits Conference (EuMIC). - Paris, 27-28 Sept. 2010. - P. 302-305. ↑
- C278.** Taking S. New process for low sheet and ohmic contact resistance of AlN/GaN MOS-HEMTs. / Taking S., Khokhar A.Z., MacFarlane D., Sharabi S., Dabiran A.M., Wasige E. // 2010 European Microwave Integrated Circuits Conference (EuMIC). - Paris, 27-28 Sept. 2010. - P. 306-309. ↑
- C279.** Astre G. Trapping related degradation effects in AlGaIn/GaN HEMT. / Astre G., Tartarin J.G., Lambert B. // 2010 European Microwave Integrated Circuits Conference (EuMIC). - Paris, 27-28 Sept. 2010. - P. 298-301. ↑
- C280.** Yore M.D. High-isolation low-loss SP7T pHEMT switch suitable for antenna switch modules. / Yore M.D., Nevers C.A., Cortese P. // 2010 European Microwave Integrated Circuits Conference (EuMIC). - Paris, 27-28 Sept. 2010. - P. 69-72. ↑
- C281.** Olivier A. High frequency performance of Tellurium σ -doped AlSb/InAs HEMTs at low power supply. / Olivier A., Noudeviwa A., Wichmann N., Roelens Y., Desplanque L., Danneville F., Dambrine G., Wallart X., Bollaert S. // 2010 European Microwave Integrated Circuits Conference (EuMIC). - Paris, 27-28 Sept. 2010. - P. 162-165. ↑
- C282.** Morkner H. High power, fully integrated SMT amplifiers with +47dBm OIP3 at 15 GHz and 6W, 38% efficiency at 30GHz using low cost, high volume PHEMT. / Morkner H., Fujii K., Ostermann B. // 2010 European Microwave Integrated Circuits Conference (EuMIC). - Paris, 27-28 Sept. 2010. - P. 412-415. ↑
- C283.** Do M.-N. AlGaIn/GaN mixer MMICs, and RF front-end receivers for C-, Ku-, and Ka-band space applications. / Do M.-N., Seelmann-Eggebert M., Quay R., Langrez D., Cazaux J.-L. // 2010 European Microwave Integrated Circuits Conference (EuMIC). - Paris, 27-28 Sept. 2010. - P. 57-60. ↑
- C284.** Douvry Y. Temperature dependent degradation modes in AlGaIn/GaN HEMTs. / Douvry Y., Hoel V., De Jaeger J., Defrance N., Sury C., Malbert N., Labat N., Curutchet A., Dua C., Oualli M., Piazza M., Bluet J., Chikhaoui W., Bru-Chevallier C. // 2010 European Microwave Integrated Circuits Conference (EuMIC). - Paris, 27-28 Sept. 2010. - P. 114-117. ↑
- C285.** Jangheon Kim. A high efficiency and multi-band/multi-mode power amplifier using a distributed second harmonic termination. / Jangheon Kim, Mkadem F., Boumaiza S. // 2010 European Microwave Integrated Circuits Conference (EuMIC). - Paris, 27-28 Sept. 2010. - P. 420-423. ↑
- C286.** Liu Z.H. Improved microwave noise and linearity performance in GaN MISHEMTs on silicon with ALD Al₂O₃ as gate dielectric. / Liu Z.H., Ng G.I., Arulkumaran S., Maung Y.K.T., Teo K.L., Foo S.C., Vicknesh S. // 2010 European Microwave Integrated Circuits Conference (EuMIC). - Paris, 27-28 Sept. 2010. - P. 41-44. ↑
- C287.** Caller G. Electrothermal and large-signal modeling of switchmode AlGaIn/GaN HEMTs. / Caller G., Faraj J., Rafei A.E., Jardel O., Jacquet J.C., Teyssier J.P., Morvan E., Piotrowicz S., Que, re R. // 2010 European Microwave Integrated Circuits Conference (EuMIC). - Paris, 27-28 Sept. 2010. - P. 266-269. ↑
- C288.** Charbonniaud C. A non linear power HEMT model operating in multi-bias conditions. / Charbonniaud C., Xiong A., Dellier S., Jardel O., Que, re, R. // 2010 European Microwave Integrated Circuits Conference (EuMIC). -

Paris, 27-28 Sept. 2010. - P. 134-137. ↑

C289. Che. Design of HEMT GaN power amplifiers with wideband control of 2nd harmonic impedances in S-Band. / Che,ron J., Campovecchio M., Barataud D., Stanislawiak M., Tolant C., Eudeline P., Floriot D., Heckmann S., Fave,de L., Temcamani F., Duperrier C. // 2010 European Microwave Integrated Circuits Conference (EuMIC). - Paris, 27-28 Sept. 2010. - P. 1-4. ↑

C290. Marinchio H. Hydrodynamic study of electronic, optical and thermal excitation of plasma waves in HEMTs. / Marinchio H., Palermo C., Sabatini G., Ziade, P., Laurent T., Shiktorov P., Starikov E., Gruz,inskis V., Nouvel P., Torres J., Pe,narier A., Blin S., Chusseau L., Varani L. // 2010 35th International Conference on Infrared Millimeter and Terahertz Waves (IRMMW-THz). - Rome, 5-10 Sept. 2010. - P. 1-2. ↑

C291. Bin Lu. Breakdown mechanism in AlGaIn/GaN HEMTs on Si substrate. / Bin Lu, Piner E.L., Palacios T. // 2010 Device Research Conference (DRC). - South Bend, IN, 21-23 June 2010. - P. 193-194. ↑

C292. Medjdoub F. Preliminary reliability at 50 V of state-of-the-art RF power GaN-on-Si HEMTs. / Medjdoub F., Marcon D., Das J., Derluyn J., Cheng K., Degroote S., Germain M., Decoutere S. // 2010 Device Research Conference (DRC). - South Bend, IN, 21-23 June 2010. - P. 195-196. ↑

C293. Hwang E. Scalability study of In_{0.7} Ga_{0.3} As HEMTs for 22nm node and beyond logic applications. / Hwang E., Mookerjee S., Hudait M.K., Datta S. // 2010 Device Research Conference (DRC). - South Bend, IN, 21-23 June 2010. - P. 61-62. ↑

C294. Ali A. Fermi level unpinning of GaSb(100) using Plasma Enhanced ALD Al₂O₃ dielectric. / Ali A., Madan H.S., Kirk A.P., Wallace R.M., Zhao D.A., Mourey D.A., Hudait M., Jackson T.N., Bennett B.R., Boos J.B., Datta S. // 2010 Device Research Conference (DRC). - South Bend, IN, 21-23 June 2010. - P. 27-30. ↑

C295. Roelens Y. Tellurium δ-doped 120nm AlSb/InAs HEMTs: towards sub-100mV electronics. / Roelens Y., Olivier A., Desplanque L., Noudeviwa A., Danneville F., Wichmann N., Wallart X., Bollaert S. // 2010 Device Research Conference (DRC). - South Bend, IN, 21-23 June 2010. - P. 53-54. ↑

C296. Selvaraj S.L. MOCVD grown normally-OFF type AlGaIn/GaN HEMTs on 4 inch Si using p-InGaIn cap layer with high breakdown. / Selvaraj S.L., Nagai K., Egawa T. // 2010 Device Research Conference (DRC). - South Bend, IN, 21-23 June 2010. - P. 135-136. ↑

C297. Tadjer M.J. Reduced self-heating in AlGaIn/GaN HEMTs using nanocrystalline diamond heat spreading films. / Tadjer M.J., Anderson T.J., Hobart K.D., Feygelson T.I., Mastro M.A., Caldwell J.D., Hite J.K., Eddy C.R., Kub F.J., Butler J.E., Melngailis J. // 2010 Device Research Conference (DRC). - South Bend, IN, 21-23 June 2010. - P. 125-126. ↑

C298. Ronghua Wang. High performance E-mode InAlN/GaN HEMTs: Interface states from subthreshold slopes. / Ronghua Wang, Xiu Xing, Tian Fang, Zimmermann T., Chuanxin Lian, Guowang Li, Saunier P., Xiang Gao, Shiping Guo, Snider G., Fay P., Jena D., Huili Xing. // 2010 Device Research Conference (DRC). - South Bend, IN, 21-23 June 2010. - P. 129-130. ↑

C299. Nidhi. T-gate technology for N-polar GaN-based self-aligned MIS-HEMTs with state-of-the-art f_{MAX} of 127 GHz: Pathway towards scaling to 30nm GaN HEMTs. / Nidhi, Dasgupta S., Brown D.F., Keller S., Speck J.S., Mishra U.K. // 2010 Device Research Conference (DRC). - South Bend, IN, 21-23 June 2010. - P. 155-156. ↑

C300. Hongwei Chen. Self-aligned enhancement-mode AlGaIn/GaN HEMTs using 25 keV fluorine ion implantation. / Hongwei Chen, Maojun Wang, Chen K.J. // 2010 Device Research Conference (DRC). - South Bend, IN, 21-23 June 2010. - P. 137-138. ↑

C301. Guowang Li. Work-function engineering in novel high Al composition Al_{0.72} Ga_{0.28} N/AlN/GaN HEMTs. / Guowang Li, Zimmermann T., Yu Cao, Chuanxin Lian, Xiu Xing, Ronghua Wang, Fay P., Xing H.G., Jena D. // 2010 Device Research Conference (DRC). - South Bend, IN, 21-23 June 2010. - P. 21-22. ↑

C302. Jacqmaer P. Fast robust gate-drivers with easily adjustable voltage ranges for driving normally-on wide-bandgap power transistors. / Jacqmaer P., Everts J., Gelagaev R., Tant P., Driesen J. // 2010 14th International Power Electronics and Motion Control Conference (EPE/PEMC). - Ohrid, 6-8 Sept. 2010. - P. T2-44-T2-51-44. ↑

- C303.** Ming Shi. Schrödinger-Poisson and Monte Carlo analysis of III-V MOSFETs for high frequency and low consumption applications. / Ming Shi, Saint-Martin J., Bournel A., Dollfus P. // 2010 International Conference on Simulation of Semiconductor Processes and Devices (SISPAD). - Bologna, 6-8 Sept. 2010. - P. 83-86. ↑
- C304.** Khmyrova I. Analysis of plasma resonances in terahertz devices with grating gate. / Khmyrova I., Yamase R., Watanabe N. // 2010 35th International Conference on Infrared Millimeter and Terahertz Waves (IRMMW-THz). - Rome, 5-10 Sept. 2010. - P. 1-2. ↑
- C305.** Li C. An In_{0.23}Ga_{0.77}As-based pHEMT-like planar Gunn diode operating at 116 GHz. / Li C., Khalid A., Lok L.B., Pilgrim N.J., Holland M.C., Dunn G.M., Cumming D.R.S. // 2010 35th International Conference on Infrared Millimeter and Terahertz Waves (IRMMW-THz). - Rome, 5-10 Sept. 2010. - P. 1-2. ↑
- C306.** Marinchio H. Hydrodynamic simulation of heterodyne terahertz detection in a field effect transistor. / Marinchio H., Palermo C., Sabatini G., Ziade, P., Shiktorov P., Starikov E., Gruz,inskiy V., Laurent T., Nouvel P., Torres J., Pe,narier A., Blin S., Chusseau L., Varani L. // 2010 35th International Conference on Infrared Millimeter and Terahertz Waves (IRMMW-THz). - Rome, 5-10 Sept. 2010. - P. 1-2. ↑
- C307.** Li Mingliang. On 10Gbps Terahertz wireless communication systems. / Li Mingliang, Wang Cong. // 2010 29th Chinese Control Conference (CCC). - Beijing, 29-31 July 2010. - P. 4180-4184. ↑
- C308.** Meierbachtol C.S. Development of a novel HEMT-based plasmonic sensor. / Meierbachtol C.S., Brown T.D., Chahal P., Shanker B. // 2010 IEEE Antennas and Propagation Society International Symposium (APSURSI). - Toronto, ON, 11-17 July 2010. - P. 1-4. ↑
- C309.** Chenyang Xue. Temperature-dependence electrical performance of GaAs-based HEMT-embedded accelerometer. / Chenyang Xue, Zhenxin Tan, Tingting Hou, Guowen Liu, Jun Liu, Binzhen Zhang. // 2010 5th IEEE International Conference on Nano/Micro Engineered and Molecular Systems (NEMS). - Xiamen, 20-23 Jan. 2010. - P. 798-801. ↑
- C310.** Rudin S. Viscous hydrodynamic model of non-linear plasma oscillations in two-dimensional gated conduction channels and application to the detection of terahertz signals. 2010 10th International Conference on Numerical Simulation of Optoelectronic Devices (NUSOD). - Atlanta, GA, 6-9 Sept. 2010. - P. 107-108. ↑
- C311.** Xiaojuan Jia. Characteristic research on an accelerated sensor based on GaAs/AlGaAs/InGaAs PHEMT. / Xiaojuan Jia, Binzhen Zhang, Jun Liu, Chenyang Xue, Tingting Hou. // 2010 5th IEEE International Conference on Nano/Micro Engineered and Molecular Systems (NEMS). - Xiamen, 20-23 Jan. 2010. - P. 417-420. ↑
- C312.** Pantellini A. Performance assessment of GaN HEMT technologies for power limiter and switching applications. / Pantellini A., Peroni M., Nanni A., Bettidi A. // 2010 European Microwave Integrated Circuits Conference (EuMIC). - Paris, 27-28 Sept. 2010. - P. 45-48. ↑
- C313.** Di Lecce V. Study of GaN HEMTs electrical degradation by means of numerical simulations. / Di Lecce V., Esposto M., Bonaiuti M., Fantini F., Chini A. // 2010 Proceedings of the European Solid-State Device Research Conference (ESSDERC). - Sevilla, 14-16 Sept. 2010. - P. 285-288. ↑
- C314.** Ming Shi. Optimization of III-V FET architectures for high frequency and low consumption applications. / Ming Shi, Saint-Martin J., Bournel A., Dollfus P. // 2010 Proceedings of the European Solid-State Device Research Conference (ESSDERC). - Sevilla, 14-16 Sept. 2010. - P. 424-427. ↑
- C315.** Sadi T. A continuous physics-based electrothermal compact model for the study of non-linearities in III-V HEMTs. / Sadi T., Schwierz F. // 2010 Proceedings of the European Solid-State Device Research Conference (ESSDERC). - Sevilla, 14-16 Sept. 2010. - P. 432-435. ↑
- C316.** Albrecht J.D. DARPA's Nitride Electronic NeXt Generation Technology Program. / Albrecht J.D., Tsu-Hsi Chang, Kane A.S., Rosker M.J. // 2010 IEEE Compound Semiconductor Integrated Circuit Symposium (CSICS). - Monterey, CA, 3-6 Oct. 2010. - P. 1-4. ↑
- C317.** Umana-Membreno G.A. Thermal broadening of two-dimensional electron gas mobility distribution in AlGaIn/AlIn/GaN heterostructures. / Umana-Membreno G.A., Stomeo T., Tasco V., Passaseo A., de Vittorio M., Faraone L. // 2010 Proceedings of the European Solid-State Device Research Conference (ESSDERC). - Sevilla, 14-16 Sept. 2010. - P. 182-185. ↑

- C318.** Lecourt F. High transconductance AlGaIn/GaN HEMT with thin barrier on Si(111) substrate. / Lecourt F., Douvry Y., Defrance N., Hoel V., De Jaeger J.C., Bouzid S., Renvoise M., Smith D., Maher H. // 2010 Proceedings of the European Solid-State Device Research Conference (ESSDERC). - Sevilla, 14-16 Sept. 2010. - P. 281-284. ↑
- C319.** Bathich K. A wideband GaN Doherty amplifier with 35 % fractional bandwidth. / Bathich K., Markos A.Z., Boeck G. // 2010 European Microwave Conference (EuMC). - Paris, 28-30 Sept. 2010. - P. 1006-1009. ↑
- C320.** Jangheon Kim. A high efficiency and multi-band/multi-mode power amplifier using a distributed second harmonic termination. / Jangheon Kim, Mkadem F., Boumaiza S. // 2010 European Microwave Conference (EuMC). - Paris, 28-30 Sept. 2010. - P. 1662-1665. ↑
- C321.** Morkner H. High power, fully integrated SMT amplifiers with +47dBm OIP3 at 15GHz and 6W, 38% efficiency at 30GHz using low cost, high volume PHEMT. / Morkner H., Fujii K., Ostermann B. // 2010 European Microwave Conference (EuMC). - Paris, 28-30 Sept. 2010. - P. 1654-1657. ↑
- C322.** Wentzel A. A voltage-mode class-s power amplifier for the 450MHz band. / Wentzel A., Meliani C., Heinrich W. // 2010 European Microwave Conference (EuMC). - Paris, 28-30 Sept. 2010. - P. 640-643. ↑
- C323.** Sledzik H. GaN based power amplifiers for broadband applications from 2 GHz to 6 GHz. / Sledzik H., Reber R., Bunz B., Schuh P., Oppermann M., Musser M., Seelmann-Eggebert M., Quay R. // 2010 European Microwave Conference (EuMC). - Paris, 28-30 Sept. 2010. - P. 1658-1661. ↑
- C324.** Ganesello F. 325GHz CPW band pass filter integrated in advanced HR SOI RF CMOS technology. / Ganesello F., Pilard R., Lepilliet S., Waldhoff N., Durand C., Boret S., Martineau B., Dambrine G., Gloria D., Rauber B., Raynaud C. // 2010 European Microwave Conference (EuMC). - Paris, 28-30 Sept. 2010. - P. 57-60. ↑
- C325.** Kuang-Yu Cheng. Development of 90nm InGaAs HEMTs and Benchmarking Logic Performance with Si CMOS. / Kuang-Yu Cheng, Chan D., Fei Tan, Huiming Xu, Feng M., Chih-Hsin Ko, Wann C. // 2010 IEEE Compound Semiconductor Integrated Circuit Symposium (CSICS). - Monterey, CA, 3-6 Oct. 2010. - P. 1-4. ↑
- C326.** Takagi K. Developing GaN HEMTs for Ka-Band with 20W. / Takagi K., Matsushita K., Kashiwabara Y., Masuda K., Nakanishi S., Sakurai H., Onodera K., Kawasaki H., Takada Y., Tsuda K. // 2010 IEEE Compound Semiconductor Integrated Circuit Symposium (CSICS). - Monterey, CA, 3-6 Oct. 2010. - P. 1-4. ↑
- C327.** Lynch J. An mHEMT Q-Band Integrated LNA and Vector Modulator MMIC. / Lynch J., Traut F.A., Benson K., Tshudy R. // 2010 IEEE Compound Semiconductor Integrated Circuit Symposium (CSICS). - Monterey, CA, 3-6 Oct. 2010. - P. 1-4. ↑
- C328.** Xiong A. A Scalable and Distributed Electro-Thermal Model of AlGaIn/GaN HEMT Dedicated to Multi-Fingers Transistors. / Xiong A., Charbonniaud C., Gatard E., Dellier S. // 2010 IEEE Compound Semiconductor Integrated Circuit Symposium (CSICS). - Monterey, CA, 3-6 Oct. 2010. - P. 1-4. ↑
- C329.** Kharabi F. A Verilog-A Large-Signal GaN HEMT Model for High Power Amplifier Design. / Kharabi F., McMacken J.R.F., Gering J.M. // 2010 IEEE Compound Semiconductor Integrated Circuit Symposium (CSICS). - Monterey, CA, 3-6 Oct. 2010. - P. 1-4. ↑
- C330.** Mahon S.J. LNA Design Based on an Extracted Single Gate Finger Model. / Mahon S.J., Dadello A., Vun P., Tarazi J., Young A.C., Heimlich M.C., Harvey J.T., Parker A.E. // 2010 IEEE Compound Semiconductor Integrated Circuit Symposium (CSICS). - Monterey, CA, 3-6 Oct. 2010. - P. 1-4. ↑
- C331.** Trejo M. Comparative Study of AlGaIn/GaN HEMTs on Free-Standing Diamond and Silicon Substrates for Thermal Effects. / Trejo M., Chabak K.D., Poling B., Gilbert R., Crespo A., Gillespie J.K., Kossler M., Walker D.E., Via G.D., Jessen G.H., Francis D., Faili F., Babic D., Ejeckam F. // 2010 IEEE Compound Semiconductor Integrated Circuit Symposium (CSICS). - Monterey, CA, 3-6 Oct. 2010. - P. 1-4. ↑
- C332.** Krishnamurthy K. A 0.1-1.8 GHz, 100 W GaN HEMT Power Amplifier Module. / Krishnamurthy K., Lieu D., Vetury R., Martin J. // 2010 IEEE Compound Semiconductor Integrated Circuit Symposium (CSICS). - Monterey, CA, 3-6 Oct. 2010. - P. 1-4. ↑
- C333.** Tessmann A. A Metamorphic HEMT S-MMIC Amplifier with 16.1 dB Gain at 460 GHz. / Tessmann A.,

Leuther A., Loesch R., Seelmann-Eggebert M., Massler H. // 2010 IEEE Compound Semiconductor Integrated Circuit Symposium (CSICS). - Monterey, CA, 3-6 Oct. 2010. - P. 1-4. ↑

C334. Deal W.R. Scaling of InP HEMT Cascode Integrated Circuits to THz Frequencies. / Deal W.R., Leong K., Mei X.B., Sarkozy S., Radisic V., Lee J., Liu P.H., Yoshida W., Zhou J., Lange M. // 2010 IEEE Compound Semiconductor Integrated Circuit Symposium (CSICS). - Monterey, CA, 3-6 Oct. 2010. - P. 1-4. ↑

C335. Xiaosen Liu. Single-Polarity Power Supply Bootstrapped Comparator for GaN Smart Power Technology. / Xiaosen Liu, Chen K.J. // 2010 IEEE Compound Semiconductor Integrated Circuit Symposium (CSICS). - Monterey, CA, 3-6 Oct. 2010. - P. 1-4. ↑

C336. Nakasha Y. E-Band 85-mW Oscillator and 1.3-W Amplifier ICs Using 0.12μm GaN HEMTs for Millimeter-Wave Transceivers. / Nakasha Y., Masuda S., Makiyama K., Ohki T., Kanamura M., Okamoto N., Tajima T., Seino T., Shigematsu H., Imanishi K., Kikkawa T., Joshin K., Hara N. // 2010 IEEE Compound Semiconductor Integrated Circuit Symposium (CSICS). - Monterey, CA, 3-6 Oct. 2010. - P. 1-4. ↑

C337. Mougnot G. Thermal and trapping phenomena assessment on AlGaIn/GaN microwave power transistor. / Mougnot G., Sommet R., Quere R., Ouarch Z., Heckmann S., Camiade M. // 2010 European Microwave Integrated Circuits Conference (EuMIC). - Paris, 27-28 Sept. 2010. - P. 110-113. ↑

C338. Sledzik H. GaN based power amplifiers for broadband applications from 2 GHz to 6 GHz. / Sledzik H., Reber R., Bunz B., Schuh P., Oppermann M., Musser M., Seelmann-Eggebert M., Quay R. // 2010 European Microwave Integrated Circuits Conference (EuMIC). - Paris, 27-28 Sept. 2010. - P. 416-419. ↑

C339. Jin-Siang Syu. Comparison on mHEMT Q-band sub-harmonic mixers with/without delay compensation. / Jin-Siang Syu, Chinchun Meng, Jen-Yi Su, Guo-Wei Huang. // 2010 European Microwave Integrated Circuits Conference (EuMIC). - Paris, 27-28 Sept. 2010. - P. 194-197. ↑

C340. Jin-Cheol Jeong. An MMIC wide-band doubly balanced resistive mixer with an active IF balun. / Jin-Cheol Jeong, In-Bok Yom, Kyung-Whan Yeom. // 2010 European Microwave Integrated Circuits Conference (EuMIC). - Paris, 27-28 Sept. 2010. - P. 333-336. ↑

C341. Diciomma R. 8W 2-8GHz solid state amplifier for phased array. / Diciomma R., Ciaccia E., Giolo G., Baccello D., Orobello B., Alleva V. // 2010 European Microwave Integrated Circuits Conference (EuMIC). - Paris, 27-28 Sept. 2010. - P. 401-403. ↑

C342. Lopez-Diaz D. A balanced resistive 210 GHz mixer with 50 GHz IF bandwidth. / Lopez-Diaz D., Kallfass I., Tessmann A., Massler H., Leuther A., Schlechtweg M., Ambacher O. // 2010 European Microwave Integrated Circuits Conference (EuMIC). - Paris, 27-28 Sept. 2010. - P. 190-193. ↑

C343. Kallfass I. An all-active MMIC-based chip set for a wideband 260-304 GHz receiver. / Kallfass I., Tessmann A., Massler H., Pahl P., Leuther A. // 2010 European Microwave Integrated Circuits Conference (EuMIC). - Paris, 27-28 Sept. 2010. - P. 53-56. ↑

C344. Diebold S. Determination of suitable mHEMT transistor dimensioning for power amplification at 210 GHz by comprehensive measurements. / Diebold S., Kallfass I., Massler H., Leuther A., Tessmann A., Pahl P., Koch S., Siegel M., Ambacher O. // 2010 European Microwave Integrated Circuits Conference (EuMIC). - Paris, 27-28 Sept. 2010. - P. 78-81. ↑

C345. Lavanga S. High Voltage Breakdown pHEMTs for C-band HPA. / Lavanga S., Chini A., Coppa A., Corsaro F., Nanni A., Pantellini A., Romanini P., Lanzieri C. // 2010 European Microwave Integrated Circuits Conference (EuMIC). - Paris, 27-28 Sept. 2010. - P. 142-145. ↑

C346. Santarelli A. Nonlinear thermal resistance characterization for compact electrothermal GaN HEMT modelling. / Santarelli A., Di Giacomo V., Cignani R., D'Angelo S., Niessen D., Filicori F. // 2010 European Microwave Integrated Circuits Conference (EuMIC). - Paris, 27-28 Sept. 2010. - P. 82-85. ↑

C347. Jardel O. GaN power MMICs for X-Band T/R modules. / Jardel O., Mazeau J., Piotrowicz S., Caban-Chastas D., Chartier E., Morvan E., Due,me P., Mancuso Y., Delage S.L. // 2010 European Microwave Integrated Circuits Conference (EuMIC). - Paris, 27-28 Sept. 2010. - P. 17-20. ↑

C348. Musser M. GaN power FETs for next generation mobile communication systems. / Musser M., Walcher

H., Maier T., Quay R., Dammann M., Mikulla M., Ambacher O. // 2010 European Microwave Integrated Circuits Conference (EuMIC). - Paris, 27-28 Sept. 2010. - P. 9-12. ↑

C349. Yong Wang. Improved AlGaIn/GaN HEMTs grown on Si substrates by MOCVD. / Yong Wang, Naisen Yu, Dongmei Deng, Ming Li, Fei Sun, Kei May Lau. // 2010 10th Russian-Chinese Symposium on Laser Physics and Laser Technologies (RCSLPLT) and 2010 Academic Symposium on Optoelectronics Technology (ASOT). - Harbin, July 28 2010-Aug. 1 2010. - P. 68-71. ↑

C350. Bentini A. Broadband resistive-inductive compensated GaN-HEMT single-FET switch. / Bentini A., Colangeli S., Ferrari M., Limiti E. // 2010 European Microwave Conference (EuMC). - Paris, 28-30 Sept. 2010. - P. 1206-1209. ↑

C351. Yuk K. Design of a high power x-band frequency tripler using a AlGaIn/GaN HEMT device. / Yuk K., Wong C., Branner G.R. // 2010 European Microwave Conference (EuMC). - Paris, 28-30 Sept. 2010. - P. 612-615. ↑

C352. Jungjoon Kim. Doherty power amplifier design employing direct input power dividing for base station applications. / Jungjoon Kim, Junghwan Moon, Daehyun Kang, Seunghoon Jee, Young Yun Woo, Bumman Kim. // 2010 European Microwave Conference (EuMC). - Paris, 28-30 Sept. 2010. - P. 866-869. ↑

C353. Medjdoub F. GaN-on-Si HEMTs above 10 W/mm at 2 GHz together with high thermal stability at 325°C. / Medjdoub F., Marcon D., Das J., Derluyn J., Cheng K., Degroote S., Vellas N., Gaquiere C., Germain M., Decoutere S. // 2010 European Microwave Integrated Circuits Conference (EuMIC). - Paris, 27-28 Sept. 2010. - P. 37-40. ↑

C354. van der Bent G. Four-channel Ku-band downconverter MMIC. / van der Bent G., de Hek P., van Dijk R., van Vliet F.E. // 2010 European Microwave Conference (EuMC). - Paris, 28-30 Sept. 2010. - P. 1074-1077. ↑

C355. Akmal M. The effect of baseband impedance termination on the linearity of GaN HEMTs. / Akmal M., Lees J., Bensmida S., Woodington S., Carrubba V., Cripps S., Benedikt J., Morris K., Beach M., McGeehan J., Tasker P.J. // 2010 European Microwave Conference (EuMC). - Paris, 28-30 Sept. 2010. - P. 1046-1049. ↑

C356. Jangheon Kim. A novel design method of highly efficient saturated power amplifier based on self-generated harmonic currents. / Jangheon Kim, Junghwan Moon, Jungjoon Kim, Boumaiza S., Bumman Kim. // 2009. EuMC 2009. European Microwave Conference. - Rome, Sept. 29 2009-Oct. 1 2009. - P. 1082-1085. ↑

C357. Martynov Y.B. Substrate design enabling to increase HEMTs open channel breakdown voltage. / Martynov Y.B., Pogorelova E.V. // 2009. CriMiCo 2009. 19th International Crimean Conference Microwave & Telecommunication Technology. - Sevastopol, 14-18 Sept. 2009. - P. 127-128. ↑

C358. Baylis C. Electrothermal nonlinear FET modeling for spectral prediction. / Baylis C., Dunleavy L. // 2009. EMC 2009. IEEE International Symposium on Electromagnetic Compatibility. - Austin, TX, 17-21 Aug. 2009. - P. 95-98. ↑

C359. Kistchinsky A. Gan solid-state microwave power amplifiers-State-of-the-art and future trends. 2009. CriMiCo 2009. 19th International Crimean Conference Microwave & Telecommunication Technology. - Sevastopol, 14-18 Sept. 2009. - P. 11-16. ↑

C360. Di Giacomo V. Modelling and design of a wideband 6-18 GHz GaN resistive mixer. / Di Giacomo V., Thouvenin N., Gaquiere C., Santarelli A., Filicori F. // 2009. EuMC 2009. European Microwave Conference. - Rome, Sept. 29 2009-Oct. 1 2009. - P. 1812-1815. ↑

C361. Yuh-Jing Hwang. A photonic-tunable cryogenically cooled W-band subharmonically-pumped GaAs HEMT diode mixer module. / Yuh-Jing Hwang, Chih-Chiang Han, Yau-De Huang. // 2009. EuMIC 2009. European Microwave Integrated Circuits Conference. - Rome, 28-29 Sept. 2009. - P. 208-211. ↑

C362. Sayed A. 5W, 0.35-8 GHz linear power amplifier using GaN HEMT. / Sayed A., Al Tanany A., Boeck G. // 2009. EuMC 2009. European Microwave Conference. - Rome, Sept. 29 2009-Oct. 1 2009. - P. 488-491. ↑

C363. van der Bent G. X-band phase-shifting dual-output balanced amplifier MMIC. / van der Bent G., de Boer T.S., van Dijk R., van der Graaf M.W., de Hek A.P., van Vliet F.E. // 2009. EuMC 2009. European Microwave Conference. - Rome, Sept. 29 2009-Oct. 1 2009. - P. 1665-1668. ↑

- C364.** Flucke J. An accurate package model for 60W GaN power transistors. / Flucke J., Schmuckle F.-J., Heinrich W., Rudolph M. // 2009. EuMIC 2009. European Microwave Integrated Circuits Conference. - Rome, 28-29 Sept. 2009. - P. 152-155. ↑
- C365.** Crispoldi F. New fabrication process to manufacture RF-MEMS and HEMT on GaN/Si substrate. / Crispoldi F., Pantellini A., Lavanga S., Nanni A., Romanini P., Rizzi L., Farinelli P., Lanzieri C. // 2009. EuMIC 2009. European Microwave Integrated Circuits Conference. - Rome, 28-29 Sept. 2009. - P. 387-390. ↑
- C366.** Jardel O. A new nonlinear HEMT model for AlGaIn/GaN switch applications. / Jardel O., Callet G., Charbonniaud C., Jacquet J.C., Sarazin N., Morvan E., Aubry R., Di Forte Poisson M.-A., Teyssier J.-P., Piotrowicz S., Quere R. // 2009. EuMIC 2009. European Microwave Integrated Circuits Conference. - Rome, 28-29 Sept. 2009. - P. 73-76. ↑
- C367.** Weber R. A novel tuning concept for wideband VCOs based on a shunt-FET. / Weber R., Kallfass I., Seelmann-Eggebert M., Leuther A. // 2009. EuMIC 2009. European Microwave Integrated Circuits Conference. - Rome, 28-29 Sept. 2009. - P. 124-127. ↑
- C368.** Piotrowicz S. Broadband AlGaIn/GaN high power amplifiers, robust LNAs, and power switches in L-band. / Piotrowicz S., Mallet-Guy B., Chartier E., Jacquet J.C., Jardel O., Lancereau D., Le Coustre G., Morvan E., Aubry R., Dua C., Oualli M., Richard M., Sarazin N., diForte-Poisson M.A., Delaire J., Mancuso Y., Delage S.L. // 2009. EuMC 2009. European Microwave Conference. - Rome, Sept. 29 2009-Oct. 1 2009. - P. 1784-1787. ↑
- C369.** Masuda S. GaN MMIC amplifiers for W-band transceivers. / Masuda S., Ohki T., Makiyama K., Kanamura M., Okamoto N., Shigematsu H., Imanishi K., Kikkawa T., Joshin K., Hara N. // 2009. EuMC 2009. European Microwave Conference. - Rome, Sept. 29 2009-Oct. 1 2009. - P. 1796-1799. ↑
- C370.** Bettidi A. X-Band GaN-HEMT LNA performance versus robustness trade-off. / Bettidi A., Corsaro F., Cetrionio A., Nanni A., Peroni M., Romanini P. // 2009. EuMIC 2009. European Microwave Integrated Circuits Conference. - Rome, 28-29 Sept. 2009. - P. 439-442. ↑
- C371.** De Jaeger J.-C. Microwave power performance on AlGaIn/GaN HEMTs on composite substrate. / De Jaeger J.-C., Hoel V., Defrance N., Douvry Y., Gaquiere C., di Forte-Poisson M.-A., Thorpe J., Lahreche H., Langer R. // 2009. EuMIC 2009. European Microwave Integrated Circuits Conference. - Rome, 28-29 Sept. 2009. - P. 144-147. ↑
- C372.** Zuniga-Juarez J.E. Two-tier L-L de-embedding method for S-parameters measurements of devices mounted in test fixture. / Zuniga-Juarez J.E., Reynoso-Hernandez J.A., Loo-Yau J.R. // 2009 73rd ARFTG Microwave Measurement Conference. - Boston, MA, 12-12 June 2009. - P. 1-5. ↑
- C373.** Ivo P. Influence of GaN cap on robustness of AlGaIn/GaN HEMTs. / Ivo P., Glowacki A., Pazirandeh R., Bahat-Treidel E., Lossy R., Wurfl J., Boit C., Trankle G. // 2009 IEEE International Reliability Physics Symposium. - Montreal, QC, 26-30 April 2009. - P. 71-75. ↑
- C374.** Rawal D.S. Study of Cl₂/BCl₃ inductively coupled plasma for selective etching of GaAs. / Rawal D.S., Malik H.K., Sehgal B.K., Muralidharan R. // 2009. ICOPS 2009. IEEE International Conference on Plasma Science-Abstracts. - San Diego, CA, 1-5 June 2009. - P. 1. ↑
- C375.** Verzellesi G. False surface-trap signatures induced by buffer traps in AlGaIn-GaN HEMTs. / Verzellesi G., Faqir M., Chini A., Fantini F., Meneghesso G., Zanon E., Danesin F., Zanon F., Rampazzo F., Marino F.A., Cavallini A., Castaldini A. // 2009 IEEE International Reliability Physics Symposium. - Montreal, QC, 26-30 April 2009. - P. 732-735. ↑
- C376.** Nakajima A. Physical mechanism of buffer-related lag and current collapse in GaN-based FETs and their reduction by introducing a field plate. / Nakajima A., Itagaki K., Horio K. // 2009 IEEE International Reliability Physics Symposium. - Montreal, QC, 26-30 April 2009. - P. 722-726. ↑
- C377.** Baylis C. Modeling considerations for GaN HEMT devices. / Baylis C., Dunleavy L., Connick R. // 2009. WAMICON '09. IEEE 10th Annual Wireless and Microwave Technology Conference. - Clearwater, FL, 20-21 April 2009. - P. 1-2. ↑
- C378.** Fathipour M. Improving performance in single field plate power High Electron Mobility Transistors

(HEMTs) based on AlGaIn/GaN. / Fathipour M., Peyvast N., Azadvari R. // 2009. ASQED 2009. 1st Asia Symposium on Quality Electronic Design. - Kuala Lumpur, 15-16 July 2009. - P. 157-161. ↑

C379. Casto M.J. AlGaIn/GaN HEMT temperature-dependent large-signal model thermal circuit extraction with verification through advanced thermal imaging. / Casto M.J., Dooley S.R. // 2009. WAMICON '09. IEEE 10th Annual Wireless and Microwave Technology Conference. - Clearwater, FL, 20-21 April 2009. - P. 1-5. ↑

C380. Wu D.Y.-T. 10W GaN inverse class F PA with input/output harmonic termination for high efficiency WiMAX transmitter. / Wu D.Y.-T., Boumaiza S. // 2009. WAMICON '09. IEEE 10th Annual Wireless and Microwave Technology Conference. - Clearwater, FL, 20-21 April 2009. - P. 1-4. ↑

C381. Sajjad A. 10 W Class AB power amplifier design for UMTS applications using GaN HEMT. / Sajjad A., Sayed A., Al Tanany A., Boeck G. // 2009. NRSC 2009. National Radio Science Conference. - New Cairo, 17-19 March 2009. - P. 1-8. ↑

C382. Elnaby M.A. An analytical expression for the I-V characteristics of AlGaIn/GaN HEMTs. / Elnaby M.A., Aziz M.A., Shalaby A.A., El-Abd A. // 2009. NRSC 2009. National Radio Science Conference. - New Cairo, 17-19 March 2009. - P. 1-7. ↑

C383. Jin He. Design of a 2.2 GHz high efficiency GaN HEMT inverse class E transmission-line power amplifier. / Jin He, Dehao Ren. // 2009. ICCAS 2009. International Conference on Communications, Circuits and Systems. - Milpitas, CA, 23-25 July 2009. - P. 746-748. ↑

C384. Yuehang Xu. Influence of the Al mole fraction on microwave noise performance of Al_xGa_{1-x}N/GaN HEMTs. / Yuehang Xu, Yunchuan Guo, Yunqi Wu, Ruimin Xu, Bo Yan. // 2009. ICCAS 2009. International Conference on Communications, Circuits and Systems. - Milpitas, CA, 23-25 July 2009. - P. 759-761. ↑

C385. Klehr A. A new concept of an ultra fast pulse picker for fs- and ps-pulses from GHz pulse-trains with semiconductor tapered elements. / Klehr A., Liero A., Hoffann T., Schwertfeger S., Erbert G., Heinrich W., Trankle G. // Lasers and Electro-Optics 2009 and the European Quantum Electronics Conference. CLEO Europe-EQEC 2009. European Conference on. - Munich, 14-19 June 2009. - P. 1. ↑

C386. Muravjov A.V. Terahertz plasmons in grating-gate AlGaIn/GaN HEMTs. / Muravjov A.V., Veksler D.B., Popov V.V., Shur M.S., Pala N., Hu X., Gaska R., Saxena H., Peale R.E. // Lasers and Electro-Optics 2009 and the European Quantum Electronics Conference. CLEO Europe-EQEC 2009. European Conference on. - Munich, 14-19 June 2009. - P. 1. ↑

C387. Xiaopeng Zhou. AlGaIn/GaN HEMT device structure optimization design. / Xiaopeng Zhou, Zhiquan Cheng, Sha Hu, Weijian Zhou, Sheng Zhang. // 2009. IPFA 2009. 16th IEEE International Symposium on the Physical and Failure Analysis of Integrated Circuits. - Suzhou, Jiangsu, 6-10 July 2009. - P. 339-343. ↑

C388. Ramadan A. Study and design of high efficiency switch mode GaN power amplifiers at L-band frequency. / Ramadan A., Martin A., Sardin D., Reveyard T., Nebus J.-M., Bouysse P., Lapierre L., Villemazet J.F., Forestier S. // 2009. ACTEA '09. International Conference on Advances in Computational Tools for Engineering Applications. - Zouk Mosbeh, 15-17 July 2009. - P. 117-120. ↑

C389. Quaglia R. Real-time FPGA-based baseband predistortion of W-CDMA 3GPP high-efficiency power amplifiers: Comparing GaN HEMT and Si LDMOS predistorted PA performances. / Quaglia R., Camarchia V., Guerrieri S.D., Lima E.G., Ghione G., Qiang Luo, Pirola M., Tinivella R. // 2009. EuMC 2009. European Microwave Conference. - Rome, Sept. 29 2009-Oct. 1 2009. - P. 342-345. ↑

C390. Mun-Woo Lee. Optimum bias for highly linear and efficient doherty power amplifier with memoryless digital predistortion. / Mun-Woo Lee, Yong-Sub Lee, Sang-Ho Kam, Yoon-Ha Jeong. // 2009. EuMC 2009. European Microwave Conference. - Rome, Sept. 29 2009-Oct. 1 2009. - P. 1441-1444. ↑

C391. ElBarkouky M. A 7 GHz FBAR overtone-based oscillator. / ElBarkouky M., Vandersteen G., Wambacq P., Rolain Y. // 2009. EuMC 2009. European Microwave Conference. - Rome, Sept. 29 2009-Oct. 1 2009. - P. 318-321. ↑

C392. Nilsson J. S-band discrete and MMIC GaN power amplifiers. / Nilsson J., Billstrom N., Rorsman N., Romanini P. // 2009. EuMC 2009. European Microwave Conference. - Rome, Sept. 29 2009-Oct. 1 2009. - P. 1848-1851. ↑

- C393.** FitzPatrick D.M. Systematic investigation of the impact of harmonic termination in the efficiency performance of above octave bandwidth microwave amplifiers. / FitzPatrick D.M., Lees J., Sheikh A., Benedikt J., Tasker P.J. // 2009. EuMC 2009. European Microwave Conference. - Rome, Sept. 29 2009-Oct. 1 2009. - P. 1445-1448. ↑
- C394.** Crispoldi F. New fabrication process to manufacture RF-MEMS and HEMT on GaN/Si substrate. / Crispoldi F., Pantellini A., Lavanga S., Nanni A., Romanini P., Rizzi L., Farinelli P., Lanzieri C. // 2009. EuMC 2009. European Microwave Conference. - Rome, Sept. 29 2009-Oct. 1 2009. - P. 1740-1743. ↑
- C395.** Dinari M. Wide band high linearity and high isolation mixer MMIC developed on GaAs 0.25μm power pHEMT technology. / Dinari M., Serru V., Camiade M., Teyssandier C., Baglieri D., Durand E., Mallet-Guy B., Plaze J.P. // 2009. EuMC 2009. European Microwave Conference. - Rome, Sept. 29 2009-Oct. 1 2009. - P. 1661-1664. ↑
- C396.** Bensmida S. Power amplifier memory-less pre-distortion for 3GPP LTE application. / Bensmida S., Morris K., Lees J., Wright P., Benedikt J., Tasker P.J., Beach M., McGeehan J. // 2009. EuMC 2009. European Microwave Conference. - Rome, Sept. 29 2009-Oct. 1 2009. - P. 1433-1436. ↑
- C397.** Wentzel A. A simplified switch-based GaN HEMT model for RF switch-mode amplifiers. / Wentzel A., Schnieder F., Meliani C., Heinrich W. // 2009. EuMIC 2009. European Microwave Integrated Circuits Conference. - Rome, 28-29 Sept. 2009. - P. 77-80. ↑
- C398.** Fornetti F. Pulsed operation and performance of commercial GaN HEMTs. / Fornetti F., Morris K.A., Beach M.A. // 2009. EuMIC 2009. European Microwave Integrated Circuits Conference. - Rome, 28-29 Sept. 2009. - P. 226-229. ↑
- C399.** Pantellini A. Gate technology and substrate property influence on GaN HEMT switch device performance. / Pantellini A., Peroni M., Nanni A., Cetronio A., Bettidi A., Giovine E. // 2009. EuMIC 2009. European Microwave Integrated Circuits Conference. - Rome, 28-29 Sept. 2009. - P. 140-143. ↑
- C400.** Chini A. RF degradation of GaN HEMTs and its correlation with DC stress and I-DLTS measurements. / Chini A., Di Lecce V., Esposto M., Meneghesso G., Zanoni E. // 2009. EuMIC 2009. European Microwave Integrated Circuits Conference. - Rome, 28-29 Sept. 2009. - P. 132-135. ↑
- C401.** Morkner H. Wafer Scale Package construction and usage for RF through millimeter wave applications. 2009. EuMIC 2009. European Microwave Integrated Circuits Conference. - Rome, 28-29 Sept. 2009. - P. 419-422. ↑
- C402.** Ramadan A. Efficiency enhancement of GaN power HEMTs by controlling gate-source voltage waveform shape. / Ramadan A., Martin A., Reveyrand T., Nebus J.-M., Bouysse P., Lapierre L., Villemazet J.F., Forestier S. // 2009. EuMC 2009. European Microwave Conference. - Rome, Sept. 29 2009-Oct. 1 2009. - P. 1840-1843. ↑
- C403.** Piotrowicz S. Broadband AlGaIn/GaN high power amplifiers, robust LNAs, and power switches in L-Band. / Piotrowicz S., Mallet-Guy B., Chartier E., Jacquet J.C., Jardel O., Lancereau D., Le Coustre G., Morvan E., Aubry R., Dua C., Oualli M., Richard M., Sarazin N., diForte-Poisson M.A., Delaire J., Mancuso Y., Delage S.L. // 2009. EuMIC 2009. European Microwave Integrated Circuits Conference. - Rome, 28-29 Sept. 2009. - P. 431-434. ↑
- C404.** Mkhitarian A. 200W discrete GaN HEMT power device in a 747mm CMC package. / Mkhitarian A., Ngo V., Baltac F., Huoping Xin. // 2009. EuMIC 2009. European Microwave Integrated Circuits Conference. - Rome, 28-29 Sept. 2009. - P. 97-100. ↑
- C405.** Bettidi A. X-band GaN-HEMT LNA performance versus robustness trade-off. / Bettidi A., Corsaro F., Cetronio A., Nanni A., Peroni M., Romanini P. // 2009. EuMC 2009. European Microwave Conference. - Rome, Sept. 29 2009-Oct. 1 2009. - P. 1792-1795. ↑
- C406.** Srinidhi E.R. Device inherent IMD reproducibility issues in GaN HEMTs. / Srinidhi E.R., Rui Ma, Kompa G., Bangert A. // 2009. EuMIC 2009. European Microwave Integrated Circuits Conference. - Rome, 28-29 Sept. 2009. - P. 108-111. ↑
- C407.** van der Bent G. X-band phase-shifting dual-output balanced amplifier MMIC. / van der Bent G., de Boer

T.S., van Dijk R., van der Graaf M.W., de Hek A.P., van Vliet F.E. // 2009. EuMIC 2009. European Microwave Integrated Circuits Conference. - Rome, 28-29 Sept. 2009. - P. 312-315. ↑

C408. Kallfass I. A 300 GHz active frequency-doubler and integrated resistive mixer MMIC. / Kallfass I., Tessmann A., Massler H., Lopez-Diaz D., Leuther A., Schlechtweg M., Ambacher O. // 2009. EuMIC 2009. European Microwave Integrated Circuits Conference. - Rome, 28-29 Sept. 2009. - P. 200-203. ↑

C409. Kallfass I. A 200 GHz active heterodyne receiver MMIC with low sub-harmonic LO power requirements for imaging frontends. / Kallfass I., Tessmann A., Massler H., Leuther A., Schlechtweg M., Ambacher O. // 2009. EuMIC 2009. European Microwave Integrated Circuits Conference. - Rome, 28-29 Sept. 2009. - P. 45-48. ↑

C410. Fan-Hsiu Huang. A linearity improved GaAs pHEMT power amplifier using common-gate/common-source circuit topology. / Fan-Hsiu Huang, Hong-Yeh Chang, Yi-Jen Chan. // 2009. EuMIC 2009. European Microwave Integrated Circuits Conference. - Rome, 28-29 Sept. 2009. - P. 491-494. ↑

C411. Nilsson J. S-band discrete and MMIC GaN power amplifiers. / Nilsson J., Billstrom N., Rorsman N., Romanini P. // 2009. EuMIC 2009. European Microwave Integrated Circuits Conference. - Rome, 28-29 Sept. 2009. - P. 495-498. ↑

C412. Chih-Chun Shen. Comparison of enhancement- and depletion-mode triple stacked power amplifiers in 0.5 μm AlGaAs/GaAs PHEMT technology. / Chih-Chun Shen, Hong-Yeh Chang, Vendelin G.D. // 2009. EuMIC 2009. European Microwave Integrated Circuits Conference. - Rome, 28-29 Sept. 2009. - P. 222-225. ↑

C413. Di Giacomo V. Modelling and design of a wideband 6-18 GHz GaN Resistive Mixer. / Di Giacomo V., Thouvenin N., Gaquiere C., Santarelli A., Filicori F. // 2009. EuMIC 2009. European Microwave Integrated Circuits Conference. - Rome, 28-29 Sept. 2009. - P. 459-462. ↑

C414. Gerbedoen J.-C. Study of ohmic contact formation on AlGaIn/GaN HEMT with AlN spacer on silicon substrate. / Gerbedoen J.-C., Soltani A., Mattalah M., Telia A., Troadec D., Abdallah B., Gautron E., De Jaeger J.-C. // 2009. EuMIC 2009. European Microwave Integrated Circuits Conference. - Rome, 28-29 Sept. 2009. - P. 136-139. ↑

C415. Ramadan A. Efficiency enhancement of GaN power HEMTs by controlling gate-source voltage waveform shape. / Ramadan A., Martin A., Reveyrand T., Nebus J.-M., Bouysse P., Lapierre L., Villemazet J.F., Forestier S. // 2009. EuMIC 2009. European Microwave Integrated Circuits Conference. - Rome, 28-29 Sept. 2009. - P. 487-490. ↑

C416. Albahrani S.A. Characterizing drain current dispersion in GaN HEMTs with a new trap model. / Albahrani S.A., Rathmell J.G., Parker A.E. // 2009. EuMC 2009. European Microwave Conference. - Rome, Sept. 29 2009-Oct. 1 2009. - P. 1692-1695. ↑

C417. Yong-Sub Lee. High-efficiency GaN HEMT power amplifier design based on inverse class-e topology. / Yong-Sub Lee, Mun-Woo Lee, Sang-Ho Kam, Yoon-Ha Jeong. // 2009. EuMC 2009. European Microwave Conference. - Rome, Sept. 29 2009-Oct. 1 2009. - P. 500-503. ↑

C418. Fujii K. 40 to 85GHz power amplifier MMICs using an optical lithography based low cost GaAs PHEMT process. / Fujii K., Stanback J., Morkner H. // 2009. EuMIC 2009. European Microwave Integrated Circuits Conference. - Rome, 28-29 Sept. 2009. - P. 503-506. ↑

C419. Masuda S. GaN MMIC amplifiers for W-band transceivers. / Masuda S., Ohki T., Makiyama K., Kanamura M., Okamoto N., Shigematsu H., Imanishi K., Kikkawa T., Joshin K., Hara N. // 2009. EuMIC 2009. European Microwave Integrated Circuits Conference. - Rome, 28-29 Sept. 2009. - P. 443-446. ↑

C420. Albahrani S.A. Characterizing drain current dispersion in GaN HEMTs with a new trap model. / Albahrani S.A., Rathmell J.G., Parker A.E. // 2009. EuMIC 2009. European Microwave Integrated Circuits Conference. - Rome, 28-29 Sept. 2009. - P. 339-342. ↑

C421. Hon P.W.C. InP, W-band, oscillator stabilized with a resonant cavity created by Wafer Level Packaging. / Hon P.W.C., Farkas D., Itoh T., Chang-Chien P.P., Lai R. // 2009. EuMIC 2009. European Microwave Integrated Circuits Conference. - Rome, 28-29 Sept. 2009. - P. 282-285. ↑

C422. Yu-Chao Lin. Low-leakage InAs/AlSb HEMT with high FT-LG product. / Yu-Chao Lin, Ta-Wei Fan,

Heng-Kuang Lin, Pei-Chin Chiu, Jen-Inn Chyi, Chih-Hsin Ko, Ta-Ming Kuan, Meng-Kuei Hsieh, Wen-Chin Lee, Wann C.H. // 2009. IPRM 09. IEEE International Conference on Indium Phosphide & Related Materials. - Newport Beach, CA, 10-14 May 2009. - P. 330-333. ↑

C423. Da-Wei Fan. Metal-oxide-HEMT on 6.1E antimonides. / Da-Wei Fan, Yu-Chao Lin, Heng-Kuang Lin, Pei-Chin Chiu, Shu-Han Chen, Jen-Inn Chyi, Chih-Hsin Ko, Ta-Ming Kuan, Meng-Kuei Hsieh, Wen-Chin Lee, Wann C.H. // 2009. IPRM 09. IEEE International Conference on Indium Phosphide & Related Materials. - Newport Beach, CA, 10-14 May 2009. - P. 326-329. ↑

C424. Stettler M. Device Simulation for Future Technologies. / Stettler M., Kotlyar R., Rakshit T., Linton T. // 2009. IWCE '09. 13th International Workshop on Computational Electronics. - Beijing, 27-29 May 2009. - P. 1-4. ↑

C425. Ashok A. Bias Induced Strain Effects, Short-Range Electron-Electron Interactions and Quantum Effects in AlGaIn/GaN HEMTs. / Ashok A., Vasileska D., Goodnick S.M., Hartin O. // 2009. IWCE '09. 13th International Workshop on Computational Electronics. - Beijing, 27-29 May 2009. - P. 1-4. ↑

C426. Chou Y.C. Manufacturable tri-stack AlSb/InAs HEMT low-noise amplifiers using wafer-level-packaging technology for light-weight and ultralow-power applications. / Chou Y.C., Chang-Chien P., Yang J.M., Nishimoto M.Y., Hennig K., Lange M.D., Zeng X., Parlee M.R., Lin C.H., Lee L.S., Nam P.S., Wojtowicz M., Barsky M.E., Oki A.K., Boos J.B., Bennett B.R., Papanicolaou N.A. // 2009. IPRM 09. IEEE International Conference on Indium Phosphide & Related Materials. - Newport Beach, CA, 10-14 May 2009. - P. 200-203. ↑

C427. Tessmann A. A 300 GHz mHEMT amplifier module. / Tessmann A., Leuther A., Hurm V., Massler H., Zink M., Kuri M., Riessle M., Losch R., Schlechtweg M., Ambacher O. // 2009. IPRM 09. IEEE International Conference on Indium Phosphide & Related Materials. - Newport Beach, CA, 10-14 May 2009. - P. 196-199. ↑

C428. Moschetti G. DC characteristics of InAs/AlSb HEMTs at cryogenic temperatures. / Moschetti G., Nilsson P.-A., Wadefalk N., Malmkvist M., Lefebvre E., Grahn J., Roelens Y., Noudeviwa A., Olivier A., Bollaert S., Danneville F., Desplanque L., Wallart X., Dambine G. // 2009. IPRM 09. IEEE International Conference on Indium Phosphide & Related Materials. - Newport Beach, CA, 10-14 May 2009. - P. 323-325. ↑

C429. Mei X.B. InGaAs/InAlAs/InP power hemt with an improved ohmic contact and an extremely high operating voltage. / Mei X.B., Farkas D., Luo W.B., Lin C.H., Lee L.J., Liu W., Liu P.H., Cavus A., Lai R. // 2009. IPRM 09. IEEE International Conference on Indium Phosphide & Related Materials. - Newport Beach, CA, 10-14 May 2009. - P. 204-206. ↑

C430. {no data available}. Title page. 2009. ISPSD 2009. 21st International Symposium on Power Semiconductor Devices & IC's. - Barcelona, 14-18 June 2009. - P. i. ↑

C431. Kobayashi K.W. Multi-decade GaN HEMT Cascode-distributed power amplifier with baseband performance. / Kobayashi K.W., YaoChung Chen, Smorchkova I., Heying B., Wen-Ben Luo, Sutton W., Wojtowicz M., Oki A. // 2009. RFIC 2009. IEEE Radio Frequency Integrated Circuits Symposium. - Boston, MA, 7-9 June 2009. - P. 369-372. ↑

C432. Pala V. GaAs pseudomorphic HEMTs for low voltage high frequency DC-DC converters. / Pala V., Varadarajan K., Chow T.P. // 2009. ISPSD 2009. 21st International Symposium on Power Semiconductor Devices & IC's. - Barcelona, 14-18 June 2009. - P. 120-123. ↑

C433. King-Yuen Wong. Integrated voltage reference and comparator circuits for GaN smart power chip technology. / King-Yuen Wong, Wanjun Chen, Chen K.J. // 2009. ISPSD 2009. 21st International Symposium on Power Semiconductor Devices & IC's. - Barcelona, 14-18 June 2009. - P. 57-60. ↑

C434. Neophytou N. Quantum Transport Simulations of InGaAs HEMTs: Influence of Mass Variations on the Device Performance. / Neophytou N., Kosina H., Rakshit T. // 2009. IWCE '09. 13th International Workshop on Computational Electronics. - Beijing, 27-29 May 2009. - P. 1-3. ↑

C435. Satou A. Numerical Simulation of Plasma Waves in High-Electron-Mobility Transistors Using Kinetic Transport Model. / Satou A., Ryzhii V., Vagidov N., Mitin V. // 2009. IWCE '09. 13th International Workshop on Computational Electronics. - Beijing, 27-29 May 2009. - P. 1-3. ↑

C436. Ping-Hsun Wu. Wi-Fi/WiMAX dual mode RF MMIC front-end module. / Ping-Hsun Wu, Shih-Ming Wang, Ming-Wei Lee. // 2009. RFIC 2009. IEEE Radio Frequency Integrated Circuits Symposium. - Boston, MA,

7-9 June 2009. - P. 289-292. ↑

C437. Grabner M. Parameter extraction of HEMT models from multibias s-parameters. / Grabner M., Dobes J. // 2009. ISCAS 2009. IEEE International Symposium on Circuits and Systems. - Taipei, 24-27 May 2009. - P. 2085-2088. ↑

C438. Leuther A. Metamorphic HEMT technology for low-noise applications. / Leuther A., Tessmann A., Kallfass I., Losch R., Seelmann-Eggebert M., Wadefalk N., Schafer F., Gallego Puyol J.D., Schlechtweg M., Mikulla M., Ambacher O. // 2009. IPRM 09. IEEE International Conference on Indium Phosphide & Related Materials. - Newport Beach, CA, 10-14 May 2009. - P. 188-191. ↑

C439. Mateos J. Monte Carlo analysis of thermal effects in GaN HEMTs. / Mateos J., Perez S., Pardo D., Gonzalez T. // 2009. CDE 2009. Spanish Conference on Electron Devices. - Santiago de Compostela, 11-13 Feb. 2009. - P. 459-462. ↑

C440. Romero M.F. Electrical and Microstructural Characteristics of Ohmic Contacts formation on AlGaIn/GaN HEMT. / Romero M.F., Jimenez A., Palacio C., Diaz D., Munoz E. // 2009. CDE 2009. Spanish Conference on Electron Devices. - Santiago de Compostela, 11-13 Feb. 2009. - P. 258-261. ↑

C441. Wentzel A. Design and Realization of an Output Network for a GaN-HEMT Current-Mode Class-S Power Amplifier at 450MHz. / Wentzel A., Meliani C., Flucke J., Ersoy E., Heinrich W. // 2009 German Microwave Conference. - Munich, 16-18 March 2009. - P. 1-4. ↑

C442. Khalil I. High Power, High Linearity and Low-Noise Hybrid RF Amplifiers Based on GaN HEMTs. / Khalil I., Rudolph M., Liero A., Neumann M., Heinrich W. // 2009 German Microwave Conference. - Munich, 16-18 March 2009. - P. 1-4. ↑

C443. Tayel M.B. Parameters Extraction for Pseudomorphic HEMTs Using Genetic Algorithms. / Tayel M.B., Yassin A.H. // 2009 International Conference on Electronic Computer Technology. - Macau, 20-22 Feb. 2009. - P. 600-603. ↑

C444. Tayel M.B. An Introduced Neural Network-Differential Evolution Model for Small Signal Modeling of PHEMTs. / Tayel M.B., Yassin A.H. // 2009 International Conference on Electronic Computer Technology. - Macau, 20-22 Feb. 2009. - P. 499-506. ↑

C445. Rodilla H. Monte Carlo Simulation of Sb-based Heterostructures. / Rodilla H., Gonzaleiz T., Pardo D., Mateos J. // 2009. CDE 2009. Spanish Conference on Electron Devices. - Santiago de Compostela, 11-13 Feb. 2009. - P. 152-155. ↑

C446. Vasallo B.G. Monte Carlo Study of an InAlAs/InGaAs Velocity Modulation Transistor. / Vasallo B.G., Gonzalez T., Pardo D., Mateos J. // 2009. CDE 2009. Spanish Conference on Electron Devices. - Santiago de Compostela, 11-13 Feb. 2009. - P. 128-131. ↑


C447. Chien-I Kuo. A 40-nm-Gate InAs/In_{0.7}Ga_{0.3}As Composite-Channel HEMT with 2200 mS/mm and 500-GHz f_T. / Chien-I Kuo, Heng-Tung Hsu, Chien-Ying Wu, Yi Chang E., Miyamoto Y., Yu-Lin Chen, Biswas D. // 2009. IPRM 09. IEEE International Conference on Indium Phosphide & Related Materials. - Newport Beach, CA, 10-14 May 2009. - P. 128-131. ↑


C448. Ha W. High performance InP HEMT technology with multiple interconnect layers for advanced RF and mixed signal circuits. / Ha W., Shinohara K., Griffith Z., Urteaga M., Chen P., Rowell P., Brar B. // 2009. IPRM 09. IEEE International Conference on Indium Phosphide & Related Materials. - Newport Beach, CA, 10-14 May 2009. - P. 115-119. ↑


C449. Lai R. Sub-MMW active integrated circuits based on 35 nm InP HEMT technology. / Lai R., Deal W.R., Radisic V., Leong K., Mei X.B., Sarkozy S., Gaier T., Samoska L., Fung A. // 2009. IPRM 09. IEEE International Conference on Indium Phosphide & Related Materials. - Newport Beach, CA, 10-14 May 2009. - P. 185-187. ↑


C450. Chak Wah Tang. Hetero-epitaxy of III-V compounds lattice-matched to InP by MOCVD for device applications. / Chak Wah Tang, Haiou Li, Zhenyu Zhong, Kai Lun Ng, Kei May Lau. // 2009. IPRM 09. IEEE International Conference on Indium Phosphide & Related Materials. - Newport Beach, CA, 10-14 May 2009. - P. 136-139. ↑


- C451. Hu W.D. Intrinsic Mechanism of Drain-Lag and Current Collapse in GaN-Based HEMTs. / Hu W.D., Chen X.S., Lu W. // 2009. WMED 2009. IEEE Workshop on Microelectronics and Electron Devices. - Boise, ID, 3-3 April 2009. - P. 1-3. ↑
- C452. Al Tanany A. Design of Class F-1 Power Amplifier Using GaN pHEMT for Industrial Applications. / Al Tanany A., Sayed A., Boeck G. // 2009 German Microwave Conference. - Munich, 16-18 March 2009. - P. 1-4. ↑
- C453. {no data available}. Committee. 2009. IPRM '09. IEEE International Conference on Indium Phosphide & Related Materials. - Newport Beach, CA, 10-14 May 2009. - P. i-iii. ↑
- C454. Yong-Sub Lee. Advanced design of an extended GaN HEMT Doherty amplifier using uneven saturation power for WiMAX applications. / Yong-Sub Lee, Mun-Woo Lee, Yoon-Ha Jeong. // 2009. RWS '09. IEEE Radio and Wireless Symposium. - San Diego, CA, 18-22 Jan. 2009. - P. 268-271. ↑
- C455. Elkhatib T.A. Enhanced terahertz detection using multiple GaAs HEMTs connected in series. / Elkhatib T.A., Veksler D.B., Salama K.N., Zhang X.-C., Shur M.S. // 2009. MTT 09. IEEE MTT-S International Microwave Symposium Digest. - Boston, MA, 7-12 June 2009. - P. 937-940. ↑
- C456. Gil Wong Choi. High efficiency Class-E tuned Doherty amplifier using GaN HEMT. / Gil Wong Choi, Hyoung Jong Kim, Woong Jae Hwang, Suk Woo Shin, Jin Joo Choi, Sung Jae Ha. // 2009. MTT 09. IEEE MTT-S International Microwave Symposium Digest. - Boston, MA, 7-12 June 2009. - P. 925-928. ↑
- C457. Chung J.W. On-wafer integration of nitrides and Si devices: Bringing the power of polarization to Si. / Chung J.W., Bin Lu, Palacios T. // 2009. MTT 09. IEEE MTT-S International Microwave Symposium Digest. - Boston, MA, 7-12 June 2009. - P. 1117-1120. ↑
- C458. Bertoluzza F. Lumped element thermal modeling of GaN-Based HEMTs. / Bertoluzza F., Sozzi G., Delmonte N., Menozzi R. // 2009. MTT 09. IEEE MTT-S International Microwave Symposium Digest. - Boston, MA, 7-12 June 2009. - P. 973-976. ↑
- C459. Reynoso-Hernandez J.A. A straightforward method to determine the parasitic gate resistance of GaN FET. / Reynoso-Hernandez J.A., Loo-Yau J.R., Zuniga-Juarez J.E., del Valle-Padilla J.L. // 2009. MTT 09. IEEE MTT-S International Microwave Symposium Digest. - Boston, MA, 7-12 June 2009. - P. 877-880. ↑
- C460. Liu Z.H. Temperature dependent microwave noise parameters and modeling of AlGaIn/GaN HEMTs on Si substrate. / Liu Z.H., Arulkumaran S., Ng G.I. // 2009. MTT 09. IEEE MTT-S International Microwave Symposium Digest. - Boston, MA, 7-12 June 2009. - P. 777-780. ↑
- C461. Prejs A. Thermal analysis and its application to high power GaN HEMT amplifiers. / Prejs A., Wood S., Pengelly R., Pribble W. // 2009. MTT 09. IEEE MTT-S International Microwave Symposium Digest. - Boston, MA, 7-12 June 2009. - P. 917-920. ↑
- C462. Darwish A.M. The dependence of GaN HEMT's frequency figure of merit on temperature. / Darwish A.M., Huebschman B., Viveiros E., Hung H.A. // 2009. MTT 09. IEEE MTT-S International Microwave Symposium Digest. - Boston, MA, 7-12 June 2009. - P. 909-912. ↑
- C463. Chin-Lung Yang. Design of a Ka-band bandpass filter with asymmetrical compact resonator. / Chin-Lung Yang, Hsien-Chin Chiu, Yi-Chyun Chiang. // 2009. MTT 09. IEEE MTT-S International Microwave Symposium Digest. - Boston, MA, 7-12 June 2009. - P. 1609-1612. ↑
- C464. Ildu Kim. Hybrid EER transmitter using highly efficient saturated power amplifier for 802.16e mobile WiMAX application. / Ildu Kim, Jangheon Kim, Junghwan Moon, Jungjoon Kim, Young Yun Woo, Bumman Kim. // 2009. MTT 09. IEEE MTT-S International Microwave Symposium Digest. - Boston, MA, 7-12 June 2009. - P. 1385-1388. ↑
- C465. Ohki T. Reliability of GaN HEMTs: current status and future technology. / Ohki T., Kikkawa T., Inoue Y., Kanamura M., Okamoto N., Makiyama K., Imanishi K., Shigematsu H., Joshin K., Hara N. // 2009 IEEE International Reliability Physics Symposium. - Montreal, QC, 26-30 April 2009. - P. 61-70. ↑
- C466. Verma A.K. Bias dependent and scalable small-signal modeling of pseudomorphic HEMTs. / Verma A.K., Chaturvedi S., Bhat K.M., Saravanan G.S., Muralidharan R. // 2009. IEDST '09. 2nd International Workshop ↑


on Electron Devices and Semiconductor Technology. - Mumbai, 1-2 June 2009. - P. 1-4. 


C467. Chieh-Kai Yang. Characterization of traps in AlGaIn/GaN HEMTs with a combined large signal network analyzer/deep level optical spectrometer system. / Chieh-Kai Yang, Roblin P., Malonis A., Arehart A., Ringel S., Poblentz C., Yi Pei, Speck J., Mishra U. // 2009. MTT 09. IEEE MTT-S International Microwave Symposium Digest. - Boston, MA, 7-12 June 2009. - P. 1209-1212. 


C468. Abouchahine M. Broadband time-domain measurement system applied to the characterization of cross-modulation in nonlinear microwave devices. / Abouchahine M., Saleh A., Neveux G., Reveyard T., Teyssier J.P., Barataud D., Nebus J.M. // 2009. MTT 09. IEEE MTT-S International Microwave Symposium Digest. - Boston, MA, 7-12 June 2009. - P. 1201-1204. 


C469. Deguchi H. A 33W GaN HEMT Doherty amplifier with 55% drain efficiency for 2.6GHz base stations. / Deguchi H., Ui N., Ebihara K., Inoue K., Yoshimura N., Takahashi H. // 2009. MTT 09. IEEE MTT-S International Microwave Symposium Digest. - Boston, MA, 7-12 June 2009. - P. 1273-1276. 


C470. Shigematsu H. C-band 340-W and X-band 100-W GaN power amplifiers with over 50-% PAE. / Shigematsu H., Inoue Y., Akasegawa A., Yamada M., Masuda S., Kamada Y., Yamada A., Kanamura M., Ohki T., Makiyama K., Okamoto N., Imanishi K., Kikkawa T., Joshin K., Hara N. // 2009. MTT 09. IEEE MTT-S International Microwave Symposium Digest. - Boston, MA, 7-12 June 2009. - P. 1265-1268. 


C471. Al Tanany A. Broadband GaN switch mode class E power amplifier for UHF applications. / Al Tanany A., Sayed A., Boeck G. // 2009. MTT 09. IEEE MTT-S International Microwave Symposium Digest. - Boston, MA, 7-12 June 2009. - P. 761-764. 


C472. Ma B.Y. DC-2 GHz low loss cryogenic InAs/AlSb HEMT switch. / Ma B.Y., Bergman J., Hacker J.B., Sullivan G., Sailer A., Brar B. // 2009. MTT 09. IEEE MTT-S International Microwave Symposium Digest. - Boston, MA, 7-12 June 2009. - P. 449-452. 


C473. Simin G. Novel RF devices with multiple capacitively-coupled electrodes. / Simin G., Gaska R., Shur M. // 2009. MTT 09. IEEE MTT-S International Microwave Symposium Digest. - Boston, MA, 7-12 June 2009. - P. 445-448. 


C474. Morgan M. Wideband medium power amplifiers using a short gate-length GaAs MMIC process. / Morgan M., Bryerton E., Karimy H., Dugas D., Gunter L., Kuanghann Duh, Xiaoping Yang, Smith P., Chao P.-C. // 2009. MTT 09. IEEE MTT-S International Microwave Symposium Digest. - Boston, MA, 7-12 June 2009. - P. 541-544. 


C475. Takagi K. Ku-band AlGaIn/GaN-HEMT with over 30% of PAE. / Takagi K., Takatsuka S., Kashiwabara Y., Teramoto S., Matsushita K., Sakurai H., Onodera K., Kawasaki H., Takada Y., Tsuda K. // 2009. MTT 09. IEEE MTT-S International Microwave Symposium Digest. - Boston, MA, 7-12 June 2009. - P. 457-460. 

C476. Changmin Lee. Design of compact-sized class-F PA for wireless handset applications. / Changmin Lee, Youngcheol Park. // 2009. MTT 09. IEEE MTT-S International Microwave Symposium Digest. - Boston, MA, 7-12 June 2009. - P. 405-408. 

C477. Tang K. Enhancement-mode GaN hybrid MOS-HEMTs with breakdown voltage of 1300V. / Tang K., Li Z., Chow T.P., Niyama Y., Nomura T., Yoshida S. // 2009. ISPSD 2009. 21st International Symposium on Power Semiconductor Devices & IC's. - Barcelona, 14-18 June 2009. - P. 279-282. 

C478. Abbasi M. A broadband 60-to-120 GHz single-chip MMIC multiplier chain. / Abbasi M., Kozhuharov R., Karnfelt C., Angelov I., Zirath H., Kallfass I., Leuther A. // 2009. MTT 09. IEEE MTT-S International Microwave Symposium Digest. - Boston, MA, 7-12 June 2009. - P. 441-444. 

C479. Kallfass I. A 144 GHz power amplifier MMIC with 11 dBm output power, 10 dB associated gain and 10 % power-added efficiency. / Kallfass I., Pahl P., Massler H., Leuther A., Tessmann A., Koch S., Zwick T. // 2009. MTT 09. IEEE MTT-S International Microwave Symposium Digest. - Boston, MA, 7-12 June 2009. - P. 429-432. 

C480. Kawasaki K. V-band 8th harmonic push-push oscillator using microstrip ring resonator. / Kawasaki K., Tanaka T., Aikawa M. // 2009. MTT 09. IEEE MTT-S International Microwave Symposium Digest. - Boston, MA, 7-12 June 2009. - P. 697-700. 

- C481.** Bryerton E.W. A W-band low-noise amplifier with 22K noise temperature. / Bryerton E.W., Xiaobing Mei, Young-Min Kim, Deal W., Yoshida W., Lange M., Uyeda J., Morgan M., Lai R. // 2009. MTT 09. IEEE MTT-S International Microwave Symposium Digest. - Boston, MA, 7-12 June 2009. - P. 681-684. ↑
- C482.** Yuk K. An improved empirical large-signal model for high-power GaN HEMTs including self-heating and charge-trapping effects. / Yuk K., Branner G.R., McQuate D. // 2009. MTT 09. IEEE MTT-S International Microwave Symposium Digest. - Boston, MA, 7-12 June 2009. - P. 753-756. ↑
- C483.** Lin-Sheng Liu. Electrothermal large-signal model of III-V FETs accounting for frequency dispersion and charge conservation. / Lin-Sheng Liu, Jian-Guo Ma, Geok-Ing Ng. // 2009. MTT 09. IEEE MTT-S International Microwave Symposium Digest. - Boston, MA, 7-12 June 2009. - P. 749-752. ↑
- C484.** Wright P. An efficient, linear, broadband class-J-mode PA realised using RF waveform engineering. / Wright P., Lees J., Tasker P.J., Benedikt J., Cripps S.C. // 2009. MTT 09. IEEE MTT-S International Microwave Symposium Digest. - Boston, MA, 7-12 June 2009. - P. 653-656. ↑
- C485.** Nakasha Y. W-band transmitter and receiver modules for 10-Gb/s impulse radio. / Nakasha Y., Sato M., Tajima T., Kawano Y., Suzuki T., Takahashi T., Makiyama K., Ohki T., Hara N. // 2009. MTT 09. IEEE MTT-S International Microwave Symposium Digest. - Boston, MA, 7-12 June 2009. - P. 553-556. ↑
- C486.** Shih S.E. Design and analysis of ultra wideband GaN dual-gate HEMT low noise amplifiers. / Shih S.E., Deal W.R., Yamauchi D., Sutton W.E., Chen Y.C., Smorchkova I., Heying B., Wojtowicz M., Siddiqui M. // 2009. MTT 09. IEEE MTT-S International Microwave Symposium Digest. - Boston, MA, 7-12 June 2009. - P. 669-672. ↑
- C487.** van der Heijden M.P. A compact 12-watt high-efficiency 2.1-2.7 GHz class-E GaN HEMT power amplifier for base stations. / van der Heijden M.P., Acar M., Vromans J.S. // 2009. MTT 09. IEEE MTT-S International Microwave Symposium Digest. - Boston, MA, 7-12 June 2009. - P. 657-660. ↑
- C488.** Zuo-Min Tsai. A compact low DC consumption 24-GHz Cascode HEMT VGA. / Zuo-Min Tsai, Jui-Chi Kao, Kun-You Lin, Huei Wang. // 2009. APMC 2009. Asia Pacific Microwave Conference. - Singapore, 7-10 Dec. 2009. - P. 1625-1627. ↑
- C489.** Yang Hou. Analysis and optimum design of impedance matching for Ka-Band cryogenic low noise amplifiers. / Yang Hou, Ruming Wen, Lingyun Li, Hengrong Cui, Rong Qian, Xiaowei Sun. // 2009. APMC 2009. Asia Pacific Microwave Conference. - Singapore, 7-10 Dec. 2009. - P. 1593-1596. ↑
- C490.** Chevaux N. New analytical expressions for the design of linear power amplifier using GaN HEMTs. / Chevaux N., De Souza M.M. // 2009. APMC 2009. Asia Pacific Microwave Conference. - Singapore, 7-10 Dec. 2009. - P. 1112-1115. ↑
- C491.** Chien-I Kuo. A novel metamorphic high electron mobility transistors with $(\text{In}_x\text{Ga}_{1-x}\text{As})_m/(\text{InAs})_n$ superlattice channel layer for millimeter-wave applications. / Chien-I Kuo, Heng-Tung Hsu, Jung-Chi Lu, Chang E.Y., Chien-Ying Wu, Miyamoto Y., Wen-Chung Tsern. // 2009. APMC 2009. Asia Pacific Microwave Conference. - Singapore, 7-10 Dec. 2009. - P. 1651-1654. ↑
- C492.** Chow Y.H. A 29dBm linear power amplifier module for IEEE 802.16e (Wimax) and LTE applications using E-mode pHEMT technology. / Chow Y.H., Tee K.G., Rajendran J., Ho S.Y., Lee M.H., Chan C.F., Liew Y.Y. // 2009. RFIT 2009. IEEE International Symposium on Radio-Frequency Integration Technology. - Singapore, Jan. 9 2009-Dec. 11 2009. - P. 92-95. ↑
- C493.** Mustafa F. RF characterization of planar dipole antenna for on-chip integration with GaAs-based schottky diode. / Mustafa F., Hashim A.M., Parimon N., Rahman S.F.A., Rahman A.R.A., Osman M.N. // 2009. APMC 2009. Asia Pacific Microwave Conference. - Singapore, 7-10 Dec. 2009. - P. 571-574. ↑
- C494.** Kuwata E. C-Ku band 120% relative bandwidth high efficiency high power amplifier using GaN HEMT. / Kuwata E., Yamanaka K., Kirikoshi T., Inoue A., Hirano Y. // 2009. APMC 2009. Asia Pacific Microwave Conference. - Singapore, 7-10 Dec. 2009. - P. 1663-1666. ↑
- C495.** Kawai S. A GaN HEMT Doherty amplifier with a series connected load. / Kawai S., Takayama Y., Ishikawa R., Honjo K. // 2009. APMC 2009. Asia Pacific Microwave Conference. - Singapore, 7-10 Dec. 2009. - P. 325-328. ↑

- C496.** Renfeng Jin. Tunable pulse generator for ultra-wideband applications. / Renfeng Jin, Halder S., Hwang J.C.M., Law C.L. // 2009. APMC 2009. Asia Pacific Microwave Conference. - Singapore, 7-10 Dec. 2009. - P. 2272-2275. ↑
- C497.** Ebrahimi M.M. Trading-off stability for efficiency in designing switching-mode GaN PAs for WiMAX applications. / Ebrahimi M.M., Helaoui M., Ghannouchi F. // 2009. APMC 2009. Asia Pacific Microwave Conference. - Singapore, 7-10 Dec. 2009. - P. 2348-2351. ↑
- C498.** Jarndal A. On the large-signal modeling of AlGaIn/GaN HEMTs for RF switching-mode power amplifiers design. / Jarndal A., Aflaki P., Degachi L., Birafane A., Kouki A., Negra R., Ghannouchi F.M. // 2009. APMC 2009. Asia Pacific Microwave Conference. - Singapore, 7-10 Dec. 2009. - P. 2356-2359. ↑
- C499.** Aflaki P. Intrinsic capacitances effects on the accuracy of the large-signal switch-based GaN device model. / Aflaki P., Negra R., Ghannouchi F.M. // 2009. APMC 2009. Asia Pacific Microwave Conference. - Singapore, 7-10 Dec. 2009. - P. 281-284. ↑
- C500.** Grebennikov A. High-efficiency transmission-line GaN HEMT inverse class F power amplifier for active antenna arrays. 2009. APMC 2009. Asia Pacific Microwave Conference. - Singapore, 7-10 Dec. 2009. - P. 317-320. ↑
- C501.** Yu Zhu. Electromagnetic only HEMT model for switch design. / Yu Zhu, Cejun Wei, Nohra G., Zhang C., Klimashov O., Hong Yin, Bartle D. // 2009. APMC 2009. Asia Pacific Microwave Conference. - Singapore, 7-10 Dec. 2009. - P. 273-276. ↑
- C502.** Ando A. A predistortion linearizer for a class-F GaN HEMT power amplifier using two independently controlled diodes. / Ando A., Takayama Y., Yoshida T., Ishikawa R., Honjo K. // 2009. APMC 2009. Asia Pacific Microwave Conference. - Singapore, 7-10 Dec. 2009. - P. 269-272. ↑
- C503.** Soga I. Thermal management for flip-chip high power amplifiers utilizing carbon nanotube bumps. / Soga I., Kondo D., Yamaguchi Y., Iwai T., Kikkawa T., Joshin K. // 2009. RFIT 2009. IEEE International Symposium on Radio-Frequency Integration Technology. - Singapore, Jan. 9 2009-Dec. 11 2009. - P. 221-224. ↑
- C504.** Deen D.A. Modeling the small signal characteristics of an ALD Al₂O₃ insulated-gate AlN/GaN high electron mobility transistor. / Deen D.A., Champlain J.G., Storm D.F., Meyer D.J., Binari S.C., Eddy C.R., Bass R. // 2009. ISDRS '09. International Semiconductor Device Research Symposium. - College Park, MD, 9-11 Dec. 2009. - P. 1-2. ↑
- C505.** Huq H.F. Analysis of physics based model of AlGaIn/GaN power HEMT with temperature compensation. / Huq H.F., Polash B. // 2009. ISDRS '09. International Semiconductor Device Research Symposium. - College Park, MD, 9-11 Dec. 2009. - P. 1-2. ↑
- C506.** Vitanov S. High-temperature modeling of AlGaIn/GaN HEMTs. / Vitanov S., Palankovski V., Maroldt S., Quay R. // 2009. ISDRS '09. International Semiconductor Device Research Symposium. - College Park, MD, 9-11 Dec. 2009. - P. 1-2. ↑
- C507.** Meyer D.J. Self-aligned ALD AlO_x T-gate footprint insulator for gate leakage current suppression in SiNx passivated AlGaIn/GaN HEMTs. / Meyer D.J., Bass R., Katzer D.S., Deen D.A., Binari S.C., Daniels K.M., Eddy C.R. // 2009. ISDRS '09. International Semiconductor Device Research Symposium. - College Park, MD, 9-11 Dec. 2009. - P. 1-2. ↑
- C508.** Huebschman B.D. Investigation of breakdown behavior for AlGaIn HEMTs. / Huebschman B.D., Darwish A., Goldsman N., Vivieros E.A., Hung A. // 2009. ISDRS '09. International Semiconductor Device Research Symposium. - College Park, MD, 9-11 Dec. 2009. - P. 1-2. ↑
- C509.** Abidin M.S.Z. Fabrication of open gate structure on GaN-based HEMT for pH sensing. / Abidin M.S.Z., Sharifabad M.E., Hashim A.M., Rahman S.F.A., Rahman A.R.A., Osman M.N. // 2009. ISDRS '09. International Semiconductor Device Research Symposium. - College Park, MD, 9-11 Dec. 2009. - P. 1-2. ↑
- C510.** Anderson T.J. Enhancement mode AlN/ultrathin AlGaIn/GaN HEMTs using selective wet etching. / Anderson T.J., Tadjer M.J., Mastro M.A., Hite J.K., Hobart K.D., Eddy C.R., Kub F.J. // 2009. ISDRS '09. International Semiconductor Device Research Symposium. - College Park, MD, 9-11 Dec. 2009. - P. 1-2. ↑

- C511.** Andrei P. Optimization of power AlGaIn/GaN vertical HEMT devices with low on-state resistance and high breakdown voltage. 2009. ISDRS '09. International Semiconductor Device Research Symposium. - College Park, MD, 9-11 Dec. 2009. - P. 1-2. ↑
- C512.** Kaho T. A compact X-band balanced frequency doubler on GaAs pHEMT 3D MMIC. / Kaho T., Yamaguchi Y., Okazaki H., Uehara K. // 2009. RFIT 2009. IEEE International Symposium on Radio-Frequency Integration Technology. - Singapore, Jan. 9 2009-Dec. 11 2009. - P. 237-240. ↑
- C513.** Liu Z.H. Analytical modeling of the temperature dependent microwave noise in AlGaIn/GaN HEMTs. / Liu Z.H., Ng G.I., Arulkumaran S. // 2009. RFIT 2009. IEEE International Symposium on Radio-Frequency Integration Technology. - Singapore, Jan. 9 2009-Dec. 11 2009. - P. 276-279. ↑
- C514.** Kok-Yan Lee. Integration of RF MEMS switch with MMIC pHEMT and passive devices on GaAs. / Kok-Yan Lee, Seah Yong Meng, Ang Kian Sen, Ng Geok Ing, Wang Hong. // 2009. RFIT 2009. IEEE International Symposium on Radio-Frequency Integration Technology. - Singapore, Jan. 9 2009-Dec. 11 2009. - P. 288-291. ↑
- C515.** Nagamine S. Multifunctional frequency converter MMIC for 38GHz band 600Mbps multi-level QAM wireless system. / Nagamine S., Ozawa F., Shirosaki T., Taniguchi T., Okada K. // 2009. RFIT 2009. IEEE International Symposium on Radio-Frequency Integration Technology. - Singapore, Jan. 9 2009-Dec. 11 2009. - P. 229-232. ↑
- C516.** Weatherford T. TCAD analysis of self heating in AlGaIn/GaN HEMTs under pulsed conditions. / Weatherford T., Wang Y., Tracey S. // 2009. IRW 09. IEEE International Integrated Reliability Workshop Final Report. - S. Lake Tahoe, CA, 18-22 Oct. 2009. - P. 159-162. ↑
- C517.** Memon N.M. Extraction of intrinsic AC parameters of mm wavelength GaAs HEMTs from measured DC characteristics. / Memon N.M., Ahmed M.M., Moiz S.A. // 2009. INMIC 2009. IEEE 13th International Multitopic Conference. - Islamabad, 14-15 Dec. 2009. - P. 1-7. ↑
- C518.** Zirath H. Integrated receivers up to 220 GHz utilizing GaAs-mHEMT technology. / Zirath H., Wadefalk N., Kuzhuharov R., Gunnarsson S.E., Cherednichenko S., Angelov I., Abbasi M., Hansson B., Vassilev V., Svedin J., Rudner S., Kallfass I., Leuther A. // 2009. RFIT 2009. IEEE International Symposium on Radio-Frequency Integration Technology. - Singapore, Jan. 9 2009-Dec. 11 2009. - P. 225-228. ↑
- C519.** Mays K.W. A 40 GHz power amplifier using a low cost high volume 0.15 um optical lithography pHEMT process. 2009. COMCAS 2009. IEEE International Conference on Microwaves, Communications, Antennas and Electronics Systems. - Tel Aviv, 9-11 Nov. 2009. - P. 1-5. ↑
- C520.** Kharche N. Performance analysis of ultra-scaled InAs HEMTs. / Kharche N., Klimeck G., Dae-Hyun Kim, del Alamo J.A., Luisier M. // 2009 IEEE International Electron Devices Meeting (IEDM). - Baltimore, MD, 7-9 Dec. 2009. - P. 1-4. ↑
- C521.** Tae-Woo Kim. 30 nm In_{0.7} Ga_{0.3} As Inverted-Type HEMTs with reduced gate leakage current for logic applications. / Tae-Woo Kim, Dae-Hyun Kim, del Alamo J.A. // 2009 IEEE International Electron Devices Meeting (IEDM). - Baltimore, MD, 7-9 Dec. 2009. - P. 1-4. ↑
- C522.** Chini A. Correlation between DC and rf degradation due to deep levels in AlGaIn/GaN HEMTs. / Chini A., Fantini F., Di Lecce V., Esposto M., Stocco A., Ronchi N., Zanon F., Meneghesso G., Zanoni E. // 2009 IEEE International Electron Devices Meeting (IEDM). - Baltimore, MD, 7-9 Dec. 2009. - P. 1-4. ↑
- C523.** Nidhi. N-polar GaN-based highly scaled self-aligned MIS-HEMTs with state-of-the-art fT_{LG} product of 16.8 GHz-μm. / Nidhi, Dasgupta S., Brown D.F., Keller S., Speck J.S., Mishra U.K. // 2009 IEEE International Electron Devices Meeting (IEDM). - Baltimore, MD, 7-9 Dec. 2009. - P. 1-3. ↑
- C524.** Ghajar M.R. High efficiency GaN class E amplifier for polar transmitter. / Ghajar M.R., Boumaiza S. // 2009 3rd International Conference on Signals, Circuits and Systems (SCS). - Medenine, 6-8 Nov. 2009. - P. 1-4. ↑
- C525.** Kaddeche M. Study of field plate effects on AlGaIn/GaN HEMTs. / Kaddeche M., Telia A., Soltani A. // 2009 International Conference on Microelectronics (ICM). - Marrakech, 19-22 Dec. 2009. - P. 362-365. ↑
- C526.** Donghyun Jin. Quantum capacitance in scaled down III-V FETs. / Donghyun Jin, Daehyun Kim, Taewoo

Kim, del Alamo J.A. // 2009 IEEE International Electron Devices Meeting (IEDM). - Baltimore, MD, 7-9 Dec. 2009. - P. 1-4. ↑

C527. Boutros K.S. Normally-off 5A/1100V GaN-on-silicon device for high voltage applications. / Boutros K.S., Burnham S., Wong D., Shinohara K., Hughes B., Zehnder D., McGuire C. // 2009 IEEE International Electron Devices Meeting (IEDM). - Baltimore, MD, 7-9 Dec. 2009. - P. 1-3. ↑

C528. Jaafar M. Improved mathematical model for the investigation of deep traps into semiconductor devices: application to Metamorphic HEMT. / Jaafar M., Aupetit-Berthelemot C., Cluzeau T., Teyssier J.P. // 2009 74th ARFTG Microwave Measurement Symposium. - Broomfield, CO, Nov. 30 2009-Dec. 4 2009. - P. 1-6. ↑

C529. Inwon Suh. Additive phase noise measurements of AlGaIn/GaN HEMTs using a large signal network analyzer and a tunable monochromatic light source. / Inwon Suh, Roblin P., Youngseo Ko, Chieh-Kai Yang, Malonis A., Arehart A., Ringel S., Poblenz C., Yi Pei, Speck J., Mishra U. // 2009 74th ARFTG Microwave Measurement Symposium. - Broomfield, CO, Nov. 30 2009-Dec. 4 2009. - P. 1-5. ↑

C530. Kumar B.N. Effect of variation of topological changes on the Equivalent Circuit Parameters of pseudomorphic HEMTs. / Kumar B.N., Srivastava G., Verma A.K., Bhat K.M., Chaturvedi S., Saravanan G.S., Muralidharan R. // 2009. ELECTRO '09. International Conference on Emerging Trends in Electronic and Photonic Devices & Systems. - Varanasi, 22-24 Dec. 2009. - P. 74-77. ↑

C531. Essen H. SUMATRA, a W-band SAR for UAV application. / Essen H., Brautigam M., Sommer R., Wahlen A., Johannes W., Wilcke J., Schlechtweg M., Tessmann A. // 2009. RADAR. International Radar Conference-Surveillance for a Safer World. - Bordeaux, 12-16 Oct. 2009. - P. 1-4. ↑

C532. Uemoto Y. GaN monolithic inverter IC using normally-off gate injection transistors with planar isolation on Si substrate. / Uemoto Y., Morita T., Ikoshi A., Umeda H., Matsuo H., Shimizu J., Hikita M., Yanagihara M., Ueda T., Tanaka T., Ueda D. // 2009 IEEE International Electron Devices Meeting (IEDM). - Baltimore, MD, 7-9 Dec. 2009. - P. 1-4. ↑

C533. {no data available}. Copyright. 2009 IEEE International Electron Devices Meeting (IEDM). - Baltimore, MD, 7-9 Dec. 2009. - P. 1. ↑

C534. Rose M.R.C. The effect of multiple gate for P1dB and PAE of AlGaAs/InGaAs HEMT. / Rose M.R.C., Osman M.N., Man A., Rasmi A., Rahim A., Yaakob S., Yahya M.R. // 2009 IEEE 9th Malaysia International Conference on Communications (MICC). - Kuala Lumpur, 15-17 Dec. 2009. - P. 890-893. ↑

C535. Bensmida S. Generic Power Amplifier linearization. / Bensmida S., Morris K., Beach M., McGeehan J. // 2009 3rd International Conference on Signals, Circuits and Systems (SCS). - Medenine, 6-8 Nov. 2009. - P. 1-5. ↑

C536. Zhiwei Bi. Characteristics analysis of gate dielectrics in AlGaIn/GaN MIS-HEMT. / Zhiwei Bi, Yue Hao, Hongxia Liu, Linjie Liu, Qian Feng. // 2009. EDSSC 2009. IEEE International Conference of Electron Devices and Solid-State Circuits. - Xi'an, 25-27 Dec. 2009. - P. 419-422. ↑

C537. Junshuai Xue. Effect of high temperature AlN interlayer on the performance of AlGaIn/GaN properties. / Junshuai Xue, Yue Hao, Jincheng Zhang, Jinyu Ni. // 2009. EDSSC 2009. IEEE International Conference of Electron Devices and Solid-State Circuits. - Xi'an, 25-27 Dec. 2009. - P. 416-418. ↑

C538. Chen K.J. GaN smart power chip technology. 2009. EDSSC 2009. IEEE International Conference of Electron Devices and Solid-State Circuits. - Xi'an, 25-27 Dec. 2009. - P. 403-407. ↑

C539. Mustafa F. RF-DC power conversion of Schottky diode fabricated on AlGaAs/GaAs heterostructure for on-chip rectenna device application in nanosystem. / Mustafa F., Parimon N., Rahman S.F.A., Hashim A.M., Osman M.N. // 2009. EDSSC 2009. IEEE International Conference of Electron Devices and Solid-State Circuits. - Xi'an, 25-27 Dec. 2009. - P. 150-153. ↑

C540. Khmyrova I. Terahertz resonant frequencies of grating-bicoupled plasma wave devices. 2009. COMCAS 2009. IEEE International Conference on Microwaves, Communications, Antennas and Electronics Systems. - Tel Aviv, 9-11 Nov. 2009. - P. 1-2. ↑

C541. Khmyrova I. Multi-cantilever HEMT-based resonant sensor. / Khmyrova I., Shestakova E. // 2009. COMCAS 2009. IEEE International Conference on Microwaves, Communications, Antennas and Electronics

Systems. - Tel Aviv, 9-11 Nov. 2009. - P. 1-4. ↑

C542. van der Bent G. Low-cost high-efficient 10-Watt X-band high-power amplifier. / van der Bent G., de Hek A.P., Bessemoulin A., van Vliet F.E. // 2009. COMCAS 2009. IEEE International Conference on Microwaves, Communications, Antennas and Electronics Systems. - Tel Aviv, 9-11 Nov. 2009. - P. 1-6. ↑

C543. Che-Kai Lin. GaN lattice matched ZnO/Pr₂O₃ film as gate dielectric oxide layer for AlGaN/GaN HEMT. / Che-Kai Lin, Ming-Yang Chen, Hsiang-Chun Wang, Chih-Wei Yang, Chao-Wei Chiu, Hsien-Chin Chiu, Kuang-Po Hsueh. // 2009. EDSSC 2009. IEEE International Conference of Electron Devices and Solid-State Circuits. - Xi'an, 25-27 Dec. 2009. - P. 408-411. ↑

C544. Lenka T.R. Microwave characteristics of Al_xGa_{1-x}N/In_xGa_{1-x}N/GaN-based HEMT using propagation delay model. / Lenka T.R., Panda A.K. // 2009. CODEC 2009. 4th International Conference on Computers and Devices for Communication. - Kolkata, 14-16 Dec. 2009. - P. 1-4. ↑

C545. Habibzadeh A. An 18Ghz LNA Ga FET high gain amplifier for WLAN. / Habibzadeh A., Moghaddasi M.N., Jalali M. // 2009 Mediterranean Microwave Symposium (MMS). - Tangiers, 15-17 Nov. 2009. - P. 1-3. ↑

C546. Kaddeche M. Modeling of AlGaIn/GaN HEMTs using field-plate technology. / Kaddeche M., Telia A., Soltani A. // 2009 3rd International Conference on Signals, Circuits and Systems (SCS). - Medenine, 6-8 Nov. 2009. - P. 1-4. ↑

C547. Chinen Koyu. Satellite-receiving-system overlay with WDM RoF on 10Gb/s link. / Chinen Koyu, Uchima Yuki. // 2009 Asia Communications and Photonics Conference and Exhibition (ACP). - Shanghai, China, 2-6 Nov. 2009. - Vol. 2009-Supplement. - P. 1-6. ↑

C548. Elkhatab T.A. Subwavelength detection of terahertz radiation using GaAs HEMTs. / Elkhatab T.A., Muravjov A.V., Veksler D.B., Stillman W.J., Zhang X.-C., Shur M.S., Kachorovskii V.Y. // 2009 IEEE Sensors. - Christchurch, 25-28 Oct. 2009. - P. 1988-1990. ↑

C549. Liang Wu. A high performance plastic air-cavity QFN solution for future potential microwave package large scale application. / Liang Wu, Qian Rong, Xiaowei Sun. // 2009. (EDAPS 2009). IEEE Electrical Design of Advanced Packaging & Systems Symposium. - Shatin, Hong Kong, 2-4 Dec. 2009. - P. 1-4. ↑

C550. Qi Zhou. High-dynamic-range zero-bias microwave detector using AlGaIn/GaN-based lateral field-effect diode. / Qi Zhou, King-Yuen Wong, Wanjun Chen, Chen K.J. // 2009. (EDAPS 2009). IEEE Electrical Design of Advanced Packaging & Systems Symposium. - Shatin, Hong Kong, 2-4 Dec. 2009. - P. 1-4. ↑

C551. Demirtas S. Critical voltage for electrical reliability of GaN high electron mobility transistors on Si substrate. / Demirtas S., del Alamo J.A. // 2009 Reliability of Compound Semiconductors Digest (ROCS). - Greensboro, NC, 11-11 Oct. 2009. - P. 53-56. ↑

C552. Dammann M. Reliability of AlGaIn/GaN HEMTs under DC- and RF-operation. / Dammann M., Casar M., Waltereit P., Bronner W., Konstanzer H., Quay R., Muller S., Mikulla M., Ambacher O., van der Wel P., Rodle T., Behtash R., Bourgeois F., Riepe K. // 2009 Reliability of Compound Semiconductors Digest (ROCS). - Greensboro, NC, 11-11 Oct. 2009. - P. 19-32. ↑

C553. Rozman D. Reliability of AlGaIn/GaN HEMT: Impact of acceleration condition on dominant degradation mechanism. / Rozman D., Knafo Y., Baksht T., Aktushev O., Kolatker G., Moskovitch S., Bunin G. // 2009 Reliability of Compound Semiconductors Digest (ROCS). - Greensboro, NC, 11-11 Oct. 2009. - P. 7-18. ↑

C554. Weatherford T. Self heating of AlGaIn/GaN HEMTs in pulsed operation. / Weatherford T., Wang Y., Tracey S. // 2009 Reliability of Compound Semiconductors Digest (ROCS). - Greensboro, NC, 11-11 Oct. 2009. - P. 59-69. ↑

C555. Chou Y.C. Reliability evaluation of hermetic GaAs HEMT MMICs using wafer-scale-assembly technology for compact and light-weight applications. / Chou Y.C., Chang-Chien P., Leung D.L., Kono R.K., Zeng X., Parlee M.R., Hennig K., Eng D.C., Trucker C., Tsai R.S., Wojtowicz M., Barsky M.E., Oki A.K., Block T. // 2009 Reliability of Compound Semiconductors Digest (ROCS). - Greensboro, NC, 11-11 Oct. 2009. - P. 141-145. ↑

C556. Jimenez J.L. Recent advances on the understanding of the physics of failure of GaN on SiC FET

technology. / Jimenez J.L., Chowdhury U. // 2009 Reliability of Compound Semiconductors Digest (ROCS). - Greensboro, NC, 11-11 Oct. 2009. - P. 57-58. ↑

C557. Pazirandeh R. Comparison of DC measurement methods to determine GaN HEMT reliability. / Pazirandeh R., Wurfl J., Trankle G. // 2009 Reliability of Compound Semiconductors Digest (ROCS). - Greensboro, NC, 11-11 Oct. 2009. - P. 41-51. ↑

C558. Ciccognani W. MMIC LNAs for Radioastronomy Applications Using Advanced Industrial 70 nm Metamorphic Technology. / Ciccognani W., Limiti E., Longhi P.E., Renvoise M. // 2009. CISC 2009. Annual IEEE Compound Semiconductor Integrated Circuit Symposium. - Greensboro, NC, 11-14 Oct. 2009. - P. 1-2. ↑

C559. Krishnamurthy K. 0.5-2.5 GHz, 10W MMIC Power Amplifier in GaN HEMT Technology. / Krishnamurthy K., Green D., Vetury R., Poulton M., Martin J. // 2009. CISC 2009. Annual IEEE Compound Semiconductor Integrated Circuit Symposium. - Greensboro, NC, 11-14 Oct. 2009. - P. 1-4. ↑

C560. Chia-Shih Cheng. High Linearity AlGaAs/InGaAs Pseudomorphic HEMT Driver Amplifier Using Tunable Field-Plate Voltage Technology. / Chia-Shih Cheng, Shao-Wei Lin, Fu J.S., Hsien-Chin Chiu. // 2009. CISC 2009. Annual IEEE Compound Semiconductor Integrated Circuit Symposium. - Greensboro, NC, 11-14 Oct. 2009. - P. 1-4. ↑

C561. Koch S. A Fully Integrated, Compound Transceiver MIMIC Utilizing Six Antenna Ports for 60 GHz Wireless Applications. / Koch S., Kallfass I., Weber R., Leuther A., Schlechtweg M., Saito S. // 2009. CISC 2009. Annual IEEE Compound Semiconductor Integrated Circuit Symposium. - Greensboro, NC, 11-14 Oct. 2009. - P. 1-4. ↑

C562. Lopez N.D. Design Method for UHF Class-E Power Amplifiers. / Lopez N.D., Hoversten J., Popovic Z. // 2009. CISC 2009. Annual IEEE Compound Semiconductor Integrated Circuit Symposium. - Greensboro, NC, 11-14 Oct. 2009. - P. 1-4. ↑

C563. Takatani S. Accurate HEMT Switch Large-Signal Device Model Derived from Pulsed-Bias Capacitance and Current Characteristics. / Takatani S., Cheng-Duan Chen. // 2009. CISC 2009. Annual IEEE Compound Semiconductor Integrated Circuit Symposium. - Greensboro, NC, 11-14 Oct. 2009. - P. 1-4. ↑

C564. Lin C.H. Sub-mW Operation of InP HEMT X-Band Low-Noise Amplifiers for Low Power Applications. / Lin C.H., Mei X.B., Chou Y.C., Lee L.S., Yang J.M., Nishimoto M.Y., Liu P.H., To R., Cavus A., Tsai R., Wojtowicz M., Lai R. // 2009. CISC 2009. Annual IEEE Compound Semiconductor Integrated Circuit Symposium. - Greensboro, NC, 11-14 Oct. 2009. - P. 1-4. ↑

C565. Maroldt S. High Efficiency Digital GaN MMIC Power Amplifiers for Future Switch-Mode Based Mobile Communication Systems. / Maroldt S., Haupt C., Kiefer R., Bronner W., Mueller S., Benz W., Quay R., Ambacher O. // 2009. CISC 2009. Annual IEEE Compound Semiconductor Integrated Circuit Symposium. - Greensboro, NC, 11-14 Oct. 2009. - P. 1-4. ↑

C566. Yohan Jeong. Broadband CPW-fed active monopole antenna for WLAN applications. / Yohan Jeong, Yong Jee. // 2009. AFRICON '09. AFRICON. - Nairobi, 23-25 Sept. 2009. - P. 1-3. ↑

C567. Zuo-Min Tsai. A 24-48 GHz cascode HEMT mixer with DC to 15 GHz IF bandwidth for astronomy radio telescope. / Zuo-Min Tsai, Jui-Chin Kao, Kun-You Lin, Huei Wang. // 2009. EuMIC 2009. European Microwave Integrated Circuits Conference. - Rome, 28-29 Sept. 2009. - P. 5-8. ↑

C568. Junghwan Moon. A highly efficient Doherty power amplifier employing optimized carrier cell. / Junghwan Moon, Young Yun Woo, Bumman Kim. // 2009. EuMIC 2009. European Microwave Integrated Circuits Conference. - Rome, 28-29 Sept. 2009. - P. 367-370. ↑

C569. Gonzalez-Garrido M.-A. Critical analysis of results for a european GaN power amplifier after first iteration. / Gonzalez-Garrido M.-A., Grajal J., Cetronio A., Marescialli L. // 2009. EuMIC 2009. European Microwave Integrated Circuits Conference. - Rome, 28-29 Sept. 2009. - P. 218-221. ↑

C570. Dinari M. Wide band high linearity and high isolation mixer MMIC developed on GaAs 0.25μm Power pHEMT technology. / Dinari M., Serru V., Camiade M., Teyssandier C., Baglieri D., Durand E., Mallet-Guy B., Plaze J.P. // 2009. EuMIC 2009. European Microwave Integrated Circuits Conference. - Rome, 28-29 Sept. 2009. - P. 308-311. ↑

- C571.** Zhen-Yu Zhang. Sub-harmonic self-oscillating mixer design using dual-mode substrate integrated waveguide cavity. / Zhen-Yu Zhang, Ke Wu. // 2009. EuMIC 2009. European Microwave Integrated Circuits Conference. - Rome, 28-29 Sept. 2009. - P. 196-199. ↑
- C572.** Morkner H. A complete 38 GHz transmit and receive chip set in low cost surface mount package. / Morkner H., Fujii K., Phan K., Kumar S. // 2009. EuMIC 2009. European Microwave Integrated Circuits Conference. - Rome, 28-29 Sept. 2009. - P. 316-319. ↑
- C573.** Kuhn J. Design of X-Band GaN MMICs using field plates. / Kuhn J., van Raay F., Quay R., Kiefer R., Peschel D., Mikulla M., Seelmann-Eggebert M., Bronner W., Schlechtweg M., Ambacher O., Thumm M. // 2009. EuMIC 2009. European Microwave Integrated Circuits Conference. - Rome, 28-29 Sept. 2009. - P. 33-36. ↑
- C574.** Hettak K. A novel size reduction of a MMIC I/Q direct down converter in uniplanar technology at 20 GHz using CPW and ACPS stubs loading for an EHF satcom terminal phased array size. / Hettak K., Verver C.J., Morin G.A., Stubbs M.G. // 2009. EuMIC 2009. European Microwave Integrated Circuits Conference. - Rome, 28-29 Sept. 2009. - P. 304-307. ↑
- C575.** Saad P. An inverse class-F GaN HEMT power amplifier with 78% PAE at 3.5 GHz. / Saad P., Nemati H.M., Thorsell M., Andersson K., Fager C. // 2009. EuMC 2009. European Microwave Conference. - Rome, Sept. 29 2009-Oct. 1 2009. - P. 496-499. ↑
- C576.** Junghwan Moon. A highly efficient Doherty power amplifier employing optimized carrier cell. / Junghwan Moon, Young Yun Woo, Bumman Kim. // 2009. EuMC 2009. European Microwave Conference. - Rome, Sept. 29 2009-Oct. 1 2009. - P. 1720-1723. ↑
- C577.** Bettidi A. X-band T/R module in state-of-the-art GaN technology. / Bettidi A., Cetronio A., Cicolani M., Costrini C., Lanzieri C., Maccaroni S., Marescialli L., Peroni M., Romanini P. // 2009. EuRAD 2009. European Radar Conference. - Rome, Sept. 30 2009-Oct. 2 2009. - P. 258-261. ↑
- C578.** Boglione L. A 5GHz WLAN amplifier with novel on-chip positive voltage switchable bias implemented in a D-pHEMT process. / Boglione L., Paradis J. // 2009. EuMC 2009. European Microwave Conference. - Rome, Sept. 29 2009-Oct. 1 2009. - P. 472-475. ↑
- C579.** Zaroni E. Long-term stability of Gallium Nitride High Electron Mobility Transistors: a reliability physics approach. / Zaroni E., Meneghesso G., Meneghini M., Tazzoli A., Ronchi N., Stocco A., Zanon F., Chini A., Verzellesi G., Cetronio A., Lanzieri C., Peroni M. // 2009. EuMIC 2009. European Microwave Integrated Circuits Conference. - Rome, 28-29 Sept. 2009. - P. 212-217. ↑
- C580.** Chi-Jeon Hwang. An ultra-low power OOK RF transceiver for wireless sensor networks. / Chi-Jeon Hwang, McGregor I., Oxland R., Whyte G., Thayne I.G., Elgaid K. // 2009. EuMC 2009. European Microwave Conference. - Rome, Sept. 29 2009-Oct. 1 2009. - P. 1323-1326. ↑
- C581.** El Maazouzi L. A 3.5 GHz 2nd harmonic tuned PA design. / El Maazouzi L., Colantonio P., Mediavilla A., Giannini F. // 2009. EuMC 2009. European Microwave Conference. - Rome, Sept. 29 2009-Oct. 1 2009. - P. 1090-1093. ↑
- C582.** Koch S. A 140 GHz Heterodyne Receiver Chipset for Passive Millimeter Wave Imaging Applications. / Koch S., Guthoerl M., Kallfass I., Leuther A., Saito S. // 2009. CISC 2009. Annual IEEE Compound Semiconductor Integrated Circuit Symposium. - Greensboro, NC, 11-14 Oct. 2009. - P. 1-4. ↑
- C583.** Khayer M.A. Modeling and performance analysis of high-speed, high-power GaN nanowire FETs. / Khayer M.A., Lake R.K. // 2009. DRC 2009 Device Research Conference. - University Park, PA, 22-24 June 2009. - P. 107-108. ↑
- C584.** De-Zhong Li. A high-power Ka-band power amplifier design based on GaAs P-HEMT technology for VSAT ODU applications. / De-Zhong Li, Cong Wang, Wen-Cheng Huang, Krishna R., Sung-Jin Cho, Shrestha B., Gear Inpyo Kyung, Nam-Young Kim. // 2009 3rd IEEE International Symposium on Microwave, Antenna, Propagation and EMC Technologies for Wireless Communications. - Beijing, 27-29 Oct. 2009. - P. 20-23. ↑
- C585.** Jae-Sung Rieh. An Overview of Semiconductor Technologies and Circuits for Terahertz Communication Applications. / Jae-Sung Rieh, Dong-Hyun Kim. // 2009 IEEE GLOBECOM Workshops. - Honolulu, HI, Nov. 30 2009-Dec. 4 2009. - P. 1-6. ↑

- C586.** Higashiwaki M. Small-signal and 30-GHz power performance of AlGaIn/GaN HFETs without back barriers. / Higashiwaki M., Yi Pei, Rongming Chu, Mishra U.K. // 2009. DRC 2009 Device Research Conference. - University Park, PA, 22-24 June 2009. - P. 105-106. ↑
- C587.** Ha W. High performance monolithic InP HBT-HEMT integration. / Ha W., Urteaga M., Griffith Z., Pierson R., Rowell P., Chen P., Brar B. // 2009. DRC 2009 Device Research Conference. - University Park, PA, 22-24 June 2009. - P. 163-164. ↑
- C588.** Kanamura M. High current operation of enhancement-mode GaN MIS-HEMTs with triple cap structure using atomic layer deposited Al₂O₃ gate insulator. / Kanamura M., Ohki T., Kikkawa T., Imanishi K., Imada T., Hara N. // 2009. DRC 2009 Device Research Conference. - University Park, PA, 22-24 June 2009. - P. 165-166. ↑
- C589.** Shinohara K. 60-nm GaN/AlGaIn DH-HEMTs with 1.0 Ω·mm Ron, 2.0 A/mm Idmax, and 153 GHz fT. / Shinohara K., Milosavljevic I., Burnham S., Corrión A., Hashimoto P., Wong D., Hu M., Butler C., Schmitz A., Willadsen P.J., Boutros K.S., Kazemi H., Micovic M. // 2009. DRC 2009 Device Research Conference. - University Park, PA, 22-24 June 2009. - P. 167-168. ↑
- C590.** Han Liu. The application analysis of GaN power devices in Radar transmitter. / Han Liu, Xin Zheng, Zhen-kun Yu. // 2009 IET International Radar Conference. - Guilin, China, 20-22 April 2009. - P. 1-5. ↑
- C591.** Yu Cao. MBE-grown buffer with high breakdown voltage for nitride HEMTs on GaN template. / Yu Cao, Zimmermann T., Huili Xing, Jena D. // 2009. ISDRS '09. International Semiconductor Device Research Symposium. - College Park, MD, 9-11 Dec. 2009. - P. 1-2. ↑
- C592.** Storm D.F. Effect of GaN buffer thickness on the electrical properties of RF-MBE grown AlGaIn/GaN HEMTs on free-standing GaN substrates. / Storm D.F., Katzer D.S., Deen D.A., Bass R., Meyer D.J., Binari S.C., Paskova T., Preble E.A., Evans K.R. // 2009. ISDRS '09. International Semiconductor Device Research Symposium. - College Park, MD, 9-11 Dec. 2009. - P. 1-2. ↑
- C593.** Eliza S.A. Modeling of floating gate AlGaIn/GaN heterostructure-transistor based sensor. / Eliza S.A., Islam S.K., Lee I., Greenbaum E., Tulip F.S. // 2009. ISDRS '09. International Semiconductor Device Research Symposium. - College Park, MD, 9-11 Dec. 2009. - P. 1-2. ↑
- C594.** Jia Guo. Ultra-scaled AlN/GaN enhancement- & depletion-mode nanoribbon HEMTs. / Jia Guo, Zimmermann T., Jena D., Huili Xing. // 2009. ISDRS '09. International Semiconductor Device Research Symposium. - College Park, MD, 9-11 Dec. 2009. - P. 1-2. ↑
- C595.** Yildirim R. Asymmetric condition computed from the four tone input GaN HEMT. / Yildirim R., Celebi F.V., Guclu Yavuzcan H., Gokrem L. // 2009. AICT 2009. International Conference on Application of Information and Communication Technologies. - Baku, 14-16 Oct. 2009. - P. 1-4. ↑
- C596.** Eshghabadi F. An MMIC receiver front-end design for 2.4GHz frequency band applications in 0.2μm GaAs pseudomorphic HEMT process. / Eshghabadi F., Dousti M., Yazdizadeh M. // 2009. AICT 2009. International Conference on Application of Information and Communication Technologies. - Baku, 14-16 Oct. 2009. - P. 1-5. ↑
- C597.** Li Ji Hao. Study on the Impact of Operating Point on Transmission Efficiency and Harmonic Suppression of T/R Module Based on Wide Bandgap Semiconductor. 2009. APSAR 2009. 2nd Asian-Pacific Conference on Synthetic Aperture Radar. - Xian, Shanxi, 26-30 Oct. 2009. - P. 951-954. ↑
- C598.** Man Hoi Wong. High performance MBE-grown N-face microwave GaN HEMTs with >70% PAE. / Man Hoi Wong, Yi Pei, Brown D.F., Keller S., Speck J.S., Mishra U.K. // 2009. DRC 2009 Device Research Conference. - University Park, PA, 22-24 June 2009. - P. 157-158. ↑
- C599.** Yamashita Y. X-band GaN HEMT advanced power amplifier unit for compact active phased array antennas. / Yamashita Y., Nakada T., Kumamoto T., Suzuki R., Tanabe M. // 2009 ICCAS-SICE. - Fukuoka, 18-21 Aug. 2009. - P. 3047-3050. ↑
- C600.** Marinkovic Z. Hybrid PKI empirical-neural bias dependent noise model of microwave transistors. / Marinkovic Z., Rancic O.P., Markovic V. // 2009. TELSIS '09. 9th International Conference on Telecommunication in Modern Satellite, Cable, and Broadcasting Services. - Nis, 7-9 Oct. 2009. - P. 44-47. ↑

- C601.** Crupi G. Combined empirical and look-up table approach for non-quasi-static modelling of GaN HEMTs. / Crupi G., Schreurs D., Caddemi A., Angelov I., Rui Liu, Germain M., De Raedt W. // 2009. TELSIKS '09. 9th International Conference on Telecommunication in Modern Satellite, Cable, and Broadcasting Services. - Nis, 7-9 Oct. 2009. - P. 40-43. ↑
- C602.** Fornetti F. Evaluation of commercial GaN HEMTs for pulsed power applications. / Fornetti F., Morris K.A., Beach M.A. // 2009 IET European Pulsed Power Conference. - Geneva, 21-25 Sept. 2009. - P. 1-4. ↑
- C603.** Chao-Wei Lin. Device performance of AlGaIn/GaN MOS-HEMTs using La₂O₃ high-k oxide gate insulator. / Chao-Wei Lin, Chih-Wei Yang, Chao-Hung Chen, Che-Kai Lin, Hsien-Chin Chiu. // 2009. ESSDERC 09. Proceedings of the European Solid State Device Research Conference. - Athens, 14-18 Sept. 2009. - P. 435-439. ↑
- C604.** Esposto M. Comparison of Cu-gate and Ni/Au-gate GaN HEMTs large signal characteristics. / Esposto M., Di Lecce V., Chini A., De Guido S., Passaseo A., De Vittorio M. // 2009. ESSDERC 09. Proceedings of the European Solid State Device Research Conference. - Athens, 14-18 Sept. 2009. - P. 431-434. ↑
- C605.** Choi Sung-Soon. Si ICL based Si₃N₄ passivation on InAlAs surface of InP-HEMT by RPECVD system. / Choi Sung-Soon, Lee Kwan-Hoon, Song Byeong-Seok. // 2009. IRMMW-THz 2009. 34th International Conference on Infrared, Millimeter, and Terahertz Waves. - Busan, 21-25 Sept. 2009. - P. 1-2. ↑
- C606.** Chung J.W. Seamless on-wafer integration of GaN HEMTs and Si(100) MOSFETs. / Chung J.W., Lee J., Piner E.L., Palacios T. // 2009. DRC 2009 Device Research Conference. - University Park, PA, 22-24 June 2009. - P. 155-156. ↑
- C607.** Brown R.J. Al_xSi_yN_z passivated AlGaIn/GaN high electron mobility transistors. / Brown R.J., Harvard E., Shealy J.R. // 2009. DRC 2009 Device Research Conference. - University Park, PA, 22-24 June 2009. - P. 153-154. ↑
- C608.** Selvaraj S.L. Enhancing the breakdown voltage by growing 9 μm thick AlGaIn/GaN HEMTs on 4 inch silicon. / Selvaraj S.L., Suzue T., Egawa T. // 2009. DRC 2009 Device Research Conference. - University Park, PA, 22-24 June 2009. - P. 283-284. ↑
- C609.** Maier D. Above 500 °C operation of InAlN/GaN HEMTs. / Maier D., Alomari M., Grandjean N., Carlin J.-F., Diforte-Poisson M.-A., Dua C., Chuvilin A., Troadec D., Gaquiere C., Kaiser U., Delage S., Kohn E. // 2009. DRC 2009 Device Research Conference. - University Park, PA, 22-24 June 2009. - P. 285-286. ↑
- C610.** Chang M.-C.F. Terahertz CMOS circuit design and applications for ultra-high data rate (100Gbps) communication. 2009. ASICON '09. IEEE 8th International Conference on ASIC. - Changsha, Hunan, 20-23 Oct. 2009. - P. 1-2. ↑
- C611.** Zimmermann T. Top-down AlN/GaN enhancement- & depletion-mode nanoribbon HEMTs. / Zimmermann T., Yu Cao, Jia Guo, Xiangning Luo, Jena D., Xing H. // 2009. DRC 2009 Device Research Conference. - University Park, PA, 22-24 June 2009. - P. 129-130. ↑
- C612.** Bin Lu. Enhancement-mode AlGaIn/GaN HEMTs with high linearity fabricated by hydrogen plasma treatment. / Bin Lu, Saadat O.I., Piner E.L., Palacios T. // 2009. DRC 2009 Device Research Conference. - University Park, PA, 22-24 June 2009. - P. 59-60. ↑
- C613.** Tangsheng Chen. X-Band Microstrip AlGaIn/GaN HEMT Power MMICs. / Tangsheng Chen, Bin Zhang, Chunjiang Ren, Gang Jiao, Weibin Zheng, Chen Chen, Kai Shao, Naibin Yang. // 2008. CSIC 08. IEEE Compound Semiconductor Integrated Circuits Symposium. - Monterey, CA, 12-15 Oct. 2008. - P. 1-4. ↑
- C614.** Inoue Y. A CW 7-12 GHz GaN Hybrid Power Amplifier IC with High PAE Using the Load-Impedance Change Compensation Technique. / Inoue Y., Kanamura M., Ohki T., Makiyama K., Okamoto N., Imanishi K., Kikkawa T., Hara N., Shigematsu H., Joshin K. // 2008. CSIC 08. IEEE Compound Semiconductor Integrated Circuits Symposium. - Monterey, CA, 12-15 Oct. 2008. - P. 1-4. ↑
- C615.** Nagasaku T. 77GHz Low-Cost Single-Chip Radar Sensor for Automotive Ground Speed Detection. / Nagasaku T., Kogo K., Shinoda H., Kondoh H., Muto Y., Yamamoto A., Yoshikawa T. // 2008. CSIC 08. IEEE Compound Semiconductor Integrated Circuits Symposium. - Monterey, CA, 12-15 Oct. 2008. - P. 1-4. ↑

- C616.** Tessmann A. A Metamorphic 220-320 GHz HEMT Amplifier MMIC. / Tessmann A., Leuther A., Massler H., Kuri M., Loesch R. // 2008. CSIC 08. IEEE Compound Semiconductor Integrated Circuits Symposium. - Monterey, CA, 12-15 Oct. 2008. - P. 1-4. ↑
- C617.** Lin-Sheng Liu. Improved Drain-Source Current Model for HEMT's with Accurate Gm Fitting in All Regions. / Lin-Sheng Liu, Jian-Guo Ma. // 2008. CSIC 08. IEEE Compound Semiconductor Integrated Circuits Symposium. - Monterey, CA, 12-15 Oct. 2008. - P. 1-4. ↑
- C618.** Piotrowicz S. State of the Art 58W, 38% PAE X-Band AlGaIn/GaN HEMTs Microstrip MMIC Amplifiers. / Piotrowicz S., Morvan E., Aubry R., Bansropun S., Bouvet T., Chartier E., Dean T., Drisse O., Dua C., Floriot D., diForte Poisson M.A., Gourdel Y., Hydes A.J., Jacquet J.C., Jardel O., Lancereau D., McLean J.O., Lecoustre G., Martin A., Ouarch Z., Reveyrand T., Richard M., Sarazin N., Thenot D., Delage S.L. // 2008. CSIC 08. IEEE Compound Semiconductor Integrated Circuits Symposium. - Monterey, CA, 12-15 Oct. 2008. - P. 1-4. ↑
- C619.** Campbell C. A Wideband Power Amplifier MMIC Utilizing GaN on SiC HEMT Technology. / Campbell C., Cathy Lee, Williams V., Ming-Yih Kao, Hua-Quen Tserng, Saunier P. // 2008. CSIC 08. IEEE Compound Semiconductor Integrated Circuits Symposium. - Monterey, CA, 12-15 Oct. 2008. - P. 1-4. ↑
- C620.** Kobayayashi K.W. A Cool, Sub-0.2 dB, Ultra-Low Noise Gallium Nitride Multi-Octave MMIC LNA-PA with 2-Watt Output Power. / Kobayayashi K.W., Yao Chung Chen, Smorchkova I., Heying B., Luo W.-B., Sutton W., Wojtowicz M., Oki A. // 2008. CSIC 08. IEEE Compound Semiconductor Integrated Circuits Symposium. - Monterey, CA, 12-15 Oct. 2008. - P. 1-4. ↑
- C621.** Shigematsu H. C-Band GaN-HEMT Power Amplifier with Over 300-W Output Power and Over 50-% Efficiency. / Shigematsu H., Inoue Y., Masuda S., Yamada M., Kanamura M., Ohki T., Makiyama K., Okamoto N., Imanishi K., Kikkawa T., Joshin K., Hara N. // 2008. CSIC 08. IEEE Compound Semiconductor Integrated Circuits Symposium. - Monterey, CA, 12-15 Oct. 2008. - P. 1-4. ↑
- C622.** Yuan-Zheng Yue. AlGaIn/GaN MOS-HEMT with Stack Gate HfO₂/Al₂O₃ Structure Grown by Atomic Layer Deposition. / Yuan-Zheng Yue, Yue Hao, Jin-Cheng Zhang. // 2008. CSIC 08. IEEE Compound Semiconductor Integrated Circuits Symposium. - Monterey, CA, 12-15 Oct. 2008. - P. 1-4. ↑
- C623.** Smith R.P. AlGaIn/GaN-on-SiC HEMT Technology Status. / Smith R.P., Sheppard S., Wu Y.-F., Heikman S., Wood S., Pribble W., Milligan J.W. // 2008. CSIC 08. IEEE Compound Semiconductor Integrated Circuits Symposium. - Monterey, CA, 12-15 Oct. 2008. - P. 1-4. ↑
- C624.** Cijvat E. A comparison of polar transmitter architectures using a GaN HEMT power amplifier. / Cijvat E., Sjolund H., Tom K., Faulkner M. // 2008. ICECS 2008. 15th IEEE International Conference on Electronics, Circuits and Systems. - St. Julien's, Aug. 31 2008-Sept. 3 2008. - P. 1075-1078. ↑
- C625.** Deal W.R. A balanced sub-millimeter wave power amplifier. / Deal W.R., Mei X.B., Radisic V., Bayuk B., Fung A., Yoshida W., Liu P.H., Uyeda J., Samoska L., Gaier T., Lai R. // 2008 IEEE MTT-S International Microwave Symposium Digest. - Atlanta, GA, 15-20 June 2008. - P. 399-402. ↑
- C626.** Nakasha Y. A 12.5-Gb/s Pulse Modulator with 6.5-ps FWHM Using 0.1-μm InP HEMTs for Ultra-Wideband Impulse Radio Communications. / Nakasha Y., Kawano Y., Suzuki T., Ohki T., Takahashi T., Makiyama K., Hirose T., Hara N. // 2008. CSIC 08. IEEE Compound Semiconductor Integrated Circuits Symposium. - Monterey, CA, 12-15 Oct. 2008. - P. 1-4. ↑
- C627.** Krishnamurthy K. RLC Matched GaN HEMT Power Amplifier with 2 GHz Bandwidth. / Krishnamurthy K., Wang D., Landberg B., Martin J. // 2008. CSIC 08. IEEE Compound Semiconductor Integrated Circuits Symposium. - Monterey, CA, 12-15 Oct. 2008. - P. 1-4. ↑
- C628.** De Groote F. High power on-wafer capabilities of a time domain load-pull setup. / De Groote F., Teyssier J.-P., Verspecht J., Faraj J. // 2008 IEEE MTT-S International Microwave Symposium Digest. - Atlanta, GA, 15-20 June 2008. - P. 100-102. ↑
- C629.** Yang Hou. An efficient technique for designing balanced vector modulators with low insertion loss. / Yang Hou, Xiaowei Sun, Lingyun Li. // 2008 IEEE MTT-S International Microwave Symposium Digest. - Atlanta, GA, USA, 15-20 June 2008. - P. 1281-1284. ↑
- C630.** Jing Lu. First-principles calculations for effects of Fluorine impurity in GaN. / Jing Lu, Mingzhi Gao,

Jinyu Zhang, Yan Wang, Zhiping Yu. // 2008. SISPAD 2008. International Conference on Simulation of Semiconductor Processes and Devices. - Hakone, 9-11 Sept. 2008. - P. 233-236. ↑

C631. Chung J.W. New Technologies for Improving the High Frequency Performance of AlGaIn/GaN High Electron Mobility Transistors. / Chung J.W., Piner E.L., Roberts J.C., Palacios T. // 2008. ENICS '08. International Conference on Advances in Electronics and Micro-electronics. - Valencia, Sept. 29 2008-Oct. 4 2008. - P. 66-71. ↑

C632. Wright P. Highly efficient operation modes in GaN power transistors delivering upwards of 81% efficiency and 12W output power. / Wright P., Sheikh A., Roff C., Tasker P.J., Benedikt J. // 2008 IEEE MTT-S International Microwave Symposium Digest. - Atlanta, GA, 15-20 June 2008. - P. 1147-1150. ↑

C633. Kangaslahti P. Low noise amplifier for 180 GHz frequency band. / Kangaslahti P., Pukala D., Gaier T., Deal W., Xiaobing Mei, Lai R. // 2008 IEEE MTT-S International Microwave Symposium Digest. - Atlanta, GA, 15-20 June 2008. - P. 451-454. ↑

C634. Yong-Sub Lee. Linearity-optimized power tracking GaN HEMT Doherty amplifier using derivative superposition technique for repeater systems. / Yong-Sub Lee, Mun-Woo Lee, Yoon-Ha Jeong. // 2008 IEEE MTT-S International Microwave Symposium Digest. - Atlanta, GA, 15-20 June 2008. - P. 427-430. ↑

C635. Piotrowicz S. Broadband hybrid flip-chip 6-18 GHz AlGaIn/GaN HEMT amplifiers. / Piotrowicz S., Aubry R., Chartier E., Jardel O., Jacquet J.C., Morvan E., Grimbert B., Lecoustre G., Delage S.L., Obregon J., Floriot D. // 2008 IEEE MTT-S International Microwave Symposium Digest. - Atlanta, GA, USA, 15-20 June 2008. - P. 1131-1134. ↑

C636. Thorsell M. Thermal characterization of the intrinsic noise parameters for AlGaIn/GaN HEMTs. / Thorsell M., Andersson K., Fagerlind M., Sudow M., Nilsson P.-A., Rorsman N. // 2008 IEEE MTT-S International Microwave Symposium Digest. - Atlanta, GA, 15-20 June 2008. - P. 463-466. ↑

C637. Zhiqun Cheng. Distributed amplifier using enhancement-mode AlGaIn/GaN HEMTs. / Zhiqun Cheng, Xiaopeng Zhou, Chen K.J. // 2008. ICCAS 2008. International Conference on Communications, Circuits and Systems. - Fujian, 25-27 May 2008. - P. 94-96. ↑

C638. El Fatimy A. Room temperature terahertz imaging by a GaAs-HEMT transistor associated with a THz time domain spectrometer. / El Fatimy A., Abraham E., Nguema E., Mounaix P., Teppe F., Knap W., Otsuji T. // 2008. IRMMW-THz 2008. 33rd International Conference on Infrared, Millimeter and Terahertz Waves. - Pasadena, CA, 15-19 Sept. 2008. - P. 1-2. ↑

C639. Lynch J.J. Low noise radiometers for passive millimeter wave imaging. / Lynch J.J., Schulman J.N., Schaffner J.H., Moyer H.P., Royter Y., Macdonald P.A., Hughes B. // 2008. IRMMW-THz 2008. 33rd International Conference on Infrared, Millimeter and Terahertz Waves. - Pasadena, CA, 15-19 Sept. 2008. - P. 1-3. ↑

C640. Raman S. The DARPA FLARE Program: Recent Advances in Ultra High Linearity RF Amplifiers. / Raman S., Tsu-Hsi Chang, Eden R.C., Pappert S. // 2008. CSIC 08. IEEE Compound Semiconductor Integrated Circuits Symposium. - Monterey, CA, 12-15 Oct. 2008. - P. 1-4. ↑

C641. Micovic M. GaN MMIC PAs for E-Band (71 GHz-95 GHz) Radio. / Micovic M., Kurdoghlian A., Moyer H.P., Hashimoto P., Hu M., Antcliffe M., Willadsen P.J., Wong W.S., Bowen R., Milosavljevic I., Yoon Y., Schmitz A., Wetzel M., McGuire C., Hughes B., Chow D.H. // 2008. CSIC 08. IEEE Compound Semiconductor Integrated Circuits Symposium. - Monterey, CA, 12-15 Oct. 2008. - P. 1-4. ↑

C642. Ortolani M. Homodyne mixing at 150 GHz in a high electron mobility transistor. / Ortolani M., Di Gaspare A., Giovine E., Evangelisti F., Doria A., Giovenale E., Gallerano G.P., Messina G., Spassovsky I., Cetronio A., Lanzieri C., Peroni M., Foglietti V. // 2008. IRMMW-THz 2008. 33rd International Conference on Infrared, Millimeter and Terahertz Waves. - Pasadena, CA, 15-19 Sept. 2008. - P. 1-2. ↑

C643. Meziani Y.M. Room temperature generation of terahertz radiation from dual grating gate HEMT's. / Meziani Y.M., Nishimura T., Handa H., Knap W., Otsuji T., Sano E., Popov V.V., Coquillat D., Teppe F. // 2008. IRMMW-THz 2008. 33rd International Conference on Infrared, Millimeter and Terahertz Waves. - Pasadena, CA, 15-19 Sept. 2008. - P. 1-2. ↑

C644. Nakajima A. Equivalent circuit model for GaN-HEMTs in a switching simulation. / Nakajima A., Takao

K., Shimizu M., Okumura H., Ohashi H. // 2008. INTELEC 2008. IEEE 30th International Telecommunications Energy Conference. - San Diego, CA, 14-18 Sept. 2008. - P. 1-4. ↑

C645. Samoska L. A G-Band multi-chip MMIC T/R module for radar applications. / Samoska L., Pukala D., Soria M., Sadowy G. // 2008. IRMMW-THz 2008. 33rd International Conference on Infrared, Millimeter and Terahertz Waves. - Pasadena, CA, 15-19 Sept. 2008. - P. 1-2. ↑

C646. Peale R.E. Tunable InGaAs/InAlAs/InP far-IR detector based on plasmon resonance. / Peale R.E., Saxena H., Buchwald W.R. // 2008. IRMMW-THz 2008. 33rd International Conference on Infrared, Millimeter and Terahertz Waves. - Pasadena, CA, 15-19 Sept. 2008. - P. 1-2. ↑

C647. Galdetskiy A.V. Elimination of parasitic generation in power X-band internally matched transistors with high associated gain. / Galdetskiy A.V., Manchenko L.V., Pashkovskii A.B., Pchelin V.A. // 2008. CriMiCo 2008. 2008 18th International Crimean Conference Microwave & Telecommunication Technology. - Sevastopol, Crimea, 8-12 Sept. 2008. - P. 75-76. ↑

C648. Sato M. InP-HEMT MMICs for passive millimeter-wave imaging sensors. / Sato M., Hirose T., Ohki T., Takahashi T., Makiyama K., Hara N., Sato H., Sawaya K., Mizuno K. // 2008. IPRM 2008. 20th International Conference on Indium Phosphide and Related Materials. - Versailles, 25-29 May 2008. - P. 1-4. ↑

C649. Lai R. Fabrication of InP HEMT devices with extremely high Fmax. / Lai R., Deal W.R., Mei X.B., Yoshida W., Lee J., Dang L., Wang J., Kim Y.M., Liu P.H., Radisic V., Lange M., Gaier T., Samoska L., Fung A. // 2008. IPRM 2008. 20th International Conference on Indium Phosphide and Related Materials. - Versailles, 25-29 May 2008. - P. 1-3. ↑

C650. Yakovleva I.B. Computer simulation of low-noise SHF amplifier using field effect transistor. / Yakovleva I.B., Sayenko V.D. // 2008. APEDE '08. International Conference on Actual Problems of Electron Devices Engineering. - Saratov, 24-25 Sept. 2008. - P. 268-273. ↑

C651. Kamitsuna H. DC-40-GHz SP4T switch IC using high-breakdown-voltage InGaAs/InP composite-channel HEMTs with an InAlP etch stopper. / Kamitsuna H., Sugiyama H., Kosugi T., Yokoyama H., Murata K., Yamane Y., Enoki T. // 2008. IPRM 2008. 20th International Conference on Indium Phosphide and Related Materials. - Versailles, 25-29 May 2008. - P. 1-2. ↑

C652. Olivier A. AlSb/InAs HEMTs on InP substrate using wet and dry etching for mesa isolation. / Olivier A., Gehin T., Desplanque L., Wallart X., Roelens Y., Dambrine G., Cappy A., Bollaert S., Lefebvre E., Malmkvist M., Grahn J. // 2008. IPRM 2008. 20th International Conference on Indium Phosphide and Related Materials. - Versailles, 25-29 May 2008. - P. 1-3. ↑

C653. Watanabe I. Simultaneous achievement of high-speed and low-noise performance of pseudomorphic InGaAs/InAlAs HEMTs. / Watanabe I., Endoh A., Mimura T., Matsui T. // 2008. IPRM 2008. 20th International Conference on Indium Phosphide and Related Materials. - Versailles, 25-29 May 2008. - P. 1-4. ↑

C654. Murata H. Optical control of InP-based HEMT millimeter-wave oscillators. / Murata H., Kobayashi N., Okamura Y., Kosugi T., Enoki T. // 2008. IPRM 2008. 20th International Conference on Indium Phosphide and Related Materials. - Versailles, 25-29 May 2008. - P. 1-2. ↑

C655. Chou Y.C. The effect of gate metals on manufacturability of 0.1 μm metamorphic AlSb/InAs HEMTs for ultralow-power applications. / Chou Y.C., Lee L.J., Yang J.M., Lange M.D., Nam P.S., Lin C.H., Quach H., Gutierrez A.L., Barsky M.E., Wojtowicz M., Oki A.K., Block T.R., Boos J.B., Bennett B.R., Papanicolaou N.A. // 2008. IPRM 2008. 20th International Conference on Indium Phosphide and Related Materials. - Versailles, 25-29 May 2008. - P. 1-4. ↑

C656. Liberati R.M. High performance future hybrid transceiver module using GaN power devices for seeker applications. / Liberati R.M., Calori M. // 2008. RADAR 08. IEEE Radar Conference. - Rome, 26-30 May 2008. - P. 1-4. ↑

C657. Ueda D. Present and future prospects of gan-based power electronics. / Ueda D., Hikita M., Nakazawa S., Nakazawa K., Ishida H., Yanagihara M., Inoue K., Ueda T., Uemoto Y., Tanaka T., Egawa T. // 2008. ICSICT 2008. 9th International Conference on Solid-State and Integrated-Circuit Technology. - Beijing, 20-23 Oct. 2008. - P. 1078-1081. ↑

- C658.** Chen K.J. Fluorine plasma ion implantation technology: a new dimension in gan device processing. 2008. ICSICT 2008. 9th International Conference on Solid-State and Integrated-Circuit Technology. - Beijing, 20-23 Oct. 2008. - P. 1074-1077. ↑
- C659.** Wen C.P. Evidence of mobile holes on GaN HFET barrier layer surface-root cause of high power transistor amplifier current collapse. / Wen C.P., Jinyan Wang, Yilong Hao, Yaohui Zhang, Keimay Lau, Tang. // 2008. ICSICT 2008. 9th International Conference on Solid-State and Integrated-Circuit Technology. - Beijing, 20-23 Oct. 2008. - P. 1090-1093. ↑
- C660.** Yeong-Her Wang. The comprehensive study of liquid phase oxidation on GaAs-based transistor applications. 2008. ICSICT 2008. 9th International Conference on Solid-State and Integrated-Circuit Technology. - Beijing, 20-23 Oct. 2008. - P. 1082-1085. ↑
- C661.** Jo-Won Lee. Road-blocks to Tera-level nanoelectronics. / Jo-Won Lee, Moonkyung Kim. // 2008. ICSICT 2008. 9th International Conference on Solid-State and Integrated-Circuit Technology. - Beijing, 20-23 Oct. 2008. - P. 37-40. ↑
- C662.** Bettidi A. Innovative T/R module in state-of-the-art GaN technology. / Bettidi A., Calori M., Cetronio A., Cicolani M., Costrini C., Lanzieri C., Maccaroni S., Marescialli L., Peroni M. // 2008. RADAR 08. IEEE Radar Conference. - Rome, 26-30 May 2008. - P. 1-5. ↑
- C663.** Jian Tang. AlGaN/AlN/GaN/InGaN/GaN DH-HEMTs with improved mobility grown by MOCVD. / Jian Tang, Xiaoliang Wang, Tangsheng Chen, Hongling Xiao, Junxue Ran, Minglan Zhang, Guoxin Hu, Chun Feng, Qifeng Hou, Meng Wei, Jinmin Li, Zhanguo Wang. // 2008. ICSICT 2008. 9th International Conference on Solid-State and Integrated-Circuit Technology. - Beijing, 20-23 Oct. 2008. - P. 1114-1117. ↑
- C664.** Ching-Sung Lee. Investigations on In_{0.2} Ga_{0.8} AsSb/GaAs high electron mobility transistors with gate passivations. / Ching-Sung Lee, Ciou-Sheng He, Wei-Chou Hsu, Ke-Hua Su, Ping-Chang Yang, Bo-i Chou, An-Yung Kao. // 2008. ICSICT 2008. 9th International Conference on Solid-State and Integrated-Circuit Technology. - Beijing, 20-23 Oct. 2008. - P. 1106-1109. ↑
- C665.** Kuan-Wei Lee. Liquid phase oxidation on InAlAs and application to gate insulator of InAlAs/InGaAs HEMT lattice-matched to InP substrate. / Kuan-Wei Lee, Hsien-Chang Lin, Ja-Hong Hsieh, Yu-Chun Cheng, Yeong-Her Wang. // 2008. IPRM 2008. 20th International Conference on Indium Phosphide and Related Materials. - Versailles, 25-29 May 2008. - P. 1-4. ↑
- C666.** Tae-Woo Kim. Fabrication of In_{0.52} Al_{0.48} As/In_{0.53} Ga_{0.47} As p-HEMT utilizing Ne-based atomic layer etching. / Tae-Woo Kim, Seung Heon Shin, Sang Duk Park, Geun Young Yeom, Jae-Hyung Jang, Jong-In Song. // 2008. IPRM 2008. 20th International Conference on Indium Phosphide and Related Materials. - Versailles, 25-29 May 2008. - P. 1-4. ↑
- C667.** Wichmann N. Fabrication technology and device performances of ultra-short 30-nm-gate pseudomorphic In_{0.52} Al_{0.48} As/In_{0.75} Ga_{0.25} As HEMTs. / Wichmann N., Shchepetov A., Duszynski I., Roelens Y., Wallart X., Dambrine G., Cappy A., Bollaert S. // 2008. IPRM 2008. 20th International Conference on Indium Phosphide and Related Materials. - Versailles, 25-29 May 2008. - P. 1-4. ↑
- C668.** Leuther A. 35 nm metamorphic HEMT MMIC technology. / Leuther A., Tessmann A., Massler H., Losch R., Schlechtweg M., Mikulla M., Ambacher O. // 2008. IPRM 2008. 20th International Conference on Indium Phosphide and Related Materials. - Versailles, 25-29 May 2008. - P. 1-4. ↑
- C669.** Craft H.S. CH029. / Craft H.S., Paisley E.A., Losego M.D., Maria J-P. // 2008. ISAF 2008. 17th IEEE International Symposium on the Applications of Ferroelectrics. - Santa Re, NM, USA, 23-28 Feb. 2008. - P. 1-2. ↑
- C670.** Yablonskii G.P. AlInGaN/GaN heterostructures with 2D electron gas and quantum wells for transistors and light emitting diodes. / Yablonskii G.P., Lutsenko E.V., Kalish H., Heuken M. // 2008. CriMiCo 2008. 2008 18th International Crimean Conference Microwave & Telecommunication Technology. - Sevastopol, Crimea, 8-12 Sept. 2008. - P. 584-585. ↑
- C671.** Craft H.S. CH029. / Craft H.S., Paisley E.A., Losego M.D., Maria J-P. // 2008. ISAF 2008. 17th IEEE International Symposium on the Applications of Ferroelectrics. - Santa Re, NM, USA, 23-28 Feb. 2008. - Vol. 1. - P. 1-2. ↑

- C672.** Ihlefeld J.F. Adsorption-controlled growth of BiFeO₃ by MBE and integration with wide band gap semiconductors. / Ihlefeld J.F., Tian W., Liu Z.K., Doolittle W.A., Bernhagen M., Reiche P., Uecker R., Ramesh R., Schlom D.G. // 2008. ISAF 2008. 17th IEEE International Symposium on the Applications of Ferroelectrics. - Santa Re, NM, USA, 23-28 Feb. 2008. - Vol. 2. - P. 1-2. ↑
- C673.** Akis R. The upper limits of cut-off frequency in ultra-short gate length InP-based p-HEMTs. / Akis R., Faralli N., Ferry D.K., Goodnick S.M., Saraniti M., Ayubi-Moak J.S. // 2008. IPRM 2008. 20th International Conference on Indium Phosphide and Related Materials. - Versailles, 25-29 May 2008. - P. 1-4. ↑
- C674.** Sung-Won Kim. W-band low-noise amplifier with 50 nm In_{0.8} GaP/In_{0.4} AlAs/In_{0.35} GaAs metamorphic HEMT. / Sung-Won Kim, Yu-Min Koh, Woo-Yeol Choi, Hyung-Tae Kim, Young-Woo Kwon, Kwang-Seok Seo. // 2008. IPRM 2008. 20th International Conference on Indium Phosphide and Related Materials. - Versailles, 25-29 May 2008. - P. 1-3. ↑
- C675.** Chien-I Kuo. Investigation of impact ionization from In_x Ga_{1-x} As to InAs Channel HEMTs for high speed and low power applications. / Chien-I Kuo, Heng-Tung Hsu, Yi Chang E., Chia-Ta Chang, Chia-Yuan Chang, Miyamoto Y. // 2008. IPRM 2008. 20th International Conference on Indium Phosphide and Related Materials. - Versailles, 25-29 May 2008. - P. 1-4. ↑
- C676.** Takahashi T. Improvement in high frequency and noise characteristics of InP-based HEMTs by reducing parasitic capacitance. / Takahashi T., Makiyama K., Hara N., Sato M., Hirose T. // 2008. IPRM 2008. 20th International Conference on Indium Phosphide and Related Materials. - Versailles, 25-29 May 2008. - P. 1-4. ↑
- C677.** Hong Wang. Channel noise in InGaAs/InP composite channel high electron mobility transistors (HEMTs). / Hong Wang, Yuwei Liu. // 2008. IPRM 2008. 20th International Conference on Indium Phosphide and Related Materials. - Versailles, 25-29 May 2008. - P. 1-3. ↑
- C678.** Mei X.B. A W-band InGaAs/InAlAs/InP HEMT Low-Noise Amplifier MMIC with 2.5dB noise figure and 19.4 dB gain at 94GHz. / Mei X.B., Lin C.H., Lee L.J., Kim Y.M., Liu P.H., Lange M., Cavus A., To R., Nishimoto M., Lai R. // 2008. IPRM 2008. 20th International Conference on Indium Phosphide and Related Materials. - Versailles, 25-29 May 2008. - P. 1-3. ↑
- C679.** Delhay G. Preliminary investigations on the Te-doped AlInSb/GaInSb heterostructures for High Electron Mobility Transistor (HEMT) applications. / Delhay G., Desplanque L., Wallart X. // 2008. IPRM 2008. 20th International Conference on Indium Phosphide and Related Materials. - Versailles, 25-29 May 2008. - P. 1-3. ↑
- C680.** Endoh A. DC and RF characteristics of InAlAs/In_{0.7} Ga_{0.3} As HEMTs at 16 K. / Endoh A., Watanabe I., Shinohara K., Mimura T., Matsui T. // 2008. IPRM 2008. 20th International Conference on Indium Phosphide and Related Materials. - Versailles, 25-29 May 2008. - P. 1-4. ↑
- C681.** Lange M.D. InAs/InGaAs composite-channel HEMT on InP: Tailoring InGaAs thickness for performance. / Lange M.D., Mei X.B., Chin T.P., Yoshida W.H., Deal W.R., Liu P.-H., Lee J., Uyeda J.J., Dang L., Wang J., Liu W., Li D.T., Barsky M.E., Kim Y.-M., Radisic V., Lai R. // 2008. IPRM 2008. 20th International Conference on Indium Phosphide and Related Materials. - Versailles, 25-29 May 2008. - P. 1-4. ↑
- C682.** Guang Yang. An 18-40 GHz ultra broadband low noise amplifier MMIC. / Guang Yang, Yunchuan Guo, Ruimin Xu. // 2008. ICMMT 2008. International Conference on Microwave and Millimeter Wave Technology. - Nanjing, 21-24 April 2008. - Vol. 2. - P. 865-867. ↑
- C683.** Yong-Sub Lee. High-efficiency doherty amplifier using GaN HEMT class-F cells for WCDMA applications. / Yong-Sub Lee, Mun-Woo, Yoon-Ha Jeong. // 2008. ICMMT 2008. International Conference on Microwave and Millimeter Wave Technology. - Nanjing, 21-24 April 2008. - Vol. 1. - P. 270-273. ↑
- C684.** Jeongwon Cha. A charge-pump based 0.35-um CMOS RF switch driver for multi-standard operations. / Jeongwon Cha, Minsik Ann, Changhyuk Cho, Chang-Ho Lee, Laskar J. // 2008. ISCAS 2008. IEEE International Symposium on Circuits and Systems. - Seattle, WA, 18-21 May 2008. - P. 452-455. ↑
- C685.** Horio K. Analysis of pulsed I-V curves and power slump in field-plate GaN-based FETs. / Horio K., Itagaki K., Nakajima A. // 2008. ICMMT 2008. International Conference on Microwave and Millimeter Wave Technology. - Nanjing, 21-24 April 2008. - Vol. 2. - P. 893-896. ↑

- C686.** Li-Yang Chen. Improved formal passivations of pseudomorphic high electron mobility transistors. / Li-Yang Chen, Shiou-Ying Cheng, Kuei-Yi Chu, Jung-Hui Tsai, Tzu-Pin Chen, Tsung-Han Tsai, Wen-Chau Liu. // 2008. IWJT '08. Extended Abstracts-2008 8th International workshop on Junction Technology. - Shanghai, 15-16 May 2008. - P. 183-186. ↑
- C687.** Huang W. Enhancement-mode gan hybrid mos-hemts with ron,sp of 20 m ω -cm². / Huang W., Li Z., Chow T.P., Niiyama Y., Nomura T., Yoshida S. // 2008. ISPSD '08. 20th International Symposium on Power Semiconductor Devices and IC's. - Orlando, FL, 18-22 May 2008. - P. 295-298. ↑
- C688.** Ning Li. Characterization of the noise performance of a cryogenically-cooled HEMT Low-Noise Amplifier. / Ning Li, Zuo Y.-X., Jian Xu, Yuan Ren, Huang S.-P., Shi S.-C. // 2008. ICMMT 2008. International Conference on Microwave and Millimeter Wave Technology. - Nanjing, 21-24 April 2008. - Vol. 1. - P. 182-185. ↑
- C689.** Tae-Woo Kim. Performance of capless self-aligned gate D- and QE-mode p-HEMTs. / Tae-Woo Kim, Jang-Soo Chun, Chul-Seung Park, Woo-Keun Song, Jong-In Song. // 2008. ICMMT 2008. International Conference on Microwave and Millimeter Wave Technology. - Nanjing, 21-24 April 2008. - Vol. 1. - P. 163-165. ↑
- C690.** Sayed A. Highly linear broadband GaN power amplifier design. / Sayed A., Boeck G. // 2008. NRSC 2008. National Radio Science Conference. - Tanta Univ., 18-20 March 2008. - P. 1-7. ↑
- C691.** Kolaklieva L. The role of Ti/Al ratio in nanolayered ohmic contacts for GaN/AlGaIn HEMTs. / Kolaklieva L., Kakanakov R., Cimalla V., Maroldt S., Niebelschutz F., Tonisch K., Ambacher O. // 2008. MIEL 2008. 26th International Conference on Microelectronics. - Nis, 11-14 May 2008. - P. 221-224. ↑
- C692.** Hsiang Chen. Effects of hot hole trapping in GaN HEMTs. / Hsiang Chen, Lai J., Preech P., Guann-Pyng Li. // 2008. IRPS 2008. IEEE International Reliability Physics Symposium. - Phoenix, AZ, April 27 2008-May 1 2008. - P. 621-622. ↑
- C693.** Apel T. Efficient three-state WCDMA PA integrated with high-performance BiHEMT HBT / E-D pHEMT process. / Apel T., Henderson T., Yu-Lung Tang, Berger O. // 2008. RFIC 2008. IEEE Radio Frequency Integrated Circuits Symposium. - Atlanta, GA, June 17 2008-April 17 2008. - P. 149-152. ↑
- C694.** Tyagi R.K. Modeling of nanoscale GaN FET in a compact 2-D model with gate stack effects. / Tyagi R.K., Ahlawat A., Pandey M., Pandey S. // 2008. MIEL 2008. 26th International Conference on Microelectronics. - Nis, 11-14 May 2008. - P. 229-232. ↑
- C695.** Jimenez J.L. X-Band GaN FET reliability. / Jimenez J.L., Chowdhury U. // 2008. IRPS 2008. IEEE International Reliability Physics Symposium. - Phoenix, AZ, April 27 2008-May 1 2008. - P. 429-435. ↑
- C696.** Vitusevich S.A. Reliability and improved performance of AlGaIn/GaN high electron mobility transistor structures. / Vitusevich S.A., Kurakin A.M., Klein N., Petrychuk M.V., Naumov A.V., Belyaev A.E. // 2008. ICCDCS 2008. 7th International Caribbean Conference on Devices, Circuits and Systems. - Cancun, 28-30 April 2008. - P. 1-5. ↑
- C697.** Sangmin Lee. Reliability assessment of AlGaIn/GaN HEMT technology on SiC for 48V applications. / Sangmin Lee, Vetry R., Brown J.D., Gibb S.R., Cai W.Z., Jinming Sun, Green D.S., Shealy J. // 2008. IRPS 2008. IEEE International Reliability Physics Symposium. - Phoenix, AZ, April 27 2008-May 1 2008. - P. 446-449. ↑
- C698.** Chou Y.C. Degradation mechanisms of 0.1 μ m AlSb/InAs HEMTs for ultralow-power applications. / Chou Y.C., Yang J.M., Lange M.D., Tsui S.S., Leung D.L., Lin C.H., Wojtowicz M., Oki A.K. // 2008. IRPS 2008. IEEE International Reliability Physics Symposium. - Phoenix, AZ, April 27 2008-May 1 2008. - P. 436-440. ↑
- C699.** Yu M. High power RF switch MMICs development in GaN-on-Si HFET technology. / Yu M., Ward R.J., Hegazi G.M. // 2008 IEEE Radio and Wireless Symposium. - Orlando, FL, 22-24 Jan. 2008. - P. 855-858. ↑
- C700.** Aflaki P. Design and implementation of an inverse class-F power amplifier with 79 % efficiency by using a switch-based active device model. / Aflaki P., Negra R., Ghannouchi F.M. // 2008 IEEE Radio and Wireless Symposium. - Orlando, FL, 22-24 Jan. 2008. - P. 423-426. ↑
- C701.** Karangu C.W. Device Modeling using Neural Network Techniques for Solid State Power Amplifier Applications. / Karangu C.W., Ogunniyi A.J., Henriquez S.L., Reece M., White C. // 2008 IEEE Sarnoff

Symposium. - Princeton, NJ, 28-30 April 2008. - P. 1-4. ↑

C702. Mikeka C. Phase Control in Small Linear Antenna Arrays Based on LNA's Parasitic Phase Shifts. / Mikeka C., Arai H. // 2008. iWAT 2008. International Workshop on Antenna Technology: Small Antennas and Novel Metamaterials. - Chiba, 4-6 March 2008. - P. 402-405. ↑

C703. Kanto K. An X-band 250W solid-state power amplifier using GaN power HEMTs. / Kanto K., Satomi A., Asahi Y., Kashiwabara Y., Matsushita K., Takagi K. // 2008 IEEE Radio and Wireless Symposium. - Orlando, FL, 22-24 Jan. 2008. - P. 77-80. ↑

C704. Joshin K. High-power and high-efficiency GaN HEMT amplifiers. / Joshin K., Kikkawa T. // 2008 IEEE Radio and Wireless Symposium. - Orlando, FL, 22-24 Jan. 2008. - P. 65-68. ↑

C705. Youngmin Kim. 60 GHz flip-chip mounted frequency doubler/PA chain MMIC with low input power and high output power. / Youngmin Kim, Sangsub Song, Kwang-Seok Seo, Youngwoo Kwon. // 2008 IEEE Radio and Wireless Symposium. - Orlando, FL, 22-24 Jan. 2008. - P. 411-414. ↑

C706. Srinidhi E.R. Optimization of broadband drain modulation in GaN HEMT devices. / Srinidhi E.R., Ma R., Markos A.Z., Kompa G. // 2008 IEEE Radio and Wireless Symposium. - Orlando, FL, 22-24 Jan. 2008. - P. 81-84. ↑

C707. Chang D.P. Design of High Performance HEMT Switch for S-band MSM of Satellite Transponder. / Chang D.P., Noh Y.S., Yom I.B. // 2008. VTC Spring 2008. IEEE Vehicular Technology Conference. - Singapore, 11-14 May 2008. - P. 2888-2891. ↑

C708. Min Han. Two-Stage 94 GHz drive Amplifiers Using 0.1- μ m Metamorphic HEMT Technology. / Min Han, Sung-Woon Moon, Jung-hun Oh, Byeong-Ok Lim, Tae-Jong Baek, Seok-Gyu Choi, Young-Hyun Baek, Yeon-Sik Chae, Hyun-Chang Park, Sam-Dong Kim, Jin Koo Rhee. // 2008. GSMM 2008. Global Symposium on Millimeter Waves. - Nanjing, 21-24 April 2008. - P. 10-13. ↑

C709. Seok Gyu Choi. Studies on Modification of Channel Material and Gate Recess Structures in Metamorphic HEMT. / Seok Gyu Choi, Young Hyun Baek, Jung Hun Oh, Min Han, Seok Ho Bang, Byoung Chul Jun, Hyun Chang Park, Jin Koo Rhee. // 2008. GSMM 2008. Global Symposium on Millimeter Waves. - Nanjing, 21-24 April 2008. - P. 6-9. ↑

C710. Kyu-Heon Cho. High Breakdown Voltage AlGaIn/GaN HEMTs by Employing Proton Implantation. / Kyu-Heon Cho, In-Hwan Ji, Young-Hwan Choi, Jiyong Lim, Young-Shil Kim, Kye-Ryung Kim, Min-Koo Han. // 2008. ISPSD '08. 20th International Symposium on Power Semiconductor Devices and IC's. - Orlando, FL, 18-22 May 2008. - P. 241-244. ↑

C711. Yong Hyun Baek. Millimeter-wave Broadband Amplifier using MHEMT. / Yong Hyun Baek, Sang Jin Lee, Tae Jong Baek, Jung Hun Oh, Seok Gyu Choi, Dong Sun Kang, Sam Dong Kim, Jin Koo Rhee. // 2008. GSMM 2008. Global Symposium on Millimeter Waves. - Nanjing, 21-24 April 2008. - P. 48-51. ↑

C712. Mohamad M. The Sensing Performance of Undoped-AlGaIn/GaN/Sapphire HEMT Hydrogen Gas Sensor. / Mohamad M., Fong Yee Meng, Hashim A.M. // 2008. AICMS 08. Second Asia International Conference on Modeling & Simulation. - Kuala Lumpur, 13-15 May 2008. - P. 985-986. ↑

C713. Kangaslahti P. Broadband Characterization of a 100 to 180 GHz Amplifier. / Kangaslahti P., Deal W.R., Mei X.B., Lai R. // 2008 IEEE Aerospace Conference. - Big Sky, MT, 1-8 March 2008. - P. 1-6. ↑

C714. Mohd Ahir Z.F. Modeling and Characterization of Capacitively Coupled Interdigital-Gated HEMT Plasma Device for Terahertz Wave Amplification. / Mohd Ahir Z.F., Zulkifli A.Z., Hashim A.M. // 2008. AICMS 08. Second Asia International Conference on Modeling & Simulation. - Kuala Lumpur, 13-15 May 2008. - P. 990-993. ↑

C715. Parimon N.B. Modeling and Characterization of Schottky Diode on AlGaAs/GaAs HEMT Structure for Rectenna Device. / Parimon N.B., Yusof S.S.B., Bin Hashim A.M. // 2008. AICMS 08. Second Asia International Conference on Modeling & Simulation. - Kuala Lumpur, 13-15 May 2008. - P. 987-989. ↑

C716. Bettidi A. High power GaN-HEMT microwave switches for X-Band and wideband applications. / Bettidi A., Cetronio A., De Dominicis M., Giolo G., Lanzieri C., Manna A., Peroni M., Proietti C., Romanini P. // 2008. RFIC 2008. IEEE Radio Frequency Integrated Circuits Symposium. - Atlanta, GA, June 17 2008-April 17 2008. -

P. 329-332. ↑

C717. Kunkee E.T. A mixed HEMT-HBT MMIC technology using MBE regrowth. / Kunkee E.T., Consolazio S., Barner J., Retelny T., Dietz G., Bogus E., Cavus A., Chen J., Uyeda J., Hsing R., Chin P., Ahkiyat A., Chua D., Clark R., Haubenstricker R., Johnson M., Nguyen T., Sahm P., Zeliash E., Lai R. // 2008 IEEE MTT-S International Microwave Symposium Digest. - Atlanta, GA, 15-20 June 2008. - P. 1067-1070. ↑

C718. Santhakumar R. Monolithic millimeter-wave distributed amplifiers using AlGaIn/GaN HEMTs. / Santhakumar R., Yi Pei, Mishra U.K., York R.A. // 2008 IEEE MTT-S International Microwave Symposium Digest. - Atlanta, GA, 15-20 June 2008. - P. 1063-1066. ↑

C719. Ma B.Y. High power AlGaIn/GaN Ku-band MMIC SPDT switch and design consideration. / Ma B.Y., Boutros K.S., Hacker J.B., Nagy G. // 2008 IEEE MTT-S International Microwave Symposium Digest. - Atlanta, GA, 15-20 June 2008. - P. 1473-1476. ↑

C720. Reynoso-Hernandez J.A. A new method for determining the gate resistance and inductance of GaN HEMTs based on the extrema points of Z11 curves. / Reynoso-Hernandez J.A., Zuniga-Juarez J.E., Zarate-de Landa A. // 2008 IEEE MTT-S International Microwave Symposium Digest. - Atlanta, GA, 15-20 June 2008. - P. 1409-1412. ↑

C721. Zawrotny K. GaAs C-band 4-bit phase shifter MMIC. / Zawrotny K., Cegielski T. // 2008. MIKON 2008. 17th International Conference on Microwaves, Radar and Wireless Communications. - Wroclaw, 19-21 May 2008. - P. 1-4. ↑

C722. Colantonio P. 0.8-4 GHz high efficiency power amplifier in GaN technology. / Colantonio P., Giannini F., Giofre R., Piazzon L. // 2008. MIKON 2008. 17th International Conference on Microwaves, Radar and Wireless Communications. - Wroclaw, 19-21 May 2008. - P. 1-4. ↑

C723. Mahon S.J. 35 dBm, 35 GHz power amplifier MMICs using 6-inch GaAs pHEMT commercial technology. / Mahon S.J., Dadello A., Fattorini A.P., Bessemoulin A., Harvey J.T. // 2008 IEEE MTT-S International Microwave Symposium Digest. - Atlanta, GA, 15-20 June 2008. - P. 855-858. ↑

C724. Meliani C. Switch-mode amplifier ICs with over 90% efficiency for Class-S PAs using GaAs-HBTs and GaN-HEMTs. / Meliani C., Flucke J., Wentzel A., Wurfl J., Heinrich W., Trankle G. // 2008 IEEE MTT-S International Microwave Symposium Digest. - Atlanta, GA, 15-20 June 2008. - P. 751-754. ↑

C725. Nemati H.M. Characterization of switched mode LDMOS and GaN power amplifiers for optimal use in polar transmitter architectures. / Nemati H.M., Fager C., Gustavsson U., Jos R., Zirath H. // 2008 IEEE MTT-S International Microwave Symposium Digest. - Atlanta, GA, 15-20 June 2008. - P. 1505-1508. ↑

C726. Chenggang Xie. A high efficiency broadband monolithic gallium nitride distributed power amplifier. / Chenggang Xie, Pavio J., Griffey D.A., Hanson A., Singhal S. // 2008 IEEE MTT-S International Microwave Symposium Digest. - Atlanta, GA, 15-20 June 2008. - P. 307-310. ↑

C727. Krishnamurthy K. Wideband 400 W pulsed power GaN HEMT amplifiers. / Krishnamurthy K., Martin J., Landberg B., Vetry R., Poulton M.J. // 2008 IEEE MTT-S International Microwave Symposium Digest. - Atlanta, GA, 15-20 June 2008. - P. 303-306. ↑

C728. Radisic V. A 330-GHz MMIC oscillator module. / Radisic V., Samoska L., Deal W.R., Mei X.B., Yoshida W., Liu P.H., Uyeda J., Fung A., Gaier T., Lai R. // 2008 IEEE MTT-S International Microwave Symposium Digest. - Atlanta, GA, 15-20 June 2008. - P. 395-398. ↑

C729. Otsuka H. Over 57% efficiency C-band GaN HEMT high power amplifier with internal harmonic manipulation circuits. / Otsuka H., Yamanaka K., Noto H., Tsuyama Y., Chaki S., Inoue A., Miyazaki M. // 2008 IEEE MTT-S International Microwave Symposium Digest. - Atlanta, GA, 15-20 June 2008. - P. 311-314. ↑

C730. Leberer R. An AlGaIn/GaN class-S amplifier for RF-communication signals. / Leberer R., Reber R., Oppermann M. // 2008 IEEE MTT-S International Microwave Symposium Digest. - Atlanta, GA, 15-20 June 2008. - P. 85-88. ↑

C731. Lopez N.D. A 65-W high-efficiency UHF GaN power amplifier. / Lopez N.D., Hoversten J., Poulton M., Popovic Z. // 2008 IEEE MTT-S International Microwave Symposium Digest. - Atlanta, GA, 15-20 June 2008. -

P. 65-68. ↑

C732. Niehenke E.C. A Q-Band MHEMT 100-mW MMIC power amplifier with 46 % power-added efficiency. / Niehenke E.C., Whelehan J., Dong Xu, Meharry D., Duh K.H.G., Smith P.M. // 2008 IEEE MTT-S International Microwave Symposium Digest. - Atlanta, GA, 15-20 June 2008. - P. 277-280. ↑

C733. Nakasha Y. A W-band wavelet generator using 0.13- μm InP HEMTs for multi-gigabit communications based on ultra-wideband impulse radio. / Nakasha Y., Kawano Y., Suzuki T., Ohki T., Takahashi T., Makiyama K., Hirose T., Hara N. // 2008 IEEE MTT-S International Microwave Symposium Digest. - Atlanta, GA, 15-20 June 2008. - P. 109-112. ↑

C734. Tomaska M. Microwave Characterization and Properties of 2 μm Gate Length AlGaIn/GaN HEMT Structures. / Tomaska M., Lalinsky T., Vanko G., Misun M. // 2008. COMITE 2008. 14th Conference on Microwave Techniques. - Prague, 23-24 April 2008. - P. 1-4. ↑

C735. Narendra K. High performance 1.5W pHEMT Distributed Power Amplifier with Adjustable Inter-Stage Cascaded Network for 10 Γ -2000 MHz. / Narendra K., Paoloni C., Limiti E., Collantes J.M. // 2008. COMITE 2008. 14th Conference on Microwave Techniques. - Prague, 23-24 April 2008. - P. 1-4. ↑

C736. Phan Hong Phuong. Genetic algorithm for optimization of HEMT model parasitic parameters. / Phan Hong Phuong, Tong Due Thanh. // 2008. ICCE 2008. Second International Conference on Communications and Electronics. - Hoi an, 4-6 June 2008. - P. 355-359. ↑

C737. Wright P. GaN Power Transistors in Narrow and Wide Bandwidth Applications. / Wright P., Lees J., Tasker P.J., Benedikt J. // 2008 IET Seminar on Wideband Receivers and Components. - London, 7-7 May 2008. - P. 1. ↑

C738. Liu S.M.J. Optical stepper based 150mm GaAs PHEMT for microwave and millimeter-wave MMIC applications. / Liu S.M.J., Cheng-Guan Yuan, Der-Wei Tu, Wu R., Huang J., Shih-Wei Yeh, Lai W., Yu P. // 2008. COMCAS 2008. IEEE International Conference on Microwaves, Communications, Antennas and Electronic Systems. - Tel-Aviv, 13-14 May 2008. - P. 1-6. ↑

C739. Wen C.P. Experimental evidence of surface mobile holes on GaN HEMT structure. / Wen C.P., Wang J.Y., Hao Y.L., Shen B. // 2008. COMCAS 2008. IEEE International Conference on Microwaves, Communications, Antennas and Electronic Systems. - Tel-Aviv, 13-14 May 2008. - P. 1-6. ↑

C740. Ciccognani W. GaN Device Technology: Manufacturing, Characterization, Modelling and Verification. / Ciccognani W., Giannini F., Limit E., Longhi P.E., Nanni M.A., Serino A., Lanzieri C., Peroni M., Romanini P., Camarchia V., Pirola M., Ghione G. // 2008. COMITE 2008. 14th Conference on Microwave Techniques. - Prague, 23-24 April 2008. - P. 1-6. ↑

C741. Shumaker J. Design of power amplifiers using high breakdown GaN HEMT devices. / Shumaker J., Ohoka M., Ui N. // 2008. COMCAS 2008. IEEE International Conference on Microwaves, Communications, Antennas and Electronic Systems. - Tel-Aviv, 13-14 May 2008. - P. 1-5. ↑

C742. Simin G. Ultra low-loss high power AlGaIn/GaN HFET switches. / Simin G., Wang J., Hu X., Yang J., Yang Z., Gaska R., Shur M. // 2008. PESC 2008. IEEE Power Electronics Specialists Conference. - Rhodes, 15-19 June 2008. - P. 85-87. ↑

C743. Yingliang Li. A novel high effective envelope-tracking amplifier for OFDM systems. / Yingliang Li, Jide-Zhao. // 2008. ICEPT-HDP 2008. International Conference on Electronic Packaging Technology & High Density Packaging. - Shanghai, 28-31 July 2008. - P. 1-3. ↑

C744. Chen Y. Predict the characteristics of a terahertz photomixer based on HEMT with the cap region from the analytical theory. / Chen Y., He J., Mou X., Wei Y., Lou H., Liu C., Lin X., Zhang X. // 2008. MIXDES 2008. 15th International Conference on Mixed Design of Integrated Circuits and Systems. - Poznan, Poland, 19-21 June 2008. - P. 431-436. ↑

C745. Huque M.A. Towards fully integrated high temperature wireless sensors using GaN-based HEMT devices. / Huque M.A., Islam S.K., Kuruganti P.T. // 2008. MWSCAS 2008. 51st Midwest Symposium on Circuits and Systems. - Knoxville, TN, 10-13 Aug. 2008. - P. 582-585. ↑

- C746.** Avignon E. Central frequency tuning considerations for Gm-C resonators in GaAs technology. / Avignon E., Guessab S., Kielbasa R. // 2008. MWSCAS 2008. 51st Midwest Symposium on Circuits and Systems. - Knoxville, TN, 10-13 Aug. 2008. - P. 558-561. ↑
- C747.** Kyu Heon Cho. Channel modulated AlGaIn/GaN HEMTs employing fluoride plasma treatment. / Kyu Heon Cho, Young Hwan Choi, Jiyong Lim, Young Shil Kim, In Hwan Ji, Min Koo Han. // 2008. PESC 2008. IEEE Power Electronics Specialists Conference. - Rhodes, 15-19 June 2008. - P. 2172-2176. ↑
- C748.** Jiyong Lim. 1.4 kV AlGaIn/GaN HEMTs employing As⁺ ion implantation on SiO₂ passivation layer. / Jiyong Lim, Young-Hwan Choi, Kyu-Heon Cho, Jihye Lee, Jo W., Min-Koo Han. // 2008. PESC 2008. IEEE Power Electronics Specialists Conference. - Rhodes, 15-19 June 2008. - P. 88-91. ↑
- C749.** Saito W. Demonstration of resonant inverter circuit for electrodeless fluorescent lamps using high voltage GaN-HEMT. / Saito W., Domon T., Omura I., Nitta T., Kakiuchi Y., Tsuda K., Yamaguchi M. // 2008. PESC 2008. IEEE Power Electronics Specialists Conference. - Rhodes, 15-19 June 2008. - P. 3324-3329. ↑
- C750.** Young Hwan Choi. AlGaIn/GaN high-electron-mobility transistor(HEMT) employing Schottky contact on the unetched region and the silicon dioxide passivation. / Young Hwan Choi, Sun Jae Kim, Jiyong Lim, Kyu Heon Cho, Young Shil Kim, In Hwan Ji, Min Koo Han. // 2008. PESC 2008. IEEE Power Electronics Specialists Conference. - Rhodes, 15-19 June 2008. - P. 2590-2593. ↑
- C751.** Li Yuan. Molecular dynamics simulation study on fluorine plasma ion implantation in AlGaIn/GaN heterostructures. / Li Yuan, Maojun Wang, Chen K.J. // 2008. ICSICT 2008. 9th International Conference on Solid-State and Integrated-Circuit Technology. - Beijing, 20-23 Oct. 2008. - P. 1094-1097. ↑
- C752.** Maojun Wang. Source injection induced off-state breakdown and its improvement by enhanced back barrier with fluorine ion implantation in AlGaIn/GaN HEMTs. / Maojun Wang, Chen K.J. // 2008. IEDM 2008. IEEE International Electron Devices Meeting. - San Francisco, CA, 15-17 Dec. 2008. - P. 1-4. ↑
- C753.** Wanjun Chen. Monolithic integration of lateral field-effect rectifier with normally-off HEMT for GaN-on-Si switch-mode power supply converters. / Wanjun Chen, King-Yuen Wong, Chen K.J. // 2008. IEDM 2008. IEEE International Electron Devices Meeting. - San Francisco, CA, 15-17 Dec. 2008. - P. 1-4. ↑
- C754.** Luisier M. Full-band and atomistic simulation of realistic 40 nm InAs HEMT. / Luisier M., Neophytou N., Kharche N., Klimeck G. // 2008. IEDM 2008. IEEE International Electron Devices Meeting. - San Francisco, CA, 15-17 Dec. 2008. - P. 1-4. ↑
- C755.** Datta Suman. Session 30: Quantum, power, and compound semiconductors devices-heterostructure high-speed devices. / Datta Suman, Nicolic Rebecca. // 2008. IEDM 2008. IEEE International Electron Devices Meeting. - San Francisco, CA, USA, 15-17 Dec. 2008. - P. 1. ↑
- C756.** Halim M.H.C. Low Noise Amplifier for front end transceiver at 5.8 GHz. / Halim M.H.C., Aziz M.Z.A.A., Othman A.R., Sahingan S.A., Selamat M.F., Aziz A.A.A. // 2008. ICED 2008. International Conference on Electronic Design. - Penang, 1-3 Dec. 2008. - P. 1-4. ↑
- C757.** Sanusi R. 15 GHz SPDT switch design using 0.15 μm GaAs technology for microwave applications. / Sanusi R., Ismail M.A., Norhapizin K., Rahim A., Marzuki A., Yahya M.R. // 2008. ICED 2008. International Conference on Electronic Design. - Penang, 1-3 Dec. 2008. - P. 1-4. ↑
- C758.** Park S.Y. Physical degradation of GaN HEMT device observed in TEM during reliability test. / Park S.Y., Floresca C., Kim M.J., Chowdhury U., Jimenes J.L., Lee C., Beam E., Sunier P., Balistreri T. // 2008 [Reliability of Compound Semiconductors Workshop] ROCS Workshop. - Monterey, CA, USA, 12-12 Oct. 2008. - P. 45-54. ↑
- C759.** Chou Y.C. Reliability evaluation of wafer-level-packaging AlSb/InAs HEMT receivers for light-weight and ultralow-power applications. / Chou Y.C., Chang-Chien P., Leung D.L., Nishimoto M.Y., Yang J.M., Hennig K., Zeng X., Parlee M.R., Eng D.C., Farkas D.S., Gutierrez A.L., Wojtowicz M., Oki A.K., Block T. // 2008 [Reliability of Compound Semiconductors Workshop] ROCS Workshop. - Monterey, CA, USA, 12-12 Oct. 2008. - P. 105-108. ↑
- C760.** Dammann M. Reliability and degradation mechanism of AlGaIn/GaN HEMTs for next generation mobile communication systems. / Dammann M., Pletschen W., Waltereit P., Bronner W., Quay R., Muller S., Mikulla M., Ambacher O., van der Wel P.J., Murad S., Rodle T., Behtash R., Bourgeois F., Riepe K., Fagerlind M.,

Sveinbjornsson E.O. // 2008 [Reliability of Compound Semiconductors Workshop] ROCS Workshop. - Monterey, CA, USA, 12-12 Oct. 2008. - P. 25-44. ↑

C761. Chung J.W. N-face GaN/AlGaIn Transistors Through Substrate Removal. / Chung J.W., Piner E., Palacios T. // 2008 Device Research Conference. - Santa Barbara, CA, 23-25 June 2008. - P. 199-200. ↑

C762. Waltereit P. High-efficiency, high-breakdown AlGaIn/GaN HEMTs with lifetimes beyond 20 years. / Waltereit P., Bronner W., Quay R., Dammann M., Muller S., Mikulla M., van Rijs F., Rodle T., Riepe K. // 2008 Device Research Conference. - Santa Barbara, CA, 23-25 June 2008. - P. 133-134. ↑

C763. Tirado J.M. Origin of the Increasing Access Resistance in AlGaIn/GaN HEMTs. / Tirado J.M., Mievillev F., Xu Zhao, Jinwook Chung, Sanchez-Rojas J.L., Palacios T. // 2008 Device Research Conference. - Santa Barbara, CA, 23-25 June 2008. - P. 203-204. ↑

C764. Man Hoi Wong. Power performance of MBE-grown N-face high electron mobility transistors with AlN back barrier. / Man Hoi Wong, Yi Pei, Rongming Chu, Rajan S., Swenson B.L., Brown D.F., Keller S., DenBaars S.P., Speck J.S., Mishra U.K. // 2008 Device Research Conference. - Santa Barbara, CA, 23-25 June 2008. - P. 201-202. ↑

C765. Mcglone D. Electrical and thermal modeling of AlGaIn/GaN HEMTs on diamond silicon substrates. / Mcglone D., Weatherford T., Gillespie J., Via G., Zimmer J. // 2008 [Reliability of Compound Semiconductors Workshop] ROCS Workshop. - Monterey, CA, USA, 12-12 Oct. 2008. - P. 3-14. ↑

C766. Costi F. Finite-element thermal modeling of N-based HEMT structures. / Costi F., Bertoluzza F., Delmonte N., Sozzi G., Menozzi R. // 2008 [Reliability of Compound Semiconductors Workshop] ROCS Workshop. - Monterey, CA, USA, 12-12 Oct. 2008. - P. 15-24. ↑

C767. Adachi T. High-Performance E-Mode AlGaIn/GaN HEMTs with LT-GaN Cap Layer Using Gate Recess Techniques. / Adachi T., Deguchi T., Nakagawa A., Terada Y., Egawa T. // 2008 Device Research Conference. - Santa Barbara, CA, 23-25 June 2008. - P. 129-130. ↑

C768. Liu Z.H. Temperature-dependent microwave noise characteristics of AlGaIn/GaN HEMTs on silicon substrate. / Liu Z.H., Arulkumaran S., Ng G.I., Xu T. // 2008 Device Research Conference. - Santa Barbara, CA, 23-25 June 2008. - P. 127-128. ↑

C769. Ciccognani W. Full W-Band High-Gain LNA in mHEMT MMIC Technology. / Ciccognani W., Giannini F., Limiti E., Longhi P.E. // 2008. EuMIC 2008. European Microwave Integrated Circuit Conference. - Amsterdam, 27-28 Oct. 2008. - P. 314-317. ↑

C770. Hasan-Abrar Z. A Low-voltage, Fully-integrated (1.5-6) GHz Low-Noise Amplifier in E-mode pHEMT Technology for Multiband, Multimode Applications. / Hasan-Abrar Z., Chow Y.H., Eng Y.W. // 2008. EuMIC 2008. European Microwave Integrated Circuit Conference. - Amsterdam, 27-28 Oct. 2008. - P. 306-309. ↑

C771. Ciccognani W. A Reflection-Type Biphase Modulator with Balanced Loads. / Ciccognani W., di Paolo F., Ferrari M., Giannini F., Limiti E. // 2008. EuMIC 2008. European Microwave Integrated Circuit Conference. - Amsterdam, 27-28 Oct. 2008. - P. 334-337. ↑

C772. Gerbedoen J.-C. Performance of Unstuck-Gate AlGaIn/GaN HEMTs on (001) Silicon Substrate at 10 GHz. / Gerbedoen J.-C., Soltani A., Defrance N., Rousseau M., Gaquiere C., De jaeger J.-C., Joblot S., Cordier Y. // 2008. EuMIC 2008. European Microwave Integrated Circuit Conference. - Amsterdam, 27-28 Oct. 2008. - P. 330-333. ↑

C773. Schuh P. GaN MMIC based T/R-Module Front-End for X-Band Applications. / Schuh P., Sledzik H., Reber R., Fleckenstein A., Leberer R., Oppermann M., Quay R., van Raay F., Seelmann-Eggebert M., Kiefer R., Mikulla M. // 2008. EuMIC 2008. European Microwave Integrated Circuit Conference. - Amsterdam, 27-28 Oct. 2008. - P. 274-277. ↑

C774. Boles T. Advanced Components for Applications in S-Band and X-Band Radars. 2008. EuMIC 2008. European Microwave Integrated Circuit Conference. - Amsterdam, 27-28 Oct. 2008. - P. 258-261. ↑

C775. di Giacomo V. Accurate Nonlinear Electron Device Modelling for Cold FET Mixer Design. / di Giacomo V., Santarelli A., Raffo A., Traverso P.A., Schreurs D., Lonac J., Resca D., Vannini G., Filicori F., Pagani M. //

2008. EuMIC 2008. European Microwave Integrated Circuit Conference. - Amsterdam, 27-28 Oct. 2008. - P. 294-297. ↑

C776. Inoue A. A Nonlinear Drain Resistance pHEMT model for Millimeter-wave High Power Amplifiers. / Inoue A., Amasuga H., Goto S., Miyazaki M. // 2008. EuMIC 2008. European Microwave Integrated Circuit Conference. - Amsterdam, 27-28 Oct. 2008. - P. 282-285. ↑

C777. Khy A. A Highly Linear (40.5-43.5) GHz MMIC Single Balanced pHEMT Resistive Up-Converter Mixer for LMDS Applications. / Khy A., Huyart B., Teillet H. // 2008. EuMIC 2008. European Microwave Integrated Circuit Conference. - Amsterdam, 27-28 Oct. 2008. - P. 418-421. ↑

C778. Scappaviva F. 10 Watt High Efficiency GaAs MMIC Power Amplifier for Space Applications. / Scappaviva F., Cignani R., Florian C., Vannini G., Filicori F., Feudale M. // 2008. EuMIC 2008. European Microwave Integrated Circuit Conference. - Amsterdam, 27-28 Oct. 2008. - P. 562-565. ↑

C779. Koch S. A Four-Antenna Transceiver MIMIC for 60 GHz Wireless Multimedia Applications. / Koch S., Kallfass I., Leuther A., Schlechtweg M., Saito S., Uno M. // 2008. EuMIC 2008. European Microwave Integrated Circuit Conference. - Amsterdam, 27-28 Oct. 2008. - P. 502-505. ↑

C780. CheYu Kuo. A Compact 20-35 GHz Quadrature Coupler using 0.15um pHEMT Coplanar Waveguide Technology. / CheYu Kuo, ChiaShih Cheng, CheYen Huang, PoYu Ke, HsienChin Chiu, Fu J.S. // 2008 China-Japan Joint Microwave Conference. - Shanghai, 10-12 Sept. 2008. - P. 636-639. ↑

C781. ChiaSong Wu. High Linearity 5.2 GHz Power Amplifier MMIC Using the Linearizer Circuit. / ChiaSong Wu, ChienHuang Chang, HsingChung Liu, TingYu Ko, HsienChin Chiu. // 2008 China-Japan Joint Microwave Conference. - Shanghai, 10-12 Sept. 2008. - P. 633-635. ↑

C782. Takahashi H. 120-GHz-band Low-noise Amplifier with 14-ps Group-delay Variation for 10-Gbit/s Data Transmission. / Takahashi H., Kosugi T., Hirata A., Murata K., Kukutsu N. // 2008. EuMIC 2008. European Microwave Integrated Circuit Conference. - Amsterdam, 27-28 Oct. 2008. - P. 430-433. ↑

C783. Kallfass I. Multiple-Throw Millimeter-Wave FET Switches for Frequencies from 60 up to 120 GHz. / Kallfass I., Diebold S., Massler H., Koch S., Seelmann-Eggebert M., Leuther A. // 2008. EuMIC 2008. European Microwave Integrated Circuit Conference. - Amsterdam, 27-28 Oct. 2008. - P. 426-429. ↑

C784. Napijalo V. 24 GHz LTCC Amplifier Using Packaged HEMTs. / Napijalo V., Cojocaru V., Yokoyama T. // 2008. EuMIC 2008. European Microwave Integrated Circuit Conference. - Amsterdam, 27-28 Oct. 2008. - P. 462-465. ↑

C785. Napijalo V. 24 GHz LTCC I/Q Mixer Using Packaged HEMTs. / Napijalo V., Cojocaru V. // 2008. EuMIC 2008. European Microwave Integrated Circuit Conference. - Amsterdam, 27-28 Oct. 2008. - P. 454-457. ↑

C786. Rongming Chu. V-Gate GaN HEMTs with 12.2 W/mm and 65% PAE at X-Band. / Rongming Chu, Likun Shen, Fichtenbaum N., Brown D., Zhen Chen, Keller S., Mishra U. // 2008 Device Research Conference. - Santa Barbara, CA, 23-25 June 2008. - P. 205-206. ↑

C787. Kitazawa S. A study of switchable dual-frequency oscillator for 60 GHz FSK modulation. / Kitazawa S., Taromaru M., Ueba M. // 2008. APMC 2008. Asia-Pacific Microwave Conference. - Macau, 16-20 Dec. 2008. - P. 1-4. ↑


C788. Muller A. AIN SAW structures for GHz applications. / Muller A., Konstantinidis G., Neculoiu D., Dinescu A., Morosanu C., Stavriniadis A., Dragoman M., Vasilache D., Buiculescu C., Petrini I., Anton C. // 2008. APMC 2008. Asia-Pacific Microwave Conference. - Macau, 16-20 Dec. 2008. - P. 1-4. ↑


C789. Yong-Sub Lee. A wideband GaN HEMT distributed power amplifier for WiMAX applications. / Yong-Sub Lee, Mun-Woo Lee, Yoon-Ha Jeong. // 2008. APMC 2008. Asia-Pacific Microwave Conference. - Macau, 16-20 Dec. 2008. - P. 1-4. ↑


C790. Gangwani P. Capacitance modeling of 120nm AlGaIn/GaN HEMT for microwave and high speed circuit applications. / Gangwani P., Gupta M., Kaur R., Pandey S., Halder S., Gupta R.S. // 2008. APMC 2008. Asia-Pacific Microwave Conference. - Macau, 16-20 Dec. 2008. - P. 1-4. ↑


- C791.** Chan-Sei Yoo. A ultrawideband low noise amplifier using metamorphic HEMT on organic substrate. / Chan-Sei Yoo, Gyeong-Sun Seol, Je-Hyun Youn, Gwang-Hoon Lee, Dongsu Kim, Sung-Won Kim, Kwang-Seok Seo, Woo-Sung Lee. // 2008. APMC 2008. Asia-Pacific Microwave Conference. - Macau, 16-20 Dec. 2008. - P. 1-4. ↑
- C792.** Yong-Sub Lee. Linearity-optimized class-E GaN HEMT Doherty amplifier. / Yong-Sub Lee, Mun-Woo Lee, Yoon-Ha Jeong. // 2008. APMC 2008. Asia-Pacific Microwave Conference. - Macau, 16-20 Dec. 2008. - P. 1-4. ↑
- C793.** Kumar S.P. DMG AlGaIn/GaN HEMT: A solution to RF and wireless applications for reduced distortion performance. / Kumar S.P., Agrawal A., Chaujar Student R., Gupta M., Gupta R.S. // 2008. APMC 2008. Asia-Pacific Microwave Conference. - Macau, 16-20 Dec. 2008. - P. 1-4. ↑
- C794.** Ando A. A high-efficiency class-F GaN HEMT power amplifier with a diode predistortion linearizer. / Ando A., Takayama Y., Yoshida T., Ishikawa R., Honjo K. // 2008. APMC 2008. Asia-Pacific Microwave Conference. - Macau, 16-20 Dec. 2008. - P. 1-4. ↑
- C795.** Cheng-Guan Yuan. Quarter-micron optical gate 6" power pHEMT technology. / Cheng-Guan Yuan, Der-Wei Tu, Liu S.M.J., Wu R., Huang J., Chen F., Shih-Wei Yeh, Lai W. // 2008. APMC 2008. Asia-Pacific Microwave Conference. - Macau, 16-20 Dec. 2008. - P. 1-4. ↑
- C796.** Yong-Hyun Baek. D-band amplifier using metamorphic HEMT technology. / Yong-Hyun Baek, Seok-Gyu Choi, Sang-Jin Lee, Tae-Jong Baek, Min Han, Jung-Hun Oh, Hui-chul Cho, Eung-Ho Rhee, Jin-Koo Rhee. // 2008. APMC 2008. Asia-Pacific Microwave Conference. - Macau, 16-20 Dec. 2008. - P. 1-4. ↑
- C797.** Osman M.N. Influence of gate width and gate finger towards noise figure of p-HEMT. / Osman M.N., Rahim A., Yahya M.R., Awang Mat A.F. // 2008. APMC 2008. Asia-Pacific Microwave Conference. - Macau, 16-20 Dec. 2008. - P. 1-4. ↑
- C798.** Krishnamoorthy S. Steady-state and transient temperature distribution in GaAs microwave circuits. / Krishnamoorthy S., Chowdhury M.H. // 2008. ICM 2008. International Conference on Microelectronics. - Sharjah, 14-17 Dec. 2008. - P. 114-117. ↑
- C799.** Tzu-Chieh Hong. Low-phase-noise, phase-locked tunable millimeter-wave signal source for calibration of W-band low-noise astronomical heterodyne receivers. / Tzu-Chieh Hong, Yuh-Jing Hwang, Wei-Ting Wong, Tashun Wei, Yo-Shen Lin. // 2008. APMC 2008. Asia-Pacific Microwave Conference. - Macau, 16-20 Dec. 2008. - P. 1-4. ↑
- C800.** Wang Y. High power X-band internally-matched AlGaIn/GaN HEMT. / Wang Y., Zhang Z.G., Feng Z., Li J.Q., Song J.B., Feng Z.H., Cai S.J. // 2008. APMC 2008. Asia-Pacific Microwave Conference. - Macau, 16-20 Dec. 2008. - P. 1-3. ↑
- C801.** Jonghyuk Jeong. A 3.7GHz GaN HEMT Doherty power amplifier using digital predistortion linearization. / Jonghyuk Jeong, Van J., Jaeyong Cho, Min-su Kim, Hanjin Cho, Kyung-hoon Lim, Sung-wook Kwon, Kyonggon Choi, Hyung-chul Kim, Sungcheol Yoo, Youngoo Yang. // 2008. APMC 2008. Asia-Pacific Microwave Conference. - Macau, 16-20 Dec. 2008. - P. 1-4. ↑
- C802.** Chien-Ying Wu. Evaluation of RF and logic performance for 40 nm InAs/InGaAs composite channel HEMTs for high-speed and low-voltage applications. / Chien-Ying Wu, Heng-Tung Hsu, Chien-I Kuo, Yi Chang E., Yu-lin Chen. // 2008. APMC 2008. Asia-Pacific Microwave Conference. - Macau, 16-20 Dec. 2008. - P. 1-4. ↑
- C803.** Fan-Hsiu Huang. A low-power subharmonic injection-locked oscillator using E/D-mode GaAs PHEMTs for Ka-band applications. / Fan-Hsiu Huang, Chi-Hsien Lin, Hong-Yeh Chang, Yi-Jen Chan. // 2008. APMC 2008. Asia-Pacific Microwave Conference. - Macau, 16-20 Dec. 2008. - P. 1-4. ↑
- C804.** Tartarin J.G. Improved robustness of AlGaIn/GaN HEMTs using Deuterium to passivate the structural defects. / Tartarin J.G., Astre G., Bary L., Chevallier J., Delage S. // 2008. COMMAD 2008. Conference on Optoelectronic and Microelectronic Materials and Devices. - Sydney, SA, July 28 2008-Aug. 1 2008. - P. 4-7. ↑
- C805.** Wanjun Chen. High-Performance AlGaIn/GaN HEMT-Compatible Lateral Field-Effect Rectifiers. / Wanjun Chen, Wei Huang, King Yuen Wong, Chen K.J. // 2008 Device Research Conference. - Santa Barbara, ↑


CA, 23-25 June 2008. - P. 287-288. 


C806. Halim M.H.C. 5-6 GHz Front End Low Noise Amplifier. / Halim M.H.C., Aziz M.Z.A.A., Othman A.R., Sahingan S.A., Selamat M.F., Aziz A.A.A. // Telecommunication Technologies 2008 and 2008 2nd Malaysia Conference on Photonics. NCTT-MCP 2008. 6th National Conference on. - Putrajaya, 26-28 Aug. 2008. - P. 136-139. 


C807. Menozzi R. Reliability of GaN-Based HEMT devices. 2008. COMMAD 2008. Conference on Optoelectronic and Microelectronic Materials and Devices. - Sydney, SA, July 28 2008-Aug. 1 2008. - P. 44-50. 


C808. Nishimura T. Broadband Terahertz Emission from Dual-Grating Gate HEMT's-Mechanism and Emission Spectral Profile. / Nishimura T., Handa H., Tsuda H., Suemitsu T., Meziani Y.M., Knap W., Otsuji T., Sano E., Ryzhii V., Satou A., Popov V.V., Coquillat D., Teppe F. // 2008 Device Research Conference. - Santa Barbara, CA, 23-25 June 2008. - P. 263-264. 


C809. Kim T.-W. Enhancement-mode 130 nm InAs p-HEMTs having f_T of 403 GHz and f_{max} of 470 GHz fabricated using atomic-layer-etching technology. / Kim T.-W., Kim D.-H., Park S.D., Shin S.H., Yeom G.Y., Jang J.H., Song J.-I. // 2008 Device Research Conference. - Santa Barbara, CA, 23-25 June 2008. - P. 211-212. 


C810. Hashizume T. Surface control of AlGaIn for the stability improvement of AlGaIn/GaN HEMTs. 2008 Device Research Conference. - Santa Barbara, CA, 23-25 June 2008. - P. 283-284. 


C811. Akis R. Simulating Pseudomorphic HEMTs: Optimizing Performance to Achieve Multi-terahertz Operating Frequencies. / Akis R., Ayubi-Moak J.S., Faralli N., Goodnick S.M., Ferry D.K., Saraniti M. // 2008 Device Research Conference. - Santa Barbara, CA, 23-25 June 2008. - P. 267-268. 


C812. Khan F.N. A GaN HEMT Class-F amplifier for UMTS/WCDMA applications. / Khan F.N., Mohammadi F.A., Yagoub M.C.E. // 2008. RFM 2008. IEEE International RF and Microwave Conference. - Kuala Lumpur, 2-4 Dec. 2008. - P. 478-482. 


C813. Shao Wei Lin. A compact size Ka band pHEMT MMIC frequency tripler using lump element balun. / Shao Wei Lin, Chia-Shih Cheng, Chien-Cheng Wei, Fu J.S., Hsien-Chin Chiu. // 2008. APMC 2008. Asia-Pacific Microwave Conference. - Macau, 16-20 Dec. 2008. - P. 1-4. 


C814. Yi-Chien Tsai. A 40-80-GHz mHEMT single-pole-double-throw switch using traveling-wave concept. / Yi-Chien Tsai, Jing-Lin Kuo, Huei Wang. // 2008. APMC 2008. Asia-Pacific Microwave Conference. - Macau, 16-20 Dec. 2008. - P. 1-4. 


C815. Kimura M. GaN X-band 43% internally-matched FET with 60W output power. / Kimura M., Yamauchi K., Yamanaka K., Noto H., Kuwata E., Otsuka H., Inoue A., Kamo Y., Miyazaki M. // 2008. APMC 2008. Asia-Pacific Microwave Conference. - Macau, 16-20 Dec. 2008. - P. 1-4. 

C816. Heng-Tung Hsu. On the noise performance of 80nm InAs/In_{0.7}Ga_{0.3}As HEMTs using gate sinking technology. / Heng-Tung Hsu, Chien-I Kuo, Chang E.Y. // 2008. APMC 2008. Asia-Pacific Microwave Conference. - Macau, 16-20 Dec. 2008. - P. 1-4. 

C817. Noh Y.S. Ku-band MMIC power amplifier with on-chip compensation gate bias circuit. / Noh Y.S., Yom I.B. // 2008. APMC 2008. Asia-Pacific Microwave Conference. - Macau, 16-20 Dec. 2008. - P. 1-4. 

C818. Anand L. High efficiency 600-mW pHEMT balance amplifier design with load pull technique. / Anand L., Kumar N., Pragash S., Ain M.F., Hassan S.I.S. // 2008. RFM 2008. IEEE International RF and Microwave Conference. - Kuala Lumpur, 2-4 Dec. 2008. - P. 483-486. 

C819. Yuehang Xu. Accurate modeling noise characteristic of microwave field-effect transistor. / Yuehang Xu, Yunchuan Guo, Yunqiu Wu, Ruimin Xu, Bo Yan. // 2008. APMC 2008. Asia-Pacific Microwave Conference. - Macau, 16-20 Dec. 2008. - P. 1-4. 

C820. Hang-Kiong Lee. A low noise figure high linearity balanced amplifier module for cellular band base station's tower mounted amplifier application using E-mode pHEMT technology. / Hang-Kiong Lee, King-CS A., Fuad H.-M., Chong-CK T. // 2008. APMC 2008. Asia-Pacific Microwave Conference. - Macau, 16-20 Dec. 2008. - P. 1-4. 

- C821.** Kuroda K. High-Efficiency GaN-HEMT Class-F Amplifier Operating at 5.7 GHz. / Kuroda K., Ishikawa R., Honjo K. // 2008. EuMC 2008. 38th European Microwave Conference. - Amsterdam, 27-31 Oct. 2008. - P. 440-443. ↑
- C822.** Schwierz F. The frequency limits of field-effect transistors: MOSFET vs. HEMT. 2008. ICSICT 2008. 9th International Conference on Solid-State and Integrated-Circuit Technology. - Beijing, 20-23 Oct. 2008. - P. 1433-1436. ↑
- C823.** Faraj J. Pulse Profiling for AlGaIn/GaN HEMTs Large Signal Characterizations. / Faraj J., De Groote F., Teyssier J.-P., Verspecht J., Quere R., Aubry R. // 2008. EuMC 2008. 38th European Microwave Conference. - Amsterdam, 27-31 Oct. 2008. - P. 757-760. ↑
- C824.** Azam S. Designing, Fabrication and Characterization of Power Amplifiers Based on 10-Watt SiC MESFET & GaN HEMT at Microwave Frequencies. / Azam S., Jonsson R., Wahab Q. // 2008. EuMC 2008. 38th European Microwave Conference. - Amsterdam, 27-31 Oct. 2008. - P. 444-447. ↑
- C825.** Wen C.P. Transient leakage current technique for MIS HEMT (Al₂O₃/AlGaIn/GaN) dielectric semiconductor interface property characterization. / Wen C.P., Jinyan Wang, Hongwei Chen, Hao Y.L., Lau K.M., Tang C.W. // 2008. ICSICT 2008. 9th International Conference on Solid-State and Integrated-Circuit Technology. - Beijing, 20-23 Oct. 2008. - P. 1440-1442. ↑
- C826.** Mun-Woo Lee. A High-Efficiency GaN HEMT Hybrid Class-E Power Amplifier for 3.5 GHz WiMAX Applications. / Mun-Woo Lee, Yong-Sub Lee, Yoon-Ha Jeong. // 2008. EuMC 2008. 38th European Microwave Conference. - Amsterdam, 27-31 Oct. 2008. - P. 436-439. ↑
- C827.** Yong-Sub Lee. High-Efficiency Class-E-Cells-Based GaN HEMT Doherty Amplifier for WCDMA Applications. / Yong-Sub Lee, Mun-Woo Lee, Yoon-Ha Jeong. // 2008. EuMC 2008. 38th European Microwave Conference. - Amsterdam, 27-31 Oct. 2008. - P. 428-431. ↑
- C828.** Hongwei Chen. Enhanced device performance of AlGaIn/GaN HEMTs using thermal oxidation of electron-beam deposited aluminum for gate oxide. / Hongwei Chen, Jinyan Wang, Chuan Xu, Min Yu, Yang Fu, Zhihua Dong, Fujun Xu, Yilong Hao, Wen C.P. // 2008. ICSICT 2008. 9th International Conference on Solid-State and Integrated-Circuit Technology. - Beijing, 20-23 Oct. 2008. - P. 1443-1446. ↑
- C829.** Weizhong Li. A design of Ka-band GaAs PHEMT power amplifier MMIC. / Weizhong Li, Longxin Peng. // 2008. ISAPE 2008. 8th International Symposium on Antennas, Propagation and EM Theory. - Kunming, 2-5 Nov. 2008. - P. 1079-1082. ↑
- C830.** Costrini C. A 20 Watt Micro-strip X-Band AlGaIn/GaN HPA MMIC for Advanced Radar Applications. / Costrini C., Calori M., Cetronio A., Lanzieri C., Lavanga S., Peroni M., Limiti E., Serino A., Ghione G., Melone G. // 2008. EuMC 2008. 38th European Microwave Conference. - Amsterdam, 27-31 Oct. 2008. - P. 1433-1436. ↑
- C831.** Scappaviva F. 10 Watt High Efficiency GaAs MMIC Power Amplifier for Space Applications. / Scappaviva F., Cignani R., Florian C., Vannini G., Filicori F., Feudale M. // 2008. EuMC 2008. 38th European Microwave Conference. - Amsterdam, 27-31 Oct. 2008. - P. 1429-1432. ↑
- C832.** Kallfass I. Multiple-Throw Millimeter-Wave FET Switches for Frequencies from 60 up to 120 GHz. / Kallfass I., Diebold S., Massler H., Koch S., Seelmann-Eggebert M., Leuther A. // 2008. EuMC 2008. 38th European Microwave Conference. - Amsterdam, 27-31 Oct. 2008. - P. 1453-1456. ↑
- C833.** Khy A. A Highly Linear (40.5-43.5) GHz MMIC Single Balanced pHEMT Resistive Up-Converter Mixer for LMDS Applications. / Khy A., Huyart B., Teillet H. // 2008. EuMC 2008. 38th European Microwave Conference. - Amsterdam, 27-31 Oct. 2008. - P. 1445-1448. ↑
- C834.** Hadziabdic D. Power Amplifier Design for E-band Wireless System Communications. / Hadziabdic D., Krozer V., Johansen T.K. // 2008. EuMC 2008. 38th European Microwave Conference. - Amsterdam, 27-31 Oct. 2008. - P. 1378-1381. ↑
- C835.** Millon B.J. Design of GaN HEMT Transistor Based Amplifiers for 5-6 GHz WiMAX Applications. / Millon B.J., Wood S.M., Pengelly R.S. // 2008. EuMC 2008. 38th European Microwave Conference. - Amsterdam, 27-31 Oct. 2008. - P. 1090-1093. ↑

- C836.** Paquay M. Alignment Verification of the PLANCK Reflector Configuration by RCS Measurements at 320 GHz. / Paquay M., Marti-Canales J., Rolo L., Forma G., Dubruel D., Wylde R., Maffei B., Doyle D., Crone G., Tauber J., Hills R. // 2008. EuMC 2008. 38th European Microwave Conference. - Amsterdam, 27-31 Oct. 2008. - P. 765-768. ↑
- C837.** Armengaud V. Design of a Ka-band MMIC Filtering LNA with a Metamorphic HEMT Technology for a Space Application. / Armengaud V., Lintignat J., Barelaud B., Jarry B., Babak L.I., Laporte C. // 2008. EuMC 2008. 38th European Microwave Conference. - Amsterdam, 27-31 Oct. 2008. - P. 1358-1361. ↑
- C838.** Hyoungjong Kim. Pulse Operation of an Inverse Class-F GaN Power Amplifier. / Hyoungjong Kim, Gilwong Choi, Jinjoo Choi. // 2008. EuMC 2008. 38th European Microwave Conference. - Amsterdam, 27-31 Oct. 2008. - P. 1177-1180. ↑
- C839.** Tomaska M. High Frequency Characterization and Properties of AlGaIn/GaN HEMT Structures. / Tomaska M., Lalinsky T., Vanko G., Misun M. // 2008. ASDAM 2008. International Conference on Advanced Semiconductor Devices and Microsystems. - Smolenice, 12-16 Oct. 2008. - P. 331-334. ↑
- C840.** Lalinsky T. Surface Acoustic Wave Excitation on SF6 Plasma Treated AlGaIn/GaN Heterostructure. / Lalinsky T., Rufer L., Vanko G., Ryger I., Hascik S., Tomaska M., Mozolova Z., Vincze A. // 2008. ASDAM 2008. International Conference on Advanced Semiconductor Devices and Microsystems. - Smolenice, 12-16 Oct. 2008. - P. 311-314. ↑
- C841.** Boudjelida B. Sub-0.5 dB NF broadband low-noise amplifier using a novel InGaAs/InAlAs/InP pHEMT. / Boudjelida B., Sobih A., Arshad S., Bouloukou A., Boulay S., Sly J., Missous M. // 2008. ASDAM 2008. International Conference on Advanced Semiconductor Devices and Microsystems. - Smolenice, 12-16 Oct. 2008. - P. 75-78. ↑
- C842.** Vanko G. Impact of SF6 Plasma on DC and Microwave Performance of AlGaIn/GaN HEMT Structures. / Vanko G., Lalinsky T., Tomaska M., Hascik S., Mozolova Z., Skriniarova J., Kostic I., Vincze A., Uherek F. // 2008. ASDAM 2008. International Conference on Advanced Semiconductor Devices and Microsystems. - Smolenice, 12-16 Oct. 2008. - P. 335-338. ↑
- C843.** Zanon F. Reliability aspects of GaN-HEMTs on composite substrates. / Zanon F., Danesin F., Tazzoli A., Meneghini M., Ronchi N., Chini A., Bove P., Langer R., Zanon E., Meneghesso G. // 2008. ASDAM 2008. International Conference on Advanced Semiconductor Devices and Microsystems. - Smolenice, 12-16 Oct. 2008. - P. 23-30. ↑
- C844.** Weijia Li. A 2.469 2.69GHz AlGaIn/GaN HEMT power amplifier for IEEE 802.16e WiMAX applications. / Weijia Li, Yan Wang, Ghione G. // 2008. ICCS 2008. 11th IEEE Singapore International Conference on Communication Systems. - Guangzhou, 19-21 Nov. 2008. - P. 1475-1479. ↑
- C845.** Khmyrova I. Frequency performance of plasmawave devices for THZ applications and the role of fringing effects. / Khmyrova I., Nishimura T., Magome N., Suemitsu T., Otsuji T. // 2008. IEEEI 2008. IEEE 25th Convention of Electrical and Electronics Engineers in Israel. - Eilat, 3-5 Dec. 2008. - P. 650-653. ↑
- C846.** Mohiuddin M. 2-D Physical Modelling of 6-doped GaAs/AlGaAs HEMT. / Mohiuddin M., Arshad S., Bouloukou A., Missous M. // 2008. ASDAM 2008. International Conference on Advanced Semiconductor Devices and Microsystems. - Smolenice, 12-16 Oct. 2008. - P. 207-210. ↑
- C847.** Hashizume T. Surface control structures for high-performance AlGaIn/GaN HEMTs. 2008. ASDAM 2008. International Conference on Advanced Semiconductor Devices and Microsystems. - Smolenice, 12-16 Oct. 2008. - P. 17-22. ↑
- C848.** Telia A. Analysis of trap states effects on the frequency-dependent capacitance and conductance of an AlGaIn/GaN heterostructure. / Telia A., Meziani A., Soltani A. // 2008. SCS 2008. 2nd International Conference on Signals, Circuits and Systems. - Monastir, 7-9 Nov. 2008. - P. 1-5. ↑
- C849.** Chaibi M. Modelling of temperature and dispersion effects in MESFET and HEMT transistors. / Chaibi M., Fernandez T., Tellez J.R., Tazon A., Aghoutane M. // 2008. INMMIC 2008. Workshop on Integrated Nonlinear Microwave and Millimetre-Wave Circuits. - Malaga, 24-25 Nov. 2008. - P. 173-175. ↑
- C850.** Bonhoun Koo. A 28-dBm pHEMT Power Amplifier Using Voltage Combiner for K-Band Applications. /

Bonhoon Koo, Changkun Park, Kyung Ai Lee, Jong-Hoon Chun, Songcheol Hong. // 2008. EuMC 2008. 38th European Microwave Conference. - Amsterdam, 27-31 Oct. 2008. - P. 293-296. ↑

C851. Huet T. A 8W High efficiency X-band Power pHEMT amplifier. / Huet T., Gruenenpuett J., Ouarch Z., Bouw D., Serru V., Camiade M., Chang C., Chaumas P. // 2008. EuMC 2008. 38th European Microwave Conference. - Amsterdam, 27-31 Oct. 2008. - P. 289-292. ↑

C852. Zamanillo J.M. The versatility of verilog-A based models on commercial microwave simulators. / Zamanillo J.M., Zamanillo I., Campelo J., Mediavilla A., Perez-Vega C., Lopez-Espi P.L., Torres R. // 2008. INMMIC 2008. Workshop on Integrated Nonlinear Microwave and Millimetre-Wave Circuits. - Malaga, 24-25 Nov. 2008. - P. 153-156. ↑

C853. Thorsell M. Characterization of the temperature dependent access resistances in AlGaIn/GaN HEMTs. / Thorsell M., Andersson K., Fagerlind M., Sudow M., Nilsson P.-A., Rorsman N. // 2008. INMMIC 2008. Workshop on Integrated Nonlinear Microwave and Millimetre-Wave Circuits. - Malaga, 24-25 Nov. 2008. - P. 17-20. ↑

C854. Cico K. InAlN/GaN MOSHEMT with Al₂O₃ insulating film. / Cico K., Gregusova D., Kuzmik J., di Forte-Poisson M.A., Lalinsky T., Pogany D., Delage S.L., Frohlich K. // 2008. ASDAM 2008. International Conference on Advanced Semiconductor Devices and Microsystems. - Smolenice, 12-16 Oct. 2008. - P. 87-90. ↑

C855. Martin A. Power and thermal design criteria of AlGaIn/GaN cascode cell for wideband distributed power amplifier. / Martin A., Reveyrand T., Campovecchio M., Quere R., Jardel O., Piotrowicz S. // 2008. INMMIC 2008. Workshop on Integrated Nonlinear Microwave and Millimetre-Wave Circuits. - Malaga, 24-25 Nov. 2008. - P. 145-148. ↑

C856. Marante R. Impact of Ron (VDD) dependence on polar transmitter residual distortion. / Marante R., Garcia J.A., Cabral P.M., Pedro J.C. // 2008. INMMIC 2008. Workshop on Integrated Nonlinear Microwave and Millimetre-Wave Circuits. - Malaga, 24-25 Nov. 2008. - P. 123-126. ↑

C857. Hasan M.T. InN-based dual channel high electron mobility transistor. / Hasan M.T., Rahman M.M., Shamsuzzaman A.N.M., Islam M.S., Bhuiyan A.G. // 2008. ICECE 2008. International Conference on Electrical and Computer Engineering. - Dhaka, 20-22 Dec. 2008. - P. 452-455. ↑

C858. Rasmi A. Design of 2-stage medium power amplifier using 0.5 μm GaAs PHEMT for wireless LAN applications. / Rasmi A., Marzuki A., Ismail M.A., Rahim A.I.A., Yahya M.R., Mat A.F.A. // TENCON 2008-2008 IEEE Region 10 Conference. - Hyderabad, 19-21 Nov. 2008. - P. 1-5. ↑

C859. Norhapizin K. Parasitic effects of spiral inductors on the performance of GaAs-based MMIC low noise amplifier. / Norhapizin K., Ismail M.A., Ismat A.R.A., Marzuki A., Yahya M.R., Mat A.F.A. // 2008. ICSE 2008. IEEE International Conference on Semiconductor Electronics. - Johor Bahru, 25-27 Nov. 2008. - P. 134-137. ↑

C860. Gonzalez-Garrido M.A. 2-6 GHz GaN MMIC Power Amplifiers for Electronic Warfare Applications. / Gonzalez-Garrido M.A., Grajal J., Cubilla P., Cetronio A., Lanzieri C., Uren M. // 2008. EuMIC 2008. European Microwave Integrated Circuit Conference. - Amsterdam, 27-28 Oct. 2008. - P. 83-86. ↑

C861. Hayati M. HEMT Transistor Noise modeling using generalized radial basis function. / Hayati M., Shamkhani A., Rezaei A., Seifi M. // 2008. ICSE 2008. IEEE International Conference on Semiconductor Electronics. - Johor Bahru, 25-27 Nov. 2008. - P. 509-513. ↑

C862. Padmaja T. A 18-40GHz Monolithic GaAs pHEMT low noise amplifier. / Padmaja T., N'Gongo R.S., Ratna P., Vasu P.S., Babu J.S., Kirty V.S.R. // 2008. MICROWAVE 2008. International Conference on Recent Advances in Microwave Theory and Applications. - Jaipur, 21-24 Nov. 2008. - P. 309-311. ↑

C863. Chattopadhyay M.K. Thermal model for AlGaIn/GaN HEMTs including self-heating effect and non-linear polarization. 2008. MICROWAVE 2008. International Conference on Recent Advances in Microwave Theory and Applications. - Jaipur, 21-24 Nov. 2008. - P. 63-65. ↑

C864. Mahajan S.S. High temperature alloyed Ag based ohmic contacts to pseudomorphic high electron mobility transistor (p-HEMT). / Mahajan S.S., Tomer A., Goyal A., Vinayak S., Sharma H.S., Sehgal B.K. // 2008. MICROWAVE 2008. International Conference on Recent Advances in Microwave Theory and Applications. - Jaipur, 21-24 Nov. 2008. - P. 312-315. ↑

- C865.** Rath S. Comparative subthreshold analysis for channel thickness variation on sub-100 nm Double Gate with Single-Gate HEMT. / Rath S., Gupta R., Gupta M., Gupta R.S. // 2008. MICROWAVE 2008. International Conference on Recent Advances in Microwave Theory and Applications. - Jaipur, 21-24 Nov. 2008. - P. 322-324. ↑
- C866.** Aggarwal R. Investigation of temperature dependent microwave performance of AlGaIn/GaN MISHFETs for high power wireless applications. / Aggarwal R., Agrawal A., Gupta M., Gupta R.S. // 2008. MICROWAVE 2008. International Conference on Recent Advances in Microwave Theory and Applications. - Jaipur, 21-24 Nov. 2008. - P. 66-68. ↑
- C867.** Alleva V. High Power Microstrip GaN-HEMT Switches for Microwave Applications. / Alleva V., Bettidi A., Cetrionio A., De Dominicis M., Ferrari M., Giovine E., Lanzierf C., Limiti E., Megna A., Peroni M., Romaninf P. // 2008. EuMIC 2008. European Microwave Integrated Circuit Conference. - Amsterdam, 27-28 Oct. 2008. - P. 194-197. ↑
- C868.** Astre G. Increased reliability of AlGaIn/GaN HEMTs versus temperature using deuterium. / Astre G., Tartarin J.G., Chevallier J., Delage S. // 2008. EuMIC 2008. European Microwave Integrated Circuit Conference. - Amsterdam, 27-28 Oct. 2008. - P. 187-189. ↑
- C869.** Tessmann A. Metamorphic MMICs for Operation Beyond 200 GHz. / Tessmann A., Kallfass I., Leuther A., Massler H., Schlechtweg M., Ambacher O. // 2008. EuMIC 2008. European Microwave Integrated Circuit Conference. - Amsterdam, 27-28 Oct. 2008. - P. 210-213. ↑
- C870.** Kumar S. 6-24 GHz Mixer Using 0.25 μ m Enhancement Mode PHEMT Technology in a Low Cost Chip Scale Package. / Kumar S., Kessler J., Morkner H. // 2008. EuMIC 2008. European Microwave Integrated Circuit Conference. - Amsterdam, 27-28 Oct. 2008. - P. 238-241. ↑
- C871.** Dahmani S. Thermal Model Extraction of GaN HEMTs for Large-Signal Modeling. / Dahmani S., Mengistu E.S., Kompa G. // 2008. EuMIC 2008. European Microwave Integrated Circuit Conference. - Amsterdam, 27-28 Oct. 2008. - P. 226-229. ↑
- C872.** ShiChang Zhong. AlGaIn/GaN HEMT with over 110 W Output Power for X-Band. / ShiChang Zhong, Tangsheng Chen, Chunjiang Ren, Gang Jiao, Chen Chen, Kai Shao, Naibin Yang. // 2008. EuMIC 2008. European Microwave Integrated Circuit Conference. - Amsterdam, 27-28 Oct. 2008. - P. 91-94. ↑
- C873.** Quay R. Efficient AlGaIn/GaN HEMT Power Amplifiers. / Quay R., van Raay F., Kuhn J., Kiefer R., Waltereit P., Zorcic M., Musser M., Bronner W., Dammann M., Seelmann-Eggebert M., Schlechtweg M., Mikulla M., Ambacher O., Thorpe J., Riepe K., van Rijs F., Saad M., Harm L., Rodle T. // 2008. EuMIC 2008. European Microwave Integrated Circuit Conference. - Amsterdam, 27-28 Oct. 2008. - P. 87-90. ↑
- C874.** Kuhn J. Balanced Microstrip AlGaIn/GaN HEMT Power Amplifier MMIC for X-Band Applications. / Kuhn J., van Raay F., Quay R., Kiefer R., Bronner W., Seelmann-Eggebert M., Schlechtweg M., Mikulla M., Ambacher O., Thumm M. // 2008. EuMIC 2008. European Microwave Integrated Circuit Conference. - Amsterdam, 27-28 Oct. 2008. - P. 95-98. ↑
- C875.** Nakajima A. Decrease in Slow Current Transients and Current Collapse in GaN-based FETs with a Filed Plate. / Nakajima A., Itagaki K., Horio K. // 2008. EuMIC 2008. European Microwave Integrated Circuit Conference. - Amsterdam, 27-28 Oct. 2008. - P. 183-186. ↑
- C876.** Cumana J. Advanced Modeling of MISHFET Devices and their Performance in Current-Mode Class-D Power Amplifiers. / Cumana J., Lautensack C., Eickelkamp M., Goliasch J., Nocolak A., Vescan A., Jansen R.H. // 2008. EuMIC 2008. European Microwave Integrated Circuit Conference. - Amsterdam, 27-28 Oct. 2008. - P. 179-182. ↑
- C877.** Wan-Cheng Tsai. Structural and electrical characteristics of lanthanum oxide gate dielectric film on GaAs pHEMT technology. / Wan-Cheng Tsai, Chao-Hung Chen, Hsien-Chin Chiu, Fu J.S. // 2008. EDSSC 2008. IEEE International Conference on Electron Devices and Solid-State Circuits. - Hong Kong, 8-10 Dec. 2008. - P. 1-4. ↑
- C878.** Da-Wei Lin. A low insertion loss GaAs pHEMT switch utilizing highly n⁺-doping AlAs etching stop layer design. / Da-Wei Lin, Feng-Tso Chien, Chih-Wei Yang, Hsien-Chin Chiu. // 2008. EDSSC 2008. IEEE International Conference on Electron Devices and Solid-State Circuits. - Hong Kong, 8-10 Dec. 2008. - P. 1-4. ↑

- C879.** Parvesh. Analytical approach for high temperature analysis of AlGaIn/GaN HEMT. / Parvesh, kaur R., Pandey S., Halder S., Gupta M., Gupta R.S. // 2008. MICROWAVE 2008. International Conference on Recent Advances in Microwave Theory and Applications. - Jaipur, 21-24 Nov. 2008. - P. 725-728. ↑
- C880.** King-Yuen Wong. Temperature dependence of AlGaIn/GaN HEMT-compatible lateral field effect rectifier. / King-Yuen Wong, Wanjun Chen, Wei Huang, Chen K.J. // 2008. EDSSC 2008. IEEE International Conference on Electron Devices and Solid-State Circuits. - Hong Kong, 8-10 Dec. 2008. - P. 1-4. ↑
- C881.** Hsin-Shun Huang. High sensitivity pH sensor using Al_xGa_{1-x}N/GaN HEMT heterostructure design. / Hsin-Shun Huang, Chao-Wei Lin, Hsien-Chin Chiu. // 2008. EDSSC 2008. IEEE International Conference on Electron Devices and Solid-State Circuits. - Hong Kong, 8-10 Dec. 2008. - P. 1-4. ↑
- C882.** Napijalo V. 24 GHz LTCC Amplifier Using Packaged HEMTs. / Napijalo V., Cojocaru V., Yokoyama T. // 2008. EuMC 2008. 38th European Microwave Conference. - Amsterdam, 27-31 Oct. 2008. - P. 1489-1492. ↑
- C883.** Takahashi H. 120-GHz-band Low-noise Amplifier with 14-ps Group-delay Variation for 10-Gbit/s Data Transmission. / Takahashi H., Kosugi T., Hirata A., Murata K., Kukutsu N. // 2008. EuMC 2008. 38th European Microwave Conference. - Amsterdam, 27-31 Oct. 2008. - P. 1457-1460. ↑
- C884.** Scappaviva F. 10 Watt high efficiency GaAs MMIC power amplifier for space applications. / Scappaviva F., Cignani R., Florian C., Vannini G., Filicori F., Feudale M. // 2008. EuWiT 2008. European Conference on Wireless Technology. - Amsterdam, 27-28 Oct. 2008. - P. 238-241. ↑
- C885.** Koch S. A Four-Antenna Transceiver MIMIC for 60 GHz Wireless Multimedia Applications. / Koch S., Kallfass I., Leuther A., Schlechtweg M., Saito S., Uno M. // 2008. EuMC 2008. 38th European Microwave Conference. - Amsterdam, 27-31 Oct. 2008. - P. 1529-1532. ↑
- C886.** Kumar S.P. RF performance investigation of DMG AlGaIn/GaN high electron mobility transistor. / Kumar S.P., Agrawal A., Chaujar R., Gupta M., Gupta R.S. // 2008. MICROWAVE 2008. International Conference on Recent Advances in Microwave Theory and Applications. - Jaipur, 21-24 Nov. 2008. - P. 306-308. ↑
- C887.** Muthukrishnan S. A novel on-chip protection circuit for RFICs implemented in D-mode pHEMT technology. / Muthukrishnan S., Iversen C., Peachey N. // 2007. EOS/ESD 29th Electrical Overstress/Electrostatic Discharge Symposium. - Anaheim, CA, 16-21 Sept. 2007. - P. 4A.3-1-4A.3-7-1. ↑
- C888.** Chou Y.C. Reliability Evaluation of 0.1 μm AlSb/InAs HEMT Low Noise Amplifiers for Ultralow-Power Applications. / Chou Y.C., Leung D.L., Luo W.B., Yang J.M., Lin C.H., Lange M.D., Kan Q.W., Farkas D.S., Boos J.B., Bennett B.R., Gutierrez A.L., Eng D.C., Wojtowicz M., Oki A., Block T. // 2007. [Reliability of Compound Semiconductors Digest] ROCS Workshop. - Portland, OR, 14-14 Oct. 2007. - P. 43-46. ↑
- C889.** Chen S.C. Reliability Study of 0.15μm MHEMT with V_{ds} 3V Bias for Amplifier Application. / Chen S.C., Chou H.C., Chou F., Hsieh I., Tu D.W., Wang Y.C., Wu C.S., Nelson S.R. // 2007. [Reliability of Compound Semiconductors Digest] ROCS Workshop. - Portland, OR, 14-14 Oct. 2007. - P. 47-63. ↑
- C890.** Lai J.B. A Fully On-Chip, Single-Ended S-Band Image Reject Mixer for High Dynamic Range Applications. / Lai J.B., Christodoulou C.G. // 2007. CSIC 2007. IEEE Compound Semiconductor Integrated Circuit Symposium. - Portland, OR, 14-17 Oct. 2007. - P. 1-4. ↑
- C891.** Yunchuan Guo. A Support Vector Machine Method for Electrothermal Modeling of Power FETs. / Yunchuan Guo, Yuehang Xu, Lei Wang, Ruimin Xu. // 2007 International Symposium on Microwave, Antenna, Propagation and EMC Technologies for Wireless Communications. - Hangzhou, 16-17 Aug. 2007. - P. 1387-1389. ↑
- C892.** Khmyrova I. Plasma effects in HEMT-like structures: Equivalent circuit model and simulation. 2007. KJMW 2007. Korea-Japan Microwave Conference. - Okinawa, 15-16 Nov. 2007. - P. 197-200. ↑
- C893.** Colantonio P. Linearity and Efficiency Optimisation in Microwave Power Amplifier Design. / Colantonio P., Giannini F., Limiti E., Nanni A., Camarchia V., Teppati V., Pirola M. // 2007 European Conference on Wireless Technologies. - Munich, 8-10 Oct. 2007. - P. 363-366. ↑
- C894.** Chin-Leong Lim. 0.5 W High Linearity Power Amplifier for Broadband Wireless (3.3 ~ 3.9 GHz). 2007. KJMW 2007. Korea-Japan Microwave Conference. - Okinawa, 15-16 Nov. 2007. - P. 9-12. ↑

- C895.** Tazzoli A. ESD robustness of AlGaIn/GaN HEMT devices. / Tazzoli A., Danesin F., Zaroni E., Meneghesso G. // 2007. EOS/ESD 29th Electrical Overstress/Electrostatic Discharge Symposium. - Anaheim, CA, 16-21 Sept. 2007. - P. 4A.4-1-4A.4-9-1. ↑
- C896.** Tapfuh-Mouafo J. Low level and high linearity amplifiers in integrated technologies for satellite receivers: Technical issues of linearization techniques. / Tapfuh-Mouafo J., Jarry B., Campovechio M., Villemazet J.F., Cazaux J.L. // 2007. PRIME 2007. Ph.D. Research in Microelectronics and Electronics Conference. - Bordeaux, 2-5 July 2007. - P. 153-156. ↑
- C897.** Farkas D.S. Demonstration of a 3-D GaAs HEMT Phase Shifter MMIC Utilizing a Five Layer BCB Process with Seven Metal Layers. / Farkas D.S., Uyeda J., Wang J., Luo W.B., Elmadjian R., Eaves D., Luo K., Lai R., Barsky M., Wojtowicz M., Oki A. // 2007. CSIC 2007. IEEE Compound Semiconductor Integrated Circuit Symposium. - Portland, OR, 14-17 Oct. 2007. - P. 1-3. ↑
- C898.** Eliza S.A. Detection of Photosystem I Reaction Centers using Chemically Derivatized High Electron Mobility Transistor. / Eliza S.A., Islam S.K., Lee I., Greenbaum E., Ericson M.N., Khan M.A. // 2007 IEEE Sensors. - Atlanta, GA, 28-31 Oct. 2007. - P. 1456-1459. ↑
- C899.** Ma B.Y. Ultra-Wideband Ultra-Low-DC-Power High Gain Differential-Input Low Noise Amplifier MMIC Using InAs/AlSb HEMT. / Ma B.Y., Bergman J., Chen P.S., Hacker J.B., Sullivan G., Brar B. // 2007. CSIC 2007. IEEE Compound Semiconductor Integrated Circuit Symposium. - Portland, OR, 14-17 Oct. 2007. - P. 1-4. ↑
- C900.** Torres J. Tunable plasma wave resonant detection of optical beating in high electron mobility transistor. / Torres J., Nouvel P., Chusseau L., Teppe F., Shchepetov A., Bollaert S. // 2007 and the International Quantum Electronics Conference. CLEOE-IQEC 2007. European Conference on Lasers and Electro-Optics. - Munich, 17-22 June 2007. - P. 1. ↑
- C901.** Tessmann A. Metamorphic HEMT Amplifier Circuits for Use in a High Resolution 210 GHz Radar. / Tessmann A., Leuther A., Massler H., Kuri M., Riessle M., Zink M., Sommer R., Wahlen A., Essen H. // 2007. CSIC 2007. IEEE Compound Semiconductor Integrated Circuit Symposium. - Portland, OR, 14-17 Oct. 2007. - P. 1-4. ↑
- C902.** {no data available}. 2007 ROCS Workshop. 2007.[Reliability of Compound Semiconductors Digest] ROCS Workshop. - Portland, OR, 14-14 Oct. 2007. - P. i. ↑
- C903.** Kharabi F. A Classic Nonlinear FET Model for GaN HEMT Devices. / Kharabi F., Poulton M.J., Halchin D., Green D. // 2007. CSIC 2007. IEEE Compound Semiconductor Integrated Circuit Symposium. - Portland, OR, 14-17 Oct. 2007. - P. 1-4. ↑
- C904.** Li-Hsien Huang. Investigation of AlGaIn/GaN metal-oxide-semiconductor high electron mobility transistors using Photoelectrochemical Oxidation Method. / Li-Hsien Huang, Shu-Hao Yeh, Ching-Ting Lee, Haipeng Tang, Bardwell J., Webb J.B. // 2007. CLEO/Pacific Rim 2007. Conference on Lasers and Electro-Optics-Pacific Rim. - Seoul, 26-31 Aug. 2007. - P. 1-2. ↑
- C905.** Shih S.E. Broadband GaN Dual-Gate HEMT Low Noise Amplifier. / Shih S.E., Deal W.R., Sutton W.E., Chen Y.C., Smorchkova I., Heying B., Wojtowicz M., Siddiqui M. // 2007. CSIC 2007. IEEE Compound Semiconductor Integrated Circuit Symposium. - Portland, OR, 14-17 Oct. 2007. - P. 1-4. ↑
- C906.** Hamada D.J.M. Wafer-level Accelerated Lifetesting of Individual Devices. / Hamada D.J.M., Roesch W.J. // 2007.[Reliability of Compound Semiconductors Digest] ROCS Workshop. - Portland, OR, 14-14 Oct. 2007. - P. 21-30. ↑
- C907.** Lin C.H. 0.1 um n+-InAs-AlSb-InAs HEMT MMIC Technology for Phased-Array Applications. / Lin C.H., Chou Y.C., Lange M.D., Yang J.M., Nishimoto M.Y., Lee J., Nam P.S., Boos J.B., Bennett B.R., Papanicolaou N.A., Tsai R.S., Gutierrez A.L., Barsky M.E., Chin T.P., Wojtowicz M., Lai R., Oki A.K. // 2007. CSIC 2007. IEEE Compound Semiconductor Integrated Circuit Symposium. - Portland, OR, 14-17 Oct. 2007. - P. 1-4. ↑
- C908.** Han Gil Bae. High-efficiency GaN class-E power amplifier with ecompact harmonic-suppression network. / Han Gil Bae, Negra R., Boumaiza S., Ghannouchi F.M. // 2007 European Conference on Wireless Technologies. - Munich, 8-10 Oct. 2007. - P. 375-378. ↑

- C909.** Malmkvist M. Characterization of insulated-gate versus schottky-gate InAs/AlSb HEMTs. / Malmkvist M., Lefebvre E., Borg M., Desplanque L., Wallart X., Dambrine G., Bollaert S., Grahn J. // 2007. EuMIC 2007. European Microwave Integrated Circuit Conference. - Munich, 8-10 Oct. 2007. - P. 24-27. ↑
- C910.** Torregrosa G. Large-Signal modeling of power GaN HEMTs including thermal effects. / Torregrosa G., Grajal J., Peroni M., Serino A., Nanni A., Cetronio A. // 2007. EuMIC 2007. European Microwave Integrated Circuit Conference. - Munich, 8-10 Oct. 2007. - P. 36-39. ↑
- C911.** Srinidhi E.R. Investigation of IMD3 in GaN HEMT based on extended volterra series analysis. / Srinidhi E.R., Kompa G. // 2007. EuMIC 2007. European Microwave Integrated Circuit Conference. - Munich, 8-10 Oct. 2007. - P. 52-55. ↑
- C912.** Murata H. Optically controllable millimeter-wave oscillator using InP-based HEMTs. / Murata H., Kobayashi N., Kosugi T., Enoki T., Okamura Y. // 2007 Asia Optical Fiber Communication and Optoelectronics Conference. - Shanghai, 17-19 Oct. 2007. - P. 66-68. ↑
- C913.** van Dijk R. Driver amplifier for 60 GHz communication systems. / van Dijk R., de Boer L., Megej A., Hoogland J., van Vliet F.E. // 2007. EuMIC 2007. European Microwave Integrated Circuit Conference. - Munich, 8-10 Oct. 2007. - P. 5-7. ↑
- C914.** Bollaert S. Benchmarking of low band gap III-V based-HEMTs and sub-100nm CMOS under low drain voltage regime. / Bollaert S., Desplanque L., Wallart X., Roelens Y., Malmkvist M., Borg M., Lefebvre E., Grahn J., Smith D., Dambrine G. // 2007. EuMIC 2007. European Microwave Integrated Circuit Conference. - Munich, 8-10 Oct. 2007. - P. 20-23. ↑
- C915.** Resca D. Scalable equivalent circuit PHEMT modelling using an EM-based parasitic network description. / Resca D., Santarelli A., Raffo A., Cignani R., Vannini G., Filicori F. // 2007. EuMIC 2007. European Microwave Integrated Circuit Conference. - Munich, 8-10 Oct. 2007. - P. 60-63. ↑
- C916.** Hoel V. AlGaIn/GaN HEMTs on epitaxies grown on composite substrate. / Hoel V., Boulay S., Gerard H., Rabaland V., Delos E., De Jaeger J.C., Di-Forte-Poisson M.A., Brylinski C., Lahreche H., Langer R., Bove P. // 2007. EuMIC 2007. European Microwave Integrated Circuit Conference. - Munich, 8-10 Oct. 2007. - P. 100-103. ↑
- C917.** Colantonio P. Simultaneous dual-band high efficiency harmonic tuned power amplifier in GaN technology. / Colantonio P., Giannini F., Giofre R., Piazzon L. // 2007. EuMIC 2007. European Microwave Integrated Circuit Conference. - Munich, 8-10 Oct. 2007. - P. 127-130. ↑
- C918.** Martin A. Design of GaN-based balanced cascode cells for wide-band distributed power amplifier. / Martin A., Reveyrand T., Campovecchio M., Aubry R., Piotrowicz S., Floriot D., Quere R. // 2007. EuMIC 2007. European Microwave Integrated Circuit Conference. - Munich, 8-10 Oct. 2007. - P. 154-157. ↑
- C919.** Rathmell J.G. Characterization and modeling of substrate trapping in HEMTs. / Rathmell J.G., Parker A.E. // 2007. EuMIC 2007. European Microwave Integrated Circuit Conference. - Munich, 8-10 Oct. 2007. - P. 64-67. ↑
- C920.** Di Giacomo V. Low-frequency dynamic drain current modeling in AlGaIn-GaN HEMTs. / Di Giacomo V., Santarelli A., Filicori F., Raffo A., Vannini G., Aubry R., Gaquiere C. // 2007. EuMIC 2007. European Microwave Integrated Circuit Conference. - Munich, 8-10 Oct. 2007. - P. 68-71. ↑
- C921.** Boulay S. AlGaIn/GaN HEMTs on (001) oriented silicon substrate based on 100nm SiN recessed gate technology for low cost device fabrication. / Boulay S., Touati S., Sar A., Hoel V., Gaquiere C., De Jacger J.C., Joblot S., Cordier Y., Semond F., Massies J. // 2007. EuMIC 2007. European Microwave Integrated Circuit Conference. - Munich, 8-10 Oct. 2007. - P. 96-99. ↑
- C922.** Billstrom N. Compact front-end filter banks for wideband multi-role AESA systems. / Billstrom N., Sandwall J. // 2007. EuRAD 2007. European Radar Conference. - Munich, 10-12 Oct. 2007. - P. 307-310. ↑
- C923.** Colantonio P. Linearity and efficiency optimisation in microwave power amplifier design. / Colantonio P., Giannini F., Limiti E., Nanni A., Camarchia V., Teppati V., Pirola M. // 2007. European Microwave Conference. - Munich, 9-12 Oct. 2007. - P. 1081-1084. ↑

- C924.** Han Gil Bae. High-efficiency GaN class-E power amplifier with compact harmonic-suppression network. / Han Gil Bae, Negra R., Boumaiza S., Ghannouchi F.M. // 2007. European Microwave Conference. - Munich, 9-12 Oct. 2007. - P. 1093-1096. ↑
- C925.** Junghwan Moon. GaN HEMT Based Doherty Amplifier for 3.5-GHz WiMAX Applications. / Junghwan Moon, Jangheon Kim, Ildu Kim, Young Yun Woo, Sungchul Hong, Han Seok Kim, Jong Sung Lee, Bumman Kim. // 2007 European Conference on Wireless Technologies. - Munich, 8-10 Oct. 2007. - P. 395-398. ↑
- C926.** Narahashi S. 2-GHz Band Cryogenically-Cooled GaN HEMT Amplifier for Mobile Base Station Receivers. / Narahashi S., Suzuki Y., Nojima T. // 2007 European Conference on Wireless Technologies. - Munich, 8-10 Oct. 2007. - P. 399-402. ↑
- C927.** Mazer S. GaAs monocycle pulse generator for UWB applications. / Mazer S., Rumelhard C., Algani C., Terre M., Deshours F. // 2007. EuRAD 2007. European Radar Conference. - Munich, 10-12 Oct. 2007. - P. 287-290. ↑
- C928.** Junghwan Moon. GaN HEMT based Doherty amplifier for 3.5-GHz WiMAX applications. / Junghwan Moon, Jangheon Kim, Ildu Kim, Young Yun Woo, Sungchul Hong, Han Seok Kim, Jong Sung Lee, Bumman Kim. // 2007. European Microwave Conference. - Munich, 9-12 Oct. 2007. - P. 1193-1196. ↑
- C929.** Sayed A. 5W highly linear GaN power amplifier with 3.4 GHz bandwidth. / Sayed A., Boeck G. // 2007. European Microwave Conference. - Munich, 9-12 Oct. 2007. - P. 1429-1432. ↑
- C930.** Flucke J. Improved design methodology for a 2 GHz class-E hybrid power amplifier using packaged GaN-HEMTs. / Flucke J., Meliani C., Schnieder F., Heinrich W. // 2007. European Microwave Conference. - Munich, 9-12 Oct. 2007. - P. 1437-1440. ↑
- C931.** Hohkawa K. P5I-1 Multiple States Switching Operation of AlGaIn /GaIn Layer Mode Device. / Hohkawa K., Koh K., Nishimura K., Shigekawa N. // 2007. IEEE Ultrasonics Symposium. - New York, NY, 28-31 Oct. 2007. - P. 2355-2358. ↑
- C932.** Narahashi S. 2-GHz band cryogenically-cooled GaN HEMT amplifier for mobile base station receivers. / Narahashi S., Suzuki Y., Nojima T. // 2007. European Microwave Conference. - Munich, 9-12 Oct. 2007. - P. 1197-1200. ↑
- C933.** van der Bent G. X-band phase shifting power amplifier MMIC for phased array transmit modules. / van der Bent G., van der Graaf M.W., van Vliet F.E. // 2007. European Microwave Conference. - Munich, 9-12 Oct. 2007. - P. 1201-1204. ↑
- C934.** de Hek A.P. A cost-effective high-power s-band 6-bit phase shifter with integrated LVCMOS control logic. / de Hek A.P., Rodenburg M., van Vliet F.E. // 2007. European Microwave Conference. - Munich, 9-12 Oct. 2007. - P. 1261-1264. ↑
- C935.** Stiebler W. Statistical Large-Signal Model Enabling Yield Optimization in High-Power Amplifier Design. / Stiebler W., Koliass P., Sanctuary J. // 2007. CSIC 2007. IEEE Compound Semiconductor Integrated Circuit Symposium. - Portland, OR, 14-17 Oct. 2007. - P. 1-4. ↑
- C936.** Rakov Yu.N. High Power Pseudomorphic HEMTs' with Doped Channel. / Rakov Yu.N., Toropov A.I., Mjakishev Yu.B., Zhuravlev K.S., Chibaev V.P. // 2007. CriMiCo 2007. 17th International Crimean Conference Microwave & Telecommunication Technology. - Crimea, 10-14 Sept. 2007. - P. 554-555. ↑
- C937.** Zhuravlev K.S. New IR Photodetector Based on GaN QWs' or QDs' Located in Barrier of AlGaIn/GaN HEMT Structure. / Zhuravlev K.S., Grinyaev S.N., Karavaev G.F., Tronc P. // 2007. CriMiCo 2007. 17th International Crimean Conference Microwave & Telecommunication Technology. - Crimea, 10-14 Sept. 2007. - P. 571-572. ↑
- C938.** Gromov D.V. Radiation Effects in Heterostructures on Gallium Arsenide. / Gromov D.V., Polevich S.A., Elesin V.V. // 2007. CriMiCo 2007. 17th International Crimean Conference Microwave & Telecommunication Technology. - Crimea, 10-14 Sept. 2007. - P. 657-658. ↑
- C939.** Mokerov V.G. X-band MMIC Low-Noise Amplifier Based on 0.15 μm GaAs PHEMT Technology. / Mokerov V.G., Gunter V.Ya., Arzhanov S.N., Fedorov Yu.V., Scherbakova M.Yu., Babak L.I., Barov A.A.,

Cherkashin M.V., Sheherman F.I. // 2007. CriMiCo 2007. 17th International Crimean Conference Microwave & Telecommunication Technology. - Crimea, 10-14 Sept. 2007. - P. 77-78. ↑

C940. Babak L.I. "Visual" Design of X-Band Two-Stage MMIC Low-Noise Amplifier. / Babak L.I., Cherkashin M.V., Sheherman F.I., Barov A.A. // 2007. CriMiCo 2007. 17th International Crimean Conference Microwave & Telecommunication Technology. - Crimea, 10-14 Sept. 2007. - P. 101-102. ↑

C941. Berejnova P.V. Heat Generation in High Power hemt's Size Estimashion. / Berejnova P.V., Lukashin V.M., Pashkovskii A.B. // 2007. CriMiCo 2007. 17th International Crimean Conference Microwave & Telecommunication Technology. - Crimea, 10-14 Sept. 2007. - P. 119-120. ↑

C942. Recht F. AlGaIn/GaN HEMTs with Large Angle Implanted Nonalloyed Ohmic Contacts. / Recht F., McCarthy L., Shen L., Poblentz C., Corrión A., Speck J.S., Mishra U.K. // 2007 65th Annual Device Research Conference. - Notre Dame, IN, 18-20 June 2007. - P. 37-38. ↑

C943. Kumar V. Self-Aligned AlGaIn/GaN High Electron Mobility Transistors. / Kumar V., Kim D.-H., Basu A., Adesida I. // 2007 65th Annual Device Research Conference. - Notre Dame, IN, 18-20 June 2007. - P. 39-40. ↑

C944. Kotani J. Analysis of lateral surface leakage in the vicinity of Schottky gates in AlGaIn/GaN HEMTs. / Kotani J., Tajima M., Hashizume T. // 2007 65th Annual Device Research Conference. - Notre Dame, IN, 18-20 June 2007. - P. 41-42. ↑

C945. Dumka D.C. AlGaIn/GaN HEMTs on Diamond Substrate. / Dumka D.C., Saunier P. // 2007 65th Annual Device Research Conference. - Notre Dame, IN, 18-20 June 2007. - P. 31-32. ↑

C946. Seoane N. Analysis of the impact of intrinsic parameter fluctuations in a 50 nm InP HEMT. / Seoane N., Garcia-Loureiro A., Kalna K., Asenov A. // 2007 Spanish Conference on Electron Devices. - Madrid, Jan. 31 2007-Feb. 2 2007. - P. 92-95. ↑

C947. Moon J.S. 10 W/mm and High PAE Field-plated AlGaIn/GaN HEMTs at Ka-band with n+GaIn Source Contact Ledge. / Moon J.S., Hashimoto P., Wong D., Hu M., Antcliffe M., McGuire C., Micovic M., Willadsen P., Chow D. // 2007 65th Annual Device Research Conference. - Notre Dame, IN, 18-20 June 2007. - P. 33-34. ↑

C948. Vitusevich S.A. Low-Noise Microwave Devices: AlGaIn/GaN High Electron Mobility Transistors and Oscillators. 2007. MSMW '07. The Sixth International Kharkov Symposium on Physics and Engineering of Microwaves, Millimeter and Submillimeter Waves and Workshop on Terahertz Technologies. - Kharkov, 25-30 June 2007. - Vol. 1. - P. 55-60. ↑

C949. Korolev A.M. Low-Noise pHEMT Amplifier Operating at Extra-Low Supply Voltage and Power. / Korolev A.M., Shulga V.M. // 2007. MSMW '07. The Sixth International Kharkov Symposium on Physics and Engineering of Microwaves, Millimeter and Submillimeter Waves and Workshop on Terahertz Technologies. - Kharkov, 25-30 June 2007. - Vol. 2. - P. 742-744. ↑

C950. Nomura T. Discrete and Half Bridge Module using GaN HFETs for High Temperature Applications more than 200°C. / Nomura T., Masuda M., Yoshida S., Yamate T., Sudo Y., Takeda J. // 2007. ISPSD '07. 19th International Symposium on Power Semiconductor Devices and IC's. - Jeju Island, 27-31 May 2007. - P. 117-120. ↑

C951. Perez S. InAlAs/InGaAs heterostructures for THz generation. / Perez S., Mateos J., Pardo D., Gonzalez T. // 2007 Spanish Conference on Electron Devices. - Madrid, Jan. 31 2007-Feb. 2 2007. - P. 127-130. ↑

C952. Gonzalez-Posada F. 2-DEG Characteristics Improvement by N₂-plasma exposure in GaN HEMT heterostructures. / Gonzalez-Posada F., Brana A.F., Romero D.L., Romero M.F., Jimenez A., Arranz A., Palacio C., Munoz E. // 2007 Spanish Conference on Electron Devices. - Madrid, Jan. 31 2007-Feb. 2 2007. - P. 154-157. ↑

C953. Nakajima A. Analysis of Drain Lag and Current Slump in GaN-Based HEMTs and MESFETs. / Nakajima A., Takayanagi H., Itagaki K., Horio K. // 2007. ISSSE '07. International Symposium on Signals, Systems and Electronics. - Montreal, Que., July 30 2007-Aug. 2 2007. - P. 193-196. ↑

C954. Yagi S. 1.8 kV AlGaIn/GaN HEMTs with High-k/Oxide/SiN MIS Structure. / Yagi S., Shimizu M.,

Okumura H., Ohashi H., Arai K., Yano Y., Akutsu N. // 2007. ISPSD '07. 19th International Symposium on Power Semiconductor Devices and IC's. - Jeju Island, 27-31 May 2007. - P. 261-264. ↑

C955. Hung C.W. Hydrogen Sensing Characteristics of a Pd/GaAs Semiconductor Transistor-Type Sensor. / Hung C.W., Chen H.I., Guo D.F., Tsa J.H., Cheng S.Y., Tsai Y.Y., Chen T.P., Liu W.C. // 2007. TRANSDUCERS 2007. International Solid-State Sensors, Actuators and Microsystems Conference. - Lyon, 10-14 June 2007. - P. 2043-2046. ↑

C956. Guangyi Xi. Studies on Uniformity of MOVPE-Grown AlGaIn/GaN HEMT Structures by Spectroscopic Ellipsometry. / Guangyi Xi, Yi Luo, Lai Wang, Hongtao Li, Yang Jiang, Dong Chen, Wei Zhao, Yanjun Han, Zhibiao Hao. // 2007. i-NOW '07. International Nano-Optoelectronics Workshop. - Beijing, July 29 2007-Aug. 11 2007. - P. 254-255. ↑

C957. Min-Woo Ha. Hot-Carrier-Stress-Induced Degradation of 1 kV AlGaIn/GaN HEMTs by Employing SiO₂ Passivation. / Min-Woo Ha, Young-Hwan Choi, Jiyong Lim, Joong-Hyun Park, Soo-Seong Kim, Chong-Man Yun, Min-Koo Han. // 2007. ISPSD '07. 19th International Symposium on Power Semiconductor Devices and IC's. - Jeju Island, 27-31 May 2007. - P. 129-132. ↑

C958. Niiyama Y. Induction heating system operation by soft switching GaN heterojunction field effect transistors. 2007. ISPSD '07. 19th International Symposium on Power Semiconductor Devices and IC's. - Jeju Island, 27-31 May 2007. - P. 157-160. ↑

C959. Di Song. Normally-off AlGaIn/GaN Low-Density-Drain HEMTs (LDD-HEMT) with Enhanced Breakdown Voltage and Suppressed Current Collapse. / Di Song, Jie Liu, Zhiqun Cheng, Tang W.C.-W., Kei May Lau, Chen K.J. // 2007. ISPSD '07. 19th International Symposium on Power Semiconductor Devices and IC's. - Jeju Island, 27-31 May 2007. - P. 257-260. ↑

C960. Huq H.F. DC Characterization and Validation of the Improved Analytical Model of AlGaIn/GaN HEMT. / Huq H.F., Islam S.K. // 2007 IEEE Region 5 Technical Conference. - Fayetteville, AR, 20-22 April 2007. - P. 175-180. ↑

C961. Kikkawa T. High F_{max} GaN-HEMT with High Breakdown Voltage for Millimeter-Wave Applications. / Kikkawa T., Makiyama K., Imanishi K., Ohki T., Kanamura M., Okamoto N., Hara N., Joshin K. // 2007. CSIC 2007. IEEE Compound Semiconductor Integrated Circuit Symposium. - Portland, OR, USA, 14-17 Oct. 2007. - P. 1-4. ↑

C962. Rosker M.J. Recent Advances in GaN-on-SiC HEMT Reliability and Microwave Performance within the DARPA WBSG-RF Program. 2007. CSIC 2007. IEEE Compound Semiconductor Integrated Circuit Symposium. - Portland, OR, 14-17 Oct. 2007. - P. 1-4. ↑

C963. Vasallo B.G. Monte Carlo Comparison Between InAlAs/InGaAs Double-Gate and Standard HEMTs. / Vasallo B.G., Gonzalez T., Pardo D., Mateos J., Wichmann N., Bollaert S., Cappy A. // 2007 Spanish Conference on Electron Devices. - Madrid, Jan. 31 2007-Feb. 2 2007. - P. 80-83. ↑

C964. Suemitsu T. Novel Plasmon-Resonant Terahertz-Wave Emitter Using a Double-Decked HEMT Structure. / Suemitsu T., Meziani Y.M., Hosono Y., Hanabe M., Otsuji T., Sano E. // 2007 65th Annual Device Research Conference. - Notre Dame, IN, 18-20 June 2007. - P. 157-158. ↑

C965. del Alamo J.A. InGaAs CMOS: a "Beyond-the-Roadmap" Logic Technology?. / del Alamo J.A., Kim D.H. // 2007 65th Annual Device Research Conference. - Notre Dame, IN, 18-20 June 2007. - P. 201-202. ↑

C966. Deal W.R. Demonstration of a S-MMIC LNA with 16-dB Gain at 340-GHz. / Deal W.R., Mei X.B., Radisic V., Yoshida W., Liu P.H., Uyeda J., Barsky M., Gaier T., Fung A., Lai R. // 2007. CSIC 2007. IEEE Compound Semiconductor Integrated Circuit Symposium. - Portland, OR, 14-17 Oct. 2007. - P. 1-4. ↑

C967. Shih S.E. A W-Band 4-Bit Phase Shifter in Multilayer Scalable Array Systems. / Shih S.E., Duan D.W., Fordham O., Tornquist K., Zeng X., Chang-Chien P., Tsai R. // 2007. CSIC 2007. IEEE Compound Semiconductor Integrated Circuit Symposium. - Portland, OR, 14-17 Oct. 2007. - P. 1-4. ↑

C968. Bessemoulin A. GaAs PHEMT Power Amplifier MMIC with Integrated ESD Protection for Full SMD 38-GHz Radio Chipset. / Bessemoulin A., Mahon S.J., Harvey J.T., Richardson D. // 2007. CSIC 2007. IEEE Compound Semiconductor Integrated Circuit Symposium. - Portland, OR, 14-17 Oct. 2007. - P. 1-4. ↑

- C969.** Krishnamurthy K. A 250W S-Band GaN HEMT Amplifier. / Krishnamurthy K., Poulton M.J., Martin J., Vetry R., Brown J.D., Shealy B. // 2007. CSIC 2007. IEEE Compound Semiconductor Integrated Circuit Symposium. - Portland, OR, 14-17 Oct. 2007. - P. 1-4. ↑
- C970.** Sano H. A 40W GaN HEMT Doherty Power Amplifier with 48% Efficiency for WiMAX Applications. / Sano H., Ui N., Sano S. // 2007. CSIC 2007. IEEE Compound Semiconductor Integrated Circuit Symposium. - Portland, OR, 14-17 Oct. 2007. - P. 1-4. ↑
- C971.** Kallfass I. A 210 GHz, Subharmonically-Pumped Active FET Mixer MMIC for Radar Imaging Applications. / Kallfass I., Massler H., Leuther A. // 2007. CSIC 2007. IEEE Compound Semiconductor Integrated Circuit Symposium. - Portland, OR, 14-17 Oct. 2007. - P. 1-4. ↑
- C972.** Tipirneni N. AlGaIn/GaN Bidirectional Power Switch. / Tipirneni N., Wang B., Monti A., Simin G. // 2007 65th Annual Device Research Conference. - Notre Dame, IN, 18-20 June 2007. - P. 97-98. ↑
- C973.** Zhao X. Schottky Drain AlGaIn/GaN HEMTs for mm-wave Applications. / Zhao X., Chung J.W., Tang H., Palacios T. // 2007 65th Annual Device Research Conference. - Notre Dame, IN, 18-20 June 2007. - P. 107-108. ↑
- C974.** Medjdoub F. Barrier layer downscaling of InAlN/GaN HEMTs. / Medjdoub F., Carlin J.-F., Gonschorek M., Feltin E., Py M.A., Knez M., Troadec D., Gaquiere C., Chuvilin A., Kaiser U., Grandjean N., Kohn E. // 2007 65th Annual Device Research Conference. - Notre Dame, IN, 18-20 June 2007. - P. 109-110. ↑
- C975.** Pala N. Drain-to-Gate Field Engineering for Improved Frequency Response of GaN-based HEMTs. / Pala N., Yang Z., Koudymov A., Hu X., Deng J., Gaska R., Simin G., Shur M.S. // 2007 65th Annual Device Research Conference. - Notre Dame, IN, 18-20 June 2007. - P. 43-44. ↑
- C976.** Horio K. Effects of Source Access Resistance on Gate lag in AlGaIn/GaN HEMTs and Current Slump Behavior. / Horio K., Nakajima A., Itagaki K. // 2007 65th Annual Device Research Conference. - Notre Dame, IN, 18-20 June 2007. - P. 67-68. ↑
- C977.** Liu J. Microwave Noise Characterization of Enhancement-Mode AlGaIn/GaN/InGaIn/GaN Double-Heterojunction HEMTs. / Liu J., Song D., Cheng Z., Tang W.C.-W., Lau K.M., Chen K.J. // 2007 65th Annual Device Research Conference. - Notre Dame, IN, 18-20 June 2007. - P. 77-78. ↑
- C978.** Mehrotra V. Electric-Field Dependence of Junction Temperature in GaN HEMTs. / Mehrotra V., Boutros K., Brar B. // 2007 65th Annual Device Research Conference. - Notre Dame, IN, 18-20 June 2007. - P. 143-144. ↑
- C979.** Barsky M. Advanced InP and GaAs HEMT MMIC technologies for MMW commercial products. / Barsky M., Biedenbender M., Xiaobing Mei, Po-Hsin Liu, Lai R. // 2007 65th Annual Device Research Conference. - Notre Dame, IN, 18-20 June 2007. - P. 147-148. ↑
- C980.** Singiseti U. Ultra-Low Resistance Ohmic Contacts to InGaAs/InP. / Singiseti U., Crook A.M., Lind E., Zimmerman J.D., Wistey M.A., Gossard A.C., Rodwell M.J.W. // 2007 65th Annual Device Research Conference. - Notre Dame, IN, 18-20 June 2007. - P. 149-150. ↑
- C981.** Chung J.W. Estimation of Trap Density in AlGaIn/GaN HEMTs from Subthreshold Slope Study. / Chung J.W., Zhao X., Palacios T. // 2007 65th Annual Device Research Conference. - Notre Dame, IN, 18-20 June 2007. - P. 111-112. ↑
- C982.** Rongming Chu. Surface Treatment for Leakage Reduction in AlGaIn/GaN HEMTs. / Rongming Chu, Likun Shen, Fichtenbaum N., Keller S., Corron A., Poblencz C., Speck J., Mishra U. // 2007 65th Annual Device Research Conference. - Notre Dame, IN, 18-20 June 2007. - P. 127-128. ↑
- C983.** Pei Y. AlGaIn/GaNHEMT with High PAE and Breakdown Voltage Grown by Ammonia MBE. / Pei Y., Suh C., Chu R., Recht F., Shen L., Corron A., Poblencz C., Speck J., Mishra U.K. // 2007 65th Annual Device Research Conference. - Notre Dame, IN, 18-20 June 2007. - P. 129-130. ↑
- C984.** Daipuria R. Silicon nitride films for passivation of pHEMT based MMIC. / Daipuria R., Dayal S., Laishram R., Mahajan S., Rawal D.S., Bhat K.M., Sharma H.S., Sehgal B.K., Muralidharan R. // 2007. IWPSD 2007. International Workshop on Physics of Semiconductor Devices. - Mumbai, 16-20 Dec. 2007. - P. 431-434. ↑



C985. Mahadeva Bhat K. Study of selective gate recess etching of InGaAs/InAlAs/InGaAs metamorphic HEMT structures using succinic acid based etchant. / Mahadeva Bhat K., Sai Saravanan G., Vyas H.P., Muralidharan R., Dhamodaran S., Jain M.K., Subrahmanyam A. // 2007. IWPSD 2007. International Workshop on Physics of Semiconductor Devices. - Mumbai, 16-20 Dec. 2007. - P. 469-471.

C986. Basak M. Modeling of a radio frequency transimpedance amplifier based on a δ -doped AlInAs-GaInAs HEMT and its performance optimization. / Basak M., Biswas A., Basu P.K. // 2007. IWPSD 2007. International Workshop on Physics of Semiconductor Devices. - Mumbai, 16-20 Dec. 2007. - P. 507-510.

C987. Kohn E. InAlN-A new barrier material for GaN-based HEMTs. / Kohn E., Medjdoub F. // 2007. IWPSD 2007. International Workshop on Physics of Semiconductor Devices. - Mumbai, 16-20 Dec. 2007. - P. 311-316.



C988. Arulkumaran S. Surface passivation effects in AlGaIn/GaN HEMTs on high-resistivity Si substrate. 2007. IWPSD 2007. International Workshop on Physics of Semiconductor Devices. - Mumbai, 16-20 Dec. 2007. - P. 317-322.

C989. Kumar S.P. 3-dimensional analytical modeling and simulation of fully depleted AlGaIn/GaN modulation doped field effect transistor. / Kumar S.P., Agrawal A., Chaujar R., Kabra S., Gupta M., Gupta R.S. // 2007. IWPSD 2007. International Workshop on Physics of Semiconductor Devices. - Mumbai, 16-20 Dec. 2007. - P. 373-376.

C990. Zmuidzinas Jonas. Superconducting microresonators for detection and multiplexing. 2007 and the 2007 15th International Conference on Terahertz Electronics. IRMMW-THz. Joint 32nd International Conference on Infrared and Millimeter Waves. - Cardiff, UK, 2-9 Sept. 2007. - P. 109.

C991. Meziani Y.M. Emission of terahertz radiation from an interdigitated grating gates high electron-mobility transistors. / Meziani Y.M., Otsuji T., Sano E. // 2007 and the 2007 15th International Conference on Terahertz Electronics. IRMMW-THz. Joint 32nd International Conference on Infrared and Millimeter Waves. - Cardiff, 2-9 Sept. 2007. - P. 466-467.

C992. Torres J. Room temperature amplification of optical-beating photoresponse in HEMTs. / Torres J., Nouvel P., Palermo C., Chusseau L., Varani L., Teppe F., Shchepetov A., Bollaert S. // 2007 and the 2007 15th International Conference on Terahertz Electronics. IRMMW-THz. Joint 32nd International Conference on Infrared and Millimeter Waves. - Cardiff, 2-9 Sept. 2007. - P. 738-739.

C993. Omura I. Gallium Nitride power HEMT for high switching frequency power electronics. / Omura I., Saito W., Domon T., Tsuda K. // 2007. IWPSD 2007. International Workshop on Physics of Semiconductor Devices. - Mumbai, 16-20 Dec. 2007. - P. 781-786.

C994. Cijvat E. A GaN HEMT power amplifier with variable gate bias for envelope and phase signals. / Cijvat E., Tom K., Faulkner M., Sjoland H. // 2007 Norchip. - Aalborg, 19-20 Nov. 2007. - P. 1-4.

C995. Richards P.L. Cosmic Microwave Background experiments-past, present and future. 2007 and the 2007 15th International Conference on Terahertz Electronics. IRMMW-THz. Joint 32nd International Conference on Infrared and Millimeter Waves. - Cardiff, 2-9 Sept. 2007. - P. 12-15.

C996. Pimenta M.N. Optical fibre CDMA for access and optical networks. / Pimenta M.N., Darwazeh I. // 2007 6th International Conference on Information, Communications & Signal Processing. - Singapore, 10-13 Dec. 2007. - P. 1-4.

C997. Adesida I. Advances in Gallium Nitride-based Electronics. / Adesida I., Kumar V. // 2007. EDSSC 2007. IEEE Conference on Electron Devices and Solid-State Circuits. - Tainan, 20-22 Dec. 2007. - P. 1-6.

C998. Ciou-Sheng He. A Novel Parameter Extraction Method for HEMT Models by Using Generic Algorithms. / Ciou-Sheng He, Wang-Yu Yang, Meng-Bi Cheng, Ke-Hua Su, Su-Jen Yu, Wei-Chou Hsu. // 2007. EDSSC 2007. IEEE Conference on Electron Devices and Solid-State Circuits. - Tainan, 20-22 Dec. 2007. - P. 241-245.



C999. Inoue A. MMIC technologies for MW and MMW applications. / Inoue A., Amasuga H., Watanabe S., Goto S., Oku T. // 2007. RFIT 007. IEEE International Workshop on Radio-Frequency Integration Technology. -

Rasa Sentosa Resort, 9-11 Dec. 2007. - P. 232-235. ↑

C1000. Luo B. Modeling of 0.15 μm InGaAs pHEMT up to 60 GHz. / Luo B., Guo Y.X., Wong S.Y., Ong L.C. // 2007. RFIT 007. IEEE International Workshop on Radio-Frequency Integration Technology. - Rasa Sentosa Resort, 9-11 Dec. 2007. - P. 286-289. ↑

C1001. Rizk M. Design and simulation of high gain PHEMT low noise amplifier (LNA). / Rizk M., Nasar M., Hafez A. // 2007. ICCES '07. International Conference on Computer Engineering & Systems. - Cairo, 27-29 Nov. 2007. - P. 253-257. ↑

C1002. Xie Chenggang. Development of GaN HEMT based High Power High Efficiency Distributed Power Amplifier for Military Applications. / Xie Chenggang, PAVIO Anthony. // 2007. MILCOM 2007. IEEE Military Communications Conference. - Orlando, FL, USA, 29-31 Oct. 2007. - P. 1-4. ↑

C1003. Kalavagunta A. Electrostatic mechanisms responsible for device degradation in AlGaIn/AlN/GaN HEMTs. / Kalavagunta A., Touboul A., Shen L., Schrimpf R.D., Reed R.A., Fleetwood D.M., Jain R.K., Mishra U.K. // 2007. RADECS 2007. 9th European Conference on Radiation and Its Effects on Components and Systems. - Deauville, 10-14 Sept. 2007. - P. 1-7. ↑

C1004. Muralidharan R. MMIC technology at Gallium Arsenide Enabling Technology Centre. 2007. IWPSD 2007. International Workshop on Physics of Semiconductor Devices. - Mumbai, 16-20 Dec. 2007. - P. 303-306. ↑

C1005. Chien-I Kuo. Evaluation of RF and Logic Performance for 80 nm InAs/InGaAs Composite Channel HEMTs Using Gate Sinking Technology. / Chien-I Kuo, Heng-Tung Hsu, Chia-Yuan Chang, Chang E.Y., Heng-Shou Hsu. // 2007. EDSSC 2007. IEEE Conference on Electron Devices and Solid-State Circuits. - Tainan, 20-22 Dec. 2007. - P. 255-258. ↑

C1006. Lee K.W. Analytical Study of the DC Characteristics on the InAlAs/InGaAs Metamorphic HEMT with Oxidized InGaAs Gate. / Lee K.W., Huang J.S., Lee F.M., Huang Y.S., Wang Y.H., Su S.C., Chao B.H., Chen C.C. // 2007. EDSSC 2007. IEEE Conference on Electron Devices and Solid-State Circuits. - Tainan, 20-22 Dec. 2007. - P. 259-262. ↑

C1007. Meziani Y.M. Generation of terahertz radiation from a new InGaP/InGaAs/GaAs Double Grating Gate HEMT Device. / Meziani Y.M., Hanabe M., Koizumi A., Ishibashi T., Uno T., Otsuji T., Sano E. // 2007. CLEO 2007. Conference on Lasers and Electro-Optics. - Baltimore, MD, 6-11 May 2007. - P. 1-2. ↑

C1008. Bumjin Kim. A High Power, High Efficiency Amplifier using GaN HEMT. / Bumjin Kim, Derickson D., Sun C. // 2007. APMC 2007. Asia-Pacific Microwave Conference. - Bangkok, 11-14 Dec. 2007. - P. 1-4. ↑

C1009. Inwon Suh. Negative input resistance and real-time active load-pull measurements of a 2.5GHz oscillator using a LSNA. / Inwon Suh, Seok Joo Doo, Roblin P., Xian Cui, Young Gi Kim, Strahler J., Vanden Bossche M., Rojas R., Hyo Dal Park. // 2007 69th ARFTG Conference. - Honolulu, HI, 8-8 June 2007. - P. 1-6. ↑

C1010. Ashok A. Monte Carlo simulation of GaN n+nn+ diode including intercarrier interactions. / Ashok A., Vasilevski D., Hartin O., Goodnick S.M. // 2007. IEEE-NANO 2007. 7th IEEE Conference on Nanotechnology. - Hong Kong, 2-5 Aug. 2007. - P. 338-341. ↑

C1011. Chia-Shih Cheng. A High Isolation 0.15 μm Depletion-Mode pHEMT SPDT Switch Using Field-Plate Technology. / Chia-Shih Cheng, Shao-Wei Lin, Chien-Cheng Wei, Hsien-Chin Chiu, Rong-Jyi Yang. // 2007. APMC 2007. Asia-Pacific Microwave Conference. - Bangkok, 11-14 Dec. 2007. - P. 1-4. ↑


C1012. Hokyun Ahn. Influence of Gate Head Dimensions on the Device performance of 0.12 μm PHEMT. / Hokyun Ahn, Jong-Won Lim, Hong-Gu Ji, Woo-Jin Chang, Jae-Kyoung Mun, Haecheon Kim. // 2007. APMC 2007. Asia-Pacific Microwave Conference. - Bangkok, 11-14 Dec. 2007. - P. 1-4. ↑


C1013. Heng-Tung Hsu. High Performance InAs-Channel HEMT for Low Voltage Millimeter Wave Applications. / Heng-Tung Hsu, Chia-Yuan Chang, Chang E.Y., Chien-I Kuo, Miyamoto Y. // 2007. APMC 2007. Asia-Pacific Microwave Conference. - Bangkok, 11-14 Dec. 2007. - P. 1-4. ↑


C1014. Vasu P.S. A MMIC control chipset for T/R modules-A SiP approach. 2007. AEMC 2007. IEEE Applied Electromagnetics Conference. - Kolkata, 19-20 Dec. 2007. - P. 1-4. ↑


- C1015.** Jarndal A. Large-Signal Model for AlGaIn/GaN HEMT for Designing High Power Amplifiers of Next Generation Wireless Communication Systems. / Jarndal A., Kompa G. // 2007. ICSPC 2007. IEEE International Conference on Signal Processing and Communications. - Dubai, 24-27 Nov. 2007. - P. 77-80. ↑
- C1016.** Basak Moumita. Analysis of a radio frequency transimpedance amplifier based on a δ -doped AlInAs-GaN HEMT and its performance optimization. / Basak Moumita, Biswas Abhijit, Basu P. K. // 2007. ICTES. IET-UK International Conference on Information and Communication Technology in Electrical Sciences (ICTES 2007). - Chennai, Tamilnadu, India, 20-22 Dec. 2007. - P. 879-883. ↑
- C1017.** Seong-Jin Yeon. Novel sloped etch process for 15nm InAlAs/InGaAs metamorphic HEMTs. / Seong-Jin Yeon, Myunghwan Park, Kwang-Seok Seo. // 2007. IEEE-NANO 2007. 7th IEEE Conference on Nanotechnology. - Hong Kong, 2-5 Aug. 2007. - P. 1152-1155. ↑
- C1018.** Hyungtae Kim. New NRZ-mode resonant tunneling bistable-to-monostable-to-bistable transition logic element operating up to 36 Gb/s. / Hyungtae Kim, Seongjin Yeon, Kwangseok Seo. // 2007. IEEE-NANO 2007. 7th IEEE Conference on Nanotechnology. - Hong Kong, 2-5 Aug. 2007. - P. 1288-1291. ↑
- C1019.** Osman M.N. Gain and cut-off frequency analysis of multiple-gated AlGaAs/InGaAs HEMTs. / Osman M.N., Zaiki Awang, Yaakob S., Yahya M.R., Mat A. // 2007. APACE 2007. Asia-Pacific Conference on Applied Electromagnetics. - Melaka, 4-6 Dec. 2007. - P. 1-4. ↑
- C1020.** Nakamura S. A design of multi-GHz continuous-time bandpass filters using 0.1- μ m HEMT technology. / Nakamura S., Ohmae U., Watanabe H., Waho T. // 2007. ECCTD 2007. 18th European Conference on Circuit Theory and Design. - Seville, 27-30 Aug. 2007. - P. 484-487. ↑
- C1021.** Heng-Tung Hsu. Accurate Performance Evaluation of HEMT Devices for High-Speed Logic Applications through Rigorous Device Modelling Technique. / Heng-Tung Hsu, Chia-Yuan Chang, Heng-Shou Hsu, Chang E.Y. // 2007. APMC 2007. Asia-Pacific Microwave Conference. - Bangkok, 11-14 Dec. 2007. - P. 1-4. ↑
- C1022.** Lautensack C. Modification of EEHEMT1 Model for Accurate Description of GaN HEMT Output Characteristics. / Lautensack C., Chalermwisutkul S., Jansen R.H. // 2007. APMC 2007. Asia-Pacific Microwave Conference. - Bangkok, 11-14 Dec. 2007. - P. 1-4. ↑
- C1023.** Ryzhii M. Detector of modulated terahertz radiation based on HEMT with mechanically floating gate. / Ryzhii M., Ryzhii V., Yabo Hu, Shur M.S. // 2007 and the 2007 15th International Conference on Terahertz Electronics. IRMMW-THz. Joint 32nd International Conference on Infrared and Millimeter Waves. - Cardiff, 2-9 Sept. 2007. - P. 754-755. ↑
- C1024.** Aflaki P. Compact Load-Coupling Network for Microwave Current Mode Class-D Power Amplifiers. / Aflaki P., Negra R., Ghannouchi F.M. // 2007. CAS 2007. International Semiconductor Conference. - Sinaia, Oct. 15 2007-Sept. 17 2007. - Vol. 1. - P. 233-236. ↑
- C1025.** Amza C. Ensemble Monte Carlo Simulation of a Pseudomorphic HEMT Structure. / Amza C., Cimpian I., Profirescu M.D. // 2007. CAS 2007. International Semiconductor Conference. - Sinaia, Oct. 15 2007-Sept. 17 2007. - Vol. 2. - P. 419-422. ↑
- C1026.** Kumar S.P. Analytical Modeling and Simulation of Potential and Electric Field Distribution in Dual Material Gate HEMT For Suppressed Short Channel Effects. / Kumar S.P., Chaujar R., Gupta M., Gupta R.S., Agrawal A. // 2007. APMC 2007. Asia-Pacific Microwave Conference. - Bangkok, 11-14 Dec. 2007. - P. 1-4. ↑
- C1027.** Janne-Wha Wu. PHEMT SP6T ICs for Quadband GSM Handset Applications. / Janne-Wha Wu, Sheng-Wen Chen, Chiun-Chau Huang, Ching-Wen Tang, Jeng-Hung Li, Chia-Wei Tsai. // 2007. APMC 2007. Asia-Pacific Microwave Conference. - Bangkok, 11-14 Dec. 2007. - P. 1-4. ↑
- C1028.** Osman M.N. Kink Effect Phenomenon in I-V Characteristic of Multiple-Gated AlGaAs/InGaAs HEMTs Device. / Osman M.N., Awang Z., Rahim A.I.A., Yaakob S., Yahya M.R., Mat A.F.A. // 2007. APMC 2007. Asia-Pacific Microwave Conference. - Bangkok, 11-14 Dec. 2007. - P. 1-4. ↑
- C1029.** Bhakuni M. A Low Current Fully Integrated Front End Module On GaAs E/D p-HEMT For 2.4 GHz Applications. / Bhakuni M., Gupta D., Vaidya R. // 2007. APMC 2007. Asia-Pacific Microwave Conference. - ↑


Bangkok, 11-14 Dec. 2007. - P. 1-4. 


C1030. Kyungtae Oh. Characterization of Electrical Memory Effects in Power Amplifier using Multi-tone Measurement. / Kyungtae Oh, Youngsup Lee, Hyunchul Ku, Dongsu Kim, Chan Sei Yoo, Woo Sung Lee. // 2007. APMC 2007. Asia-Pacific Microwave Conference. - Bangkok, 11-14 Dec. 2007. - P. 1-4. 


C1031. Seon-eui Hong. Preamplifier for fiber-optic Millimeter wave Wireless LAN. / Seon-eui Hong, Young-jun Chong, Jeong-won Lim, Dong-young Kim, Haecheon Kim, Hyun-kyu Yu. // 2007. APMC 2007. Asia-Pacific Microwave Conference. - Bangkok, 11-14 Dec. 2007. - P. 1-4. 


C1032. Zirath H. Newly developed chip sets for 60 GHz radio communication systems. / Zirath H., Gunnarsson S.E., Ferndahl M., Kozhuharov R., Karnfelt C. // 2007. RFIT 007. IEEE International Workshop on Radio-Frequency Integration Technology. - Rasa Sentosa Resort, 9-11 Dec. 2007. - P. 102-106. 


C1033. Flucke J. Improved design methodology for a 2 GHz class-E hybrid power amplifier using packaged GaN-HEMTs. / Flucke J., Meliani C., Schnieder F., Heinrich W. // 2007. EuMIC 2007. European Microwave Integrated Circuit Conference. - Munich, 8-10 Oct. 2007. - P. 639-642. 


C1034. Congwen Yi. Reliability of Enhancement-mode AlGaIn/GaN HEMTs Fabricated by Fluorine Plasma Treatment. / Congwen Yi, Ruonan Wang, Wei Huang, Tang W.C.-W., Lau K.M., Chen K.J. // 2007. IEDM 2007. IEEE International Electron Devices Meeting. - Washington, DC, 10-12 Dec. 2007. - P. 389-392. 


C1035. Villanueva A. Drain Corrosion in RF Power GaAs PHEMTs. / Villanueva A., del Alamo J.A., Hisaka T., Ishida T. // 2007. IEDM 2007. IEEE International Electron Devices Meeting. - Washington, DC, 10-12 Dec. 2007. - P. 393-396. 


C1036. Yu-Cheng Hsu. Single-chip RF Front-end MMIC using InGaAs E/DpHEMT for 3.5 GHz WiMAX applications. / Yu-Cheng Hsu, Ping-Hsun Wu, Cheng-Chung Chen, Jian-Yu Li, Sheng-Feng Lee, Wu-Jing Ho, Cheng-Kuo Lin. // 2007. EuMIC 2007. European Microwave Integrated Circuit Conference. - Munich, 8-10 Oct. 2007. - P. 419-422. 


C1037. de Boer L. Integrated 48 GHz LO chain for 60 GHz communication systems. / de Boer L., van Dijk R., Megej A., Hoogland J., van Vliet F.E. // 2007. EuMIC 2007. European Microwave Integrated Circuit Conference. - Munich, 8-10 Oct. 2007. - P. 471-473. 


C1038. Sayed A. 5W Highly Linear GaN power amplifier with 3.4 GHz bandwidth. / Sayed A., Boeck G. // 2007. EuMIC 2007. European Microwave Integrated Circuit Conference. - Munich, 8-10 Oct. 2007. - P. 631-634. 

C1039. Lai R. Sub 50 nm InP HEMT Device with Fmax Greater than 1 THz. / Lai R., Mei X.B., Deal W.R., Yoshida W., Kim Y.M., Liu P.H., Lee J., Uyeda J., Radisic V., Lange M., Gaier T., Samoska L., Fung A. // 2007. IEDM 2007. IEEE International Electron Devices Meeting. - Washington, DC, 10-12 Dec. 2007. - P. 609-611. 

C1040. Seong-Jin Yeon. 610 GHz InAlAs/In_{0.75}GaAs Metamorphic HEMTs with an Ultra-Short 15-nm-Gate. / Seong-Jin Yeon, Myonghwan Park, JeHyuk Choi, Kwangseok Seo. // 2007. IEDM 2007. IEEE International Electron Devices Meeting. - Washington, DC, 10-12 Dec. 2007. - P. 613-616. 

C1041. Chou C. 0.1 μ m In_{0.2}Al_{0.8}Sb-InAs HEMT low-noise amplifiers for ultralow-power applications. / Chou C., Lange M.D., Bennett B.R., Boos J.B., Yang J.M., Papanicolaou N.A., Lin C.H., Lee L.J., Nam P.S., Gutierrez A.L., Farkas D.S., Tsai R.S., Wojtowicz M., Chin T.P., Oki A.K. // 2007. IEDM 2007. IEEE International Electron Devices Meeting. - Washington, DC, 10-12 Dec. 2007. - P. 617-620. 

C1042. Nanjo T. Remarkable Breakdown Voltage Enhancement in AlGaIn Channel HEMTs. / Nanjo T., Takeuchi M., Suita M., Abe Y., Oishi T., Tokuda Y., Aoyagi Y. // 2007. IEDM 2007. IEEE International Electron Devices Meeting. - Washington, DC, 10-12 Dec. 2007. - P. 397-400. 

C1043. Meneghesso G. Characterisation of AlGaIn/GaN HEMT epitaxy and devices on composite substrates. / Meneghesso G., Ongaro C., Zanon E., Brylinski C., di Forte-Poisson M.A., Hoel V., de Jaeger J.C., Langer R., Lahreche H., Bove P., Thorpe J. // 2007. IEDM 2007. IEEE International Electron Devices Meeting. - Washington, DC, 10-12 Dec. 2007. - P. 401-404. 

C1044. Wu Y.-F. High-voltage Millimeter-Wave GaN HEMTs with 13.7 W/mm Power Density. / Wu Y.-F., Moore M., Abrahamsen A., Jacob-Mitos M., Parikh P., Heikman S., Burk A. // 2007. IEDM 2007. IEEE

International Electron Devices Meeting. - Washington, DC, 10-12 Dec. 2007. - P. 405-407. ↑

C1045. Yamamoto T. A 9.5-10.5GHz 60W AlGaIn/GaN HEMT for X-band high power application. / Yamamoto T., Mitani E., Inoue K., Nishi M., Sano S. // 2007. EuMIC 2007. European Microwave Integrated Circuit Conference. - Munich, 8-10 Oct. 2007. - P. 173-175. ↑

C1046. Mitani E. A kW-class AlGaIn/GaN HEMT pallet amplifier for S-band high power application. / Mitani E., Aojima M., Sano S. // 2007. EuMIC 2007. European Microwave Integrated Circuit Conference. - Munich, 8-10 Oct. 2007. - P. 176-179. ↑

C1047. Colantonio P. Linearity and efficiency optimisation in microwave power amplifier design. / Colantonio P., Giannini F., Limiti E., Nanni A., Camarchia V., Teppati V., Pirola M. // 2007. EuMIC 2007. European Microwave Integrated Circuit Conference. - Munich, 8-10 Oct. 2007. - P. 283-286. ↑

C1048. Tangsheng Chen. X-Band 11W AlGaIn/GaN HEMT power MMICs. / Tangsheng Chen, Bin Zhang, Gang Jiao, Chunjiang Ren, Chen Chen, Kai Shao, Naibin Yang. // 2007. EuMIC 2007. European Microwave Integrated Circuit Conference. - Munich, 8-10 Oct. 2007. - P. 162-164. ↑

C1049. Roff C. Optimising AlGaIn/GaN HFET designs for high efficiency. / Roff C., Sheikh A., Benedikt J., Tasker P.J., Hilton K.P., Maclean J.O., Hayes D.G., Uren M.J., Martin T. // 2007. EuMIC 2007. European Microwave Integrated Circuit Conference. - Munich, 8-10 Oct. 2007. - P. 165-168. ↑

C1050. Takagi K. Ku-band AlGaIn/GaN HEMT with over 30W. / Takagi K., Kashiwabara Y., Masuda K., Matsushita K., Sakurai H., Onodera K., Kawasaki H., Takada Y., Tsuda K. // 2007. EuMIC 2007. European Microwave Integrated Circuit Conference. - Munich, 8-10 Oct. 2007. - P. 169-172. ↑

C1051. Narahashi S. 2-GHz band cryogenically-cooled GaN HEMT amplifier for mobile base station receivers. / Narahashi S., Suzuki Y., Nojima T. // 2007. EuMIC 2007. European Microwave Integrated Circuit Conference. - Munich, 8-10 Oct. 2007. - P. 399-402. ↑

C1052. van der Bent G. X-band Phase Shifting Power Amplifier MMIC for phased array transmit modules. / van der Bent G., van der Graaf M.W., van Vliet F.E. // 2007. EuMIC 2007. European Microwave Integrated Circuit Conference. - Munich, 8-10 Oct. 2007. - P. 403-406. ↑

C1053. Hardcastle I. 30 GHz (Ka-band) VSAT DVB-RCS Mixer-Driver multifunction MMIC. / Hardcastle I., Melvin S., Mayock J., Collar A., Simpson P., Brookbanks M., Bisby I. // 2007. EuMIC 2007. European Microwave Integrated Circuit Conference. - Munich, 8-10 Oct. 2007. - P. 415-418. ↑

C1054. Sigyun Jeong. High efficiency distributed amplifier using optimum transmission line. / Sigyun Jeong, Heungjae Choi, Yongchae Jeong, Kenney J.S., Chuldong Kim. // 2007. EuMIC 2007. European Microwave Integrated Circuit Conference. - Munich, 8-10 Oct. 2007. - P. 287-290. ↑

C1055. Han Gil Bae. High-efficiency GaN class-E power amplifier with compact harmonic-suppression network. / Han Gil Bae, Negra R., Boumaiza S., Ghannouchi F.M. // 2007. EuMIC 2007. European Microwave Integrated Circuit Conference. - Munich, 8-10 Oct. 2007. - P. 295-298. ↑

C1056. Junghwan Moon. GaN HEMT based Doherty amplifier for 3.5-GHz WiMAX Applications. / Junghwan Moon, Jangheon Kim, Ildu Kim, Young Yun Woo, Sungchul Hong, Han Seok Kim, Jong Sung Lee, Bumman Kim. // 2007. EuMIC 2007. European Microwave Integrated Circuit Conference. - Munich, 8-10 Oct. 2007. - P. 395-398. ↑

C1057. Hyeonnam Kim. Extraction of effective trap density and gate length in AlGaIn/GaN HEMTs based on pulsed I-V characteristics. / Hyeonnam Kim, Wu Lu. // 2007 International Semiconductor Device Research Symposium. - College Park, MD, 12-14 Dec. 2007. - P. 1-2. ↑

C1058. Koudymov A.N. Current collapse and reliability mechanisms in GaN HEMTs. / Koudymov A.N., Shur M.S., Simin G.S. // 2007 International Semiconductor Device Research Symposium. - College Park, MD, 12-14 Dec. 2007. - P. 1-2. ↑

C1059. Liu D. 80nm In_{0.52}Al_{0.48}As/In_{0.53}Ga_{0.47}As/InAs_{0.3}P_{0.7} Composite channel HEMT with an fT of 280GHz. / Liu D., Hudait M., Lin Y., Ringel S.A., Lu W. // 2007 International Semiconductor Device Research Symposium. - College Park, MD, 12-14 Dec. 2007. - P. 1-2. ↑

- C1060.** Eliza S.A. Analysis of AlGaIn/GaN HEMT modulated by photosystem I reaction centers. / Eliza S.A., Islam S.K., Lee I., Greenbaum E. // 2007 International Semiconductor Device Research Symposium. - College Park, MD, 12-14 Dec. 2007. - P. 1-2. ↑
- C1061.** Rosker M. The coming revolution in RF electronics. 2007 International Semiconductor Device Research Symposium. - College Park, MD, 12-14 Dec. 2007. - P. 1. ↑
- C1062.** Lingjia Li. Gate I-V characteristics degradation in AlGaIn/AlN/GaN HEMTs. / Lingjia Li, Skowronski M. // 2007 International Semiconductor Device Research Symposium. - College Park, MD, 12-14 Dec. 2007. - P. 1-2. ↑
- C1063.** Li-Hsien Huang. Investigation of AlGaIn/GaN/AlGaIn metal -oxide-semiconductor high electron mobility transistors. / Li-Hsien Huang, Chien-liang Lu, Ching-Ting Lee. // TENCON 2007-2007 IEEE Region 10 Conference. - Taipei, Oct. 30 2007-Nov. 2 2007. - P. 1-3. ↑
- C1064.** Chung-Yeh Wu. A High-Sensitive Pd/InGaP transistor hydrogen sensor. / Chung-Yeh Wu, Chin-Tien Lin, Yen-I Chou, Chieng-Chi Tung, Wen-Chau Liu, Huey-Ing Chen. // 2007. ESSDERC 2007. 37th European Solid State Device Research Conference. - Munich, 11-13 Sept. 2007. - P. 442-445. ↑
- C1065.** Pullia A. High-resolution alpha-particle spectroscopy with an hybrid SiC/GaN detector/front-end detection system. / Pullia A., Bertuccio G., Maiocchi D., Caccia S., Zocca F. // 2007. NSS 07. IEEE Nuclear Science Symposium Conference Record. - Honolulu, HI, Oct. 26 2007-Nov. 3 2007. - Vol. 2. - P. 1516-1520. ↑
- C1066.** Dae-Hyun Kim. Impact of lateral engineering on the logic performance of sub-50 nm InGaAs HEMTs. / Dae-Hyun Kim, del Alamo J.A. // 2007 International Semiconductor Device Research Symposium. - College Park, MD, 12-14 Dec. 2007. - P. 1-2. ↑
- C1067.** Maoliu Lin. Application of linearization modeling technology for nonlinear RF power devices. / Maoliu Lin, Xiaojie Hua, Hongjian Sun, Jing Jiang. // TENCON 2007-2007 IEEE Region 10 Conference. - Taipei, Oct. 30 2007-Nov. 2 2007. - P. 1-4. ↑
- C1068.** Shih-Ming Wang. A single chip dual-band low noise amplifier. / Shih-Ming Wang, Cheng-Chung Chen. // TENCON 2007-2007 IEEE Region 10 Conference. - Taipei, Oct. 30 2007-Nov. 2 2007. - P. 1-4. ↑
- C1069.** Saito W. Current Collapseless High-Voltage GaN-HEMT and its 50-W Boost Converter Operation. / Saito W., Kuraguchi M., Takada Y., Tsuda K., Saito Y., Omura I., Yamaguchi M. // 2007. IEDM 2007. IEEE International Electron Devices Meeting. - Washington, DC, 10-12 Dec. 2007. - P. 869-872. ↑
- C1070.** Andrei P. Redesign and optimization of semiconductor devices. / Andrei P., Liviu Oniciuc. // 2007 International Semiconductor Device Research Symposium. - College Park, MD, 12-14 Dec. 2007. - P. 1-2. ↑
- C1071.** Gangwani P. 2-Dimensional simulation and characterization of deep-submicron AlGaIn/GaN HEMTs for high frequency applications. / Gangwani P., Kaur R., Pandey S., Haldar S., Gupta M., Gupta R.S. // 2007 International Semiconductor Device Research Symposium. - College Park, MD, 12-14 Dec. 2007. - P. 1-2. ↑
- C1072.** Dae-Hyun Kim. Logic Performance of 40 nm InAs HEMTs. / Dae-Hyun Kim, del Alamo J.A. // 2007. IEDM 2007. IEEE International Electron Devices Meeting. - Washington, DC, 10-12 Dec. 2007. - P. 629-632. ↑
- C1073.** Waldron N. 90 nm Self-aligned Enhancement-mode InGaAs HEMT for Logic Applications. / Waldron N., Dae-Hyun Kim, del Alamo J.A. // 2007. IEDM 2007. IEEE International Electron Devices Meeting. - Washington, DC, 10-12 Dec. 2007. - P. 633-636. ↑
- C1074.** Uemoto Y. 8300V Blocking Voltage AlGaIn/GaN Power HFET with Thick Poly-AlN Passivation. / Uemoto Y., Shibata D., Yanagihara M., Ishida H., Matsuo H., Nagai S., Batta N., Ming Li, Ueda T., Tanaka T., Ueda D. // 2007. IEDM 2007. IEEE International Electron Devices Meeting. - Washington, DC, 10-12 Dec. 2007. - P. 861-864. ↑
- C1075.** Vitanov S. Normally-off AlGaIn/GaN HEMTs with InGaIn cap layer: A theoretical study. / Vitanov S., Palankovski V. // 2007 International Semiconductor Device Research Symposium. - College Park, MD, 12-14 Dec. 2007. - P. 1-2. ↑
- C1076.** Medjdoub F. Thermal stability of 5 nm barrier InAlN/GaN HEMTs. / Medjdoub F., Alomari M., Carlin J. -

F., Gonschorek M., Feltin E., Py M.A., Grandjean N., Kohn E. // 2007 International Semiconductor Device Research Symposium. - College Park, MD, 12-14 Dec. 2007. - P. 1-2. ↑

C1077. Cao Y. Ultrathin MBE-Grown AlN/GaN HEMTs with record high current densities. / Cao Y., Deen D., Simon J., Bean J., Su N., Zhang J., Fay P., Xing H., Jena D. // 2007 International Semiconductor Device Research Symposium. - College Park, MD, 12-14 Dec. 2007. - P. 1-2. ↑

C1078. Kumar S.P. Two-dimensional analytical sub-threshold modeling and simulation of Gate Material Engineered HEMT for enhanced carrier transport Efficiency. / Kumar S.P., Agrawal A., Chaujar R., Gupta M., Gupta R.S. // 2007 International Semiconductor Device Research Symposium. - College Park, MD, 12-14 Dec. 2007. - P. 1-2. ↑

C1079. Huque M.A. Effect of the aspect ratio in AlGaIn/GaN HEMT's DC and small signal parameters. / Huque M.A., Eliza S.A., Rahman T., Huq H.F., Islam S.K. // 2007 International Semiconductor Device Research Symposium. - College Park, MD, 12-14 Dec. 2007. - P. 1-2. ↑

C1080. Young-Hwan Choi. AlGaIn/GaN HEMT without Schottky contact on the dry-etched region for high breakdown voltage. / Young-Hwan Choi, Jiyong Lim, In-Hwan Ji, Kyu-Heon Cho, Young-Shil Kim, Min-Koo Han. // 2007 International Semiconductor Device Research Symposium. - College Park, MD, 12-14 Dec. 2007. - P. 1-2. ↑

C1081. Weber R. A PLL-Stabilized W-Band MHEMT Push-Push VCO with Integrated Frequency Divider Circuit. / Weber R., Kuri M., Lang M., Tessmann A., Seelmann-Eggebert M., Leuther A. // 2007. IEEE/MTT-S International Microwave Symposium. - Honolulu, HI, 3-8 June 2007. - P. 653-656. ↑

C1082. Inoue Y. Degradation-Mode Analysis for Highly Reliable GaN-HEMT. / Inoue Y., Masuda S., Kanamura M., Ohki T., Makiyama K., Okamoto N., Imanishi K., Kikkawa T., Hara N., Shigematsu H., Joshin K. // 2007. IEEE/MTT-S International Microwave Symposium. - Honolulu, HI, 3-8 June 2007. - P. 639-642. ↑

C1083. Parker A.E. Robust Extraction of Access Elements for Broadband Small-signal FET Models. / Parker A.E., Mahon S.J. // 2007. IEEE/MTT-S International Microwave Symposium. - Honolulu, HI, 3-8 June 2007. - P. 783-786. ↑

C1084. Zarate-de Landa A. A New and Better Method for Extracting the Parasitic Elements of On-Wafer GaN Transistors. / Zarate-de Landa A., Zuniga-Juarez J.E., Reynoso-Hernandez J.A., Maya-Sanchez M.C., Piner E.L., Linthicum K.J. // 2007. IEEE/MTT-S International Microwave Symposium. - Honolulu, HI, 3-8 June 2007. - P. 791-794. ↑

C1085. Hong Yin. A new physics-based compact model for AlGaIn/GaN HFETs. / Hong Yin, Bilbro G.L., Trew R.J. // 2007. IEEE/MTT-S International Microwave Symposium. - Honolulu, HI, 3-8 June 2007. - P. 787-790. ↑

C1086. Kobayashi K.W. A 2 Watt, Sub-dB Noise Figure GaN MMIC LNA-PA Amplifier with Multi-octave Bandwidth from 0.2-8 GHz. / Kobayashi K.W., Yao Chung Chen, Smorchkova I., Tsai R., Wojtowicz M., Oki A. // 2007. IEEE/MTT-S International Microwave Symposium. - Honolulu, HI, 3-8 June 2007. - P. 619-622. ↑

C1087. Jardel O. A Drain-Lag Model for AlGaIn/GaN Power HEMTs. / Jardel O., De Groote F., Charbonniaud C., Reveyrand T., Teyssier J.P., Quere R., Floriot D. // 2007. IEEE/MTT-S International Microwave Symposium. - Honolulu, HI, 3-8 June 2007. - P. 601-604. ↑

C1088. Shen L. Deep-recessed GaN HEMTs using selective etch technology exhibiting high microwave performance without surface passivation. / Shen L., Pei Y., McCarthy L., Poblencz C., Corrión A., Fichtenbaum N., Keller S., Denbaars S.P., Speck J.S., Mishra U.K. // 2007. IEEE/MTT-S International Microwave Symposium. - Honolulu, HI, 3-8 June 2007. - P. 623-626. ↑

C1089. Meharry D.E. Multi-Watt Wideband MMICs in GaN and GaAs. / Meharry D.E., Lender R.J., Kanin Chu, Gunter L.L., Beech K.E. // 2007. IEEE/MTT-S International Microwave Symposium. - Honolulu, HI, 3-8 June 2007. - P. 631-634. ↑

C1090. Ming-Yih Kao. AlGaIn/GaN HEMTs with PAE of 53% at 35 GHz for HPA and Multi-Function MMIC Applications. / Ming-Yih Kao, Lee C., Hajji R., Saunier P., Hua-Quen Tserng. // 2007. IEEE/MTT-S International Microwave Symposium. - Honolulu, HI, 3-8 June 2007. - P. 627-629. ↑

- C1091.** Negra R. Switch-based GaN HEMT model suitable for highly-efficient RF power amplifier design. / Negra R., Chu T.D., Helaoui M., Boumaiza S., Hegazi G.M., Ghannouchi K. // 2007. IEEE/MTT-S International Microwave Symposium. - Honolulu, HI, 3-8 June 2007. - P. 795-798. ↑
- C1092.** Crescenzi E.J. A 2.5 Watt 3.3-3.9 GHz Power Amplifier for WiMAX Applications using a GaN HEMT in a Small Surface-Mount Package. / Crescenzi E.J., Wood S.M., Prejs A., Pengelly R.S., Pribble W. // 2007. IEEE/MTT-S International Microwave Symposium. - Honolulu, HI, 3-8 June 2007. - P. 1111-1114. ↑
- C1093.** Yong-Sub Lee. Applications of GaN HEMTs and SiC MESFETs in High Efficiency Class-E Power Amplifier Design for WCDMA Applications. / Yong-Sub Lee, Yoon-Ha Jeong. // 2007. IEEE/MTT-S International Microwave Symposium. - Honolulu, HI, 3-8 June 2007. - P. 1099-1102. ↑
- C1094.** Koch S. An Analogue, 4:2 MUX/DEMUX Front-End MIMIC for Wireless 60 GHz Multiple Antenna Transceivers. / Koch S., Kallfass I., Weber R., Leuther A., Schlechtweg M., Uno M. // 2007. IEEE/MTT-S International Microwave Symposium. - Honolulu, HI, 3-8 June 2007. - P. 1121-1124. ↑
- C1095.** Sungchul Hong. High Efficiency GaN HEMT Power Amplifier optimized for OFDM EER Transmitter. / Sungchul Hong, Young Yun Woo, Ildu Kim, Jangheon Kim, Junghwan Moon, Han Seok Kim, Jong Sung Lee, Bumman Kim. // 2007. IEEE/MTT-S International Microwave Symposium. - Honolulu, HI, 3-8 June 2007. - P. 1247-1250. ↑
- C1096.** Jeng-Han Tsai. A Miniature 38-48 GHz MMIC Sub-Harmonic Transmitter With Post-Distortion Linearization. / Jeng-Han Tsai, Hong-Yuan Yang, Che-Chung Kuo, Tian-Wei Huang. // 2007. IEEE/MTT-S International Microwave Symposium. - Honolulu, HI, 3-8 June 2007. - P. 1133-1136. ↑
- C1097.** Lefebvre B. A K-band low cost plastic packaged high linearity Power Amplifier with integrated ESD protection for Multi-band Telecom applications. / Lefebvre B., Bouw D., Lhortolary J., Chang C., Tranchant S., Camiade M. // 2007. IEEE/MTT-S International Microwave Symposium. - Honolulu, HI, 3-8 June 2007. - P. 825-828. ↑
- C1098.** Amasuga H. A High Power and High Breakdown Voltage Millimeter-Wave GaAs pHEMT with Low Nonlinear Drain Resistance. / Amasuga H., Inoue A., Goto S., Kunii T., Yamamoto Y., Oku T., Ishikawa T. // 2007. IEEE/MTT-S International Microwave Symposium. - Honolulu, HI, 3-8 June 2007. - P. 821-824. ↑
- C1099.** Wallis R.E. Advances in Microwave Technology for the MESSENGER Mission to Mercury. / Wallis R.E., Sheng Cheng, Malouf P.M., Stilwell R.K. // 2007. IEEE/MTT-S International Microwave Symposium. - Honolulu, HI, 3-8 June 2007. - P. 939-942. ↑
- C1100.** Bokatius M. Overcoming pHEMT Linearity Dependence on Fundamental Input Tuning by Digital Pre-Distortion. / Bokatius M., Lefevre M., Miller M. // 2007. IEEE/MTT-S International Microwave Symposium. - Honolulu, HI, 3-8 June 2007. - P. 1067-1070. ↑
- C1101.** Bokatius M. High Gain, High Efficiency 12V pHEMT Power Transistors for WiMAX Applications. / Bokatius M., Moore K., Miller M. // 2007. IEEE/MTT-S International Microwave Symposium. - Honolulu, HI, 3-8 June 2007. - P. 1063-1066. ↑
- C1102.** Lhortolary J. A new nonlinear HEMT model allowing accurate simulation of very low IM3 levels for high-frequency highly linear amplifiers design. / Lhortolary J., Chang C., Reveyrand T., Camiade M., Campovecchio M., Obregon J. // 2007. IEEE/MTT-S International Microwave Symposium. - Honolulu, HI, 3-8 June 2007. - P. 589-592. ↑
- C1103.** Hoon Hee Chung. A Bandpass $\Delta\Sigma$ DDFS-Driven 19GHz Frequency Synthesizer for FMCW Automotive Radar. / Hoon Hee Chung, Lyles U., Copani T., Bakaloglu B., Kiaei S. // 2007. ISSCC 2007. Digest of Technical Papers. IEEE International Solid-State Circuits Conference. - San Francisco, CA, 11-15 Feb. 2007. - P. 126-591. ↑
- C1104.** Sugimoto M. Vertical device operation of AlGaIn/GaN HEMTs on free-standing n-GaN substrates. / Sugimoto M., Ueda H., Kanechika M., Soejima N., Uesugi T., Kachi T. // 2007. PCC '07 Power Conversion Conference-Nagoya. - Nagoya, 2-5 April 2007. - P. 368-372. ↑
- C1105.** Deal W.R. Advanced MMIC for Passive Millimeter and Submillimeter Wave Imaging. / Deal W.R., Yujiri L., Siddiqui M., Lai R. // 2007. ISSCC 2007. Digest of Technical Papers. IEEE International Solid-State Circuits Conference. - San Francisco, CA, 11-15 Feb. 2007. - P. 126-591. ↑

Conference. - San Francisco, CA, 11-15 Feb. 2007. - P. 572-622.

C1106. Ogunniyi A.J. Accurate Modeling of Drain Current Derivatives of MESFET/HEMT Devices for Intermodulation Analysis. / Ogunniyi A.J., Henriquez S.L., Karangu C.W., Dickens C., White C. // 2007. ISCAS 2007. IEEE International Symposium on Circuits and Systems. - New Orleans, LA, 27-30 May 2007. - P. 1013-1016. ↑

C1107. Waho T. A Four-Resonant-Tunneling-Diode (4RTD) NAND/NOR Logic Gate. / Waho T., Yamada A., Okuyama H., Khorenko V., Do T., Prost W. // 2007. ISCAS 2007. IEEE International Symposium on Circuits and Systems. - New Orleans, LA, 27-30 May 2007. - P. 129-132. ↑

C1108. Coffie R. Temperature and Voltage Dependent RF Degradation Study in Algan/gan HEMTs. / Coffie R., Chen Y., Smorchkova I.P., Heying B., Gambin V., Sutton W., Chou Y.-C., Luo W.-B., Wojtowicz M., Oki A. // 2007. proceedings. 45th annual. ieee international Reliability physics symposium. - Phoenix, AZ, 15-19 April 2007. - P. 568-569. ↑

C1109. Chang Woo Jin. 60 GHz Amplifier MMICs and Module for 60 GHz WPAN System. / Chang Woo Jin, Lim Jong Won, Ahn Ho Kyun, Kim Haecheon, Yu Hyun Kyu. // 2007 IEEE Radio and Wireless Symposium. - Long Beach, CA, 9-11 Jan. 2007. - P. 377-380. ↑

C1110. Grinyaev S.N. Novel IR Photodetectors Based on GaN/AlGaIn HEMT with QWs or QDs in the Barrier. / Grinyaev S.N., Karavaev G.F., Zhuravlev K.S., Tronc P. // 2007. SIBCON '07. Siberian Conference on Control and Communications. - Tomsk, 20-21 April 2007. - P. 248-254. ↑

C1111. Raboch J. Restrictions in Using Large Signal and Small Signal Models of FET Transistors. / Raboch J., Hoffmann K. // 2007. 17th International Conference Radioelektronika. - Brno, 24-25 April 2007. - P. 1-4. ↑

C1112. Randus M. Broadband Medium-Power Transistor Amplifier 12-18 GHz. / Randus M., Hoffmann K. // 2007. 17th International Conference Radioelektronika. - Brno, 24-25 April 2007. - P. 1-5. ↑

C1113. Ducatteau D. Non Linear RF Device Characterization in Time Domain using an Active Loadpull Large Signal Network Analyzer. / Ducatteau D., Werquin M., Grimbert B., Morvan E., Theron D., Gaquiere C. // 2007. IMTC 2007. IEEE Instrumentation and Measurement Technology Conference Proceedings. - Warsaw, 1-3 May 2007. - P. 1-5. ↑

C1114. Giancesello F. 1.8 dB insertion loss 200 GHz CPW band pass filter integrated in HR SOI CMOS Technology. / Giancesello F., Gloria D., Montusclat S., Raynaud C., Boret S., Dambrine G., Lepilliet S., Martineau B., Pilard R. // 2007. IEEE/MTT-S International Microwave Symposium. - Honolulu, HI, 3-8 June 2007. - P. 453-456. ↑

C1115. {no data available}. WE2A: Low Noise CMOS and Low Power HEMT Technologies. 2007. IEEE/MTT-S International Microwave Symposium. - Honolulu, HI, USA, 3-8 June 2007. - P. 439. ↑

C1116. Simin G. High-power III-Nitride Integrated Microwave Switch with capacitively-coupled contacts. / Simin G., Yang G., Shur M. // 2007. IEEE/MTT-S International Microwave Symposium. - Honolulu, HI, 3-8 June 2007. - P. 457-460. ↑

C1117. Shih-Fong Chao. A 40-GHz MMIC SPDT Bandpass Filter Integrated Switch. / Shih-Fong Chao, Che-Chung Kuo, Zou-Min Tsai, Huei Wang. // 2007. IEEE/MTT-S International Microwave Symposium. - Honolulu, HI, 3-8 June 2007. - P. 483-486. ↑

C1118. Yeong-Chang Chou. Manufacturable and Reliable 0.1 μm AlSb/InAs HEMT MMIC Technology for Ultra-Low Power Applications. / Yeong-Chang Chou, Yang J.M., Lin C.H., Lee J., Lange M., Tsai R., Nam P., Nishimoto M., Gutierrez A., Quach H., Lai R., Farkas D., Wojtowicz M., Chin P., Barsky M., Oki A., Boos J.B., Bennett B.R. // 2007. IEEE/MTT-S International Microwave Symposium. - Honolulu, HI, 3-8 June 2007. - P. 461-464. ↑

C1119. Brown J.D. Voltage Dependent Characteristics of 48V AlGaIn/GaN High Electron Mobility Transistor Technology on Silicon Carbide. / Brown J.D., Lee S., Lieu D., Martin J., Vetury R., Poulton M.J., Shealy J.B. // 2007. IEEE/MTT-S International Microwave Symposium. - Honolulu, HI, 3-8 June 2007. - P. 303-306. ↑

C1120. Yu-Cheng Hsu. Single-chip Dual-Mode Power Amplifier MMIC using GaAs E-pHEMT for

WiMAX/WLAN Applications. / Yu-Cheng Hsu, Shih-Ming Wang, Cheng-Chung Chen, Wu-Jing Ho, Cheng-Kuo Lin. // 2007. IEEE/MTT-S International Microwave Symposium. - Honolulu, HI, 3-8 June 2007. - P. 159-162. ↑

C1121. Yaochung Chen. Survivability of AlGaIn/GaN HEMT. / Yaochung Chen, Coffie R., Wen-Ben Luo, Wojtowicz M., Smorchkova I., Benjamin Heying, Young-Min Kim, Aust M.V., Oki A. // 2007. IEEE/MTT-S International Microwave Symposium. - Honolulu, HI, 3-8 June 2007. - P. 307-310. ↑

C1122. Tessmann A. Metamorphic H-Band Low-Noise Amplifier MMICs. / Tessmann A., Leuther A., Massler H., Bronner W., Schlechtweg M., Weimann G. // 2007. IEEE/MTT-S International Microwave Symposium. - Honolulu, HI, 3-8 June 2007. - P. 353-356. ↑

C1123. Deal W.R. A 245-GHz MMIC Amplifier with 80- μ m Output Periphery and 12-dB Gain. / Deal W.R., Mei X.B., Radisic V., Yoshida W., Liu P.H., Uyeda J., Barsky M., Gaier T., Fung A., Samoska L., Lai R. // 2007. IEEE/MTT-S International Microwave Symposium. - Honolulu, HI, 3-8 June 2007. - P. 329-332. ↑

C1124. Jung-Sheng Huang. An Analytical Model and Measurement on the InAlAs/InGaAs High-Electron-Mobility Transistor with Oxidized InAlAs Gate. / Jung-Sheng Huang, Kuan-Wei Lee, Fang-Ming Lee, Yung-Sheng Huang, Yeong-Her Wang. // 2007. IPRM 07. IEEE 19th International Conference on Indium Phosphide & Related Materials. - Matsue, 14-18 May 2007. - P. 114-117. ↑

C1125. Hyung Sup Yoon. Characteristics of 80 nm T-Gate Metamorphic HEMTx with 60 % Indium Channel. / Hyung Sup Yoon, Jae Yeob Shim, Dong Min Kang, Ju Yeon Hong, Kyung Ho Lee. // 2007. IPRM 07. IEEE 19th International Conference on Indium Phosphide & Related Materials. - Matsue, 14-18 May 2007. - P. 110-113. ↑

C1126. Lefebvre E. (Cl₂/Ar) ICP/RIE Dry Etching of Al(Ga) Sb FOR AlSb/InAs HEMTs. / Lefebvre E., Borg M., Malmkvist M., Grahn J., Desplanque L., Wallart X., Roelens Y., Dambrine G., Cappy A., Bollaert S. // 2007. IPRM 07. IEEE 19th International Conference on Indium Phosphide & Related Materials. - Matsue, 14-18 May 2007. - P. 125-128. ↑

C1127. Chee Leong Tan. Evidence of Existence of Different Surface States in INP-Based High Electron Mobility Transistors (HEMTs). / Chee Leong Tan, Hong Wang, Radhakrishnan K. // 2007. IPRM 07. IEEE 19th International Conference on Indium Phosphide & Related Materials. - Matsue, 14-18 May 2007. - P. 118-120. ↑

C1128. Borg M. DC and RF Performance of 0.2-0.4 μ m Gate Length InAs/AlSb HEMTs. / Borg M., Lefebvre E., Malmkvist M., Desplanque L., Wallart X., Roelens Y., Dambrine G., Cappy A., Bollaert S., Grahn J. // 2007. IPRM 07. IEEE 19th International Conference on Indium Phosphide & Related Materials. - Matsue, 14-18 May 2007. - P. 67-70. ↑

C1129. Lai R. High Performance and High Reliability of 0.1 μ m InP HEMT MMIC Technology on 100 mm InP Substrates. / Lai R., Chou Y.C., Lee L.J., Liu P.H., Leung D., Kan Q., Mei X., Lin C.H., Farkas D., Barsky M., Eng D., Cavus A., Lange M., Chin P., Wojtowicz M., Block T., Oki A. // 2007. IPRM 07. IEEE 19th International Conference on Indium Phosphide & Related Materials. - Matsue, 14-18 May 2007. - P. 63-66. ↑

C1130. Nannen I. InP-HEMT-TIA with Differential Optical Input Using Vertical High Topology Pin-Diodes. / Nannen I., Poloczek A., Matiss A., Brockerhoff W., Regolin I., Tegude F.-J. // 2007. IPRM 07. IEEE 19th International Conference on Indium Phosphide & Related Materials. - Matsue, 14-18 May 2007. - P. 107-109. ↑

C1131. Murata H. Optical Response of InP-based High-Electron Mobility Transistor and its Applications to High-Speed Photo-Detectors and Signal Converters. / Murata H., Kobayashi N., Okamura Y., Kosugi T., Enoki T. // 2007. IPRM 07. IEEE 19th International Conference on Indium Phosphide & Related Materials. - Matsue, 14-18 May 2007. - P. 84-86. ↑

C1132. Meziani Y.M. Self Oscillation of the Plasma Waves in a Dual Grating Gates HEMT Device. / Meziani Y.M., Hanabe M., Koizumi A., Otsuji T., Sano E. // 2007. IPRM 07. IEEE 19th International Conference on Indium Phosphide & Related Materials. - Matsue, 14-18 May 2007. - P. 534-537. ↑

C1133. Ganesello F. 65 nm HR SOI CMOS Technology: emergence of Millimeter-Wave SoC. / Ganesello F., Montusclat S., Martineau B., Gloria D., Raynaud C., Boret S., Dambrine G., Lepilliet S., Pilard R. // 2007 IEEE Radio Frequency Integrated Circuits (RFIC) Symposium. - Honolulu, HI, 3-5 June 2007. - P. 555-558. ↑

C1134. Morkner H. A Single Chip 802.11abgn Enhancement Mode PHEMT MMIC with dual LNAs, Switches, and Distortion Compensation Power Amplifiers. / Morkner H., Vice M., Karakucuk M., Abey W., Lan Nguyen,

Kessler J., Ruebusch R. // 2007 IEEE Radio Frequency Integrated Circuits (RFIC) Symposium. - Honolulu, HI, 3-5 June 2007. - P. 365-368. ↑

C1135. Kobayashi K.W. 1-Watt Conventional and Cascoded GaN-SiC Darlington MMIC Amplifiers to 18 GHz. / Kobayashi K.W., YaoChung Chen, Smorchkova I., Tsai R., Wojtowicz M., Oki A. // 2007 IEEE Radio Frequency Integrated Circuits (RFIC) Symposium. - Honolulu, HI, 3-5 June 2007. - P. 585-588. ↑

C1136. Tayrani R. A Spectrally pure 5.0 W, High PAE, (6-12 GHz) GaN Monolithic Class E Power Amplifier for Advanced T/R Modules. 2007 IEEE Radio Frequency Integrated Circuits (RFIC) Symposium. - Honolulu, HI, 3-5 June 2007. - P. 581-584. ↑

C1137. Lijian He. A new Linearization technique of Power Amplifier. / Lijian He, Wanrong Zhang, Wei Zhang, Hongyun Xie, Dongyue Jin, Yang Wang, Yongping Sha, Jianjun Qiu, Pan Gao. // 2007. ICMMT '07. International Conference on Microwave and Millimeter Wave Technology. - Builin, 18-21 April 2007. - P. 1-4. ↑

C1138. Cai Shuicheng. 0-80GHz 0.15 μm GaAs PHEMT Distributed Amplifier for Optic-Fiber Transmission Systems. / Cai Shuicheng, Wang Zhigong. // 2007. ICMMT '07. International Conference on Microwave and Millimeter Wave Technology. - Builin, 18-21 April 2007. - P. 1-3. ↑

C1139. Angelov I. Direct Extraction Techniques for Thermal Resistance of MESFET and HEMT Devices. / Angelov I., Karnfelt C. // 2007 IEEE Radio Frequency Integrated Circuits (RFIC) Symposium. - Honolulu, HI, 3-5 June 2007. - P. 351-354. ↑

C1140. Rosker M.J. The Present State of the Art of Wide-Bandgap Semiconductors and Their Future. 2007 IEEE Radio Frequency Integrated Circuits (RFIC) Symposium. - Honolulu, HI, 3-5 June 2007. - P. 159-162. ↑

C1141. King-Yuen Wong. Planar Two-dimensional Electron Gas (2DEG) IDT SAW Filter on AlGaN/GaN Heterostructure. / King-Yuen Wong, Tang W., Kei May Lau, Chen K.J. // 2007. IEEE/MTT-S International Microwave Symposium. - Honolulu, HI, 3-8 June 2007. - P. 2043-2046. ↑

C1142. Zmuidzinas J. Technology for Submillimeter Astronomy. 2007. IEEE/MTT-S International Microwave Symposium. - Honolulu, HI, 3-8 June 2007. - P. 1861-1864. ↑

C1143. Kallfass I. A Broadband Frequency Sixtupler MIMIC for the W-Band with >7 dBm Output Power and >6 dB Conversion Gain. / Kallfass I., Massler H., Tessmann A., Leuther A., Schlechtweg M., Weimann G. // 2007. IEEE/MTT-S International Microwave Symposium. - Honolulu, HI, 3-8 June 2007. - P. 2169-2172. ↑

C1144. Gaquiere C. AlInN/GaN a suitable HEMT device for extremely high power high frequency applications. / Gaquiere C., Medjdoub F., Carlin J.-F., Vandenbrouck S., Delos E., Feltin E., Grandjean N., Kohn E. // 2007. IEEE/MTT-S International Microwave Symposium. - Honolulu, HI, 3-8 June 2007. - P. 2145-2148. ↑

C1145. Sato M. 94-GHz Band High-Gain and Low-Noise Amplifier Using InP-HEMTs for Passive Millimeter Wave Imager. / Sato M., Hirose T., Ohki T., Sato H., Sawaya K., Mizuno K. // 2007. IEEE/MTT-S International Microwave Symposium. - Honolulu, HI, 3-8 June 2007. - P. 1775-1778. ↑

C1146. Iyomasa K. GaN HEMT 60W Output Power Amplifier with Over 50% Efficiency at C-Band 15% Relative Bandwidth Using Combined Short and Open Circuited Stubs. / Iyomasa K., Yamanaka K., Mori K., Noto H., Ohtsuka H., Nakayama M., Yoneda S., Kamo Y., Isota Y. // 2007. IEEE/MTT-S International Microwave Symposium. - Honolulu, HI, 3-8 June 2007. - P. 1255-1258. ↑

C1147. Yamanaka K. C-band GaN HEMT Power Amplifier with 220W Output Power. / Yamanaka K., Mori K., Iyomasa K., Ohtsuka H., Noto H., Nakayama M., Kamo Y., Isota Y. // 2007. IEEE/MTT-S International Microwave Symposium. - Honolulu, HI, 3-8 June 2007. - P. 1251-1254. ↑

C1148. Yamamoto T. 50% Drain Efficiency Doherty Amplifier with Optimized Power Range for W-CDMA Signal. / Yamamoto T., Kitahara T., Hiura S. // 2007. IEEE/MTT-S International Microwave Symposium. - Honolulu, HI, 3-8 June 2007. - P. 1263-1266. ↑

C1149. Ui N. A 80W 2-stage GaN HEMT Doherty Amplifier with 50dBc ACLR, 42% Efficiency 32dB Gain with DPD for W-CDMA Base station. / Ui N., Sano H., Sano S. // 2007. IEEE/MTT-S International Microwave Symposium. - Honolulu, HI, 3-8 June 2007. - P. 1259-1262. ↑

- C1150.** Rodwell M. Frequency Limits of InP-based Integrated Circuits. / Rodwell M., Lind E., Griffith Z., Bank S.R., Crook A.M., Singiseti U., Wistey M., Burek G., Gossard A.C. // 2007. IPRM 07. IEEE 19th International Conference on Indium Phosphide & Related Materials. - Matsue, 14-18 May 2007. - P. 9-13. ↑
- C1151.** del Alamo J.A. Beyond CMOS: Logic Suitability of InGaAs HEMTs. / del Alamo J.A., Dae-Hyun Kim. // 2007. IPRM 07. IEEE 19th International Conference on Indium Phosphide & Related Materials. - Matsue, 14-18 May 2007. - P. 51-54. ↑
- C1152.** Watanabe I. 35-nm-Gate In_{0.7}Ga_{0.3}As/In_{0.52}Al_{0.48}As HEMT with 520-GHz f_T. / Watanabe I., Endoh A., Mimura T., Matsui T. // 2007. IPRM 07. IEEE 19th International Conference on Indium Phosphide & Related Materials. - Matsue, 14-18 May 2007. - P. 28-31. ↑
- C1153.** Mei X.B. 35nm InP HEMT for Millimeter and Sub-Millimeter Wave Applications. / Mei X.B., Yoshida W., Deal W., Liu P.H., Lee J., Uyeda J., Dang L., Wang J., Liu W., Barsky M., Kim Y.M., Lange M., Chin T.P., Radisic V., Gaier T., Fung A., Lai R. // 2007. IPRM 07. IEEE 19th International Conference on Indium Phosphide & Related Materials. - Matsue, 14-18 May 2007. - P. 59-62. ↑
- C1154.** Takahashi T. InAlAs/InGaAs HEMTs with Minimum Noise Figure of 1.0 dB AT 94 GHz. / Takahashi T., Sato M., Makiyama K., Hirose T., Hara N. // 2007. IPRM 07. IEEE 19th International Conference on Indium Phosphide & Related Materials. - Matsue, 14-18 May 2007. - P. 55-58. ↑
- C1155.** Leuther A. 50 nm MHEMT Technology for G- and H-Band MMICs. / Leuther A., Tessmann A., Dammann M., Schworer C., Schlechtweg M., Mikulla M., Losch R., Weimann G. // 2007. IPRM 07. IEEE 19th International Conference on Indium Phosphide & Related Materials. - Matsue, 14-18 May 2007. - P. 24-27. ↑
- C1156.** Shinohara K. Extremely High gm>2.2 S/mm and f_T>550 GHz in 30-nm Enhancement-Mode InP-HEMTs with Pt/Mo/Ti/Pt/Au Buried Gate. / Shinohara K., Wonill Ha, Rodwell M.J.W., Brar B. // 2007. IPRM 07. IEEE 19th International Conference on Indium Phosphide & Related Materials. - Matsue, 14-18 May 2007. - P. 18-21. ↑
- C1157.** Liu P.H. High Gain G-Band MMIC Amplifiers Based on Sub-50 nm Gate Length InP HEMT. / Liu P.H., Yoshida W., Lee J., Dang L., Wang J., Liu W., Uyeda J., Li D., Mei X.B., Deal W., Barsky M., Kim Y.M., Lange M., Chin T.P., Radisic V., Gaier T., Fung A., Lai R. // 2007. IPRM 07. IEEE 19th International Conference on Indium Phosphide & Related Materials. - Matsue, 14-18 May 2007. - P. 22-23. ↑